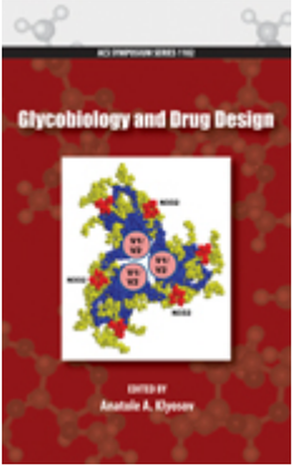

ACS SYMPOSIUM SERIES 1102

Glycobiology and Drug Design

EDITED BY

Anatole A. Klyosov

Downloaded by 89.163.35.42 on June 13, 2012 | http://pubs.acs.org
Publication Date (Web): June 12, 2012 | doi: 10.1021/bk-2012-1102.fw001

Glycobiology and Drug Design

Downloaded by 89.163.35.42 on June 13, 2012 | http://pubs.acs.org
Publication Date (Web): June 12, 2012 | doi: 10.1021/bk-2012-1102.fw001

ACS SYMPOSIUM SERIES **1102**

Glycobiology and Drug Design

Anatole A. Klyosov, Editor
Galectin Therapeutics

Downloaded by 89.163.35.42 on June 13, 2012 | http://pubs.acs.org
Publication Date (Web): June 12, 2012 | doi: 10.1021/bk-2012-1102.fw001

Sponsored by the
ACS Division of Carbohydrate Chemistry

American Chemical Society, Washington, DC

Distributed in print by Oxford University Press, Inc.

Downloaded by 89.163.35.42 on June 13, 2012 | http://pubs.acs.org
Publication Date (Web): June 12, 2012 | doi: 10.1021/bk-2012-1102.fw001

Library of Congress Cataloging-in-Publication Data

Glycobiology and drug design / Anatole A. Klyosov, editor ; sponsored by the ACS Division of Carbohydrate Chemistry.
p. cm. -- (ACS symposium series ; 1102)
Includes bibliographical references and index.
ISBN 978-0-8412-2765-1 (alk. paper)
1. Drugs--Design. 2. Glycomics. 3. Drug development. 4. Carbohydrate drugs. I. Klesov, A. A. (Anatolii
Alekseevich) II. American Chemical Society. Division of Carbohydrate Chemistry.
RS420.G59 2012
615.1’9--dc23
2012012730

The paper used in this publication meets the minimum requirements of American National Standard for Information Sciences—Permanence of Paper for Printed Library Materials, ANSI Z39.48n1984.

Copyright © 2012 American Chemical Society

Distributed in print by Oxford University Press, Inc.

All Rights Reserved. Reprographic copying beyond that permitted by Sections 107 or 108 of the U.S. Copyright Act is allowed for internal use only, provided that a per-chapter fee of $40.25 plus $0.75 per page is paid to the Copyright Clearance Center, Inc., 222 Rosewood Drive, Danvers, MA 01923, USA. Republication or reproduction for sale of pages in this book is permitted only under license from ACS. Direct these and other permission requests to ACS Copyright Office, Publications Division, 1155 16th Street, N.W., Washington, DC 20036.

The citation of trade names and/or names of manufacturers in this publication is not to be construed as an endorsement or as approval by ACS of the commercial products or services referenced herein; nor should the mere reference herein to any drawing, specification, chemical process, or other data be regarded as a license or as a conveyance of any right or permission to the holder, reader, or any other person or corporation, to manufacture, reproduce, use, or sell any patented invention or copyrighted work that may in any way be related thereto. Registered names, trademarks, etc., used in this publication, even without specific indication thereof, are not to be considered unprotected by law.

PRINTED IN THE UNITED STATES OF AMERICA

Downloaded by 89.163.35.42 on June 13, 2012 | http://pubs.acs.org
Publication Date (Web): June 12, 2012 | doi: 10.1021/bk-2012-1102.fw001

Foreword

The ACS Symposium Series was first published in 1974 to provide a mechanism for publishing symposia quickly in book form. The purpose of the series is to publish timely, comprehensive books developed from the ACS sponsored symposia based on current scientific research. Occasionally, books are developed from symposia sponsored by other organizations when the topic is of keen interest to the chemistry audience.

Before agreeing to publish a book, the proposed table of contents is reviewed for appropriate and comprehensive coverage and for interest to the audience. Some papers may be excluded to better focus the book; others may be added to provide comprehensiveness. When appropriate, overview or introductory chapters are added. Drafts of chapters are peer-reviewed prior to final acceptance or rejection, and manuscripts are prepared in camera-ready format.

As a rule, only original research papers and original review papers are included in the volumes. Verbatim reproductions of previous published papers are not accepted.

ACS Books Department

Preface

Six years have passed since the book *Carbohydrate Drug Design* (edited by Anatole A. Klyosov, Zbigniew J. Witczak, and David Platt, Oxford University Press, 2006) was published, which brought a great deal of new knowledge to this area of study. Since then, however, literally thousands of peer-reviewed papers have been published. In the area of galectins alone — which are lectins, specific to galactose, and which carry many important functions directly related to angiogenesis, inflammation, immune response, trigger many intra- and intercellular signals when they interact with galectin blockers or stimulants, and are responsible for many different pathologies, as briefly described in Chapter 2 of the book — more than 300 articles are published each year.

A great many papers appear every day on such themes as molecular recognition in carbohydrate drug design, multivalent glycans and glycoconjugates, low molecular weight inhibitors of receptors involved in carbohydrate drug recognition, structure–function relationships in glycobiology of drug design, glycomimetic interactions in drug design, bioassays in carbohydrate drug design, carbohydrate-based anti-glioma drug design, anti-diabetes drug design, lectins in disease, intracellular functions related to glycobiology of drug design, extracellular functions in drug design and their role in immunity, carbohydrate drugs and angiogenesis, carbohydrate drugs and inflammation, carbohydrate drugs and tissue fibrogenesis, carbohydrate drug design and infections, carbohydrate drug design in renal and lung fibrosis, knockout mice and drug design, glycobiology and drugs aimed at autoimmune disorders, carbohydrate drugs against lymphoid malignancies, carbohydrate drug design against thrombosis, carbohydrate drugs against melanomas, a translational rational in carbohydrate drug design, carbohydrate drug design for multiple sclerosis, in cardiac diseases, in ophthalmology, and at least in a hundred more different pathologies currently under study with carbohydrate drugs.

Of course it would be impossible to address all of these topics in a single volume; and although that is not the intention of this book, it should be noted that many of the above-mentioned subjects are explored here.

During the past several years, it has become increasingly clear that carbohydrates, which can be targeted to specific diseases, represent a whole new dimension in drug design. Characterized by a variety of terms — *specific recognition, lectins*, and *molecular diversity*, just to cite a few — this new dimension based on carbohydrates essentially has introduced a new *language* to chemistry, biochemistry, and related disciplines.

Vocabulary has been building so fast, in fact, that most professional chemists (i.e., practitioners who are among the few who work in the area of carbohydrates)

Downloaded by 89.163.35.42 on June 13, 2012 | http://pubs.acs.org
Publication Date (Web): June 12, 2012 | doi: 10.1021/bk-2012-1102.pr001

Downloaded by 89.163.35.42 on June 13, 2012 | http://pubs.acs.org
Publication Date (Web): June 12, 2012 | doi: 10.1021/bk-2012-1102.pr001

may sometimes feel a bit illiterate. This book will help them and many other scientists to better understand the current state of the art and the challenges that remain in successfully consummating matches of carbohydrate-based drugs and the deadly diseases they target.

Only four books have been published previously in this area, directed to drug design: *Carbohydrates in Drug Design* (by Z.J. Witczak and K. Nieforth, editors, 1997); *Complex Carbohydrates in Drug Research: Structural and Functional Aspects* (Klaus Boch, Henrik Clausen, and Dennis Boch, editors, 1998); *Carbohydrates-Based Drug Discovery* (by C.-H. Wong, editor, 2003); and *Carbohydrate Drug Design* (cited above, 2006). The current book complements and extends these preceding volumes in several critical ways. It includes preclinical studies and clinical trials of carbohydrate-based drugs in progress as well as analyzing their delivery, biocompatibility, clearance, and metabolic pathways. Further, this book explores a number of other features of carbohydrate drugs and their targets, such as the structure of antibodies with unusually high-affinity for carbohydrates, and protein–glycan interactions and their inhibitors. Galactomannans and thio-, imino-, nitro-, and aminosugars are particularly considered with respect to their structural and functional impacts.

It is our hope that this volume will not only update existing publications on carbohydrate-based drug design but also further shape the emerging data and thinking in this new area. This book also includes several chapters on carbohydrate-based vaccines and carbohydrate-based treatment of some infections, along with new data on the chemistry of carbohydrates and the computation of carbohydrate structures. An overview of these chapters is given in the last several sections of Chapter 1, entitled "Cancer and a combination carbohydrate-assisted chemotherapy," "Carbohydrate-based HIV vaccines," "Polysaccharides and infections," "Aminosugars," and "Computation studies."

Last, but not least, I have the pleasure of thanking my wife Gail, who also holds a Ph.D. in chemistry, and who provided me with great support and tolerated the many evenings and weekends I spent preparing this book.

Anatole A. Klyosov

Galectin Therapeutics Inc.
7 Wells Avenue
Newton, MA 02459

Downloaded by CORNELL UNIV on June 14, 2012 | http://pubs.acs.org
Publication Date (Web): June 12, 2012 | doi: 10.1021/bk-2012-1102.ot001

Editor's Biography

Anatole A. Klyosov

Anatole A. Klyosov, Ph.D., D.Sc., is Chief Scientist and founder of Galectin Therapeutics, a public company, and a co-inventor of the patented technology based on galectin blockers, which often control angiogenesis, inflammation, and immune response in humans. Previously, Dr. Klyosov was Professor of Biochemistry at Harvard Medical School for eight years, and also Vice President of Research and Development of a biotechnology and polymer engineering public company in the Boston area. Prior to that period, he was Professor and Head of the Carbohydrates Research Laboratory at the Institute of Biochemistry, Russian Academy of Sciences. Dr. Klyosov is Fellow, the World Academy of Art and Science (since 1989), holds over 50 U.S. and international patents, has published more than 250 peer-reviewed scientific articles, written books on enzymes, carbohydrates, polymers, and biotechnology, and edited three books: *Enzyme Engineering; Carbohydrates in Drug Design*; and *Galectins*. Dr. Klyosov earned his Ph.D. and D.Sc. degrees in physical chemistry from Moscow University.

Downloaded by 89.163.35.42 on June 13, 2012 | http://pubs.acs.org
Publication Date (Web): June 12, 2012 | doi: 10.1021/bk-2012-1102.ch001

Chapter 1

Carbohydrates and Drug Design

Anatole A. Klyosov*

Galectin Therapeutics, 7 Wells Avenue, Newton, MA 02459
***Klyosov@galectintherapeutics.com**

In order to design a target-specific drug, the designer should know – in an ideal situation – both the target and the structure of the drug candidate, or at least the most important structural elements of the latter, specific for the target. That is when biology and chemistry meet each other. In this particular case it is glycobiology and carbohydrate chemistry. Both of them acting in concert provide a guidance mechanism for sick cells, enabling drugs to arrive there with precision and act properly, that is effectively and without (or with minimum) of side effects. Conversely, carbohydrates can be employed by sick cells to defend themselves against drugs. Furthermore, some sick cells (such as cancer cells) can even use carbohydrate-dependent biological molecules as a weapon, for instance, to disable the immune system and stay "transparent" for the defense system of the body. All these cases are considered as examples in this book. This introductory chapter presents a brief overview of the FDA-approved prescription drugs which contain carbohydrate moieties as part of their structures (typically, removal of the sugar eliminates the therapeutic value of the drug), Besides, this chapter introduces the following aspects of glycobiology and drug design covered, or, sometimes, touched upon in this book, such as galectin-targeted drug design, carbohydrate-assisted chemotherapy of cancer, carbohydrate-based HIV-vaccines, polysaccharide and infections, aminosugars, and computational studies of carbohydrates in the glycosylation reactions.

In Glycobiology and Drug Design; Klyosov, A.;
ACS Symposium Series; American Chemical Society: Washington, DC, 2012.

A good drug is a target-specific drug; its users can expect high efficiency and few, if any, side effects. Target specificity also means recognition, and this is where carbohydrates come in. While many drugs contain carbohydrates as part of their molecules, other drugs – lacking carbohydrates covalently bound to their molecules – can be guided by them. Carbohydrates' value is that they provide a guidance mechanism for sick cells, enabling drugs to arrive there with precision and act properly. On the other hand, carbohydrates can provide a defence mechanism to sick or deadly cells, preventing a drug to act properly.

This book covers, or, in some places, touches on – all these aspects of carbohydrates in drug design, with transition in glycobiology, particularly when biological mechanisms and their manifestation *in vivo* are considered. This chapter introduces the book's content in accordance with the following seven categories, described below:

1. Carbohydrate drugs
2. Glycobiology of galectin-related diseases
3. Cancer and a combination carbohydrate-assisted chemotherapy
4. Carbohydrate-based HIV-1 vaccines
5. Polysaccharides and infections
6. Aminosugars
7. Computational studies

Downloaded by 89.163.35.42 on June 13, 2012 | http://pubs.acs.org
Publication Date (Web): June 12, 2012 | doi: 10.1021/bk-2012-1102.ch001

1. Carbohydrate Drugs

A few dozen FDA-approved prescription drugs contain carbohydrate moieties as part of their structures. Typically, removal of the sugar eliminates the therapeutic value of the drug. These drugs can be divided into five categories, as follows:

- Monosaccharide conjugates
- Disaccharides and disaccharide conjugates
- Trisaccharides
- Oligosaccharides and polysaccharides
- Macrolides

1.1. Monosaccharide Conjugates

Monosaccharide conjugates include, in turn, four groups of prescription drugs:

- Anthracycline antibiotics and agents
    - Doxorubicin
    - Daunorubicin
    - Epirubicin
    - Idarubicin

Downloaded by 89.163.35.42 on June 13, 2012 | http://pubs.acs.org
Publication Date (Web): June 12, 2012 | doi: 10.1021/bk-2012-1102.ch001

- Nucleotides and nucleosides and their analogs
    - Fludarabine Phosphate
    - Stavudine
    - Adenosine
    - Gemcitabine
    - Ribavirin
    - Acadesine

- Polyenes
    - Amphotericin B

- Other agents
    - Etoposide
    - Lincomycin
    - Clindamycin
    - Pentostatin

1.1.1. Anthracycline Antibiotics and Agents

The first group is represented by cytotoxic anthracycline antibiotics of microbial origin (**Doxorubicin** and **Daunorubicin**) or their semi-synthetic derivatives (**Epirubicin** and **Idarubicin**).

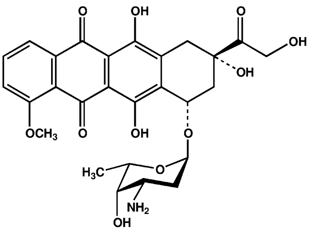

Doxorubicin

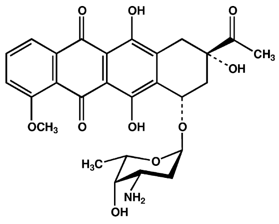

Daunorubicin

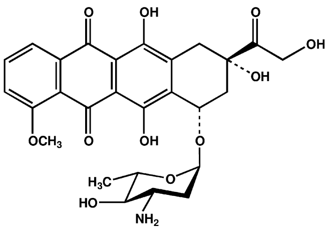

Epirubicin

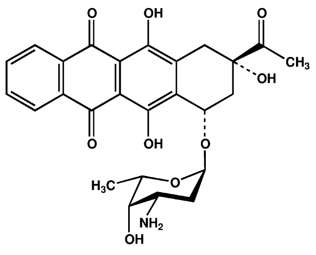

Idarubicin

Downloaded by 89.163.35.42 on June 13, 2012 | http://pubs.acs.org
Publication Date (Web): June 12, 2012 | doi: 10.1021/bk-2012-1102.ch001

All of these drugs are potent neoplastic agents consisting of a naphthacenequinone nucleus linked through a glycosidic bond at ring atom 7 to an amine sugar, daunosamine. All of them bind to nucleic acid, presumably by specific intercalation of the planar anthracycline nucleus with the DNA double helix, between nucleotide base pairs, with consequent inhibition of nucleic acids (DNA and RNA) and protein synthesis. They all inhibit topoisome rase II activity by stabilizing the DNA-topoisomerase II complex, blocking the ligation-religation reaction. All of these drugs show the cytotoxic effect on malignant cells and – as side effects – on various organs. Intercalation inhibits nucleotide replication and action of DNA and RNA polymerases. All of them induce apoptosis, which may be an integral component of the cellular action related to antitumor therapeutic effects as well as toxicities.

1.1.2. Nucleotides and Nucleosides and Their Analogs

The second group of monosaccharide drugs is represented by an assortment of nucleotides and nucleosides and their synthetic analogs. Among them are:

- Potent neoplastic agents, such as **Fludarabine Phosphate** (fluorinated arabinofuranosyladenine 5′-monophosphate), whose metabolic products inhibit DNA synthesis. This drug is indicated for the treatment of patients with B-cell chronic lymphocytic leukemia, while another such agent **Gemcitabine** (2′-deoxy-2′,2′-difluorocytidine), is a nucleoside analogue that inhibits DNA synthesis and exhibits antitumor activity.

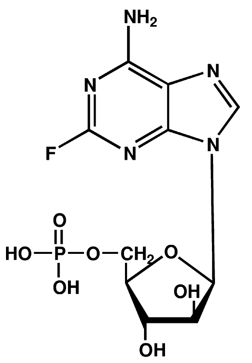

Fludarabine Phosphate

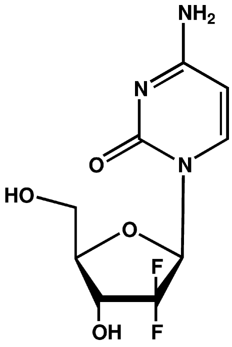

Gemcitabine

- Drugs active against the human immunodeficiency virus (HIV) such as **Stavudine**, a synthetic thymidine nucleoside analog. This drug is a derivative of deoxythymidine, which inhibits the replication of HIV in human cells.

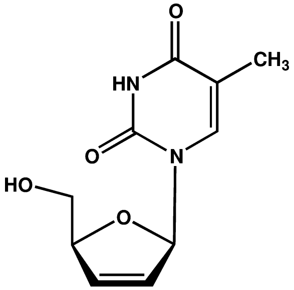

Stavudine

- An antiarrhythmic drug **Adenosine** (6-amino-9-β-D-ribofuranosyl-9-H-purine), which presents in all cells of the body and apparently activates purine receptors (cell-surface adenosine receptors). These molecules in turn activate relaxation of vascular smooth muscle through a number of biochemical events, and they are therefore indicated in patients with paroxysmal supraventricular tachycardia.

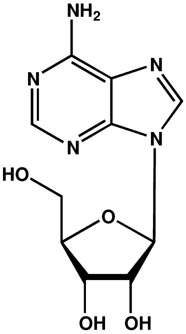

Adenosine

- The first synthetic, non-interferon type antiviral drug **Ribavirin** (ribofuranosyl-triazole derivative), a nucleoside analog, which is particularly active against respiratory syncytial virus (RSV)

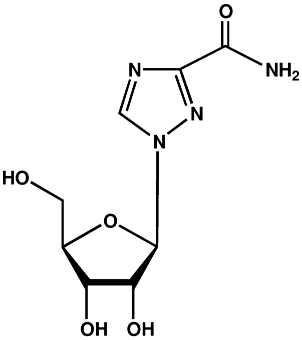

Ribavirin

Downloaded by 89.163.35.42 on June 13, 2012 | http://pubs.acs.org
Publication Date (Web): June 12, 2012 | doi: 10.1021/bk-2012-1102.ch001

- A cardioprotective agent **Acadesine**, a ribofuranosyl-imidazole derivative and a purine nucleoside analog, which is employed in particular in coronary artery bypass graft surgery.

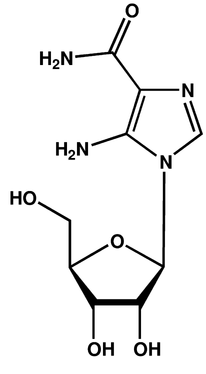

Acadesine

1.1.3. Polyenes

The third group, polyenes, is exemplified by **Amphotericin B**, which is an antifungal antibiotic of microbial origin. Amphotericin B is a 3-Amino-3,6-dideoxy-β-D-mannopyranosyl derivative of an octahydroxypolyene containing seven carbon-carbon double bonds in a macrocyclic 38-member ring. The drug changes the permeability of the cell membrane of susceptible fungi by binding to sterols in the membrane. This binding causes leakage of intracellular content – and, as a consequence, cell death.

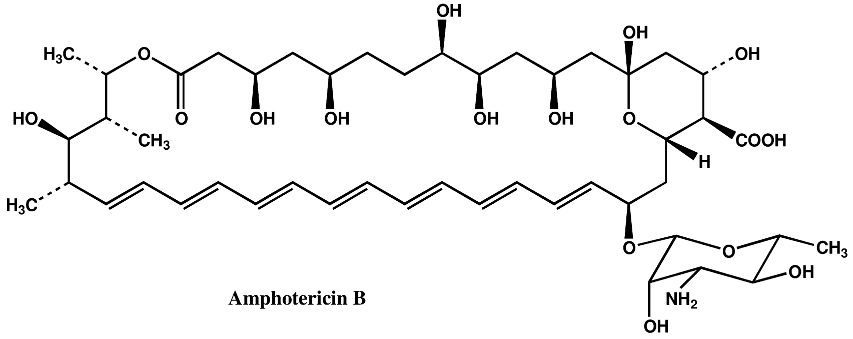

Amphotericin B

1.1.4. Other Agents

The forth group of monosaccharide drugs contains a number of assorted compounds, such as:

Downloaded by 89.163.35.42 on June 13, 2012 | http://pubs.acs.org
Publication Date (Web): June 12, 2012 | doi: 10.1021/bk-2012-1102.ch001

Downloaded by 89.163.35.42 on June 13, 2012 | http://pubs.acs.org
Publication Date (Web): June 12, 2012 | doi: 10.1021/bk-2012-1102.ch001

- The cancer chemotherapeutic agent **Etoposide**, a semi-synthetic β-D-glucopyranoside derivative of podophyllotoxin.

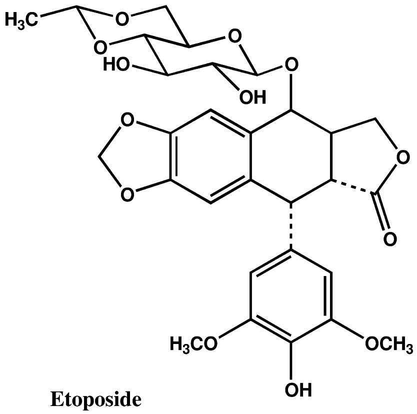
H3C
O
O
O
HO
OH
O
O
O
O
O
H3CO
OCH3
OH

Etoposide

- An antibacterial antibiotic of microbial origin **Lincomycin**, which is a derivative of 1-thio-D-*erythro*-α-D-*galacto*-octopyranoside,

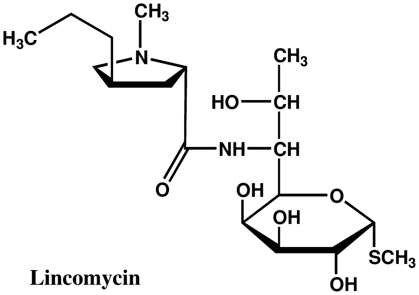
CH3
H3C
N
CH3
HO—CH
NH—CH
O
OH
O
OH
SCH3
OH

Lincomycin

- A semisynthetic antibiotic, **Clindamycin**, which is a derivative of 1-thio-L-*threo*-α-D-*galacto*-octopyranoside and produced from Lincomycin. Clindamycin is indicated in the treatment of infections caused by susceptible anaerobic bacteria, streptococci, pneumococci, and staphylococci.

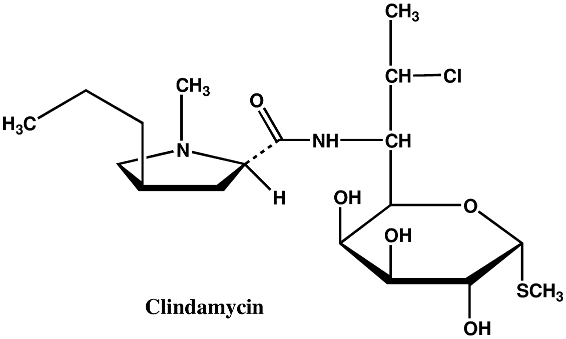
CH3
CH—Cl
CH3
O
H3C
NH
CH
N
H
OH
O
OH
SCH3
OH

Clindamycin

- An antitumor drug, **Pentostatin**, that inhibits RNA and DNA synthesis by being a direct inhibitor of enzymes adenosine deaminase and ribonucleotide reductase, particularly in cells of the lymphoid system.

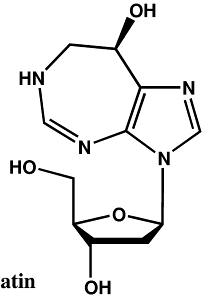

Pentostatin

Downloaded by 89.163.35.42 on June 13, 2012 | http://pubs.acs.org
Publication Date (Web): June 12, 2012 | doi: 10.1021/bk-2012-1102.ch001

1.2. Disaccharides and Disaccharide Conjugates

The next subcategory of prescription carbohydrate drugs, disaccharides and their conjugates, is represented by the following medications:

- An antipeptic and antiulcerative drug, **Sucralfate**, which is a β-D-fructofuranosyl-α-D-glucopyranoside basic aluminum sucrose sulfate complex. It accelerates healing of duodenal ulcers, in part by inhibiting pepsin activity in gastric juice.

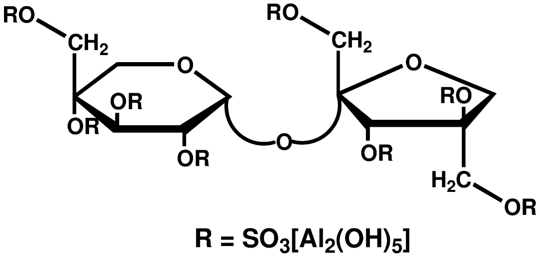

Sucralfate

- A synthetic colonic acidifier Lactulose, 4-O-β-D-galactosyl-D-fructose, which promotes laxation.

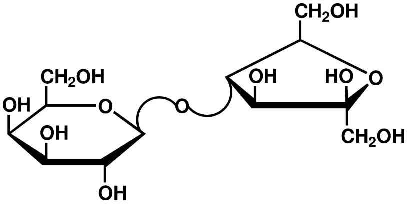

Lactulose

- A microbial amphoteric tricyclic glycopeptide antibiotic, **Vancomycin**, which inhibits bacterial cell-wall biosynthesis. Vancomycin is active against staphylococci, streptococci, enterococci, and diphtheroids, and it is indicated for treatment of systemic infections.

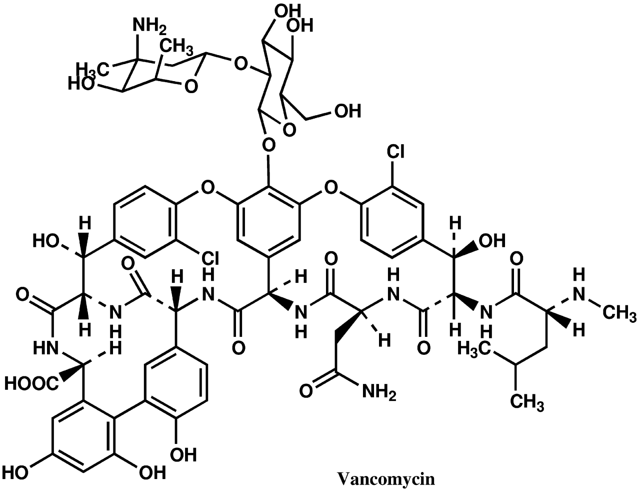

Vancomycin

1.3. Trisaccharides

The third category, trisaccharides and their conjugates, is represented by the following two prescription drugs:

An antibacterial aminoglycoside antibiotic of microbial origin, **Tobramycin**, which is a derivative of an aminoglucopyranosyl-ribohexopyranosyl-L-streptamine. The drug acts primarily by disrupting protein synthesis through altering cell membrane permeability, thereby breaching the cell envelope and causing eventual cell death. It is indicated for the management of cystic fibrosis patients,

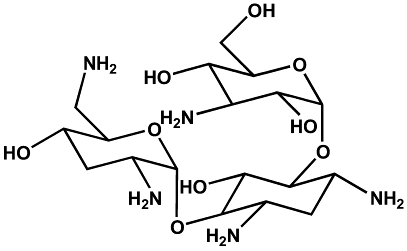

Tobramycin

- A cardiac glycoside, **Digoxin**, that belongs to a closely related group of drugs of plant origin and that contains a sugar and a cardenolide; the sugar part consists of (O-2,6-dideoxy-β-D-*ribo*-hexapyranosyl)3. Digoxin inhibits sodium-potassium ATPase, that in turn leads to an increase in the intracellular concentration of sodium and calcium. This results in a chain of biochemical events that have multiple effects on cardiac muscle and the cardiovascular system in general.

Downloaded by 89.163.35.42 on June 13, 2012 | http://pubs.acs.org
Publication Date (Web): June 12, 2012 | doi: 10.1021/bk-2012-1102.ch001

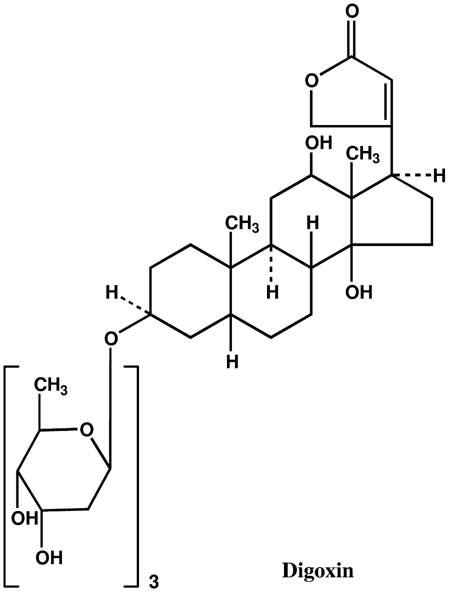

Downloaded by 89.163.35.42 on June 13, 2012 | http://pubs.acs.org
Publication Date (Web): June 12, 2012 | doi: 10.1021/bk-2012-1102.ch001

1.4. Oligosaccharides and Polysaccarides

Prescription drugs made of oligosaccharides and polysaccharides include two principal groups:

- Heparin and heparin-like saccharides
    - Heparin
    - Enoxaparin
    - Tinzaparin
    - Dalteparin
    - Danaparoid
    - Pentosan polysulfate
- Complex oligosaccharides
    - Streptomycin
    - Neomycin
    - Acarbose

1.4.1. Heparin and Heparin-like Saccharides

The first group is represented by heparin and a series of its low-molecular weight fragments and analogs, all of them being antithrombotic agents.

Heparin is a heterogeneous group of glycosaminoglycans, straight-chain anionic mucopolysaccharides that have anticoagulant activity; in particular they inhibit formation of fibrin clots in blood. These drugs' variably sulfated polysaccharide chains are composed of repeating units of D-glucosamine and L-iduronic or D-glucuronic acids.

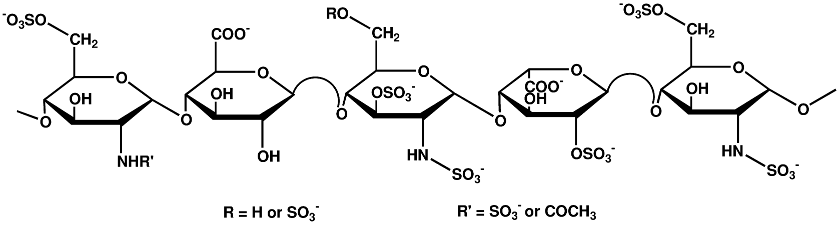

Heparin

Enoxaparin, **Tinzaparin** and **Dalteparin** are all prepared by controlled depolymerization of Heparin or its derivatives. This is accomplished by alkaline degradation, enzymatic hydrolysis, and nitrous acid fragmentation, respectively. **Danaparoid** is a complex glycosaminoglycuronan whose active components are heparan sulfate, dermatan sulfate, and chondroitin sulfate. Finally, **Pentosan Polysulfate** is a semi-synthetic sulfated heparin-like oligomer. Composed of β-D-xylopyranose residues, it shows anticoagulant and fibrinolytic effects.

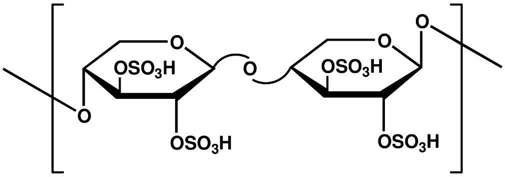

Pentosan Polysulfate

1.4.2. Complex Oligosaccharides

The group of complex oligosaccharides contains two fundamentally different kinds of prescription drugs. The first are bactericidal aminoglycoside antibiotics of microbial origin, **Streptomycin** and **Neomycin**, which act by interfering with normal protein synthesis. Streptomycin is usually available as the sulfate (2:3) salt,

Downloaded by 89.163.35.42 on June 13, 2012 | http://pubs.acs.org
Publication Date (Web): June 12, 2012 | doi: 10.1021/bk-2012-1102.ch001

Downloaded by 89.163.35.42 on June 13, 2012 | http://pubs.acs.org
Publication Date (Web): June 12, 2012 | doi: 10.1021/bk-2012-1102.ch001

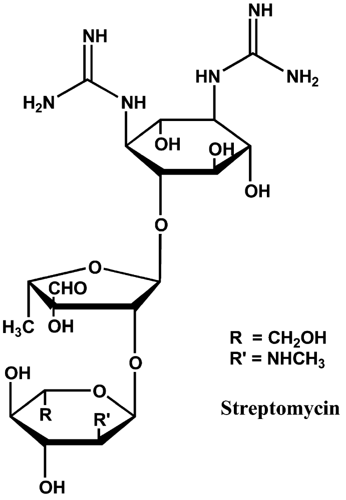

Streptomycin

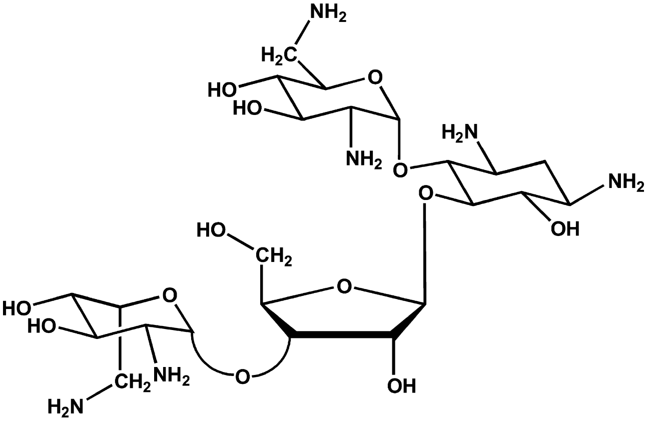

Neomycin

The second kind of complex oligosaccharide **Acarbose**, also of microbial origin, inhibits α-glucosidase and delays the digestion of ingested carbohydrates, making the drug beneficial for the management of type 2 diabetes mellitus.

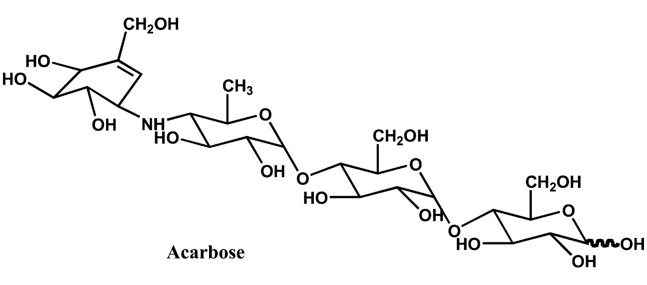

Acarbose

Downloaded by 89.163.35.42 on June 13, 2012 | http://pubs.acs.org
Publication Date (Web): June 12, 2012 | doi: 10.1021/bk-2012-1102.ch001

1.5. Macrolides

The fifth and final subcategory of prescription carbohydrate drugs is represented by macrolide group of antibiotics, of which there are four. The first, **Erythromycin**, is of microbial origin; it appears to inhibit protein synthesis in susceptible organisms by binding to ribosomal subunits and thereby inhibiting translocation of aminoacyl transfer-RNA. The other three – **Dirithromycin**, **Clarithromycin** and **Azithromycin** – are semi-synthetic macrolide antibiotics derived of Erythromycin. Dirithromycin is a pro-drug that is transformed during intestinal absorption into an anti-bacterial active form, Erythromycylamine. Clarithromycin is 6-O-methylerythromycin. Azithromycin is N-methyl-11-aza-10-deoxo-10-dihydroerythromycin.

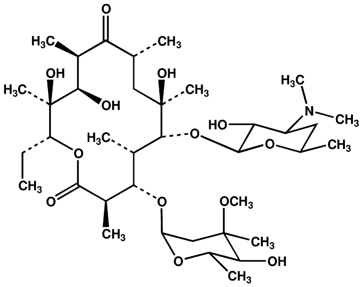

Erythromycin

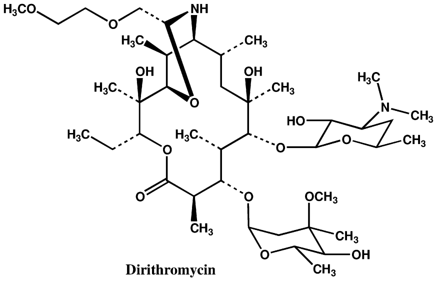

Dirithromycin

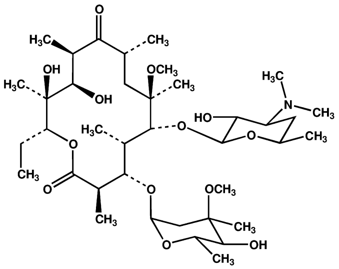

Clarithromycin

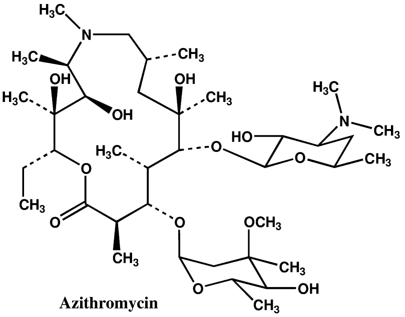

Azithromycin

Among these near-forty carbohydrate drugs are some of the most widely used prescription drugs in the United States. Based on a total of more than three billion U.S. prescriptions (for all drugs), the following carbohydrate drugs make it into the top 200:

- Digoxin (Lanoxin, **Glaxo SmithKline**; Digitek, **Bertek**)
- Azithromycin (Zithromax, **Pfizer**)
- Clarithromycin (Biaxin, **Abbott**)
- Neomycin (**Baush & Lomb**)
- Erythromycin (Ery-Tab, **Abbott**)
- Tobramycin (Tobradex, **Alcon**)

An essential component of these drugs (five of which are antibiotics), as well of all other carbohydrate drugs described in this chapter, is their sugar moiety. Removal of the sugar residue typically leads to elimination of the drug's therapeutic properties. On the other hand, addition of a certain sugar moiety sometimes enhances the recognized potential of the drug at the target level. This approach is exemplified in the section "Cancer" of this book – particularly in the chapter "Synthesis and Biological Activity of Galactomycin and Doxo-Davanat, New Conjugates of Doxorubicin with D-galactose and 1,4-β-D-galactomannan" (Chapter 5).

2. Cancer and a Combination Carbohydrate-Assisted Chemotherapy

Downloaded by 89.163.35.42 on June 13, 2012 | http://pubs.acs.org
Publication Date (Web): June 12, 2012 | doi: 10.1021/bk-2012-1102.ch001

Doxorubicin consists of an aglycone, named adriamycinone, and the aminosugar residue daunosamine attached via α(1→4) linkage to 7-hydroxy group of the aglycone. The drug is considered one of the most active antitumor agents. Unfortunately, by virtue of its mechanism of action, which is directed at replication, transcription, and recombination of DNA, the drug shows severe side effects. This has stimulated several studies aimed at chemical modification of doxorubicin sugar moiety in order to reduce side effects, or to increase the drug efficacy, or both.

Authors of the above-mentioned chapter 5 in this book, Anna Tevyashova et al, have elongated doxorubicin at its sugar part by linking it to a stable D-galactose residue, which was chosen because of the important role that galactose-specific receptors – called galectins – play in tumor development. The best of six synthesized derivatives, in which D-galactose had the α-anomeric configuration and the two sugar residues were linked via 1→6 bond was, tentatively named Doxo-Galactose. It had a lower toxicity and a higher efficacy compared to the parent doxorubicin when tested on mice bearing lymphocite leukemia P-388 at single and multiple i.v. injection regimens. While doxorubicin showed the maximal antitumor effect of 70 percent (increase of lifespan) at the MTD (maximal tolerated dose) of 7 mg/kg, Doxo-Galactose showed a 118-percent increase of lifespan and no toxicity at 40 mg/kg. Moreover, Doxo-Galactose did not show any cumulative toxic effect, unlike the parent doxorubicin, which caused progressive toxicity at triple injection (q2d x 3) at almost 20-times lower doses than Doxo-Galactose. For its part, Doxo-Galactose showed 20 to 60 times lower cytotoxicity, using different cell lines, compared to that by doxorubicin.

Another doxorubicin derivative (Doxo-Davanat) described in the chapter was its conjugate with a polymeric galactomannan (DAVANAT®). This drug, which carried about 10 percent of doxorubicin residues by weight, had cytotoxicity some 20 to 90 times lower than that of doxorubicin.

Two other chapters in the same Cancer section of this book (Chapters 3 and 4) describe preclinical and clinical (Phase I and II) studies using a polysaccharide, a galactomannan of plant origin employing 5-FU (5-fluorouracil), that enhances chemotherapy of colon cancer. Just by mixing 5-FU and GM-CT-01 (which was partially degraded under controlled conditions; the trade name DAVANAT®) in the right proportions and introducing the two combined ingredients i.v., median tumor volume of mice bearing human colon cancer (COLO 205 and HT-29) decreased by 17 percent to 65 percent and median survival time (in days) increased to from 100 percent to 150 and even to 190 percent. A radiolabel study has indicated that 5-FU and GM-CT-01 apparently showed synergism in entering a cancer tumor, and the same two compounds interfered with each other when entering the liver. This might explain how the combination might show a better antitumor activity and lower toxicity toward healthy cells and organs.

The two chapters also describe a phase I clinical trial of GM-CT-01 co-administered with 5-FU in patients with refractory solid tumors. The study was initiated to evaluate the safety and tolerability of escalating doses of GM-CT-01 (30 to 280 mg/m^2) in the presence and absence of 500 mg/m^2 5-FU in patients with advances solid tumors. Twenty-six patients had completed the study, and the combination of GM-CT-01 and 5-FU was found to be well tolerated. Chapter 5 describes Phase I and Phase II clinical trials in some detail.

Downloaded by 89.163.35.42 on June 13, 2012 | http://pubs.acs.org
Publication Date (Web): June 12, 2012 | doi: 10.1021/bk-2012-1102.ch001

3. Galectins

A separate chapter (Chapter 2) in this book describes galectins, which are specific galactose-binding receptors made of protein. They are built into cellular membranes, or cell-wall structures, they are also located in the cytoplasm, and they are located in the cell nucleus. In other words, galectins are truly promiscuous with respect to their location. All galectins show an affinity to galactose residues, attached to other organic compounds, such as in lactose [(β-D-Galactosido)-D-glucose], N-acetyl-lactosamine, poly-N-acetyl-lactosamine, galactomannans, fragments of pectins, etc. After a tight binding to a galectin, something happens on the cell, within the cell, and/or between the cells. In other words, galactose ligands either intercept the inter- and/or intra-cellular communications, or enhance them. Galectins serve as sort of cellular antennae, which either are blocked (hence, those galactose ligands serve as galectin blockers), or stimulated (galectin enhancers). To secure such a multifunctional job in many different places (cell membrane, cytoplasm, cell nucleus), nature has created as many as 15 different galectins, known of today, which have already been identified, isolated, and in some cases characterized – structurally and functionally (Galectins, ed. by Klyosov, A.A. et al, 2008)

The interest to galectins is so high, that after their discovery, or, rather, recognition of them as a separate family of galactose-specific lectins having a clear similarity in their structural motifs, the amount of their publications reached almost 3500 by November 2011. Chapter 2 explains reasons of such an interest, and outlines a number of approaches in diagnostics and therapy based on funtions of galectins and their specificity to their ligands, galectin blockers. The chapter lists more than hundred of various pathologies which are controlled, or assisted, or accompanied by galectins.

Galectins turned out to be instrumental in many extremely important biomedical functions, such as inflammation (and cancer is an extreme case of inflammation), angiogenesis (blood supply, including that to cancer tumor cells),

Downloaded by 89.163.35.42 on June 13, 2012 | http://pubs.acs.org
Publication Date (Web): June 12, 2012 | doi: 10.1021/bk-2012-1102.ch001

immune response (they were shown to turn off the "friend or foe" immune recognition system), cancer cell migration (leading to metastasis). There is no surprise, that a number of academic publications on galectins, on their structure and functions, have been rising exponentially for the last thirty years (see the graph in Chapter 2). It should be mentioned here, that the very term "galectins" was coined only 17 years ago (Barondes et al, 1994), and for 14 preceding years scientists had been studying what they had called "galactose-binding proteins".

There is a great surprise, though, that Big Pharma has not shown any detectable interest as yet in galectins and galectin therapeutics, that is targeting galectins by aiming at diseases associated with angiogenesis, inflammation, immune response, cell migration, chemoresistance, and many serious and mortal pathologies. It cannot be explained by lack of information in the area, and those more than 3500 publications on galectins in academic journals speak for their importance; there is a book, though only one on the market, solely devoted to galectins (Galectins, John Wiley & Sons, 2008, 279 pp); there was a special Symposium "Galectins" under the guidance of the American Chemical Society (Boston, August 2007), which has attracted world leading scientists on galectins. Chapter 2 summarizes the latest data with the most recent references – out of more than 100 references more than two-thirds are references to publications of 2010-2011.

4. Carbohydrate-Based HIV-1 Vaccines

Two chapters (6 and 7) in this book offer an overview of the use of carbohydrate-based vaccines against HIV/AIDS.

Generally, vaccines are a large group of approved products that include some of the world's oldest pharmaceuticals. They are targeted against such conditions as adenovirus, MMR (measles, mumps, rubella), influenza, rabies, hepatitis B, polio, DTP (diphtheria, tetanus, pertussis), typhoid, encephalitis, and varicella. Use of vaccines has practically eradicated some historic diseases and led to a lower need for prophylaxis (*1*). While traditionally employed to prevent the spread of infectious diseases, a new market is emerging for therapeutic vaccines as potential treatments for a wide range of chronic illnesses (*2*) such as cancer and HIV; other viral infections like hepatitis, human papilloma virus, and herpes; and autoimmune disorders such as multiple sclerosis, rheumatoid arthritis, lupus, and maybe even drug addiction.

The therapeutic-vaccine industry, which had estimated worldwide revenues of $80 million in 2004, is still in its infancy, and the market awaits its first largely successful product ("blockbuster").Yet there are at least nine vaccines anticipated to launch in the near future, which means that this market may soon experience enormous growth – possibly reaching, according to some predictions, over $2 billion by 2006 (*2*). These nine vaccines are all late-stage candidates, in Phase III and above, and are primarily targeted against cancer. They include autologous vaccines (whereby each patient is treated with drug derived from his or her own tumor cell, allowing for truly personalized medicine) and allogeneic vaccines (which consist of antigens specific to a particular type of cancer).

There are no HIV vaccines among these about-to-be newcomers to the market. Although it has been 20 years since the HIV virus was identified, and numerous therapies have emerged, no HIV vaccine yet exists. One vaccine candidate, AIDSVAX, a recombinant HIV *gp120* protein developed by VaxGen, failed to improve HIV protection in clinical trials performed in North America, Europe and Asia. At least three other vaccine candidates are currently tested in clinical trials, all in Phase I. One of these trials, initiated by Walter Reed Army Institute of Research and AVANT Immunotherapeutics, is evaluating the safety and immunogenicity of LFn-p24 vaccine. This drug, which uses bacterial vectors removed of their toxins, delivers target antigens into human cells and induces a cell-mediated immune response. Specifically, the vaccine consists of a detoxified anthrax-derived polypeptide fused to the HIV-1 *gag* p24 protein.

Another HIV vaccine, which is currently being developed by Merck, is also in its international trial. This candidate uses replication-defective adenovirus (which causes the common cold) to express the HIV *gag* gene – *gag* being HIV's core protein. Yet another vaccine candidate was created by Chiron. It is used in the form of microparticle-delivered *gag* DNA plasmids in combination with a protein-based formulation (*3*).

A wide variety of other HIV vaccine candidates are being considered on a research level, with investigations so numerous that they cover practically every conceivable target site in the virus and the immune system. Many vaccine candidates contain DNA for the *gag* and *pol* genes; pol includes three enzymes crucial for HIV replication. Gag and pol are considered good candidates for developing AIDS vaccines because they are relatively constant across different virus strains and account for a large percentage of total virus protein (*4*).

AIDS prophylactics present a new challenge for the vaccine approach. Traditionally, only a few types of vaccines – made primarily from attenuated or killed pathogens or from attenuated or deactivated toxins – have been used as antigens to trigger an adaptive immune response. However, because AIDS is so deadly and frightening, few researchers seriously consider the use of attenuated live or killed virus as a vaccine; and in any case this would not likely be acceptable to the public. Hence the best alternative is to use the new genetic engineering technologies for vaccine development (*4*). For instance, fragments of the virus – specifically, viral envelope proteins – and not purified from viruses but instead are synthesized separately in bacteria through genetic engineering techniques. These approaches are surveyed in the abovementioned two chapters.

It makes eminent sense that these two articles are included in this volume. As one of them says: "Pathogen glycosylation is often perceived as a barrier to immune recognition and, by extension, to vaccine design. This notion is perhaps best illustrated in the case of HIV-1, where the glycosylation of the viral surface glycoproteins (gp120 and gp41) appear to profoundly affect the antibody response to the virus and likely contributes to viral immune evasion. The carbohydrate chains, which cover a substantial portion of the antigenic surface of HIV-1, are poorly immunogenic and act as a shield to prevent antibody recognition of the viral particle… Therefore, in principle, the glycosylation of HIV-1 should be considered a target for vaccine design" (D. Calarese et al., Chapter 7).

Downloaded by 89.163.35.42 on June 13, 2012 | http://pubs.acs.org
Publication Date (Web): June 12, 2012 | doi: 10.1021/bk-2012-1102.ch001

And according to the other paper: "In order to achieve persistent infection, HIV has evolved strong defense mechanisms to evade immune recognition, including … heavy glycosylation of the envelope, switch of conformations, and formation of oligomeric envelope spikes. Therefore, the design of an immunogen capable of inducing broadly neutralizing antibody responses remains a major goal in HIV vaccine development… Accumulating data have suggested that the carbohydrate portion of HIV envelope can also serve as attractive targets for HIV-1 vaccine development. Carbohydrates account for about half of the molecular weight of the outer envelope glycoprotein gp120, which cover a large area of the surface of the envelope and play a major protective role for viral immune evasion… The present review intends to provide an overview on our understanding of the structure and biological functions of the HIV-1 carbohydrates, and on how the information might be explored for developing carbohydrate-based vaccines against HIV/AIDS" (Lai-Xi Wang, Chapter 6).

5. Polysaccharides and Infections

Disseminated fungal infections that generally result from the inhalation of airborne spores of pathogenic molds are called systemic mycoses. These diseases typically start with a primary pulmonary infection and can advance into a secondary, life-threatening conditions. Some patients may develop progressive disease that spreads to other parts of the body.

Systemic mycoses, unlike superficial cutaneous and subcutaneous mycoses (which affect the skin, hair, and nails), involve the blood and internal organs. They are subdivided into primary systemic mycoses, which occur regardless of the host's health; and opportunistic systemic mycoses, that occur in hosts with weakened immune systems. Opportunistic mycoses, typically caused by pathogens such as *Aspergillus*, *Cryptococcus* and *Candida*, are being observed with increasing frequency in patients compromised by disease or drug treatment.

Normally, fungi live in a healthy balance with other microorganisms in the human body. However, factors such as antibiotics, prescribed medications, or poor diet can negatively affect this balance, resulting in the accelerated growth of opportunistic microorganisms such as *Candida* yeasts that in turn leads to a systemic fungal infection. Yeast overgrowth, which produces chemicals toxic to the body, is often referred to as candidosis.

Candida infections are thought to affect over 40 million people in the United States, both men and women. *Candida* are single-cell fungal yeasts, and they are considered to be one of the most prolific organisms. There are many *Candida* species, such as *Candida albicans*, *C. krusei*, *C. tropicalis*, *C. glabrata*, *C. parapsilosis*, *C. guilliermondii*, *C. lusitaniae*, *C. dubliniensis*. *Candida albicans* is the most frequently isolated causative agent of candidal infection in humans (accounting for more than 50 percent of cases) and is generally accepted as the most pathogenic species of the genus *Candida*. However, in recent years non-*C. albicans* species – such as *C. glabrata* (10 to 30 percent), *C. parapsilopsis* (10 to 20 percent), *C. tropicalis* (10 to 20 percent), *C. krusei*, and *C. lusitaniae* – have been recovered with increasing frequency from cases of candidiasis (*5*). All of

Downloaded by 89.163.35.42 on June 13, 2012 | http://pubs.acs.org
Publication Date (Web): June 12, 2012 | doi: 10.1021/bk-2012-1102.ch001

them produce different enzymes, including proteases, lipases, phospholipases, esterases, phosphatases, that most probably are able to cause damage to host cells *in vivo* (*6*).

Some *Candida* species are known to rapidly acquire decreased susceptibility to antifungal antibiotics and other agents, such as fluconazole and amphotericin B (*5*). Other species are considered to be inherently resistant to the agents. And some *Candida* species can survive in the hospital environment, thus increasing the chance of nosocomial transmission. Hence there is a necessity for targeted and effective antifungal therapy and hospital infection control measures.

This is a subject considered in the chapter titled "Cationic Polysaccharides in the Treatment of Pathogenic *Candida* Infections" (A.M. Ben-Josef at al., Chapter 5) in this book. The paper shows that glucosamine-based cationic polysaccharides isolated and purified from the cell wall of the fungus *Mucor rouxii* and from crab's chitin possess a significant *in vitro* and *in vivo* fungicidal activity against azole-resistant *Candida* species, particularly *Candida albicans*. The authors offer experimental evidence that the polysaccharides bind very rapidly, tightly, and practically irreversibly to the *Candida* cell wall, suggesting that the binding occurs at the wall's carbohydrate-recognition domains. The data show that these cationic polysaccharides possess superior antifungal properties (compared to known antifungal agents such as amphotericin B and azoles) and that they hold great promise of becoming clinically advanced and useful drugs.

6. Aminosugars

Two chapters in this book (Chapter 9 and 10) are dedicated to syntheses of aminosugars, a group of carbohydrates widely represented in prescription drugs. These include the anthracycline antibiotics Doxorubicin, Daunorubicin, Epirubicin, and Idarubicin; the antifungal antibiotic Amphotericin B; antibacterial antibiotics Lincomycin and Clindamycin; the tricyclic glycopeptide antibiotic Vancomycin; the antibacterial aminoglycoside antibiotic Tobramycin; glycosaminoglycans Heparin, Enoxaparin, Tinzaparin and Dalteparin; complex oligosaccharides Streptomycin, Neomycin, and Acarbose; and the macrolide antibiotics Erythromycin, Dirithromycin, Clarithromycin, and Azithromycin.

In their chapter titled "Systematic Synthesis of Aminosugars and Their Stereoselective Glycosylation" (Chapter 10) J. Wang and C.-W. T. Chang introduce glycodiversification, a concept aimed – in this particular case - at replacing original aminosugars in naturally occurring antibiotics with synthetic aminosugars. To show one way of accomplishing this, the authors discuss systematic synthesis of aminosugars through the regio- and stereoselective incorporation of amino groups on pyranoses.

A related chapter is titled "Synthetic Methods to Incorporate α-Linked 2-Amino-2-Deoxy-D-Glucopyranoside and 2-Amino-2-Deoxy-D-Galactopyranoside Residues into Glycoconjugate Structures" (R. Kerns and P. W. Chang, Chapter 9). Here the authors present a similar approach to introducing variably substituted and differentially modified α-D-glucosamine and α-D-galactosamine residues into glycoconjugate structures in order to synthesize

Downloaded by 89.163.35.42 on June 13, 2012 | http://pubs.acs.org
Publication Date (Web): June 12, 2012 | doi: 10.1021/bk-2012-1102.ch001

many important bioactive glycoconjugates and their structural analogs. The emphasis in the chapter is on 2-amino-2-deoxy-D-hexopyranoside residues and their alpha-linked isomers.

7. Computational Studies

Proteins have long been known as a challenge for computer modeling. But the complexity of proteins pales in comparison to that of carbohydrates. Only lately has the enormous task of modeling carbohydrates been made possible, thanks in part to giant strides in computer power and speed.

Computational studies of carbohydrates are described in a chapter titled “Practical Applications of Computational Studies of the Glycosylation Reaction”, by D.M. Whitfield and T. Nukada (Chapter 11). The authors describe their development of a new algebra – to quantitatively describe the conformations of six-membered rings that dominate the chemistry of carbohydrates – and its use in calculations aimed at understanding the mechanism of glycosylation reactions, both enzymatic and “common chemical”, and at optimizing it. More specifically, the authors studied the mechanism of the acyl transfer reaction to the acceptor alcohol with neighboring group participation via a proposed transition state.

The chapter improves our current understanding of the conformations of pyranose sugars with protecting groups, and it is expected to give organic chemists a better tool for designing stereoselective glycosylation reactions.

Note

This is an updated version of a chapter that previously appeared in *Carbohydrate Drug Design* (ACS Symposium Series 932), edited by Klyosov et al. and published in 2006.

Downloaded by 89.163.35.42 on June 13, 2012 | http://pubs.acs.org
Publication Date (Web): June 12, 2012 | doi: 10.1021/bk-2012-1102.ch001

References

1. Sellick, I. Streamlining conjugate vaccine production. *Genet. Eng. News* **2004**, *24* (16), 48–52.
2. Ellis, R. Therapeutic vaccines gain growing interest. *Genet. Eng. News* **2004**, *24* (21), 25–28.
3. Filmore, D. HIV vaccine testing. *Mod. Drug Discovery* **2004** (August), 11.
4. Lesney, M. S. Vaccine futures. *Mod. Drug Discovery* **2002** (March), 35–40.
5. Yokoyama, K.; Biswas, S. K.; Miyaji, M.; Nishimura, K. Identification and phylogenetic relationship of the most common pathogenic *Candida* species inferred from mitochondrial cytochrome *b* gene sequences. *J. Clin. Microbiol.* **2000**, *38*, 4503–4510.
6. Rodrigues, A. G.; Pina-Vaz, C.; Costa-de-Oliveira, S.; Tavares, C. Expression of plasma coagulase among pathogenic *Candida* species. *J. Clin. Microbiol.* **2003**, *41*, 5792–5793.

Downloaded by UNIV OF DELAWARE MORRIS LIB on June 14, 2012 | http://pubs.acs.org
Publication Date (Web): June 12, 2012 | doi: 10.1021/bk-2012-1102.ch002

Chapter 2

Galectin-Targeted Drug Design

Anatole A. Klyosov[*]

Galectin Therapeutics, 7 Wells Avenue, Newton, MA 02459
[*]Klyosov@galectintherapeutics.com

Galectins are specific galactose-binding proteins, that is galactose-specific lectins. Galectins are truly promiscuous with respect to their location - they are built into cellular membranes, they are located in the cytoplasm, and they reside in the cell nucleus. All galectins show an affinity to galactose residues, attached to other organic compounds, typically in di- and oligosaccharides, in polysaccharides (such as in galactomannans and pectin and its fragments), in glycoproteins. Galactose itself does not bind to galectins, or binds so weakly that the binding can hardly be detected. After a tight binding of a galectin blocker to galectin, something happens on the cell, within the cell, and/or between the cells - it turns out that galactose ligands either intercept the inter- and/or intra-cellular communications, or enhance them. Galectins serve as sort of cellular antennae, which either are blocked (hence, those galactose ligands serve as galectin blockers), or stimulated (galectin enhancers). To secure such a multifunctional job in many different places (cell membrane, cytoplasm, cell nucleus), nature has created as many as 15 different galectins, known today, which have already been identified, isolated, and in some cases characterized – structurally and functionally. Galectins are instrumental to many crucial biological functions, such as inflammation (including cancer which represents an extreme case of inflammation), angiogenesis (blood supply, including that to cancer tumor cells), immune response (they were shown to turn off the "friend or foe" immune recognition system), cancer cell migration (leading to metastasis). Therefore there should be no surprise in the number of publications on galectins, on their structures and functions which reached by the end of

In Glycobiology and Drug Design; Klyosov, A.;
ACS Symposium Series; American Chemical Society: Washington, DC, 2012.

2011 staggering 3516 of peer-review papers. The very term "galectins" was coined only 18 years ago, and for the preceding 15 years scientists had been reporting on what they called "galactose-binding proteins". This overview paper covers some basis of the clinical manifestations often associated with galectins, such as tumor angiogenesis, inflammation, and immune response, as well as galectins-based diagnostics and clinical survival prognosis in patients. With respect to galectin therapeutics and its underlying mechanisms, cancer, heart failure, liver diseases and many other diseases are partly covered or mentioned, a list of which includes 126 pathologies, either galectin-dependent or galectin-accompanied. Some polymer galectin blockers are described, such as galactomannans and pectins and its fragments, and some experimental data are described related to galectin therapy in solid cancer tumor clinical trials, in cardiovascular diseases, in asthma, in arthritis, in malignant gliomas, as well as galectins as indicators in various pathologies, and some general aspects of galectins in human diseases and potential of galectin therapy.

Downloaded by UNIV OF DELAWARE MORRIS LIB on June 14, 2012 | http://pubs.acs.org
Publication Date (Web): June 12, 2012 | doi: 10.1021/bk-2012-1102.ch002

1. Introduction

By the beginning of 2012, the number of publications on galectins reached 3516 and counting (Fig. 1).

What is the reason for such a steep rise of interest in galectins? What are galectins?

Galectins are specific galactose-binding proteins. They are built into cellular membranes, or cell-wall structures. They are also located in the cytoplasm, i.e. in that part of a cell enclosed by the cell membrane, and filled with liquid and gel and contains many components called organelles; galectins also are located in the cell nucleus. In other words, galectins are truly promiscuous with respect to their location. All galectins show an affinity to galactose residues, attached to other organic compounds, such as in lactose [(β-D-Galactosido)-D-glucose], N-acetyl-lactosamine, poly-N-acetyllactosamine, galactomannans, fragments of pectins, etc. Galactose by itself does not bind to galectins, or binds so weakly that the binding can hardly be detected. After a tight binding to a galectin, something happens on the cell, within the cell, and/or between the cells. It turns out that galactose ligands either intercept the inter- and/or intra-cellular communications, or enhance them. Galectins serve as sort of cellular antennae, which either are blocked (hence, those galactose ligands serve as galectin blockers), or stimulated (galectin enhancers). To secure such a multifunctional job in many different places (cell membrane, cytoplasm, cell nucleus), nature has created as many as 15 different galectins, known today, which have already been identified, isolated, and in some cases characterized – structurally and functionally (Galectins, ed. by Klyosov, A.A. et al, John Wiley & Sons, 2008).

Downloaded by UNIV OF DELAWARE MORRIS LIB on June 14, 2012 | http://pubs.acs.org
Publication Date (Web): June 12, 2012 | doi: 10.1021/bk-2012-1102.ch002

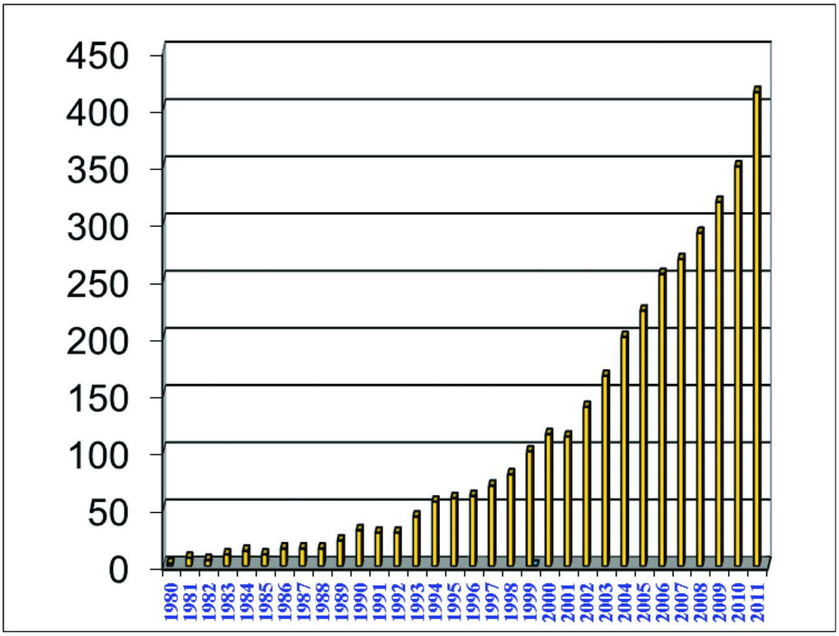

Figure 1. PubMed (U.S. National Library of Medicine, Medical Institutes of Health) records on academic publications on galectins, total 3516 by January 1, 2012.

Proteins that specifically bind sugars (galactose is a sugar, a carbohydrate) are called lectins. Lectins which specifically bind galactose are called galectins. They are numbered from 1 through 15, such as galectin-1, galectin-3, galectin-7 and so on, up to galectin-15. Lectins are not unfamiliar to scientists, and they have been studied since the end of the 19th century. Those times lectins were defined as proteins which agglutinate erythrocytes. Much later, in the 1960-s, it was found that lectins can agglutinate other types of cells, and that they are specific sugar-binding proteins. More recently lectins have been established to be recognition molecules, playing some very important functions on cell surface – cytoplasm – nucleus (intra-cellular) and cell-cell (inter-cellular) communications. Often those communications lead to pathologies, such as to malignancy, and/or mediate malignancy in progress, and/or contribute to metastasis. In the last 15 years, it was shown that not only malignancy, but more than one hundred various pathologies are controlled, or assisted by, or accompanied by lectins (see the last part of this article).

Galectins are instrumental to many crucial biological functions, such as inflammation (and cancer is an extreme case of inflammation), angiogenesis (blood supply, including that to cancer tumor cells), immune response (they were shown to turn off the “friend or foe” immune recognition system), cancer cell migration (leading to metastasis). It is for this reason that there should be no surprise in the number of publications on galectins, on their structures and functions (see the graph above). It should be mentioned here, that the very term

Downloaded by UNIV OF DELAWARE MORRIS LIB on June 14, 2012 | http://pubs.acs.org
Publication Date (Web): June 12, 2012 | doi: 10.1021/bk-2012-1102.ch002

"galectins" was coined only 18 years ago (*1*), and for the preceding 15 years (see Fig. 1) scientists had been reporting on what they called "galactose-binding proteins".

Galectins, as with many other lectins, present a challenge to researchers in terms of quantitative description of ligand-receptor interactions, which is density-dependent when glycan epitopes are located on the surface of cells. In other words, a quantitative description for galectin-cell interactions should include the density and number of glycan epitopes on the surface of cells, as well as the dissociation constant (K_d) that is not a single, well-defined (at least in theory) value as with respect to monovalent glycans in solution, but a relative $K_{d(eff)}$ value that includes density and number of epitopes on the cell surface (*2*).

Surprisingly, however, Big Pharma has not demonstrate appreciable interest as yet in galectins and in developing galectin-targeted therapeutics against such physiologies and pathologies as angiogenesis, inflammation, immune response, cell migration, chemoresistance, etc. (see the last part of this article). This oversight cannot be explained by lack of information in this area. As mentioned above, there are those 3500+ publications on galectins already in academic journals that speak to the importance of galectins, and there is a book (although only one on the market), solely devoted to galectins (*3*), from a special Symposium "Galectins" under the guidance of the American Chemical Society (Boston, August 2007) that attracted world leading scientists in the galectin field.

Before turning to galectin-based therapeutics and their potential (and results obtained to date) against specific pathologies, we will briefly consider some clinical manifestations associated with galectins, and the apparent mechanisms of action of selected galectin-targeted drug candidates. We will also provide some references on key reviews and some of the most recent papers on the subject.

2. Some Basis of Clinical Manifestations Often Associated with Galectins

2.1. Tumor Angiogenesis

Tumor growth depends on a continuous blood supply to deliver oxygen, nutrients, and other biologically important factors to the tumor. The growth of new capillaries from preexisting blood vessels is called neovascularization or angiogenesis, which is a complex process involving e.g. endothelial cell activation, disruption of vascular basement membranes, proliferation of endothelial cells and their migration. This multistep cellular process, the molecular machinery, leading to growth of new vessels into the tumor, hence, tumor angiogenesis, is dependent on a number of galectins, among them galectin-1, -2, -3, -4, -8, which presumably play important roles in mediating cell-cell and cell-matrix interactions.

For example, galectin-1-null mice showed much slower tumor growth because of reduced tumor angiogenesis. Galectin-3 stimulates capillary tube formation *in vitro* and angiogenesis *in vivo*. It has been shown that vessel walls of normal lymphoid tissues do not express galectin-1, while blood vessel walls of lymphomas express it in relation to their vascular density. These and other relevant data are reviewed in (*4*, *5*), as well as in other recent articles. A recent study (*6*) notes: "Recent studies have shown that a carbohydrate-binding protein, galectin-3, is a novel pro-angiogenic molecule. The mechanism by which galectin-3 promotes angiogenesis remains unknown". In the follow-up study (*7*) the authors confirmed that angiogenesis is heavily influenced by VEGF-A and by VEGF receptor 2 (VEGF-R2), which is glycosylated like most cell surface proteins, although, as the authors mentioned, the function of VEGF-R2 with respect to its glycosylation pattern is poorly characterized. The authors have shown that galectin-3 interacts with the EGF and TGFβ receptors, retaining them on the plasma membrane and altering their signal transduction via phosphorylation of VEGF-R2 in endothelial cells. The authors concluded that galectin-3 contributes to the plasma membrane retention and proangiogenic function of VEGF-R2.

Another review (*8*) has noted that "galectin-3 is an important regulator of a broad range of cancer cell activities and plays important roles in cancer cell growth, transformation, apoptosis, angiogenesis, adhesion, invasion and metastasis. Such a divergent influence of galectin-3 on cancer cell activities derives from its multiple inter- and sub-cellular localizations where it interacts with a range of different binding partners".

It was also shown that galectin-3 promotes adhesion of disseminating tumor cells to vascular endothelium *in vitro* and experimental metastasis *in vivo*. Furthermore, the presence of galectin-2, -3, -4, and -8 enhances cancer-endothelial adhesion by interaction with the TF epitope (Gal-β-1,3GalNAc α-) disaccharide on cancer-associated MUC1 glycan and promote cancer-endothelial adhesion (*9*).

Nearly this same group of galectins (galectins-1, -3, -4, and -8) are expressed in human colon and rectal cancer, and upregulated during colorectal cancer development and metastasis. Their upregulation has been correlated with cancer cell growth, apoptosis, and angiogenesis (*10*).

Galectin-8 is a rather common target when deciphering the angiogenesis-related processes, and it was suggested to be one of the "pro-angiogenic" lectins. Galectin-8 is a bivalent "tandem-repeat"–type galectin, whose two carbohydrate-recognition domains are connected covalently by a linker peptide. This galectin is expressed both in the cytoplasm and nucleus in endothelial cells of normal and tumor vessels; hence, it might play an essential role in the regulation of angiogenesis in general and tumor angiogenesis in particular (*11*).

Recently, it was shown that tumor cells can stimulate tumor angiogenesis by secretion of galectin-1 in wild-type mice; however, this effect is hampered in galectin-1-null mice (*12*). The authors concluded that galectin-1 is a pro-angiogenic factor.

A significant study describing the role of galectin-1 in angiogenesis and immune dysregulation in murine cancer was recently published (*13*). It was shown that galectin-1 is a tumor promoting protein produced by cancer cells, and that the low-molecular weight galectin blocker, thiodigalactoside (TDG), a non-metabolized drug candidate, suppressed tumor growth, angiogenesis, immune cell dysregulation. Furthermore, intra-tumoral (B16F10 melanoma and breast cancer model) injection of TDG significantly increased the level of tumor-infiltrating CD8+ lymphocytes, and TDG treatment of tumors in nude

Downloaded by UNIV OF DELAWARE MORRIS LIB on June 14, 2012 | http://pubs.acs.org
Publication Date (Web): June 12, 2012 | doi: 10.1021/bk-2012-1102.ch002

Downloaded by UNIV OF DELAWARE MORRIS LIB on June 14, 2012 | http://pubs.acs.org
Publication Date (Web): June 12, 2012 | doi: 10.1021/bk-2012-1102.ch002

mice, defective in T cell immunity, reduced angiogenesis and slowed tumor growth by ~ 30% less than in immunocompetent mice. At the same time, Dings et al. (*14*) showed that anti-angiogenic compounds could also enhance T-cell mediated anti-tumor responses and function as angiostatic adjuvants to immunotherapy against cancer. These are apparently the first cases demonstrating that low-molecular weight galectin-1 blockers are potential immune system modulating anti-cancer agents.

2.2. Inflammation

Inflammation is probably the most general term for pathologies in which galectins play an important role. Hundreds and thousands of studies – literally – can be cited in this section. However, we will restrict examples to several recent studies that illustrate the subject of this short overview.

Simply stated, inflammation as a side effect or a pathology where angiogenesis is in the wrong place. In these instances, there is a need to suppress inflammatory responses. Galectins were recognized as major players in regulating inflammatory responses; however, the data obtained still do not provide a clear picture. Some galectins appear to suppress responses of inflammatory cells, while some galectins stimulate and promote them. It seems that the specific effect of a galectin depends on the targeted cell, its microenvironment (such as a pattern of the specific glycosylation of target cells), and the inflammatory stimulus. It is for this reason that many authors choose to use indirect language when describing results of their studies on galectins, such as "attenuating inflammatory responses", "potentiating", "associating", "contributing to the balance", "play a role", "still remain to be elucidated". It may well be that many of these studies are performed *in vitro* and employ recombinant galectins, typically lacking their glycosylated part (if any, since most structures of galectins were conducted on recombinant galectins anyway) (*15*). Where more relevant studies were conducted, for instance, with galectin-3-null mice, it was found that galectin-3 promotes inflammatory responses (reviewed by Liu et al, in (*16*)). In a number of cases, galectins can accompany inflammatory responses, and often it is hard to determine whether the appearance of galectins (as an elevated expression) post-injury is causal or a "biomarker" case.

For example, spine cord injury in rats induces secondary tissue damage that is associated with inflammation, and up to six months post-injury, a cluster of genes (including that of galectin-3) has been reported to show elevated expression in macrophages. The authors (*17*) concluded that "inflammation-related genes are chronically up-regulated after spinal cord injury".

Galectin-4 was found to induce the inflammatory cytokine IL-6, "known to contribute to the progression of the disease" (*16*).

Steatosis was significantly less pronounced in galectin-3 null mice compared to wild type [gal-3 (+/+)] mice. NASH (nonalcoholic steatohepatitis), which was invariably detected in galectin-3 (+/+) mice on an atherogenic diet, was much less pronounced and was found in only 38% of these galectin-3 null mice (*18*).

Galectin-3 is a key player in the liver fibrosis (see below), an inflammatory disease, as well as in liver cirrhosis, idiopathic lung fibrosis, and chronic pancreatitis, all of which are associated with upregulation of galectin-3 (for a review see (*19*). These authors noted that besides fibrosis, galectin-3 also plays an important role in other inflammatory responses, such as cardiac remodeling and renal models of inflammation.

Experiments with galectin-3-null mice have shown that when those mice have been infected with African trypanosomiasis (*Trypanosoma brucei* infection in mice), they manifest significantly lower levels of anemia (which is due to a sustained type 1 cytokine-mediated inflammation and hyperactivation of M1 macrophages) and survive twice as long as wild type mice (*20*).

Another interesting study (*21*) has shown that it is not just galectin-3 that contributes to development of rheumatoid arthritis (RA), also an inflammatory disease, but it may be some of its polymorphic forms. Indeed in synovium of RA, an elevated expression of galectin-3 has been found; however, the allelic carriage of LGALS3 +292C was increased in RA patients (151 RA patients and 182 healthy subjects as control) from 66.9% in RA vs. 52.7% in control. The two polymorphic forms (SNP) of galectin-3 gene were located at rs4644 and rs4652 sites in the DNA.

Almost at the same time, another study (*22*) showed that galectin-3 is present in the inflamed synovium in patients with rheumatoid arthritis, and plays a pathogenic role in the development and progression of antigen-induced arthritis. The authors showed that the joint inflammation and bone erosion in mice were markedly suppressed in galectin-3 null mice as compared with wild-type mice. The reduced arthritis in galectin-3 null mice was accompanied by decreased levels of proinflammatory cytokines.

Henderson and Sethi (*23*) noted that galectin-3 is a specific regulator of many biological systems, including inflammation. For example, in acute tissue damage, galectin-3 is a key component in the host defense against microbes, such as *Streptococcus pneumoniae*. However, if tissue injury becomes repetitive, galectin-3 also appears to be involved in the transition to chronic inflammation, facilitating the walling off of tissue injury with fibrogenesis and organ scarring. Therefore galectin-3 can be viewed as a regulatory molecule acting at various stages along the continuum from acute inflammation to chronic inflammation and tissue fibrogenesis. The authors of this review noted that targeted effects aimed at galectin-3 expression may present “a potentially novel therapeutic strategy in the treatment of a broad range of inflammatory diseases”.

That is what galectin therapy is about. More on it is described later in this article.

According to Norling et al (*24*), evidence is accruing that indicates that galectins fall into this category of immunoregulatory mediators, signifying their potential as prospective novel anti-inflammatory agents. In their review, they describe the immunoregulatory bioactivities of three members of the galectin superfamily, galectin-1, -3 and -9. As the authors emphasize, these galectins are emerging as pertinent players in the modulation of acute and chronic inflammatory diseases, autoimmunity and cancer, and thus are being increasingly recognized as molecular targets for innovative drug discovery.

Again, this is what galectin therapy is all about.

Downloaded by UNIV OF DELAWARE MORRIS LIB on June 14, 2012 | http://pubs.acs.org
Publication Date (Web): June 12, 2012 | doi: 10.1021/bk-2012-1102.ch002

Downloaded by UNIV OF DELAWARE MORRIS LIB on June 14, 2012 | http://pubs.acs.org
Publication Date (Web): June 12, 2012 | doi: 10.1021/bk-2012-1102.ch002

2.3. Immune Response

The immune system works – by a very simplified description – through two separate arms. One operates through immune cells called macrophages that engulf pathogens and other debris and alert adaptive immune cells called T cells, which after activation multiply and attack and kill pathogen-infected cells and/or engage another type of immune cell called B cells, which produce pathogen-blocking antibodies. Another arm operates through immune cells called dendritic cells, which also activate T cells.

T cells, or T lymphocytes, play a crucial role in the immune response, or cell-mediated immunity. T cells include a number of subsets which are very important for the protective function of the body – T helper cells, cytotoxic T cells, memory T cells, regulatory T cells, natural killer T cells, etc. In response to an antigen, T cells release various cytokines (signaling molecules, which activate other T cells) and cytolytic/cell killing molecules to destroy the “invader”, such as different pathogens and cancer tumors.

Some galectins can disable T cells by inducing apoptosis. For example, galectin-1 induces apoptosis in activated human T cells. Apparently, galectin-1 does it through the binding to some of T cell surface glycoproteins, such as CD7, CD43, and CD45, which in turn leads to T cell death. That is why many types of solid tumors, including colorectal cancer tumors, breast cancer tumors, melanomas, bladder, ovarian, thyroid, gynecological cancers, and other tumors overexpress various galectins, including those on the tumor surface. Those galectins, galectin-1 and -3 among them, exert apoptotic and immunosuppressive effects, which makes cancer tumor “transparent” to the immune system, and contributes to tumor survival, its angiogenesis (see above), as well as tumor progression and metastasis (reviewed in Liu et al, in (*16*, *25*)).

A recent study (*26*) identified galectin-1 as an intracellular binding partner of Bam32, the B lymphocyte adaptor molecule which is strongly induced during human dendritic cell maturation. These authors noted that galectin-1demonstrates many immunological activities, among them regulating immune responses via regulatory T cells modulation.

Galectin-1 is also an important element along with its immunoregulatory activity in controlling immune cell trafficking, dendritic cell physiology, and T-cell fate (*27*).

Galectin-9 plays a role in a murine acute lung injury by preferentially suppressing macrophage function to release pro-inflammatory cytokines through down-regulation of Toll-like receptors. In those experiments, mice were pretreated with galectin-9 by subcutaneous injection prior to intranasal LPS inoculation, and the authors found that galectin-9 suppresses pathological changes in acute lung-injured mice by reducing levels of pro-inflammatory cytokines and chemokines, such as tumor necrosis factor (TNF)-α, IL-1b, IL-6, decreased neutrophils, and increased IL-10 (*28*).

Another work on galectin-9 has shown that by binding to T cell Ig mucin-3 (Tim-3) expressed on different cells, galectin-9 mediates two important functions: triggering T cell death and activating innate immune cells. The authors found some indications that two carbohydrate recognition domains of galectin-9 (N- and C-terminal regions) have different activities in promoting T cell death (*29*).

Robert Kiss and his Laboratory of Experimental Immunology in Leuven, Belgium, continue to uncover the role of galectin-1 in immunotherapy for brain cancer as an important player in glioma-mediated immune escape (*30–32*). It was shown that galectin-1 is abundantly expressed in high-grade glioma, and active specific immunotherapy by dendritic cell vaccination apparently generates an anti-tumoral immune response, when accompanied by down-regulation of counteracting tolerogenic signals (*32*).

A recent study (*33*) notes – "galectin-3 is strongly expressed in thyroid carcinomas but not in benign tumors or normal glands". Anaplastic thyroid carcinomas are deadly tumors that are highly invasive, particularly into bone (there are two more types of malignant thyroid tumors – papillary and follicular). The authors of the study concluded that galectin-3 contributes to thyroid carcinoma malignancy.

In another study, Zhu et al. (*34*) reported that expression of galectin-3 in papillary thyroid carcinoma (PTC) [40 cases of papillary microcarcinoma, 74 cases of classic PTC, and several rare variants in 155 PTC cases have been considered] occurred in 92% (142/155) of all cases, and was found to be at much higher levels than that in the control group.

3. Galectins-Based Diagnostics and Clinical Survival Prognosis in Patients. Galectin Therapeutics and Its Underlying Mechanisms

It is obvious from the above discussion that galectins are elevated on the surface of tumor cells (as well as being found in their intracellular compartments). Galectins can be detected by various analytical means (typically by various modifications of ELISA tests). The use of galectins is already under study as new and reliable histological tumor markers, because their presence correlates with clinical aggressiveness of the tumor and the patient survival prognosis. Furthermore, since galectins are associated with inflammatory responses, which are not restricted to tumors (cancer can be considered as an extreme case of an inflammation), an elevated level of some galectins in the bloodstream can be a readout for prognoses of other inflammatory diseases. A few examples are given in this section.

3.1. Cancer

Expression of galectin-3 in patients with colorectal cancer following surgery and/or under chemotherapy treatment and the relationship of galectin-3 expression and clinical aspects or tumor evolution have been studied in 75 samples of colorectal tissues (*35*). The highest percentage of staining cells (an immunohistochemical test for galectin-3 expression) appeared in the most advanced cancer. The immunoexpression of galectin-3 was strong or moderate in 42% of the colorectal tumors. Patients with strong or moderate immunoexpression

Downloaded by UNIV OF DELAWARE MORRIS LIB on June 14, 2012 | http://pubs.acs.org
Publication Date (Web): June 12, 2012 | doi: 10.1021/bk-2012-1102.ch002

Downloaded by UNIV OF DELAWARE MORRIS LIB on June 14, 2012 | http://pubs.acs.org
Publication Date (Web): June 12, 2012 | doi: 10.1021/bk-2012-1102.ch002

of galectin-3 died or had recurrence more frequently. The authors noted that galectin-3 cytoplasmatic immunoexpression seems to be a prognostic factor in colorectal cancer, because a higher risk of recurrence had been observed in tumors with a high score of galectin-3.

A high level of expression of galectin-3 was found in malignant lesions of breast (n = 60) compared with that in benign breast lesions (n = 30) (*36*). Besides, the 5-year survival rate and mean survival period were significantly lower in the gal-3 expression positive cases than those in the negative cases of breast cancer. The authors concluded that the expressive level of gal-3 might have important effect on the carcinogenesis, progression and biologic behaviors of breast cancer, and that the positive cases of gal-3 expression might have poor prognosis.

Canesin et al. provide an example of galectin-3 expression in bladder cancer (*37*). Galectin-3 expression was assessed by transcript profiling (U133A arrays) in a series or frozen bladder tumors (n = 105). Immunohistochemistry was performed on tissue arrays containing bladder tumors (n = 389) to evaluate associations of protein expression patterns of galectin-3 with proliferation, apoptosis, and clinical pathologic variables. Galectin-3 protein levels were then quantified in 160 urinary specimens of bladder cancer patients and controls by ELISA test. It was found that galectin-3 gene expression levels increased in invasive tumors as compared with non-muscle invasive lesions and were associated with poor survival in patients with advanced disease. Protein expression patterns also correlated galectin-3 with tumor stage, grade, and apoptosis, and overall survival in patients with tumors. Furthermore, galectin-3 urinary levels segregated bladder cancer patients from controls with high diagnostic accuracy. The authors (*37*) concluded that galectin-3 can be considered as a biomarker for bladder cancer diagnostics, staging, and outcome prognosis.

Galectin-3 is considered to be the most well-studied molecular candidate for thyroid cancer diagnosis. Despite great variance in methodology, the majority of immunohistochemical studies found that galectin-3 was differentially expressed in thyroid carcinoma compared with benign and normal thyroid specimens. This suggests that galectin-3 is a good diagnostic marker for thyroid cancer. The authors (*38*) noted that, on the other hand, galectin-3 genomic expression studies have shown inconsistent results for diagnostic utility and are not recommended. They emphasized that consideration of galectin-3 as a diagnostic marker for thyroid cancer represents a promising avenue for future study, and its clinical application could significantly reduce the number of diagnostic thyroid operations and thus positively impact the current management of thyroid nodular disease. A separate study (*39*) has also shown that galectin-3 demonstrated highest specificity and sensitivity in the diagnosis of thyroid cancer.

Prostate cancer, which is the second most common cancer and the second leading cause of cancer death in men, can be effectively treated if it is diagnosed at an early stage when the tumor is confined to the prostate. The PSA test and screening method, which has been widely used for detection of prostate cancer, is unreliable due to the high prevalence of false positive and false negative results. A recent study (*40*) points out that epigenetic alterations, including hyper-methylation of gene promoters, are believed to be early events in neoplastic progression, and thus these methylated genes can serve as biomarkers for the detection of cancer from clinical specimens. This study considers methylated galectin-3 DNA sequence during prostate carcinogenesis and evaluates its usefulness for early detection of prostate cancer in tissue biopsies, serum, and urine.

Galectin-3 expression as a prognostic marker or therapeutic target has been immunohistochemically studied in epithelial ovarian carcinoma (EOC), in which levels of galectin-3, mainly cytoplasmic in location, were evaluated in 71 patients with 54 serous, 13 endometrioid, and 4 mucinous ovarian carcinomas. In vitro, Gal-3 was inhibited using siRNA to evaluate its role in cell growth and sensitivity to chemotherapeutic agents in ovarian carcinoma cell lines. High Gal-3 expression was observed in a majority (88.7%) of the EOCs but not in normal ovarian tissues, and it was correlated with shorter progression-free survival of patients, 43.1 and 49.5 months, respectively (*41*).

Galectin-3 has also been suggested to be a marker of disease progression in primary cutaneous melanoma (PCM) in patients due to its over-expression in the pathology. To examine this point, galectin-3 expression was evaluated using immunohistochemistry in 104 PCM samples, two-thirds of those were superficial spreading (SSM) and one-third was nodular melanomas (NM). Significant differences in galectin-3 expression between SSM and NM was observed, and increased galectin-3 expression was positively correlated with tumor thickness, Clark and Breslow stage, mitotic rate, presence of tumor ulceration, lymphatic invasion, positive sentinel lymph node and distant metastases. The data showed an association between increased galectin-3 expression and reduced recurrence-free survival, as well as with reduced disease-specific survival. The authors concluded that galectin-3 could serve as an additional prognostic marker of disease progression and metastasis in patients with PMC (*42*).

All of the above examples are related to galectin-3. However, this simply reflects the attention that researchers have paid to galectin-3 and the availability of test kits for galectin-3. Recently, galectin-8 was shown to be a robust biomarker for recurrence of bladder cancer (*43*), as demonstrated by galectin-8 staining patterns from 162 samples of non-muscle-invasive transitional cell carcinoma, 25 samples of muscle-invasive transitional cell carcinoma, and 10 samples of normal urothelium. Loss of galectin-8 was associated with the likelihood of tumor recurrence, with no significance for tumor progression. Patients whose specimens showed weak galectin-8 expression had a shorter recurrence-free interval (42 vs. 12 months). All of the 10 normal urothelium samples showed high galectin-8 expression. Decreased staining was found to be associated with higher tumor stages and grades. The authors concluded that loss of galectin-8 might be an early step in the development of malignant lesions of the bladder and a significant independent predictor of recurrence.

Aside from galectin-3 and -8, galectin-1 and -4 have been reported to be clinically significant as colorectal cancer markers (*44*). These authors showed early on that galectin-1 is over-expressed in colorectal carcinoma (CRC) tissues. In this paper, they showed in 105 CRC patients and 100 healthy volunteers (control) that levels of circulating galectin-1 and -4 reflect the presence of CRC and/or its state of progression. Circulating levels of galectin-1/-3/-4 in plasma of CRC patients were significantly higher compared to those in controls. Galectin-1

Downloaded by UNIV OF DELAWARE MORRIS LIB on June 14, 2012 | http://pubs.acs.org
Publication Date (Web): June 12, 2012 | doi: 10.1021/bk-2012-1102.ch002

Downloaded by UNIV OF DELAWARE MORRIS LIB on June 14, 2012 | http://pubs.acs.org
Publication Date (Web): June 12, 2012 | doi: 10.1021/bk-2012-1102.ch002

and -4 levels significantly decreased post surgery, and the level of galectin-4 in most patients fell below the threshold value. The levels of circulating galectin-4 significantly increased as tumor stage progressed, whereas those for galectin-1 were relatively high at an early stage. These data suggested that galectin-4 may be a tumor biomarker for use in patient follow-ups, while galectin-1 could be used potentially for tumor screening.

In terms of galectin-1-based diagnostic screening, the Nicolay group in Eindhoven, The Netherlands, have employed molecular MRI and a novel galectin-1-targeting peptide, Anginex, with liposome-based nanoparticles to assess and combat tumor growth *in vivo* (*45*, *46*).

3.2. Heart Failure

From the pathological perspective, heart failure is the result of myocardial injury or hemodynamic overload, which goes beyond mechanical dysfunction. From the viewpoint of biomedical research, heart failure is the result of interplay of a number of biochemical factors, or risk factors, collectively referred to as biomarkers. Those biomarkers in heart failure include brain natriuretic peptides, inflammatory markers, neurohormones (such as aldosterone), cardiorenal markers, and galectin-3, which is considered to be a novel biomarker (*47*, *48*). Aside from this, heart failure is associated with a number of pathophysiologic mechanisms, including inflammation, tissue remodeling, endocrine signaling, and interactions with the renal and nervous systems. The authors (*49*) found galectin-3 to be among some novel biomarkers.

A recent study (*50*) has shown that an elevated galectin-3 level was associated with advanced age, poor renal function and predicted all-cause mortality (hazard ratio 1.86, 95% confidence interval 1.36 to 2.54). These data were based on measured plasma galectin-3 levels in 133 subjects with chronic heart failure (HF) and 45 with advanced decompensated HF using echocardiographic and hemodynamic evaluations. In the chronic HF cohort, median plasma galectin-3 level was 13.9 ng/ml (interquartile range 12.1 to 16.9). In multivariate analysis, galectin-3 remained an independent predictor of all-cause mortality after adjusting for age and other myocardial indications. The authors reported that galectin-3 level, however, did not predict the combined end point of all-cause mortality, cardiac transplantation, or HF hospitalization. In the advanced decompensated HF cohort, there was no relationship between galectin-3 levels and echocardiographic or hemodynamic indexes. The authors concluded that high plasma galectin-3 levels were associated with renal insufficiency and poorer survival in patients with chronic systolic HF.

It was found recently that the level of galectin-3 in plasma (determined using a novel ELISA kit, Galectin-3 Assay™, BG Medicine, Waltham, MA) is a prognostic marker in patients with chronic heart failure (HF), and a significant predictor of mortality risk. In the Netherlands study (*51*) 232 patients with chronic HF have been studied, of which during a follow-up period of 6.5 years 98 patents died. The upper level of galectin-3 in plasma considered normal was 17.7 ng/mL. Half of the patients had galectin-3 plasma levels above the recommended upper limit, and the median value was 18.6±7.8 ng/mL. Generally, older patients had higher levels of galectin-3 in plasma. Also, higher levels of galectin-3 were associated with renal disfunction in patients, and even with body mass index. The later, apparently, should not be surprising, since it is known that heart failure risk is generally associated with body weight. Overall, those 98 patients who died during the follow-up period had galectin-3 levels of 20.1±8.1 ng/mL, which the authors of the study considered significantly higher compared to those of the survivors, 17.5±7.4 ng/mL.

The authors (*51*) describe similar studies, including a study (*52*) in which galectin-3 was measured in 599 patients with acute dyspnea who presented to the emergency room, of whom 209 were diagnosed as "acute heart failure". Again, galectin-3 levels were higher in those with acute heart failure (9.2 ng/mL) than in those who did not (6.9 ng/mL). The same study was described by (de Boer et al, 2010) who reported that galectin-3 was the most powerful predictor in a short-term prognosis (60 days, primary end-point rehospitalization caused by heart failure or all-cause mortality, n = 17).

The study was later extended to 592 heart failure patients (*53*) with preserved and reduced left ventricular ejection fraction (LVEF), and results were compared this to other biomarkers. The patients had been hospitalized for HF and were followed for 18 months. The primary end-point of the study was a composite of all-cause mortality and HF hospitalization. The observed doubling of galectin-3 levels was associated with a hazard ratio (HR) of 1.97 (1.62-2.42) for the primary outcome. After correction for age, gender, and other factors, such as diabetes, the HR was 1.38 (1.07-1.78). Changes of galectin-3 levels after 6 months did not add prognostic information to the base-line value, however, the predictive value of galectin-3 was stronger in patients with preserved LVEF (n = 114) compared to patients with reduced LVEF. The authors concluded that galectin-3 is an independent marker for outcome in HF and appears to be particularly useful in HF patients with preserved LVEF.

In another study (*54*), galectin-3 levels in 55 patients with end-stage HF were compared with those in 40 healthy controls, and again galectin-3 levels were higher in HF patients (11 ng/mL) than in control (4.1 mg/mL). Furthermore, patients who died or developed multi-organ failure had significantly higher galectin-3 levels compared to those who successfully bridged to transplantation.

In yet another recent study (*55*) 115 patients presenting to the emergency room with acute dysphonea and diagnosed with heart failure (ADHF) have their galectin-3 level measured. Those patients who had galectin-3 levels above the medial value had a 63% mortality in the following four years; patients with less that the median value has a 37% mortality. Therefore, as the authors noted, a single admission galectin-3 level predicts mortality to four years, independent of echocardiographic markers of disease severity.

The authors (*51*) conclude – "*it would be tempting to speculate that blockade or inhibition of galectin-3 could have favorably affect this process and be a target for treatment, but to our knowledge, such data are not (yet) available*".

In the same manner, Liu et al (*16*) have concluded – "*Overall, current information suggests that inhibitors of some galectins, such as galectin-3, may be useful for treatment of inflammatory diseases*".

Downloaded by UNIV OF DELAWARE MORRIS LIB on June 14, 2012 | http://pubs.acs.org
Publication Date (Web): June 12, 2012 | doi: 10.1021/bk-2012-1102.ch002

Downloaded by UNIV OF DELAWARE MORRIS LIB on June 14, 2012 | http://pubs.acs.org
Publication Date (Web): June 12, 2012 | doi: 10.1021/bk-2012-1102.ch002

Similarly, Lefranc et al (*5*) have concluded their paper – "*The possibility exists that such antigalectin-1 compounds could be evaluated in clinical trials (in association with cytotoxic agents) in the near future*".

Another citation (*19*) – "*Future studies should focus on galectin-3 biology to better address the usefulness of galectin-3 as a biomarker and probe the usefulness of anti-galectin-3 therapy in treating heart failure*".

In this overview, we will show (see below) that this is exactly the aim of galectin therapy, which we have been developing since 2000 and have successfully demonstrated thus far in Phase I and Phase II clinical trials on cancer patients, as well as with experimental animals bearing other inflammatory pathologies. Furthermore we have shown that the principal mechanism of action of the drug candidate, DAVANAT, which is a modified galactomannan, is the strong blocking of galectin-1 and galectin-3. In other words, DAVANAT is a galectin blocker. *In vitro*, the binding constant for DAVANAT with isolated and purified galectin-1 and -3 was found to be in the micromolar range (~10 μM), but with a stoichiometry of binding 3 to 6 molecules of galectin-1 to one molecule of DAVANAT (molecular weight of 59 kDa). In cell cultures, DAVANAT showed 50% of its maximum biological activity (at saturation) at 3.1-3.8 μg/mL, that is 60-70 nM. The same maximum biological activity was reached only at 5 mM (about 120,000 times greater) with N-acetyllactosamine (LacNAc, or Gal-β 1,4-GlcNAc), one of the most specific ligands for galectins.

3.3. Liver Diseases

Galectin-3 is known to be involved in liver fibrosis. As mentioned above, galectin-3 appears to be involved in the transition to chronic inflammation, facilitating the walling off of tissue injury with fibrogenesis and organ scarring. Therefore, galectin-3 may be viewed as a regulatory molecule acting at various stages along the continuum from acute inflammation to chronic inflammation and tissue fibrogenesis (*23*).

A recent study of 33 patients with alcoholic liver cirrhosis and 11 patients with normal liver function has shown higher galectin-3 in portal venous serum compared to hepatic venous serum (HVS) in patients with normal liver function, which suggested hepatic removal of galectin-3 (*56*). However, galectin-3 was cleared by healthy livers, but not from cirrhotic livers, and subsequently HVS and SVS (systemic venous blood) galectin-3 levels were significantly increased in patients with liver cirrhosis compared to controls. In summary, systemic, portal and hepatic levels of galectin-3 were found to be negatively associated with liver function in patients with alcoholic liver cirrhosis.

Another study questioning the importance of galectin-3 in liver disease to non-alcoholic fatty liver disease (*57*) concluded that galectin-3 can hardly serve as a biomarker of human metabolic liver alterations. In this study, serum levels of galectin-3 in 71 patients with NAFLD and 39 controls were assayed, and it was shown that they did not differ in patients with NAFLD (median 4.1 ng/mL; interquartile range: 1.5-5.5 ng/mL) compared with healthy controls (median 3.1 ng/mL; interquartile range: 0.8-7.5 ng/mL).

3.4. Other Diseases

As an example, we describe here a role of galectin-3 in Behçet's disease (BD), or Silk Road disease, a rare immune-mediated systemic vasculitis, often manifested by mucous membrane ulceration and ocular involvements. This 2-year study involved 131 subjects, 39 of which were BD active, 31 inactive, 22 disease controls with leucocytoclastic vasculitis confirmed with a skin biopsy, and 39 healthy control subjects. It was found that serum galectin-3 levels were significantly higher in active BD patients compared to inactive BD patients and healthy control subjects. There was no significant difference between the leucocytoclastic vasculitis and active BD patients. Serum galectin-3 levels were positively correlated with clinical activity scores of active BD patients. In addition, galectin-3 levels were significantly higher during the active disease period when compared with the inactive period during follow-ups. It was also reported that patients with vascular involvement had significantly higher galectin-3 levels than other active BD patients (*58*).

Since galectins are known as immunomodulators of diverse inflammatory diseases, a number of them were examined with respect to their expression and localization in multiple sclerosis lesions (*59*), specifically, in control white matter (CWM). Among 11 different galectins tested, those which were present at detectable levels in CWM were galectins-1, -3, -8 and -9, and their expression was significantly enhanced in active multiple sclerosis (MS) lesions, namely in macrophages, astrocytes, and endothelial cells. Galectin-9 showed a distinctly different intracellular localization in microglia/macrophages when comparing active and inactive MS lesions. In active lesions, it was mainly found in nuclei, while in inactive lesions, it was primarily located in the cytoplasm. The authors (ibid.) concluded that some galectins are associated with multiple sclerosis pathology.

In a series of papers (*60–63*), St-Pierre, Sato et al. have suggested a role for galectin-1 as a host factor that influences HIV-1 pathogenesis by increasing its drug resistance. In brief, galectin-1 increases HIV-1 infectivity by accelerating its binding to susceptible cells. By comparison, galectin-3 does not show similarity with galectin-1 in this regard. It seems that galectin-1 directly binds to HIV-1 through recognition of clusters of N-linked glycans on the viral envelope gp120, by binding to CD_4, the host receptor for gp120. In turn, it results in promoting of virus attachment and infection events, since viral adhesion is a rate-limiting step for HIV-1 entry. The authors have tested some glycosides, such as mercaptododecyl glycosides with a terminal β-galactosyl group, and for some derivatives found "high binding responses" with galectin-3, -4, and 8. This opens possibilities in developing new drugs to prevent and treat HIV-1 infection.

4. Some Basis for Galectin Therapy and Specific Examples

Clearly, one of the obvious approaches to galectin therapy would be to design galectin blockers that specifically inhibit galectins, and examine those inhibitors against certain pathologies, first, of course, in experimental animal models. This, however, is not so easy. First of all, "classical" ligands of galectins are rather

Downloaded by UNIV OF DELAWARE MORRIS LIB on June 14, 2012 | http://pubs.acs.org
Publication Date (Web): June 12, 2012 | doi: 10.1021/bk-2012-1102.ch002

Downloaded by UNIV OF DELAWARE MORRIS LIB on June 14, 2012 | http://pubs.acs.org
Publication Date (Web): June 12, 2012 | doi: 10.1021/bk-2012-1102.ch002

weak binders, and are not really applicable as drugs. For example, lactose (4-O-β-D-Galactopyranosyl-D-glucose) binds to galectin-3 with K_d between 0.2 and 1 mM, to galectin-4 with K_d of 0.9-2.0 mM, and quite poorly binds to galectin-7, -10, 13 ((*15*) and references therein). N-acetyllactosamine binds better, however, still not good enough to become a drug: 50 μM with galectin-1, 34-200 μM with galectin-3, 1-2 mM with galectin-4 (ibid).

4.1. Galectin Blockers

There are only three groups of galectin ligands which can be considered as potential galectin blockers for biomedical applications. One group is comprised of low-molecular weight organic molecules, specifically designed to inhibit galectins (*64*, *65*). The other group is exemplified with modified citrus pectins. The third group is represented with 1,4-β-D-galactomannans, particularly GM-CT-01 (see below).

4.1.1. Small Galectin Ligands Molecules as Potential Galectin Blockers

A group of researchers at Lund University, Sweden, is active at synthesizing small organic compounds, derivatives of galactose, and testing them with respect to different galectins (*65*). Their strategy so far has been unsuccessful with inhibiting galectin-1, since apparent K_d values indicated rather weak binding, varying from 40 μM (digalactosyl sulfone) and 313 μM (C-galactoside derivative) to 1.25 mM (3-O-triazolylmethyl galactose derivative). Inhibitors of galectin-4, -7, and -9 were also relatively unsuccessful, with K_d values as high as 160 μM (2,3-dibenzoyl taloside, galectin-4), 23 μM; 140 μM (3′-thiourea lacNac and phenyl thio-galactoside derivatives, respectively, galectin-7), and 540 μM (3′-triazolyl mannoside, galectin-9). Inhibitors of galectin-3 were the most potent of all, with K_d values as low as 29 nM (3,3′-ditriazolyl thiodigalactoside), 50 nM (3,3′-diamido thiodigalactoside), 320 nM (3′-amido lacNAC derivative), and 660 nM (3′-triazolyl lacNac derivative).

One might have thought that these new inhibitors of galectin-3 would have significant potential for biomedicine; however, the reality of the situation was much more complex. The thiodigalactoside diester galectin-3 inhibitor (K_d = 660 nM; named Td131_1), when tested against papillary thyroid cancer (PTC) cell lines and human *ex vivo* PTC, actually increased the percentage of apoptotic cells in a dose-dependent manner (with 100-600 μM of the inhibitor, that is in the 150-1000 higher concentrations compared with the K_d value). However, this treatment was found to be largely ineffective in terms of the chemosensitivity of PTC cell lines to doxorubicin, which is normally enhanced upon suppression of galectin-3. Administration of as much as 0.6 mM of the thiodigalactoside compound actually decreased the IC_{50} of doxorubicin by 43-46%, or showed no detectable change in e.g. caspase-3 or PAEP cleavage (*66*).

The Mayo lab at the University of Minnesota has taken an alternative approach by designing compounds that target galectin-1 at a site different from the canonical β-galactoside binding site. Initially, they designed a peptide 33mer, called Anginex, based on structural and compositional features common to many anti-angiogenic proteins (e.g. endostatin, angiostatin, PF4, thrombospondin, gamma interferon-inducible protein-10 (IP-10), tumor necrosis factor, BPI, thrombospondin type 1 repeat peptides, Flt-1 peptide) (*67*, *68*). Anginex was shown to effectively inhibit tumor angiogenesis and tumor growth in mouse models (*69*) by targeting galectin-1 (*70*). Subsequently, these researchers were able to design peptidomimetics of Anginex (6DBF7 and PTX008) that were reduced in size and peptidic character from the peptide 33mer. 6DBF7 has only 13 amino acid residues, 20 less than parent Anginex, and maintains a requisite anti-parallel β-sheet fold via a dibenzofuran β-turn mimetic scaffold (*71*). PTX008 is a fully non-peptidic calixarene-scaffolded compound (a.k.a. compound 0118 in (*64*)) that displays chemical substituents to approximate the molecular dimensions and amphipathic features of Anginex and 6DBF7. All three compounds (Anginex, 6DBF7 and PTX008) target galectin-1 and function similarly *in vitro* and *in vivo* in terms of e.g. inhibiting endothelial cell proliferation, angiogenesis, and tumor growth (*64*, *69*, *71*). Moreover, in targeting galectin-1, they are quite different from traditional sugar-based compounds, because they act as allosteric inhibitors of galectin-1 carbohydrate ligand binding (*72*). A Swiss-based company, OncoEthix Inc. is currently taking PTX008 into Phase I clinical trials.

Downloaded by UNIV OF DELAWARE MORRIS LIB on June 14, 2012 | http://pubs.acs.org
Publication Date (Web): June 12, 2012 | doi: 10.1021/bk-2012-1102.ch002

4.1.2. Modified Citrus Pectin as a Potential Galectin Blocker

Modified citrus pectin (MCP) is a product of partial degradation of highly branched citrus pectin. Despite numerous studies published since 1992 (*73*), none of them showed a structure of a MCP, except for some vague wording about “linear” and “hairy” parts of the polymer. “Average” molecular weights of various MCPs range from about 10,000 to 120,000 Da; however, these are only crude estimates. Each MCP variant likely represents a wide range of molecules of various molecular weights.

In initial studies in the 1990’s and the first half of the 2000’s, it was assumed that MCPs bind to galectin-3, although this was more conjecture than experimentally-based fact (e.g., (*74*, *75*), and references therein). The first studies showed that iv injection of B16-F1 murine melanoma cells with MCP into mice resulted in a significant decrease of lung colonization, unlike injection of non-modified pectin solution, which led to the opposite effect, i.e. an increase of lung colonization (*73*). Besides, MCP inhibited B16-F1 melanoma cells adhesion to laminin and asialofetuin –induced homotypic aggregation (*74*). MCP was also found to be active by oral intake in mice (as a 1 and 2.5 mg/mL in drinking water solutions), reducing tumor growth, angiogenesis, and spontaneous metastasis *in vivo* (*76*). MCP (a code name GCS-100) was shown to induce apoptosis in various multiple myeloma cell lines, growth of which was induced by adhesion to bone marrow stromal cells (*75*). It should be noted that GCS-100 by itself did not alter galectin-3 expression, but was active in that regard in a mixture with dexamethasone (ibid.).

MCP was found to be active in the suppression of liver metastasis of colon cancer in mice (*16*). Mice fed with a drinking water solution of MCP in concentrations of 0 (control), 10, 25, and 50 mg/mL showed rates of liver metastasis of 100%, 80%, 73%, and 60%, respectively, and median volumes from primary lesions in the spleen of 1.51, 0.93, 0.77 and 0.70 cm^3, respectively.

Commercially available fractionated pectin powder (FPP) [molecular weight of pectin fragments and their distribution in FPP was not available, and the meaning of the term “fractionated” was unclear, whether the “native”, pH-untreated pectin was fractionated or fractionation was performed with its partially degraded form] was shown to be capable of inducing apoptosis in human prostate cancer cells, and the level of apoptosis was reported to be 40 times above that in untreated cells. Interestingly, PectaSol (pH-treated citrus pectin) had little or no apoptotic activity, even though there were no detectable (or significant) differences found among the pectins (*77*). The pattern is complicated by the fact that chemical removal of ester linkages in FPP (by mild alkaline treatment) which yield homogalacturonan oligosaccharides, completely destroyed the apoptotic activity. Conversely, removing galacturonosyl carboxymethylesters and/or breaking the nonmethylesterified homopolygalacturonan chains in FPP by enzymatic treatment (with pectinmethylesterase and/or emdopolygalacturonase) did not significantly reduce the apoptotic activity of FPP. Furthermore, heat treatment (by autoclaving) of citrus pectin solutions led to the induction of significant levels of apoptosis comparable to that of FPP (ibid.). In other words, the biological activity of citrus pectin can be modulated by chemical and physical (which apparently lead to chemical effects) means, which makes the picture not easily manageable in order to obtain a reproducible drug formulation.

Apparently, the first time the interaction of pectin fragments, galactans (from potato pectin) with galectin-3 (in fact, it was the recombinant form of human Gal3) was demonstrated in 2009 (*78*). The galactans contain 88% galactose residues (6% galacturonic acid, 3% arabinose, and 3% rhamnose). For a comparison, rhamnogalacturonan 1 (containing 12% galactose, 62% galacturonic acid, 20% rhamnose, 3% arabinose) and polygalacturonic acid from MCP (96% galacturonic acid, 1% galactose, 1.2% rhamnose, 1% xylose, 0.2% arabinose) were also tested for their interaction with galectin-3. It was found that all three compounds, fluorescently labeled, bind to galectin-3 at pH 7.2 (at which pH galectin-3 is positively changed), but not at pH 12, at which only galactans retained a high level of binding to Gal-3.

A more recent article supporting this last conclusion reported an effect of a galactan from an almost pure pectic rhamnogalacturonan 1 (from okra pods) on the proliferation and apoptosis of highly metastatic B16-F10 melanoma cells *in vitro* (*79*). The study suggests that the pectic galactan induced apoptosis in melanoma cells by interacting with galectin-3.

The inhibitory effect of citrus pectin on the proliferative capacity of several malignant carcinoma and erythroleukemia cell lines was studied at various doses of the pectin, and it was suggested that the observed antiproliferative effect may be due to this pectin’s ability to inhibit galectin expression (*80*).

One more study was based on the known ability of galectin-3 to be upregulated in acute kidney injury, and was aimed at suppressing galectin-3 with

Downloaded by UNIV OF DELAWARE MORRIS LIB on June 14, 2012 | http://pubs.acs.org
Publication Date (Web): June 12, 2012 | doi: 10.1021/bk-2012-1102.ch002

Downloaded by UNIV OF DELAWARE MORRIS LIB on June 14, 2012 | http://pubs.acs.org
Publication Date (Web): June 12, 2012 | doi: 10.1021/bk-2012-1102.ch002

MCP. Indeed, MCP-treated mice demonstrated reduced levels of galectin-3 in association with decreased renal fibrosis, macrophages, proinflammatory cytokine expression and apoptosis. However, levels of other renal galectins, galectin-1 and -9, were unchanged (*81*).

It was observed long ago that in patients with advanced cancer, tumor progressed despite the presence of tumor-infiltrating lymphocytes (TIL), resulting from a spontaneous T-cell response against their tumor. In other words, anti-tumoral T cells become ineffective. It was suggested that this ineffectiveness resulted from either an acquired resistance of tumor cells to the immune attack, or because TIL becomes functionally impaired ((*82*) and references therein). The authors suggested that the impairing effect was caused by intratumoral galectin-3, and that galectin blockers could improve anti-tumor immunity *in vivo*. Indeed, these authors found that two polymeric galactose-containing compounds, pectin-derived GCS-100 and DAVANAT, a galactomannan from *C. tetragonoloba*, detached galectin-3 from TIL and boosted secretion of IFN-γ (*82*, *83*).

A recent review article, which summarizes various biological effects of MCP possibly due to its binding galectin-3, has been published (*84*).

4.2. Galactomannans. GM-CT-01 (DAVANAT®) as a Drug Candidate in Galectin Therapy

Since the founding of Pro-Pharmaceuticals Inc. (presently Galectin Therapeutics Inc.) in 2000 (www.galectintherapeutics.com), we have initiated a strategy to target galectins for cancer therapy, as well as for other inflammatory diseases. Our approach is based on producing galactose-containing polysaccharides that function as galectin ligands (galectin antagonists) and interfere with their function. To this end, the company has manufactured DAVANAT®, a modified galactomannan, through a patented method of controlled chemical degradation of natural galactomannans ((*85*); U.S. Pat. No. 6,645,946, 6,914,055, 6,982,255, 7,012,068, 7,893,252, Pat. Australia No. 272022B2, Pat. Japan No. 4744782). Since galactomannans are present in nearly all plants, an understandable effort was made by us to identify a source of an industrial significance and scale, that is readily available for subsequent processing, with the goal of having an inexpensive drug that would be affordable to patients. Unfortunately, this is not the case for the great majority of chemotherapy drugs on the market. After studying a number of galactomannans from various plant sources, we chose galactomannans from the seeds of *Cyamopsis tetragonoloba*, a readily available product typically imported from Pakistan and India in ton quantities for use as a gel in the food industry. With regard to galactomannans, this source is about 50% pure. However, the natural galactomannans have molecular weights of well over one million Da and are water-insoluble. Our task was to make it pure and readily water soluble, and be able to characterize the resulting oligo- or polysaccharides, as being capable of effectively binding to galectins (particularly to galectin-1 and/or -3), being non-toxic (according to FDA standards) in test animals and then in humans, and having desirable therapeutic properties. This task was accomplished in preclinical and Phase I and

Phase II clinical studies, completed in 2006 and 2008, respectively. Results are described in detail in (*85–87*), submitted to and agreed upon by the FDA. Also, a number of US patents were granted (see above) with respect to preparation of the galactose-based polysaccharide (later obtained a trademark DAVANAT®), and its therapeutic usage. In 2011, the name GM-CT-01 was assigned to the particular DAVANAT® compound which was filed with the FDA in a form of the Drug Master File.

It is well known that galactomannans in general and those from *Cyamopsis tetragonoloba* in particular consist of two sugar residues: galactose and mannose. Its backbone is made of mannose, and approximately every second mannose residue carries a galactose substituent, Fig. 2 (*85*, *87*). The average repeating unit of DAVANAT® is made up of seventeen β-D-Man residues and ten α-D-Gal residues, and an average polymeric molecule contains approximately 12 of such repeating units, at an average molecular weight of about 55 kDa. (54,550±210 Da according to a recent QC test at Sigma-Aldrich Co.). GM-CT-01 compound for clinical trials has a specified molecular weight in the range of 42,000 to 60,000 Da.

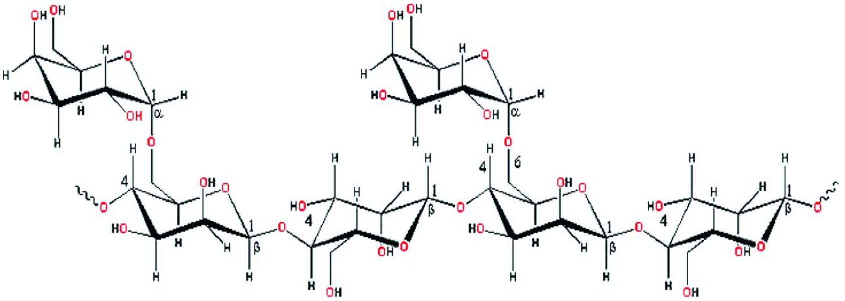

Figure 2. Structure of the basic repeating building block of DAVANAT. Each DAVANAT® molecule consists of 54 such units (86)

Identification of its molecular structure was done using the chemical analysis and the ^{1}H- and ^{13}C-NMR spectroscopy (*87*), its absolute molecular weight was determined using HPLC/RI-MALLS and a ZIMM plot analysis (ibid.), where MALLS stands for the Multi-Angle Laser Light Scattering, which was used for the Refractive Index (RI) measurements. Aside from this, the weight-averaged molecular weight of DAVANAT® was measured by pulsed field gradient NMR diffusion spectroscopy in our recent work (*88*) as 59±8 KDa.

Compared with many other known polysaccharides, galactomannans have repeated galactose singular side residues that could readily interact with galactose-specific receptors such as galectins on the tumor cell surface, modulate the tumor surface physiology, and potentially affect delivery of drugs to the tumor. In fact, such an interaction between DAVANAT® and galectin-1 was recently shown and characterized by us in terms of its specificity, dissociation constant and stoichiometry of binding (*89*, *90*). As far as we know, DAVANAT® is the first polymeric carbohydrate-based drug candidate proven to be an effective ligand for galectin-1 (*89*), with an apparent binding avidity of 60-70 nM, tested

Downloaded by UNIV OF DELAWARE MORRIS LIB on June 14, 2012 | http://pubs.acs.org
Publication Date (Web): June 12, 2012 | doi: 10.1021/bk-2012-1102.ch002

in a bioassay system (CD4+ and CD8+ tumor infiltrating lymphocytes, with interferon-γ secreted as a readout of the assay) (*83*).

4.2.1. Galectin Therapy in Solid Cancer Tumor Clinical Trials, Phase I and II

Only clinical trial data available in the public domain are presented in this book, specifically in some detail in Chapter 4. First, in a series of pre-clinical studies, we demonstrated that DAVANAT® is not toxic and increases the efficacy of 5-FU against cancer. This was shown in a number of animal studies in which

(a) toxicity of 5-FU in mice was practically eliminated when it was injected i.v. along with DAVANAT® at the dose of 5-FU above LD_{50} (*86*)
(b) a quadrupling tumor growth median time for human colon tumor COLO205 subcutaneously implanted in NCr-nu mice was increased from 12.5 days (control, no treatment) to 23.7 days (75 mg/kg of 5-FU), and to 56 days (120 mg/kg of DAVANAT® + 75 mg/kg of 5-FU), with median tumor volume at the end point being 2058 mm^3, 2254 mm^3 and 379 mm^3, respectively (*85*)
(c) a similar in-kind effect was observed when another human colon tumor, HT-29, was s.c. implanted in NU/NU-nuBR mice and treated with 5-FU+leucovorin (45+25 mg/kg, respectively) or with the same plus 120 mg/kg of DAVANAT®; the respective median time to quadrupling of tumor volume was 13.3, 15.3, and 23.5 days, with a median tumor volume at the end point being 1318, 1120, and 729 mm^3, respectively, (ibid.)
(d) dose escalation of DAVANAT® from 6 to 600 mg/kg in COLO205 human tumor-bearing mice treated with 5-FU (48 mg/kg/dose) has shown that the highest median time to quadrupling of tumor volume and the smallest tumor volume at the endpoint were achieved with 120 and 600 mg/kg DAVANAT® dose (16.5-16.2 days compared to 8.7 days for 5-FU alone, and 540-588 mm^3 compared to 800 mm^3 for 5-FU alone, respectively). (ibid.)

These studies, along with many others, including toxicity studies in rats and dogs, mutagenicity studies which included Ames bacterial reverse mutation assays for DAVANAT® itself and in a combination with 5-FU in bacterial assays using *Salmonella typhimurium* strains TA97a, TA98, TA100, TA1535 and *Escherichia coli* strain WP2 *uvr*A (pKM101), in which no evidence of mutagenic toxicity was detected at any concentration level tested, as well as radiolabel studies in tumored (COLO205-treated) and non-tumored male athymic NCr-nu mice are described in detail in our publications (*85*, *86*). Based on these and other studies, which had comprised the full scope of pre-clinical investigations required by the FDA, the FDA allowed us to move into Phase I clinical studies to test DAVANAT® in conjunction with 5-FU, first with 30 to 280 mg/m^2/day (0.74 to 6.9 mg/kg/day) of DAVANAT® co-administered with 500 mg/m^2/day of 5-FU (Phase I), and after the non-toxicity of DAVANAT® was established as the principal result of Phase I, the FDA had allowed DAVANAT® to move into Phase II with the highest dose

Downloaded by UNIV OF DELAWARE MORRIS LIB on June 14, 2012 | http://pubs.acs.org
Publication Date (Web): June 12, 2012 | doi: 10.1021/bk-2012-1102.ch002

Downloaded by UNIV OF DELAWARE MORRIS LIB on June 14, 2012 | http://pubs.acs.org
Publication Date (Web): June 12, 2012 | doi: 10.1021/bk-2012-1102.ch002

established as 280 mg/m^2/day of DAVANAT® being co-administered with 5-FU at 500 mg/m^2/day dose according to the approved – for Phase II – clinical regimen.

A Phase I dose-escalating safety clinical trial (NCT00054977) was initiated by Pro-Pharmaceuticals as a sponsor on January 27, 2003, and completed in April 11, 2005. The study was conducted in the following locations: Florida Oncology Associates (Jacksonville, FL), Ochsner Cancer Institute (New Orleans, LA), University of Michigan Comprehensive Cancer Center (Ann Arbor, MI), Hematology/Oncology Private Practice (Howell, NJ), and Dartmouth-Hitchcock Medical Center (Lebanon, NH) [http://clinicaltrials.gov/ct2/show/NCT00054977]. The study had the official title: "**A Phase I Open-Label Study to Evaluate the Safety and Tolerability of Escalating Doses of DAVANAT (A Galactomannan Derivative) in the Presence and Absence of 5-Fluorouracil (5-FU) in Subjects With Advanced Solid Tumors**". Patients that were enrolled in the study had different types of solid tumors and had failed standard, approved treatments. This study evaluated the tolerability of six rising doses of DAVANAT® alone ranging from 30 to 280 mg/m2 and then in combination with 5-FU (500 mg/m2) over 2 cycles of therapy. A total of 40 patients enrolled in the study.

A Phase II safety and efficacy clinical trial (NCT00110721) was initiated by Pro-Pharmaceuticals as a sponsor on May 1, 2005, completed on January 31, 2008, and conducted in the following locations: Hematology-Oncology Associates of the Treasure Coast (Port St. Lucie, FL), Ochsner Clinic Foundation (New Orleans, LA), University of Michigan Comprehensive Cancer Center (Ann Arbor, MI), Medical Oncology and Hematology (Waterbury, CT), Shaare Zedek Medical Center, Oncology (Jerusalem, Israel), and Soroka University Medical Center (Beer-Sheva, Israel) [http://clinicaltrials.gov/ct2/show/NCT00110721]. It had the official title: "**A Phase II, Multi-Center, Open-Label Trial to Evaluate the Efficacy and Safety of Intravenous DAVANAT in Combination With 5-Fluorouracil When Administered in Monthly Cycles as Third- or Fourth-Line Therapy for Metastatic Colorectal Cancer**". Patients that were enrolled in this study had a histologically proven adenocarcinoma of the colon or rectum, and had documentation of locally advanced or metastatic colorectal cancer not amenable to curative surgery or radiotherapy, and had one or more measurable lesion(s) according to RESIST (Response Evaluation Criteria in Solid Tumors) criteria. Furthermore, eligible subjects were those who had unresectable, locally advanced and/or metastatic colorectal cancer that progressed during or after receiving treatment with at least two lines of therapy, which collectively must have included at a minimum all of the following agents: 5-FU or capecitibine, irinotecan, and oxaliplatin. Simply put, this Phase II experimental study using DAVANAT® was their last resort. All preceding treatments with approved therapies failed in their cases. A standard dose of 280 mg/m^2 DAVANAT® and 500 mg/m^2 5-FU was given in monthly cycles for at least two cycles, or until their disease progressed.

Some milestones of the both studies were as follows:

(a) DAVANAT® was non-toxic, and a DLT (dose limiting toxicity) was not reached,

(b) 70% of the patients were stabilized at the highest DAVANAT® dose (280 mg/m^2/day),
(c) when co-administered with DAVANAT®, the half-life of 5-FU increased in the bloodstream of patients from 6-22 min (historical data for 5-FU alone) to 28-137 min,
(d) a 46% increase in longevity of patients (based on the Median Overall Survival) was achieved compared with the Best Standard of Care, and
(e) a 41% reduction of SAE (Serious Adverse Effects) was achieved compared to the Best Standard of Care.

Downloaded by UNIV OF DELAWARE MORRIS LIB on June 14, 2012 | http://pubs.acs.org
Publication Date (Web): June 12, 2012 | doi: 10.1021/bk-2012-1102.ch002

It should be emphasized that all patients in these Phase I and II clinical trials had failed their prior cancer therapies, including 5-FU, Xeloda®, Avastin®, Erbitux®, oxaliplatin, irinotecan. The majority of them had colorectal cancer (53%), following up with pancreatic cancer (13%) and others, such as hepatocellular, biliary (cholangiocarcinoma), gastric, breast, ovarian, appendiceal, testicular, prostate, and unknown primary cancers. 60% of the patients failed prior surgery, and 30% failed prior radiotreatment. 100% of the patients in Phase II have failed prior chemotherapy and/or other systemic therapies. 58% of the patients failed prior 5-FU treatment.

Based on these data, objections for Galectin Therapeutics to move into a Phase III clinical trial was not expressed by the FDA.

5. More Examples of Galectin Therapy: Potential and Some Experimental Results

5.1. Galectin Therapy in Cardiovascular Diseases

Heart failure is generally defined as a failure of the heart to supply sufficient blood volume to meet the requirements of the body. Heart failure is the result of myocardial injury or hemodynamic overload, which goes beyond mechanical dysfunction; heart failure is associated with a number of pathophysiologic mechanisms, including inflammation, tissue remodeling, endocrine signaling, and interactions with the renal and nervous systems; it is the result of interplay of a number of biochemical factors, collectively referred to a biomarkers. One of the novel biomarkers is galectin-3.

We have described above a series of studies (*19*, *47–55*) which quite convincingly showed an importance of galectin-3 in heart failure and mortality. Clearly, galectin therapy aimed at blocking galectin-3 (and maybe some other galectins, still not identified in the pathology) might be a strategic approach in curative cardiology.

5.2. Galectin Therapy in Asthma: A Potential

Asthma is a chronic disease characterized by airway inflammation, airway hyperresponsiveness, reversible airway obstruction, predominance of Th2 cells and eosinophilic inflammation. A number of studies point at an important role of galectins in these outcomes and mechanisms leading to them. The following are

Downloaded by UNIV OF DELAWARE MORRIS LIB on June 14, 2012 | http://pubs.acs.org
Publication Date (Web): June 12, 2012 | doi: 10.1021/bk-2012-1102.ch002

several examples of such studies, which show the involvement of galectin-3, -7, -9 and -10 in the allergic disorder.

Ge et al (*91*) have investigated a murine model of chronic allergic airway inflammation aiming at the role played by galectin-3 in airway remodeling, a characteristic feature of asthma that leads to airway dysfunction and poor clinical outcome in humans. They have found that the higher degree of airway remodeling in wild-type mice was associated with higher Gal-3 expression. Furthermore, using galectin-3-null mice they found diminished remodeling of the airways with significantly reduced mucus secretion, subepithelial fibrosis, smooth muscle thickness, and peribronchial angiogenesis. The authors concluded that Gal-3 promotes airway remodeling via airway recruitment of inflammatory cells, specifically eosinophils, and the development of a Th2 phenotype, as well as increased expression of eosinophil-specific chemokines and profibrogenic and angiogenic mediators (*91*).

In one particular study, galectin-3 was not a target but the encoded agent, using a gene therapy approach, which employed plasmid encoding galectin-3 in chronic asthmatic mice. This was shown to improve Th2 allergic inflammation. Another model under study was a mouse model of chronic airway inflammation, with therapeutic galectin-3 delivered by gene therapy. The microarray approach has resulted in finding a correlation between galectin-3 treatment and inhibition of cytokine signaling proteins in lungs which act as negative regulators of cytokine signaling, and play an important role in immune response by controlling the balance between Th1 and Th2 cells. The authors concluded that Gal-3 treatment could be a valuable therapeutic approach in allergic disease (*92*).

Galectin-9 was found to play a potential role in the pathogenesis of asthma (*93*). Galectin-9 is an eosinophil chemoattractant and inducer of Th1 cell apoptosis. The authors used a group of BALB/c mice sensitized and challenged with ovalbumin, which develop airway inflammation and mucus hypersecretion, and found that galectin-9 protein levels were elevated in lungs of those mice compared to controls. The authors concluded that galectin-9 contributes to the development of allergic airway inflammation (*93*).

Galectin-9 was also found to inhibit allergic inflammation of the airway and airway hyperresponsiveness (AHR) by modulating CD44-dependent leukocyte recognition of the extracellular matrix (*94*). However, in their work, human galectin-9 was given by intravenous injection to mice during antigen challenge.

The study (*95*) reported that galectin-9 and Tim-3 mRNA levels in lungs increased in mice with asthma and significantly correlated with the levels of blood Th1/Th2 cytokines; hence, they are closely related to inflammatory process in asthma. Rosiglitazone treatment has apparently decreased the expression of galectin-9 and Tim-3. This was shown in a group of 45 BALB/c SPF female mice which were randomized into control group and asthma groups with and without rosiglitazone intervention. Also, it has been shown that the expression of galectin-9 and Tim-3 mRNA was positively correlated with blood IL-4 level, but negatively correlated with blood IFN-γ level (*95*).

A recent review (*96*) considers an important role of galectin-9 in health and disease, and in asthma among those. In normal physiology, galectin-9 appears to be a pivotal modulator of T-cell immunity by inducing apoptosis in specific

T-cell subpopulations. However, since these T-cell populations are associated with autoimmunity, inflammatory disease, and graft rejection, it was found that application of exogenous (such as recombinant) galectin-9 may limit pathogenic T-cell activity in various preclinical models of autoimmunity and allograft graft rejection. In many solid cancers, the loss of galectin-9 expression is closely associated with metastatic progression, and treatment with recombinant galectin-9 prevents metastatic spread in various preclinical cancer models. The review discusses the therapeutic potential of galectin-9 in various diseases, including autoimmunity, asthma, infection, and cancer.

Galectin-10 mRNA was found to be over-expressed in aspirin-induced asthma (AIA), suggesting a novel candidate gene and a potentially innovative pathway for mucosal inflammation in aspirin intolerance (*97*). The choice of the model was made following the observation that in sensitive patients, aspirin is associated with nasal and bronchial inflammation, eliciting local symptoms.

The following study by Rogerio et al (*98*) does not mention galectins specifically; however, it identifies some “D-galactose-binding lectin” from *Synadenium carinatum* latex. The lectin, which is very likely a galectin, increased interferon-gamma and IL-10 in an asthma inflammatory model, suggesting that it might induce a TH2 to TH1 shift in the adaptive immune response. Extracts from this latex are widely used in popular medicine to treat a great number of inflammatory disorders.

Another galectin, galectin-7, was found to be involved in asthma development in children (*99*). Asthmatic and non-asthmatic children were compared, and galectin-7 was found to be 8-fold greater in bronchial epithelial cells from asthmatic children. Furthermore, bronchial epithelial cell apoptosis also increased in asthma *in vivo*.

5.3. Galectin Therapy in Arthritis: A Potential

Arthritis is an inflammatory disease of one or more joints in the body, and is a collective term. There are more than a hundred types of arthritis, rheumatoid arthritis (RA) is just one of them, but probably the most known. RA is a chronic, systemic inflammatory disorder that may affect many tissues and organs, and destroys cartilages or bones at the joints. RA is initiated by self-attack using own immune system, but the detail of pathological mechanism is unclear. Since different forms of arthritis are inflammatory in their nature, it can be expected that galectins are involved in them. This indeed was confirmed in a number of studies, with galectin-3 and galectin-9 making the most studies.

The following are several examples of studies on involvement galectins in arthritis.

Galectin-1, which is recognized to play a profound role in modulating adaptive immune responses by altering the phenotype and fate of T cells, was a target in a mouse Gal-1 human Ig chimera (Gal-1hFc). At high concentrations, Gal-1hFc induced apoptosis in Gal-1 ligand(+) Th1 and Th17 cells, leukemic cells, and granulocytes from synovial fluids of patients with rheumatoid arthritis (*100*).

In a recent study of Wang et al (*101*) lentiviral vectors encoding galectin-3 small hairpin RNA (shRNA) and galectin-1, as well as two control vectors

Downloaded by UNIV OF DELAWARE MORRIS LIB on June 14, 2012 | http://pubs.acs.org
Publication Date (Web): June 12, 2012 | doi: 10.1021/bk-2012-1102.ch002

expressing luciferase shRNA and green fluorescent protein, were individually injected intra-articularly into the ankle joints of rats with collagen-induced arthritis, and their treatment responses were monitored by measuring the clinical, radiological and histological changes. The authors showed that both knockdown of galectin-3 and overexpression of galectin-1 induced higher percentages of antigen-induced T-cell death in the lymph node cells from arthritic rats. Based on the data obtained the authors suggest a hypothetical model of a cross talk between galectin-1 and galectin-3 in the circumstance of rheumatoid joints, and implicate galectin-3 and galectin-1 as potential therapeutic targets for the treatment of rheumatoid arthritis.

Li et al (*102*) investigated an involvement of galectin-3 in the regulatory process of inflammatory bone resorption in rats with adjuvant-induced arthritis (AA rats) accompanying severe bone destruction in the ankle joints. The protein level of galectin-3 in the ankle-joint extracts was markedly augmented at week 3 after adjuvant injection, at the time when severe bone destruction was observed. Immunohistochemical analysis revealed an extremely high expression of galectin-3 in macrophages and granulocytes infiltrated in the area of severe bone destruction. Besides, recombinant galectin-3 was added to *in vitro* culture systems, and found to markedly inhibit the formation of osteoclasts in cultures of murine osteoclast precursor cell line as well as in rat bone marrow culture systems. This inhibition was not observed by heat-inactivated galectin-3 or by galectin-7. Furthermore, *in vivo* studies clearly showed a significant suppression of bone destruction and osteoclast recruitment accompanying arthritis, when galectin-3 was injected into the cavity of ankle joint of AA rats. The authors concluded that abundant galectin-3 observed in the area of severe bone destruction may act as a negative regulator for the upregulated osteoclastogenesis accompanying inflammation to prevent excess bone destruction.

The following study (*22*) was brought about by the observation that galectin 3 is present in the inflamed synovium in patients with rheumatoid arthritis, hence, it might be associated with the pathogenesis of this disease. A murine model of arthritis was employed in the study, in which wild-type (WT) and galectin 3-deficient (galectin 3(-/-)) mice were subjected to antigen-induced arthritis (AIA) through immunization with methylated bovine serum albumin. It was found that the joint inflammation and bone erosion of AIA were markedly suppressed in galectin 3(-/-) mice as compared with WT mice, and the reduced arthritis in galectin 3(-/-) mice was accompanied by decreased levels of antigen-specific IgG and proinflammatory cytokines. The frequency of IL-17-producing cells in the spleen was reduced in galectin 3(-/-) mice as compared with WT mice. Besides, exogenously added recombinant galectin 3 could partially restore the reduced arthritis and cytokines in galectin 3(-/-) mice. The authors concluded that galectin 3 plays a pathogenic role in the development and progression of AIA and that the disease severity is accompanied by alterations of antigen-specific IgG levels, systemic levels of TNFα and IL-6, and frequency of IL-17-producing T cells.

The following study (*21*) has been already described in Inflammation Section. It was shown that it is not just galectin-3 that contributes to development of rheumatoid arthritis (RA), but may be some of its polymorphic forms. Indeed, in synovium of RA an elevated expression of galectin-3 has been demonstrated,

Downloaded by UNIV OF DELAWARE MORRIS LIB on June 14, 2012 | http://pubs.acs.org
Publication Date (Web): June 12, 2012 | doi: 10.1021/bk-2012-1102.ch002

Downloaded by UNIV OF DELAWARE MORRIS LIB on June 14, 2012 | http://pubs.acs.org
Publication Date (Web): June 12, 2012 | doi: 10.1021/bk-2012-1102.ch002

however, the allelic carriage of LGALS3 +292C was increased in RA patients (151 RA patients and 182 healthy subjects as control) from 66.9% in RA vs. 52.7% in control.

The importance of galectin-9 in rheumatoid arthritis was discussed in the study (*103*), in which galectin-9 is considered as a ligand of TIM-3, a novel transmembrane protein that is involved in the regulation of T-helper 1 (Th1)-cell-mediated immunity, and containing T-cell immunoglobulin- and mucin-domain. The goal of the study was to investigate the expressions of TIM-3 along with galectin 9 with respect to disease activity in rheumatoid arthritis (RA). Blood was collected from 39 RA patients and 31 healthy controls, and blood leucocyte TIM-3 and Gal-9 mRNA levels and RA disease activity were determined. It was found that TIM-3 mRNA expression was significantly higher in the synovial tissue (ST) of RA patients than in the ST of osteoarthritis (OA) patients. The authors concluded that TIM-3 and its interaction with Gal-9 are closely associated with RA disease activity and may play an important role in the pathogenesis of RA. Besides, in addition to the negative regulatory effect of Gal-9 mediated through the TIM-3-Gal-9 pathway, Gal-9 may exert its suppressive effect on RA disease activity by modulation of regulatory T (Treg) cells.

The study described above was part of a more general work by the authors (*104*) aimed at the role of expression of TIM-3 from CD4+ T cells from rheumatoid arthritis (RA) patients and healthy controls, and a contribution of galectin-9 to apoptosis of CD4+ T cells in these patients. It was shown that TIM-3 mRNA expression was significantly lower in CD4+ T cells from RA patients compared with those in healthy controls. CD4+ T cell survival (as measured by MTT assay when incubated with Gal-9) was significantly higher in RA patients than in healthy controls.

Apoptotic activity of CD4+ T cells from healthy controls increased with graded doses of Gal-9 (between 0 and 90 nM). However, apoptotic activity of CD4+ T cells from RA patients did not change despite the stimulation with Gal-9. Gal-9-mediated apoptosis of CD4+ T cells is dysfunctional in RA patients. The authors concluded that TIM-3 and its interaction with Gal-9 may play an important role in the pathogenesis of RA and may represent a potential therapeutic target (*104*).

Galectin-9 was found to suppress collagen-induced arthritis (CIA) in a mouse model in a dose-dependent manner (*105*). Such suppression was observed even when treatment was started on 7 days after the booster, indicating its preventive and therapeutic effects. The authors have suggested that galectin-9 ameliorates CIA by suppressing the generation of Th17, promoting the induction of regulatory T cells.

In was found that the synovial fluid (SF) cells from rheumatoid arthritis (RA) patients express and secrete galectin-8, to a concentration of 25-65 nM, well within the concentration of Gal-8 required to induce apoptosis of SF cells (*106*). Besides, Gal-8 was found to be a novel high-affinity ligand of CD44vRA, a specific CD44 variant, with an apparent binding constant of 6 nM (*106*). Besides, it was found that galectin-1 was found to be overexpressed in rheumatoid arthritis (RA) synovium (*107*).

Contrary (or in addition) to the data in the above item, galectin-3 was found to be expressed in the synovial tissue of patients with rheumatoid arthritis (RA), particularly at sites of joint destruction (*108*).

Earlier data by the same authors (as in item 6) showed that galectin 3 is not only involved in inflammation, but also contribute to the activation of synovial fibroblasts. The intracellular accumulation of galectin 3 can be enhanced by TNFalpha. In contrast, the authors found that expression of galectin-1 was not uniform in different RA specimens, and was never found at sites of invasion. The authors concluded that galectin 3 represents novel markers of disease activity in rheumatoid arthritis (*109*).

Downloaded by UNIV OF DELAWARE MORRIS LIB on June 14, 2012 | http://pubs.acs.org
Publication Date (Web): June 12, 2012 | doi: 10.1021/bk-2012-1102.ch002

5.4. Galectin Therapy in Malignant Gliomas: A Potential

Malignant gliomas are the most common primary brain tumors. A clinical prognosis in those pathologies is rather bleak, making an average survival time around one year in unselected series ((*110*), and references therein). The immune response of the patients typically is not effective, due to high migratory capacity of the brain tumor and its aggressive growth. It was suggested that a number of galectins, such as galectin-1, -3, -4, and -8 contribute to malignant gliomas growth and resistance against antineoplastic therapy (ibid.). In an earlier work the authors have provided evidences of a role of galectin-1 in the regulation of glioma cell proliferation and migration (*111*). The authors concluded that targeting galectin-1 (and possibly other galectins) may have therapeutic benefits in the treatment of malignant glioma.

As it was described above in this Chapter, Robert Kiss and his Laboratory of Experimental Immunology in Leuven, Belgium, continue to uncover the role of galectin-1 in immunotherapy for brain cancer as an important player in glioma-mediated immune escape (*30–32*). It was shown that galectin-1 is abundantly expressed in high-grade glioma, and active specific immunotherapy by dendritic cell vaccination apparently generates an anti-tumoral immune response, when accompanied by down-regulation of counteracting tolerogenic signals (*32*), see also (*112–116*).

5.5. Galectins Are Indicators in Other Pathologies, Just a Few Examples

An elevated level of galectin-9 was observed in patients with allergy to insulin (*117*). The elevation of galectin-9 (22.5-fold) was more than an order of magnitude compared with that for other four inflammatory biomarkers monitored in the study (1.4-7.3-fold, the highest was for eosinophil count).

Galectin-3 was suggested as a biomarker for amyotrophic lateral sclerosis (ALS), a neurodegenerative disease (*118*), after studying the appropriate mice model and then validating the finding in human tissues. 1299 proteins have been studying, of which 14 proteins were found to be dramatically altered in the ALS mice compared with the two control groups. Galectin-3 emerged as a lead biomarker candidate on the basis of its differential expression as assessed by immunoblot and immunocytochemistry as compared to controls and because it is a secreted protein that could be measured in human biofluids. Spinal cord

Downloaded by UNIV OF DELAWARE MORRIS LIB on June 14, 2012 | http://pubs.acs.org
Publication Date (Web): June 12, 2012 | doi: 10.1021/bk-2012-1102.ch002

tissue from ALS patients also exhibited 2-fold increased levels of galectin-3 when compared to controls.

The expression pattern of galectin-1 was determined in 73 vulvar tissues by a standard immunohistochemical method: 12 benign vulvar specimen, 41 vulvar intraepithelial lesions (VIN), according to their differentiation were subdivided into VIN I, II and III and 20 invasive squamous cell carcinomas (ISCC). The immunohistochemical analyses showed that the intensity of galectin-1 expression on stromal cells next to the neoplastic cells steadily increased according to the pathological grade: benign vulvar tissue <VIN I<VIN II<VIN IIVIN III<ISCC ($p<0.0001$). In epithelial cells, negative or weak reactivity for galectin-1 was observed. These findings indicate that the galectin-1 expression on stromal cells increases with the histopathological grade of vulvar tissues, and it can be suggested that these changes might be associated with the progression of vulvar neoplasia (*119*).

5.6. Galectins in Human Diseases and Potential of Galectin Therapy

As it was described in the very beginning of this article, as many as 3516 articles have been published, in which galectins were considered either from strictly "biochemical point of view", as a component of cellular systems, or as a protein which was isolated, purified and characterized, or as a diagnostic tool signaling about a certain pathology. Very few of those papers were considering specific drug candidates, aiming at galectins and achieved positive clinical results, such as described above and in Chapter 4 with the example of GM-CT-01. With this drug candidate, a GMP drug form have been prepared, described in a full-size Drug Master File, presented to the FDA, and tested in Phase I and Phase II clinical trials. More than 50 submissions to the FDA have been done over the last 9 years, in which every detail of the animal experiments and the human trials was described. It seems there is no such work with respect to galectin therapy has been done to date.

In other words, most (and practically all) of those 3500+ papers on galectins are academic studies. This is very important and beneficial for galectin therapy. In order to analyze the published papers with respect to human diseases and pathologies, we have considered the most recent thousand articles, from December 2011 back through August 2007, and broke them into categories according to diseases and pathologies. In more than one-third of those articles certain diseases and pathologies have been mentioned. They are listed below from the most frequent disease (thyroid carcinoma) which have been studied in 63 publications in connection with overexpressed galectins, and/or activated K-Ras, and/or considered galectins as a diagnostic tool (such as galectin-3), etc. Clearly, to design a drug aiming at galectin-3 and galectin-1 (and maybe at some other galectins, promoting thyroid tumors) would be an important achievement of galectin therapy.

The following is the list, with the second column indicating a number of publications according to PubMed, in which a specific disease was identified and galectins were mentioned in association with the disease (in the order of that number). Some diseases could be combined under more general names, however, we prefer to be more specific at the expense of extending the list:

1.	Thyroid carcinoma	63
2.	Colorectal/gastric cancer/adenoma	54
3.	Heart failure/myocardial dysfunction/injury	42
4.	Breast cancer	37
5.	Papillary thyroid carcinoma	31
6.	Pancreatic cancer/adenocarcinoma	25
7.	Melanoma	22
8.	Rheumatoid arthritis/osteoarthritis	21
9.	Oral/laryngeal squamous cell carcinoma	20
10.	Prostate cancer/adenocarcinoma	16
11.	Diabetes	13
12.	Glioma-associated cancer/glioblastoma	12
13.	Preeclampsia	11
14.	Follicular thyroid adenomas/carcinomas	10
15.	Ovarian cancer	10
16.	Cancer, carcinoma (non-specified)	10
17.	Hepatocellular carcinoma	9
18.	Asthma/lung inflammation	9
19.	Pituitary tumors/adenocarcinoma/blastoma	9
20.	Spinal cord injury	9
21.	Bladder cancer	7
22.	Liver fibrosis	7
23.	Lung cancer/non-small cell lung cancer	7
24.	Renal carcinoma	7
25.	Myelogeneous leukemia	5
26.	Ischemia (non-specified)	5
27.	HIV-1	5
28.	Lymphoid malignancies/lymphomas	4
29.	Human cervical (epithelial) adenocarcinoma	4
30.	Multiple sclerosis	4
31.	Ophthalmology	4
32.	Nasopharyngeal carcinoma	4
33.	Renal fibrosis	4
34.	NASH	4
35.	Lung diseases/pneumonia	3
36.	Neuroblastoma	3
37.	Myeloma, multiple myeloma	3
38.	Lupus erythematosus	3
39.	Brain cancer	3
40.	Cholangiocarcinoma	3
41.	Hypoxic-ischemic brain injury	3
42.	Malignant mesothelioma	3
43.	Head and neck cancer	2
44.	Ulcer/ulcerative colitis	2

Downloaded by UNIV OF DELAWARE MORRIS LIB on June 14, 2012 | http://pubs.acs.org
Publication Date (Web): June 12, 2012 | doi: 10.1021/bk-2012-1102.ch002

Downloaded by UNIV OF DELAWARE MORRIS LIB on June 14, 2012 | http://pubs.acs.org
Publication Date (Web): June 12, 2012 | doi: 10.1021/bk-2012-1102.ch002

45. T-cell leukemia/lymphoma	2
46. Venous thrombosis	2
47. Cancer vaccines	2
48. Malaria	2
49. Chondrosarcoma	2
50. Trypanosomiasis	2
51. Gynecological cancer	2
52. Lymphocytic leukemia	2
53. Nasal polyposis	2
54. Cartilage tumor	2
55. Lymphoblastic leukemias	2
56. Adenoid cystic carcinoma	2
57. Servical squamous cell carcinoma	2
58. Celiac disease	2
59. Amyotrophic lateral sclerosis	2
60. Hodgkin lymphoma	2
61. Chronic lymphocytic leukemia	2
62. Malignant pheochromocytoma	2
63. Cystic fibrosis	2
64. Parathyroid carcinoma	2
65. Glaucoma	2
66. Tongue carcinoma	2
67. Invasive globular carcinoma	2
68. Cardiomyopathy	2
69. Renal ischemia	2
70. Carcinomas of the endometrium	2
71. Liver ischemia	2
72. Diabetic nephropathy	2
73. Cutaneous melanoma	2
74. Forebrain ischemia	2

The following diseases for which connections with galectins were found (at least one publication), are as follows:

75. Nasal papilloma
76. Intestinal inflammation
77. Proliferative vitreoretinopathy
78. Hepatitis C
79. Invasive trophoblasts
80. Liver cancer
81. Kaposi’s sarcoma
82. Invasive pathogens
83. Pilocytic astrocytomas
84. Peripheral nerve injury
85. Psoriasis/skin inflammation

Downloaded by UNIV OF DELAWARE MORRIS LIB on June 14, 2012 | http://pubs.acs.org
Publication Date (Web): June 12, 2012 | doi: 10.1021/bk-2012-1102.ch002

86. Atopic dermatitis
87. Encephalomyelitis
88. Cystic tumors of the pancreas
89. Nephritis
90. Renal injury
91. Venereal diseases
92. Intestinal fibrosis
93. Digestive diseases
94. Parkinson's disease
95. Malignant endothelia
96. Corticotroph adenomas
97. Pneumococcal meningitis
98. Esophageal cancer
99. Connective tissue disease
100. Histocytic sarcoma
101. Eosinophilic pneumonia
102. Cell carcinoma
103. Leiomyosarcoma
104. Endometrioid adenocarcinoma
105. Large cell lymphoma
106. Testicular cancer
107. Thyroiditis
108. Ductal adenocarcinoma
109. Myeloid leukemia
110. Leukemia (non-specified)
111. Ischemic stroke
112. Salivary gland tumor
113. Ulcerative colitis
114. Crohn's disease
115. Acute kidney injury
116. Liver cirrhosis
117. Encephalitis
118. Cardiac toxicity (non-specified)
119. Behcet's disease
120. GVH disease
121. Serous carcinomas
122. Cerebral ischemia
123. Choriocarcinoma
124. Fibrosis (non-specified)
125. Insulin allergy
126. Spindle cell oncocytoma

References

1. Barondes, S. H.; Castronovo, V.; Cooper, D. N. W.; Cummings, R. D.; Drickamer, K.; Feizi, T.; Gitt, M. A.; Hirabayashi, J.; Hughes, C.; Ken-ichi, K.; Leffler, H.; Liu, F. T.; Lotan, R.; Mercurio, A. M.; Monsigny, M.; Pillai, S.; Poirer, F.; Raz, A.; Rigby, P. W. J.; Rini, J. M.;

Downloaded by UNIV OF DELAWARE MORRIS LIB on June 14, 2012 | http://pubs.acs.org
Publication Date (Web): June 12, 2012 | doi: 10.1021/bk-2012-1102.ch002

Wang, J. L. Galectins: A Family of Animal a-Galactoside-Binding Lectins. *Cell* **1994**, *76*, 597–98.

2. Dam, T. K.; Brewer, C. F. Lectins as pattern recognition molecules: the effects of epitope density in innate immunity. *Glycobiology* **2010**, *20*, 270–279.
3. *Galectins*; Klyosov, A. A., Witzhak, Z. A., Platt, D., Eds.; John Wiley & Sons: 2008.
4. Camby, I.; Le Mercier, M.; Lefranc, F.; Kiss, R. Galectin-1: a small protein with major functions. *Glycobiology* **2006**, *16*, 137R–157R.
5. Lefranc, F.; Le Mercier, M.; Mathieu, V.; Kiss, R. Galectin-1, cancer cell migration, angiogenesis, and chemoresistance. In *Galectins*; Klyosov, A. A., Witzhak, Z. A., Platt, D., Eds.; John Wiley & Sons: Hoboken, NJ, 2008 pp 157−191.
6. Markowska, A. I.; Liu, F. T.; Panjwani, N. Galectin-3 is an important mediator of VEGF- and bFGF-mediated angiogenic response. *J. Exp. Med.* **2010** (e-publication).
7. Markowska, A. I.; Jefferies, K. C.; Panjwani, N. Galectin-3 protein modulates cell surface expression and activation of vascular endothelial growth factor receptor 2 in human endothelial cells. *J. Biol. Chem.* **2011**, *286* (34), 29913–29921.
8. Newlaczyl, A. U.; Yu, L. G. Galectin-3 – A jack-of-all-trades in cancer. *Cancer Lett.* **2011** (Epub ahead of print).
9. Barrow, H.; Guo, X.; Wandall, H. H.; Pedersen, J. W.; Fu, B.; Zhao, Q.; Chen, C.; Rhodes, J. M.; Yu, L. G. Serum galectins -2, -4 and -8 are greatly increased in colon and breast cancer patients and promote cancer cell adhesion to blood vascular endothelium. *Clin. Cancer Res.* **2011** (Epub ahead of print).
10. Barrow, H.; Rhodes, J. M.; Yu, L. G. The role of galectins in colorectal cancer progression. *Int. J. Cancer* **2011b**, *129*, 1–8.
11. Delgado, V. M.; Nugnes, L. G.; Colombo, L. L.; Troncoso, M. F.; Fernandez, M. M.; Malchiodi, E. L.; Frahm, I.; Croci, D. O.; Compagno, D.; Rabinovich, G. A.; Wolfenstein-Todel, C.; Elola, M. T. *FASEB J.* **2011**, *25*, 242–254.
12. Thijssen, V. L.; Barkan, B.; Shoji, H.; Aries, I. M.; Mathieu, V.; Deltour, L.; Hackeng, T. M.; Kiss, R.; Kloog, Y.; Poirier, F.; Griffioen, A. W. Tumor cells secrete galectin-1 to enhance endothelial cell activity. *Cancer Res.* **2010**, *70*, 6216–6224.
13. Ito, K.; Scott, S. A.; Cutler, S.; Dong, L. F.; Neuzil, J.; Blanchard, H.; Ralph, S. J. Thiodigalactoside inhibits murine cancer by concurrently blocking effects of galectin-1 on immune dysregulation, angiogenesis and protection against oxidative stress. *Angiogenesis* **2011**, *14*, 293–307.
14. Dings, R. P. M.; Vang, K. B.; Castermans, K.; Popescu, F. E.; Zhang, Y.; Noesser, E.; oude Egbrink, M. G. A.; Mescher, M. F.; Farrar, M. A.; Griffioen, A. W.; Mayo, K. H. *Enhancement Clin. Cancer Res.* **2011**, *17*, 3134–3145.

15. Klyosov, A. A. Galectins and their functions in plain language. In *Galectins*; Klyosov, A. A., Witzhak, Z. A., Platt, D., Eds.; John Wiley & Sons: Hoboken, NJ, 2008; pp 9–31.
16. Liu, F.-T.; Hsu, D. K.; Yang, R.-Y.; Chen, H.-Y.; Saesuga, J. Galectins in regulation of inflammation and immunity. In *Galectins*; Klyosov, A. A., Witzhak, Z. A., Platt, D., Eds.; John Wiley & Sons: Hoboken, NJ, 2008; pp 97−113.
17. Byrnes, K. R.; Washington, P. M.; Knoblach, S. M.; Hoffman, E.; Faden, A. I. Delayed inflammatory mRNA and protein expression after spinal cord injury. *J. Neuroinflammation* **2011**, *8*, 130.
18. Iacobini, C.; Menini, S.; Ricci, C.; Fantauzzi, C. B.; Scipioni, A.; Salvi, L.; Gordone, S.; Delucchi, F.; Serino, M.; Federici, M.; Pricci, F.; Pugliese, G. Galectin-3 ablation protects mice from diet-induced NASH: a major scavenging role for galectin-3 in liver. *J. Hepatol.* **2011**, *54*, 975–983.
19. de Boer, R. A.; Yu, L.; van Veldhuisen, D. J. Galectin-3 in cardiac remodeling and heart failure. *Curr. Heart Failure Rep.* **2010**, *7*, 1–8.
20. Vankrunkelsven, A.; De Ceulaer, K.; Hsu, D.; Liu, F. T.; De Baetselier, P.; Stijlemans, B. Lack of galectin-3 alleviates trypanosomiasis-associated anemia of inflammation. *Immunobiology* **2010**, *215*, 833–841.
21. Hu, C. Y.; Chang, S. K.; Wu, C. S.; Tsai, W. I.; Hsu, P. N. Galectin-3 gene (LGALS3) +292C allele is a genetic predisposition factor for rheumatoid arthritis in Taiwan. *Clin. Rheumatol.* **2011**, *30*, 1227–1233.
22. Forsman, H.; Islander, U.; Andreasson, E.; Andersson, A.; Onnheim, K.; Karlstrom, A.; Savman, K.; Magnusson, M.; Brown, K. L.; Karlsson, A. Galectin 3 aggravates joint inflammation and destruction in antigen-induced arthritis. *Arthritis Rheum.* **2011**, *63*, 445–454.
23. Henderson, N. C.; Sethi, T. The regulation of inflammation by galectin-3. *Immunol. Rev.* **2009**, *230*, 160–171.
24. Norling, L. V.; Perretti, M.; Cooper, D. Endogenous galectins and the control of the host inflammatory response. *J. Endocrinol.* **2009**, *201*, 169–184.
25. Cummings, R. D.; Liu, F. T. In *Essentials of Glycobiology*, 2nd ed.; Varki, A., Cummings, R. D., Esko, J. D., Freeze, H. H., Stanley, P., Bertozzi, C. R., Hart, G. W., Etzler, M. E., Eds.; Cold Spring Harbor Laboratory Press: Cold Spring Harbor, NY, 2009; Chapter 33.
26. Ortner, D.; Grabher, D.; Hermann, M.; Kremmer, E.; Hofer, S.; Heufler, C. The adaptor protein Bam32 in Human dendritic cells participates in the regulation of MHC Class I-induced CD8+ T cell activation. *J. Immunol.* **2011**, *187*, 3972–3978.
27. Cooper, D.; Llarregui, J. M.; Pesoa, S. A. Q.; Croci, D. O.; Perretti, M.; Rabinovich, G. A. Multiple functional targets of the immunoregulatory activity of galectin-1: control of immune cell trafficking , dendritic cell physiology, and T-cell fate. *Methods Enzymol.* **2010**, *480*, 199–244.
28. Kojima, K.; Arikawa, T.; Saita, N.; Goto, E.; Tsumura, S.; Tanaka R.; Masunaga, A.; Niki, T.; Oomizu, S.; Hirashima, M.; Kohrogi, H. Galectin-9 attenuates acute lung injury by expanding CD14- plasmacytoid dendritic cell-like macrophages. *Am. J. Respir. Crit. Care Med.* **2011** (Epub ahead of print).

Downloaded by UNIV OF DELAWARE MORRIS LIB on June 14, 2012 | http://pubs.acs.org
Publication Date (Web): June 12, 2012 | doi: 10.1021/bk-2012-1102.ch002

29. Li, Y.; Feng, J.; Geng, S.; Wei, H.; Chen, G.; Li, X.; Wang, L.; Wand, R.; Peng, H.; Han, G.; Shen, B.; Li, Y. The N- and C-terminal carbohydrate recognition domains of galectin-9 contribute differently to its multiple functions in innate immunity and adaptive immunity. *Mol. Immunol.* **2011**, *48*, 670–677.
30. Lefranc, F.; Sadeghi, N.; Camby, I.; Metens, T.; Dewitte, O.; Kiss, R. Present and potential future issues in glionlastoma treatment. *Expert Rev. Anticancer Ther.* **2006**, *6*, 719–732.
31. Lefranc, F.; Marhieu, V.; Kiss, R. Galectin-1 mediated biochemical controls of melanoma and glioma aggressive behavior. *World J. Biol. Chem.* **2011**, *2*, 193–201.
32. Verschuere, T.; De Vleeschouwer, S.; Lefranc, F.; Kiss, R.; Van Gool, S. W. Galectin-1 and immunotherapy for brain cancer. *Expert Rev. Neurother.* **2011**, *11*, 533–543.
33. Levy, R; Grafi-Cohen, M; Kraiem, Z.; Kloog, Y. Galectin-3 promotes chronic activation of K-Ras and differentiation block in malignant thyroid carcinomas. *Mol. Cancer Ther.* **2010**, *9*, 2208–2219.
34. Zhu, X.; Sun, T.; Lu, H.; Zhou, X.; Lu, Y.; Cai, X.; Zhu, X. Diagnostic significance of CK19, RET, galectin-3 and HBME-1 expression for papillary thyroid carcinoma. *J. Clin. Pathol.* **2010** (e-publication ahead of print).
35. Povegliano, Z. L.; Oshima, C. T.; de Oliveira Lima, F.; Andrade Scherholz, P. L.; Manoukian, F. N. Immunoexpression of Galectin-3 in Colorectal Cancer and its Relationship with Survival. *J. Gastrointest. Cancer* **2010** (e-publication ahead of print).
36. Chen, G.; Zou, Q.; Yang, Z. Expression of galectin-3 and Sambucus nigra agglutinin and its clinicopathological significance in benign and malignant lesions of breast. *Zhong Nan Da Xue Xue Bao Yi Xue Ban* **2010**, *35*, 584–589 (in Chinese).
37. Canesin, G.; Gonzalez-Peramato, P.; Palou, J.; Urrutia, M.; Cordón-Cardo, C.; Sánchez-Carbayo, M. Galectin-3 expression is associated with bladder cancer progression and clinical outcome. *Tumour Biol.* **2010**, *31*, 277–285.
38. Chiu, C. G.; Strugnell, S. S.; Griffith, O. L.; Jones, S. J.; Gown, A. M.; Walker, B.; Nabi, I. R.; Wiseman, S. M. Diagnostic utility of galectin-3 in thyroid cancer. *Am. J. Pathol.* **2010**, *176*, 2067–2081.
39. Sethi, K.; Sarkar, S.; Das, S.; Mohanty, B.; Mandal, M. Biomarkers for the diagnosis of thyroid cancer. *J. Exp. Ther. Oncol.* **2010**, *8*, 341–352.
40. Ahmed, H. Promoter Methylation in Prostate Cancer and its Application for the Early Detection of Prostate Cancer Using Serum and Urine Samples. *Biomark. Cancer* **2010**, *2*, 17–33.
41. Kim, M. K.; Sung, C. O.; Do, I. G.; Jeon, H. K.; Song, T. J.; Park, H. S.; Lee, Y. Y.; Kim, B. G.; Lee, J. W.; Bae, D. S. Overexpression of Galectin-3 and its clinical significance in ovarian carcinoma. *Int. J. Clin. Oncol.* **2011**, *16*, 352–358.
42. Buljan, M.; Situm, M.; Tomas, D.; Milošević, M.; Krušlin, B. Prognostic value of galectin-3 in primary cutaneous melanoma. *J. Eur. Acad. Dermatol. Venereol.* **2011**, *25*, 1174–1181.

Downloaded by UNIV OF DELAWARE MORRIS LIB on June 14, 2012 | http://pubs.acs.org
Publication Date (Web): June 12, 2012 | doi: 10.1021/bk-2012-1102.ch002

43. Kramer, M. W.; Waalkes, S.; Serth, J.; Hennenlotter, J.; Tezval, H.; Stenzl, A.; Kuczyk, M. A.; Merseburger, A. S. Decreased galectin-8 is a strong marker for recurrence in urothelial carcinoma of the bladder. *Urol. Int.* **2011**, *87*, 143–150 (Epub 2011 Jul 14).
44. Watanabe, M.; Takemasa, I.; Kaneko, N.; Yokoyama, Y.; Matsuo, E.; Iwasa, S.; Mori, M.; Matsuura, N.; Monden, M.; Nishimura, O. Clinical significance of circulating galectins as colorectal cancer markers. *Oncol Rep.* **2011**, *25*, 1217–1226.
45. Mulder, W. J. M.; van der Schaft, D. W. J.; Hautvast, P. A. I.; Strijkers, G. J.; Koning, G. A.; Storm, G.; Mayo, K. H.; Griffioen, A. W.; Nicolay, K. Early *in vivo* assessment of angiostatic therapy efficacy by molecular MRI. *FASEB J.* **2007**, *21*, 378–383.
46. Kluza, E.; van der Schaft, D. W. J.; Hautvast, P. A. I.; Mulder, W. J. M.; Mayo, K. H.; Griffioen, A. W.; Strijkers, G. J.; Nicolay, K. Synergistic targeting of a_Vb_3 integrin and galectin-1 with heteromultivalent paramagnetic liposomes for combined MR imaging and treatment of angiogenesis. *Nano Lett.* **2010**, *10*, 52–58.
47. Bohm, M.; Voors, A. A.; Ketelslegers, J. M.; Schirmer, S. H.; Turgonyl, E.; Bramlage, P.; Zannad, F. Biomarkers: optimizing treatment guidance in heart failure. *Clin. Res. Cardiol.* **2011** (Epub ahead of print).
48. Ueland, T.; Aukrust, P.; Broch, K.; Aakhus, S.; Skårdal, R.; Muntendam, P.; Gullestad, L. Galectin-3 in heart failure: high levels are associated with all-cause mortality. *Int. J. Cardiol.* **2011**, *150*, 361–364.
49. Yanavitski, M.; Givertz, M. M. Novel biomarkers in acute heart failure. *Curr. Heart Fail. Rep.* **2011**, *8*, 206–21.
50. Tang, W. H.; Shrestha, K.; Shao, Z.; Borowski, A. G.; Troughton, R. W.; Thomas, J. D.; Klein, A. L. Usefulness of plasma galectin-3 levels in systolic heart failure to predict renal insufficiency and survival. *Am. J. Cardiol.* **2011**, *108*, 385–90.
51. Lok, D. J.; Van Der Meer, P.; de la Porte, P. W.; Lipsic, E.; Van Wijngaarden, J.; Hillege, H. L.; van Veldhuisen, D. J. Prognostic value of galectin-3, a novel marker of fibrosis, in patients with chronic heart failure: data from the DEAL-HF study. *Clin. Res. Cardiol.* **2010**, *99*, 323–328.
52. van Kimmenade, R. R.; Januzzi, J. L., Jr.; Ellinor, P. T.; Sharma, U. C.; Bakker, J. A.; Low, A. F.; Martinez, A.; Crijns, H. J.; MacRae, C. A.; Menheere, P. P.; Pinto, Y. M. Utility of amino-terminal pro-brain natriuretic peptide, galectin-3, and apelin for the evaluation of patients with acute heart failure. *J. Am. Coll. Cardiol.* **2006**, *48*, 1217–1224.
53. de Boer, R. A.; Lok, D. J.; Jaarsma, T.; van der Meer, P.; Voors, A. A.; Hillege, H. L.; van Veldhuisen, D. J. Predictive value of plasma galectin-3 levels in heart failure with reduced and preserved ejection fraction. *Ann. Med.* **2011**, *43*, 60–68.
54. Milting, H.; Ellinghaus, P.; Seewald, M.; Cakar, H.; Bohms, B.; Kassner, A.; Körfer, R.; Klein, M.; Krahn, T.; Kruska, L.; El Banayosy, A.; Kramer, F. Plasma biomarkers of myocardial fibrosis and remodeling in terminal heart failure patients supported by mechanical circulatory support devices. *J. Heart Lung Transplant* **2008**, *27*, 589–596.

Downloaded by UNIV OF DELAWARE MORRIS LIB on June 14, 2012 | http://pubs.acs.org
Publication Date (Web): June 12, 2012 | doi: 10.1021/bk-2012-1102.ch002

55. Shah, R. V.; Chen-Tournoux, A. A.; Picard, M. H.; van Kimmenade, R. R.; Januzzi, J. L. Galectin-3, cardiac structure and function, and long-term mortality in patients with acutely decompensated heart failure. *Eur. J. Heart Failure* **2010**, *12*, 826–832.
56. Wanninger, J.; Weigert, J.; Wiest, R.; Bauer, S.; Karrasch, T.; Farkas, S.; Scherer, M. N.; Walter, R.; Weiss, T. S.; Hellerbrand, C.; Neumeier, M.; Schäffler, A.; Buechler, C. Systemic and hepatic vein galectin-3 are increased in patients with alcoholic liver cirrhosis and negatively correlate with liver function. *Cytokine* **2011**, *55*, 435–40.
57. Yilmaz, Y.; Eren, F.; Kurt, R.; Yonal, O.; Polat, Z.; Senates, E.; Bacha, M.; Imeryuz, N. Serum galectin-3 levels in patients with nonalcoholic fatty liver disease. *Clin. Biochem.* **2011**, *44*, 955–958.
58. Ozden, M. G.; Caycı, Y. T.; Tekin, H.; Coban, A. Y.; Aydın, F.; Sentürk, N.; Bek, Y.; Cantürk, T.; Turanlı, A. Y. Serum galectin-3 levels in patients with Behçet's disease: association with disease activity over a long-term follow-up. *J. Eur. Acad. Dermatol. Venereol.* **2011**, *25*, 1168–1173.
59. Stancic, M.; van Horssen, J.; Thijssen, V. L.; Gabius, H. J.; van der Valk, P.; Hoekstra, D.; Baron, W. Increased expression of distinct galectins in multiple sclerosis lesions. *Neuropathol. Appl. Neurobiol.* **2011**, *37*, 654–671.
60. St-Pierre, C.; Ouellet, M.; Tremblay, M. J.; Sato, S. Galectin-1 and HIV-1 Infection. *Methods Enzymol.* **2010**, *480*, 267–294.
61. St-Pierre, C.; Ouellet, M.; Giguère, D.; Ohtake, R.; Roy, R.; Sato, S.; Tremblay, M. J. Galectin-1 specific inhibitors as a new class of compounds to treat HIV-1 infection. *Antimicrob. Agents Chemother*. **2011** (Epub ahead of print, PMID:22064534).
62. St-Pierre, C.; Manya, H.; Ouellet, M.; Clark, G. F.; Endo, T.; Tremblay, M. J.; Sato, S. Host-Soluble Galectin-1 Promotes HIV-1 Replication through a Direct Interaction with Glycans of Viral gp120 and Host CD4. *J. Virol.* **2011**, *85*, 11742–11751.
63. Murakami, T.; Yoshioka, K.; Sato, Y.; Tanaka, M.; Niwa, O.; Yabuki, S. Synthesis and galectin-binding activities of mercaptododecyl glycosides containing a terminal β-galactosyl group. *Bioorg. Med. Chem. Lett.* **2011**, *21*, 1265–1269.
64. Dings, R. P. M.; Chen, X.; Hellebrekers, D. M. E. I.; van Eijk, L. I.; Hoye, T. R.; Griffioen, A. W.; Mayo, K. H. Design of non-peptidic topomimetics of anti-angiogenic proteins with anti-tumor activities. *J. Natl. Can. Inst.* **2006**, *98*, 932–936.
65. Oberg, C. T.; Leffler, H.; Nilsson, U. J. Inhibition of galectins with small molecules. *Chimia* **2011**, *65*, 18–23.
66. Lin, C.-L.; Whang, E. E.; Donner, D. B.; Jiang, X.; Price, B. D.; Carothers, A. M.; Delaine, T.; Leffler, H.; Nilsson, U. J.; Nose, V.; Moore, F. D.; Ruan, D. T. Activates Apoptosis and Enhances Both Chemosensitivity Galectin-3 Targeted Therapy with a Small Molecule Inhibitor. *Mol. Cancer Res.* **2009**, *7*, 1655–1662.
67. Griffioen, A. W.; van der Schaft, D.; Barandsz-Janson, A.; Cox, A.; Struijker-Boudier, H. A.; Hillen, H. F. P.; Mayo, K. H. Anginex, a designed Peptide that Inhibits angiogenesis. *Biochem. J.* **2001**, *354*, 233–242.

Downloaded by UNIV OF DELAWARE MORRIS LIB on June 14, 2012 | http://pubs.acs.org
Publication Date (Web): June 12, 2012 | doi: 10.1021/bk-2012-1102.ch002

Downloaded by UNIV OF DELAWARE MORRIS LIB on June 14, 2012 | http://pubs.acs.org
Publication Date (Web): June 12, 2012 | doi: 10.1021/bk-2012-1102.ch002

68. Dings, R. P. M.; Mayo, K. H. A journey in structure-based discovery: from designed peptides to protein-surface topomimetics as antibiotic and antiangiogenic agents. *Acc. Chem. Res.* **2007**, *40*, 1057–1065.
69. Dings, R. P. M.; Hargittai, B.; Haseman, J.; Griffioen, A. W.; Mayo, K. H. Anti-tumor activity of the novel angiogenesis inhibitor anginex. *Cancer Lett.* **2003**, *194*, 55–66.
70. Thijssen, V. L. J. L.; Postel, R.; Brandwijk, R. J. M. G. E.; Dings, R. P. M.; Nesmelova, I.; Satijn, S.; Verhofstad; Nakabeppu, Y.; Baum, L. G.; Bakkers, J.; Mayo, K. H.; Poirier, F.; Griffioen, A. W. Galectin-1 is essential in tumor angiogenesis and is a target for anti-angiogenesis therapy. *Proc. Natl. Acad. Sci. U.S.A.* **2006**, *103*, 15975–15980.
71. Mayo, K. H.; Dings, R. P. M.; Flader, C.; Nesmelova, I.; Hargittai, B.; van der Schaft; van Eijk, L. I.; Walek, D.; Haseman, J.; Hoye, T. R.; Griffioen, A. W. Design of a Partial-Peptide Mimetic of Anginex with Antiangiogenic and Anticancer Activity. *J. Biol. Chem.* **2003**, *278*, 45746–45752.
72. Dings, R. P. M.; Miller, M. C.; Raymond, E.; Nesmelova, I.; Astorgues-Xerri, L.; Kumar, N.; Serova, M.; Mayo, K. H. Anti-tumor agent calixarene 0118 targets human galectin-1 as an allosteric inhibitor of carbohydrate binding. *J. Med. Chem.* **2012**, in press.
73. Platt, D.; Raz, A. Modulation of the lung colonization of B16-F1 melanoma cells by citrus pectin. *J. Natl. Cancer Inst.* **1992**, *84*, 438–442.
74. Inohara, H.; Raz, A. Effects of natural complex carbohydrate (citrus pectin) on murine melanoma cell properties related to galectin-3 functions. *Glycoconjugate J.* **1994**, *11*, 527–532.
75. Chauhan, D.; Li, G.; Podar, K.; Hideshima, T.; Neri, P.; He, D.; Mitsiades, N.; Richardson, P.; Chang, Y.; Schindler, J.; Carver, B.; Anderson, K. C. A novel carbohydrate-based therapeutic GCS-100 overcomes bortezomib resistance and enhances dexamethasone-induced apoptosis in multiple myeloma cells. *Cancer Res.* **2005**, *65*, 8350–8358.
76. Nangia-Makker, P.; Hogan, V.; Honjo, Y.; Baccarini, S.; Tait, L.; Bresalier, R.; Raz, A. Inhibition of human cancer cell growth and metastasis in nude mice by oral intake of modified citrus pectin. *J. Natl. Cancer Inst.* **2002**, *94*, 1854–1862.
77. Jackson, C. L.; Dreaden, T. M.; Theobald, L. K.; Tran, N. M.; Beal, T. L.; Eid, M.; Gao, M. Y.; Shirley, R. B.; Stoffel, M. T.; Kimar, M. V.; Mohnen, D. M. Pectin induces apoptosis in human prostate cancer cells: correlation of apoptotic function with pectin structure. *Glycobiology* **2007**, *17*, 805–819.
78. Gunning, A. P.; Bongaerts, R. J.; Morris, V. J. Recognition of galactan components of pectin by galectin-3. *FASEB J.* **2009**, *23*, 415–424.
79. Vayssade, M.; Sengkhamparn, N.; Verhoef, R.; Delaigue, C.; Goundiam, O.; Vigneron, P.; Voragen, A. G.; Schols, H. A.; Nagel, M. D. Antiproliferative and proapoptotic actions of okra pectin on B16F10 melanoma cells. *Phytother. Res.* **2010**, *24*, 982–989.
80. Bergman, M.; Djaldetti, M.; Salman, H.; Bessler, H. Effect of citrus pectin on malignant cell proliferation. *Biomed. Pharmacother.* **2010**, *64*, 44–47.
81. Kolatsi-Joannou, M.; Price, K. L.; Winyard, P. J.; Long, D. A. Modified citrus pectin reduces galectin-3 expression and disease severity

in experimental acute kidney injury. *PLoS One* **2011**, *6*, e18683; doi:10.1371/journal.pone.0018683.

82. Demotte, N.; Wieërs, G.; Van Der Smissen, P.; Moser, M.; Schmidt, C.; Thielemans, K.; Squifflet, J. L.; Weynand, B.; Carrasco, J.; Lurquin, C.; Courtoy, P. J.; van der Bruggen, P. A galectin-3 ligand corrects the impaired function of human CD4 and CD8 tumor-infiltrating lymphocytes and favors tumor rejection in mice. *Cancer Res.* **2010**, *70*, 7476–88.
83. Demotte, N.; Wieers, G.; Klyosov, A.; van der Bruggen, P. Is it possible to correct the impaired function of human tumor-infiltrating lymphocytes? Presented at Keystone Symposium on Molecular and Cellular Biology. New Frontiers at the Interface of Immunity and Glycobiology, March 6−11, 2011, Lake Louise, AB, Canada; Abstract 23F112011.
84. Glinsky, V. V.; Raz, A. Modified citrus pectin anti-metastatic properties: one bullet, multiple targets. *Carbohydr Res* **2009**, *344* (14), 1788–1791 (Epub 2008 Sep 26).
85. Klyosov, A. A.; Platt, D.; Zomer, E. Preclinical Studies of Anticancer Efficacy of 5-Fluorouracil when Co-Administered with the 1,4-beta-D-Galactomannan. *Preclinica* **2003**, *1*, 175–186.
86. Klyosov, A. A.; Zomer, E.; Platt, D. Davanat® and colon cancer: preclinical and clinical (Phase I) studies. In *Carbohydrate Drug Design*; ACS Symposium Series 932; Klyosov, A. A., Witczak, Z. J., Platt, D., Eds.; American Chemical Society: Washington, DC, 2006; pp 67−104.
87. Platt, D.; Klyosov, A. A.; Zomer, E. Development of a polysaccharide as a vehicle to improve the efficacy of chemotherapeutics. In *Carbohydrate Drug Design*; ACS Symposium Series 932; Klyosov, A. A., Witczak, Z. J., Platt, D., Eds.; American Chemical Society: Washington, DC, 2006; pp 49−66.
88. Miller, M.; Klyosov, A. A.; Platt, D.; Mayo, K. Using Pulse Field Gradient NMR Diffusion Measurements to Define Molecular Size Distributions in Glycan Preparations. *Carbohydr. Res.* **2009a**, *344*, 1205–1212.
89. Miller, M. C.; Klyosov, A. A.; Mayo, K. H. The α-galactomannan Davanat binds galectin-1 at a site different from the conventional galectin carbohydrate binding domain. *Glycobiology* **2009b**, *19*, 1034–1045.
90. Miller, M. C.; Nesmelova, I. V.; Platt, D.; Klyosov, A. A.; Mayo, K. H. The carbohydrate-binding domain on galectin-1 is more extensive for a complex glycan than for simple saccharides: implications for galectin-glycan interactions at the cell surface. *Biochem. J.* **2009c**, *421*, 211–221.
91. Ge, X. N.; Bahaie, N. S.; Kang, B. N.; Hosseinkhani, M. R.; Ha, S. G.; Frenzel, E. M.; Liu, F. T.; Rao, S. P.; Sriramarao, P. Allergen-induced airway remodeling is impaired in galectin-3-deficient mice. *J. Immunol.* **2010**, *185*, 1205–1214.
92. López, E.; Zafra, M. P.; Sastre, B.; Gámez, C.; Lahoz, C.; del Pozo, V. Gene expression profiling in lungs of chronic asthmatic mice treated with galectin-3: downregulation of inflammatory and regulatory genes. *Mediators Inflammation* **2011**, 823279 (Epub 2011 Mar 20, 2011).
93. Sziksz, E.; Kozma, G. T.; Pállinger, E.; Komlósi, Z. I.; Adori, C.; Kovács, L.; Szebeni, B.; Rusai, K.; Losonczy, G.; Szabó, A.; Vannay, A. Galectin-9 in

Downloaded by UNIV OF DELAWARE MORRIS LIB on June 14, 2012 | http://pubs.acs.org
Publication Date (Web): June 12, 2012 | doi: 10.1021/bk-2012-1102.ch002

allergic airway inflammation and hyper-responsiveness in mice. *Int. Arch. Allergy Immunol.* **2010**, *151*, 308–317.

94. Katoh, S.; Ishii, N.; Nobumoto, A.; Takeshita, K.; Dai, S. Y.; Shinonaga, R.; Niki, T.; Nishi, N.; Tominaga, A.; Yamauchi, A.; Hirashima, M. Galectin-9 inhibits CD44-hyaluronan interaction and suppresses a murine model of allergic asthma. *Am. J. Respir. Crit. Care Med.* **2007**, *176*, 27–35.
95. Zhang, Z. Y.; Luan, B.; Feng, X. X. To study the expression of Galectin-9 and Tim-3 in lungs of mice with asthma and the effect of rosiglitazone (PPAR-γ agonist) on their expression. *Zhongguo Dang Dai Er Ke Za Zhi* **2011**, *13*, 406–410 (in Chinese).
96. Wiersma, V. R.; de Bruyn, M.; Helfrich, W.; Bremer, E. Therapeutic potential of Galectin-9 in human disease. *Med. Res. Rev.* **2011**, doi: 10.1002/med.20249 (Epub ahead of print).
97. Devouassoux, G.; Pachot, A.; Laforest, L.; Diasparra, J.; Freymond, N.; Van Ganse, E.; Mougin, B.; Pacheco, Y. Galectin-10 mRNA is overexpressed in peripheral blood of aspirin-induced asthma. *Allergy* **2008**, *63*, 125–31.
98. Rogerio, A. P.; Cardoso, C. R.; Fontanari, C.; Souza, M. A.; Afonso-Cardoso, S. R.; Silva, E. V.; Koyama, N. S.; Basei, F. L.; Soares, E. G.; Calixto, J. B.; Stowell, S. R.; Dias-Baruffi, M.; Faccioli, L. H. Anti-asthmatic potential of a D-galactose-binding lectin from Synadenium carinatum latex. *Glycobiology* **2007**, *17*, 795–804.
99. Yin, G. Q.; Zhao, S. Y.; Guo, S. P.; Zhao, Y. H.; Liu, X. C.; Jiang, Z. F. Galectin-7 is associated with bronchial epithelial cell apoptosis in asthmatic children. *Zhonghua Er Ke Za Zhi* **2006**, *44*, 523–526 (in Chinese).
100. Cedeno-Laurent, F.; Barthel, S. R.; Opperman, M. J.; Lee, D. M.; Clark, R. A.; Dimitroff, C. J. Development of a nascent galectin-1 chimeric molecule for studying the role of leukocyte galectin-1 ligands and immune disease modulation. *J. Immunol.* **2010**, *185*, 4659–4672.
101. Wang, C. R.; Shiau, A. L.; Chen, S. Y.; Cheng, Z. S.; Li, Y. T.; Lee, C. H.; Yo, Y. T.; Lo, C. W.; Lin, Y. S.; Juan, H. Y.; Chen, Y. L.; Wu, C. L. Intra-articular lentivirus-mediated delivery of galectin-3 shRNA and galectin-1 gene ameliorates collagen-induced arthritis. *Gene Ther.* **2010** (e-publication ahead of print).
102. Li, Y. J.; Kukita, A.; Teramachi, J.; Nagata, K.; Wu, Z.; Akamine, A.; Kukita, T. A possible suppressive role of galectin-3 in upregulated osteoclastogenesis accompanying adjuvant-induced arthritis in rats. *Lab. Invest.* **2009**, *89*, 26–37.
103. Lee, J.; Oh, J. M.; Hwang, J.; Ahn, J.; Bae, E. K.; Won, J.; Koh, E. M.; Cha, H. S. Expression of human TIM-3 and its correlation with disease activity in rheumatoid arthritis. *Scand. J. Rheumatol.* **2011a**, *40*, 334–440.
104. Lee, J.; Park, E. J.; Noh, J. W.; Hwang, J. W.; Bae, E. K.; Ahn, J. K.; Koh, E. M.; Cha, H. S. Underexpression of TIM-3 and Blunted Galectin-9-Induced Apoptosis of CD4+ T Cells in Rheumatoid Arthritis. *Inflammation* **2011b** (Epub ahead of print).
105. Seki, M.; Oomizu, S.; Sakata, K. M.; Sakata, A.; Arikawa, T.; Watanabe, K.; Ito, K.; Takeshita, K.; Niki, T.; Saita, N.; Nishi, N.; Yamauchi, A.; Katoh, S.; Matsukawa, A.; Kuchroo, V.; Hirashima, M. Galectin-9 suppresses the

Downloaded by UNIV OF DELAWARE MORRIS LIB on June 14, 2012 | http://pubs.acs.org
Publication Date (Web): June 12, 2012 | doi: 10.1021/bk-2012-1102.ch002

generation of Th17, promotes the induction of regulatory T cells, and regulates experimental autoimmune arthritis. *Clin. Immunol.* **2008**, *127*, 78–88.

106. Eshkar, S. L.; Ronen, D.; Levartovsky, D.; Elkayam, O.; Caspi, D.; Aamar, S.; Amital, H.; Rubinow, A.; Golan, I.; Naor, D.; Zick, Y.; Golan, I. The involvement of CD44 and its novel ligand galectin-8 in apoptotic regulation of autoimmune inflammation. *J. Immunol.* **2007**, *179*, 1225–1235.
107. Kim, C. W.; Cho, E. H.; Lee, Y. J.; Kim, Y. H.; Hah, Y. S.; Kim, D. R. Disease-specific proteins from rheumatoid arthritis patients. *J. Korean Med. Sci.* **2006**, *21*, 478–84.
108. Neidhart, M.; Zaucke, F.; von Knoch, R.; Jüngel, A.; Michel, B. A.; Gay, R. E.; Gay, S. Galectin-3 is induced in rheumatoid arthritis synovial fibroblasts after adhesion to cartilage oligomeric matrix protein. *Ann. Rheum. Dis.* **2005**, *64*, 419–424.
109. Ohshima, S.; Kuchen, S.; Seemayer, C. A.; Kyburz, D.; Hirt, A.; Klinzing, S.; Michel, B. A.; Gay, R. E.; Liu, F. T.; Gay, S.; Neidhart, M. Galectin 3 and its binding protein in rheumatoid arthritis. *Arthritis Rheum.* **2003**, *48*, 2788–2795.
110. Strik, H. M.; Kolodziej, M.; Oertel, W.; Bäsecke, J. Glycobiology in Malignant Gliomas: Expression and Functions of Galectins and Possible Therapeutic Options. *Curr Pharm Biotechnol.* **2011**, PMID:21605067 (Epub ahead of print).
111. Strik, H. M.; Schmidt, K.; Lingor, P.; Tönges, L.; Kugler, W.; Nitsche, M.; Rabinovich, G. A.; Bähr, M. Galectin-1 expression in human glioma cells: modulation by ionizing radiation and effects on tumor cell proliferation and migration. *Oncol. Rep.* **2007**, *18*, 483–488.
112. Bruyère, C.; Madonna, S.; Van Goietsenoven, G.; Mathieu, V.; Dessolin, J.; Kraus, J. L.; Lefranc, F.; Kiss, R. JLK1486, a bis 8-hydroxyquinoline-substituted benzylamine, displays cytostatic effects in experimental gliomas through MyT1 and STAT1 activation and, to a lesser extent, PPARγ activation. *Transl. Oncol.* **2011a**, *4* (3), 126–37.
113. Bruyère, C.; Abeloos, L.; Lamoral-Theys, D.; Senetta, R.; Mathieu, V.; Le Mercier, M.; Kast, R. E.; Cassoni, P.; Vandenbussche, G.; Kiss, R.; Lefranc, F. Temozolomide modifies caveolin-1 expression in experimental malignant gliomas *in vitro* and *in vivo*. *Transl. Oncol.* **2011b**, *4*, 92–100.
114. Bruyère, C.; Mijatovic, T.; Lonez, C.; Spiegl-Kreinecker, S.; Berger, W.; Kast, R. E.; Ruysschaert, J. M.; Kiss, R.; Lefranc, F. Temozolomide-induced modification of the CXC chemokine network in experimental gliomas. *Int. J. Oncol.* **2011c**, *38*, 1453–64.
115. Suñol, M.; Cusi, V.; Cruz, O.; Kiss, R.; Lefranc, F. Immunohistochemical analyses of alpha1 and alpha3 Na+/K+-ATPase subunit expression in medulloblastomas. *Anticancer Res.* **2011**, *31*, 953–958.
116. Le Calvé, B.; Rynkowski, M.; Le Mercier, M.; Bruyère, C.; Lonez, C.; Gras, T.; Haibe-Kains, B.; Bontempi, G.; Decaestecker, C.; Ruysschaert, J. M.; Kiss, R.; Lefranc, F. Long-term in vitro treatment of human glioblastoma cells with temozolomide increases resistance in vivo through up-regulation

Downloaded by UNIV OF DELAWARE MORRIS LIB on June 14, 2012 | http://pubs.acs.org
Publication Date (Web): June 12, 2012 | doi: 10.1021/bk-2012-1102.ch002

of GLUT transporter and aldo-keto reductase enzyme AKR1C expression. *Neoplasia* **2011**, *12*, 727–739. *Neoplasia* **2011**, *13* (9), 886 (Erraturm; 5 p following).

117. Chagan-Yasutan, H.; Shiratori, B.; Siddiqi, U. R.; Saitoh, H.; Ashino, Y.; Arikawa, T.; Hirashima, M.; Hattori, T. The increase of plasma galectin-9 in a patient with insulin allergy: a case report. *Clin. Mol. Allergy* **2010**, *11*, 8–12.
118. Zhou, J. Y.; Afjehi-Sadat, L.; Asress, S.; Duong, D. M.; Cudkowicz, M.; Glass, J. D.; Peng, J. Galectin-3 Is a candidate biomarker for amyotrophic lateral sclerosis: discovery by a proteomics approach. *J. Proteome Res.* **2010** (e-publication ahead of print).
119. Kohrenhagen, N.; Voelker, H. U.; Kapp, M.; Dietl, J.; Kämmerer, U. The expression of galectin-1 in vulvar neoplasia. *Anticancer Res.* **2010**, *30*, 1547–1552.

Downloaded by UNIV OF DELAWARE MORRIS LIB on June 14, 2012 | http://pubs.acs.org
Publication Date (Web): June 12, 2012 | doi: 10.1021/bk-2012-1102.ch002

Downloaded by CORNELL UNIV on June 13, 2012 | http://pubs.acs.org
Publication Date (Web): June 12, 2012 | doi: 10.1021/bk-2012-1102.ch003

Chapter 3

Development of a Galactomannan Polysaccharide as a Vehicle To Improve the Efficacy of Chemotherapeutics

Eliezer Zomer,[1] Anatole A. Klyosov,[1,*] and David Platt[2]

[1]Galectin Therapeutics, 7 Well Avenue, Newton, MA 02459
[2]Pro-Pharmaceuticals, 7 Well Avenue, Newton, MA 02459
[*]Klyosov@galectintherapeutics.com

The GMP process has been developed for manufacturing of GM-CT-01 (DAVANAT®), a modified galactomannan from *Cyamopsis tetragonoloba*, or guar gum. The material was structurally identified and characterized by standard analytical techniques, as well as by ^{13}C Nuclear Magnetic Resonance (^{13}C-NMR), Size Exclusion Chromatography with Multi Angle Laser Light Scattering (SEC-MALLS) for the molecular weight determination, and by Anion Exchange Liquid Chromatography with Pulsed Amperometric Detection (AELC-PAD) for carbohydrate composition and to establish the uniformity and purity of the final products. Both in the manufacturing of the bulk material and the final drug product, precautions were taken to control degradation by either thermal or microbial/enzymatic activity. As a parental i.v., the slow dissolving polymer was formulated as a sterile solution to make it easy to handling in a hospital. The shelf life of the polymer solution has been estimated to be at least nine years at room temperature. Pre-clinical studies with 5-fluorouracil, doxorubicin, irinotecan and cisplatin have shown no detectable toxicity along with a noticeable efficacy enhancement in both colon and breast cancer models in nude mice. Phase I and II clinical studies have been conducted, and the Drug Master File was submitted to the FDA in 2009.

In Glycobiology and Drug Design; Klyosov, A.;
ACS Symposium Series; American Chemical Society: Washington, DC, 2012.

Downloaded by CORNELL UNIV on June 13, 2012 | http://pubs.acs.org
Publication Date (Web): June 12, 2012 | doi: 10.1021/bk-2012-1102.ch003

Introduction

A background for galactose-containing compounds' anti-cancer activity has been established in a few studies showing that galactoside-containing carbohydrate and galactoside specific lectins disturbed cell association and may affect tumor development and metastasis (*1–12*).

In vitro studies have shown that galactoside-binding proteins on the tumor cell surface interact with terminal D-galactoside residues located on adjacent cells, thus mediating cellular attachment and the potential for metastasis (*1*, *2*). Many studies showed that tumor cells contain multiple lectins, specific to galactose residues, and located on the cell surface, in cytoplasm and in the cell nucleus. These lectins are called galectins, and 15 of them have been discovered and described, some of them in detail ((*13*) and references therein). It was also shown that tumor cells commonly express galectins as agents associated with their malignancy, which perform multiple functions related to angiogenesis, inflammation, immune response (ibid.).

We report here that a linear galactose-containing polymer – galactomannan – interacts with cancer drugs and positively affects their anti-tumor activity. Although structures like cyclodextrins have been shown to entrap a variety of hydrophobic drugs and improve their solubility and delivery, this was the first time that co-administration of polysaccharides along with chemotherapeutics has been proven effective in animal models, as well as in humans. It was shown in Phase I of the clinical trials, aimed at the evaluation of toxicity of the galactomannan, and in Phase II, aimed as evaluation of its efficacy along with a known chemotherapy drug, 5-fluorouracil (see, for example, (*14*, *15*) and references therein).

This galactomannan, the chemical structure of which is shown below, was named DAVANAT®, and the respective trade mark has been obtained. However, since then we have found that other galactomannans of a different structure can also serve as tight ligands for galectins, and can be considered as drug candidates. Therefore a new nomenclature has been developed, and DAVANAT® as such was renamed as GM-CT-01, where GM stands to galactomannan, CT designates the natural source (in this particular case it is *Cyamopsis tetragonoloba*), and 01 shows its number in the drug candidate pipeline. Therefore, in this overview we use the new nomenclature.

From the development state, raw material qualification and characterization and GMP processing of GM-CT-01 have been a high priority in obtaining consistently positive enhancement of 5-fluorouracil (5-FU) activity against human colon tumor models. As a parental i.v., the polysaccharide was formulated as a sterile solution to make it easy to handle in a hospital. The shelf life of GM-CT-01 solution has been confirmed to exceed many years at refrigerated conditions and at least nine years at room temperature. It is not important for the FDA since it does not require reporting of stability exceeding three years, it is important to know from the scientific viewpoint. In addition to 5-FU, pre-clinical studies with doxorubicin, irinotecan and cisplatin have shown reduction in toxicity, while significantly enhanced anti-cancer activity in human colon, breast and melanoma xenographic models in nude mice.

Polymeric carbohydrates have been long used in separation techniques to trap specific chemicals in a three-dimension matrix. As it was mentioned above, structures like cyclodextrins have been shown to entrap a variety of hydrophobic drugs and improve their solubility and delivery. We have employed a different approach, that is to study carbohydrate polymers for chemotherapeutics, targeting tumor-lectin binding moieties, galectins. A variety of galactomannans exist naturally, and a few were selected because of their high homogeneity and uniform structure. These molecules have been modified (while maintaining the linear structure of the mannose backbone with galactose residues at approximately every second mannose residue) to improve systemic solubility.

Multiple studies have shown (see Chapter 2 in this book) that galectins mediate various types of cellular interactions, modulate cell–cell and cell–matrix interactions. Galectins act as receptors that are involved in selective intercellular adhesion, cell migration, and recognition of circulating glycoproteins. Many experimental agents – including monoclonal antibodies, simple sugars, and some polysaccharides like pectin fragments – are known to interact *in vitro* with the lectins on the cancer cell surface. Some of these agents inhibit the development of tumor cell colony formation (*3*, *16–19*). The galactomannan with its exposed galactose residues has previously been shown to interact with hepatoma cell lectins and reversed by lactose, and thus potentially modulate their physiological actions. Initially it was believed that galectins are β-galactoside specific lectins (*1*), however, it was recently shown that galactomannans, which are α-galactose derivatives "mounted" on a polymeric β-D-mannopyranosyl backbone, tightly interact with some galectins, as shown by the NMR experiments (*20*).

It is believed that lectins mediate various types of cellular interactions, and some of them have been studied for the last 20 years. These studies have resulted in identification of more than a dozen lectins, some of them turned out to be tumor-associated galectins. A few glycoproteins that allegedly interact with these lectins have also been identified. Some of them reportedly result in inhibition of tumor cell colony development, as described above. Even simple carbohydrates such as methyl-α-D-lactoside and lacto-N-tetrose have been shown to slightly inhibit metastasis of B16 melanoma cells, while D-galactose and arabinogalactose inhibit liver metastasis of L-1 sarcoma cells (*21*).

Despite advances in chemotherapeutic regimens for metastatic colorectal cancer, as well as other solid tumors, patients refractory to these therapies represent a large unmet medical need. For example, 5-FU is used alone or in a combination with many other chemotherapeutic agents for treatment of solid tumors, particularly colorectal, breast, hepatic, and gastric cancers (*22*, *23*). These combinations, while marginally improving efficacy, may increase toxicity. It is reasonable to hypothesize, however, that more specific targeting of efficacious chemotherapeutic agents such as 5-FU to tumor cells could result in higher response rates along with reduced toxicity.

Compared to many other known polysaccharides, galactomannans have multiple single-sidechain galactose units. These units might readily interact with galactose-specific receptors such as galectins on the tumor cell surface, modulate the tumor surface physiology, and potentially affect delivery of 5-FU to the tumor.

Downloaded by CORNELL UNIV on June 13, 2012 | http://pubs.acs.org
Publication Date (Web): June 12, 2012 | doi: 10.1021/bk-2012-1102.ch003

Downloaded by CORNELL UNIV on June 13, 2012 | http://pubs.acs.org
Publication Date (Web): June 12, 2012 | doi: 10.1021/bk-2012-1102.ch003

This hypothesis has been proven in our studies, and results are described in this chapter and the next.

GM-CT-01 is a chemically modified galactomannan from the seeds of *Cyamopsis tetragonoloba*. The natural ("initial") galactomannan has too large a molecular weight to be water-soluble, but after a controlled molecular-weight reduction it acquires a good solubility in water, up to 100 mg/mL.

In animal models of colorectal cancer, GM-CT-01 enhances the antitumor activity of 5-FU. Galectin Therapeutics is developing GM-CT-01 for use in humans as a potential enhancer of the antitumor activity of 5-FU against solid tumors that include (but are not limited to) those of colorectal, breast, lung (non-small cell), gastric, pancreatic, hepatic, ovarian, prostate, and head and neck cancers. As far as we know, GM-CT-01 is the first polymeric carbohydrate-based drug candidate proven to be an effective ligand for galectin-1 (*20*), with an apparent binding constant of 60-70 nM, tested in a bioassay system (CD4+ and CD8+ tumor infiltrating lymphocytes, with interferon-γ secreted as a readout of the assay) (*24*).

With its exposed galactose residues, GM-CT-01 might readily interact with carbohydrate-binding proteins on the cell surface and thus block the physiological actions of these carbohydrate-binding proteins.

In clinical trials GM-CT-01 was evaluated in combination with 5-FU in patients with solid tumors who have filed proven surgical, radiation, and chemotherapeutic regimens. It is described in more detail in the next chapter.

Description and Structural Identification of GM-CT-01 (Davanat®)

Physical Description

GM-CT-01 is a white, water soluble (up to 100 mg/mL) polysaccharide obtained by partial and controlled chemical cleavage of the storage polysaccharide from seeds of *Cyamopsis tetragonoloba*, commercially available as guar gum flour. Its chemical formula can be expressed as [(1→4)-linked β-D-mannopyranosyl]$_{17}$-[(1→6)-linked-α-D-galactopyranose]$_{10}$}$_{12}$ with average molecular weight of 51,000 Dalton, and mannose to galactose ratio of 1.7. In other words, the polymer is a linear (1→4)-β-D-Mannopyranosyl backbone to which a single α-D-Galactopyranosyl residue is attached by (1→6) linkage randomly to every other mannopyranose (Figures 1 and 2) (Klyosov & Platt, US Patent No. 6,645,946).

Chemical names of the galactomannan are 1,4-β-D-Galactomannan, or [(1→6)-α-D-galacto-(1→4)-β-D-mannan].

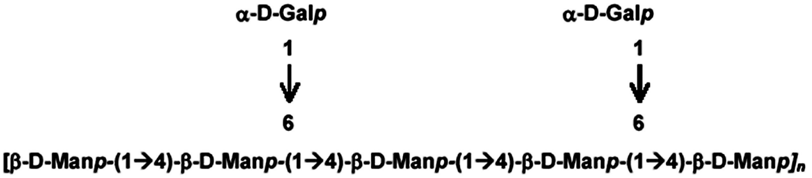

$$[\beta\text{-D-Man}p\text{-}(1\rightarrow4)\text{-}\overset{\substack{\alpha\text{-D-Gal}p\\1\\\downarrow\\6}}{\beta\text{-D-Man}p}\text{-}(1\rightarrow4)\text{-}\beta\text{-D-Man}p\text{-}(1\rightarrow4)\text{-}\overset{\substack{\alpha\text{-D-Gal}p\\1\\\downarrow\\6}}{\beta\text{-D-Man}p}\text{-}(1\rightarrow4)\text{-}\beta\text{-D-Man}p]_n$$

Figure 1. The building block of GM-CT-01

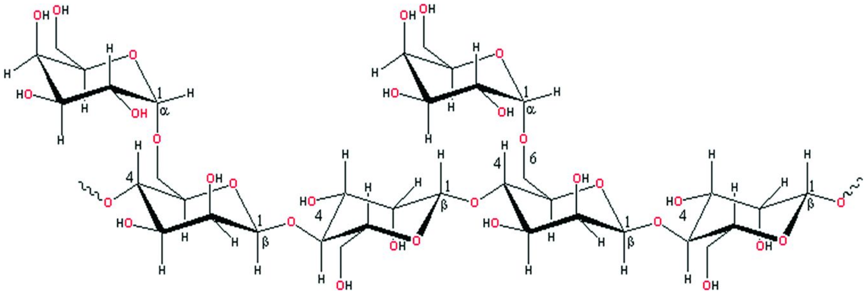

Figure 2. Stereochemical configuration of GM-CT-01

Composition of the Final Formulation

GM-CT-01 is packaged sterile as 60 mg/mL solution in 10 mL normal saline, and is dispensed in single-use glass vials with rubber stoppers. Each vial has a permanently affixed label on it with the lot number, volume in vial, manufacturing date, concentration, storage conditions (2–8°C), along with the Galectin Therapeutics (former Pro-Pharmaceuticals) name and address plus the statement “Caution: New Drug. Limited by Federal Laws to Investigational Use”.

This clinical solution should be stored in a locked, refrigerated space with access limited to study personnel.

Manufacturing

GM-CT-01 was manufactured from a commercial flour of *Cyamopsis tetragonoloba* (guar gum, galactomannan) using controlled thermal/acidic degradation and purification through copper salt complex and multiple ethanol washes. The typical yield of GM-CT-01 was 50 percent (w/w from the initial guar gum). To assure a pharmaceutical-grade product, extra specifications were put in place. Thus the prime raw material has minimum microbial contamination and consistent chemical structure, and purity suitable for pharmaceutical manufacturing. The purification procedure results in GM-CT-01 that is more than 98-percent pure (formalized calculations show purity of 100±2 percent).

Downloaded by CORNELL UNIV on June 13, 2012 | http://pubs.acs.org
Publication Date (Web): June 12, 2012 | doi: 10.1021/bk-2012-1102.ch003

Analytical Identification

While the purity and composition of mannose and galactose were established by AELC-PAD method, the polysaccharide structure was established with ^{1}H-NMR and ^{13}C NMR spectra. In Figure 3 the NMR spectrum is given, along with that of a purified galactomannan from carob (locust-bean) gum for comparative purposes. An easy identification of the two principal sugar residues – that is, mannose and galactose – comes from two peaks in ^{1}H-NMR, at 4.8 p.p.m. and 5.0 p.p.m. (doublet), respectively, given that the ratio of mannose to galactose (Man/Gal) in the galactomannan from guar gum is 1.7, and from carob gum is 4.3.

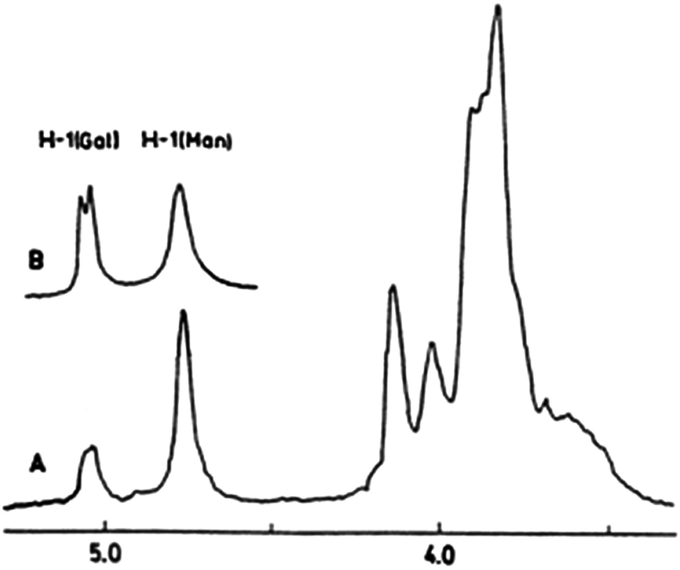

Figure 3. ^{1}H NMR Spectra (99.6 MHz) of galactomannan from carob gum (A) and GM-CT-01 (B) in D_2O solutions (10 mg/mL) at pD 7 and 90°C

Downloaded by CORNELL UNIV on June 13, 2012 | http://pubs.acs.org
Publication Date (Web): June 12, 2012 | doi: 10.1021/bk-2012-1102.ch003

The ^{13}C-NMR spectrum of GM-CT-01 (Figure 4) shows detailed positions of the chemical shifts and their intensity, and it confirms the above chemical structure of GM-CT-01. All three sugar structures – that is, α-D-galactopyranosyl, 4-O-β-D-mannopyranosyl (unsubstituted), and 4,6-di-O-β-D-manno-pyranosyl (substituted) – are seen in the NMR spectrum. The positions of signals from C1 to C6 for all three sugars – G-1 to G-6, M-1 to M-6, and GM-1 to GM-6, respectively – are shown in the above figure as well. (The positions of G-2 and G-4, M-1 and GM-1, M-2 and GM-2, M-3 and GM-3, and M-4 and GM-4 are coincided within these pairs).

The positions of signals for galactose in the NMR spectrum completely correspond to those of carbon atoms of free galactopyranose, providing evidence for the absence of substituents at positions of Gal units in the galactomannan. Substitution of certain mannose residues is at C-6 (because of the shift of the signal from 63.6 ppm for "normal" unsubstituted methylene carbon to a “substituted” one at 69.6 ppm, along with a shift of the adjacent C-5 signal from a “normal” 78 ppm to 76.4 ppm). The 63.6 p.p.m. shift for the methylene carbons are well documented.

C-1 of galactose residue is involved in formation of a galactoside bond (compared to C-1 free of galactose that in the NMR spectrum had a lowfield shift +6.5 ppm). Mannose residues are attached to each other “head-to-tail”, forming the β (1→4) backbone chain. There are unsubstituted Man-Man pairs along with substituted, Man(Gal)-Man, Man-Man(Gal), and Man(Gal)-Man(Gal).

The NMR of galactomannans from guar gum, carob gum, and clover seeds in the region of C-4 (Man) resonance (split into three peaks) is used to identify each with highest peak at high field (corresponding to unsubstituted Man-Man pairs) and is observed for a galactomannan from carob gum (Man/Gal = 3.8). The lowest peak corresponds to a galactomannan from clover seeds (Man/Gal = 1.4), and the intermediate peak corresponds to GM-CT-01 from *Cyamopsis tetragonoloba* (with a Man/Gal = 1.7). This also can be calculated from frequencies for unsubstituted and substituted Man residues, measured from C-4 (Man) resonance.

The relative frequency of unsubstituted Man-Man pairs in GM-CT-01 was 22 percent, that of Man(Gal)-Man and Man-Man(Gal) total was 48 percent, and that of totally substituted pairs Man(Gal)-Man(Gal) was 30 percent (from intensities of the split C-4 signals into their respective three lines/peaks).

Downloaded by CORNELL UNIV on June 13, 2012 | http://pubs.acs.org
Publication Date (Web): June 12, 2012 | doi: 10.1021/bk-2012-1102.ch003

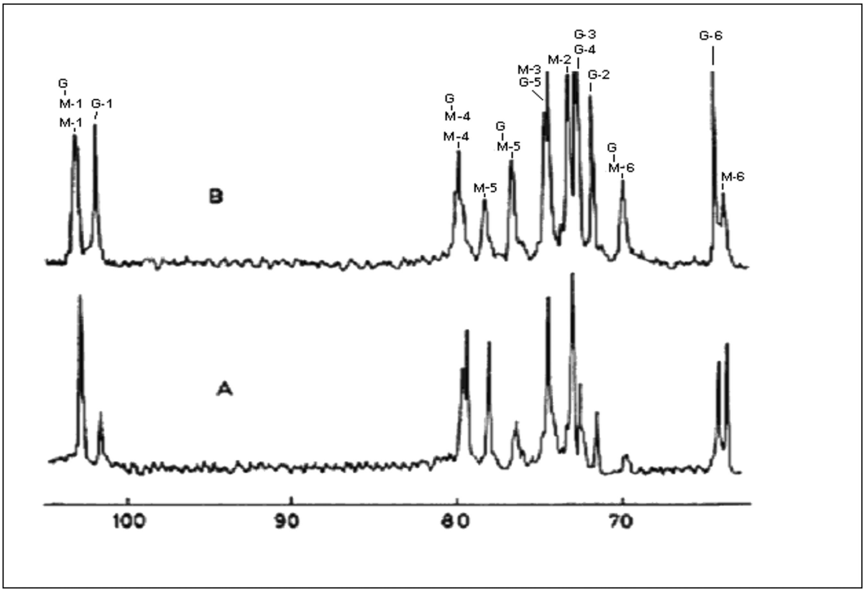

Figure 4. The ^{13}C-NMR spectrum of GM-CT-01 compared with purified galactomannan from Carob (locust-bean) Gum (Chemical shifts: G - galactose carbons, M - mannose carbons)

Downloaded by CORNELL UNIV on June 13, 2012 | http://pubs.acs.org
Publication Date (Web): June 12, 2012 | doi: 10.1021/bk-2012-1102.ch003

The ^1H-NMR signals for the GM-CT-01 galactose anomeric protons appear at approximately 4.9 ppm (doublet). The signals for the GM-CT-01 mannose anomeric protons appear at approximately 4.6 ppm (broad signal). These signals are completely separated from those of the free monosaccharides: the galactose alpha proton at 5.1 and beta at 4.5 ppm, the mannose alpha at 4.8 ppm and beta at 5.0 ppm. The ratio of mannose to galactose units was calculated at 1.67 for this working reference standard produced at 1 Kg batch size (Figure 5). This type of linkage is a well-established fact in galactomannans of plant origin.

The spectra were recorded at 3-percent solution of D_2O at 30°C on the Bruker AM-300 NMR spectrometer, with an operating frequency on carbon nuclei of 75.4 MHz. Acetone was used as an internal standard (31.45 ppm).

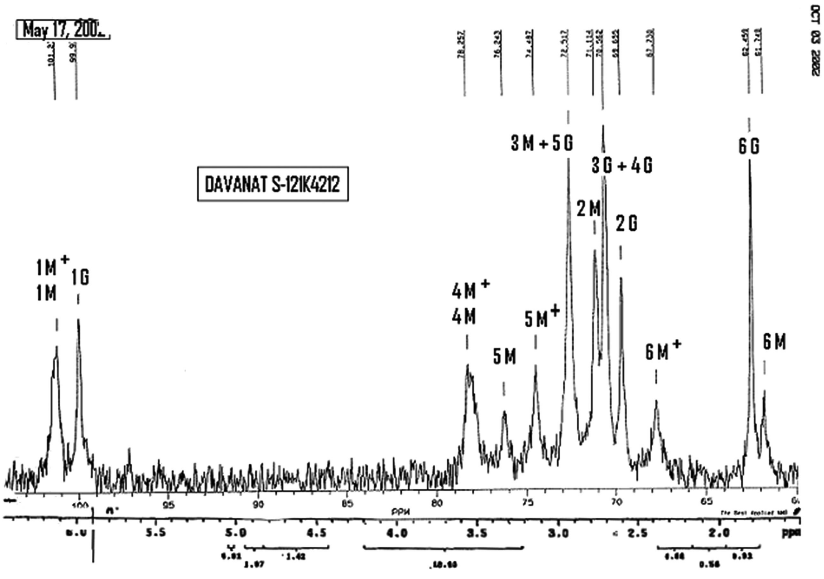

Figure 5. The ^1H-NMR spectrum of GM-CT-01. Lot # S-12K4212

This NMR spectrum clearly shows all three sugar units: D-galactopyranosyl (G on the spectrum), 4-O-β-D-mannopyranosyl- (M); and 4,6-di-O-β-D-mannopyranosyl- (M+).

The position of signals for galactose (except for C-1) in the NMR spectrum completely corresponds to those of carbon atoms free of galactopyranose, providing evidence for the absence of substituents at positions C-2 to C-6. C-1 of galactose residue is bound to the mannan backbone, with NMR spectrum revealing a low field shift of +6.4 ppm.

Substitution of substantial mannose residues is at C-6 (because of the shift of the signal from 62.3 ppm for a “normal” unsubstituted methylene carbon to a “substituted” one at 67.7 ppm, along with a shift of the adjacent C-5 signal from a “normal” 77.4 ppm to 74.5 ppm). The 62.3 p.p.m. shift for the methylene carbons is well documented (see footnote to Table 1).

A lowfield shift of C-1 and C-4 indicates that mannosyl residues are involved in the formation of a 1-4 glycoside bond. The ratio of mannose to galactose in the galactomannan is 1.67, which is confirmed by the NMR spectrum obtained at 60°C.

Table 1. Position and interpretation of signals of the ^{13}C-NMR spectrum of GM-CT-01

Monosaccharide residue	*Chemical shift, p.p.m.*					
	C-1	*C-2*	*C-3*	*C-4*	*C-5*	*C-6*
α-D-Galactopyranosyl-	99.9	69.6	70.6	70.6	72.5	62.5
α-D-Galactopyranose[a]	93.5	69.6	70.4	70.6	71.7	62.4
4-O-β-D-Mannopyranosyl-	101.2	71.1	72.5	78.3	76.2	61.7
4,6-di-O-β-D-Mannopyra-	101.2	71.1	72.5	78.3	74.5	67.7
nosyl-β-D-Mannopyranose	94.9	72.5	74.3	67.9	77.4	62.3

[a] Data presented for comparison, see Lipkind G.M., Shashkov A.S., Knirel Yu.A., Vinogradov E.V., Kochetkov N.K. (1988) *Carbohydrate Research* 175, 59-75.

Quantitation of GM-CT-01 and Determination of Molecular Weight by HPLC/RI-MALLS

In order to characterize the molecular-weight average and distribution throughout the research-and-development and scale-up phases, Galectin Therapeutics has adapted the GPC/RI-MALLS technique by using a ZIMM plot analysis (Figure 6). This analytical method was incorporated as the basic procedure into the Drug Certificate of Analysis specification.

The use of dual monitoring of the HPLC elution profile of GM-CT-01 provides us with two important chemical specifications of GM-CT-01 – that is, the quantitative measurement by the Refractive Index signal and the absolute molecular weight by the Multi-Angle Laser Light Scattering (MALLS) detector. Furthermore, these methods provide data on molecular stability and breakdown derivatives of GM-CT-01.

Two chromatograms (see Figure 7) are given for comparison purposes: 1) Blank (control); and 2) GM-CT-01 (Standard B3a), 30µl, injected at 8 mg/ml. The system is as follows: column packed with Phenomenex, Polysep GFC and a mobile phase of 50 mM Acetate, 0.1M NaCl, pH 5.0 at flow rate of 1 ml/min.

High Performance Liquid Chromatography (HPLC) using Gel Permeation Chromatography (GPC) separation technology is a well-established technique for the characterization of polymers. GPC in combination with Refractive Index (RI) detection and Multi-Angle Laser Light Scattering (MALLS) create a powerful tool for the determination of molecular weights of polymeric carbohydrates.

Downloaded by CORNELL UNIV on June 13, 2012 | http://pubs.acs.org
Publication Date (Web): June 12, 2012 | doi: 10.1021/bk-2012-1102.ch003

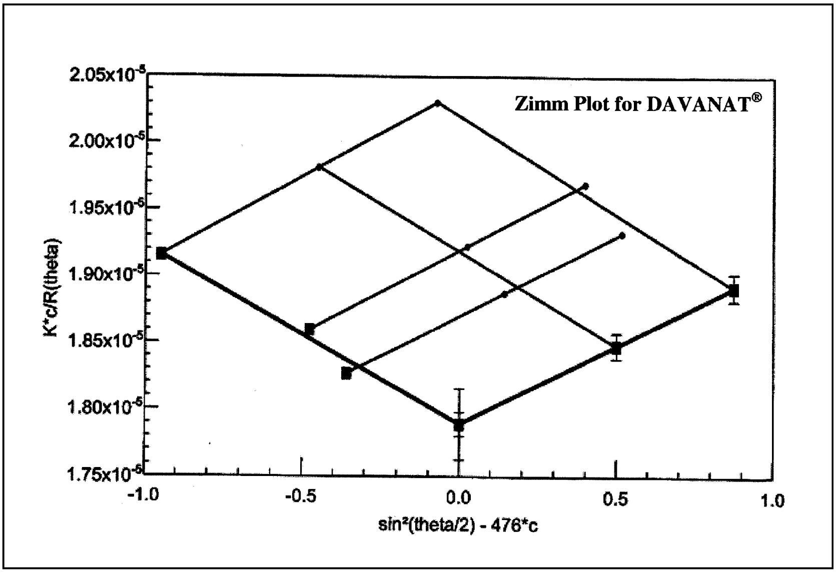

Figure 6. ZIMM plot of GM-CT-01 generated with descending concentrations

During the chromatographic run, the MALLS detector (placed in turn at many different angles) measures the degree of light scattering of a laser beam. The output of the light-scattering detector is proportional to the multiplication product of the concentration and the molecular weight of macromolecules, whereas the RI detector signal is proportional to the concentration only. Therefore, at any elution time, the molecular weight of the polymer eluting from the column can be calculated from the MALLS and RI signals.

The specification range for molecular weight of GM-CT-01 (M_w, see below) is 42,000 to 60,000 Da. As an example of a typical measurement, a recent QC test of bulk product produced the following results in triplicate: 54,780 Da, 54,500 Da, and 54,360 Da. Average molecular weight was 54,550±210 Da.

All the analytical methods described above are fully validated.

It should be noted that the manufactured GM-CT-01 materials have a rather narrow molecular weight distribution (in terms of number-average M_n, weight-average M_w, and z-average M_z molecular weights), which shows a good length-wise uniformity of the drug candidate. Below are several examples of GM-CT-01 materials manufactured, dispensed, and tested in different times for the last 9 years, between 2002 and 2011 (for different lots of GM-CT-01):

M_n = 41,420 Da
M_w = 53,780 Da
M_z = 73,010 Da

M_n = 41,490 Da
M_w = 58,560 Da
M_z = 75,880 Da

Downloaded by CORNELL UNIV on June 13, 2012 | http://pubs.acs.org
Publication Date (Web): June 12, 2012 | doi: 10.1021/bk-2012-1102.ch003

$M_n = 37{,}990$ Da
$M_w = 54{,}780$ Da
$M_z = 83{,}880$ Da

$M_n = 39{,}040$ Da
$M_w = 48{,}010$ Da
$M_z = 58{,}610$ Da

One can see that the M_w values (average is 53,780±4,360 Da) are well within the specification of the material (42,000 to 60,000 Da).

Downloaded by CORNELL UNIV on June 13, 2012 | http://pubs.acs.org
Publication Date (Web): June 12, 2012 | doi: 10.1021/bk-2012-1102.ch003

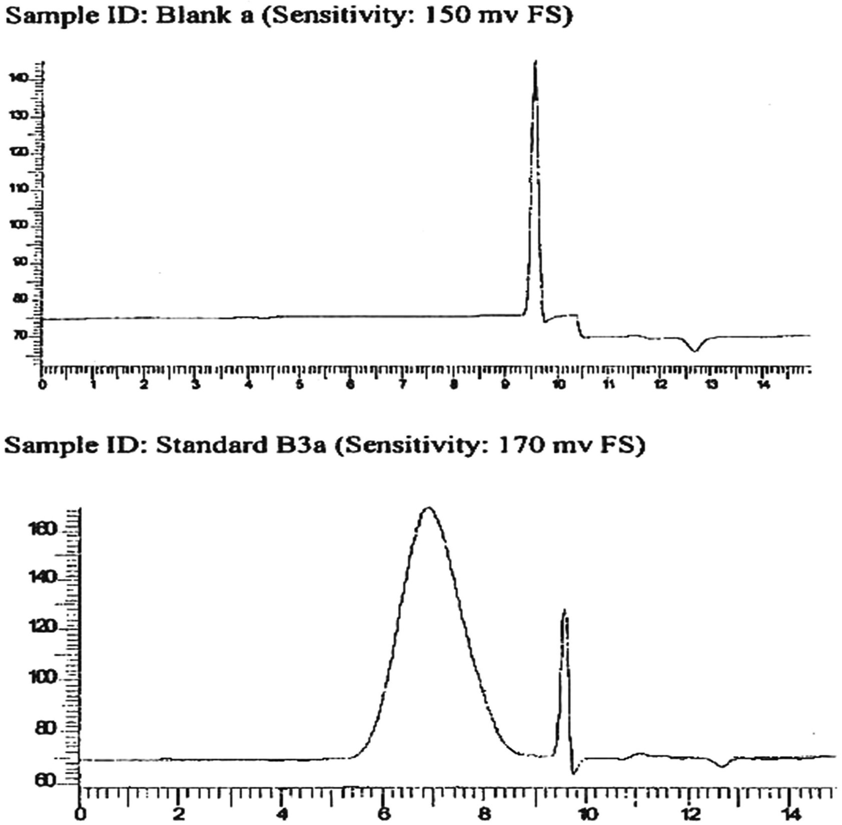

Figure 7. HPLC profile of GM-CT-01 using refractive index monitoring

Downloaded by CORNELL UNIV on June 13, 2012 | http://pubs.acs.org
Publication Date (Web): June 12, 2012 | doi: 10.1021/bk-2012-1102.ch003

Stability Studies

GM-CT-01 is very stable both in the dry-powder form and in water solutions (0.9% saline solution). We have employed three different experimental techniques for testing stability: a shelf-life study for the dry powder, an accelerated study, and a study of stress under various (and harsh) experimental conditions.

Some results of the shelf-life study for GM-CT-01 packaged dry powder (GMP Drug Substance) are shown in Table 2.

Table 2. Shelf life and accelerated thermal stability of GM-CT-01 by molecular weight data[a]

Testing	*Analysis Date*	*Molecular Weight (Daltons)*				
		Bulk Storage	*% of Initial*	*25°C 60%RH*	*40°C 75%RH*	*65°C 85% RH*
Initial Sigma C of A	02-Jun-02	54,760[b]	NA			
10 Day	29-Jul-03			50,537	49,320	47,931
30 Day	19-Aug-03			50,480	50,523	44,436
60 Day	22-Sep-03			49,783	49,603	43,438
90 Day	21-Nov-03			47,643	49,160	19,408[c]
180 Day	21-Jan-04			48,347	49,900	NT
270 Day	16-Apr-04			46,887	47,573	NT
360 Day	27-Jul-04			49,733	44,877	NT
	20-Mar-09			51,100[d]	NT	NT
	5-May-09			50,810	50,250	NT
	4-Sep-09			51,690[d]	NT	NT
PPD Bulk Release Testing	03-Feb-04	54,547	99.6			

[a] By GPC-MALLS of GM-CT-01 packaged dry powder at room temperature and accelerated storage of 40°C and 65 °C at 75% and 85% relative humidity. [b] Initial value is the mean. 10 Day values obtained at both storage conditions. [c] Separate experiments. NT - not tested. [d] In vials, 60 mg/mL solution, manufactured in 2002, dispensed in vials in September 2005.

The table shows that changes in molecular weight of GM-CT-01 after seven years of storage at 25°C and 40°C occur not significantly, and mainly within a reasonable margin of error. The same is related to the liquid, dissolved form of GM-CT-01.

Downloaded by CORNELL UNIV on June 13, 2012 | http://pubs.acs.org
Publication Date (Web): June 12, 2012 | doi: 10.1021/bk-2012-1102.ch003

For the accelerated study, GM-CT-01 powder in 1000 mg amounts was placed in polyethylene containers which were tightly closed in the packaging room at the temperature and humidity of the bulk product. The containers were exposed to the respective thermal and humidity conditions of the accelerated test, while the control was run at an average temperature of 25°C. The molecular weight was used to estimate 10-percent loss of the initial polysaccharide. An Arrhenius calculation was then used to estimate the shelf-life:

$$\mathbf{ln\ k = A - E/RT}$$

Where:

k = kinetic rate constant, or reaction rate
A= constant
E = activation energy
R = gas constant
T = absolute temperature of incubation

The plotting of reaction rates against 1/T allows the calculation of rate at any temperature, and thus it provides a prediction of shelf-life (time to 90-percent potency).

The Arrhenius plot using individual-concentration data points, and assuming the reaction is first-order, calculated the activation energy to be E = 98,000 J/mol and predicted shelf-life of over 3 years at 25°C. In reality, as Table 2 shows, it was much longer.

A drug master file Type II (DAVANAT® API-DMF No 21629) was submitted to the FDA on May 16, 2008 through Sigma-Aldrich Manufacturing, LLC (SAFC). The DMF was updated annually in 2009 and 2010 with additional 360 day stability data. A letter of Authorization for the DMF was submitted to the FDA by Sigma-Aldrich for change of ownership to Galectin therapeutics Inc. All those studies have been submitted to the US FDA.

Galectin Therapeutics tested GM-CT-01 drug product under long term 5°C/ ambient RH and accelerated 25°C/60% RH conditions for up to 4 years.

For the stress study, GM-CT-01 solutions at 0.9 to 60 mg/mL were first exposed to temperatures 80°C and 110°C at pH 5.0, 7.0, and 9.2. At 110°C, the first-order kinetic rate constant for depolymerization of GM-CT-01 was 0.021 min^{-1} at both pH 5.0 and pH 9.2, and 0.077 min^{-1} at pH 7.0. This corresponds to the respective half-life times of 33 min at 110°C and pH 5.0 and 9.2, and 90 min at the same temperature and pH 7.0.

Extended stability studies of GM-CT-01 sterile solutions of 30 and 60 mg/mL at –70°C to 65°C were carried out for a duration of 30 days to two years, in the absence and presence of 5-FU (10 to 50 mg/mL) in saline (pH 6.8 and 9.2). The frozen solutions were tested after thawing for 30 days. The molecular weight of GM-CT-01 after these freezing-thawing steps was practically the same, within experimental errors, and no precipitation was observed. These studies predict stability at room temperature for over two years.

The stability study was also performed by using the AELC/PAD method, which can monitor free galactose and mannose as well as low-molecular-weight oligomers, the likely degradation products of GM-CT-01. The method combines Anion Exchange Liquid Chromatography (AELC) and Pulsed Amperometric Detection (PAD). The data showed that practically no free galactose appeared in the course of depolymerization of GM-CT-01, with Arrhenius plot-based predictions of the stability (in terms of free galactose and mannose formation) for 5000 years! Therefore the Man-Gal covalent bond in GM-CT-01 is extremely stable compared to the Man-Man bond in GM-CT-01.

Stability and Quantitative Determination of GM-CT-01 and 5-FU

The 5-FU was analyzed in 0.9% Saline, pH 9.2 using HPLC with UV detection at 254 nm. Stock solutions for 5-FU and GM-CT-01 were in the range of 0.64 to 5.5 mg/mL, and 0.8 to 8.0 mg/mL, respectively. The procedure was applicable (after dilution for the analysis) at concentrations of 5-FU from 0.0128 to 0.128 mg/mL, and GM-CT-01 from 0.8 to 8.0 mg/mL. At these concentration ranges, both of the analyses were linear, reproducible, and highly accurate.

Both 5-FU and GM-CT-01 amounts were calculated, based on data of Table 3, to likely be stable at room temperature for a long time period, and certainly over three years.

Compatibility Studies

The study was performed to evaluate compatibility of GM-CT-01 and 5-FU with clinical infusion and filtration system used for preparation of chemotherapeutics. Solutions were prepared in accord with standard pharmacist instructions. Stock solutions of 65 mL of 8.9 mg/mL GM-CT-01 and 15.9-mg/mL 5-FU were prepared in duplicate and placed in 60-mL syringes.

A 5-mL aliquot was taken from each preparation, and the remainder was filtered through either a 0.22 mm MILLEX GP or GV filter and injected into an emptied Baxter 100 mL 0.9% Saline bag using two sterile 30-mL syringes with 16-gauge needles. Each preparation was maintained in its respective container at room temperature for 20 hours, at which time collections were made at 5 minutes and 25 minutes by pumping the sample through an 84” Primary Solution Tubing Set at a flow rate of 2 mL per minute. A Sabratek i.v. pump was used for the sample collection. The target formulation concentrations of 8.9 mg/mL of GM-CT-01 and 15.9 mg/mL of 5-FU used in the study were selected based on maximum dose expected for humans weighing 75 kg.

All analysis sets met the system suitability criteria described in the individual methods; the results are shown in Tables 3 and 4. Appearance and pH were noted for each of the samples. All solutions were clear and colorless. No interference was introduced by either filter type that would affect the quantification of GM-CT-01 and 5-FU. The actual measures of mg/mL found and percent-recovery obtained are reported in Tables 4 and 5.

Downloaded by CORNELL UNIV on June 13, 2012 | http://pubs.acs.org
Publication Date (Web): June 12, 2012 | doi: 10.1021/bk-2012-1102.ch003

Table 3. A compatibility study with 5-FU at elevated temperatures and pH of 9.2 predicts the stability of the combination of 5-FU and GM-CT-01 for over 12 months

Temperature C°	*GM-CT-01 Clinical Solution Thermal Stability*		
	10 days	30 days	60 days
5 (Control)	100%	100%	100%
25	100%	100%	100%
40	95%	94%	91%
65	93%	92%	87%

Table 4. Recovery Results for MILLEX GP, 0.22 µm Filter

Component	*pH*	*Sample Time (min)*	*Actual mg/mL*	*Theoretical mg/mL*	*% Recovery*
Control	9.01	0	9.773	8.9	109.8
GM-CT-01	9.00	5	9.694	8.9	108.9
	9.00	25	9.094	8.9	102.2
Control	9.01	0	15.576	15.9	98.0
5-FU	9.00	5	15.548	15.9	97.8
	9.00	25	15.302	15.9	96.2

Table 5. Recovery Results for MILLEX GV, 0.22 µm Filter

Component	*pH*	*Sample Time (min)*	*Actual mg/mL*	*Theoretical mg/mL*	*% Recovery*
Control	9.02	0	8.988	8.9	101.0
GM-CT-01	8.98	5	9.172	8.9	103.1
	8.99	25	8.889	8.9	99.9
Control	9.02	0	15.589	15.9	98.0
5-FU	8.98	5	15.751	15.9	99.1
	8.99	25	15.719	15.9	98.9

Downloaded by CORNELL UNIV on June 13, 2012 | http://pubs.acs.org
Publication Date (Web): June 12, 2012 | doi: 10.1021/bk-2012-1102.ch003

The quantitative results for GM-CT-01 and 5-FU, using either a MILLEX GP 0.22-μm filter or MILLEX GV 0.22, show that the filtered-fraction solutions were within 10 percent of the control solution. Hence both the MILLEX GP 0.22-μm and the MILLEX GV 0.22 filters and the infusion system were compatible with the combined solution of GM-CT-01/5-Fluorouracil, at the dose tested of 576 mg and 1035 mg in 60mL 0.9% sodium chloride for injection.

Pre-Clinical Data

Results of the pre-clinical studies of GM-CT-01 alone and in combination with 5-FU are described in the next chapter. Here we briefly mention some other chemotherapy drugs tested in combination with GM-CT-01: Camptosar®, or irinotecan (IRI); Adriamycin®, or doxorubicin (DOX), Platinol® or cisplatin (CIS), and Eloxatin® or oxaliplatin (OXA).

The pre-clinical studies employed nude mice at convertional-chemotherapy drug's tolerated doses, calculated from published literature to give approximately 50% inhibition of tumor growth. GM-CT-01 alone and a drug alone were given intravenously once every four days for a total of four injections (q4d x 4). GM-CT-01 was used at 30 and 120 mg/kg/dose, or co-administered as one injection on the same treatment schedule. Three tumors – colon tumors COLO 205 and HT-29, and mammary tumor ZR-75-1 – were used.

The selected doses were well below LD_{50}, and weight loss was insignificant. Implanted tumors grew well in all mice, and when tumors reached an average size of 100-150 mg, the treatment started. The median time required to quadruple of tumor volume was used to estimate growth rate and effect of GM-CT-01 on the chemotherapy. The average experiment lasted 35 to 60 days. The results for 14 studies with three tumor models can be summarized as follows: The average overall improvement of tumor growth inhibition was equal to 26 percent, with average improvement of 27 percent, 28 percent, 25 percent, 22 percent, and 14 percent for 5-FU, irinotecan, cisplatin, oxaliplatin, and doxorubicin, respectively.

Clinical Studies, Phase I and II

Results of the clinical studies of GM-CT-01 alone and in combination with 5-FU are described in the next chapter. Briefly, GM-CT-01 was tested at doses of 30 to 280 mg/m^2/day (0.74 to 6.9 mg/kg/day) co-administered with 500 mg/m^2/day of 5-FU (Phase I), and after the non-toxicity of DAVANAT® was established as the principal result of Phase I, GM-CT-01 was tested in Phase II at the highest dose established as 280 mg/m^2/day being co-administered with 5-FU at 500 mg/m^2/day dose, according to the approved clinical regimen. The official titles of the studies were: "**A Phase I Open-Label Study to Evaluate the Safety and Tolerability of Escalating Doses of DAVANAT (A Galactomannan Derivative) in the Presence and Absence of 5-Fluorouracil (5-FU) in Subjects With Advanced Solid Tumors**" and "**A Phase II, Multi-Center, Open-Label Trial to Evaluate the Efficacy and Safety of Intravenous DAVANAT in Combination With 5-Fluorouracil When Administered in Monthly Cycles as Third- or Fourth-Line Therapy for Metastatic Colorectal Cancer**". All

Downloaded by CORNELL UNIV on June 13, 2012 | http://pubs.acs.org
Publication Date (Web): June 12, 2012 | doi: 10.1021/bk-2012-1102.ch003

Downloaded by CORNELL UNIV on June 13, 2012 | http://pubs.acs.org
Publication Date (Web): June 12, 2012 | doi: 10.1021/bk-2012-1102.ch003

preceding treatments with approved therapies failed in their cases. In the Phase II study all (100%) patients had a primary diagnosis of colorectal cancer, and all (100%) patients had received prior therapy for their cancer, as indicated above. As reported in the "Final Clinical Study Report, Phase II Study, IND Number 64,034 of January 31, 2008", "no patient died on study". An additional principal quotation from the clinical study report is as follows: "No apparent trend was seen with regard to change from Baseline in any clinical laboratory parameter during treatment with DAVANAT/5-FU" (the Report, Summary of Safety, p. 1010). A few examples of the milestones of the both studies was achieved as described in the study Reports:

- (a) DAVANAT® was non-toxic, and a DLT (dose limiting toxicity) was not reached,
- 70% of the patients were stabilized at highest DAVANAT® dose level (280 $mg/m^2/day$) level,
- a 46% increase in longevity of the patients (based on the Median Overall Survival) was achieved compared with the Best Standard of Care,
- a 41% reduction of SAE (Serious Adverse Effects) was achieved compared to the Best Standard of Care.

It should be emphasized that all the patients in the Phase I and II clinical trials were those who failed their prior cancer therapies including 5-FU, Xeloda®, Avastin®, Erbitux®, oxaliplatin, irinotecan. The majority of them had colorectal cancer (53%), following up with pancreatic cancer (13%) and other, such as hepatocellular, biliary (cholangiocarcinoma), gastric, breast, ovarian, appendiceal, testicular, prostate, and unknown primary cancers. 60% of the patients failed prior surgery, and 30% failed prior radiotreatment. 100% of the patients in Phase II have failed prior chemotherapy and/or other systemic therapies. 58% of the patients failed prior 5-FU treatment.

More detailed description of the both studies is given in the next chapter of this book.

Note

This is an updated version of a chapter that previously appeared in *Carbohydrate Drug Design* (ACS Symposium Series 932), edited by Klyosov et al. and published in 2006.

References

1. Barondes, S. H.; Castronovo, V.; Cooper, D. N.; Cummings, R. D.; Drickamer, K.; Feizi, T.; Gitt, M. A.; Hirabayashi, J.; Hughes, C.; Kasai, K. Galectins: a family of beta-galactosidase-binding lectins. *Cell* **1994**, *76*, 597–598.
2. Beuth, J.; Ko, H. L.; Oette, K.; Pulverer, G.; Roszkowski, K.; Uhlenbruck, G. Inhibition of liver metastasis in mice by blocking hepatocyte lectins with

arabinogalactan infusions and D-galactose. *J. Cancer Res. Clin. Oncol.* **1987**, *113*, 51–55.

3. Fukuda, M. N.; Ohyama, C.; Lowitz, K.; Matsuo, O.; Pasqualini, R.; Ruoslahti, E. A peptide mimic of E-selectin ligand inhibits sialyl Lewis X-dependent lung colonization of tumor cells. *Cancer Res* **2000**, *60*, 450–456.
4. Gabius, H.-J.; Wu, A. M. Galectins as regulators of tumor growth and invasion by targeting distinct cell surface glycans and implications for drug design. In *Galectins*; Klyosov, A. A., Witzhak, Z. J., Platt, D., Eds.; John Wiley & Sons: 2008; pp 71−85.
5. Byrd, J. C.; Bresalier, R. S. Galectin-3 in the progression and metastasis of colorectal neoplasia. In *Galectins*; Klyosov, A. A., Witzhak, Z. J., Platt, D., Eds.; John Wiley & Sons: 2008; pp 193−221.
6. Rabinovich, G. A. Galectin-1 as a potential cancer target. *Br. J. Cancer* **2005**, *92*, 1188–1192.
7. Yang, R. Y.; Rabinovich, G. A.; Liu, F. T. Galectins: structure, function and therapeutic potential. *Expert Rev. Mol. Med.* **2008**, *10*, e17.
8. Salatino, M.; Croci, D. O.; Bianco, G. A.; Ilarregui, J. M.; Toscano, M. A.; Rabinovich, G. A. Galectin-1 as a potential therapeutic target in autoimmune disorders and cancer. *Expert Opin. Biol. Ther.* **2008**, *8*, 45–57.
9. Liu, F. T.; Rabinovich, G. A. Galectins: regulators of acute and chronic inflammation. *Ann. N. Y. Acad. Sci.* **2010**, *1183*, 158–182.
10. Fukumori, T.; Kanayama, H. O.; Raz, A. The role of galectin-3 in cancer drug resistance. *Drug Resist. Updates* **2007**, *10*, 101–108.
11. Nakahara, S.; Raz, A. Biological modulation by lectins and their ligands in tumor progression and metastasis. *Anticancer Agents Med. Chem.* **2008**, *8*, 22–36.
12. Nangia-Makker, P.; Wang, Y.; Raz, T.; Tait, L.; Balan, V.; Hogan, V.; Raz, A. Cleavage of galectin-3 by matrix metalloproteases induces angiogenesis in breast cancer. *Int. J. Cancer* **2010**, *127*, 2530–2541.
13. Klyosov, A. A. Galectins and their functions in plain language. In *Galectins*; Klyosov, A. A., Witzhak, Z. J., Platt, D., Eds.; John Wiley & Sons: 2008; pp 9−31.
14. Bocci, G.; Danesi, R.; Di Paolo, A. D.; Innocenti, F.; Allegrini, G.; Falcone, A.; Melosi, A.; Battistoni, M.; Barsanti, G.; Conte, P. F.; Del Tacca, M. Comparative pharmacokinetic analysis of 5-fluorouracil and its major metabolite 5-fluoro-5,6-dihydrouracil after conventional and reduced test dose in cancer patients. *Clin. Cancer Res.* **2000**, *6*, 3032–3037.
15. Klyosov, A. A.; Platt, D.; Zomer, E. Preclinical Studies of Anticancer Efficacy of 5-Fluorouracil when Co-Administered with the 1,4-beta-D-Galactomannan. *Preclinica* **2003**, *1*, 175–186.
16. Ohyama, C.; Tsuboi, S.; Fukuda, M. Dual roles of sialyl Lewis X oligosaccharides in tumor metastasis and rejection by natural killer cells. *EMBO J.* **1999**, *18*, 1516–1525.
17. Platt, D.; Raz, A. Modulation of the lung colonization of B16-F1 melanoma cells by citrus pectin. *J. Natl. Cancer Inst.* **1992**, *84*, 438–442.

Downloaded by CORNELL UNIV on June 13, 2012 | http://pubs.acs.org
Publication Date (Web): June 12, 2012 | doi: 10.1021/bk-2012-1102.ch003

18. Raz, A; Lotan, R. Endogenous galactoside-binding lectins: a new class of functional tumor cell surface molecules related to metastasis. *Cancer Metastasis Rev.* **1987**, *6*, 433–452.
19. Zhang, J.; Nakayama, J.; Ohyama, C.; Suzuki, A.; Fukuda, M.; Fukuda, M. N. Sialyl Lewis X-dependent lung colonization on B16 melanoma cells through a selectin-like endothelian receptor distinct from E- or P-selectin. *Cancer Res.* **2002**, *62*, 4194–4198.
20. Miller, M. C.; Klyosov, A. A.; Mayo, K. H. The α-galactomannan Davanat binds galectin-1 at a site different from the conventional galectin carbohydrate binding domain. *Glycobiology* **2009**, *19*, 1034–1045.
21. Some Antineoplastic and Immunosuppressive Agents. *IARC Monographs on the Evaluation of the Carcinogenic Risk of Chemicals to Humans*; WHO, International Agency for Research on Cancer: May 1981; Vol. 26, p 217−235.
22. Kannagi, R. Carbohydrate-mediated cell adhesion involved in hematogenous metastasis of cancer. *Glycoconjugate J.* **1997**, *14*, 577–584.
23. Lehmann, S.; Kuchler, S.; Theveniau, M.; Vincendon, G.; Zanetta, J. P. An endogenous lectin and one of its neuronal glycoprotein ligands are involved in contact guidance of neuron migration. *Proc. Natl. Acad. Sci. U.S.A.* **1990**, *87*, 6455–6459.
24. Demotte, N.; Wieers, G.; Klyosov, A.; van der Bruggen, P. Is it possible to correct the impaired function of human tumor-infiltrating lymphocytes? Presented at Keystone Symposium on Molecular and Cellular Biology. New Frontiers at the Interface of Immunity and Glycobiology, March 6−11, 2011. Lake Louise, AB, Canada; Abstract 23F11.

Downloaded by CORNELL UNIV on June 13, 2012 | http://pubs.acs.org
Publication Date (Web): June 12, 2012 | doi: 10.1021/bk-2012-1102.ch003

Downloaded by STANFORD UNIV GREEN LIBR on June 14, 2012 | http://pubs.acs.org
Publication Date (Web): June 12, 2012 | doi: 10.1021/bk-2012-1102.ch004

Chapter 4

DAVANAT® (GM-CT-01) and Colon Cancer: Preclinical and Clinical (Phase I and II) Studies

Anatole Klyosov,[1,*] Eliezer Zomer,[1] and David Platt[2]

[1]Galectin Therapeutics, 7 Well Avenue, Newton, MA 02459
[2]Pro-Pharmaceuticals, 7 Well Avenue, Newton, MA 02459
[*]Klyosov@galectintherapeutics.com

DAVANAT® (trade name) or GM-CT-01 (operational name) is the galactomannan isolated from seeds of *Cyamopsis tetragonoloba*, or Guar gum, and subjected to a controlled partial chemical degradation. A backbone of the galactomannan is composed of (1→4)-linked β-D-mannopyranosyl units, to which single α-D-galactopyranosyl is attached by (1→6)-linkage. Chemical names of the galactomannan are 1,4-β-D-Galactomannan, or [(1→6)-α-D-galacto-(1→4)-β-D-mannan]. The average repeating unit of GM-CT-01 consists of seventeen β-D-Man residues and ten α-D-Gal residues (Man/Gal ratio is 1.7), and an average polymeric molecule contains approximately 12 of such repeating units (for the average molecular weight of 51,000 Da, though the specification permits it to be within 42 to 60 thousand Dalton). GM-CT-01 has been tested alone and in combination with a chemotherapy drug 5-Fluorouracil (5-FU) in pre-clinical studies, and in Phase I and Phase II of the clinical studies, as well as in the pre-clinical studies in combination with some other chemotherapy drugs such as Camptosar®, or irinotecan (IRI); Adriamycin®, or doxorubicin (DOX), Platinol® or cisplatin (CIS), and Eloxatin® or oxaliplatin (OXA). The pre-clinical studies employed nude mice at conventional-chemotherapy drug's tolerated doses, calculated to give approximately 50% inhibition of tumor growth. GM-CT-01 alone and a drug alone were given intravenously once every four days for a total of four injections (q4d x 4). GM-CT-01 was used at 30 and 120 mg/kg/dose, or co-administered as one injection on the same treatment schedule. Three tumors – colon tumors COLO 205 and HT-29, and mammary tumor ZR-75-1 – were used. The selected doses were well below LD_{50}, and weight loss was insignificant. The average experiment in the preclinical studies lasted 35 to 60 days. Fourteen studies with three tumor models have resulted in the average overall improvement of tumor growth inhibition of 26 percent, with average improvement of 27 percent, 28 percent, 25 percent, 22 percent, and 14 percent for 5-FU, irinotecan, cisplatin, oxaliplatin, and doxorubicin, respectively. In the clinical studies (Phase I) GM-CT-01 was tested at doses of 30 to 280 $mg/m^2/day$ (0.74 to 6.9 mg/kg/day) co-administered with 500 $mg/m^2/day$ of 5-FU, and after the non-toxicity of DAVANAT® was established as the principal result of Phase I, GM-CT-01 was tested in Phase II at the highest dose established as 280 $mg/m^2/day$ being co-administered with 5-FU at 500 $mg/m^2/day$ dose, according to the approved clinical regimen. All preceding treatments with approved therapies failed in their cases. In the Phase II study all (100%) patients had a primary diagnosis of colorectal cancer, and all (100%) patients had received prior therapy for their cancer, as indicated above. As reported in the "Final Clinical Study Report, Phase II Study, IND Number 64,034 of January 31, 2008", "no patient died on study". It was shown that: (a) DAVANAT® was non-toxic, and a DLT (dose limiting toxicity) was not reached, (b) 70% of the patients were stabilized at highest DAVANAT® dose level (280 $mg/m^2/day$) level, (c) a 46% increase in longevity of the patients (based on the Median Overall Survival) was achieved compared with the Best Standard of Care, and (d) a 41% reduction of SAE (Serious Adverse Effects) was achieved compared to the Best Standard of Care. Phase II clinical studies was successfully complete, and objections for Galectin Therapeutics to move into a Phase III clinical trial was not expressed by the FDA.

Downloaded by STANFORD UNIV GREEN LIBR on June 14, 2012 | http://pubs.acs.org
Publication Date (Web): June 12, 2012 | doi: 10.1021/bk-2012-1102.ch004

Introduction

As it was described in the preceding Chapter in this book, the galactomannan, chemical structure of which is shown below, was named DAVANAT®, and the respective trade mark has been received in the beginning of the 2000-s. However, then we have found that other galactomannans of a different structure can also serve as tight ligands for galectins, and can be considered as drug candidates as well. Therefore a new nomenclature has been developed, and DAVANAT® as such was renamed as GM-CT-01, where GM stands to galactomannan, CT designates the natural source (in this particular case it is *Cyamopsis tetragonoloba*), and 01 shows its number in the drug candidate pipeline. Therefore, in the preceding chapter and in this overview we use the new nomenclature, unless we refer to the FDA documents in which the former name was used.

GM-CT-01 is being developed to enhance the efficacy of anti-neoplastic drugs by targeting specific receptors, possibly, but not necessarily, galectins, present on cancer cells. Since GM-CT-01 consists of a polymeric mannose backbone carrying galactose side chains, and, as it was directly shown (NMR studies), capable to interact with some galectins (in fact, with galectin-1, -3, -7, -9) , that is receptors specific for galactose residues (both β- and α-galactose, as it was recently shown (*1*)), the initial idea was to use GM-CT-01 as a kind of a chaperon along with 5-fluorouracil (5-FU) to facilitate its delivery into the cancer cell. A choice of 5-FU as a chemotherapy drug in a combination with GM-CT-01 was based on a fact that for over 40 years 5-FU has been the standard first-line agent in the treatment of metastatic colorectal cancer.

Preliminary animal studies with a variety of soluble galactomannan oligomers from various plant sources have shown promising response to the combination therapy of 5-FU along with 1,4-β-D-galactomannan of a certain molecular weight, with mannose to galactose ratio of 1.7. Fortunately, such a galactomannan can be obtained from a readily available source, namely guar gum (*Cyamopsis tetragonoloba*), by controlled partial depolymerization. The water-soluble galactomannan of molecular weight 51,000 Da (42,000 to 60,000 Da for different industrial batches, see the preceding Chapter in this book) was thoroughly characterized and selected for process optimization and manufacturing of GM-CT-01, and tested *in vivo* in animals for both efficacy and overall reduction of toxicity. In particular, GM-CT-01 has been shown to increase the anti-tumor activity of 5-FU in mice. Based on data obtained it was proposed that GM-CT-01 may potentiate the efficacy of 5-FU by changing its tissue distribution and targeting its delivery to the tumor cell. Later it was found that GM-CT-01 binds to galectin-1 and galectin-3, among other galectins, and upregulate some cellular mechanisms (see, e.g. (*2*)).

In June of 2003 the FDA has allowed to test DAVANAT® (GM-CT-01) in a formulation with and without 5-FU in Phase I clinical trials. This multi-center, open label study was designed for cancer patients with different type of solid tumors who have failed standard, approved surgical, radiation, and chemotherapeutical regimen.

In November of 2003 the US Patent (No. 6,645,946) was granted to Pro-Pharmaceuticals that protects methods and compositions with respect to galactomannan co-administered with a therapeutic agent (5-FU among them) for reducing toxicity of the agent. Since then four more US Patents were granted (Nos. 6,914,055; 6,982,255; 7,012,068; 7,893,252), the last one in February 2011, as well as Patent of Australia (No. 272022B2, February 17, 2011) and Patent of Japan (No. 4744782, May 20, 2011), and twenty US and International patent applications were filed.

Chemistry of GM-CT-01

GM-CT-01 is the galactomannan isolated from seeds of guar gum, *Cyamopsis tetragonoloba*, and subjected to a controlled partial chemical degradation (Klyosov & Platt, US Patent No. 6,645,946, and others, see above). A backbone

Downloaded by STANFORD UNIV GREEN LIBR on June 14, 2012 | http://pubs.acs.org
Publication Date (Web): June 12, 2012 | doi: 10.1021/bk-2012-1102.ch004

Downloaded by STANFORD UNIV GREEN LIBR on June 14, 2012 | http://pubs.acs.org
Publication Date (Web): June 12, 2012 | doi: 10.1021/bk-2012-1102.ch004

of the galactomannan is composed of (1→4)-linked β-D-mannopyranosyl units, to which single α-D-galactopyranosyl is attached by (1→6)-linkage.

Chemical names of the galactomannan are 1,4-β-D-Galactomannan, or [(1→6)-α-D-galacto-(1→4)-β-D-mannan].

Structural formula of the galactomannan:

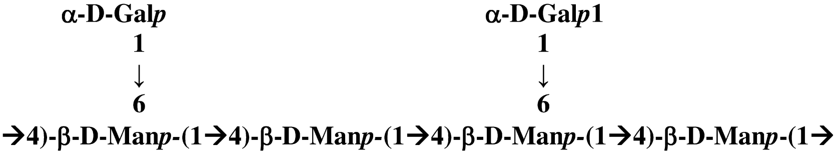

$$\rightarrow 4)\text{-}\overset{\begin{array}{c}\alpha\text{-D-Gal}p\\ 1\\ \downarrow\\ 6\end{array}}{\beta\text{-D-Man}p}\text{-}(1\rightarrow 4)\text{-}\beta\text{-D-Man}p\text{-}(1\rightarrow 4)\text{-}\overset{\begin{array}{c}\alpha\text{-D-Gal}p1\\ 1\\ \downarrow\\ 6\end{array}}{\beta\text{-D-Man}p}\text{-}(1\rightarrow 4)\text{-}\beta\text{-D-Man}p\text{-}(1\rightarrow$$

The average repeating unit of GM-CT-01 consists of seventeen β-D-Man residues and ten α-D-Gal residues (Man/Gal ratio is 1.7), and an average polymeric molecule contains approximately 12 of such repeating units (for the average molecular weight of 51,000 Da).

Stereochemical configuration

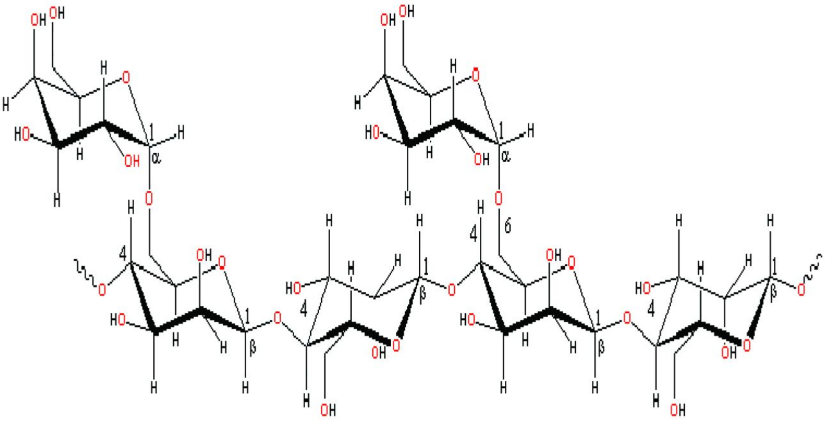

Isolation, Purification, Identification

Isolation and purification procedure of GM-CT-01, when started from a commercial *Cyamopsis tetragonoloba* guar gum flour, contains five principal steps:

- Aqueous extraction of galactomannan
- Controlled partial depolymerization
- Recovering as insoluble copper complex
- Recovering from the copper complex
- Ethanol repeated precipitation

The final yield of GM-CT-01 is typically 50% from the weight of guar gum flour.

For the manufacturing of GM-CT-01, extra specifications have been established with the supplier of guar gum to warrant a uniform and consistent product suitable for pharmaceutical manufacturing.

The purification procedure results in a pure GM-CT-01 as white powder with solubility in water more than 60 mg/mL, molecular weight of 51,000 Da (generally between 42,000 and 60,000 Da), and mannose/galactose ratio of 1.7.

^{1}H-NMR and ^{3}H-NMR spectra of GM-CT-01 are described in the preceding chapter.

Downloaded by STANFORD UNIV GREEN LIBR on June 14, 2012 | http://pubs.acs.org
Publication Date (Web): June 12, 2012 | doi: 10.1021/bk-2012-1102.ch004

GM-CT-01 Mutagenicity Studies

Mutagenicity studies that were conducted included two Ames bacterial reverse mutation assays in which GM-CT-01 was evaluated by itself in the first study and combined with 5-FU in the second study. The test articles in both studies were evaluated in bacterial assays using *Salmonella typhimurium* strains TA97a, TA98, TA100, TA1535 and *Escherichia coli* strain WP2 *uvr*A (pKM101), both in the presence and absence of an exogenous metabolic activation system. No evidence of mutagenic activity was detected in either GM-CT-01 or GM-CT-01 + 5-FU. Evidence of toxicity was not detected at any concentration level, namely from 5 to 2,000 µg per plate.

Expected New Cancer Cases and Deaths

The total (expected) number of new cases of cancer in 2009 was 1,479,350 (both sexes), of which the first five causes were lung and bronchus (219,440), breast (194,280), prostate (192,280), colorectal (106,100), and urinary bladder (70,980) (*3*).

The total number of deaths due to cancer in 2009 was 562,340, of which the first five cases were lung and bronchus (159,390), colorectal (49,920), breast (40,610), pancreas (35,240), and prostate (27,360) (ibid).

Approximately 25% of patients with colorectal adenocarcinoma present with distant metastases, and an additional 20% develop metastases during their lifetime (*4*, *5*). Although survival from this disease has improved by approximately 8% over the past two decades largely due to earlier detection, advances in the treatment of advanced colorectal cancer are largely attributed to modifications of or additions to regimens centered around 5-FU.

5-FU: Chemistry and Drug Description

5-Fluorouracil remains the first line chemotherapeutic agent for the treatment of metastatic colorectal cancer. 5-FU is a highly toxic drug with a narrow margin of safety. It is effective against carcinoma of the colon, rectum, breast, stomach and pancreas, slows or stops growth of cancer cells and their spread in the body. 5-FU is a fluorinated pyrimidine. Chemically, it is 5-fluoro-2,4

(1H,3H)-pyrimidinedione, or 2,4-dioxo-5-fluoropyrimidine, a relatively small molecule:

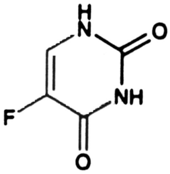

The method of chemical synthesis of 5-FU was described in the US Patent Nos. 2,802,005 and 2,885,396, issued in 1957 and 1959, and the patents' protection have long expired.

The following description of 5-FU is referenced in the Physician's Drug Reference which we consider as a reliable and FDA accepted source. 5-FU blocks the methylation reaction of deoxyuridylic acid to thymidylic acid, and thereby interferes with the synthesis of DNA and to a lesser extent inhibits the formation of RNA. Since DNA and RNA are essential for cell division and grows, the effect of 5-FU creates a thymine deficiency, which provokes unbalanced growth and death of the cell. The effect of DNA and RNA deprivation are most marked on those cells which grow more rapidly and which take up 5-FU at a more rapid rate, that is, cancer cells.

In patients, 7%-12% of 5-FU is excreted unchanged in the urine in six hours; of this 90% is excreted in the first hour. The remaining 88%-93% of the administered dose is metabolized, primarily in the liver. The inactive metabolites are excreted in the urine over the next 3 to 4 hours. Overall, 90% of the dose is accounted for during the first 24 hrs following i.v. administration. The mean half-life of elimination of 5-FU from plasma is approximately 16 minutes, with a range of 8 to 20 minutes, and is dose dependent. No intact 5-FU can be detected in the plasma three hours after i.v. administration.

5-FU is typically manufactured for intravenous administration. Following the injection, 5-FU distributes into tumors, intestinal mucosa, bone marrow, liver and other tissues throughout the body. It diffuses readily across the blood-brain barrier and distributes into cerebrospinal fluid and brain tissue.

The drug shows an extreme toxicity. Severe hematological toxicity, gastrointestinal hemorrhage and even death may result from the use of 5-FU, despite meticulous selection of patients and careful adjustment of dosage. Generally, a therapeutic response is unlikely to occur without some evidence of toxicity. Severe toxicity is more likely in poor risk patients, although fatalities may be encountered occasionally even with patients in relatively good condition.

Acute nausea and vomiting occurs frequently and may be severe. Stomatitis (sores in the mouth) and esophagopharyngitis may occur, and some patients have fever blister-like sores. These effects may be severe leading to gastrointestinal ulceration and bleeding. Anorexia, diarrhea, temporary loss of hair (alopecia), skin rash, increased skin and/or vein darkening, fatigue (2-3 days after injection) are commonly seen during therapy. Almost all patients lose all body hair, though temporarily, since 5-FU kills the hair cells.

Downloaded by STANFORD UNIV GREEN LIBR on June 14, 2012 | http://pubs.acs.org
Publication Date (Web): June 12, 2012 | doi: 10.1021/bk-2012-1102.ch004

Besides, there is a high incidence of bone marrow depression (decreased blood count), primarily of leukocytes. Rapidly falling white blood cell count often occurs during treatment with 5-FU, thereby diminishing the infection fighting activity of the body. 5-FU therapy is counter indicated for patients in a poor nutritional state and those with depressed bone marrow function. It is incompatible with doxorubicin, another powerful anti-cancer chemotherapeutic drug.

The administration of 5-FU has been associated with the occurrence of hand-foot syndrome, resulting in the symmetrical swelling of the palms and soles. This syndrome causes a tingling sensation of hands and feet, which may progress to pain when holding objects or walking in the few days following administration.

Animal studies of 5-FU have shown a number of negative causes, such as teratogenic effects and malformations, including skeletal defects.

Despite the described side effects, 5-FU has been the mainstay for therapy of colorectal cancer for the last 2 decades. Generally, fluoropyrimidines, especially 5-FU, have been used in standard chemotherapy regimens for a number of solid tumors including colorectal, breast, non-small cell carcinoma of the lung (NSCCL), gastric, pancreatic, ovarian and head and neck tumors. Schedule modification of 5-FU administration including prolonged intravenous infusion, and pharmacokinetic modulation has produced improved response rates and tolerability; however, this has not always translated into improved survival.

Bolus intravenous injection (i.v.) therapy, which was the standard of care until approximately a decade ago, produced response rates ranging from 11 to 18%. The intensity of exposure to 5-FU as measured by the area under the concentration vs. the time curve, correlates well with anti-tumor activity but also with toxicity. Regimens which include 5 days of treatment every 3 weeks produce mucositis (stomatitis), diarrhea and neutropenia. Regimens aimed at enhancing the duration of thymidylate synthase inhibition by continuous i.v. infusion or bolus injection in combination with leucovorin (folinic acid) have improved response rates ranging from 22 to 38%. Continuous infusion regimens can result in hand-foot syndrome (see above) in approximately 20% of patients, mucositis is similar in continuous infusion compared with bolus therapy, but diarrhea and neutropenia are less frequent by the continuous infusion route.

Despite advances in chemotherapeutic regimens for metastatic colorectal cancer as well as other solid tumors, patients refractory to these therapies represent a large unmet medical need. Many clinical trials are currently underway investigating new chemotherapeutic agents and regimens, antisense oligonucleotides, as well as biologics including monoclonal antibodies to various cell surface tumor proteins. It is reasonable to hypothesize that more specific targeting of efficacious chemotherapeutic agents, such as 5-FU, to tumor cells could result in higher response rates along with reduced toxicity. In vitro studies have shown that tumor galactoside-binding proteins on the cell surface interact with terminal D-galactoside residues located on adjacent cells, thus mediating cellular attachment and the potential for metastasis. Hence, the initial idea for developing GM-CT-01 which represents a relatively rigid backbone (poly-mannose) carrying galactose residues. Phase I clinical trial described below investigated the safety and tolerability of GM-CT-01, which has been shown

Downloaded by STANFORD UNIV GREEN LIBR on June 14, 2012 | http://pubs.acs.org
Publication Date (Web): June 12, 2012 | doi: 10.1021/bk-2012-1102.ch004

in preclinical studies, also described below, to enhance the efficacy of 5-FU in mouse models of human colorectal cancer without increasing toxicity.

Pre-Clinical *in Vivo* Toxicity Studies

Non-Clinical Safety Studies

Acute toxicology studies of GM-CT-01 were performed in mice, rats and dogs and subchronic toxicology studies were performed in rats and dogs. The following is a summary of the findings of these studies (*6*).

Toxicity on Mice

LD_{50} for 5-FU in mice is equal to 340 mg/kg, or 1,020 mg/m^2 i.v. (Physician's Desk Reference, 1994, p.1925).

In accord with this value, 5-FU in the single i.v. dose of 409 mg/kg (1227 mg/m^2) in our experiments caused death in 3/5 mice after 13-16 days. However, single i.v. doses of 112 mg/kg (336 mg/m^2) of GM-CT-01 or 417/222 mg/kg (1251/666 mg/m^2) 5-FU/GM-CT-01 produced no clinical signs of toxicity, death or decreased weight gain in mice (n=5 /group).

Toxicity on Rats

Single Dose Study. LD_{50} for 5-FU in rats is equal to 165 mg/kg, or 990 mg/m^2 i.v. (Physician's Desk Reference, 1994, p.1925).

In our experiments, in rats (n=5/sex/group), single i.v. doses of 140 mg/kg (840 mg/m^2) of 5-FU alone, 72 mg/kg (432 mg/m^2) of GM-CT-01 alone, or 140/72 mg/kg of the combination produced no deaths in any of the groups. Toxic changes in body weight, feed consumption, and hematology were somewhat less severe in the rats injected with the combination, versus those injected with 5-FU alone.

Subchronic Studies. Three subchronic rat studies were performed with i.v. injection for four consecutive days with 28-day or 52-day recovery periods.

In the first, 28-day study, research grade unfiltered GM-CT-01 alone and in combination with 5-FU was injected. However, it was found that this low grade GM-CT-01 produced mild granulomatous foci in the rat lungs. In this study, low grade GM-CT-01 was injected singly daily i.v. dose of 48 mg/kg (288 mg/m^2) for four consecutive days, or 5-FU in the same regime at the same dose of 48 mg/kg, or three following combinations of 5-FU/ GM-CT-01 in the same regime at 24/13 mg/kg, 36/19 mg/kg, or 48/25 mg/kg at a rate of 1 mL/min for four consecutive days. The four doses of 5-FU (192 mg/kg total) produced mortality in 7 out of 8 rats. With combinations of 24/13, 36/19 and 48/25 mg/kg 5-FU/ GM-CT-01 mortality was 1/8, 2/8 and 7/8, respectively. Alopecia, severe transient decreases in body weight and feed consumption, and transient depression of erythrocyte parameters and platelets were observed in all groups receiving 5-FU. Lesions in unscheduled-death animals were primarily due to the expected action of 5-FU

Downloaded by STANFORD UNIV GREEN LIBR on June 14, 2012 | http://pubs.acs.org
Publication Date (Web): June 12, 2012 | doi: 10.1021/bk-2012-1102.ch004

on the hematopoietic and lymphoid systems, with secondary bacterial invasion and disseminated hemorrhage due to effects on coagulation. At the study day 5 necropsy, lesions included pronounced hypocellularity of the bone marrow, lymphoid atrophy of the thymus and atrophy of villi in the various segments of the small intestine. All of it is considered due to the expected action of 5-FU. One can see that the low grade GM-CT-01 albeit produced mold complications in lungs, did not increase toxicity in combination with of 5-FU compared with 5-FU alone.

In the second, 56-day study, employing groups of 15 male and female rats, GMP grade GM-CT-01 has been used at 48 and 96 mg/kg/day (288 or 576 mg/m^2/day) dose. It was i.v. injected alone for four consecutive days, at a slower rate (0.1 mL/min, rather than 1.0 mL/min in the preceding study). Five animals of each sex were sacrificed at days 5, 28 and 56.

Only one (out of 30 rats examined) isolated and non-consistent histologic finding in the lung was associated with trace-level granulomatous inflammation of the lung of rats that-were i.v. dosed for four consecutive days with 96 mg/kg/day of GM-CT-01 and sacrificed at Study Day 5 (but not at Day 28 or 56). Male rats given GM-CT-01 at 96 mg/kg (a dose 2-fold greater than the highest dose used in the first study) and sacrificed on Day 28 had an increased incidence of trace-level interstitial inflammation in the lungs but had no histologic evidence of granulomatous inflammation. Male rats given GM-CT-01 at 96 mg/kg and sacrificed on Day 56 had an increased incidence of trace-level alveolar macrophage accumulation but again, no histologic evidence of granulomatous inflammation. However, those lesions (pulmonary interstitial inflammation and alveolar macrophage accumulation) were morphologically similar to lesions that are commonly encountered as incidental findings in the lungs of laboratory rats. Except the few rats mentioned, none of others showed any histologic evidence of said lesions.

The third study was extended to a separate 56-day injection and recovery period using GMP grade GM-CT-01 at 96 and 192 mg/kg/day (576 and 1152 mg/m^2/day) dose i.v. injected once daily for four consecutive days at a fast rate of 1 mL/min (at a concentration of 9.6 and 19.2 mg/mL, respectively). None of the 30 rats injected with the 96 mg/kg/day dose of GM-CT-01 were affected. Rats injected with 192 mg/kg/day of GM-CT-01 have shown minimal to mild granulomatous focal inflammation and minimal amounts of birefringent and/or non-birefringent foreign bodies in lung tissues. These findings were most notable in animals injected with the unfiltered GM-CT-01 solution at 192 mg/kg and sacrificed on Day 5 (24 hours after the last dose). The inflammation is considered to be reversible in rats, based on the fact that the high incidence of mild interstitial inflammation observed on Study Day 5 was reduced to control levels, and the presence of foreign bodies was also decreased substantially, by Study Day 28. In addition, the cellular constituents of the granulomatous foci changed to a more quiescent pattern with time and became less prominent by Study Day 56. However, complete resolution was not evident by Study Day 56.

Based on these studies it was concluded that GMP GM-CT-01 clinical solutions, up to a dose of 15 mg/kg (555 mg/m^2, injection solution 9 mg/mL), is safe for human use and poses no undue risk to health. The starting dose in human subjects was suggested to be 30 mg/m^2, which is approximately 10-fold

Downloaded by STANFORD UNIV GREEN LIBR on June 14, 2012 | http://pubs.acs.org
Publication Date (Web): June 12, 2012 | doi: 10.1021/bk-2012-1102.ch004

lower than the minimal 288 mg/m^2 dose of GM-CT-01 (48 mg/kg) used in the rat repeat dose safety study described above, that produced the same low level of lung inflammation noted in control animals injected with saline.

Toxicity on Dogs

Single Dose Study. LD_{50} for 5-FU in dogs is equal to 31.5 mg/kg, or 630 mg/m^2 i.v. (Physician's Desk Reference, 1994, p.1925).

In our experiments, in beagle dogs (n=2/group), single i.v. injections of 28.5 mg/kg (570 mg/m^2) of 5-FU alone, 15 mg/kg (300 mg/m^2) of GM-CT-01 alone, or 28.5/15 mg/kg of the combination resulted in the death of 2/2 dogs injected with 5-FU, 2/4 dogs injected with the combination and 0/2 dogs (no deaths) receiving GM-CT-01 alone. The surviving dogs remained clinically normal and had no treatment-related changes in body weight, feed consumption, ECG tracings, clinical pathology or gross tissue changes during the 21-day study period.

Subchronic Studies. A 28-day subchronic beagle dog study was performed with i.v. single daily injection for four consecutive days. Dogs in six groups, each group contained 4 males and 4 females, were injected with saline (control group), 5-FU alone (6 mg/kg/day, or 120 mg/m^2/day), GM-CT-01 alone (12 mg/kg/day, or 240 mg/m^2/day), or three following combinations of 5-FU/ GM-CT-01 in the same regime at 4/2 mg/kg, 6/3.2 mg/kg, or 6/6 mg/kg.

There were no death in dogs injected with GM-CT-01 alone. With 5-FU alone (6 mg/kg/day), mortality (dead or moribund sacrificed) occurred in all males (4/4 dead) between Study days 2 and 5. With the 4/2 mg/kg/day combination of 5-FU/ GM-CT-01, mortality occurred in ¾ males. With the 6/3.2 mg/kg/day combination, mortality was in 2/4 males, and with the 6/6 mg/kg/day combination, mortality occurred in ¼ females, while all other females and all males were alive (7/8 were alive).

Adverse effects in 5-FU groups included ataxia, prostration, vocalization, convulsions, tremors, hypersensitivity to touch, aggressive behavior (resulting in only three doses being given to the 6/3.2 of 5-FU/ GM-CT-01 group), emesis, salivation, soft stools and decreased red cell parameters and platelet counts. Gross/ microscopic changes in unscheduled-death animals included congestion of one or more organs (suggesting cardiovascular dysfunction) and atrophy of the mucosa of the GI tract. At the Study Day 5 necropsy, treatment-related histological changes were largely limited to the 5-FU females. At Study Day 29 necropsy, there were no remarkable changes in the survivors. GM-CT-01 at 240 mg/m^2/day produced no observed adverse effects.

Pre-Clinical Efficacy Studies, in Mice. Enhancement of Anti-Cancer Efficacy of 5-Fluorouracil When Co-Administered with GM-CT-01

In this section, we describe the principal results of three pre-clinical efficacy studies that employed GM-CT-01. We have shown that co-administration of GM-

Downloaded by STANFORD UNIV GREEN LIBR on June 14, 2012 | http://pubs.acs.org
Publication Date (Web): June 12, 2012 | doi: 10.1021/bk-2012-1102.ch004

Downloaded by STANFORD UNIV GREEN LIBR on June 14, 2012 | http://pubs.acs.org
Publication Date (Web): June 12, 2012 | doi: 10.1021/bk-2012-1102.ch004

CT-01 along with 5-FU by i.v. injection to mice bearing human colon tumors (COLO 205 and HT-29) significantly increased efficacy of the 5-FU. This section describes the principal results of three separate pre-clinical studies, employing (1) COLO 205-bearing mice at one dose of GM-CT-01 and 5-FU, (2) COLO 205-bearing mice at escalating GM-CT-01 doses in combination with 5-FU, and (3) HT-29-bearing mice at two GM-CT-01 doses in combination with 5-FU with and without leucovorin.

The studies have shown a GM-CT-01 dose-related effect with a maximum efficacy at 120 mg/kg/dose (360 mg/m^2/dose) of GM-CT-01. Effect of an additional oral administration of leucovorin was minimal. Combination of GM-CT-01 with 5-FU, compared to 5-FU alone, resulted in the decrease of median tumor volume in mice to 17%-65% and the increase of mean survival time (days) to 150%-190%, respectively.

Study 1. Effect of GM-CT-01 on Efficacy of 5-FU in NCr-*nu* Mice with Subcutaneous (s.c.) Implants of COLO 205 Human Colon Tumor at One GM-CT-01 Dose

This study employed a relatively high dose of 5-FU (75 mg/kg/dose) that exceeded the maximum tolerated dose in mice. The data are shown in Table 1 and Figure 1. Their statistical analysis is illustrated in Table 2.

Untreated control tumors grew well in all mice, with the median number of days for quadrupling the tumor volume equal to 12.5 days. There was no tumor regression after 56 days of the study, and there was practically no tumor reduction. Median tumor volume increased from 111 mm^3 at treatment initiation (in this case with saline only) to 2058 mm^3 after 5-8 weeks. Mean survival time was equal to 14.2 days.

A dosage of 75 mg/kg/dose of 5-FU (that is, 225 mg/kg total dose over 8 days) was in excess of the maximum tolerated dosage and produced treatment-related deaths for three mice out of ten within two weeks. The treatment caused a delay in the median to quadrupling the tumor volume from 12.5 to 23.7 days. Again, there was no tumor regression after 56 days of the study; however, two relatively small tumors were observed that grew from 75 mm^3 each, at initiation of treatment, to 126 mm^3 and 567 mm^3 by the end of the study. Median tumor volume increased from 101 mm3 at treatment initiation to 2254 mm^3 after 56 days of the study. Mean survival time shifted from 14.2 days (untreated control animals) to 23.7 days.

GM-CT-01, at a dosage of 120 mg/kg/dose administered alone on a q4d (one every 4 days) x 3 schedule, was well-tolerated. No deaths or body weight loss was observed. The median number of days to quadrupling the tumor volume equaled 15.5 days, which is slightly longer than the value for untreated animals (12.5 days). There was no tumor regression after 56 days of study, however, two relatively small tumors (compared to median tumor volume) were observed that grew from 100 mm^3 and 126 mm^3, at initiation of treatment, to 270 mm^3 and 729 m^3, respectively, by the end of the study. Median tumor volume increased from 100 mm^3, at treatment initiation, to 1813 mm^3 after 56 days of the study, which is noticeably less compared to 2058 mm^3 for untreated animals, and 2254 mm^3 for

5-FU (75 mg/kg/dose)-treated animals. Mean survival time was prolonged from 14.2 days (untreated control animals) to 19.2 days.

Co-administration of GM-CT-01 (120 mg/kg/dose) and 5-FU (75 mg/kg/dose) on a q4d x 3 schedule resulted in a remarkable effect, which caused a significant delay in quadrupling of the tumor volume from 12.5 days for untreated animals (control) and 23.7 and 15.5 days for 5-FU alone and GM alone, respectively, to 56.0 days for their combination. There was one tumor that completely disappeared by the end of the study. Two more tumors were relatively small in size, less than 20% that the control value, by the end of the study. Overall, median tumor volume increased from 111 mm^3 at treatment initiation to only 379 mm^3 after 56 days of study, a value significantly less than that for untreated animals or animals treated with 5-FU alone. Mean survival time increased from 14.2 days (untreated control animals) and 23.7 days (5-FU treatment) to 44.2 days for the combination treatment.

Downloaded by STANFORD UNIV GREEN LIBR on June 14, 2012 | http://pubs.acs.org
Publication Date (Web): June 12, 2012 | doi: 10.1021/bk-2012-1102.ch004

Table 1. Tumor volumes, dynamics of tumor volumes, and survival time for COLO 205 human tumor-bearing mice treated with 5-FU (75 mg/kg/dose), GM-CT-01 (120 mg/kg/dose) and their combination (75 mg/kg/dose and 120 mg/kg/dose, respectively) on q4d x 3 schedule

	Saline (control)	*5-FU 75 mg/kg*	*GM-CT-01 120 mg/kg*	*5-FU + GM-CT-01® 75 mg/kg + 120 mg/kg*
Median time to quadrupling of tumor volume (days)	12.5	23.7	15.5	56.0
Median tumor volume (mm^3) at the endpoint (56 days after treatment initiation)	2058	2254	1813	379
Mean survival time (days)	14.2	23.7	19.2	44.2

Downloaded by STANFORD UNIV GREEN LIBR on June 14, 2012 | http://pubs.acs.org
Publication Date (Web): June 12, 2012 | doi: 10.1021/bk-2012-1102.ch004

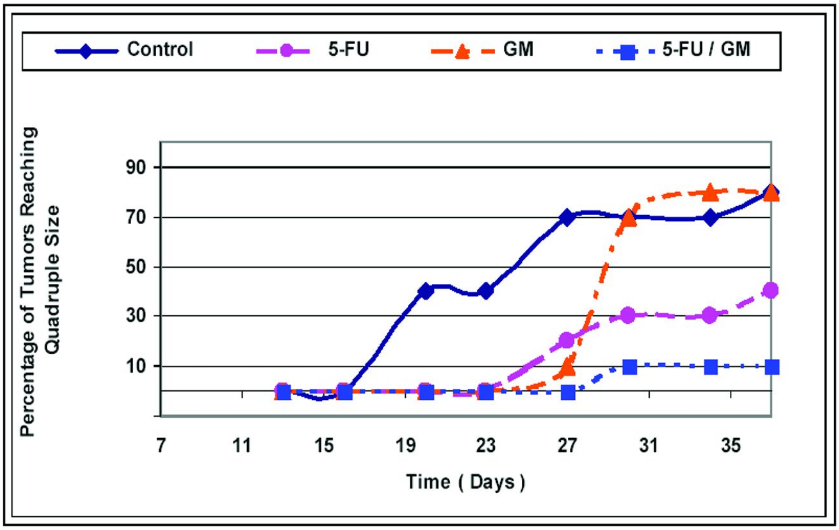

Figure 1. Effect of GM-CT-01 (120 mg/kg/dose), 5-FU (75 mg/kg/dose) and their combination in q4dx3 regimen on tumor volume in NCr-nu mice with s.c. implants of COLO 205 human colon tumor (Study 1). The upper curve is the control (no 5-FU and the galactomannan), the middle curve is for 5-FU alone, the lowest curve is for the combination of 5-FU and GM-CT-01.

Table 2. Statistical analysis of tumor volumes for COLO 205 human tumor-bearing mice treated with 5-FU (75 mg/kg/dose), GM-CT-01 (120 mg/kg/dose) and their combination on q4d x 3 schedule, for all data points (from the day of treatment initiation onward)

Treatment Group	***N (observations)***	***Mean***	***p-value***[a]	***p-value***[b]
Control	146	1174	--	<0.0001
GM-CT-01	162	962	0.0237	<0.0001
5-FU	118	652	<0.0001	0.0004
5-FU + GM-CT-01	103	358	<0.0001	--

[a] one-sided t-test p-value, compared to the control (untreated animals) [b] one-sided t-test p-value, compared to the 5-FU + GM-CT-01 treatment.

Study 2. Effect of GM-CT-01 on Efficacy of 5-FU in NCr-*nu* Mice with s.c. Implants of COLO 205 Human Colon Tumor at an Escalated GM-CT-01 Dose

The principal differences from the first study were: (i) there were four consecutive injections, not three, (ii) there were four doses of GM-CT-01 tested, not one, and (iii) 5-FU was administered (i.v.) at a more well-tolerated dose of 5-FU (48 mg/kg), compared to that used in the first study (see above). The data are shown in Table 3 and Figure 2. Results of their statistical analysis are provided below in Table 4.

No mice died in this study. As in the preceding study, untreated control tumors grew well in all mice. The median number of days to quadrupling the tumor volume equaled 7.2 days. No tumor regression or reduction occurred after 13 days of the study. Median tumor volume increased from 162 mm^3, at treatment initiation (in this case with saline only), to 1288 mm^3 after 13 days.

Downloaded by STANFORD UNIV GREEN LIBR on June 14, 2012 | http://pubs.acs.org
Publication Date (Web): June 12, 2012 | doi: 10.1021/bk-2012-1102.ch004

Table 3. Dynamics of tumor volumes for COLO 205 human tumor-bearing mice treated with 5-FU (48 mg/kg/dose), GM-CT-01, and their combination on q4d x 4 treatment schedule

	Saline, control	*5-FU 48 mg/kg*	*GM-CT-01 120 mg/kg*	*5-FU (48 mg/kg) + GM-CT-01 in dose (mg/kg):*			
				6	*30*	*120*	*600*
Median time to quadrupling of tumor volume (days)	7.2	8.7	6.9	14.8	13.5	16.5	16.2
Median tumor volume (mm^3) at the endpoint (13 days after treatment initiation)	1288	800	1152	715	695	540	588

Downloaded by STANFORD UNIV GREEN LIBR on June 14, 2012 | http://pubs.acs.org
Publication Date (Web): June 12, 2012 | doi: 10.1021/bk-2012-1102.ch004

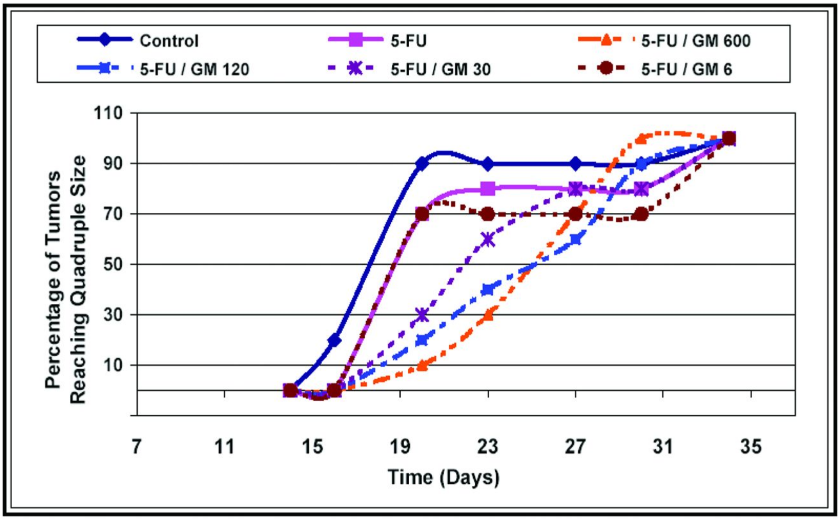

Figure 2. Effect of GM-CT-01 at escalating doses (6, 30, 120 and 600 mg/kg/dose), 5-FU (48 mg/kg/dose) and their combination in q4dx4 regimen on tumor volume in NCr-nu mice with s.c. implants of COLO 205 human colon tumor (Study 2). The upper curve is the control.

A dosage of 48 mg/kg/dose of 5-FU (192 mg/kg total dose over 12 days) was well tolerated and produced some growth delay in the median number of days to quadrupling the tumor volume, increasing it from 7.2 to 8.7 days. Two tumors in the group of 10 mice were significantly (three times or more) smaller, compared with the median tumor size, after 13 days of treatment, growing from 100 and 163 mm^3 at initiation of treatment to 270 mm^3 and 138 mm^3, respectively, by the end of the study. Median tumor volume increased from 172 mm^3 at treatment initiation to 800 mm^3 after 13 days of the study, which was less than the control value 1288 mm^3.

Co-administration of 5-FU (48 mg/kg/dose) and GM-CT-01 (6, 30, 120, and 600 mg/kg/dose) on a q4d x 4 schedule was well-tolerated at all dosages tested and caused a significant delay in quadrupling the tumor volume, from 7.2 days for untreated animals (control) and 8.7 and 6.9 days for 5-FU alone and GM-CT-01 alone, to 14.8, 13.5, 16.5, and 16.2 days, respectively (Table 3). The best results were obtained with a combination of 5-FU and 120 mg/kg/dose GM-CT-01, which resulted in a median tumor volume of 540 mm^3 at day 13, the day after the final day of treatment, compared with that of 800 mm^3 for 5-FU treatment alone. Also, the median number of days for quadrupling the tumor volume was almost twice as much for the 5-FU plus GM-CT-01 120 mg/kg/dose than for the 5-FU alone (Table 3).

Downloaded by STANFORD UNIV GREEN LIBR on June 14, 2012 | http://pubs.acs.org
Publication Date (Web): June 12, 2012 | doi: 10.1021/bk-2012-1102.ch004

Table 4. Statistical analysis of tumor volume for COLO 205 human tumor-bearing mice treated with 5-FU (48 mg/kg/dose), GM-CT-01, and their combination on q4dx4 schedule, at Day 13 after treatment initiation, that is the next day after treatment completion, and for all data points (from the day of treatment initiation onward).

Treatment Group	*Mean, at Day 13 (N=10)*	*p-value*[a]	*Mean, for all data points (N=50)*	*p-value*[b]
Control	1232	0.0055	652	0.00359
5-FU	736	--	419	--
5-FU + GM-CT-01 6 mg/kg/dose	646	0.2496	392	0.3149
5-FU + GM-CT-01 30 mg/kg/dose	594	0.1259	356	0.1201
5-FU + GM-CT-01 120 mg/kg/dose	544	0.0773	342	0.0740
5-FU + GM-CT-01 600 mg/kg/dose	576	0.0904	335	0.0509

[a] one-sided t-test p-value, compared to the 5-FU alone treatment, at the next day after treatment completion (Day 13). [b] one-sided t-test p-value, compared to the 5-FU alone treatment, for all data points.

Study 3. Effect of GM-CT-01 on Efficacy of 5-FU in NU/NU-*nu*BR Mice with s.c. Implants of HT-29 Human Colon Tumor

The principal differences from the second study were: (i) another tumor (HT-29) was used, and (ii) leucovorin was added to the treatment regimen. The data are shown in Table 5 and Figure 3. Their statistical analysis is provided in Table 6.

As in the two preceding studies, control (untreated) tumors grew well in all mice, with a median of 13.3 days for quadrupling of the tumor volume. Median tumor volume increased from 196 mm^3, at treatment initiation (day 7 after tumor implantation), to 1318 mm^3 after 26 days.

A dosage of 48 mg/kg/dose of 5-FU (192 mg/kg total dose over 12 days of the treatment) along with an oral administration of leucovorin as described above was within the maximum tolerated dosage, producing no treatment-related deaths in the group of 10 mice within three weeks. The treatment caused a delay of two days for the quadrupling of the tumor volume (from 13.3 to 15.3 days). Median tumor volume increased from 179 mm^3, at treatment initiation, to 1120 mm^3 on study day 26. Co-administration of 5-FU with GM-CT-01 (30 mg/kg/dose), along with an oral dose of leucovorin as described above, brought further delay in tumor growth, particularly in the first half of the study: quadrupling of the tumor occurred from 15.3 days without GM-CT-01 to 18.1 days with GM-CT-01 (Table 5).

Table 5. Tumor volumes and dynamics of tumor volumes for HT-29 human tumor-bearing mice treated with 5-FU (48 mg/kg/dose), leucovorin (25 mg/kg/dose), GM-CT-01 and their combination on q4dx4 treatment schedule

	Saline (control)	*GM-CT-01 (120 mg/kg) + leucovorin (25 mg/kg)*	*5-FU (48 mg/kg) + leucovorin (25 mg/kg) + GM-CT-01 (mg/kg):*		
			0	*30*	*120*
Median time to quadrupling of tumor volume (days)	13.3	12.5	15.3	18.1	23.5
Median tumor volume (mm^3) at the endpoint (26 days after treatment initiation)	1318	1595	1120	1521	729

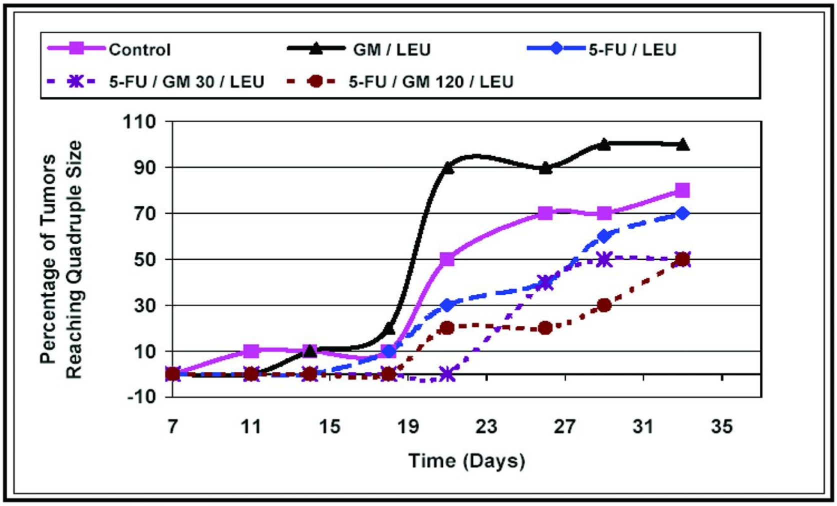

Figure 3. Effect of GM-CT-01 (30 and 120 mg/kg/dose), 5-FU (48 mg/kg/dose) and leucovorin (p.o., 25 mg/kg/dose) and their combination in q4dx4 regimen on tumor volume in NU/NU-nuBR mice with s.c. implants of HT-29 human colon tumor carcinoma (Study 3). The second from the top curve is the control. The upper curve is for the galactomannan and leucovorin.

Downloaded by STANFORD UNIV GREEN LIBR on June 14, 2012 | http://pubs.acs.org
Publication Date (Web): June 12, 2012 | doi: 10.1021/bk-2012-1102.ch004

Downloaded by STANFORD UNIV GREEN LIBR on June 14, 2012 | http://pubs.acs.org
Publication Date (Web): June 12, 2012 | doi: 10.1021/bk-2012-1102.ch004

Table 6. Statistical analysis of tumor volume for HT-29 human tumor-bearing mice treated with combinations of 5-FU (48 mg/kg/dose), leucovorin (25 mg/kg/dose), and GM-CT-01 on q4dx4 schedule, at day 26 after treatment initiation (the final day of the study) and for all data points (from the day of treatment initiation onward).

Treatment Group	*Mean, at Day 26 (N=7-10)*	*Mean, for all data points (N=71-80)*	*p-value, for all data points*
Control	1624	801	0.0778[a] 0.4559[b]
5-FU + leucovorin	1438	633	0.0778[c]
5-FU + leucovorin + GM-CT-01 30 mg/kg/dose	1519	540	0.1796[a]
5-FU + leucovorin + GM-CT-01 120 mg/kg/dose	816	455	0.0259[a] 0.0003[c]

[a] one-sided t-test p-value, compared to the 5-FU + leucovorin treatment. [b] two-sided t-test p-value, compared to GM-CT-01 + leucovorin treatment. [c] one-sided t-test p-value, compared to control (untreated animals).

Increasing the GM-CT-01 dose to 120 mg/kg/dose in co-administration with 5-FU on a q4d x 4 schedule along with an oral administration of leucovorin, as described above, again produced a significant delay in quadrupling of the tumor volume: from 13.3 days for untreated control animals and 15.3 days for 5-FU/leucovorin-treated animals to 23.5 days for animals treated with all three drugs. Furthermore, when all three drugs were used in combination, one tumor completely disappeared four weeks after treatment initiation, two more tumors were of a relatively small size (269 and 352 mm^3) by the end of the study, and three additional tumors were practically stabilized at a volume of well below 1000 mm^3. Overall, median tumor volume increased from 176 mm^3 at treatment initiation to only 729 mm^3 at study day 26 (significantly less than the 1318 mm^3 for untreated animals and 1120 mm^3 for 5-FU plus leucovorin-treated animals).

Statistical Evaluation

In summary, statistical evaluation of the data indicates the following.

In the first study (COLO 205 tumors treated with a high 5-FU dose), there was a significant advantage for 5-FU plus GM-CT-01 versus control ($p<0.0001$) and versus GM-CT-01 alone ($p<0.0001$). The difference between 5-FU plus GM-CT-01 and 5-FU was significant at a confidence level higher than 99%.

In the second study (COLO 205 tumors treated with a low 5-FU dose), there was a significant advantage for 5-FU plus GM-CT-01 120 mg/kg/dose versus 5-FU alone (with a 93%-95% confidence level), which numerically favored the combination of 5-FU with GM-CT-01.

Downloaded by STANFORD UNIV GREEN LIBR on June 14, 2012 | http://pubs.acs.org
Publication Date (Web): June 12, 2012 | doi: 10.1021/bk-2012-1102.ch004

In the third study (HT-29 tumors), there was a significant advantage for 5-FU/leucovorin plus GM-CT-01 120 mg/kg/dose versus 5-FU/leucovorin with 97% confidence level, which again numerically favored the combination of 5-FU/leucovorin with GM-CT-01.

The described studies form an experimental basis for our long-range goal of discovering mechanism-based chemotherapy agents that reduce the toxicity and increase the efficacy of co-administered antineoplastic agents. Co-administration of 5-FU with GM-CT-01 with certain chemical structures (including a specific Man/Gal ratio and molecular size/weight), which might specifically interact with galactose-specific lectins (galectins) on tumor cell surface (on recent data on the specificity of galectins see below), apparently facilitates delivery of 5-FU into cancer cells. While details of this mechanism are not within the scope of the present publication, the current observations were basic for determining the logistics and the experimental design of the preclinical efficacy studies described in this paper.

A physical combination of GM-CT-01 with 5-FU was filed with the FDA as a part of a specific IND and was approved for clinical trials in 2002. Summarized in Figure 4, GM-CT-01 increases the efficacy of 5-FU in tumor-bearing mice, in terms of decreasing median tumor volume and increasing mean survival time. GM-CT-01 co-administered along with 5-FU by i.v. once every four days for a total of three injections (study 1) or four injections (studies 2 and 3) results in the decrease of median tumor volume to 18%, 42%, and 55% compared to control (untreated animals), and to 17%, 68% and 65%, respectively, compared to 5-FU alone. Furthermore, the co-administration of GM-CT-01 and 5-FU compared to 5-FU alone results in the increase of mean survival time (days) to 190%, 190%, and 150%, for the three studies, respectively. The significance of these findings is increased because the effects were reproduced in kind using two different human colon tumors (COLO 205 and HT-29), as documented by two independent commercial testing facilities (Southern Research Institute and Charles River Laboratories).

Experimental Details

GM-CT-01, employed in this work, was thoroughly characterized using high-performance liquid chromatography (HPLC), multi-angle laser light scattering (MALLS), nuclear magnetic resonance (NMR), and quantitative chemical analysis, as described above. All of the solutions for i.v. injections were subjected to a tight quality control, using HPLC analysis in a linear range of GM-CT-01 and 5-FU concentrations. In addition, leucovorin did not interfere with GM-CT-01 when both compounds were combined with 5-FU (study 3). This non-clinical data has important clinical implications, because GM-CT-01 /5-FU may be administered in the future to patients treated with the 5-FU/leucovorin combinations.

Downloaded by STANFORD UNIV GREEN LIBR on June 14, 2012 | http://pubs.acs.org
Publication Date (Web): June 12, 2012 | doi: 10.1021/bk-2012-1102.ch004

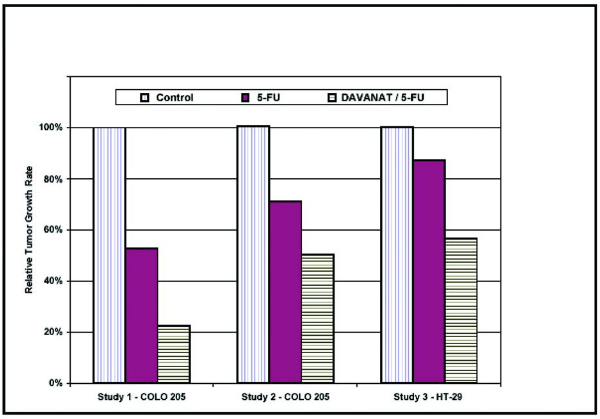

The left bar - untreated control animals, the middle bar – 5-FU alone or in the presence of leucovorin (study 3), the right bar - 5-FU + GM (studies 1 and 2) or 5-FU + GM + leucovorin (study 3).

Figure 4. Enhancement of 5-FU efficacy with GM-CT-01 on two human colon cancer tumors in mice in three separate efficacy studies: Study 1, mice bearing COLO 205 human colon tumor (5-FU 75 mg/kg/dose, GM-CT-01 120 mg/kg/dose); Study 2, mice bearing the same tumor (5-FU 48 mg/kg/dose, GM-CT-01 120 mg/kg/dose); Study 3, mice bearing HT-29 human colon carcinoma (5-FU 48 mg/kg/dose, GM-CT-01 120 mg/kg/dose, leucovorin p.o. 25 mg/kg/dose).

Efficacy Experiments on Tumor-Bearing Mice: GM-CT-01, 5-FU, Leucovorin (in Study 3), and Their Combinations

In the first two studies, male NCr-*nu* athymic nude mice (Frederick Cancer Research and Development Center, Frederick, MD, and Taconic Farms, Germantown, NY, respectively) were acclimated in the laboratory one week prior to experimentation. The animals were housed in microisolator cages, five per cage, and using a 12-hour light/dark cycle. Weight of the animals was in the range of: (i) 25-34 g on day 13 of the first study (day of treatment initiation), (ii) 21-33 g on day 14 of the second study (day of treatment initiation), and (iii) 24-25 g on day 7 of the third study (day of treatment initiation). In the third study, female NU/NU-*nu*BR athymic nude mice were housed as in the previous two studies. All animals in the three studies received sterilized tap water and sterile rodent food *ad libitum*. The animals were observed daily and clinical signs were noted. The mice were healthy and had not been previously used in other experimental procedures. The mice were randomized and were comparable at the initiation of treatment in all three studies.

The first two efficacy studies were conducted as follows. Thirty- to -forty milligram fragments from an *in vivo* passage of COLO 205 human colon tumor were implanted s.c. in mice near the right axillary area using a 12-gauge trocar needle. Tumors were allowed to reach 75-198 mm^3 in size/volume before the start of treatment. A sufficient number of mice were implanted, so that tumors in a volume range as narrow as possible were selected for the trial on the day of treatment initiation (day 13 or 14 after tumor implantation in the first and second study, respectively). Those animals selected with tumors in the proper size range were divided into the various treatment groups of 10 mice in each. The median tumor volumes in each treatment group ranged from 94 to 117 mm^3 in the first study and from 150 to 172 mm^3 in the second study.

In the third efficacy study, human colon carcinoma (HT-29) cells were injected (with $5x10^6$ cells) into the right lateral thorax of 70 female nude mice, of which 50 tumor-bearing mice were used on the study. Tumors were allowed to reach 100-200 mm^3 in volume before the start of treatment. Those animals selected with tumors in the proper size range were divided into five treatment groups of 10 mice in each. The median tumor volumes in each treatment group ranged from 172 to 196 mm^3.

Study duration was 70 days after tumor implantation or 56 days after treatment initiation in the first study; 27 days after tumor implantation or 13 days after treatment initiation in the second study; and 33 days after tumor implantation or 26 days after treatment initiation in the third study.

The s.c. tumors were measured, and the animals were weighed twice weekly starting with the first day of treatment. Tumor volume was determined by caliper measurements (mm) and using the formula for an ellipsoid sphere: $LxW^2/2=mm^3$, where L and W refer to the dimensions for length and width collected at each measurement.

Downloaded by STANFORD UNIV GREEN LIBR on June 14, 2012 | http://pubs.acs.org
Publication Date (Web): June 12, 2012 | doi: 10.1021/bk-2012-1102.ch004

Drug Formulation and Administration

Study 1

There were a total of four groups of 10 animals each, s.c.-implanted with COLO 205 human colon tumor xenografts. The groups were treated i.v. on day 13 after tumor implantation on q4d x 3 schedule as follows: (i) saline (NaCl, 0.9%), (ii) 5-FU, 75 mg/kg/dose (225 mg/m^2/dose), (iii) GM-CT-01, 120 mg/kg/dose (360 mg/m^2/dose), and (iv) 5-FU (75 mg/kg/dose) plus GM-CT-01 (120 mg/kg/dose).

5-FU was formulated in fresh saline on each day of treatment at a concentration of 3.75 mg/mL, pH 9.2. In the groups where GM-CT-01 and 5-FU were co-administered, GM-CT-01 powder was dissolved in the 5-FU solution to yield GM-CT-01 concentration of 6 mg/mL and 5-FU concentration of 3.75 mg/mL. Both individual compounds and their mixture were administered according to exact body weight, with the injection volume being 0.2 mL/10 g body weight.

Study 2

There were a total of seven groups of 10 animals each, implanted s.c. with COLO 205 human colon tumor xenografts. The groups were treated by i.v. on day 14 after tumor implantation on q4d x 4 schedule as follows: (i) Saline (NaCl, 0.9%), (ii) 5-FU (48 mg/kg/dose), (iii) GM-CT-01 (120 mg/kg/dose), (iv) 5-FU

(48 mg/kg/dose) plus GM-CT-01 (6 mg/kg/dose), (v) 5-FU (48 mg/kg/dose) plus GM-CT-01 (30 mg/kg/dose), (vi) 5-FU (48 mg/kg/dose) plus GM-CT-01 (120 mg/kg/dose), and (vii) 5-FU (48 mg/kg/dose) plus GM-CT-01® (600 mg/kg/dose).

5-FU was formulated in fresh saline on each day of treatment at a concentration of 4.8 mg/mL, at pH 9.2. In the groups where GM-CT-01 and 5-FU were co-administered, GM-CT-01 powder was dissolved in the 5-FU solution to yield GM-CT-01 concentration of 0.6, 3.0, 12, and 60 mg/mL and 5-FU concentration of 4.8 mg/mL.

Study 3

There were a total of five groups of 10 animals each, implanted s.c. with HT-29 human colon carcinoma xenografts. The groups were treated (i.v., except leucovorin) on day 7 after tumor implantation on q4d x 4 schedule as follows: (i) saline (NaCl, 0.9%), (ii) GM-CT-01 (120 mg/kg/dose) plus leucovorin (by mouth [p.o.], 25 mg/kg/dose), (iii) 5-FU (48 mg/kg/dose) plus leucovorin (p.o., 25 mg/kg/dose), (iv) 5-FU (48 mg/kg/dose) plus GM-CT-01 (30 mg/kg/dose) plus leucovorin (p.o., 25 mg/kg/dose), and (v) 5-FU (48 mg/kg/dose) plus GM-CT-01 (120 mg/kg/dose) plus leucovorin (p.o., 25 mg/kg/dose). Leucovorin was administered by oral gavage (p.o.) two hours after the injection (*via* tail vein), at a dose of 25 mg/kg/dose on the same q4d x 4 schedule.

GM-CT-01 was formulated in 0.9% sterile fresh saline on each day of treatment at a concentration of 12 mg/mL. Leucovorin powder (clinical formulation, leucovorin calcium for injection) was reconstituted with 0.9% sterile saline to yield a concentration of 2.5 mg/mL. 5-FU and combinations of 5-FU with GM-CT-01 were formulated as in study 2. Both individual compounds and their mixture were administered according to exact body weight with injection volume being 0.1 mL/10 g body weight.

Statistical Methods

Study 1

All available tumor volume data points in all animal groups (control and treatment groups), from the day of treatment initiation onward, were evaluated using unpaired one-sided Student's t-test. This was justified, since the research hypothesis (and its experimental proof) that combination of 5-FU and GM-CT-01 decreases tumor volumes compared to control, GM-CT-01 alone, and 5-FU alone was directional and permitted a one-tail test of significance. In these calculations, only animals that were alive at the time of the post-baseline evaluation were included, as well as in the calculations of the means and medians. The major comparisons of interest were against the 5-FU plus GM-CT-01combination. For these comparisons, the combination treatment served as the reference group, while remaining treatment variables were converted into three indicator variables.

The data were modeled using PROC MIXED with the indicator treatment variables, time, and the resulting interaction terms. The CONTRAST and

Downloaded by STANFORD UNIV GREEN LIBR on June 14, 2012 | http://pubs.acs.org
Publication Date (Web): June 12, 2012 | doi: 10.1021/bk-2012-1102.ch004

LSMEANS (using Dunnett's adjustment for multiple comparisons) procedures were used to evaluate the differences between the combination treatment group and the three other treatment groups.

Study 2

The mean tumor weighs were calculated for day 27, which was the day after treatment was complete, and at each post-baseline time. The serial tumor volumes were each analyzed using a longitudinal growth model to evaluate the post-baseline slopes for each treatment group from day 16 through day 27. The model used all available tumor volume data, since no animals died or were sacrificed before the final visit in this study. The major comparisons of interest were against the 5-FU alone group; comparisons against the control (untreated group of animals) and GM-CT-01 alone groups are also provided for completeness. Statistical evaluation was performed as described above for the preceding study.

Study 3

The mean tumor volumes were calculated for each post-baseline time. In these calculations, only animals that were alive at the time of the post-baseline evaluation were included. The serial tumor volumes were analyzed using a longitudinal growth model to evaluate the post-baseline slopes for each treatment group from day 11 through day 33. The model used all available tumor volume assessments, however, no data was included if animals died or were sacrificed before the final visit. The major comparisons of interest were against the 5-FU plus leucovorin group. The data were modeled using statistical tools as described above.

These results, observed for treatment of cancer-bearing mice (COLO 205 human colon tumor-bearing male athymic NCr-*nu* mice and HT-29 human colon tumor-bearing female CRL:NU-NU-*nu*BR mice) with a combination of 5-FU and GM-CT-01 in the presence and absence of leucovorin are in marked contrast to the results in cancerous mice treated with 5-FU alone or in the presence of leucovorin. Hence, the data, described in this Chapter, show that GM-CT-01combined with 5-fluorouracil (in the presence or absence of leucovorin), increases efficacy of the drug.

Ligand Specificity of Galectins and Binding of GM-CT-01 to Galectin-1

All galectins exhibit affinity for lactose [4-(β-D-galactosido)-D-glucose, or Galβ1→4Glc] and N-acetyl lactosamine [4-(β-D-galactosido)-D-acetylglucosamine, or Galβ1→ 4GlcNAc]. That is why initially a common opinion was formed in the literature that galectins are specific for beta-anomer

Downloaded by STANFORD UNIV GREEN LIBR on June 14, 2012 | http://pubs.acs.org
Publication Date (Web): June 12, 2012 | doi: 10.1021/bk-2012-1102.ch004

Downloaded by STANFORD UNIV GREEN LIBR on June 14, 2012 | http://pubs.acs.org
Publication Date (Web): June 12, 2012 | doi: 10.1021/bk-2012-1102.ch004

of galactose. GM-CT-01, however, contains alpha-anomer of galactose. Nevertheless, the discoverers of GM-CT-01 believed that a stereoconfiguration of small saccharides such as lactose and its low-molecular weight derivatives cannot fully characterize the specificity of galectins, particularly related to polysaccharides.

This consideration turned out to be true. In 2002 it was found (*7*) that alpha-linked galactose rather than beta-linked galactose (as in N-acetyl lactosamine) serves as a specific ligand for some galectins. Furthermore, it was shown that the N-acetyl galactosamine motif is not cancer tumor specific (*8*).

Then it was shown, that some galectins are specific to long carbohydrate sequences, such as poly-N-acetyllactosamine chains (*9*), with the binding being much stronger compared to N-acetyllactosamine.

Finally, it was shown in 2009 that GM-CT-01 binds to galectin-1 and galectin-3 – in a low micromolar range with purified galectins (1), and down to nanomolar range with galectin-containing cells (*2*).

Binding of GM-CT-01 to galectin-1 was studied using ^{15}N-^{1}H HSQC (heteronuclear single quantum coherence) and PFG (pulse field gradient) NMR spectroscopy. The experiments are described in detail in (*1*, *10*). Briefly, galectin-1 binds GM-CT-01 with an apparent equilibrium dissociation constant of 10 μM, compared to 48 μM for galacto-rhamnogalacturonan, GRG (10) and to 260 μM for lactose. In other words, α-galactose-based GM-CT-01 binds to galectin-1 significantly more tightly compared to that of β-galactose-containing GRG and β-D-Galactosido-D-glucose. Ironically, galectin-1, as well as all other known galectins, 15 of which are commonly considered as only β-galactoside binding lectins. This belief was first described as a principal guideline in the area of galectins at the introducing of the term in 1994 (*11*), and has been maintained since then in the literature (*12*).

Furthermore, it was found that about three to six galectin-1 molecules on average binds to one GM-CT-01 molecule, and the GM-CT-01 binding domain covers a relatively large area on the surface of galectin-1, which runs across the dimmer interface primarily on the side of galectin-1 molecule opposite to the lactose and GRG binding site. As a result, lactose and GM-CT-01 do not compete with each other for the binding. This was apparently the main reason why the binding site for GM-CT-01 and maybe other α-galactosides was missing until now, since competition with lactose was the principal methodology in searching for galectin ligands.

It was also found by us that mannan (constituting the polymeric backbone of GM-CT-01) also interacts with the same galactomannan binding domain on galectin-1, but with at least 10-fold lower affinity. This supports the role of α-galactose units in GM-CT-01 in the relatively strong binding to galectin-1 (*1*). ^{15}N-enriched galectin-1 was employed for the NMR experiments. As GM-CT-01 is added to solution of 1 or 2 mg/mL of the galectin-1, resonances of the latter are differentially decreased in intensity (broadened) at molar ratios of galectin-1 to GM-CT-01 of 10:1 to 40:1, which indicates that galectin-1 interacts with GM-CT-01. The observed differential intensity change or broadening of galectin-1 resonances is primarily the result of exchange between/among galectin-1 and binding sites on GM-CT-01 that occurs on the intermediate chemical shift time scale. By using these HSQC data in terms of HSQC resonance broadening mapping, galectin-1 residues most affected by binding GM-CT-01 were identified, by plotting fractional changes in galectin-1 HSQC resonance intensities versus the amino acid sequence of galectin-1 (*1*). An example of such analysis is shown in Figure 5. It has led to Figure 6 which shows the region with which GM-CT-01 interacts on the face of galectin-1, while lactose binds on the opposite side of galectin-1. The binding site of GM-CT-01 comprises a rather broad swath that traverses the galectin-1 dimer interface.

Downloaded by STANFORD UNIV GREEN LIBR on June 14, 2012 | http://pubs.acs.org
Publication Date (Web): June 12, 2012 | doi: 10.1021/bk-2012-1102.ch004

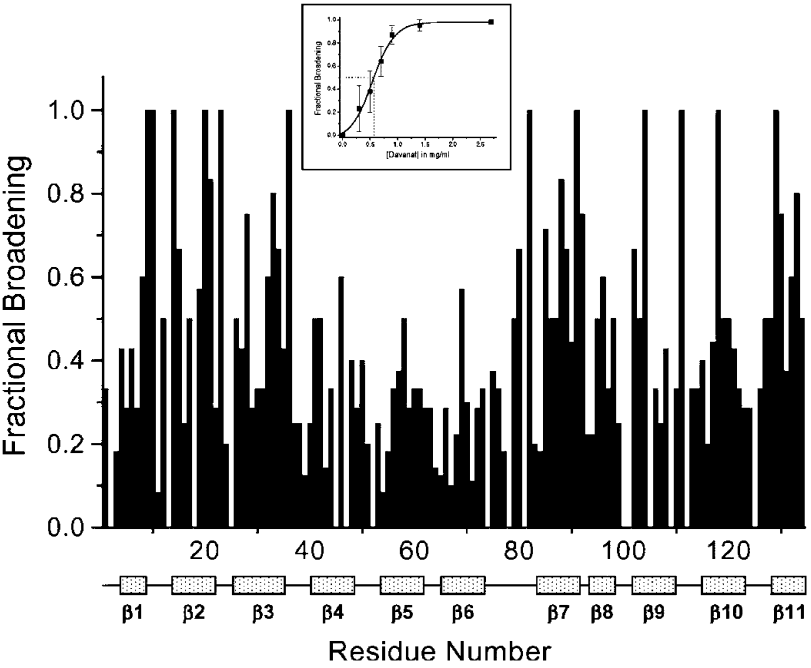

Figure 5. Gal-1/GM-CT-01 binding from HSQC resonance broadening map. Fractional changes in gal-1 resonance intensities observed at a gal-1: GM-CT-01 molar ratio (30:1) where most gal-1 resonances are still apparent versus the amino acid sequence of gal-1. A value of 1 indicates that the resonance associated with that particular residue is no longer apparent, and a value of zero indicates no change in resonance intensity. The eleven β-strands in gal-1 are identified below the residue number. The inset shows the average fractional change (±SE) in gal-1 HSQC resonance intensities versus the concentration (mg/mL) of GM-CT-01. The solid line represents a sigmoidal fit to the average of these values at each point (1).

Downloaded by STANFORD UNIV GREEN LIBR on June 14, 2012 | http://pubs.acs.org
Publication Date (Web): June 12, 2012 | doi: 10.1021/bk-2012-1102.ch004

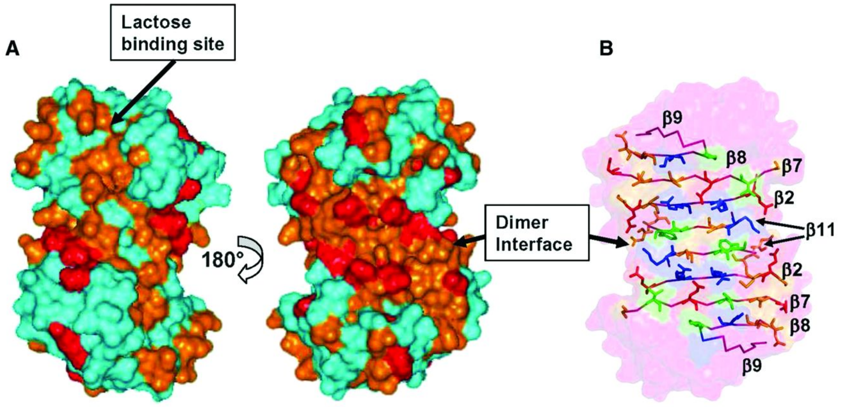

*Figure 6. GM-CT-01 binding domain on galectin-1. (**A**) Residues on the folded structure of galectin-1 that have been most affected by binding to GM-CT-01 are the darkest ones. The X-ray structure of lactose-bound human galectin-1 has been used in this figure (1). The orientation at the left shows the face of the dimmer where GM-CT-01 binds. The galectin-1 dimer interface is also indicated. The orientation at the right shows the opposite side of the dimer where lactose binds. (**B**) Illustration of galectin-1 residues in the GM-CT-01 binding domain.*

The HSQC data were also used for estimation the apparent binding affinity of galectin-1 to GM-CT-01 in terms of the dissociation constant (K_d), by plotting the average fractional change in galectin-1 HSQC resonance intensities as a function of GM-CT-01 concentration, as shown in the insert to Figure 3, with the solid line showing the fit to the data with an apparent K_d value of 10 μM. This value represents a weighed average over all binding sites on the glycan (*1*, *10*). The significance and implication of this value comparatively with those for β-ghalactose-containing polysaccharide and lactose is discussed above. Using the same procedure it was shown that β-1,4-mannan (weight-average molecular weight of 50 kDa, obtained from *Saccharomyces cerevisiae*, Sigma-Aldrich, St. Louis, MO) binds to galectin-1 much weaker, with an apparent K_d of 140 μM. Therefore, it is α-galactose residues which provide much stronger binding of GM-CT-01 to galectin-1 (as it was indicated above, β-1,4-mannan comprises the backbone of GM-CT-01 molecule).

It was shown (*1*) that lactose (Gal-β1,4-Glc) binds to free galectin-1 and to galectin-1-GM-CT-01 complex with the K_d values of 260 and 250 μM, respectively, that was essentially the same affinity. This confirmed the HSQC data that GM-CT-01 and lactose binds to different sites on galectin-1 surface. Furthermore, it was observed that lactose and GM-CT-01 bind galectin-1 simultaneously. All the above data confirmed that GM-CT-01 not only binds to galectin-1, but binds to yet unknown strong binding site on galectin-1 surface, which could not be identified using lactose, a standard reference ligand for galectins.

Radiolabel Studies

Tissue Distribution of Radiolabeled (Tritiated) GM-CT-01 in Tumored (COLO 205-Treated) and Non-Tumored Male Athymic NCr-nu Mice in the Presence and Without 5-FU

Experimental Details

Downloaded by STANFORD UNIV GREEN LIBR on June 14, 2012 | http://pubs.acs.org
Publication Date (Web): June 12, 2012 | doi: 10.1021/bk-2012-1102.ch004

Male NCr-*nu* athymic nude mice (Charles Rivers Laboratories, Raleigh, NC) were acclimated and housed as described above. The first set of animals (a total of 18 mice) were non-tumored mice. The second set of 18 mice were tumored as follows. Thirty- to -forty mg fragments from an *in vivo* passage of COLO 205 human colon tumor were implanted subcutaneously (s.c.) in mice as described above, and allowed to grow. Tumors were allowed to reach 245-392 mg in weight before the start of treatment. A sufficient number of mice were implanted so that tumors in a weight range as narrow as possible were selected for the trial on the day of treatment initiation. Those animals selected with tumors in the proper size range were divided into the various treatment groups.

Tritiation of GM-CT-01 was performed as follows. 12.8 mg of GM-CT-01 was dissolved in 2.0 mL of water and exposed to 25 Curies of tritium gas in the presence of Pd/BaSO4 catalyst (120 mg, totally insoluble in water). After one hour the gas supply was removed, the catalyst was filtered away, and the aqueous solution of GM-CT-01 was evaporated to dryness repeatedly (four-fold, adding water), until no labile tritium was found. Total yield of the labeled GM-CT-01 was 3.8 mC_i, specific radioactivity was 300 μC_i/mg.

All 36 mice, divided into 18 groups, were given a single intravenous injection of cold or tritiated GM-CT-01 (either 6 or 60 mg/kg) or of a combination of GM-CT-01 (60 mg/kg, cold or tritiated) and 5-FU (114 mg/kg) on the same day. Non-labeled GM-CT-01 was formulated in saline, and tritiated GM-CT-01 was added to the solution so that each animal received 10 μC_i of radioactivity. 5-FU was dissolved in the solution containing GM-CT-01 (at a concentration of 6 mg/mL). All dosing solutions (100 μL each) were counted in duplicate.

Two mice per group were bled at 1, 6, and 24 hrs after injection, and plasma was prepared. Animals were then sacrificed; livers, kidneys, lungs, and tumors (from tumored animals) were collected, weighed and flash-frozen for further analysis.

After weighing, livers were dissolved in 10 mL of Soluene 350 (Packard Instruments, Downers Grove, IL) and incubated first for 4 hrs at 50°C, and at room temperature, until tissues were solubilized. One mL of the resulting solution was counted in a scintillation counter as a single sample. Based on tissue weight and the sample volume, the number of μC_i of tritiated GM-CT-01 per gram of tissue was calculated.

Kidneys were treated in the same manner, but dissolved in two mL of Soluene. After the tissue was solubilized at room temperature, 15 mL of Safety Solve scintillation fluid (Research Products International, Mount Prospect, IL) was added and samples were incubated overnight. Five mL of the resulting solution were diluted in 15 mL of Safety Solve and counted in a scintillation counter as a single sample. Lungs were treated in the same manner but dissolved

Downloaded by STANFORD UNIV GREEN LIBR on June 14, 2012 | http://pubs.acs.org
Publication Date (Web): June 12, 2012 | doi: 10.1021/bk-2012-1102.ch004

in one mL of Soluene. Plasma samples (50 µL each) were placed direct into Safety Solve and counted as a single sample.

After weighing, tumors were dissolved in one or two mL of Soluene and incubated for three days at 50°C to solubilize. 15 mL of Safety Solve were then added and samples were incubated overnight at room temperature. Two mL of water were then added and samples were counted in a scintillation counter as a single sample.

The data are shown in Table 7.

Statistical Evaluation

The statistical evaluation was based on two separate series of 18 mice per series to trace and quantify the labeled GM-CT-01 in organs/tissues (tumor, liver, kidneys, lung, and plasma); one series consisted of 18 healthy mice, while the other series consisted of 18 tumor-bearing mice. Each series of 18 mice was treated with 2 mice for each of the following nine possible treatments with GM-CT-01 at 60 mg/kg with each of 2 mice sacrificed at 1, 6, and 24 hours; GM-CT-01 at 6 mg/kg with each of 2 mice sacrificed at 1, 6, and 24 hours; GM-CT-01 at 60 mg/kg + 5-FU 114mg/kg with each of 2 mice sacrificed at 1, 6, and 24 hours, as described above. The percentages of ^{3}H- GM-CT-01 recovered per organ and tumor (µC$_i$ /gram) was used for analyses; plasma outcome (µC$_i$ /ml) was counted from the entire sample.

The assessment of radiolabel uptake was challenging with only two mice per treatment-sacrifice time combination and occasional outliers. To address the number of mice per group, pooling tests were performed to determine if non-tumored mice could be pooled with tumored mice in the evaluation of kidneys, liver, lungs, and plasma; successful pooling would increase the number of mice per group to four. Further pooling was assessed for the two GM-CT-01 treatment groups; this would potentially increase sample size per group to eight. To address possible outliers, all outcomes for each individual mouse was visually compared to the other mice in the series-treatment-time combination; the four possible tumored and non-tumored mice outcomes were considered in this evaluation since any sigma-based rule would have excluded none or both observations if applied separately to the two different series.

Analysis of variance was used to test for pooling across the two series and across the two GM-CT-01 treatments. Each organ (as well as plasma) was assessed separately; tumor could only be assessed for the two GM-CT-01 treatments. The sample sizes were large enough to detect a 1.0 effect size difference between groups being compared. Results were then combined to the maximum extent allowed by pooling. Results were run both including and excluding the outliers. The primary analyses were those that excluded the outliers.

SAS (Version 6.12, Cary, NC) was used for all analyses. PROC ANOVA was used for pooling tests, while PROC FREQ was used to estimate means and standard deviations.

Table 7. Distribution of radiolabeled GM-CT-01 alone (at 6 or 60 mg/kg), and in the presence of 5-FU (60 mg/kg of GM-CT-01 and 114 mg/kg of 5-FU) in tissues of tumored (by implanting COLO 205 human colon cancer) and non-tumored mice

	1 hr after injection	*6 hr after injection*	*24 hrs after injection*
Liver			
μC$_i$ of ^{3}H- GM-CT-01 per liver, total	0.262	0.196	0.169
Same, with 5-FU	0.173	0.155	0.132
Same, per 1 g of liver (no 5-FU)	0.219	0.146	0.129
Same, with 5-FU	0.134	0.134	0.106
Tumor			
μC$_i$ of ^{3}H- GM-CT-01 per tumor, total	0.203	0.138	0.114
Same, with 5-FU	0.218	0.249	0.146
Same, per 1 g of tumor (no 5-FU)	0.123	0.092	0.066
Same, with 5-FU	0.154	0.104	0.075
Plasma			
μC$_i$ of ^{3}H- GM-CT-01 per mL of plasma	0.201	0.095	0.106
Same, with 5-FU	0.192	0.116	0.078
Kidney			
μC$_i$ of ^{3}H- GM-CT-01 per kidney, total	0.120	0.060	0.040
Same, with 5-FU	0.125	0.065	0.032
Same, per 1 g of kidney (no 5-FU)	0.302	0.131	0.087
Same, with 5-FU	0.286	0.168	0.080
Lungs			
μC$_i$ of ^{3}H- GM-CT-01 per lungs, total	0.019	0.012	0.011
Same, with 5-FU	0.017	0.011	0.008
Same, per 1 g of lungs (no 5-FU)	0.117	0.063	0.060
Same, with 5-FU	0.092	0.075	0.049

Downloaded by STANFORD UNIV GREEN LIBR on June 14, 2012 | http://pubs.acs.org
Publication Date (Web): June 12, 2012 | doi: 10.1021/bk-2012-1102.ch004

Downloaded by STANFORD UNIV GREEN LIBR on June 14, 2012 | http://pubs.acs.org
Publication Date (Web): June 12, 2012 | doi: 10.1021/bk-2012-1102.ch004

Principal Results

It was observed that GM-CT-01 freely binds to liver, kidney, lung, tumor, and plasma, and did not reach limits of the binding, e.g. did not reach saturation of the binding between the 6 mg/kg and 60 mg/kg doses. When 6 mg/kg (with a relative radioactivity of 1.0) and 60 mg/kg (with a relative radioactivity of 0.1) doses of GM-CT-01 were administered, the amount of bound radioactive GM-CT-01 was the same; that is, the amount of bound GM-CT-01 increased 10-fold for the 10-times higher dose.

The distribution of radioactivity in whole tissues as well as per weight or volume (in plasma) was practically identical for 6 and 60 mg/kg of GM-CT-01, hence, the respective data were pooled for Table 7. Also, the distribution of radioactivity in whole tissues as well as per weight or volume (in plasma) was practically identical for tumored and non-tumored animals (except in tumors, that obviously were present only in tumored animals), hence, the respective data were pooled for Table 7. Overall, the data in Table 7 are average for eight animals, except the data for tumors, that are average for four animals.

The principal results following from Table 7 are:

(1) In the presence of 5-FU the amount of GM-CT-01 in the tumor increases, and stays increased in the course of clearance of GM-CT-01.
(2) In the presence of 5-FU the amount of GM-CT-01 in the liver decreases, and stays decreased in the course of clearance of GM-CT-01.

In summary, major findings from this study indicated that tritiated GM-CT-01 freely binds to liver, kidney, lung, tumor, and plasma. Saturation of binding did not occur at concentrations of 6 to 60 mg/kg (18 to 180 mg/m^2). Tissue distribution of ^{3}H- GM-CT-01 was independent of the injected dose and did not change its pattern when 5-FU (342 mg/m^2) was combined with ^{3}H- GM-CT-01. ^{3}H- GM-CT-01 elimination from plasma, kidneys, lungs and tumor in the various groups was rapid. An average of approximately 50% of the one-hour radioactivity was detected at 6 hours except in tumor-bearing mice, where the radioactivity in tumor samples from mice treated with 6 or 60 mg/kg of ^{3}H- GM-CT-01 with or without 5-FU averaged approximately 72% remaining after 6 hours. Elimination of 3H- GM-CT-01 from the liver was more gradual than in other tissues, and on average, more than 50% of the radioactivity detected at one hour after injection was still present at 24 hours. 5-FU and GM-CT-01 work in a synergism when delivered into the tumor. This might explain why GM-CT-01 in a combination with 5-FU **increases efficacy** of the drug against COLO 205 human colon tumor, bearing by mice (see above).

At the same time, 5-FU and GM-CT-01 work as antagonists (apparently, compete with each other for the same binding sites in the liver) when delivered into the liver.

Statistical Analysis

Outlier Assessments. There were four outliers identified at the mice level. These outliers were:

- Two tumored mice at 24 hours, GM-CT-01 60 mg/kg; values were in the 0.000-0.002 range for liver, kidneys, lungs, tumor, and plasma.
- One tumored mouse at 1 hour, GM-CT-01 60 mg/kg + 5-FU 114 mg/kg; values consistently elevated relative to other values for liver, kidneys, lungs, tumor, and plasma.
- One non-tumored mouse at 1 hour, GM-CT-01 60 mg/kg; values consistently elevated relative to other values for liver, kidneys, lungs, and plasma.

No other outliers were identified at the organ, plasma, or tumor level. Analyses were run including and excluding these 4 mice.

Pooling Assessments. The goal was to test if:

1. Data from non-tumored and tumored mice could be merged for organs and plasma.
2. Both GM-CT-01 6 and 60 mg/kg doses data could be merged for organs, plasma, and for tumor.

As it was demonstrated by including outliers and excluding outliers, pooling is warranted for combining data for non-tumored and tumored mice for liver and lungs (the unpaired differences between non-tumored and tumored data are ≤0.02 for all treatment groups at 1, 6, and 24 hours), while kidneys and plasma remained skewed with higher levels in tumored mice after outlier removal (largest differences seen in the GM-CT-01 60 mg/kg groups at 1 hour). The key point is that pooling is justified for the non-tumored and tumored data for liver, the most critical organ. Pooled data for liver and lungs are provided in Table 7. Is it was shown, ANOVA analyses did not reject the null hypothesis of no difference (implying that the two series could be pooled) for each organ and plasma, despite the small sample sizes and low power.

Then, as it was demonstrated by including outliers and excluding outliers, pooling is warranted for combining GM-CT-01 doses of 6 mg/kg vs 60 mg/kg for tumors (<0.01 differences after outlier exclusions), while it is not as evident for lungs (up to 0.04 differences after outlier exclusions), liver (up to 0.06 differences after outlier exclusions), kidneys (up to 0.06 differences after outlier exclusions), and plasma (up to 0.07 differences after outlier exclusions). There was no skewing favoring either dose. The key point is that pooling is justified for the two GM-CT-01 doses for tumor, the other critical site for assessing uptake. ANOVA analyses confirmed the ability to pool GM-CT-01 6 mg/kg and 60 mg/kg data for each organ, plasma, and tumor.

Downloaded by STANFORD UNIV GREEN LIBR on June 14, 2012 | http://pubs.acs.org
Publication Date (Web): June 12, 2012 | doi: 10.1021/bk-2012-1102.ch004

Downloaded by STANFORD UNIV GREEN LIBR on June 14, 2012 | http://pubs.acs.org
Publication Date (Web): June 12, 2012 | doi: 10.1021/bk-2012-1102.ch004

Pooled data (across GM-CT-01 doses) for tumors were considered including outliers and excluding outliers. The resulting standard deviations of the combined tumor data (after GM-CT-01 doses pooling) were 0.0044 at 1 hour, 0.0333 at 6 hours, and 0.0057 at 24 hours after outlier exclusions; corresponding standard deviations for the GM-CT-01 + 5-FU group were 0.090 at 1 hour, 0.0141 at 6 hours, and 0.0014 at 24 hours after outlier exclusions. Higher levels were seen for GM-CT-01 + 5-FU versus pooled GM-CT-01 doses at 1 hour (0.032), at 6 hours (0.012), and at 24 hours (0.009); the 24 hour difference reached statistical significance after outlier exclusions. As it was found with including outliers and excluding outliers, statistical significance also held at 24 hours if data were limited to just the GM-CT-01 60 mg/kg group after outliers were excluded. Thus, **more GM-CT-01 reached the tumor in the presence of 5-FU**.

In summary, *in vivo* pharmacology studies indicate that GM-CT-01 enhances the antineoplastic effects of 5-FU. GM-CT-01 is not mutagenic, either by itself or combined with 5-FU, in bacterial reverse mutation assays. Toxicity studies in mice, rats and dogs have shown GM-CT-01 to have a very low potential for toxicity and a capacity for ameliorating some of the toxic side effects of 5-FU.

Compared to many other known polysaccharides, GM-CT-01 has multiple side-chain galactose units that should readily interact with galactose-specific receptors such as galectins on the tumor cell surface, modulate the tumor surface physiology and potentially affect delivery of 5-FU to the tumor.

To the best of our knowledge, (a) no simple sugar drugs, aimed at interactions with lectins, such as GM-CT-01, are available in clinical practice, (b) none of these carbohydrates are able to increase *in vivo* efficacy of known chemotherapy drugs, such as 5-FU, doxorubicin, or others, widely used in cancer chemotherapy, and (c) none of them are able to increase *in vivo* efficacy of any other drug when co-administered.

Clinical Studies, Phase I

January 27, 2003, a Phase I open-label study was initiated to evaluate the safety and tolerability of escalating doses of GM-CT-01 (30 mg/m^2 to 280 mg/m^2) in the presence and absence of 500 mg/m^2 5-FU in subjects with advanced solid tumors. This Clinical trial (NCT00054977) was completed in April 11, 2005. The study was conducted in the following locations: Florida Oncology Associates (Jacksonville, FL), Ochsner Cancer Institute (New Orleans, LA), University of Michigan Comprehensive Cancer Center (Ann Arbor, MI), Hematology/Oncology Private Practice (Howell, NJ), and Dartmouth-Hitchcock Medical Center (Lebanon, NH) [http://clinicaltrials.gov/ct2/show/NCT00054977]. The study had the official title: "**A Phase I Open-Label Study to Evaluate the Safety and Tolerability of Escalating Doses of DAVANAT (A Galactomannan Derivative) in the Presence and Absence of 5-Fluorouracil (5-FU) in Subjects With Advanced Solid Tumors**". Patients that were enrolled in the study were those who had different types of solid tumors, and who had failed standard, approved treatments. This study evaluated the tolerability of six rising doses of DAVANAT® alone ranging from 30 to 280 mg/m2 and then in combination with

Downloaded by STANFORD UNIV GREEN LIBR on June 14, 2012 | http://pubs.acs.org
Publication Date (Web): June 12, 2012 | doi: 10.1021/bk-2012-1102.ch004

5-FU (500 mg/m2) over 2 cycles of therapy. A total of 40 patients enrolled in the study.

The study type was interventional, the study design: treatment, non-randomized, open label, uncontrolled, single group assignment, safety/efficacy study. Types of cancer – colorectal, lung, breast, head and neck, and prostate cancer. Excluded were patients with central nervous system (CNS) metastases or primary CNS tumors.

Besides general eligibility criteria (at least 18 years of age, not pregnant or breast feeding, no current alcohol or illicit drugs abuse, patients having other significant medical, psychiatric, or social conditions which, in the investigators' opinion, may compromise the patient's safety in participating in this study, etc), enrolled patients should have had a documented histologic or cytologic recurrent or metastatic solid tumor that is not amenable to curative surgery, radiotherapy, or conventional chemotherapy of proven value. Also, patients must have had completed previous therapy (chemotherapeutic agents or other therapies including radiation) at least four weeks prior to study entry, the same time period must have been elapsed after a major surgery and patients must have been recovered from effects, at least two weeks must have elapsed after minor surgery, and the patient should have had a life expectancy of at least 12 weeks. Excluded from the study were the patients who had congestive heart failure or any other medical condition that could be adversely affected by intravenous infusion of up to approximately 200 mL of fluid over 60 minutes.

The study consisted of two cycles: different doses of GM-CT-01 (as described below) were given alone in Cycle 1, and in combination with 5-FU (500 mg/m^2) in Cycle 2. Patients were on study from February 10, 2003. In patients who had cancer that could be measured by MRI (magnetic resonance imaging) and CT (computerized tomography) scan, it was determined whether the tumors changed in size (got bigger, smaller or stayed the same) after Cycle 2.

The study was designed to determine:

- The Maximum Tolerated Dose (MTD) and Dose Limiting Toxicities (DLT) of GM-CT-01 alone.
- The safety and side effects of GM-CT-01 when given alone and in combination with 5-FU. To define the MTD and DLT of GM-CT-01 when administered concurrently with 500 mg/m^2 of 5-FU.
- To determine the pharmacokinetic profile of 5-FU in the presence of GM-CT-01.
- To determine the pharmacokinetic profile of GM-CT-01 (the effect of GM-CT-01 on the amount of 5-FU at different times in the body) at doses from 30 mg/m^2 to 280 mg/m^2 of GM-CT-01.
- The effect of GM-CT-01 plus 5-FU on tumor size in patients with measurable disease.

Patients had a screening period followed by two 28 day cycles. In cycle 1, GM-CT-01 alone was administered i.v. on days 1 to 4, and in cycle 2, 5-FU plus GM-CT-01 was administered on days 1 to 4, for a total of approximately 90 days on study.

Prior to administration of study drug, a female patient should have a negative pregnancy test. Besides, the patients should have had AST and ALT (liver function) < 2.5 times the upper limit of normal (ULN); total bilirubin < 1.5, hematopoietic parameters WBC > 3000 per mm3; granulocyte count > 1,500 per mm3; platelet count > 100,000 per mm^3, creatinine (renal) less or equal to ULN, and Dlco (pulmonary, carbon dioxide diffusing capacity) higher or equal 60% of predicted.

A letter directed to patients stated: "You have been invited to participate in a clinical research study because you have a solid tumor that has returned or a metastatic (spreading through your body) solid tumor that cannot be cured by surgery, radiotherapy, or standard chemotherapy. (….) The study will involve up to 40 subjects".

GM-CT-01 was supplied as a 60 mg/mL solution in normal saline with 10 mL contained in a single use glass vial which is stored at 4-8°C. Dose escalation was proceeded in cohorts of 3 patients with ascending doses of GM-CT-01 alone ranging from 30 to 280 mg/m^2 and in combination with 500 mg/m^2 5-FU.

According to the study schedule, three to six patients are to be entered into the study at each of six doses of GM-CT-01, or until the Maximum Tolerated Dose (MTD) is reached. Then, a total of ten patients are to be entered at this determined MTD, or at the highest dosing level if a MTD is not determined. A total time period for the participation for each patient was scheduled to approximately 90 days. If the cancer has not spread further, the patient would have received additional cycles of GM-CT-01 plus 5-FU.

An evaluation of tumor size was made by an MRI and/or CT scan (see above).

A more detailed schedule for a first cohort (30 mg/m^2 dose of GM-CT-01) was as follows (after a 30-day patients screening):

Cycle 1. Treatment of the first cohort (three to six patients) with GM-CT-01 alone (through an intravenous line into the vein once a day for 30 min for four consecutive days), record of all side effects

- Day 1 - blood laboratory tests (hematology, chemistry, coagulation)
- Day 1 - GM-CT-01 i.v. infusion at a starting dose of 30 mg/m^2
- Day 2 - GM-CT-01 i.v. infusion (30 mg/m^2)
- Day 3 - GM-CT-01 i.v. infusion (30 mg/m^2)
- Day 4 - blood laboratory tests (hematology, chemistry, coagulation)
- Day 4 - GM-CT-01 i.v. infusion (30 mg/m^2)
- Day 14 (±2) - blood laboratory tests (hematology and chemistry), record of all side effects
- Day 15-27 - Follow-up.
- Day 28(±2) - blood laboratory tests (hematology, chemistry, coagulation, pregnancy test if female), record of all side effects, limited physical examination, CEA (a special marker for cancer), electrocardiogram, a tumor evaluation, MRI and/or CT scan of the chest, abdomen and pelvis, a lung test, and record of adverse events.

Downloaded by STANFORD UNIV GREEN LIBR on June 14, 2012 | http://pubs.acs.org
Publication Date (Web): June 12, 2012 | doi: 10.1021/bk-2012-1102.ch004

Downloaded by STANFORD UNIV GREEN LIBR on June 14, 2012 | http://pubs.acs.org
Publication Date (Web): June 12, 2012 | doi: 10.1021/bk-2012-1102.ch004

If no side effects were noted that would have prevented the patient from proceeding to Cycle 2, the 5-FU/GM-CT-01mixture was administered through an intravenous line as follows:

Cycle 2. Treatment with GM-CT-01 (30 mg/m^2) in combination with 500 mg/m^2 of 5-FU (once a day for 30 min for four consecutive days), record of all side effects.

- Day 1 - blood laboratory tests (hematology, chemistry, coagulation)
- Day 1 - GM-CT-01/5-FU (30/500 mg/m^2) i.v. infusion, and a blood laboratory test to determine 5-FU concentration at different times following infusion: immediately following infusion (at 0 minutes), 5, 10, 20, 30, 45, 60 minutes, 2, 4, 6, and 8 hours after GM-CT-01 and 5-FU administration.
- Day 2 - GM-CT-01/5-FU (30/500 mg/m^2) i.v. infusion, and a blood laboratory test to determine 5-FU concentration immediately following the infusion
- Day 3 - GM-CT-01/5-FU (30/500 mg/m^2) i.v. infusion, and a blood laboratory test to determine 5-FU concentration immediately following the infusion
- Day 4 - blood laboratory tests (hematology, chemistry, coagulation)
- Day 4 - GM-CT-01/5-FU (30/500 mg/m^2) i.v. infusion, and a blood laboratory test to determine 5-FU concentration at different times during 8 hours following infusion, as indicated above.
- Day 14 (±2) - blood laboratory tests (hematology and chemistry), record of all side effects
- Day 15-27 - Follow-up.
- Day 28 - blood laboratory tests (hematology, chemistry, coagulation, pregnancy test if female), record of all side effects, limited physical examination, CEA (a special marker for cancer), electrocardiogram, a tumor evaluation, CT scan of the chest, abdomen and pelvis, a lung test, and record of adverse events.

Interpatient dose escalation was proceeded with the following doses of GM-CT-01: 30, 60, 100, 150, 210, and 280 mg/m^2. There was no intrapatient dose escalation of GM-CT-01. The dose of 5-FU remained at 500 mg/m^2 for all six cohorts throughout the study.

Chemistry included electrolytes (sodium, potassium, chloride, bicarbonate, calcium, phosphate), blood urea nitrogen (BUN), creatinine, total cholesterol, albumin, total protein, uric acid, lactate dihydrogenase (LDH), liver enzymes - aspartate aminotransferase (AST), alanine aminotransferase (ALT), alkaline phosphatase (ALK), total bilirubin, glucose, carcinoembrionic antigen (CEA).

Key pharmacokinetic parameters of 5-FU included an area under the plasma concentration-time curve (AUC), systemic clearance (CL), apparent volume of distribution (Vd), and eliminationhalf-time ($t_{1/2}$). Anti-tumor efficacy in patients with measurable disease was descriptively evaluated for response at the end of Cycle 2.

Table 8. Patients tolerance with respect to GM-CT-01 and GM-CT-01/5-FU doses in Cycles 1 and 2. 5-FU doses in Cycle 2 were of 500 mg/m^2

Dose of DAVANAT® (mg/m^2)	*Patients Enrolled*	*Diagnoses*	*Completed Cycle 1*	*Completed Cycle 2*	*DLT Event*
30	4	3 Colorectal 1 Hepatocellular	3	3	None
60	6	5 Colorectal 1 Hepatocellular	6	6	Grade 3
100	5	4 Colorectal 1 Pancreatic	5	3	ALT/ SGPT
150	3	2 Colorectal 1 Prostate	3	3	None
210	4	3 Colorectal 1 Ovarian	4	3	None
280	3	1 Colorectal 1 Pancreatic 1 Spindle Cell Tumor	3	2	None

Dose escalation of GM-CT-01 alone for the next cohort was proceeded after the preceding cohort (three to six patients) complete Cycle 1 with no patient experienced DLT. In this case the preceding cohort was advanced to Cycle 2, and the next cohort of three to six patients was escalated to next dose of GM-CT-01.

If, however, one of patients in the preceding cohort experienced DLT by Day 28 in Cycle 1, three more patients were added to the same dose level of GM-CT-01 alone, and six patients total were treated at the same dose and the remaining patients with no DLT were advanced to Cycle 2.

If two patients in the preceding cohort experienced DLT by Day 28 in Cycle 1, the dose escalation stopped and this current dose of GM-CT-01 was defined as MTD. If the drug was tolerated by five of six patients, the dose was escalated in the next cohort of three patients.

Once MTD is established (or highest dose was administered), total of ten patients were enrolled at MTD or the highest dose to further define the pharmacokinetics at this dose. Any new lung abnormality observed on CT scan was considered as DLT.

The same dose escalation criteria and assessment of DLT and MTD applied to GM-CT-01 alone was applied to the combination of each dose of GM-CT-01 plus 5-FU. When DLT was observed in one patient per cohort in Cycle 2 with the combination of GM-CT-01 plus 5-FU, then the subsequent cohort of patients completing Cycle 1 at the next dose level was de-escalated to the GM-CT-01 dose level at which DLT occurred in combination with 5-FU for their second cycle.

Downloaded by STANFORD UNIV GREEN LIBR on June 14, 2012 | http://pubs.acs.org
Publication Date (Web): June 12, 2012 | doi: 10.1021/bk-2012-1102.ch004

Of the first 25 patients with advanced solid neoplasms not amenable to curative surgery, radiotherapy, or chemotherapy of proven value, injected with GM-CT-01, 20 completed Cycle 2 of the study through November 2004.

Intravenous infusion of up to 280 mg/m^2 of DAVANAT® alone and in combination with 5-FU was found to be well tolerated (Table 8). DLT has not been reached at the final dose level of 280 mg/m^2. Toxicity of GM-CT-01 plus 5-FU were similar to those expected for 5-FU alone at this dose and schedule.

Response Evaluation Criteria in solid tumors at the end of Cycle 2 showed nine patients with stable disease, nine with progressive disease and two with non-measurable disease. Six of nine stabilized patients received additional cycles of GM-CT-01 plus 5-FU. It was also established that GM-CT-01 did not alter the pharmacokinetics of 5-FU in patient samples.

Downloaded by STANFORD UNIV GREEN LIBR on June 14, 2012 | http://pubs.acs.org
Publication Date (Web): June 12, 2012 | doi: 10.1021/bk-2012-1102.ch004

Clinical Studies, Phase II

A Phase II safety and efficacy clinical trial (NCT00110721) was initiated by Pro-Pharmaceuticals as a sponsor on May 1, 2005, completed on January 31, 2008, and conducted in the following locations: Hematology-Oncology Associates of the Treasure Coast (Port St. Lucie, FL), Ochsner Clinic Foundation (New Orleans, LA), University of Michigan Comprehensive Cancer Center (Ann Arbor, MI), Medical Oncology and Hematology (Waterbury, CT), Shaare Zedek Medical Center, Oncology (Jerusalem, Israel), and Soroka University Medical Center (Beer-Sheva, Israel) [http://clinicaltrials.gov/ct2/show/NCT00110721]. It had the official title: "**A Phase II, Multi-Center, Open-Label Trial to Evaluate the Efficacy and Safety of Intravenous DAVANAT in Combination With 5-Fluorouracil When Administered in Monthly Cycles as Third- or Fourth-Line Therapy for Metastatic Colorectal Cancer**". Patients that were enrolled in the study were those who had a histologically proven adenocarcinoma of the colon or rectum, and had documentation of locally advanced or metastatic colorectal cancer not amenable to curative surgery or radiotherapy, and had one or more measurable lesion(s) according to RESIST (Response Evaluation Criteria in Solid Tumors) criteria. Furthermore, eligible subjects were those who had unresectable, locally advanced and/or metastatic colorectal cancer that progressed during or after receiving treatment with at least two lines of therapy, which collectively must have included at a minimum all of the following agents: 5-FU or capecitibine, irinotecan, and oxaliplatin. Simply put, this Phase II experimental study using GM-CT-01 was their last resort. All preceding treatments with approved therapies failed in their cases. A standard dose of 280 mg/m^2 GM-CT-01 and 500 mg/m^2 5-FU was given in monthly cycles for at least two cycles, or until their disease progressed.

A total of 20 patients enrolled in the study. All (100%) patients had a primary diagnosis of colorectal cancer, and all (100%) patients had received prior therapy for their cancer, as indicated above. As reported in the "Final Clinical Study Report, Phase II Study, IND Number 64,034 of January 31, 2008", "no patient died on study". An additional principal quotation from the clinical study report is as follows: "No apparent trend was seen with regard to change from Baseline in any clinical laboratory parameter during treatment with GM-CT-01/5-FU" (the Report, Summary of Safety, p. 1010). Mucositis as a Severe Adverse Event is not mentioned in the Report, since monitoring for this indication, unless it is grade 3 or 4, was not performed for this Phase II trial, as well as the aforementioned Phase I trial. In other words, no mucositis of grade 3 or 4 was observed in Phase I and II of the study. More details on mucositis in the patients are given in the following section.

Other milestones of the both studies were as follows:

(a) GM-CT-01 was non-toxic, and a DLT (dose limiting toxicity) was not reached,
(b) 70% of the patients were stabilized at highest GM-CT-01 dose level (280 mg/m^2/day) level,
(c) when co-administered with GM-CT-01, the half-life of 5-FU increased in the bloodstream of the patients from 6-22 min (historical data for 5-FU alone) to 28-137 min,
(d) a 46% increase in longevity of the patients (based on the Median Overall Survival) was achieved compared with the Best Standard of Care,
(e) a 41% reduction of SAE (Serious Adverse Effects) was achieved compared to the Best Standard of Care.

Downloaded by STANFORD UNIV GREEN LIBR on June 14, 2012 | http://pubs.acs.org
Publication Date (Web): June 12, 2012 | doi: 10.1021/bk-2012-1102.ch004

It should be emphasized that all the patients in the Phase I and II clinical trials were those who failed their prior cancer therapies including 5-FU, Xeloda®, Avastin®, Erbitux®, oxaliplatin, irinotecan. The majority of them had colorectal cancer (53%), following up with pancreatic cancer (13%) and other, such as hepatocellular, biliary (cholangiocarcinoma), gastric, breast, ovarian, appendiceal, testicular, prostate, and unknown primary cancers. 60% of the patients failed prior surgery, and 30% failed prior radiotreatment. 100% of the patients in Phase II have failed prior chemotherapy and/or other systemic therapies. 58% of the patients failed prior 5-FU treatment.

Among the key inclusion criteria were one or more measurable lesion(s) according to RESIST criteria, ECOG performance status of 2 or less, and life expectancy of 3 months or more. There were 40 end-stage patients in Phase I, and 20 end-stage patients in the Phase II clinical studies. 43% of the patents treated with the GM-CT-01-5-FU combination showed Objective Response with more than 30% tumor shrinkage. With such inclusion criteria, the 46% increase of longevity of the patients and 41% drop in serious adverse effects, which were reduced to common adverse events, such as general gastrointestinal disorders (nausea, vomiting, diarrhea, constipation, fatigue), as well as the observation that GM-CT-01 co-administered with 5-FU did not appear to be associated with any systematic changes in biochemical indications of the patients, can be considered as a truly remarkable achievement. Based on these data, objections for Galectin Therapeutics to move into a Phase III clinical trial was not expressed by the FDA.

Downloaded by STANFORD UNIV GREEN LIBR on June 14, 2012 | http://pubs.acs.org
Publication Date (Web): June 12, 2012 | doi: 10.1021/bk-2012-1102.ch004

A Note on Mucositis

Overall, 97 cancer patients have been treated with a regimen including GM-CT-01 and 5-FU. Together, 60 patients were treated in the aforementioned Phase I (NCT00054977, 40 patients) and Phase II (NCT00110721, 20 patients) trials. In another Phase II trial, which was a first line study for patients diagnosed with Cholangiocarcinoma ("Study to Test the Benefit and Safety of GM-CT-01 in Combination With 5-FU to Treat Bile Duct and Gall Bladder Cancer", NCT00386516, http://clinicaltrials.gov/ct2/show/NCT00386516), 20 patients were treated at three US sites that included Boston Medical Center (Boston MA), University of Michigan Comprehensive Cancer Center (Ann Arbor, MI), Barrett Cancer Center (Cincinnati, OH), and Tampa General Hospital (Tampa, FL). In another Phase II trial, which was a first Line study for patients diagnosed with Colorectal Cancer ("A new Agent DAVANAT in Combination With 5-FU, Avastin and Leucovorin in Subjects With Colorectal Cancer", NCT00388700, http://clinicaltrials.gov/ct2/show/NCT00388700, 10 patients were treated at four sites in Israel that included Sheba Medical Center (Tel Hashomer), Kaplan Medical Center (Rechovot), Rambam Medical Center (Haifa), and Sourasky Medical Center (Tel Aviv).

Lastly, to date, Galectin Therapeutics has sponsored 7 patients for treatment in compassionate use studies. All the Phase I, Phase II, and compassionate use studies were conducted according to regimens developed by Galectin Therapeutics. 280 mg/m^2 of GM-CT-01 and 500 mg/m^2 of 5-FU were administered i.v. for 30 min, and the procedure was repeated four days in a row. Then, after a 28-day break, the procedure was repeated, or the patient was discharged. Besides standard biochemical tests (AST and ALT, total bilirubin, hematopoietic parameters, WBC, RBC, platelet count, hemoglobin, granulocyte count, creatinin, Dlco, etc.), effect of GM-CT-01/5-FU on mortality and ancillary clinical indications, including Eastern Cooperative Oncology Group (ECOG) performance status, quality of life, carcinoembrionic and antigen (CEA) levels were monitored in accordance with the FDA requirements

Remarkably, **not a single case of mucositis of grade 3 or 4 was observed**. As such, SAEs reportable to the FDA were not encountered for mucositis. Furthermore, according to literature, even lower doses of 5-FU, such as 370 mg/m^2 and 360-480 mg/m^2 (*13*, *14*) caused mucositis, up to grade 3 and 4.

Specifically, data on mucositis in all the 97 patients are as follows:

In Phase I, 40 patients were treated with GM-CT-01 (30 to 280 mg/m^2) and 5-FU (500 mg/m^2). 21 of them were male and 19 were female. 35 of them (~88%) were Caucasian, four (10%) were African American, and one was Hispanic. The median age was 64.5 years and ranged from 35 to 82 years. Adverse effects were all reported to the FDA, and included anemia, dehydration, gastrointestinal disorders (nausea, diarrhea, vomiting, abdominal pain, constipations, abdominal distention, dyspepsia, flatulence), general disorders (fatigue, pyrexia, asthenia), infections and infestations (urinary tract infection, rhinitis), weight decrease, anorexia, back pain, arthralgia, nervous system disorders (headache, dizziness, neuropathy), respiratory, thoracic, and mediastinal disorders (dyspnoea, cough), skin and subcutaneous tissue disorders (rash, palmar-plantar erythrodysaesthesia syndrome), as well as others. Serious adverse events (grades 3 and 4) included anemia, dehydration, hemorrhage, severe abdominal pain, constipation, nausea, and vomiting. Only two of the events, anemia and dehydration, were classified as "possibly related" to the treatment. Mucositis was not among them. In fact, only three subjects out of 40 (7.5%) had a mild form of mucositis: one, grade 2, "severity – mild", 500 mg/m^2 of 5-FU + 280 mg/m^2 of GM-CT-01; another, grade 1, 500 mg/m^2 + 60 mg/m^2 of GM-CT-01, and third, grade 2, "severity – moderate", 500 mg/m^2 + 280 mg/m^2 of GM-CT-01.

In other studies – Phase II, Third or Fourth-Line Therapy for Metastatic Colorectal Cancer, with 20 patients enrolled (NCT00110721); Phase II, Colorectal Cancer in Patients Unable to Tolerate Intensive Chemotherapy, with 10 patients enrolled (NCT00388700); Phase II, Gall Bladder and Bile Duct Cancer, with 20 patients enrolled (NCT00386516); and Compassionate Use Trials (EIND) with 7 patients treated - there was not a single case of mucositis grades 3 and 4 reported. In all these studies, 5-FU/ GM-CT-01 at dose 500 mg/m^2-280 mg/m^2 was employed, except the study NCT00386516, in which 600 mg/m^2 of 5-FU was used (with 280 mg/m^2 of GM-CT-01). Therefore, total only 3 cases of mild mucositis (grades 1 and 2) were observed in 97 patients. This can be compared to the data of a clinical trial (54,74) in which 61% of the patients had mucositis of grade 2, and 78% of grades 2-4 in the control group, treated with 5-FU.

Hence, data in progress show that GM-CT-01/5-FU is well tolerated and dose limiting toxiciy was not reached in this study. Disease was stabilized in 45% of the initial 20 patients who completed the trial through November 2004. The tolerability of GM-CT-01 given with 5-FU warrants further testing for safety and efficacy in a Phase II clinical trial.

Downloaded by STANFORD UNIV GREEN LIBR on June 14, 2012 | http://pubs.acs.org
Publication Date (Web): June 12, 2012 | doi: 10.1021/bk-2012-1102.ch004

Note

This is an updated version of a chapter that previously appeared in *Carbohydrate Drug Design* (ACS Symposium Series 932), edited by Klyosov et al. and published in 2006.

Acknowledgments

We thank colleagues from Southern Research Institute (SRI) and Charles River Laboratories for conducting animal studies, Drs. Yulia Maxuitenko (SRI, Birmingham, AL) and Philip T. Lavin (Averion, Framingham, MA) for conducting statistical analysis of the data, Drs. Mildred Christian and Robert Diener (Argus International, Horsham, PA) for discussing the data and the manuscript, and Drs. Marilyn Pike, Jyotsna Fuloria, Yousif Abubaker, Raymond Perez, and Merk Zalupsli for conducting clinical trials of GM-CT-01.

References

1. Miller, M. C.; Klyosov, A. A.; Mayo, K. H. The α-galactomannan Davanat binds galectin-1 at a site different from the conventional galectin carbohydrate binding domain. *Glycobiology* **2009**, *19*, 1034–1045.
2. Demotte, N.; Wieers, G.; Klyosov, A.; van der Bruggen, P. Is it possible to correct the impaired function of human tumor-infiltrating lymphocytes? Presented at Keystone Symposium on Molecular and Cellular Biology. New Frontiers at the Interface of Immunity and Glycobiology; March 6−11, 2011; Lake Louise, AB, Canada; Abstract 23F11.
3. *The World Almanac and Book of Facts*; 2010; p. 155.
4. Some Antineoplastic and Immunosuppressive Agents. WHO, International Agency for Research on Cancer. *IARC Monographs on the Evaluation of the Carcinogenic Risk of Chemicals to Humans*; 1981;Vol. 26, pp 217− 235.
5. *Novel Approaches to Selective Treatments of Human Solid Tumors: Laboratory and Clinical Correlation*; Advances in Experimental Medicine and Biolology Series; Rustum, Y. M., Ed.; Plenum Press: 1994; Vol. 339, p 319.
6. Klyosov, A. A.; Platt, D.; Zomer, E. Preclinical studies of anticancer efficacy of 5-Fluorouracil when co-administered with the 1,4-β-D-galactomannan. *Preclinica* **2003**, *1*, 175–186.
7. Appukuttan, P. S. Terminal alpha-linked galactose rather than N-acetyl lactosamine is ligand for bovine heart galectin-1 in N-linked oligosaccharides of glycoproteins. *J. Mol. Recognit.* **2002**, *15*, 180–187.
8. Chacko, B. K.; Appukuttan, P. S. Peanut (Arachis hypogaea) lectin recognizes alpha-linked galactose, but not N-acetyl lactosamine in N-linked oligosaccharide terminals. *Int. J. Biol. Macromol.* **2001**, *28*, 365–371.
9. Stowell, S. R.; Dias-Baruffi, M.; Pentilla, L.; Renkonen, O.; Kwame Nyame, A.; Cummings, R. Human galectin-1 recognition of poly-N-acetyllactosamine and chimeric polysaccharides. *Glycobiology* **2004**, *14*, 157–167.
10. Miller, M. C.; Nesmelova, I. V.; Platt, D.; Klyosov, A. A.; Mayo, K. H. The carbohydrate-binding domain on galectin-1 is more extensive for a complex glycan than for simple saccharides: implications for galectin-glycan interactions at the cell surface. *Biochem. J.* **2009**, *421*, 211–221.
11. Barondes, S. H.; Castronovo, V.; Cooper, D. N. W.; Cummings, R. D.; Drickamer, K.; Feizi, T.; Gitt, M. A.; Hirabayashi, J.; Hughes, C.; Ken-ichi, K.; Leffler, H.; Liu, F. T.; Lotan, R.; Mercurio, A. M.; Monsigny, M.; Pillai, S.; Poirer, F.; Raz, A.; Rigby, P. W. J.; Rini, J. M.; Wang, J. L. Galectins: A Family of Animal β-Galactoside-Binding Lectins. *Cell* **1994**, *76*, 597–98.
12. *Galectins*; Klyosov, A. A., Witzhak, Z. A., Platt, D., Eds.; John Wiley & Sons: 2008, p 279.
13. Di Paolo, A.; Danesi, R.; Falcone, A.; Cionini, L.; Vannozzi, F.; Masi, G.; Allegrini, G.; Mini, E.; Bocci, G.; Conte, P. F.; Del Tacca, M. Relationship between 5-fluorouracil disposition, toxicity and dihydropyrimidine

Downloaded by STANFORD UNIV GREEN LIBR on June 14, 2012 | http://pubs.acs.org
Publication Date (Web): June 12, 2012 | doi: 10.1021/bk-2012-1102.ch004

dehydrogenase activity in cancer patients. *Ann. Oncol.* **2001**, *12*, 1301–1306.

14. Malet-Martino, M.; Martino, R. Clinical studies of three oral prodrugs of 5-fluorouracil (capecitabine, UFT, S-1): A review. *The Oncologist* **2002**, *7*, 288–323.

Downloaded by STANFORD UNIV GREEN LIBR on June 14, 2012 | http://pubs.acs.org
Publication Date (Web): June 12, 2012 | doi: 10.1021/bk-2012-1102.ch004

Downloaded by STANFORD UNIV GREEN LIBR on June 13, 2012 | http://pubs.acs.org
Publication Date (Web): June 12, 2012 | doi: 10.1021/bk-2012-1102.ch005

Chapter 5

Synthesis and Biological Activity of Galactomycin and DoxoDavanat, New Conjugates of Doxorubicin with D-Galactose and 1,4-β-D-Galactomannan

**Anna N. Tevyashova,[1] Anatole A. Klyosov,[2,*] Eugenia N. Olsufyeva,[1]
Maria N. Preobrazhenskaya,[1] and Eliezer Zomer[2]**

**[1]Gause Institute of New Antibiotics, Russian Academy of Medical Sciences,
Moscow 119021, Russia
[2]Galectin Therapeutics Inc., 7 Well Avenue, Newton, MA 02459
*Klyosov@galectintherapeutics.com**

An overview of structure and antitumor properties of anthracyclines is presented, with examples of daunorubicin, doxorubicin, carminomycin, idarubicin, pyrromycin, musettamycin, and marcellomycyn, which are widely used in the treatment of numerous solid tumors and hematological malignancies. Anthracycline antibiotics consist of an aglycone and a sugar moiety, while the aglycone consists of a tetracyclic ring with adjacent quinone-hydroquinone groups in rings C-B, and the sugar is attached by a glycoside bond at the C-7 of the ring A. In the case of said antibiotics the sugar moiety is called daunosamine (2,3,6-tridesoxy-3-amino-L-*lyxo*-hexapyranose). Each of said anthracyclines has its own therapeutic profile, as well as a toxicity profile, and – among other properties – a profile of multi-drug resistance of tumor cells, mediated by a decreased intracellular drug accumulation. In order to alleviate those undesirable features of both the drugs and the tumor cells, chemical modification of anthracycline antibiotics has been undertaken in this work, as ac promising direction in drug design. The main reason is that the carbohydrate moiety in anthracycline antibiotics is recognized by the tumor cells which makes it crucial for the cytotoxic activity of the drugs, directed at a nuclear enzymes DNA topoisomerases I and II that in

In Glycobiology and Drug Design; Klyosov, A.;
ACS Symposium Series; American Chemical Society: Washington, DC, 2012.

Downloaded by STANFORD UNIV GREEN LIBR on June 13, 2012 | http://pubs.acs.org
Publication Date (Web): June 12, 2012 | doi: 10.1021/bk-2012-1102.ch005

turn involved in the processes of replication, transcription and recombination of DNA. We have synthesized a series of new N-substituted derivatives of doxorubicin and carminomycin, including doxorubicin derivatives containing D-galactose with hydrophilic (1-deoxyglucit-1-yl) or hydrophobic (benzyl or 3-methoxybenzyl) spacers, and test their cytotoxic and antitumor activities in comparison with the parent antibiotics. Up to now no methods for the conjugation of the 3′-amino group of daunosamine moiety with aldoses have been published. Compound Galactopyranosyl-(1→6)-*O*-1-deoxy-*D*-glucit-1-yl]doxorubicin, that showed the best antitumor properties, was named Galactomycin. It was two orders of magnitude less cytotoxic than doxorubicin for murine leukemia L1210/0 cell line. The developed type of modification of anthracycline antibiotics did not influence the ability of the drug to kill tumor cells which are resistant to doxorubicin. Importantly, novel derivatives of doxorubicin and 14-hydroxycarminbomycin were much better soluble in water in comparison with the parent antibiotics. Furthermore, the introduction of substituents containing hydroxyl groups into the amino group of daunosamine moiety of the anthracycline increases the ability of antibiotics to inhibit topoisomerase I. *In vivo* studies the maximum tolerated dosages were 40-60 mg/kg for Galactomycin (single i.v. injection, BDF_1 mice ($C_{57}Bl$ x DBA_2, males), as compared to 7-10 mg/kg for doxorubicin. The antitumor activity for these compounds was studied on mice bearing lymphocyte leukemia P-388 at single and multiple (q2d x 3) i.v. injection regimens. Remarkably, Galactomycin did not show any cumulative toxic effect at the triple dose of 40 mg/kg (120 mg/kg total dose), and induced ILS equal to 133%. Hence, Galactomycin may be of interest for supportive therapy. Since it was shown that DAVANAT®, a modified galactomannan of plant origin (see Chapters 3 and 4 in this book) increases efficacy and reduces toxicity of 5-Fluorouracil (5-FU) we have synthesized a conjugate of doxorubicin and galactomannan that would act like a double prodrug, that is liberating both doxorubicin and DAVANAT® in *in vivo* conditions and, importantly, in proximity to galactose/mannose specific receptors. This Chapter describes synthesis and biological activity of two DAVANAT®-doxorubicin conjugates (DoxoDavanat-1 and -2), and resulting from (a) a direct covalent binding of the two compounds, and (b) the linking of doxorubicin to DAVANAT® *via* a L-lysyl-bridge. It was shown that the both DoxoDavanat derivatives are much less cytotoxic compared Doxorubicin.

Introduction

Anthracyclines are members of a very important class of antitumor agents that have been used for many years in the treatment of numerous solid tumors and hematological malignancies. First anthracycline antibiotics, daunorubicin (**1**, Fig. 1) and doxorubicin (**2**, Fig. 1), have been isolated early in the 1960s and are still widely used for cancer chemotherapy (*1*, *2*). Anthracycline antibiotics consist of an aglycone and a sugar moiety. The aglycone consists of a tetracyclic ring with adjacent quinone-hydroquinone groups in rings C-B. The sugar is attached by a glycoside bond at the C-7 of the ring A. In the case of daunorubicin (**1**), doxorubicin (**2**), carminomycin (**3**) and idarubicin (**4**), which have differences in the aglycone part of the molecule, the sugar moiety is called daunosamine (2,3,6-tridesoxy-3-amino-L-*lyxo*-hexapyranose).

Doxorubicin (**2**, Fig. 1), which is a 14-hydroxyl derivative of daunorubicin (**1**), is one of the most widely used chemotherapeutic agents (*3*, *4*). Doxorubicin is an essential component of treatment of breast cancer, childhood solid tumors, soft tissue sarcomas, while daunorubicin is used mainly in treatment of acute lymphoblastic or myeloblastic leukemia. Carminomycin (**3**, Fig. 1) is an active antitumor natural anthracycline antibiotic, which differs from daunorubicin by the absence of methyl group in the 4-position of the aglycone moiety. Carminomycin proved to be active for the treatment of metastatic breast cancer, soft tissue sarcomas and acute lymphoblastic or myeloblastic leukemia (*5*). Idarubicin (**4**, Fig. 1), an analog obtained from daunorubicin after removal of the 4-methoxy group in the ring D, is active for the treatment of acute myelogenous leukemia, multiple myeloma, non-Hodgkin's lymphoma, and breast cancer (*6*). The broader spectrum of activity of idarubicin compared with daunorubicin may be attributed to increased lipophilicity and cellular uptake.

A natural disaccharide compound 4′-O-α-daunosaminyl-daunorubicin (**5**, Fig.1) is known, in which a second daunosamine residue is bound by α(1→4) glycosidic linkage to the first one; however, the second sugar in this case does not provide improvement in cytotoxic or antitumor activity [(*2*), pp. 38-46; (*7*)]. On the contrary, it was shown that natural mono-, di- and three-saccharide derivatives of ε-pyrromycinone (Fig.2), namely pyrromycin (**6**), musettamycin (**7**) and marcellomycin (**8**) possess a progressively increased antitumor activity with the increase in the length of the oligosaccharide chain.

Pyrromycin (**6**) contains a 3′-amino sugar (L-rhodosamine, or N,N-dimethyl-L-daunosamine) chemically attached via α(1→4) linkage to 7-hydroxy group of the cyclohexene ring (such as in doxorubicin); the addition of a second sugar residue, 2-deoxy-L-fucose, at the 4′-position of the first aminated sugar makes musettamycin (**7**), and a further addition of a third sugar residue, also 2-deoxy-L-fucose, at the 4′-position of the second sugar makes marcellomycin (**8**) (*7*, *8*). The authors note that the increase in the length of the oligosaccharide chain in this series of natural anthracyclines is correlated with an increase in their DNA-binding affinity. However, DNA-binding activity of trisaccharide derivatives of the pyrromycinone series does not correlate with its antitumor potency.

Downloaded by STANFORD UNIV GREEN LIBR on June 13, 2012 | http://pubs.acs.org
Publication Date (Web): June 12, 2012 | doi: 10.1021/bk-2012-1102.ch005

Downloaded by STANFORD UNIV GREEN LIBR on June 13, 2012 | http://pubs.acs.org
Publication Date (Web): June 12, 2012 | doi: 10.1021/bk-2012-1102.ch005

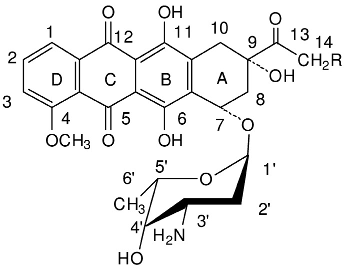
O
OH
O
1
12
11
10
9
13
14
2
CH2R
D
C
B
A
OH
3
8
4
5
6
7
O
OCH3
O
OH
6'
5'
O
1'
CH3
2'
4'
3'
H2N
HO

1. R = H, Daunorubicin
2. R=OH, Doxorubicin

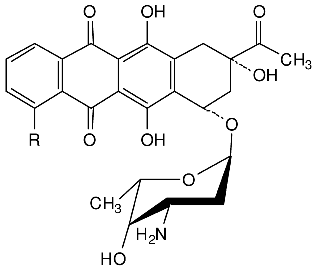
O
OH
O
CH3
OH
O
R
O
OH
O
CH3
H2N
HO

3. R=OH, Carminomycin
4. R=H, Idarubicin

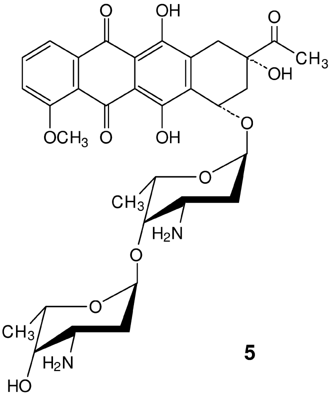
O
OH
O
CH3
OH
O
OCH3
O
OH
O
CH3
H2N
O
O
CH3
H2N
HO

5

*Figure 1. Structure of anthracycline antibiotics (## **1-5**).*

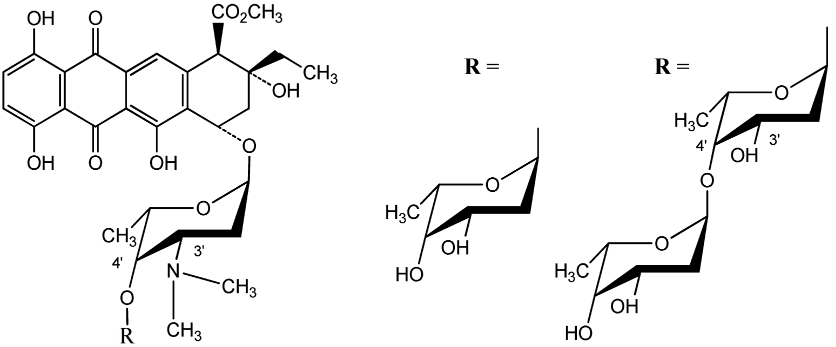
OH
O
CO2CH3
CH3
OH
OH
O
OH
O
O
CH3
3'
4'
N
CH3
O
R
CH3
R =
O
H3C
OH
HO
R =
O
H3C
4'
OH
3'
O
O
H3C
OH
HO

6. **R =H**, **Pyrromycin** 7. **Musettamycin** 8. **Marcellomycin**

*Figure 2. Structures of anthracycline antibiotics (## **6-8**).*

Downloaded by STANFORD UNIV GREEN LIBR on June 13, 2012 | http://pubs.acs.org
Publication Date (Web): June 12, 2012 | doi: 10.1021/bk-2012-1102.ch005

The mechanism by which anthracyclines inhibit cancer is still not completely clear and multiple pathways are thought to be involved in the cytotoxicity of this class of anticancer drugs (*9*). Antibiotics interfere with cell replication, by acting on DNA at several levels showing an effect in every phase of the cell cycle. It is likely that the therapeutic activity of anthracyclines is mediated by their insertion into the DNA of replicating cells and inhibition of topoisomerase I and II enzymes (*10*), thereby preventing DNA and RNA synthesis. Anthracyclinone part of the anthracyclines is responsible for the DNA intercalation, while the daunosamine moiety and the cyclohexene ring take part in minor groove binding and interaction with enzymes.

In addition to the desired effect of destroying cancer cell, anthracicline antibiotics, and Doxorubicin among them, also damage non-cancer cells resulting in side effects for the patient. These side effects limit the dose and duration of treatment with these agents.

The toxic effects of therapy with anthracyclines include nausea and vomiting, alopecia totalis (especially for doxorubicin) and myelosupresion. The most serious effect of multiple anthracycline administration is myocardial degeneration, causing congestive cardiac failure which has limited the therapeutic potential of these drugs (*11–15*).

The other serious problem is multi-drug resistance (MDR) of tumor cells to cytostatic agents, including anthracyclines, mediated by a decreased intracellular drug accumulation (*16*). This phenomenon is mediated by ATP binding cassette transporters that efflux their substrates out of the cell. In the growing list of these transporters, P-glycoprotein (Pgp, ABCB1), a 140-170 kDa plasma membrane associated pump, remains a major molecular determinant of MDR. Another mechanism of MDR initiation is alterations of the genes and the proteins involved into the control of apoptosis (especially p53 and Bcl-2) (*6*).

Because of the toxicity associated with anthracyclines, especially the dose-related cardiomyopathy, and problem of the resistance of the tumor cells to existing drugs, an extensive search has been made for anthracycline analogs that are free of cardiotoxicity and/or are active against MDR-tumor cells. One of the promising directions of chemical modification of anthracycline antibiotics is modification of the sugar residue. The carbohydrate moiety is an essential fragment of anthracycline antibiotics; it is recognized to be crucial for the cytotoxic activity of anthracyclines, directed at a nuclear enzymes DNA topoisomerases I and II that in turn are involved in the processes of replication, transcription and recombination of DNA. Several studies have been carried out aiming at chemical modification of carbohydrate moiety of the anthracyclines in hope to enhance the recognition potential of the drug at the target level.

One of the approaches aiming at obtaining anthracycline derivatives with better chemotherapeutical index is synthesis of different conjugates of anthracyclines with carbohydrates.

Novel anthracyclines with disaccharides lacking the amino group in the first (aglycone linked) sugar, were designed (Fig. 3, **9a,b-11a,b**) (*17–24*). The 3′-amino group in the first sugar was replaced by a hydroxyl group, and the second sugar residue was bound to the first one *via* an α(1→4) linkage.

Downloaded by STANFORD UNIV GREEN LIBR on June 13, 2012 | http://pubs.acs.org
Publication Date (Web): June 12, 2012 | doi: 10.1021/bk-2012-1102.ch005

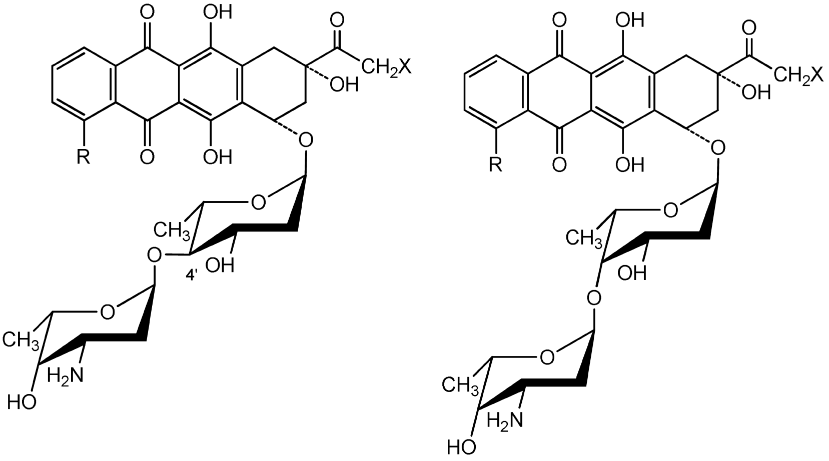

9a. **R = OCH_3, X = H;**
10a. R = X = H;
11a. R = H, X = OH

9b. **R = OCH_3, X = H;**
10b. R = X = H;
11b. R = H, X = OH, (MEN 10755)

Figure 3. Structures of anthracycline antibiotics (## 9a,b-11a,b).

Analogs of daunorubicin (**9a,b**), idarubicin (**10a,b**) and 4-demethoxy-doxorubicin (**11a,b**) in which daunosamine residue was substituted with the disaccharide L-daunosaminyl-α-(1→4)-2-deoxy-L-rhamnosyl (**a**-series) or L-daunosaminyl-α-(1→4)-2-deoxy-L-fucosyl (**b**-series), with the rhamnosyl and fucosyl residues directly linked to the aglycone *via* α(1→4) linkage were obtained (*17–24*). *In vitro* studies of the antitumor activity (using large panel of human tumor cell lines of different histotypes) of the obtained compounds revealed that in most cases the substitution of the daunosamine for the disaccharide moiety dramatically reduced cytotoxicity, by 20 to 1000 times. The only idarubicin derivative, 3′-(L-daunosaminyl-α-(1→4)-2-deoxy-L-fucosyl)-idarubicin (**10b**), conferred a cytotoxic potency and antitumor efficacy (on mice bearing cervical carcinoma and ovarian carcinoma) not significantly lower than that of doxorubicin (*21*). Further studies showed that doxorubicin analog, 4-demethoxy-3′-(L-daunosaminyl-α-(1→4)-2-deoxy-L-fucosyl)-doxorubicin (MEN 10755, Sabarubicin) (**11b**) was the best candidate in this series of disaccharide anthracycline analogs. This new compound showed comparable or higher cytotoxic activity and antitumor efficacy compared to doxorubicin, but also a reduced accumulation compared with the latter in all tissues investigated, such as heart, kidney, liver (*16*, *21*). The high antitumor activity of MEN-10755 in human tumor xenografts, including doxorubicin-resistant xenografts, and its unique pharmacological and biological properties made this novel disaccharide analogue an interesting candidate for clinical evaluation. MEN 10755 (**11b**) is currently investigated in phase II clinical trial (*25*, *26*). It was demonstrated that sabarubicin (MEN 10755) has significant single agent anti-cancer activity, and is well tolerated, in patients with extensive stage small cell lung cancer (*26*).

Another approach is based on usage of various conjugates of anthracyclines with carbohydrates as anthracycline prodrugs. Upon activation, the prodrugs are undergoing spontaneous reaction leading to formation of active anti-cancer drugs. The authors' principal premise is that doxorubicin and its analogs modified at the 3′-amino group are inactive, and their cytotoxic activity develops only after the hydrolysis of the ester or glycoside group and "activation" of the pro-drug to active drug.

A monosaccharide moiety is generally attached to 3′-amino group of the daunosamine through self-eliminating benzyloxycarbonyl spacer. These prodrugs were designed as a part of a two-step directed enzyme prodrug therapy (DEPT). Anthracycline pro-drugs, designed for their activation by human glucosidases, including glucuronidases and esterases were described (*27*, *28*).

For example, anthracycline prodrugs as possible substrates for human β-glucuronidase, contain *p*-hydroxybenzyloxycarbonyl spacer incorporated between the anthracycline moiety and β-glucuronic acid (for example, daunorubicin prodrug **11**, Fig. 4) (*27*).

The spacer is self-eliminated after hydrolysis by β-glucuronidase *via* 1,6-elimination. These prodrugs showed a 100-fold reduction in toxicity *in vitro* when compared to doxorubicin. *In vivo* data suggested that these pro-drugs were much less toxic compared to the parent agent (daunorubicin or doxorubicin respectively) and showed a somewhat better chemotherapeutic activity compared to the parent antibiotic. However, as noted in (*28*), these prodrugs did not make it to the clinic due to problems of large doses required and increased cost of synthesis.

A similar approach was used for the design of the anthracycline prodrugs, activated by *E. coli* β-galactosidase. Self-eliminating *p*-hydroxybenzyloxycarbonyl spacer (with different substituents in aromatic moiety or without them) was incorporated between the anthracycline moiety and β-galactose (for example, daunorubicin prodrug **13**, Fig.5) (*29*). These prodrugs were nearly one million-fold more toxic to human A375 melanoma cells in culture in the presence of *E. coli* β-galactosidase than in the absence of the enzyme (*30*). However, antitumor evaluation of these analogs in the experiments *in vivo* was not published, probably because of the complexity of localization of the enzyme in tumor.

Serious disadvantages, such as increased cost of the synthesis, large doses required, problems with the localization of the enzyme used for the prodrug activation and others, limit the use of such prodrugs.

Another interesting approach for improving targeted delivery of anthracyclines to a given neoplasm may be that of linking the drug to polymers recognized by receptors expressed in that particular tumor. It should be noted that polymer conjugation is of increasing interest in pharmaceutical chemistry as vehicle for target delivery of drugs having biological or physicochemical limitations (*31*). These compounds may show extended circulating life *in vivo* and, more importantly, make use of the enhanced permeability and retention effects observed in tumor cells. Currently many polymer-conjugated drugs,

Downloaded by STANFORD UNIV GREEN LIBR on June 13, 2012 | http://pubs.acs.org
Publication Date (Web): June 12, 2012 | doi: 10.1021/bk-2012-1102.ch005

including anthracycline polymeric pro-drugs, are investigated. Among them are monoclonal antibodies, polyethylene glycol, polyglutamate. Polysaccharides are among the most prospective candidates for polymeric carriers.

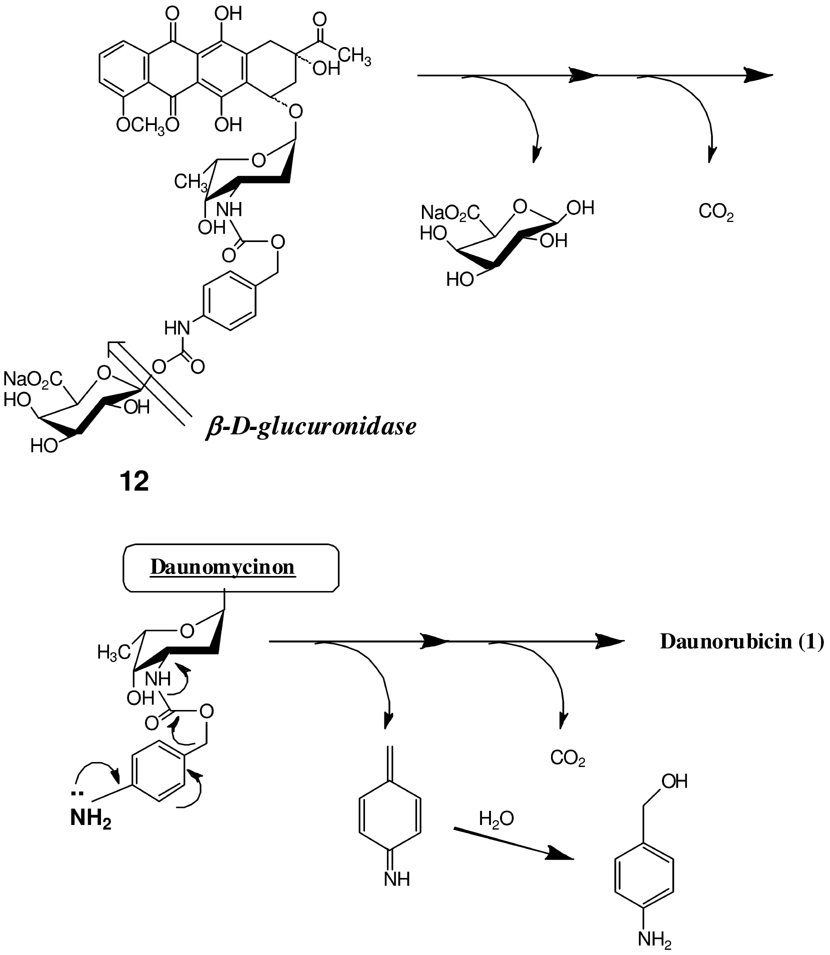
O
OH
O
CH3
OH
OCH3O
OH
O
O
CH3
NH
OH
O
O
HN
O
O
NaO2C
O
HO
OH
HO
β-D-glucuronidase
12
NaO2C
O
OH
HO
OH
HO
CO2
Daunomycinon
H3C
O
NH
OH
O
O
NH2
Daunorubicin (1)
NH
CO2
H2O
OH
NH2

*Figure 4. Activation of β-glucuronide daunorubicin prodrug (# **12**).*

Downloaded by STANFORD UNIV GREEN LIBR on June 13, 2012 | http://pubs.acs.org
Publication Date (Web): June 12, 2012 | doi: 10.1021/bk-2012-1102.ch005

Downloaded by STANFORD UNIV GREEN LIBR on June 13, 2012 | http://pubs.acs.org
Publication Date (Web): June 12, 2012 | doi: 10.1021/bk-2012-1102.ch005

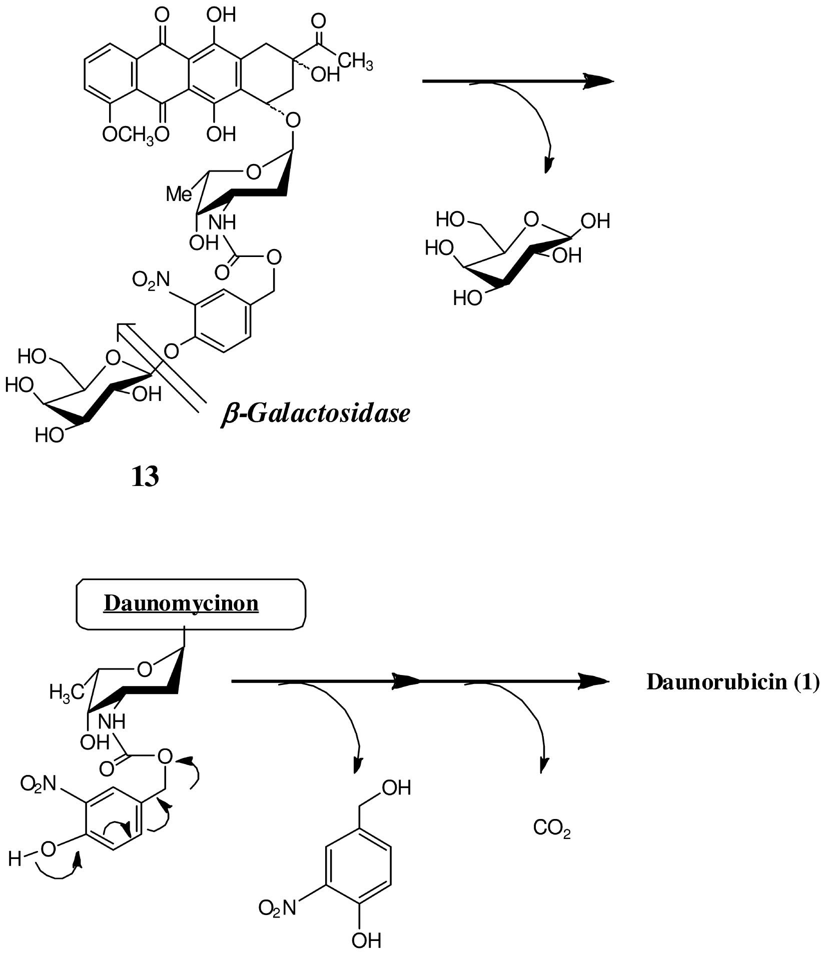

*Figure 5. Activation of β-galactosidase daunorubicin prodrug (# **13**).*

As natural biomaterials, polysaccharides are highly stable, safe, non-toxic, hydrophilic and biodegradable. In addition, polysaccharides have abundant resources in nature and low cost in their processing. Polysaccharides have a large number of reactive groups, a wide range of molecular weight, varying chemical composition, which contribute to their diversity in structure and in property. Due to the presence of various derivable groups on molecular chains, polysaccharides can be easily modified chemically and biochemically, resulting in many kinds of polysaccharide derivatives. Also, polysaccharides have advantage over other polymers as they may be naturally hydrolyzed by enzymes and metabolized in specific organs, and can provide sustained effect with target delivery. Orally administrated drugs frequently use polysaccharide vehicle for sustained delivery

Downloaded by STANFORD UNIV GREEN LIBR on June 13, 2012 | http://pubs.acs.org
Publication Date (Web): June 12, 2012 | doi: 10.1021/bk-2012-1102.ch005

and colon specific delivery, while parenteral administration is used to target specific organs like joints (hyaluronic acid) or liver (pullulan) (*32*). But, till now only in a few cases, polysaccharides were used as drug-carriers for the anthracycline antibiotics (*33*).

In this study we have considered two different types of anthracycline derivatives, aiming at reducing the drug toxicity, increasing its efficacy, or both. In one case we modified the initial drug with a stable galactose residue, which was chosen because of the important role that galactose-specific receptors, galectins, play in tumor development (*34*, *35*). One of the most promising drug-candidates in this series of anthracycline derivatives, namely, conjugate of doxorubicin with melibiose, was named Galactomycin. In the second case we have synthesized a conjugate of doxorubicin with a water-soluble 1,4-β-D-galactomannan of a certain structure, trade name DAVANAT® (*36*). The conjugates of doxorubicin and DAVANAT® were synthesized in two different chemical forms, and tentatively named DoxoDavanat-1 and -2. A new approach that is being examined in our work, aims at a double-functional anti-cancer effect of drug candidates, that is composed of a “core” chemotherapy drug (doxorubicin in this case) which is covalently attached to a galactose-branched polymer, that can interact with galactose-specific receptors of tumor surfaces, such as galectins, and results in a better drug delivery.

Galactomycin(s)

In recent years, a series of anthracycline derivatives containing sugar moieties connected to the antibiotic through alkyl- or acyl-type spacers were synthesized in connection with gene-directed enzyme prodrug therapy (GDEPT) (*29*, *37*). In these cases, the sugar moieties serve as enzyme-specific functional groups of the anthracycline substrate. When a spacer is hydrolyzed by specific enzymes in the target tissue, the inactive prodrug is activated into the initial drug. The goal of our research, on the contrary, was to modify the initial drug with a stable galactose residue aiming at an increased chemotherapeutic activity.

We have synthesized a series of new N-substituted derivatives of doxorubicin and carminomycin, including doxorubicin derivatives containing D-galactose with hydrophilic (1-deoxyglucit-1-yl) or hydrophobic (benzyl or 3-methoxybenzyl) spacers, and test their cytotoxic and antitumor activities in comparison with the parent antibiotics (*38–40*). Up to now no methods for the conjugation of the 3′-amino group of daunosamine moiety with aldoses have been published.

In the first stage of our research, we studied the possibility of 3′-*N*-substitution of daunorubicin (**1**) by reductive alkylation with *D*-glucose or *D*-galactose in the presence of $NaBH_3CN$. Although the reductive *N*-alkylation of anthracycline antibiotics has been widely studied neither mono- nor disaccharides have been used in this reaction. By this method 3′-(1-deoxy-*D*-glucit-1-yl) - and 3′-(1-deoxy-*D*-galactit-1-yl) derivatives of 13-(R,S)-dihydro-daunorubicin (**14, 15**) were isolated in ~ 20 % yields (Scheme 1).

Downloaded by STANFORD UNIV GREEN LIBR on June 13, 2012 | http://pubs.acs.org
Publication Date (Web): June 12, 2012 | doi: 10.1021/bk-2012-1102.ch005

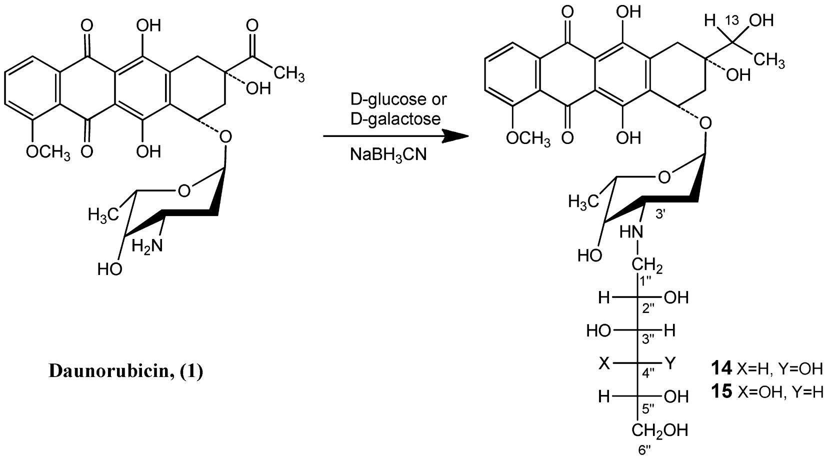

Daunorubicin, (1)

14 X=H, Y=OH
15 X=OH, Y=H

*Scheme 1. Synthesis of monosaccharide conjugates of 13-(R,S)-dihydrodaunorubicin (## **14,15**).*

To protect the 13-CO group of the antibiotics from the reduction, the 13-dimethyl ketal of 14-bromodaunorubicin (**16**) or the 13-dimethyl ketal of 14-bromocarminomycin (**17**) were used as the starting compounds, obtained from daunorubicin (**1**) or carminomycin (**3**), respectively. To introduce the *D*-galactose substituent, the disaccharides 6-*O*-α-*D*-galactopyranosyl-*D*-glucose (melibiose) (**18**) and 4-*O*-β-*D*-galactopyranosyl-*D*-glucose (lactose) (**19**) were used. 3′*N*-[α-*D*-Galactopyranosyl-(1→6)-*O*-1-deoxy-*D*-glucit-1-yl]doxorubicin (**20**), 3′*N*-[α-*D*-galactopyrano-syl-(1→6)-*O*-1-deoxy-*D*-glucit-1-yl]-14-hydroxy-carminomycin (**21**) and 3′*N*-[β-*D*-galactopy-ranosyl-(1→4)-*O*-1-deoxy-*D*-glucit-1-yl]doxorubicin (**22**) were obtained in 20, 8 and 8% yields, respectively, starting from **16** or **17** and melibiose (**18**) or lactose (**19**) with the use of $NaBCNH_3$ after hydrolysis of the intermediate bromoketals **20a**, **21a** and **22a** (Scheme 2). *D*-Galactose has the α-anomeric configuration in compounds **20** and **21**, and the β-configuration in compound **22**; the polyhydroxylated hexit-1-yl spacer in compound **22** is shorter and more branched as compared to that in compounds **20** and **21**. Compound **20** that showed the best antitumor properties (see below Table 1) was named Galactomycin.

In the first stage of the synthesis of the conjugates of doxorubicin with *D*-galactose linked to the antibiotic through the hydrophobic spacer (**30** and **31**), 3-methoxy-4-*O*-(2,3,4,6-tetra-*O*-acetyl-β-*D*-galactopyranosyl)oxybenzaldehyde (**26**) and 4-*O*-(2,3,4,6-tetra-*O*-acetyl-β-*D*-galactopyrano-syl)oxybenzaldehyde (**27**) were obtained by the reaction of 2,3,4,6-tetra-*O*-acetyl-α-*D*-galactopyranosyl bromide (**25**) with vanillin (**23**) or 4-hydroxybenzaldehyde (**24**), respectively (Scheme 3). Reductive alkylation of the 3′ amino group of 16 with compounds **26** or **27** by the use of $NaBCNH_3$ gave the corresponding derivatives of the 13-dimethylketal of 14-bromodaunorubicin (**28** and **29**). After desacetylation of the galactose moiety in **28** and **29** with $NaOCH_3$ in methanol followed by acid

Downloaded by STANFORD UNIV GREEN LIBR on June 13, 2012 | http://pubs.acs.org
Publication Date (Web): June 12, 2012 | doi: 10.1021/bk-2012-1102.ch005

hydrolysis of intermediates **30a** and **31a**, the desired doxorubicin derivatives **30** and **31** were obtained (Scheme 3).

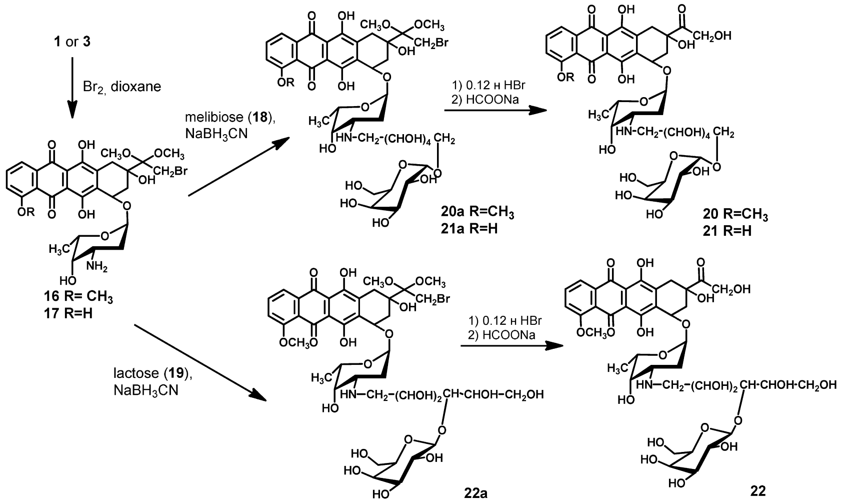

*Scheme 2. Synthesis of conjugates of doxorubicin and carminomycin with melibiose or lactose (compounds # **20-22**).*

3′*N*-(1-Deoxy-*D*-glucit-1-yl)doxorubicin (**32**), 3′*N*-(1-deoxy-*D*-galact-1-yl)doxorubicin (**33**), 3′-N-(1-desoxy-D-galactit-1-yl)-14-hydroxycarminomycin (**34**) and 3′-N-(1-deoxy-D-arabinos-1-yl)-14-hydroxycarminomycin (**35**) were obtained by the similar scheme (Scheme 2) from **16** or **17** and *D*-glucose or *D*-galactose or D-arabinose, correspondingly (Fig. 6).

Thin-layer chromatography (TLC) and high-performance liquid chromatography (HPLC) analyses showed that Galactomycin (compound **20**), as well as compounds **21**, **22**, and **30** through **35** were homogeneous, and contain no admixed daunorubicin, doxorubicin or carminomycin. Under conditions of drastic acid hydrolysis (1N HCl, 105°C, 1 h.) compounds **20, 22, 30,** and **31** produce the aglycone adriamycinone plus galactose, as demonstrated by TLC and paper chromatography, using authentic compounds as standards). Compound **21** produce the aglycone 14-hydroxycarminomycinone plus galactose, compounds **14** and **15** under similar conditions produced 13-(R,S)-dihydrodaunomicinone, compounds **32** and **33** gave adriamycinone, compounds **34** and **35** – 14-hydroxycarminomycinone. NMR investigation permitted identification of all signals in the aglycone, spacers, and carbohydrate moieties, and mass-spectral data showed the correct molecular weights (*38–40*).

Downloaded by STANFORD UNIV GREEN LIBR on June 13, 2012 | http://pubs.acs.org
Publication Date (Web): June 12, 2012 | doi: 10.1021/bk-2012-1102.ch005

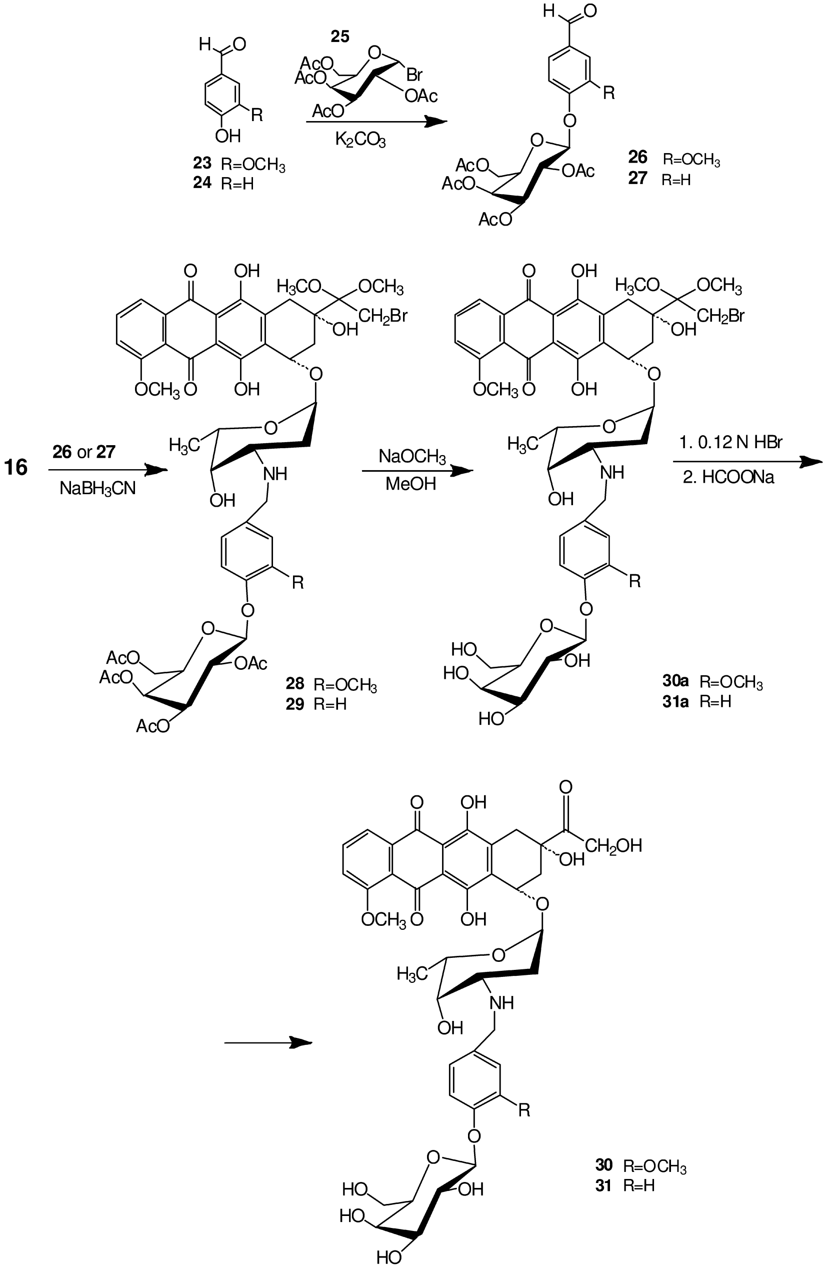
25
K_2CO_3
23 R=OCH_3
24 R=H
26 R=OCH_3
27 R=H
16
26 or 27
$NaBH_3CN$
NaOCH$_3$
MeOH
1. 0.12 N HBr
2. HCOONa
28 R=OCH_3
29 R=H
30a R=OCH_3
31a R=H
30 R=OCH_3
31 R=H

*Scheme 3. Synthesis of conjugates of doxorubicin with D-galactose with hydrophobic spacer (## **30**, **31**).*

Downloaded by STANFORD UNIV GREEN LIBR on June 13, 2012 | http://pubs.acs.org
Publication Date (Web): June 12, 2012 | doi: 10.1021/bk-2012-1102.ch005

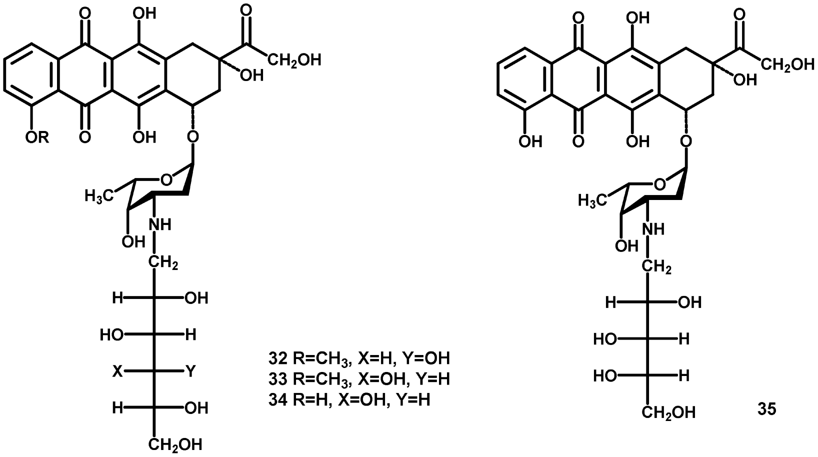

*Figure 6. Structure of monosaccharide derivatives of doxorubicin (## **32, 33**) and 14-hydroxycarminomycin (## **34, 35**).*

Antitumor Activity

The cytotoxicity of new anthracycline derivatives was tested on different cultured tumor cell lines. On the whole, addition of polyhydroxylated residues (yielding compounds **32** - **35**) or introduction of the D-galactose residue attached to the 3′-amino group of doxorubicin or 14-hydroxycarminomycin *via* hydrophilic or hydrophobic spacer (compounds **20** - **22**, **30**, **31**) resulted in a decrease of cytotoxicity in comparison with the parent antibiotics doxorubicin or 14-hydroxycarminomycin, respectively (*38–40*). For example, Galactomycin (**20**) and compound **22** are two orders less cytotoxic than doxorubicin for murine leukemia L1210/0 cell line: for GalactomycinIC_{50} (50 % inhibitory concentration) = 21 μM (L1210/0) and for **22** IC_{50} = 24 μM, whereas for doxorubicin IC_{50}= 0.213 μM. The developed type of modification of anthracycline antibiotics didn't influence on the ability of the drug to kill tumor cells which are resistant to doxorubicin. Novel doxorubicin derivatives were inactive towards tumor cells resistant to doxorubicin (K562i/S9 and MCF-7Dox), while N-substituted derivatives of 14-hydroxycarminomycin (as the parent antibiotic 14-hydroxycarminomycin), namely, compounds **21, 35** and **25** were similarly active for wild type cells and their multidrug resistant (MDR) sublines, K562i/S9 and MCF-7Dox (*39*).

Importantly, novel derivatives of doxorubicin and 14-hydroxycarminbomycin were much better soluble in water in comparison with the parent antibiotics. Some of the novel derivatives were tested for their ability to inhibit the activity of topoisomerase I, one of the enzymes modifying the DNA conformation. On the whole, the introduction of substituents containing hydroxyl groups into the amino group of daunosamine moiety of the anthracycline increases the ability of antibiotics to inhibit topoisomerase I (*40*). The bulky hydrophilic substituents (such as in **21**) appear to prevent the recognition of DNA binding sites by the enzyme and/or induce a local disturbance in the conformation of nucleotide chains. Compounds which were most active in *in vitro* testes were studied in *in vivo* experiments.

In vivo studies revealed differences in the antitumor properties of Galactomycin and compound **22.** The maximum tolerated dosages (MTD) were 40-60 mg/kg for Galactomycin, 60-80 mg/kg for **22**, and >60 mg/kg for both **30** and **31** (single i.v. injection, BDF$_1$ mice (C$_{57}$Bl x DBA$_2$, males), as compared to 7-10 mg/kg for doxorubicin. The antitumor activity for these compounds was studied on mice bearing lymphocyte leukemia P-388 at single and multiple (q2d x 3) i.v. injection regimens (Table 1).

Downloaded by STANFORD UNIV GREEN LIBR on June 13, 2012 | http://pubs.acs.org
Publication Date (Web): June 12, 2012 | doi: 10.1021/bk-2012-1102.ch005

Single Injection Regimen

When **22** was *i.v.* injected to mice with P-388 (BDF$_1$ mice) 24 h post *i.p.* implantation of the tumor, 65 % ILS at the dose of 40 mg/kg was achieved. Galactomycin was more active than compound **22**: at the dose of 20 mg/kg it induced 79 % ILS and at 40 mg/kg 118 % ILS (without toxic effects). A dose of 60 mg/kg showed some toxicity. The maximal antitumor effect of doxorubicin was 70 % at the MTD dose of 7 mg/kg. Compounds **30** and **31** at doses of 40 and 60 mg/kg induced ILS in the range of 35-44% (**30**) and 52-59% (**31**), respectively.

Multiple Injection Regimens

Multiple injections of doxorubicin revealed an increased toxicity of the drug, apparently due to its cumulative toxic effect. Compared to a single dose regimen, when at the dose of 7 mg/kg there was no toxic deaths (70% ILS), triple injection of doxorubicin with 2-day intervals (q2d x 3) at 2.3 mg/kg each dose (6.9 mg/kg total dose) resulted in four toxic deaths out of seven animals. However, Galactomycin did not show any cumulative toxic effect at the triple dose of 40 mg/kg (120 mg/kg total dose), and induced ILS equal to 133%. Hence, Galactomycin may be of interest for supportive therapy.

This study shows that doxorubicin derivatives containing at the nitrogen atom of the daunosamine moiety a polyhydroxylated spacer connected in turn with the D-galactose moiety, and particularly Galactomycin, may afford compounds having lower toxicity and better pharmaceutical index compared to the parent doxorubicin. Furthermore, this study shows that the α-anomeric configuration of D-galactose rather than β-, and/or a longer length of the spacer (six carbon atoms rather than four in this particular case of Galactomycin and compound **22** may result in a more efficacious drug candidate in this series.

Downloaded by STANFORD UNIV GREEN LIBR on June 13, 2012 | http://pubs.acs.org
Publication Date (Web): June 12, 2012 | doi: 10.1021/bk-2012-1102.ch005

Table 1. Antitumor activity of Galactomycin (20) and compounds 22, 30, and 31 [*i.v.* injection to mice (BDF_1 C_{57} B1 x DBA_2, males) with P388, 24 h *i.p.* post implantation of tumor] in comparison with doxorubicin

Compound	*Dose (mg/kg)*	*Injection (i.v.) regimen*	*Toxic death*	*ILS, %*[a]
Control	--	--	0/10	0
Doxorubicin	7	Single	0/6	70
Doxorubicin	14	Single	2/6	--
Galactomycin **20**	20	Single	0/6	79
Galactomycin **20**	40	Single	0/6	118
Galactomycin **20**	60	Single	1/6	--
22	40	Single	0/6	65
22	80	Single	1/6	--
30	40	Single	0/6	35
30	60	Single	0/6	44
31	40	Single	0/6	52
31	60	Single	0/6	59
Doxorubicin	2.3	q2 x 3[b]	4/7	--
Galactomycin **20**	20	q2 x 3[b]	0/10	79
Galactomycin **20**	40	q2 x 3[b]	0/10	133

[a] Increase of lifespan; [b] 24 h post *i.p.* tumor implanting

DoxoDavanat

Earlier it was shown (*41*), and described in chapter "DAVANAT® and colon cancer: Preclinical and clinical (Phase I) studies" above, that co-administration of a soluble 1,4-β-D-galactomannan (GM, x:y~1:0.7, Scheme 4) along with antitumor drug 5-fluorouracil (5-FU) by *i.v.* injection to mice bearing human colon tumors (COLO 205 and HT-29) significantly increased efficacy of the 5-FU. Combination of the galactomannan with 5-FU, compared to 5-FU alone, resulted in the decrease of median tumor volume to 17-65% and the increase of mean survival time (days) to 150-190%.

Data from a Phase II trial for end-stage colorectal cancer patients showed that DAVANAT® in combination with 5-FU extended median survival by 46% compared with the best standard of care as determined by the patients' physicians. Clinical trial results also showed that patients experienced fewer serious adverse side effects of chemotherapy which has the potential to reduce hospitalizations and improve quality of life. Recently, the U.S. Food & Drug Administration (FDA) DAVANAT® approved pivotal, randomized, controlled, and blinded Phase III trials of DAVANAT® co-administered with standard chemotherapy for second line treatment of patients with metastatic colorectal cancer.

Downloaded by STANFORD UNIV GREEN LIBR on June 13, 2012 | http://pubs.acs.org
Publication Date (Web): June 12, 2012 | doi: 10.1021/bk-2012-1102.ch005

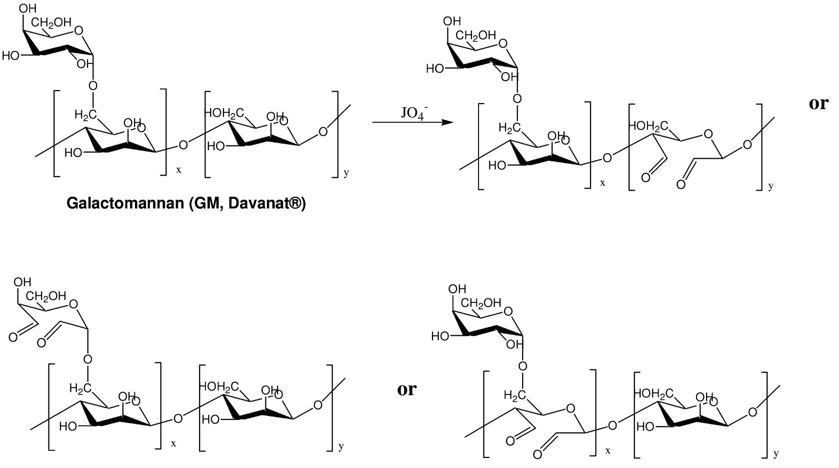

Scheme 4. Activation of galactomannan (Davanat®). Dialdehyde formation from different GM subunits.

Compared to many other polysaccharides, galactomannans have multiple side-chain galactose units that may readily interact with galactose-specific receptors such as galectins on the tumor cell surface, modulate the tumor surface physiology and potentially affect delivery of drug to the tumor. The aim of our research was the synthesis of a conjugate of doxorubicin and galactomannan that would act like a double prodrug, that is liberating both doxorubicin and DAVANAT® in *in vivo* conditions and, importantly, in proximity to galactose/manose specific receptors.

Earlier conjugates of doxorubicin with different polysaccharides were described (*33*). In most cases doxorubicin was bound to a polysaccharide through amine bond. Typically, a polysaccharide was activated to a dialdehyde derivative by periodate oxidation. In other words, for the introduction of the anthracycline antibiotic, the reductive alkylation of doxorubicin with the oxidized polysaccharide was used (*42*). However, the reduction of the Schiff base led to simultaneous reduction of 13-keto group of doxorubicin resulting in an N-alkyl derivative of 13-(R,S)-dihydrodoxorubicin, as it takes place in the case of daunorubicin (see Scheme 1). 13-(R,S)-Dihydrodoxorubicin is less active then doxorubicin. Besides, doxorubicin conjugates obtained by this method cannot be considered as doxorubicin prodrugs, as no proof that the antibiotic can be released from the polymer in physiological conditions was shown. That is why we selected binding doxorubicin to the galactomannan *via* imine bond (Schiff base), in anticipation that the conjugate will be stable in both mild basic and neutral conditions, and will slowly liberate doxorubicin in mild acid conditions.

In this Chapter we describe synthesis and biological activity of two DAVANAT®-doxorubicin conjugates, tentatively named DoxoDavanat-1 and -2, and resulting from (a) a direct covalent binding of the two compounds, and (b) the linking of doxorubicin to DAVANAT® *via* a L-lysyl-bridge.

Downloaded by STANFORD UNIV GREEN LIBR on June 13, 2012 | http://pubs.acs.org
Publication Date (Web): June 12, 2012 | doi: 10.1021/bk-2012-1102.ch005

The initial water-soluble 1,4-β-D-galactomannan (DAVANAT®) was obtained by a controlled partial chemical degradation of a high molecular weight galactomannan from *Cyamopsistetragonoloba*, or guar gum (*36*, *41*, *43*) and further purification under Good Manufacturing Practice (GMP) conditions (Chapter "DAVANAT®: A modified galactomannan that enhances chemotherapeutics. Chemistry, manufacturing, control" in this book). Molecular weight of the obtained DAVANAT® was 54,000 Da (MALLS, or Multi-Angle Laser Light Scattering), 95,000 Da (viscometry), or 92,000 Da (GPC, or gel permeation chromatography). Mannose/galactose ratio (by the NMR and chemical analysis after complete acid hydrolysis) of DAVANAT®was 1.7 (*41*). DAVANAT® was activated to a dialdehyde derivative by periodate oxidation (Scheme 4) with a subsequent purification using gel permeation chromatography.

Purified activated DAVANAT® was coupled with doxorubicin to form a Schiff base (Scheme 5, the example for one of the variants of dialdehyde-GM is shown) (*43*). A series of experiments aimed at various degrees of oxidation of DAVANAT® and performed with various amounts of doxorubicin showed that a conjugate was soluble in water only at a relatively low content of doxorubicin in the conjugate, about 5% by weight. The obtained DoxoDavanat-1 behaved at gel-filtration and dialyses similarly with the initial DAVANAT®.

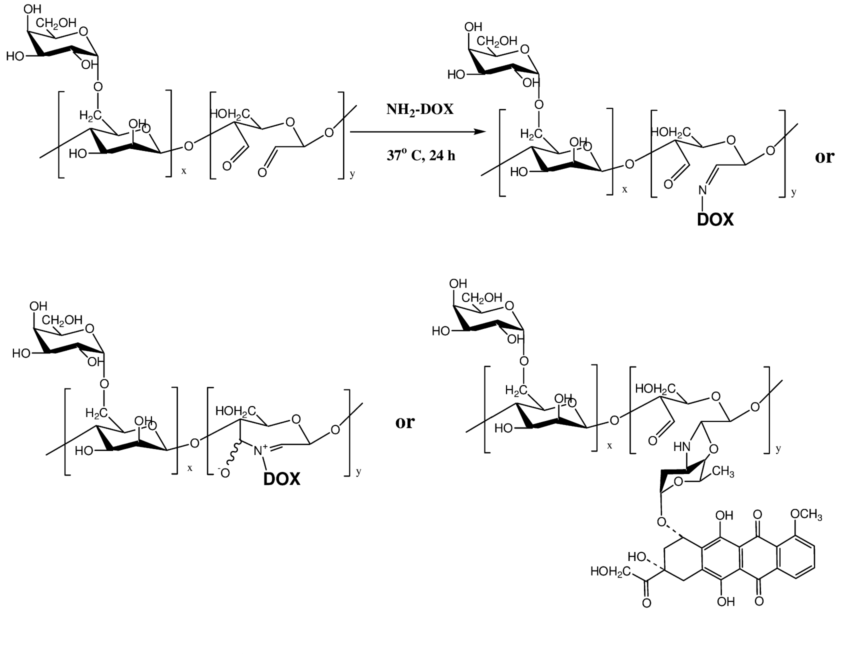

Scheme 5. Synthesis of DoxoDavanat-1. Plausible structure of doxorubicin-GM imine conjugates.

Molecular weight of DoxoDavanat-1 was 95,000 Da (GPC), while for the starting DAVANAT® it was 92,000 Da when determined on the same column.

The final preparation of DoxoDavanat-1 was obtained as a pink powder, and it contained 5% of doxorubicin covalently attached to the initial DAVANAT®, as

Downloaded by STANFORD UNIV GREEN LIBR on June 13, 2012 | http://pubs.acs.org
Publication Date (Web): June 12, 2012 | doi: 10.1021/bk-2012-1102.ch005

evaluated by UV absorption at 490 nm. It did not contain free doxorubicin. UV absorbance spectra of DoxoDavanat-1 and free doxorubicin revealed that their characteristic absorbance peaks were practically identical.

A plausible cyclic imine structure for the obtained DoxoDavanat-1 is shown on Scheme 5. Linear structure or a combination of the two cannot be excluded.

In order to further increase the amount of doxorubicin in the conjugate, DoxoDavanat-2 was synthesized, in which a doxorubicin derivative carried an additional amino group. For this purpose 3′N-L-lysyl-doxorubicin was chosen, taking into account its higher water-solubility compared to doxorubicin.

DoxoDavanat-2 was synthesized from the initial DAVANAT® and 3′N-L-lysyl-doxorubicin (**39**) (*43*). L-Lysine was converted to N^{α},N^{ε}-Di-(9*H*-fluorenylmethoxycarbonyl)-L-lysine (**36**), using N-(9*H*-fluorenylmethoxycarbonyloxy)-succinimide in the presence of dicyclohexylcarbodiimide (Scheme 6). Then, N^{ε}-di-(9*H*-fluorenylmethoxycarbonyl)-L-lysyl]oxysuccinimide (**37**), *in situ* was obtained. It was coupled with doxorubicin in the next step, into 3N′-[N^{α},N^{ε}-Di-(9*H*-fluorenylmethoxycarbonyl)-L-lysyl]-doxorubicin (**38**), which was then, in the next step, deblocked into 3′N-L-lysyl-doxorubicin (**39**) with 67% yield (re. doxorubicin). The structure of 3′N-L-lysyl-doxorubicin (**39**) was confirmed using NMR and ESI-mass spectrometry. DAVANAT® was oxidized (activated) as described above (Scheme 4) and conjugated with hydrochloride of **39** to give DoxoDavanat-2 (Scheme 7).

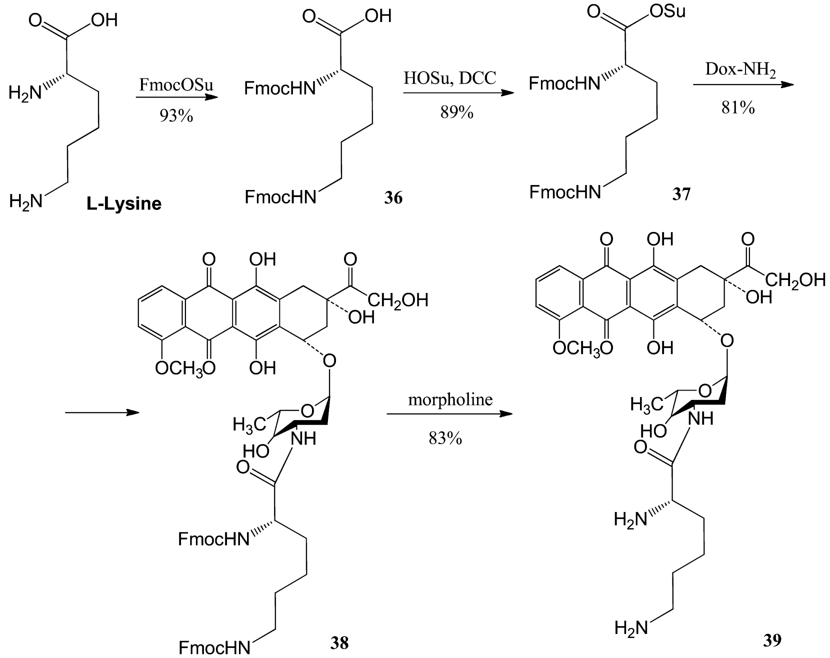

Scheme 6. Synthesis of 3′N-L-lysyl-doxorubicin.

Downloaded by STANFORD UNIV GREEN LIBR on June 13, 2012 | http://pubs.acs.org
Publication Date (Web): June 12, 2012 | doi: 10.1021/bk-2012-1102.ch005

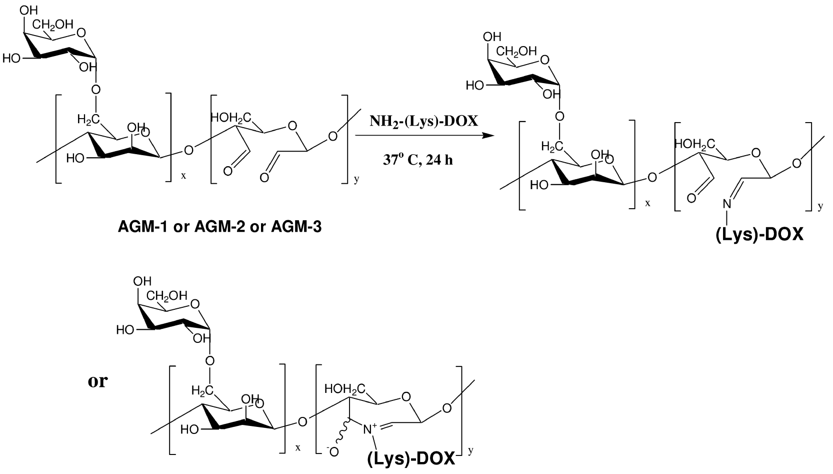

Scheme 7. Synthesis of DoxoDavanat-2. Plausible structure of 3'N-L-lysyl-doxorubicin-GM imine conjugates.

DoxoDavanat-2 was purified using dialysis and GPC. The final preparation was obtained as dark red powder containing 10% of covalently bound doxorubicin, as evaluated by UV absorption at 490 nm. Molecular weight of DoxoDavanat-2 was 98,000 Da (GPC), compared to 92,000 Da for the initial DAVANAT®.

Table 2. ED_{50} (growth inhibition activity) for doxorubicin, Galactomycin, DoxoDavanat-1 and -2 towards three cancer cell lines

Doxorubicin and its derivatives	***ED_{50}, µg/mL***		
	B16-F1 mouse melanoma cells	***MCF-7 (HTB-22) human breast cancer cells***	***HT-29 (HTB-38) human colon cancer cells***
Doxorubicin	0.01-0.02	0.08-0.12	0.2-0.3
Galactomycin **20**	0.4-0.6	1.7-2.6	1.5-2.2
DoxoDavanat-1	0.5-0.8	3.0-4.4	13-20
DoxoDavanat-2	>50	>50	>50

Cytotoxicity

Cytotoxic activities of Doxorubicin, Galactomycin, DoxoDavanat-1 and DoxoDavanat-2 have been tested using the B16-F1 mouse melanoma cells, MCF-7 (HTB-22) human breast cancer cells, and HT-29 (HTB-38) human colon cancer cells. Data are shown in Table 2. One can see that Doxorubicin is much more cytotoxic compared to all its derivatives. *In vivo* experiments are in progress.

Downloaded by STANFORD UNIV GREEN LIBR on June 13, 2012 | http://pubs.acs.org
Publication Date (Web): June 12, 2012 | doi: 10.1021/bk-2012-1102.ch005

References

1. Brockmann, H. Anthracyclinones and Anthracyclines. (Rhodomycinone, Pyrromycinone and Their Glycosides). *Fortschr. Chem. Org. Naturst.* **1963**, *21*, 121–182.
2. Arcamone F. *Doxorubicin: Anti-Cancer Antibiotics, Medicinal Chemistry Series*; Academic Press: 1981; Vol. 17.
3. Hutchinson C. R. The Biosynthesis of Tetracycline and Anthracycline Antibiotics. In *Antibiotics IV Biosynthesis*; Corcoran, J. W., Ed.; Springer-Verlag: 1981; pp 1−11.
4. White, R. J. Anthracyclines. In *Biochemistry and Genetic Regulation of Commercially Important Antibiotics*; Vining, L. C., Ed.; Addison Wesley: 1983; pp 277−291.
5. Brazhnikova, M. G.; Zbarsky, V. B.; Ponomarenko, V. I.; Potapova, N. P. Physical and Chemical Characteristics and Structure of Carmimomycin, a New Antitumor Antibiotic. *J. Antibiotics* **1974**, *27*, 254–259.
6. Minottu, G.; Menna, P.; Salvatorelli, E.; Cairo, G.; Gianni, L. Anthracyclines: Molecular Advances and Pharmacologic Development in Antitumor Activity. *Pharmacol. Rev.* **2004**, *56*, 185–209.
7. Zunino, F.; Pratesi, G.; Perego, P. Role of the Sugar Moiety in The Pharmacological Activity of Anthracyclines: Development of a Novel Series of Disaccharide Analogs. *Biochem. Pharmacol.* **2001**, *61*, 933–938.
8. DuVernay, V. H. Molecular Pharmacology of Anthracycline Antitumor Antibiotics. In *Cancer and Chemotherapy*; Academic Press: New York, 1981; Vol. III; pp 233−271.
9. Gewirtz, D. A Critical Evaluation of The Mechanisms of Action Proposed for The Antitumor Effects of The Anthracycline Antibiotics Adriamycin and Daunorubicin. *Biochem. Pharmacol.* **1999**, *57*, 727–741.
10. Denny, W. A. Emerging DNA Topoisomerase Inhibitors as Anticancer Drugs. *Expert Opin. Emerging Drugs* **2004**, *9*, 105–133.
11. Reynolds, J. E. F., Ed. *Martindale: The Extra Pharmacopoeia*, 28th ed.; London: The Pharmaceutical Press, 1982; pp 205−208.
12. McEvoy, G. K., Ed. *American Hospital Formulary Service: Drug information 1991*; American Society of Hospital Pharmacists: Bethesda, 1991; pp 527−530.
13. Pinedo, H. M., Chabner, B. A., Eds. *Cancer Chemotherapy/7: The EORTC Cancer Chemotherapy Annual*; New York: Elsevier Science Publishing Co Inc: 1985; pp 57−75.
14. Creasey, W. A.; McIntosh, L. S.; Brescia, T.; Odujinrin, O.; Aspnes, G. T.; Murray, E.; Marsh, J. C. Clinical Effects and Pharmacokinetics of Different Dosage Schedules of Adriamycin. *Cancer Res.* **1976**, *36*, 216–221.
15. Bachur, N. R. Adriamycin (NS-123127) Pharmacology. *Cancer Chemother. Rep.* **1975**, *6*, 153–158.
16. Leslie, E. M.; Deeley, R. G.; Cole, S. P. Multidrug Resistance Proteins: Role of P-Glycoprotein, MRP1, MRP2, and BCRP (ABCG2) in Tissue Defense. *Toxicol. Appl. Pharmacol.* **2005**, *204* (3), 216–237.

Downloaded by STANFORD UNIV GREEN LIBR on June 13, 2012 | http://pubs.acs.org
Publication Date (Web): June 12, 2012 | doi: 10.1021/bk-2012-1102.ch005

17. Gonzalez-Paz, O.; Polizzi, D.; De Cesare, M.; Zunino, F.; Bigioni, M.; Maggi, C. A.; Manzini, S.; Pratesi, G. Tissue Distribution, Antitumor Activity and *in vivo* Apoptosis Induction by MEN10755 in Nude Mice. *Eur. J. Cancer* **2001**, *37*, 431–437.
18. Horton, D.; Priebe, W.; Sznaidman, M. L.; Varela, O. Synthesis and Antitumor Activity of Anthracycline Disaccharide Glycosides Containing Daunosamine. *J. Antibiot.* **1993**, *46*, 1720–1730.
19. Animati, F.; Arcamone, F.; Giannini, G.; Lombardi, P.; Monteagudo, E. *S-Fluoro-Anthracyclines, Processes for Their Preparation and Pharmaceutical Compositions Containing Them.* U.S. Patent No. 5,814,608, September 29, 1998.
20. Animati, F.; Berettoni, M.; Cipollone, A.; Franciotti, M.; Lombardi, P.; Monteagudo, E.; Arcamone, F. New Anthracycline Disaccharides Synthesis of L-daunosaminyl-α-(1→4)-2-deoxy-L-rhamnosyl and of L-daunosaminyl-α-(1→4)-2-deoxy-L-fucosyl daunorubicin analogues. *J. Chem. Soc,. Perkin Trans I* **1996**, 1327–1329.
21. Arcamone, F.; Animati, F.; Bigioni, M.; Capranico, G.; Caserini, C.; Cipollone, A.; De Cesare, M.; Ettorre, A.; Guano, F.; Manzini, S.; Monteagudo, E.; Pratesi, G.; Salvatore, C.; Supino, R.; Zunino, F. Configurational Requirements of The Sugar Moiety for The Pharmacological Activity of Anthracycline Disaccharides. *Biochem. Pharmacol.* **1999**, *57*, 1133–1139.
22. Arcamone, F.; Animati, F.; Berettoni, M.; Bigioni, M.; Capranico, G.; Casazza, A. M.; Caserini, C.; Cipollone, A.; De Cesare, M.; Franciotti, M.; Lombardi, P.; Madami, A.; Manzini, S.; Monteagudo, E.; Polizzi, D.; Pratesi, G.; Righetti, S. C.; Salvatore, C.; Supino, R.; Zunino, F. Doxorubicin Disaccharide Analogue: Apoptosis-Related Improvement of Efficacy *in vivo*. *J. Natl. Cancer Inst.* **1997**, *89*, 1217–1223.
23. Pratesi, G.; Monestiroli, S. V. Preclinical Evaluation of New Anthracyclines. *Curr. Med. Chem.* **2001**, *8*, 9–13.
24. Pratesi, G.; De Cesare, M.; Caserini, C.; Perego, P.; Dal Bo, L.; Polizzi, D.; Supino, R.; Bigioni, M.; Manzini, S.; Iafrate, E.; Salvatore, C.; Casazza, A.; Arcamone, F.; Zunino, F. Improved Efficacy and Enlarged Spectrum of Activity of a Novel Anthracycline Disaccharide Analogue of Doxorubicin Against Human Tumor Xenografts. *Clin. Cancer Res.* **1998**, *4*, 2833–2839.
25. Caponigro, F.; Willemse, P.; Sorio, R.; Floquet, A.; van Bell, S.; Demol, J.; Tambaro, R.; Comandini, A.; Capriati, A.; Adank, S.; Wanders, D. Phase II Study of Sabarubicin (MEN-10755) as Second Line Therapy in Patients with Locally Advanced or Metastatic Platinum/Taxane Resistant Ovarian Cancer. *Invest. New Drugs* **2005**, *23*, 85–89.
26. O'Byrne, K. J.; Dunlop, D.; Eberhardt, W. E.; Gillissen, A.; Wagner, T. O.; Capriati, A.; Dickgreber, N. Phase II Study of Sabarubicin (MEN 10755) in Newly Diagnosed Patients With Extensive Stage Small Cell Lung Cancer (ESCLC): Final Report. *J. Clin. Oncol.* **2008**, *26*, Abstr. 19043.
27. Leenders, R. G. G.; Gerrits, K. A. A.; Ruijtenbeek, R.; Scheeren, H. W.; Haisma, H. J.; Boven, E. β-Glucuronyl Carbamate Based Pro-moieties Designed for Prodrugs in ADEPT. *Tetrahedron Lett.* **1995**, *36*, 1701–1704.

28. Kenten, J.; Simpson, D. M. *Compounds and Methods for The Selective Treatment of Cancer and Bacterial Infections*. U.S. Patent No. 6,218,519, April 17, 2001.
29. Ghosh, A. K.; Khan, S.; Marini, F.; Nelson, A.; Farquhar, D. A Daunorubicin β-Galactoside Prodrug for Use in Conjunction with Gene-Directed Enzyme Prodrug Therapy. *Tetrahedron Lett.* **2000**, *41*, 4871–4874.
30. Bakina, E.; Farquhar, D. Intensely Cytotoxic Anthracycline Prodrugs: Galactosides. *Anticancer Drug Des.* **1999**, *14*, 607–615.
31. Damen, E. W. P.; de Groot, F. M. H.; Scheeren, H. W. Novel Anthracycline Prodrugs. *Expert Opin. Ther. Patents* **2001**, *11* (4), 651–666.
32. Ahmad, S.; Tester, R. Polysaccharides as Drug Carries. Presented at 22nd International carbohydrate Symposium, Glasgow, UK, 23−27 July, 2004; C37.
33. Domb, A. J.; Benita, S.; Polacheck, I.; Linden, G. *Conjugates of Biologically Active Substances*. U.S. Patent No 6,011,008, Jan. 4, 2000.
34. Barondes, S. H.; Castronovo, V.; Cooper, D. N. W.; Cummings, R. D.; Drickamer, K.; Feizi, T.; Gitt, M. A.; Hirabayashi, J.; Hudges, C.; Kasai, K.-I.; Leffler, H.; Liu, F.-T.; Lotan, R.; Mercurio, A. M.; Monsigny, M.; Pillai, S.; Poirer, F.; Raz, A.; Rigby, P. W. J.; Rini, J. M.; Wang, J. L. Galectins: A Family of Animal beta-Galactoside-Binding Lectins. *Cell* **1994**, *76*, 597–598.
35. Lotan, R.; Ito, H.; Yasui, W.; Yokozaki, H.; Lotan, D.; Tahara, E. Expression of a 31-kDa Lactoside-Binding Lectin in Normal Human Gastric Mucosa and in Primary and Metastatic Gastric Carcinomas. *Int. J. Cancer* **1994**, *56*, 474–480.
36. Klyosov, A. A.; Platt, D. *Delivery of a Therapeutic Agent in a Formulation for Reduced Toxicity*. U.S. Patent No. 6,645,946, November 11, 2003.
37. Houba, P. H. J.; Boven, E.; Erkelens, C. A. M.; Leenders, R. G. G.; Scheren, J. W.; Pinedo, H. M.; Haisma, H. J. The efficacy of the anthracycline prodrug daunorubicin-GA3 in human overian cancer xenoggragts. *Br. J. Cancer* **1998**, *78* (12), 1600–1606.
38. Olsufyeva, E. N.; Tevyashova, A. N.; Trestchalin, I. D.; Preobrazhenskaya, M. N.; Platt, D.; Klyosov, A. A. Synthesis and Antitumor Activity of New D-Galactose-Containing Derivatives of Doxorubicin. *Carbohydr. Res.* **2003**, *338*, 1359–1367.
39. Tevyashova, A. N.; Shtil, A. A; Olsufyeva, E. N.; Simonova, V. S.; Samusenko, A. V.; Preobrazhenskaya, M. N. Carminomycin, 14-Hydroxycarminomycin and Its Novel Carbohydrate Derivatives Potently Kill Human Tumor Cells and Their Multidrug Resistant Variants. *J. Antibiotics* **2004**, *57*, 143–150.
40. Dezhenkova, L. G.; Tevyashova, A. N.; Olsuf’eva, E. N.; Treshchalin, I. D.; Shtil, A. A.; Preobrazhenskaya, M. N. Anthracycline Antibiotics and Their Derivatives, Inhibitors of Topoisomerase I. *Russ. J. Bioorg. Chem.* **2008**, *34*, 387–389.
41. Klyosov, A. A.; Platt, D.; Zomer, E. Preclinical Studies of Anticancer Efficacy of 5-Fluorouracil When Co-Administered With The 1,4-β-D-Galactomannan. *Preclinica* **2003**, *1* (4), 175–186.

Downloaded by STANFORD UNIV GREEN LIBR on June 13, 2012 | http://pubs.acs.org
Publication Date (Web): June 12, 2012 | doi: 10.1021/bk-2012-1102.ch005

42. Ouchi, T.; Matsumoto, M.; Ihara, K.; Ohya, Y. Synthesis and Cytotoxicity of Oxidized Galactomannan/ADR Conjugate. *Pure Appl. Chem.* **1997**, *A34* (6), 975–989.

43. Tevyashova, A. N.; Olsfyeva, E. N.; Preobrazhenskaya, M. N.; Klyosov, A. A.; Zomer, E.; Platt, D. New Conjugates of Antitumor Antibiotic Doxorubicin with Water-Soluble Galactomannan: Synthesis and Biological Activity. *Russ. J. Bioorg. Chem* **2007**, *33* (1), 139–145.

Downloaded by STANFORD UNIV GREEN LIBR on June 13, 2012 | http://pubs.acs.org
Publication Date (Web): June 12, 2012 | doi: 10.1021/bk-2012-1102.ch005

Downloaded by PENNSYLVANIA STATE UNIV on June 14, 2012 | http://pubs.acs.org
Publication Date (Web): June 12, 2012 | doi: 10.1021/bk-2012-1102.ch006

Chapter 6

Carbohydrate-Based Vaccines against HIV/AIDS

Lai-Xi Wang*

Institute of Human Virology and Department of Biochemistry and Molecular Biology, University of Maryland School of Medicine, 725 West Lombard Street, Baltimore, MD 21201, USA
***LWang@ihv.umaryland.edu**

The human immunodeficiency virus (HIV) is the cause of AIDS. Despite tremendous efforts in the past two decades, an effective HIV/AIDS vaccine capable of inducing broadly neutralizing antibody response in humans is still not on the horizon. HIV has evolved a number of mechanisms to escape the host immune surveillance, which account for the difficulties in HIV vaccine development. The outer envelope glycoprotein gp120 is heavily glycosylated. The carbohydrates cover a major area of the protein surface and constitute a strong defense mechanism for the virus to evade host immune attacks. Accumulating evidence has implicated that the HIV-1 carbohydrates themselves could also serve as targets for vaccines. A notable example is the broadly neutralizing antibody 2G12 that exerts its anti-HIV activity by targeting a novel oligomannose cluster on gp120. Moreover, the recent discovery of a number of glycan-dependent broadly neutralizing antibodies from HIV-infected "elite controllers", including PG9, PG16, and the PGT series antibodies, raises new hope for designing a carbohydrate-based vaccine. The present review provides an overview on the structure and function of HIV-1 carbohydrates as well as their relevance to HIV vaccine design. Recent work on the synthesis and antigenicity of HIV-1 carbohydrate epitopes and their mimics is highlighted.

In Glycobiology and Drug Design; Klyosov, A.;
ACS Symposium Series; American Chemical Society: Washington, DC, 2012.

Introduction

The acquired immunodeficiency syndrome (AIDS) is caused by the infection of human immunodeficiency virus (HIV) (*1–3*). HIV type 1 (HIV-1) is the human retrovirus that causes the global epidemic of HIV/AIDS. Since the identification of the first case in 1981, AIDS has become one of the deadliest diseases in human medical history. According to the statistics from the World Health Organization, some 30 million people had died of the disease and over 34 million people are currently living with HIV/AIDS (*4*). The epidemic is still expanding. Most people agree that the best hope to stop the worldwide HIV/AIDS epidemic is the development of an effective HIV vaccine (*5–11*).

Vaccination has been successful in controlling some of the worst infectious diseases in human history. For example, vaccines have virtually eradicated polio (*12*, *13*) and smallpox (*14*, *15*), which once took millions of lives on the earth. Vaccination has also played a key role in combating common flu. Therefore, it was once expected that a vaccine would follow closely behind upon the identification of HIV as the cause of AIDS. However, developing an effective HIV vaccine has proven to be much more difficult and complicated than anticipated. The first large-scale, phase III clinical trial (a 5000-person, 3-year trial) of a candidate vaccine, AIDSVAX (a genetically engineered version of monomeric gp120), was completed in 2003 but yielded only disappointing results. The vaccine raised weak neutralizing antibodies and did not show protective effects in humans (*16*). In another large-scale preventive HIV vaccine trial that involved more than 16,000 health individuals (The RV144 clinical trial) showed that the gp120-based ALVAC/AIDSVAX prime-boost HIV vaccine regimen could confer 31% protection in HIV transmission over 3.5 years upon immunization (*9*, *10*, *17*). This is the first large-scale clinical trial that showed statistically clear protective efficacy of an IHV vaccine.

HIV has evolved strong defense mechanisms to evade immune recognition in order to achieve persistent infection, including frequent mutation of neutralizing epitopes, heavy glycosylation of the envelope, switch of conformations, and formation of oligomeric envelope spikes (*5*, *18–20*). Each level of the HIV's defenses provides an additional dimension of complexity in vaccine design. A number of excellent reviews have been published to address the general scientific obstacles and strategies in HIV-1 vaccine development (*5–11*, *19–25*). For an effective HIV-1 vaccine, at least one of the following two types of immune effectors must be elicited: the neutralizing antibodies that bind and clean up the virus (humoral immunity) (*11*, *19*), or the HIV-specific cytotoxic T lymphocytes (CTL) that recognize and kill infected cells (cellular immunity) (*26*, *27*). While CTL alone may not be sufficient to prevent HIV infection, experiments in animal models have proved that sufficient levels of broadly neutralizing antibodies can protect animals against viral challenge (*28*, *29*). Therefore, the design of an immunogen capable of inducing broadly neutralizing antibody responses remains a major goal in HIV vaccine development.

Work on antibody-based HIV-1 vaccines has hitherto focused on the protein backbone and related peptide fragments of the viral envelope glycoproteins. However, frequent sequence mutation of the neutralizing epitopes poses a major

Downloaded by PENNSYLVANIA STATE UNIV on June 14, 2012 | http://pubs.acs.org
Publication Date (Web): June 12, 2012 | doi: 10.1021/bk-2012-1102.ch006

Downloaded by PENNSYLVANIA STATE UNIV on June 14, 2012 | http://pubs.acs.org
Publication Date (Web): June 12, 2012 | doi: 10.1021/bk-2012-1102.ch006

challenge for the conventional vaccine approaches. New concepts need to be developed in HIV vaccine design. Accumulating data have suggested that the carbohydrate portions of HIV-1 envelope may serve as attractive targets for HIV-1 vaccine development. Carbohydrates account for about half of the molecular weight of the outer envelope glycoprotein gp120, which cover a large area of the surface of the envelope and play a major protective role for viral immune evasion. Immunological and biochemical studies have indeed implicated the existence of novel carbohydrate epitopes on HIV-1 envelope. For example, the epitope of the broadly neutralizing antibody 2G12 has been characterized as a unique cluster of high-mannose type oligosaccharides located on HIV-1 gp120 (*30–33*). More recently, a new class of glycan-dependent, broadly neutralizing antibodies has been isolated from HIV-infected "elite controllers", including the somatic variants PG9 and PG16 and the PGT class antibodies such as PGT121-137 and PGT141-145 (*34–38*). These antibodies neutralize various primary HIV-1 strains across clades with remarkable breadth and potency (*34–38*). Two recent X-ray structural studies have identified novel glycopeptide antigenic structures at the V1/V2 and V3 regions as the epitopes of antibody PG9 and PGT127/PGT128, implicating a new paradigm of antigen recognition by these antibodies (*39*, *40*). The present review intends to provide an overview on our understanding of the structure and biological functions of the HIV-1 carbohydrates, and on how this information might be explored for developing carbohydrate-based vaccines against HIV/AIDS. Recent work on the design, synthesis, and antigenicity of various HIV-1 carbohydrate antigens and their mimics is highlighted.

Structural Features of Glycosylation of HIV-1 Gp120

HIV-1 has two envelope glycoproteins, gp120 and gp41. A typical gp120 molecule contains about 24 consensus N-glycosylation sites (NXS/T). Some early immunochemical studies also implicated the existence of O-linked glycosylations in gp120 (*41–43*). But direct structural evidence for the existence of O-glycans on HIV-1 gp120 is lacking. Basics of glycobiology and AIDS were discussed in two excellent earlier reviews (*44*, *45*). Discussed here are some major findings and recent progresses on the structural studies. Several groups have investigated the structures of HIV-1 gp120 N-glycans from both virus-derived and recombinant gp120, which were found to be highly heterogeneous and diverse (*46–54*). On the other hand, the transmembrane envelope glycoprotein gp41 has four conserved N-glycosylation sites that are normally occupied by N-glycans (*55*, *56*). However, to the best of our knowledge, the types of the N-glycans on each of the glycosylation sites of gp41 have not been fully characterized.

Analysis of the glycosylation pattern of the HIV-1IIIB gp120 expressed in Chinese hamster ovary (CHO) cells has revealed that all the 24 potential N-glycosylation sites are utilized for carbohydrate attachment. These include 13 sites for complex type oligosaccharides and 11 sites for high-mannose type or hybrid type oligosaccharides (*48*). Glycosylation site-specific analysis of HIV-1gp120 from different strains including JR-FL and CON-S indicated major differences in glycosylation site occupancy, thye nature and profiling of the

Downloaded by PENNSYLVANIA STATE UNIV on June 14, 2012 | http://pubs.acs.org
Publication Date (Web): June 12, 2012 | doi: 10.1021/bk-2012-1102.ch006

glycans, and the antibody's accessibility of the antigens (*51*, *52*). As for the complex type N-glycans on gp120, bi-, tri-, and tetra-antennary structures, with varied degree of sialylations, were characterized (*46*, *47*, *49–52*). In addition, a significant portion of the complex type oligosaccharides of the virus-derived gp120 was found to bear bisecting N-acetylglucosamine residues (*49*). The structural diversity of HIV-1 N-glycans is also dependent on the types of infected cells where the virus was derived, and on the expression system where the recombinant gp120 was produced. For example, the N-glycans of the recombinant gp120 produced in insect cells were found to be of high-mannose type but not complex type (*57*, *58*). There was also evidence for the presence of Fuc-α-(1-3) or α-(1-4)-GlcNAc moieties beyond the chitobiose core in the N-glycans of HIV-1 gp120 (*59*). Moreover, sulfation of GlcNAc residues of complex type N-glycans was characterized on both HIV-1 gp120 and gp160 produced in the human lymphoblastoid cell line Molt-4 (*60*).

On the other hand, the significantly high numbers of high-mannose type oligosaccharides are unusual for a mammalian glycoprotein. A high density of high-mannose type oligosaccharides was observed for free, virus-derived gp120, as well as the gp120 associated with HIV-1 infected lymphoblastoid (H9) cells. In one study, high-mannose type structures (Man_5 to Man_9) was shown to be approximate 60% of the total sugar chains (*49*); in another investigation, the high-mannose type structures (Man_7 to Man_9) account for 80% of the total N-glycans for T cell-associated gp120, and 50% for the free virus-derived gp120 with Man_8 and Man_9 as the main components (*47*). More recent studies further demonstrated that the virion-associated envelope glycoprotein gp120 from primary isolates of HIV-1 (clades A, B, and C) and from the simian immunodeficiency virus presented predominantly high-mannose type N-glycans ranging from Man5GlcNAc2 to Man9GlcNAc2, which was in stark contrast to recombinant gp120 that bears both high-mannose type and complex type N-glycans (*53*, *54*).

Clustering of oligosaccharides on the viral surface is another feature of HIV-1 glycosylation. The three-dimension structure of de-glycosylated gp120 was resolved (*61*, *62*). The core gp120 structure allowed an investigation on how the carbohydrates were globally distributed on the surface of the HIV-1 gp120. Remodeling of N-glycans on the de-glycosylated core revealed that a great deal of gp120 surface was covered by a carbohydrate coat (*20*, *61*, *62*). These N-glycans shield some receptor-binding regions of the protein backbone, and limit the access of neutralizing antibodies.

Since the HIV-1 carbohydrates are produced by the host glycosylation machinery and may appear as "self" to the immune system, the dense glycosylation would reduce the potential of the underneath protein backbone to serve as immunological targets. The dense glycosylation region on gp120 is thus called immunologically "silent" surface (*62*). Interestingly, when the types of oligosaccharides of N-glycans are sorted out at each glycosylation site, the high-mannose type N-glycans appear to be clustered together on one surface, while the complex type N-glycans are clustered as a distinct domain on another area of the surface, with little structural overlap of the two domains (*50*). The presence of the two distinct oligosaccharide clusters, together with some

Downloaded by PENNSYLVANIA STATE UNIV on June 14, 2012 | http://pubs.acs.org
Publication Date (Web): June 12, 2012 | doi: 10.1021/bk-2012-1102.ch006

"unusual" structures in the subunit oligosaccharides (e.g., fucosylation, sulfation, and bisecting structures), may provide new carbohydrate targets for vaccine development.

Biological Functions of HIV-1 N-Glycosylation

Effects of Glycosylation on the Antigenicity and Immunogenicity of the Viral Envelope

Early studies have demonstrated that N-glycosylation of HIV-1 affects the processing and maturation of the envelope glycoproteins and the infectivity of the virus (*63–65*). Glycosylation is also necessary for the correct folding of HIV-1 gp120 (*66*). Meanwhile, compelling data have shown that N-glycans of gp120 exert profound effects on the antigenicity and immunogenicity of the viral envelope glycoproteins. The dense carbohydrate shield forms a strong barrier to help protect HIV from immune recognition and limit effectiveness of antibody neutralization.

Strong evidence has come from the studies in rhesus monkeys with simian immunodeficiency virus (SIV) mutants lacking N-glycans in the V1 region of the envelope (*67*). When glycosylation sites were removed from the V1 loop of the SIV gp120, not only did the resulting mutants become much more sensitive to antibody neutralization, but the glycosylation mutants also exhibited greatly enhanced immunogenicity in the animals, eliciting much better immune responses that are reactive to both mutants and the wild-type virus (*67*). Similarly, it was also reported that deleting the V1/V2 loops from HIV-1 gp120, as well as removing other specific N-glycosylation sites on the HIV-1 envelope glycoprotein, rendered the underneath protein domains more vulnerable to antibody binding and dramatically increased viral sensitivity to antibody neutralizations (*68–73*).

On the other hand, a recent analysis of the mutations in the envelope glycoproteins by sequencing the gp160 genes of multiple escape viruses revealed a "dynamic glycosylation" as a new mechanism for HIV to evade neutralizing antibodies (*74*). It was found that a high frequency of mutations occurred at the consensus N-glycosylation sites (NXS/T) during chronic and persistent infections. Strikingly, a mutation at the old glycosylation site was usually companied with an insertion of an alternative N-glycosylation site nearby, resulting in a reposition or shifting of the N-glycans. The glycosylation mutants became more resistant to antibody neutralization. That is, HIV-1 escapes neutralizing antibodies by selected changes in N-glycan packing, but maintaining the global glycosylation, e.g., the total number of N-glycans, relatively constant. The so-called "evolving glycan shield" represents a new strategy for HIV-1 to maintain persistent replication in the face of an evolving antibody repertoire.

Carbohydrates as Ligands for HIV-1 Infection and Transmission

In addition to a strong defensive role for HIV immune evasion, the viral surface N-glycans was also implicated to play an active role in HIV-1 infection and transmission. It was proposed that immature dendritic cells, which are primary

Downloaded by PENNSYLVANIA STATE UNIV on June 14, 2012 | http://pubs.acs.org
Publication Date (Web): June 12, 2012 | doi: 10.1021/bk-2012-1102.ch006

antigen-presenting cells and are richly expressed in the skin and at the mucosal surfaces, are the first cells targeted by HIV-1 during transmission (*75*, *76*). A recently identified, dendritic cell specific C-type lectin, DC-SIGN, was found to be able to bind to HIV-1 envelope gp120 and to mediate the migration of HIV from the mucosal infection sites to secondary lymphoid organs, where the virus infects T cells (*77*, *78*).

More detailed studies on molecular levels suggested that the interaction between HIV-1 gp120 and dendritic cells was carbohydrate dependent, and the high-mannose type oligosaccharides on HIV-1 gp120 served as ligands for DC-SIGN being expressed on dendritic cells (*79–85*). In addition, HIV-1 oligosaccharides such as the high-mannose type oligosaccharides and those N-glycans with terminal fucose and N-acetylglucosamine residues may serve as ligands for mannose receptors richly expressed on macrophages. The specific carbohydrate-receptor interactions may facilitate the viral infection of macrophages and may also have an influence on the viral tropism (*86–89*).

Carbohydrate Antigens on HIV-1

The Epitope of the Broadly Neutralizing Antibody 2G12

The identification of conserved and accessible epitopes on HIV-1 is an essential step for vaccine development. The characterization of the epitopes of some broadly neutralizing antibodies provides important clues on rational immunogen design. Until recently, only a few monoclonal antibodies, including 2F5, 4E10, b12, and 2G12, were characterized that showed broadly neutralizing activities against both laboratory-adapted and primary HIV isolates (*6–9*, *11*). The epitopes of 2F5 and 4E10 were mapped to the C-terminal ectodomain of the transmembrane envelope glycoprotein gp41 (*90–93*), whereas the epitopes for the neutralizing antibodies b12 and 2G12 were characterized on the outer envelope glycoprotein gp120 (*30–32*, *94*, *95*).

Among the broadly HIV-neutralizing antibodies so far identified, the human monoclonal antibody 2G12 is unique, as it seems that it targets "purely" carbohydrate antigens on HIV-1 viral surface. Several pieces of evidence suggest that the epitope of 2G12 is a unique cluster of high-mannose type oligosaccharides (oligomannose) on HIV-1 gp120. Initial mutational studies indicated that the oligomannose sugar chains at the *N*-glycosylation sites N295, N332, N339, N386, N392, and N448 might be involved in 2G12 recognition (*30*). Two recent studies further proposed that the epitope of 2G12 might consist of several Manα1-2Man moieties contributed by the oligomannose sugar chains at sites N295, N332, and N392 that form a unique cluster on gp120 (*31*, *32*).

Systematic mutational studies suggested that peptide portions of gp120 are not directly involved in the binding of 2G12, but serve primarily as a rigid scaffold to hold the oligomannose sugars in proximity to form a unique cluster (*30–32*). The X-ray crystal structures of Fab 2G12 and its complexes with disaccharide Manα1,2Man and high-mannose oligosaccharide $Man_9GlcNAc_2$ were recently solved (*33*).

The X-ray structural study revealed an unusual domain-swapped structure, in which the V_H domains of 2G12 exchange in its two Fab regions so that an extended multivalent binding surface is created to accommodate an oligomannose cluster. Based on the X-ray structure, a model was proposed for the recognition between 2G12 and the N-glycans on gp120. The model implicated the binding of the N-glycans of N332 and N392 in the primary combining sites, with a potential binding of the N-glycan at N339 to the secondary binding site at the V_H/V_H' interface. All the evidence pointed to the fact that the epitope of broadly neutralizing antibody 2G12 is a novel oligomannose cluster on gp120. Although high-mannose oligosaccharide moiety exists in some human glycoproteins, such a high-density, clustering oligomannose structure as the 2G12 epitope has not been found in normal human glycoproteins so far. Therefore, the unique carbohydrate antigenic structure on HIV-1 gp120 provides an ideal template for designing a vaccine that may generate HIV-neutralizing antibodies but will not raise cross-reactivity or auto immune reactions in humans.

Downloaded by PENNSYLVANIA STATE UNIV on June 14, 2012 | http://pubs.acs.org
Publication Date (Web): June 12, 2012 | doi: 10.1021/bk-2012-1102.ch006

The Novel Glycopeptide Epitopes for Broadly Neutralizing Antibodies PG9 and PG16 and the PGT Series Monoclonal Antibodies

A new class of glycan-dependent, broadly neutralizing antibodies has recently been isolated from HIV-infected “elite controllers”. These antibodies, including the somatic variants PG9 and PG16 and the PGT series antibodies (PGT121-137 and PGT141-145) neutralize various primary HIV-1 strains across clades with remarkable breadth and potency (*34–38*). The PG9 and PG16 can neutralize 70-80% of circulating HIV-1 isolates (*34*). Moreover, the PGT series monoclonal antibodies are up to 10-fold more potent than PG9 and PG16, and 100-fold more potent than the previously reported prototype neutralizing antibodies such as b12, 2G12, 2F5 and 4E10 (*38*). Interestingly, epitope mapping suggest that this new class of antibodies exerts their neutralization by targeting the conserved N-glycans located in the V1/V2 and V3 domains (N160 and N156 of the V1/V2 region, or N322 and N301 of the V3 region, HXB2 numbering), together with a strand of peptide in the variable domain (*34–38*). These studies suggest that novel glycopeptides within the variable domains constitute the epitopes of the broadly neutralizing antibodies. Two recent X-ray structural studies have confirmed this notion (*39*, *40*). In one study, the structure of antibody PG9 in complex with a scaffolded V1/V2 domain of primary HIV-1 clade C strains (CAP45 and ZM109) was solved, indicating that PG9 recognized two N-glycans (at N160 and N156) and a peptide strand of the HIV-1 V1/V2 domain (*39*). In another study, the structure of PGT128 complexed with a glycosylated outer domain of JR-FL gp120 was solved, and the atomic level structural analysis revealed that PGT128 could penetrate the glycan shield to recognize two conserved N-glycans (N322 and N301) as well as a short β-strand peptide segment at the stem of the V3 domain (*40*). Taken together, these structural studies provide a valuable template for HIV vaccine design.

Other Potential Carbohydrate Epitopes on HIV-1 Envelope

Besides antibody 2G12, some other anti-carbohydrate antibodies were also reported to exhibit anti-HIV properties (*96–99*). For example, natural IgM anti-carbohydrate antibodies in baby rabbit serum that are specific for high-mannose oligosaccharides are able to effectively lyse virus-coated CD4+ T cells, regardless the virus strains (*96*). The observations implicated the existence of new potential carbohydrate epitopes on HIV-1 envelope glycoproteins other than the 2G12 epitope that was characterized as a novel oligomannose cluster. The structural analysis of HIV-1 glycosylations also revealed some unusual structures, such as the notable Fucα1,3 or α(1,4)GlcNAc moieties beyond the chitobiose core and the sulfated GlcNAc structure in certain context of the N-glycans. These structures, when coming together to form a unique configuration (clustering) on the envelope, may generate novel antigenic structures that are not expressed in normal human glycoproteins. In analogy to the clustering domain of high-mannose type oligosaccharides, a clustering domain of some complex type N-glycans was also present on the HIV-1 gp120 (*50*), which may also provide potential antigenic structures. Moreover, when an extended HIV-1 peptide portion is considered in the context, certain HIV-1 glycopeptides would be expected to constitute novel epitopes. This notion was reinforced by the recent discovery of a new class of glycan-dependent, broadlyneutralizing antibodies, such as PG9, PG16, and PGT128, the epitopes of wich are novel glycopeptides located in the V1/V2 and V3 regions of gp120. All these carbohydrate antigenic structures could have potentials for HIV-1 vaccine design.

Towards Carbohydrate-Based Vaccines against HIV/AIDS

The frustrating situation with conventional protein-based HIV vaccines urges the exploration of new vaccine approaches. As described above, the dense carbohydrate coat on HIV-1 envelope provides a strong defense for the virus to evade humoral immune recognition. However, this strong shield is not completely seamless. Accumulating evidence suggested that the HIV-1 surface carbohydrates themselves could also be targets for developing anti-HIV strategy. For example, a potent anti-HIV protein cyanovirin-N, isolated from a cyanobacterium, exerts its potent and broad-spectrum inhibitory activity against HIV-1 through tight binding to the high-mannose type oligosaccharides (Man_9 and Man_8) of gp120 (*100*, *101*). Some lectins (carbohydrate-binding proteins) specific for oligomannose structures also demonstrated anti-HIV-1 activities in *in vitro* assays (*102–112*).

Downloaded by PENNSYLVANIA STATE UNIV on June 14, 2012 | http://pubs.acs.org
Publication Date (Web): June 12, 2012 | doi: 10.1021/bk-2012-1102.ch006

From the vaccine development perspective, the most notable example is the discovery of the carbohydrate-specific neutralizing antibody 2G12. Thus, the carbohydrate epitope of 2G12, a unique oligomannose cluster, provides an excellent template for vaccine design. Several groups, including ours, have already begun to explore its potential in the hope of developing a carbohydrate-based vaccine against HIV/AIDS.

Binding of High-Mannose Type Oligosaccharide Subunits to 2G12

Structural analysis indicated that HIV-1 expressed an array of high-mannose type oligosaccharides, ranging from Man_5, Man_6, Man_7, Man_8, to Man_9 (*47*, *49*, *50*). Although it was demonstrated that 2G12 recognizes an oligosaccharide cluster consisting of several high-mannose type oligosaccharides on gp120, and biochemical analysis suggested that Manα1,2Man residues were crucial for the recognition (*31*, *32*), it was hitherto not clear how the distinct oligomannose subunits (Man5-Man9) behave individually in the binding to 2G12. The information is important for selecting the right ‘building block” for making epitope mimics. Accordingly, we prepared three typical HIV-1 high-mannose type oligosaccharides, namely $Man_5GlcNAc$, $Man_6GlcNAc$, and $Man_9GlcNAc$ (Figure 1) and examined their affinity to 2G12 by competitive inhibition of 2G12 binding to immobilized gp120. The competitive enzyme-linked immunosorbent assay (ELISA) experiments gave an IC_{50} (concentration for 50% inhibition) of 0.96 mM, 70 mM, and 200 mM for $Man_9GlcNAc$, $Man_6GlcNAc$, and $Man_5GlcNAc$ oligosaccharides, respectively (*113*).

The results suggest that Man_9GlNAc is 74-fold and 210-fold more effective in inhibition of 2G12 binding than $Man_6GlcNAc$ and $Man_5GlcNAc$, respectively. The much higher affinity of $Man_9GlcNAc$ to 2G12 than that of $Man_5GlcNAc$ or $Man_6GlcNAc$ provides direct evidence that terminal Manα1,2Man linkages are essential for the antibody-epitope recognition. In comparison, $Man_9GlcNAc$ contains three terminal Manα1,2Man linkages, $Man_6GlcNAc$ contains one, whereas $Man_5GlcNAc$ does not have any terminal Manα1,2Man moiety. The results are consistent with previous observations from the binding of 2G12 to glycosidase-treated gp120. For example, treatment of gp120 with *Aspergillus saitoi* mannosidase, which selectively removes terminal Manα1,2Man linkages without touching the Manα1,3Man or Manα1,6Man residues on gp120, significantly reduced the binding of gp120 to 2G12 (*32*).

Our direct binding studies further suggest that the larger high-mannose oligosaccharide such as $Man_9GlcNAc$ is the favorable subunit on gp120 for 2G12 recognition. Therefore, if native high-mannose type oligosaccharides would be considered for incorporation into an immunogen design, the larger oligosaccharide such as Man_9 should be the choice as the favorable “building block”.

Downloaded by PENNSYLVANIA STATE UNIV on June 14, 2012 | http://pubs.acs.org
Publication Date (Web): June 12, 2012 | doi: 10.1021/bk-2012-1102.ch006

Downloaded by PENNSYLVANIA STATE UNIV on June 14, 2012 | http://pubs.acs.org
Publication Date (Web): June 12, 2012 | doi: 10.1021/bk-2012-1102.ch006

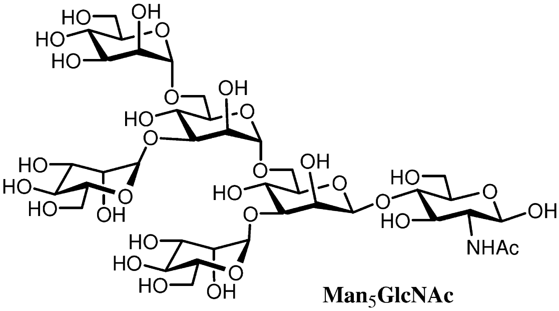

Man$_5$GlcNAc

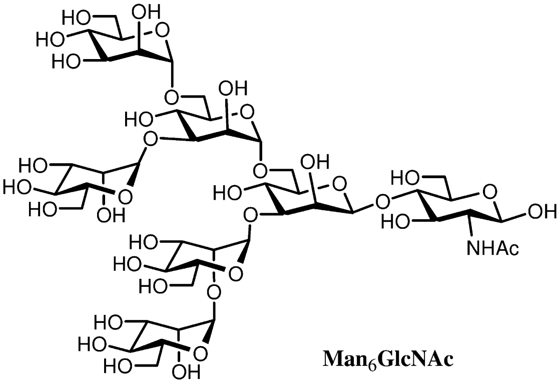

Man$_6$GlcNAc

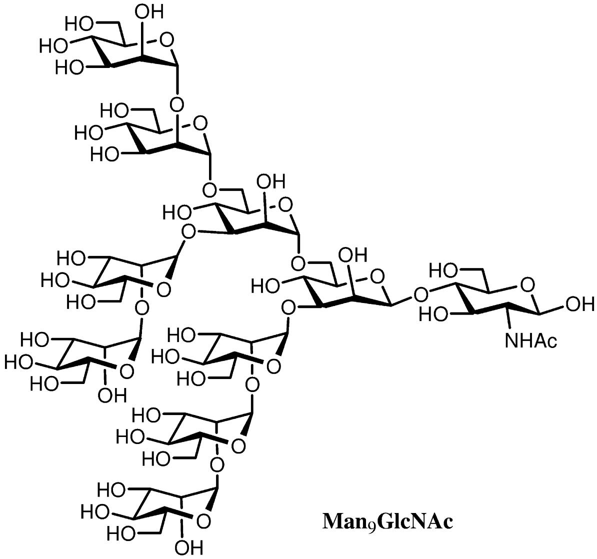

Man$_9$GlcNAc

Figure 1. Structures of typical HIV-1 high-mannose type oligosaccharides.

Downloaded by PENNSYLVANIA STATE UNIV on June 14, 2012 | http://pubs.acs.org
Publication Date (Web): June 12, 2012 | doi: 10.1021/bk-2012-1102.ch006

In another development related to 2G12 epitope, Wong *et al* synthesized a series of oligosaccharides with varied number and configuration of Manα1,2Man residues, using a programmable, reactivity-based one-pot synthetic method (*114*). The synthetic oligosaccharides, together with the standard oligosaccharide $Man_9GlcNAc_2$, were evaluated for their ability to inhibit the binding of 2G12 to immobilized gp120 in an ELISA assay. The structures and relative inhibitory activities (at 2 mM concentration) of the synthetic oligosaccharides are listed in Figure 2. Comparison between the trimannose **2** (15% inhibition at 2 mM) and tetramannose **3** (79% inhibition at 2 mM) suggested that adding up of an extra α1,2-linked mannose at an appropriate location could significantly enhance its binding efficiency. Pentamannose **4** (79% inhibition at 2 mM), which possesses a divalent Manα1,2Man configuration, shows similar activity to the tetramannose **3** that has two sequential Manα1,2Man units. Interestingly, the heptamannose **5** (65% inhibition at 2 mM), which contains an additional Manα1,2Manα1,2Man branch at the 6-position of the core mannose in **3**, does not show further increased affinity over **3**. It is interesting to observe that the tetramannose **3** exhibited similar affinity to antibody 2G12 as the native $Man_9GlcNAc_2$, which showed 71% inhibition at 2mM in the competitive assay.

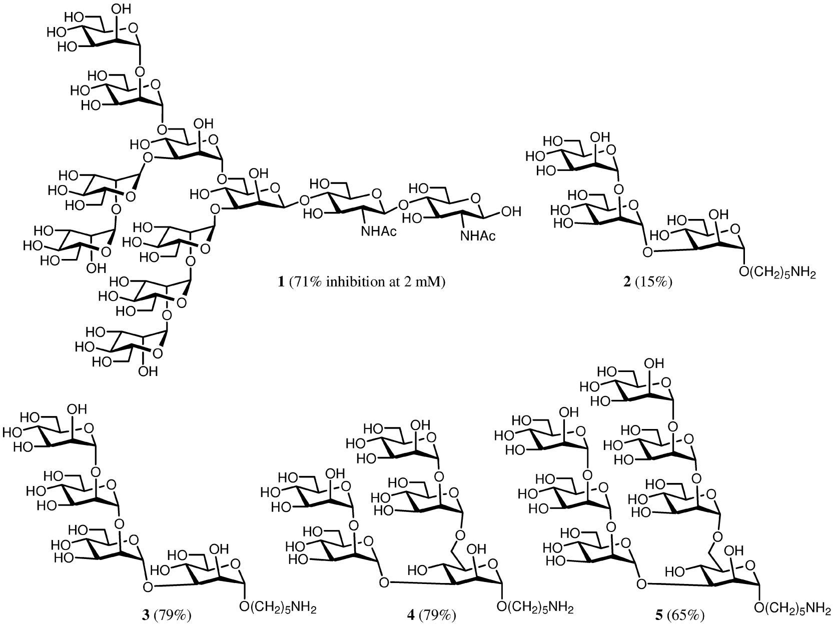

1 (71% inhibition at 2 mM)

2 (15%)

3 (79%)

4 (79%)

5 (65%)

Figure 2. Structures of the synthetic oligomannose compounds.

Downloaded by PENNSYLVANIA STATE UNIV on June 14, 2012 | http://pubs.acs.org
Publication Date (Web): June 12, 2012 | doi: 10.1021/bk-2012-1102.ch006

Synthesis and Antigenicity of Template-Assembled Oligomannose Clusters as the Mimics of 2G12 Epitope

Although Man_9 and the synthetic oligosaccharides, tetramannose (**3**) and pentamannose (**4**), showed enhanced affinity to 2G12 over other oligosaccharides so far tested, the affinity is still too weak. The mM-range exhibited by these oligosaccharide subunits are far away from the nM-range exhibited by the binding of HIV-1 gp120 to 2G12. We reasoned that assembly of oligomannose such as Man_9 on a suitable scaffold molecule should provide novel oligosaccharide clusters that may mimic or capture 2G12 epitope as it is presented on HIV-1 gp120.

To test the hypothesis, we synthesized bi-, tri- and tetra-valent Man_9 clusters based on a galactopyranoside scaffold (Figure 3). The choice of a galactopyranoside as a template was based on the following considerations. When a galactopyranoside is used as the scaffold to present the oligosaccharides, the oligosaccharide chains being installed at C-3, 4, and 6 positions will face above the galactose ring to form a cluster, while the oligomannose sugar chain at position C-2 is likely to be located on the flank of the cluster. We expect that this arrangement will at least partially mimic the spatial orientation of the carbohydrate epitope of antibody 2G12, which most likely include the N-glycans at N295, N332, and N392 (*31*, *32*). The distances between each pair of the Asn residues, N295-N332, N332-N392, and N295-N392 , were measured to be 5.8, 20.3, and 23.6 Å, respectively, based on the reported structure of gp120 core (*62*). By adjusting the length of the spacer, we expect that the distances among the conjugating sites in the synthetic cluster could fall in the range as measured on the gp120 core.

The key step for the oligosaccharide cluster synthesis was the chemoselective ligation between a thiol-tagged oligosaccharide and a maleimide-functionalized template (*113*). We have previously used this type of ligation for preparing large and complex multivalent peptides and glycoconjugates (*115–118*). The SH-tagged high-mannose oligosaccharide, Man_9-SH, was prepared in two steps: the selective N-acylation of the free amino group in $Man_9GlcNAc_2Asn$ with N-succinimidyl S-acetylthioacetate (SATA) (*119*) and subsequent removal of the S-acetyl group by treatment with hydroxylamine. The bi-, tri-, and tetravalent maleimide cluster, MC-1, MC-2, and MC-3 were prepared through functional group manipulations on ethyl α-D-galactopyranoside (*115*, *118*).

Chemoselective ligation between the Man_9-SH and the maleimide clusters proceeded very efficiently in a phosphate buffer (pH 6.6) containing acetonitrile to give the corresponding oligosaccharide clusters in high yields. On the other hand, a dimer of $Man_9GlcNAc_2Asn$ was prepared through oxidation of Man_9-SH (Figure 3). All the products were purified by reverse- phase HPLC and characterized by electron spray ionization-mass spectroscopy (ESI-MS) (*113*).

The affinity of the synthetic clusters was evaluated by a competitive inhibition of 2G12 binding to the immobilized HIV-1 gp120 in an ELISA assay. The IC50 data were deduced to be 0.4, 0.13, 0.044, and 0.013 mM for Man9-dimer, Bi-Man9, Tri-Man9, and Tetra-Man9, respectively. If IC_{50} was taken as an indication for relative affinity, the affinity of the tetravalent cluster (Tetra-Man_9)

to antibody 2G12 would be 73-fold higher than that of subunit $Man_9GlcNAc_2Asn$. On the other hand, the tri- and bi-valent oligomannose clusters are 22- and 7-fold more effective than $Man_9GlcNAc_2Asn$ in binding to 2G12. Another interesting finding from our binding studies came from the two bivalent oligomannose compounds, Bi-Man_9 and Man_9-dimer. The Bi-Man_9, which has a longer distance between the two Man_9 subunits, is 3-fold more effective than the Man_9-dimer in inhibition of 2G12 binding to gp120. The results suggest that control of the geometry and the distance between the oligosaccharide subunits is important to achieve a tight binding to antibody 2G12. It should be pointed out that although the synthetic oligosaccharide clusters reached a *micromolar* level in binding to 2G12, the affinity is still much lower than that of HIV-1 gp120, which binds to 2G12 at a *nanomolar* level. Therefore, further optimization of the epitope mimics is necessary.

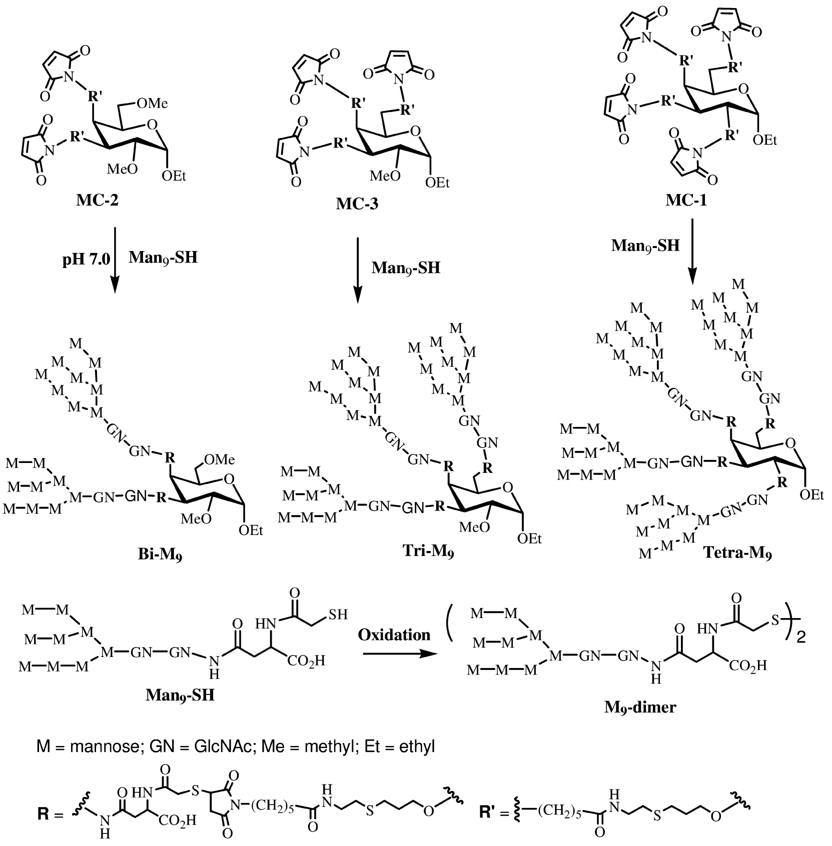

Figure 3. Structures and synthesis of a set of synthetic oligomannose clusters.

Downloaded by PENNSYLVANIA STATE UNIV on June 14, 2012 | http://pubs.acs.org
Publication Date (Web): June 12, 2012 | doi: 10.1021/bk-2012-1102.ch006

In exploring new scaffold for assembling mimics of 2G12 epitope, we synthesized a trivalent oligomannose cluster using cholic acid as the scaffold molecule (*120*) (Figure 4). The design of such an oligosaccharide cluster was based on the proposed model for the recognition between 2G12 and HIV-1 glycans, which suggested that the N-glycans at N295 and N332 of gp120 would bind to the primary combining sites of 2G12, while the N-glycan at N339 might interact with the secondary binding site of 2G12 (*33*). Therefore, the cholic acid-based oligomannose cluster was made to mimic the oligosaccharide cluster formed by the N-glycans from the N295, N332, and N339 sites. The cluster was synthesized in two key steps: introduction of maleimide functionality at the 3α, 7α, and 12α-positions of cholic acid and chemoselective ligation of the maleimide cluster with Man_9-SH. Binding studies revealed that the synthetic oligomannose cluster was 46-fold more effective than subunit $Man_9GlcNAc_2Asn$ in inhibiting 2G12-binding to HIV-1 gp120. This cholic acid-based mimic showed a moderate enhancement in the 2G12-affinity when compared to the trivalent, galactoside-scaffolded mimic. A free amino group introduced at the C24 position of the cluster would facilitate its coupling to a carrier protein to provide a functional immunogen.

Downloaded by PENNSYLVANIA STATE UNIV on June 14, 2012 | http://pubs.acs.org
Publication Date (Web): June 12, 2012 | doi: 10.1021/bk-2012-1102.ch006

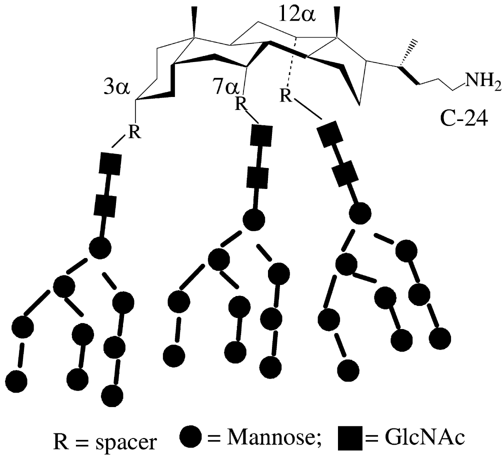

Figure 4. Structure of the synthetic, cholic acid-based oligomannose cluster.

In another study, novel oligomannose clusters were designed that contains four copies of selected fluorinated D1 arm tetrasaccharides built on a cyclic peptide template (*121*). The oligomannose clusters were successfully assembled on a cyclic decapeptide template using the the copper(I)-catalyzed alkyne-azide 1,3-dipolar cycloaddition (CuAAC) reaction to introduce four units of a synthetic D1 arm tetrasaccharide (Manα1,2Manα1,2Manα1,3Manα-) on one face of the template and two T-helper epitope peptides on the other face of the template

Downloaded by PENNSYLVANIA STATE UNIV on June 14, 2012 | http://pubs.acs.org
Publication Date (Web): June 12, 2012 | doi: 10.1021/bk-2012-1102.ch006

(Figure 5). Surface plasmon resonance (SPR) binding studies indicated that while single D1 arm tetrasaccharide had only weak affinity for human antibody 2G12, the corresponding template-assembled oligosaccharide clusters showed high affinity to antibody 2G12, indicating a clear clustering effect in 2G12 recognition. Interestingly, the binding study revealed that the fluorinated D1 arm cluster, in which the 6-OH of the terminal mannosyl residue was replaced with a fluorine atom, showed a distinct kinetic model in 2G12 binding as compared with the cluster of the natural D1 arm oligosaccharides. Moreover, the oligosaccharide clusters with varied length of spacers showed different affinities for 2G12, suggesting that an appropriate spatial orientation of the sugar chains in the cluster was crucial for high affinity binding to antibody 2G12. It would be interesting to test whether these florinated oligomannose could serve as an effective immunogen to raise better antibody responses than the native D1 arm Man4 clusters.

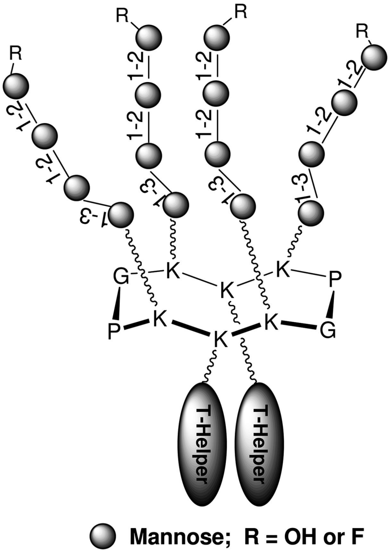

Figure 5. Structure of the cyclic peptide-based oligomannose clusters carrying the D1 arm Man4 and selectively fluorinated Man4 units.

In yet another independent study, Danishefsky and co-workers also designed cyclic peptide-template oligomannose clusters, in which 2 or 3 copies of synthetic Man9GlcNAc2 moiety were grafted on the template (Figure 6) (*122*). Again, binding studies indicated a clear clustering effect of the synthetic mimics. That is, the trivalent had a higher affinity for antibody 2G12 than the divalent compound. In addition, a suitable functional handle (a thiol group) was introduced into the construct, making it suitable for conjugating to a carier protein to provide a glycoconjugate vaccine.

Downloaded by PENNSYLVANIA STATE UNIV on June 14, 2012 | http://pubs.acs.org
Publication Date (Web): June 12, 2012 | doi: 10.1021/bk-2012-1102.ch006

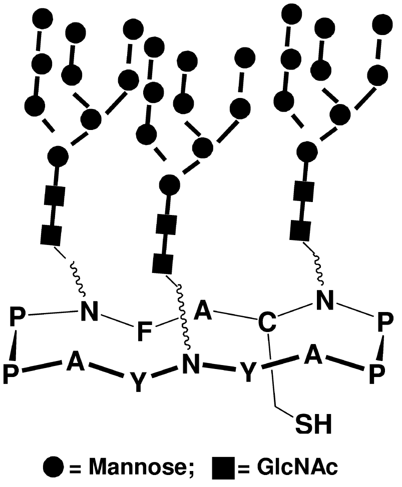

Figure 6. Structure of the cyclic peptide-based oligomannose cluster carrying three Man9GlcNAc2 units.

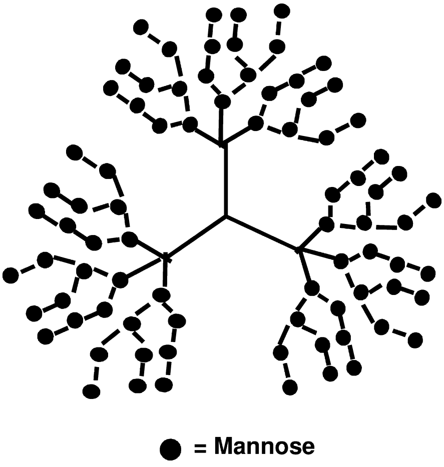

Figure 7. Structure of the synthetic glyco-dendrimers carrying multiple copies of Man9GlcNAc2 units.

More recently, Wong and co-workers designed a series of oligomannose dendrimers containing multiple copies of the D1 arm tetrasaccharide (Man4) and the full-size high-mannose oligosaccharide (Man9), but lacking the inner two GlcNAc moieties (*123*). The oligomannose dendrimers were synthesized on an AB3 type dendrimeric skeleton and the CuAAC click chemistry was used to assemble the dendrimers (Figure 7). Binding studies with 2G12 indicated that some of the higher dendrimers carrying 9-25 copies of the Man4 and/or Man9 units could bind to 2G12 very efficiently, with an IC_{50} in the range of nM concentrations. In a competitive assay, the Man9-containing dendrimers were particularly efficient in inhibiting the interactions between gp120 and 2G12 or DC-SIGN, suggesting that these synthetic glyco-dendrmers could well mimic the dense high-mannose carbohydrate antigens on HIV-1 gp120. Thus, there is a potential to use these synthetic glyco-dendrimers for the development of both carbohydrate vaccine candidates and antiviral agents.

Downloaded by PENNSYLVANIA STATE UNIV on June 14, 2012 | http://pubs.acs.org
Publication Date (Web): June 12, 2012 | doi: 10.1021/bk-2012-1102.ch006

HIV-1 Glycopeptides as Potential Targets for HIV-1 Vaccine Design

While novel HIV-1 carbohydrates, such as the epitope of 2G12, should be further investigated for HIV vaccines, certain HIV-1 glycopeptides may have a greater potential to form unique epitopes (antigenic determinants) on HIV-1 than sugar chains alone. It seems that the epitopes of the recently discovered glycan-dependent, broadly neutralizing antibodies, such as PG9, PG16, and the PGT series antibodies, fall into this category. To explore this potential, first of all, it is necessary to develop efficient methods for constructing the HIV-1 glycopeptides of interest, which are hitherto not easy to synthesize (*124–131*).

For the purpose, we initiated a project aiming to construct various HIV-1 glycopeptides by a chemoenzymatic approach, and to apply them as components for HIV-1 vaccines. The first, native HIV-1 glycopeptides that we synthesized were the gp120 fragment derived from the sequence 336-342, which contains the N339 N-glycan as part of the 2G12 epitope (Figure 8). Endoglycosidase (ENGase)-catalyzed oligosaccharide transfer was used as the key step for the glycopeptide synthesis (*132–135*). First, the acceptor GlcNAc-peptide was synthesized by automatic peptide synthesis. Homogeneous glycoforms of the gp120 peptide containing Man_9, Man_6, and Man_5 N-glycans, respectively, were then constructed using endo-β-*N*-acetylglucosaminidase from *Arthrobacter* (Endo-A) as the key enzyme. Using $Man_9GlcNAc_2Asn$ as the glycosyl donor and the chemically synthesized GlcNAc-peptide as the glycosyl acceptor, the Endo-A catalyzed transglycosylation gave the Man_9-glycopeptide in 28% isolated yield. Similarly, Transglycosylation using $Man_5GlcNAc_2Asn$ and $Man_6GlcNAc_2Asn$ as the glycosyl donors, which were prepared through pronase digestion of chicken ovalbumin, gave the Man_5-and Man_6-glycopeptides in 25% and 27% yields, respectively. Interestingly, it was observed that Endo-A was equally efficient for transferring all high-mannose type oligosaccharides, making it particularly useful for constructing an array of high-mannose type N-glycopeptides (*136*).

Downloaded by PENNSYLVANIA STATE UNIV on June 14, 2012 | http://pubs.acs.org
Publication Date (Web): June 12, 2012 | doi: 10.1021/bk-2012-1102.ch006

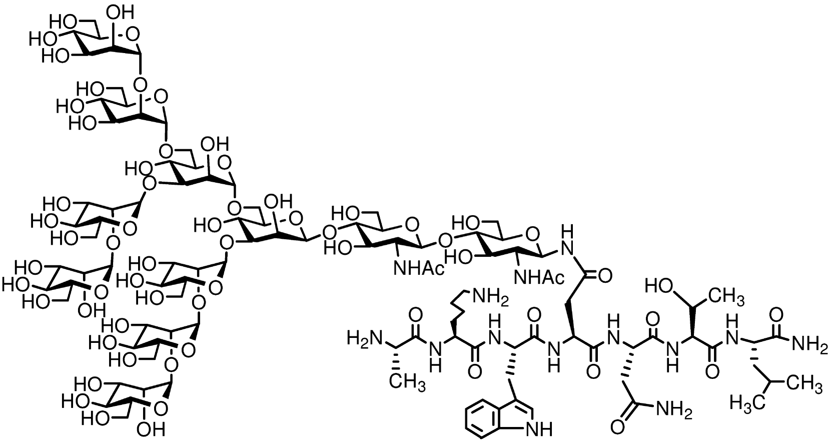

M9-gp120(336-342)

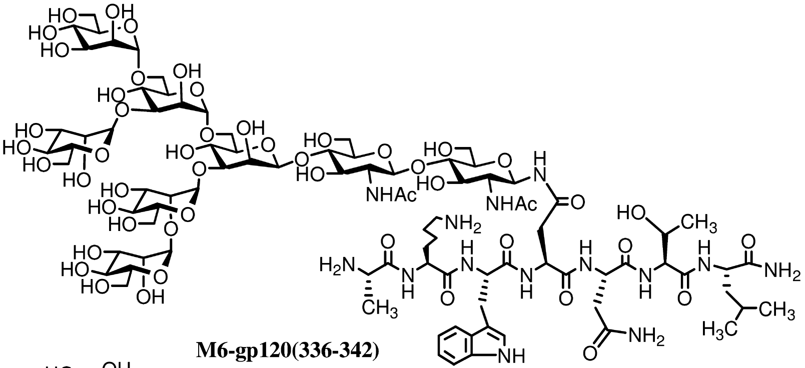

M6-gp120(336-342)

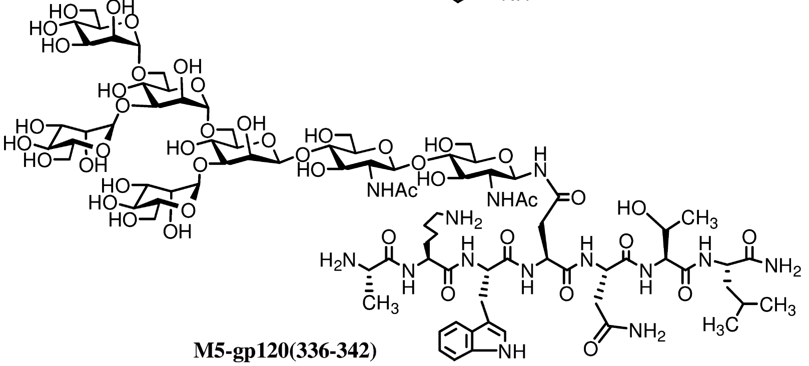

M5-gp120(336-342)

Figure 8. Structures of the synthetic gp120 glycopeptides.

While the englycosidase-catalyzed transglycosylation allows a highly convergent assembly of complex glycopeptides, two major issues remained: the relatively low transglycosylation efficiency and the hydrolysis of the transglycosylation products. Major progresses have been made in recent years to address these problems. First, the exploration of synthetic sugar oxazoline, the presumed enzymatic reaction intermediate, as donor substrate significantly enhanced the transglycosylation efficiency (*137–141*); secondly, site-directed mutagenesis led to the discovery of novel glycosynthases, the endoglycosidase mutants that are able to use the highly activated sugar oxazoline as donor substrate for transglycosylation, but are devoid of product hydrolysis activity (*142–146*). With these advances in synthetic methodology, some complex HIV-1 gp120 and gp41 glycopeptides were prepared in a concise manner in high yields (*137*, *142*, *147*, *148*). For example, HIV-1 V3 glycopeptides carrying two N-linked pentasaccharides (at the conserved N-glycosylation sites N295 and N332) were successfully synthesized by this chemoenzymatic method (Figure 9). The synthesis consisted of two key steps: a solid-phase synthesis of the cyclic, 47-mer V3 domain peptide containing two GlcNAc residues and an Endo-A catalyzed transglycosylation that simultaneously added two N-glycan moieties to the polypeptide from the oligosaccharide oxazoline to provide the final glycopeptide. The synthetic glycopeptide was used to probe the effects of glycosylation on the global conformations and protease-sensitivity of HIV-1 V3 domain. It is expected that this convergent and efficient chemoenzymatic strategy will be further exexplored for assembling various complex HIV-1 glycopeptide antigens, such as the putative epitopes of the recently discovered broadly neutralizing antibodies (PG9, PG16, PGT121-137, and PGT141-145), for evaluating their potential in HIV-1 vaccine design.

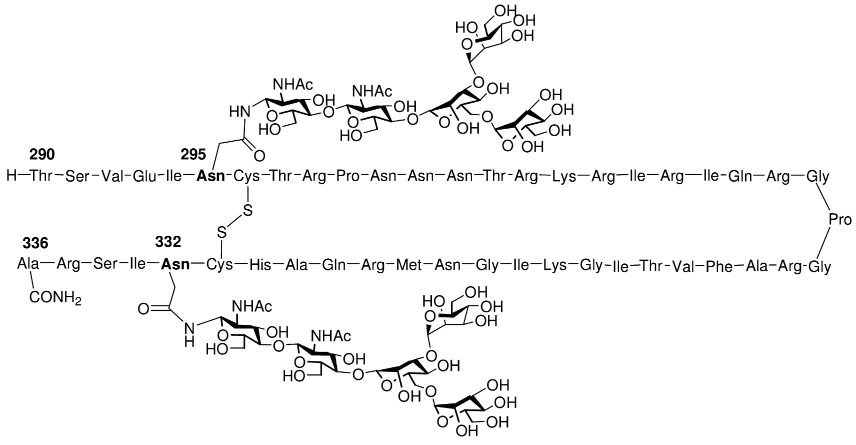
290
295
H–Thr–Ser–Val–Glu–Ile–Asn–Cys–Thr–Arg–Pro–Asn–Asn–Asn–Thr–Arg–Lys–Arg–Ile–Arg–Ile–Gln–Arg–Gly
Pro
336
332
Ala–Arg–Ser–Ile–Asn–Cys–His–Ala–Gln–Arg–Met–Asn–Gly–Ile–Lys–Gly–Ile–Thr–Val–Phe–Ala–Arg–Gly
CONH2
NHAc
HN
HO
OH
O
S

Figure 9. Structures of the synthetic HIV-1 V3 glycopeptides carrying N-glycans at the N295 and N332 conserved glycosylation sites.

In contrast to chemoenzymatic synthesis, Danishefsky *et al* launched a total chemical synthesis of HIV-1 gp120 glycopeptides carrying either a hybrid type or a high-mannose type N-glycans (*149*, *150*). The total synthesis consists of the pre-assembly of the full-size N-glycans by multiple step chemical synthesis, and the convergent coupling of the N-glycans with a selectively protected peptide containing a free aspartic acid. The structures of the two gp120 glycopeptides

Downloaded by PENNSYLVANIA STATE UNIV on June 14, 2012 | http://pubs.acs.org
Publication Date (Web): June 12, 2012 | doi: 10.1021/bk-2012-1102.ch006

synthesized were shown in Figure 10. The synthetic glycopeptides contains a hybrid or high-mannose type N-glycan at the N332 glycosylation site, which was part of the 2G12 epitope. Interestingly, a subsequent binding study indicated that while the synthetic high-mannose type glycopeptide showed only marginal affinity for antibody 2G12, the corresponding glycopeptide dimer (formed through an intermolecular disulfide linkage) demonstrated a moderate affinity to 2G12, further indicating the requirement of multivalency in 2G12 binding (*151*). Moreover, the hybrid glycan containing glycopeptide did not show any affinity for 2G12. This study provided the first direct evidence indicating that hybrid N-glycan was not part of the 2G12 epitope.

Downloaded by PENNSYLVANIA STATE UNIV on June 14, 2012 | http://pubs.acs.org
Publication Date (Web): June 12, 2012 | doi: 10.1021/bk-2012-1102.ch006

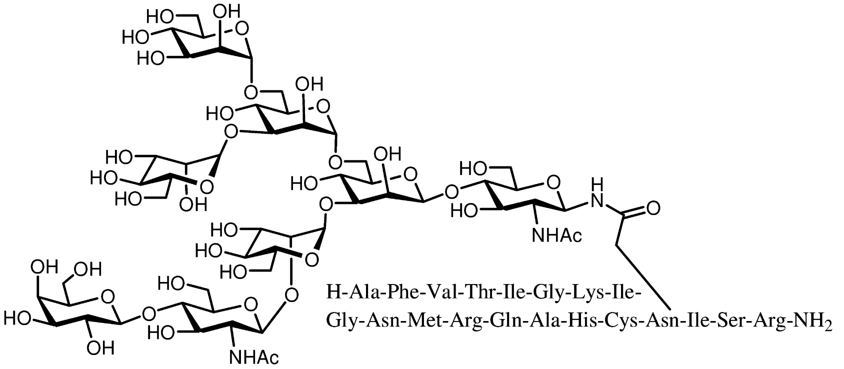
H-Ala-Phe-Val-Thr-Ile-Gly-Lys-Ile-
Gly-Asn-Met-Arg-Gln-Ala-His-Cys-Asn-Ile-Ser-Arg-NH2
NHAc

Hybrid type gp120 fragment (316-335)

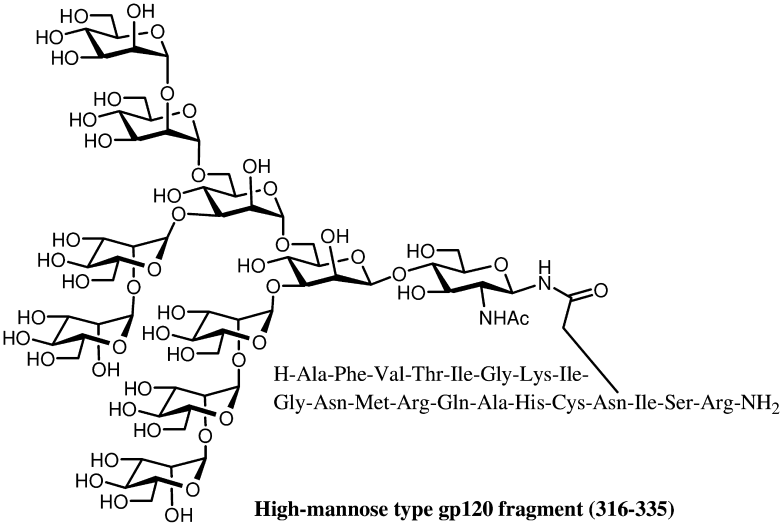
H-Ala-Phe-Val-Thr-Ile-Gly-Lys-Ile-
Gly-Asn-Met-Arg-Gln-Ala-His-Cys-Asn-Ile-Ser-Arg-NH2
NHAc

High-mannose type gp120 fragment (316-335)

Figure 10. Structures of the two gp120 glycopeptides synthesized by total chemical synthesis.

Preliminary Immunization Studies with Synthetic Glycoconjugate Immunogens

With the progress in the design and synthesis of 2G12 epitope mimics, several attempts have been made to evaluate the immunogenicity of the synthetic mimics. It should be pointed out that HIV-1 carbohydrates themselves are generally poorly immunogenic. To improve their immunogenicity, the synthetic carbohydrate antigens are usually conjugated to a carrier protein such as KLH or BSA to fulfill a functional immunogen. Thus, we have conjugated the galactose-scaffolded Man9GlcNAc2 tetravalent construct to KLH and used the resulting KLH-conjugates to immunize rabbits (*152*). This first immunization study showed that the synthetic glycoconjuate raised moderate anti-carbohydrate IgG type antibodies. In addition, the anti-sera showed weak cross-reactivity to HIV-1 gp120. However, the anti-sera did not demonstrate any neutralizing activity againt HIV-1 in a preliminary HIV-neutralizing assay. These results suggest that either the glycoconjugate failed to raise any HIV-neutralizing antibodies or the neutralizing activity was too low to detect.

In another study, Danishefsky and co-workers covalently linked their cyclic peptide-based Man9GlcNAc2 divalent construct to the outer membrane protein complex (OMPC) carrier and evaluated its immunogenicity in two animal species (guinea pigs and rhesus macaques) (*153*). It was found that the glycoconjugate raised carbohydrate-specific antibodies. However, these antibodies showed only poor cross-reactivity to recombinant gp160 and, again, the anti-sera failed to neutralize a panel of HIV-1 isolates.

The Scripps group led by Burton, Wong, and Finn also evaluated the immunogenicity of several Man4 and Man9-containing glycoconjugates, in which the synthetic glycan lacks the two GlcNAc moieties (*154*, *155*). In one study, the synthetic D1 arm tetrasaccharide (Man4) was conjugated to BSA and the resulting BSA-(Man4)14 conjugate was used to immunize rabbits (*154*). In another study, the synthetic Man4 and Man9 were coupled to surface lysines on the icosahedral capsids of bacteriophage Q beta and cowpea mosaic virus (CPMV), and the resulting glycoconjugates were used for immunization (*155*). In both cases, high titers of anti-mannose antibodies were raised. However, none of the antibodies showed cross-reactivity with HIV-1 envelope, neither did they possess HIV-neutralizing activity. Given the fact that the glycoconjugates containing the full-size N-glycan with two GlcNAc moieties, Man9GlcNAc2, could raise antibibodies that were at least moderately cross-reactive with HIV-1 envelope (*152*, *153*), the present study implicates that the innermost two GlcNAc moieties in the N-glycan may play a role in determining the appropriate orientation of the N-glycans in the construct. A side-by-side test may be required to clarify this point. Recently, Geng and co-workers reported that a yeast mutant expressing exclusively Man8GlcNAc2 N-glycans was able to raise carbohydrate-specific IgG antibodies cross-reactive with monomeric HIV-1 gp120, but not with the native gp120 trimer displayed on HIV-1 (*156*, *157*). However, the yeast-elicited antibodies could efficiently neutralize virions expressing exclusively high-mannose N-linked glycans (*156*). These results suggest that both the nature of the high-mannose N-glycan and the way it

Downloaded by PENNSYLVANIA STATE UNIV on June 14, 2012 | http://pubs.acs.org
Publication Date (Web): June 12, 2012 | doi: 10.1021/bk-2012-1102.ch006

is presented in the construct are critical for raising envelope-reactive and HIV-neutralizing antibodies.

Conclusion

Carbohydrate-based conjugate vaccines have been developed for eliciting protective immunity against many pathogens such as bacteria (*158*, *159*). Carbohydrate-based cancer vaccines have also been under extensive research and some candidates have moved to clinical trials (*160–163*). However, carbohydrate antigens have not been adequately exploited for HIV-1 vaccine design, despite their abundance on HIV-1 surface. The existence of the broadly neutralizing antibody 2G12 and the characterization of its epitope as a novel oligosaccharide cluster on HIV-1 gp120 raised a possibility of developing a carbohydrate-based vaccine against HIV/AIDS. The 2G12-binding studies with natural and synthetic high-mannose oligosaccharides described in this article have yielded useful information that defines the structural requirement for the antibody recognition of the oligosaccharide subunits. The design and synthesis of template-assembled oligosaccharide clusters as mimics of 2G12 epitope has made it one step closer towards an HIV vaccine. Nevertheless, only limited progress has been made in eliciting gp120 cross-reactive antibodies and so far none of these synthetic glycoconjugate vacccines have elicited HIV-neutralizing antibodies except the recent promising finding with a yeast mutant, indicating the challenge in pursuing a carbohydrate-based HIV vaccine. On the other hand, the recent discovery of novel glycopeptide antigens in the varial domains as the putative epitopes of the new class of broadly HIV-neutralizing antibodies, including PG9, PG16, and the PGT series antibodies, raises new hope in the field. Future work should be directed to further characterization of the neutralizing epitopes and the evaluation of various HIV-1 glycopeptide constructs as vaccine candidates.

Downloaded by PENNSYLVANIA STATE UNIV on June 14, 2012 | http://pubs.acs.org
Publication Date (Web): June 12, 2012 | doi: 10.1021/bk-2012-1102.ch006

Note

This is an updated version of a chapter that previously appeared in *Carbohydrate Drug Design* (ACS Symposium Series 932), edited by Klyosov et al. and published in 2006.

Acknowledgments

The HIV vaccine work in my group was supported in part by the Institute of Human Virology, University of Maryland Biotechnology Institute, and the National Institutes of Health (NIH grants AI054354 and AI067111 to LXW).

References

1. Gallo, R. C. *Science* **2002**, *298*, 1728–1730.
2. Montagnier, L. *Science* **2002**, *298*, 1727–1728.
3. Gallo, R. C.; Montagnier, L. *N. Engl. J. Med.* **2003**, *349*, 2283–2285.

Downloaded by PENNSYLVANIA STATE UNIV on June 14, 2012 | http://pubs.acs.org
Publication Date (Web): June 12, 2012 | doi: 10.1021/bk-2012-1102.ch006

4. UNAIDS 2011.
5. Nabel, G. J. *Nature* **2001**, *410*, 1002–1007.
6. Burton, D. R.; Desrosiers, R. C.; Doms, R. W.; Koff, W. C.; Kwong, P. D.; Moore, J. P.; Nabel, G. J.; Sodroski, J.; Wilson, I. A.; Wyatt, R. T. *Nat. Immunol.* **2004**, *5*, 233–236.
7. Zolla-Pazner, S. *Nat. Rev. Immunol.* **2004**, *4*, 199–210.
8. Stamatatos, L.; Morris, L.; Burton, D. R.; Mascola, J. R. *Nat. Med.* **2009**, *15*, 866–870.
9. Vaccari, M.; Poonam, P.; Franchini, G. *Expert Rev. Vaccines* **2010**, *9*, 997–1005.
10. Kim, J. H.; Rerks-Ngarm, S.; Excler, J. L.; Michael, N. L. *Curr. Opin. HIV AIDS* **2010**, *5*, 428–434.
11. Kwong, P. D.; Mascola, J. R.; Nabel, G. J. *Cold Spring Harbor Perspect. Biol.* **2011**, *3*, a007278.
12. Melnick, J. L. *Clin. Microbiol. Rev.* **1996**, *9*, 293–300.
13. Sutter, R. W.; Tangermann, R. H.; Aylward, R. B.; Cochi, S. L. *Infect. Dis. Clin. North Am.* **2001**, *15*, 41–64.
14. Gross, C. P.; Sepkowitz, K. A. *Int. J. Infect. Dis.* **1998**, *3*, 54–60.
15. Hilleman, M. R. *Vaccine* **2000**, *18*, 1436–1447.
16. Cohen, J. *Science* **2003**, *300*, 28–29.
17. Rerks-Ngarm, S.; Pitisuttithum, P.; Nitayaphan, S.; Kaewkungwal, J.; Chiu, J.; Paris, R.; Premsri, N.; Namwat, C.; de Souza, M.; Adams, E.; Benenson, M.; Gurunathan, S.; Tartaglia, J.; McNeil, J. G.; Francis, D. P.; Stablein, D.; Birx, D. L.; Chunsuttiwat, S.; Khamboonruang, C.; Thongcharoen, P.; Robb, M. L.; Michael, N. L.; Kunasol, P.; Kim, J. H. *N. Engl. J. Med.* **2009**, *361*, 2209–2220.
18. Calarota, S. A.; Weiner, D. B. *AIDS* **2003**, *17* (Suppl 4), S73–84.
19. Burton, D. R. *Nat. Rev. Immunol.* **2002**, *2*, 706–713.
20. Wyatt, R.; Sodroski, J. *Science* **1998**, *280*, 1884–1888.
21. Moore, J. P.; Burton, D. R. *Nat. Med.* **1999**, *5*, 142–144.
22. Ho, D. D.; Huang, Y. *Cell* **2002**, *110*, 135–138.
23. Graham, B. S. *Annu. Rev. Med.* **2002**, *53*, 207–221.
24. Wang, L. X. *Curr. Pharm. Des.* **2003**, *9*, 1771–1787.
25. Wang, L. X. *Curr. Opin. Drug Discovery Dev.* **2006**, *9*, 194–206.
26. McMichael, A. J.; Rowland-Jones, S. L. *Nature* **2001**, *410*, 980–987.
27. Barouch, D. H.; Santra, S.; Schmitz, J. E.; Kuroda, M. J.; Fu, T. M.; Wagner, W.; Bilska, M.; Craiu, A.; Zheng, X. X.; Krivulka, G. R.; Beaudry, K.; Lifton, M. A.; Nickerson, C. E.; Trigona, W. L.; Punt, K.; Freed, D. C.; Guan, L.; Dubey, S.; Casimiro, D.; Simon, A.; Davies, M. E.; Chastain, M.; Strom, T. B.; Gelman, R. S.; Montefiori, D. C.; Lewis, M. G.; Emini, E. A.; Shiver, J. W.; Letvin, N. L. *Science* **2000**, *290*, 486–492.
28. Mascola, J. R.; Stiegler, G.; VanCott, T. C.; Katinger, H.; Carpenter, C. B.; Hanson, C. E.; Beary, H.; Hayes, D.; Frankel, S. S.; Birx, D. L.; Lewis, M. G. *Nat. Med.* **2000**, *6*, 207–210.
29. Baba, T. W.; Liska, V.; Hofmann-Lehmann, R.; Vlasak, J.; Xu, W.; Ayehunie, S.; Cavacini, L. A.; Posner, M. R.; Katinger, H.; Stiegler, G.;

Downloaded by PENNSYLVANIA STATE UNIV on June 14, 2012 | http://pubs.acs.org
Publication Date (Web): June 12, 2012 | doi: 10.1021/bk-2012-1102.ch006

Bernacky, B. J.; Rizvi, T. A.; Schmidt, R.; Hill, L. R.; Keeling, M. E.; Lu, Y.; Wright, J. E.; Chou, T. C.; Ruprecht, R. M. *Nat. Med.* **2000**, *6*, 200–206.

30. Trkola, A.; Purtscher, M.; Muster, T.; Ballaun, C.; Buchacher, A.; Sullivan, N.; Srinivasan, K.; Sodroski, J.; Moore, J. P.; Katinger, H. *J. Virol.* **1996**, *70*, 1100–1108.
31. Sanders, R. W.; Venturi, M.; Schiffner, L.; Kalyanaraman, R.; Katinger, H.; Lloyd, K. O.; Kwong, P. D.; Moore, J. P. *J. Virol.* **2002**, *76*, 7293–7305.
32. Scanlan, C. N.; Pantophlet, R.; Wormald, M. R.; Ollmann Saphire, E.; Stanfield, R.; Wilson, I. A.; Katinger, H.; Dwek, R. A.; Rudd, P. M.; Burton, D. R. *J. Virol.* **2002**, *76*, 7306–7321.
33. Calarese, D. A.; Scanlan, C. N.; Zwick, M. B.; Deechongkit, S.; Mimura, Y.; Kunert, R.; Zhu, P.; Wormald, M. R.; Stanfield, R. L.; Roux, K. H.; Kelly, J. W.; Rudd, P. M.; Dwek, R. A.; Katinger, H.; Burton, D. R.; Wilson, I. A. *Science* **2003**, *300*, 2065–2071.
34. Walker, L. M.; Phogat, S. K.; Chan-Hui, P. Y.; Wagner, D.; Phung, P.; Goss, J. L.; Wrin, T.; Simek, M. D.; Fling, S.; Mitcham, J. L.; Lehrman, J. K.; Priddy, F. H.; Olsen, O. A.; Frey, S. M.; Hammond, P. W.; Kaminsky, S.; Zamb, T.; Moyle, M.; Koff, W. C.; Poignard, P.; Burton, D. R. *Science* **2009**, *326*, 285–289.
35. Walker, L. M.; Simek, M. D.; Priddy, F.; Gach, J. S.; Wagner, D.; Zwick, M. B.; Phogat, S. K.; Poignard, P.; Burton, D. R. *PLoS Pathog.* **2010**, *6*, e1001028.
36. Doores, K. J.; Burton, D. R. *J. Virol.* **2010**, *84*, 10510–10521.
37. Bonsignori, M.; Hwang, K. K.; Chen, X.; Tsao, C. Y.; Morris, L.; Gray, E.; Marshall, D. J.; Crump, J. A.; Kapiga, S. H.; Sam, N. E.; Sinangil, F.; Pancera, M.; Yongping, Y.; Zhang, B.; Zhu, J.; Kwong, P. D.; O'Dell, S.; Mascola, J. R.; Wu, L.; Nabel, G. J.; Phogat, S.; Seaman, M. S.; Whitesides, J. F.; Moody, M. A.; Kelsoe, G.; Yang, X.; Sodroski, J.; Shaw, G. M.; Montefiori, D. C.; Kepler, T. B.; Tomaras, G. D.; Alam, S. M.; Liao, H. X.; Haynes, B. F. *J. Virol.* **2011**, *85*, 9998–10009.
38. Walker, L. M.; Huber, M.; Doores, K. J.; Falkowska, E.; Pejchal, R.; Julien, J. P.; Wang, S. K.; Ramos, A.; Chan-Hui, P. Y.; Moyle, M.; Mitcham, J. L.; Hammond, P. W.; Olsen, O. A.; Phung, P.; Fling, S.; Wong, C. H.; Phogat, S.; Wrin, T.; Simek, M. D.; Principal Investigators, P. G.; Koff, W. C.; Wilson, I. A.; Burton, D. R.; Poignard, P. *Nature* **2011**, *477*, 466–470.
39. McLellan, J. S.; Pancera, M.; Carrico, C.; Gorman, J.; Julien, J. P.; Khayat, R.; Louder, R.; Pejchal, R.; Sastry, M.; Dai, K.; O'Dell, S.; Patel, N.; Shahzad-ul-Hussan, S.; Yang, Y.; Zhang, B.; Zhou, T.; Zhu, J.; Boyington, J. C.; Chuang, G. Y.; Diwanji, D.; Georgiev, I.; Kwon, Y. D.; Lee, D.; Louder, M. K.; Moquin, S.; Schmidt, S. D.; Yang, Z. Y.; Bonsignori, M.; Crump, J. A.; Kapiga, S. H.; Sam, N. E.; Haynes, B. F.; Burton, D. R.; Koff, W. C.; Walker, L. M.; Phogat, S.; Wyatt, R.; Orwenyo, J.; Wang, L. X.; Arthos, J.; Bewley, C. A.; Mascola, J. R.; Nabel, G. J.; Schief, W. R.; Ward, A. B.; Wilson, I. A.; Kwong, P. D. *Nature* **2011**, *480*, 336–343.
40. Pejchal, R.; Doores, K. J.; Walker, L. M.; Khayat, R.; Huang, P. S.; Wang, S. K.; Stanfield, R. L.; Julien, J. P.; Ramos, A.; Crispin, M.; Depetris, R.; Katpally, U.; Marozsan, A.; Cupo, A.; Maloveste, S.; Liu, Y.; McBride, R.;

Ito, Y.; Sanders, R. W.; Ogohara, C.; Paulson, J. C.; Feizi, T.; Scanlan, C. N.; Wong, C. H.; Moore, J. P.; Olson, W. C.; Ward, A. B.; Poignard, P.; Schief, W. R.; Burton, D. R.; Wilson, I. A. *Science* **2011**, *334*, 1097–1103.

41. Hansen, J. E.; Clausen, H.; Nielsen, C.; Teglbjaerg, L. S.; Hansen, L. L.; Nielsen, C. M.; Dabelsteen, E.; Mathiesen, L.; Hakomori, S. I.; Nielsen, J. O. *J. Virol.* **1990**, *64*, 2833–2840.
42. Hansen, J. E.; Nielsen, C.; Arendrup, M.; Olofsson, S.; Mathiesen, L.; Nielsen, J. O.; Clausen, H. *J. Virol.* **1991**, *65*, 6461–6467.
43. Hansen, J. E.; Jansson, B.; Gram, G. J.; Clausen, H.; Nielsen, J. O.; Olofsson, S. *Arch. Virol.* **1996**, *141*, 291–300.
44. Feizi, T.; Larkin, M. *Glycobiology* **1990**, *1*, 17–23.
45. Feizi, T. In *Carbohydrates in Chemistry and Biology*; Wiley-VCH: 2000; Vol. 4, pp 851−863.
46. Mizuochi, T.; Spellman, M. W.; Larkin, M.; Solomon, J.; Basa, L. J.; Feizi, T. *Biochem. J.* **1988**, *254*, 599–603.
47. Geyer, H.; Holschbach, C.; Hunsmann, G.; Schneider, J. *J. Biol. Chem.* **1988**, *263*, 11760–11767.
48. Leonard, C. K.; Spellman, M. W.; Riddle, L.; Harris, R. J.; Thomas, J. N.; Gregory, T. J. *J. Biol. Chem.* **1990**, *265*, 10373–10382.
49. Mizuochi, T.; Matthews, T. J.; Kato, M.; Hamako, J.; Titani, K.; Solomon, J.; Feizi, T. *J. Biol. Chem.* **1990**, *265*, 8519–8524.
50. Zhu, X.; Borchers, C.; Bienstock, R. J.; Tomer, K. B. *Biochemistry* **2000**, *39*, 11194–11204.
51. Go, E. P.; Chang, Q.; Liao, H. X.; Sutherland, L. L.; Alam, S. M.; Haynes, B. F.; Desaire, H. *J. Proteome Res.* **2009**, *8*, 4231–4242.
52. Go, E. P.; Irungu, J.; Zhang, Y.; Dalpathado, D. S.; Liao, H. X.; Sutherland, L. L.; Alam, S. M.; Haynes, B. F.; Desaire, H. *J. Proteome Res.* **2008**, *7*, 1660–1674.
53. Bonomelli, C.; Doores, K. J.; Dunlop, D. C.; Thaney, V.; Dwek, R. A.; Burton, D. R.; Crispin, M.; Scanlan, C. N. *PLoS One* **2011**, *6*, e23521.
54. Doores, K. J.; Bonomelli, C.; Harvey, D. J.; Vasiljevic, S.; Dwek, R. A.; Burton, D. R.; Crispin, M.; Scanlan, C. N. *Proc. Natl. Acad. Sci. U.S.A.* **2010**, *107*, 13800–13805.
55. Perrin, C.; Fenouillet, E.; Jones, I. M. *Virology* **1998**, *242*, 338–345.
56. Lee, W. R.; Yu, X. F.; Syu, W. J.; Essex, M.; Lee, T. H. *J. Virol.* **1992**, *66*, 1799–1803.
57. Yeh, J. C.; Seals, J. R.; Murphy, C. I.; van Halbeek, H.; Cummings, R. D. *Biochemistry* **1993**, *32*, 11087–11099.
58. Butters, T. D.; Yudkin, B.; Jacob, G. S.; Jones, I. M. *Glycoconjugate J.* **1998**, *15*, 83–88.
59. Bolmstedt, A.; Biller, M.; Hansen, J. E.; Moore, J. P.; Olofsson, S. *Arch. Virol.* **1997**, *142*, 2465–2481.
60. Shilatifard, A.; Merkle, R. K.; Helland, D. E.; Welles, J. L.; Haseltine, W. A.; Cummings, R. D. *J. Virol.* **1993**, *67*, 943–952.
61. Kwong, P. D.; Wyatt, R.; Robinson, J.; Sweet, R. W.; Sodroski, J.; Hendrickson, W. A. *Nature* **1998**, *393*, 648–659.

Downloaded by PENNSYLVANIA STATE UNIV on June 14, 2012 | http://pubs.acs.org
Publication Date (Web): June 12, 2012 | doi: 10.1021/bk-2012-1102.ch006

Downloaded by PENNSYLVANIA STATE UNIV on June 14, 2012 | http://pubs.acs.org
Publication Date (Web): June 12, 2012 | doi: 10.1021/bk-2012-1102.ch006

62. Wyatt, R.; Kwong, P. D.; Desjardins, E.; Sweet, R. W.; Robinson, J.; Hendrickson, W. A.; Sodroski, J. G. *Nature* **1998**, *393*, 705–711.
63. Pal, R.; Hoke, G. M.; Sarngadharan, M. G. *Proc. Natl. Acad. Sci. U.S.A.* **1989**, *86*, 3384–3388.
64. Lee, W. R.; Syu, W. J.; Du, B.; Matsuda, M.; Tan, S.; Wolf, A.; Essex, M.; Lee, T. H. *Proc. Natl. Acad. Sci. U.S.A.* **1992**, *89*, 2213–2217.
65. Johnson, W. E.; Sauvron, J. M.; Desrosiers, R. C. *J. Virol.* **2001**, *75*, 11426–11436.
66. Li, Y.; Luo, L.; Rasool, N.; Kang, C. Y. *J. Virol.* **1993**, *67*, 584–588.
67. Reitter, J. N.; Means, R. E.; Desrosiers, R. C. *Nat. Med.* **1998**, *4*, 679–684.
68. Wyatt, R.; Moore, J.; Accola, M.; Desjardin, E.; Robinson, J.; Sodroski, J. *J. Virol.* **1995**, *69*, 5723–5733.
69. Cao, J.; Sullivan, N.; Desjardin, E.; Parolin, C.; Robinson, J.; Wyatt, R.; Sodroski, J. *J. Virol.* **1997**, *71*, 9808–9812.
70. Kolchinsky, P.; Kiprilov, E.; Bartley, P.; Rubinstein, R.; Sodroski, J. *J. Virol.* **2001**, *75*, 3435–3443.
71. Kolchinsky, P.; Kiprilov, E.; Sodroski, J. *J. Virol.* **2001**, *75*, 2041–2050.
72. Li, Y.; Rey-Cuille, M. A.; Hu, S. L. *AIDS Res. Hum. Retroviruses* **2001**, *17*, 1473–1479.
73. Li, Y.; Cleveland, B.; Klots, I.; Travis, B.; Richardson, B. A.; Anderson, D.; Montefiori, D.; Polacino, P.; Hu, S. L. *J. Virol.* **2008**, *82*, 638–651.
74. Wei, X.; Decker, J. M.; Wang, S.; Hui, H.; Kappes, J. C.; Wu, X.; Salazar-Gonzalez, J. F.; Salazar, M. G.; Kilby, J. M.; Saag, M. S.; Komarova, N. L.; Nowak, M. A.; Hahn, B. H.; Kwong, P. D.; Shaw, G. M. *Nature* **2003**, *422*, 307–312.
75. Rowland-Jones, S. L. *Curr. Biol.* **1999**, *9*, R248–250.
76. Grouard, G.; Clark, E. A. *Curr. Opin. Immunol.* **1997**, *9*, 563–567.
77. Geijtenbeek, T. B.; Kwon, D. S.; Torensma, R.; van Vliet, S. J.; van Duijnhoven, G. C.; Middel, J.; Cornelissen, I. L.; Nottet, H. S.; KewalRamani, V. N.; Littman, D. R.; Figdor, C. G.; van Kooyk, Y. *Cell* **2000**, *100*, 587–597.
78. Snyder, G. A.; Ford, J.; Torabi-Parizi, P.; Arthos, J. A.; Schuck, P.; Colonna, M.; Sun, P. D. *J. Virol.* **2005**, *79*, 4589–4598.
79. Mitchell, D. A.; Fadden, A. J.; Drickamer, K. *J. Biol. Chem.* **2001**, *276*, 28939–28945.
80. Feinberg, H.; Mitchell, D. A.; Drickamer, K.; Weis, W. I. *Science* **2001**, *294*, 2163–2166.
81. Hong, P. W.; Flummerfelt, K. B.; de Parseval, A.; Gurney, K.; Elder, J. H.; Lee, B. *J. Virol.* **2002**, *76*, 12855–12865.
82. Su, S. V.; Hong, P.; Baik, S.; Negrete, O. A.; Gurney, K. B.; Lee, B. *J. Biol. Chem.* **2004**, *279*, 19122–19132.
83. Hong, P. W.; Nguyen, S.; Young, S.; Su, S. V.; Lee, B. *J. Virol.* **2007**, *81*, 8325–8336.
84. Hong, P. W.; Nguyen, S.; Young, S.; Su, S. V.; Lee, B. *J. Virol.* **2007**.
85. Feinberg, H.; Castelli, R.; Drickamer, K.; Seeberger, P. H.; Weis, W. I. *J. Biol. Chem.* **2007**, *282*, 4202–4209.

86. Shepherd, V. L.; Lee, Y. C.; Schlesinger, P. H.; Stahl, P. D. *Proc. Natl. Acad. Sci. U.S.A.* **1981**, *78*, 1019–1022.
87. Stahl, P. D.; Rodman, J. S.; Miller, M. J.; Schlesinger, P. H. *Proc. Natl. Acad. Sci. U.S.A.* **1978**, *75*, 1399–1403.
88. Larkin, M.; Childs, R. A.; Matthews, T. J.; Thiel, S.; Mizuochi, T.; Lawson, A. M.; Savill, J. S.; Haslett, C.; Diaz, R.; Feizi, T. *AIDS* **1989**, *3*, 793–798.
89. Ji, X.; Gewurz, H.; Spear, G. T. *Mol. Immunol.* **2005**, *42*, 145–152.
90. Conley, A. J.; Kessler, J. A., II; Boots, L. J.; McKenna, P. M.; Schleif, W. A.; Emini, E. A.; Mark, G. E., III; Katinger, H.; Cobb, E. K.; Lunceford, S. M.; Rouse, S. R.; Murthy, K. K. *J. Virol.* **1996**, *70*, 6751–6758.
91. Parker, C. E.; Deterding, L. J.; Hager-Braun, C.; Binley, J. M.; Schulke, N.; Katinger, H.; Moore, J. P.; Tomer, K. B. *J. Virol.* **2001**, *75*, 10906–10911.
92. Zwick, M. B.; Labrijn, A. F.; Wang, M.; Spenlehauer, C.; Saphire, E. O.; Binley, J. M.; Moore, J. P.; Stiegler, G.; Katinger, H.; Burton, D. R.; Parren, P. W. *J. Virol.* **2001**, *75*, 10892–10905.
93. Stiegler, G.; Kunert, R.; Purtscher, M.; Wolbank, S.; Voglauer, R.; Steindl, F.; Katinger, H. *AIDS Res. Hum. Retroviruses* **2001**, *17*, 1757–1765.
94. Burton, D. R.; Pyati, J.; Koduri, R.; Sharp, S. J.; Thornton, G. B.; Parren, P. W.; Sawyer, L. S.; Hendry, R. M.; Dunlop, N.; Nara, P. L.; Lamacchia, M.; Garratty, E.; Stiehm, E. R.; Bryson, Y. T.; Moore, J. P.; Ho, D. D.; Barbas, C. F. *Science* **1994**, *266*, 1024–1027.
95. Saphire, E. O.; Parren, P. W.; Pantophlet, R.; Zwick, M. B.; Morris, G. M.; Rudd, P. M.; Dwek, R. A.; Stanfield, R. L.; Burton, D. R.; Wilson, I. A. *Science* **2001**, *293*, 1155–1159.
96. Gerencer, M.; Barrett, P. N.; Kistner, O.; Mitterer, A.; Dorner, F. *AIDS Res. Hum. Retroviruses* **1998**, *14*, 599–605.
97. Arendrup, M.; Sonnerborg, A.; Svennerholm, B.; Akerblom, L.; Nielsen, C.; Clausen, H.; Olofsson, S.; Nielsen, J. O.; Hansen, J. E. *J. Gen. Virol.* **1993**, *74*, 855–863.
98. Hansen, J. E.; Nielsen, C.; Clausen, H.; Mathiesen, L. R.; Nielsen, J. O. *Antiviral Ress* **1991**, *16*, 233–242.
99. Tomiyama, T.; Lake, D.; Masuho, Y.; Hersh, E. M. *Biochem. Biophys. Res. Commun.* **1991**, *177*, 279–285.
100. Bolmstedt, A. J.; O'Keefe, B. R.; Shenoy, S. R.; McMahon, J. B.; Boyd, M. R. *Mol. Pharmacol.* **2001**, *59*, 949–954.
101. Shenoy, S. R.; Barrientos, L. G.; Ratner, D. M.; O'Keefe, B. R.; Seeberger, P. H.; Gronenborn, A. M.; Boyd, M. R. *Chem. Biol.* **2002**, *9*, 1109–1118.
102. Ezekowitz, R. A.; Kuhlman, M.; Groopman, J. E.; Byrn, R. A. *J. Exp. Med.* **1989**, *169*, 185–196.
103. Hansen, J. E.; Nielsen, C. M.; Nielsen, C.; Heegaard, P.; Mathiesen, L. R.; Nielsen, J. O. *AIDS* **1989**, *3*, 635–641.
104. Balzarini, J.; Schols, D.; Neyts, J.; Van Damme, E.; Peumans, W.; De Clercq, E. *Antimicrob. Agents Chemother.* **1991**, *35*, 410–416.
105. Gattegno, L.; Ramdani, A.; Jouault, T.; Saffar, L.; Gluckman, J. C. *AIDS Res. Hum. Retroviruses* **1992**, *8*, 27–37.

Downloaded by PENNSYLVANIA STATE UNIV on June 14, 2012 | http://pubs.acs.org
Publication Date (Web): June 12, 2012 | doi: 10.1021/bk-2012-1102.ch006

Downloaded by PENNSYLVANIA STATE UNIV on June 14, 2012 | http://pubs.acs.org
Publication Date (Web): June 12, 2012 | doi: 10.1021/bk-2012-1102.ch006

106. Hammar, L.; Hirsch, I.; Machado, A. A.; De Mareuil, J.; Baillon, J. G.; Bolmont, C.; Chermann, J. C. *AIDS Res. Hum. Retroviruses* **1995**, *11*, 87–95.
107. Saifuddin, M.; Hart, M. L.; Gewurz, H.; Zhang, Y.; Spear, G. T. *J. Gen. Virol.* **2000**, *81*, 949–955.
108. Huskens, D.; Ferir, G.; Vermeire, K.; Kehr, J. C.; Balzarini, J.; Dittmann, E.; Schols, D. *J. Biol. Chem.* **2010**, *285*, 24845–24854.
109. Balzarini, J.; Van Laethem, K.; Daelemans, D.; Hatse, S.; Bugatti, A.; Rusnati, M.; Igarashi, Y.; Oki, T.; Schols, D. *J. Virol.* **2007**, *81*, 362–373.
110. Balzarini, J.; Van Herrewege, Y.; Vermeire, K.; Vanham, G.; Schols, D. *Mol. Pharmacol.* **2007**, *71*, 3–11.
111. Balzarini, J. *Antiviral Chem. Chemother.* **2007**, *18*, 1–11.
112. Turville, S. G.; Vermeire, K.; Balzarini, J.; Schols, D. *J. Virol.* **2005**, *79*, 13519–13527.
113. Wang, L. X.; Ni, J.; Singh, S.; Li, H. *Chem. Biol.* **2004**, *11*, 127–134.
114. Lee, H. K.; Scanlan, C. N.; Huang, C. Y.; Chang, A. Y.; Calarese, D. A.; Dwek, R. A.; Rudd, P. M.; Burton, D. R.; Wilson, I. A.; Wong, C. H. *Angew. Chem., Int. Ed.* **2004**, *43*, 1000–1003.
115. Wang, L. X.; Ni, J.; Singh, S. *Bioorg. Med. Chem.* **2003**, *11*, 129–136.
116. Li, H.; Wang, L. X. *Org. Biomol. Chem.* **2003**, *1*, 3507–3513.
117. Ni, J.; Singh, S.; Wang, L. X. *Bioconjugate Chem.* **2003**, *14*, 232–238.
118. Ni, J.; Powell, R.; Baskakov, I. V.; DeVico, A.; Lewis, G. K.; Wang, L. X. *Bioorg. Med. Chem.* **2004**, *12*, 3141–3148.
119. Duncan, R. J.; Weston, P. D.; Wrigglesworth, R. *Anal. Biochem.* **1983**, *132*, 68–73.
120. Li, H.; Wang, L. X. *Org. Biomol. Chem.* **2004**, *2*, 483–488.
121. Wang, J.; Li, H.; Zou, G.; Wang, L. X. *Org. Biomol. Chem.* **2007**, *5*, 1529–1540.
122. Krauss, I. J.; Joyce, J. G.; Finnefrock, A. C.; Song, H. C.; Dudkin, V. Y.; Geng, X.; Warren, J. D.; Chastain, M.; Shiver, J. W.; Danishefsky, S. J. *J. Am. Chem. Soc.* **2007**, *129*, 11042–11044.
123. Wang, S. K.; Liang, P. H.; Astronomo, R. D.; Hsu, T. L.; Hsieh, S. L.; Burton, D. R.; Wong, C. H. *Proc. Natl. Acad. Sci. U.S.A.* **2008**, *105*, 3690–3695.
124. Gamblin, D. P.; Scanlan, E. M.; Davis, B. G. *Chem. Rev.* **2009**, *109*, 131–163.
125. Wang, L. X. *Carbohydr. Res.* **2008**, *343*, 1509–1522.
126. Bennett, C. S.; Wong, C. H. *Chem. Soc. Rev.* **2007**, *36*, 1227–1238.
127. Buskas, T.; Ingale, S.; Boons, G. J. *Glycobiology* **2006**, *16*, 113R–136R.
128. Grogan, M. J.; Pratt, M. R.; Marcaurelle, L. A.; Bertozzi, C. R. *Annu. Rev. Biochem.* **2002**, *71*, 593–634.
129. Sears, P.; Wong, C. H. *Science* **2001**, *291*, 2344–2350.
130. Herzner, H.; Reipen, T.; Schultz, M.; Kunz, H. *Chem. Rev.* **2000**, *100*, 4495–4538.
131. Arsequell, G.; Valencia, G. *Tetrahedron: Asymmetry* **1999**, *10*, 3045–3094.
132. Wang, L. X.; Fan, J. Q.; Lee, Y. C. *Tetrahedron Lett.* **1996**, *37*, 1975–1978.
133. Wang, L. X.; Tang, M.; Suzuki, T.; Kitajima, K.; Inoue, Y.; Inoue, S.; Fan, J. Q.; Lee, Y. C. *J. Am. Chem. Soc.* **1997**, *119*, 11137–11146.

134. Mizuno, M.; Haneda, K.; Iguchi, R.; Muramoto, I.; Kawakami, T.; Aimoto, S.; Yamamoto, K.; Inazu, T. *J. Am. Chem. Soc.* **1999**, *121*, 284–290.
135. Wang, L. X.; Singh, S.; Ni, J. In *Synthesis of Carbohydrates through Biotechnology*; Wang, P. G., Ichikawa, Y., Eds.; American Chemical Society: Washington, DC, 2004; pp 73−92.
136. Singh, S.; Ni, J.; Wang, L. X. *Bioorg. Med. Chem. Lett.* **2003**, *13*, 327–330.
137. Li, B.; Zeng, Y.; Hauser, S.; Song, H.; Wang, L. X. *J. Am. Chem. Soc.* **2005**, *127*, 9692–9693.
138. Li, B.; Song, H.; Hauser, S.; Wang, L. X. *Org. Lett.* **2006**, *8*, 3081–3084.
139. Zeng, Y.; Wang, J.; Li, B.; Hauser, S.; Li, H.; Wang, L. X. *Chem. Eur. J.* **2006**, *12*, 3355–3364.
140. Ochiai, H.; Huang, W.; Wang, L. X. *J. Am. Chem. Soc.* **2008**, *130*, 13790–13803.
141. Wei, Y.; Li, C.; Huang, W.; Li, B.; Strome, S.; Wang, L. X. *Biochemistry* **2008**, *47*, 10294–10304.
142. Umekawa, M.; Huang, W.; Li, B.; Fujita, K.; Ashida, H.; Wang, L. X.; Yamamoto, K. *J. Biol. Chem.* **2008**, *283*, 4469–4479.
143. Huang, W.; Li, C.; Li, B.; Umekawa, M.; Yamamoto, K.; Zhang, X.; Wang, L. X. *J. Am. Chem. Soc.* **2009**, *131*, 2214–2223.
144. Schwarz, F.; Huang, W.; Li, C.; Schulz, B. L.; Lizak, C.; Palumbo, A.; Numao, S.; Neri, D.; Aebi, M.; Wang, L. X. *Nat. Chem. Biol.* **2010**, *6*, 264–266.
145. Umekawa, M.; Li, C.; Higashiyama, T.; Huang, W.; Ashida, H.; Yamamoto, K.; Wang, L. X. *J. Biol. Chem.* **2010**, *285*, 511–521.
146. Umekawa, M.; Higashiyama, T.; Koga, Y.; Tanaka, T.; Noguchi, M.; Kobayashi, A.; Shoda, S.; Huang, W.; Wang, L. X.; Ashida, H.; Yamamoto, K. *Biochim. Biophys. Acta* **2010**, *1800*, 1203–1209.
147. Li, H.; Li, B.; Song, H.; Breydo, L.; Baskakov, I. V.; Wang, L. X. *J. Org. Chem.* **2005**, *70*, 9990–9996.
148. Huang, W.; Groothuys, S.; Heredia, A.; Kuijpers, B. H.; Rutjes, F. P.; van Delft, F. L.; Wang, L. X. *ChemBioChem* **2009**, *10*, 1234–1242.
149. Mandal, M.; Dudkin, V. Y.; Geng, X.; Danishefsky, S. J. *Angew. Chem., Int. Ed.* **2004**, *43*, 2557–2561.
150. Geng, X.; Dudkin, V. Y.; Mandal, M.; Danishefsky, S. J. *Angew. Chem., Int. Ed.* **2004**, *43*, 2562–2565.
151. Dudkin, V. Y.; Orlova, M.; Geng, X.; Mandal, M.; Olson, W. C.; Danishefsky, S. J. *J. Am. Chem. Soc.* **2004**, *126*, 9560–9562.
152. Ni, J.; Song, H.; Wang, Y.; Stamatos, N. M.; Wang, L. X. *Bioconjugate Chem.* **2006**, *17*, 493–500.
153. Joyce, J. G.; Krauss, I. J.; Song, H. C.; Opalka, D. W.; Grimm, K. M.; Nahas, D. D.; Esser, M. T.; Hrin, R.; Feng, M.; Dudkin, V. Y.; Chastain, M.; Shiver, J. W.; Danishefsky, S. J. *Proc. Natl. Acad. Sci. U.S.A.* **2008**, *105*, 15684–15689.
154. Astronomo, R. D.; Lee, H. K.; Scanlan, C. N.; Pantophlet, R.; Huang, C. Y.; Wilson, I. A.; Blixt, O.; Dwek, R. A.; Wong, C. H.; Burton, D. R. *J. Virol.* **2008**, *82*, 6359–6368.

Downloaded by PENNSYLVANIA STATE UNIV on June 14, 2012 | http://pubs.acs.org
Publication Date (Web): June 12, 2012 | doi: 10.1021/bk-2012-1102.ch006

155. Astronomo, R. D.; Kaltgrad, E.; Udit, A. K.; Wang, S. K.; Doores, K. J.; Huang, C. Y.; Pantophlet, R.; Paulson, J. C.; Wong, C. H.; Finn, M. G.; Burton, D. R. *Chem. Biol.* **2010**, *17*, 357–370.
156. Agrawal-Gamse, C.; Luallen, R. J.; Liu, B.; Fu, H.; Lee, F. H.; Geng, Y.; Doms, R. W. *J. Virol.* **2011**, *85*, 470–480.
157. Luallen, R. J.; Agrawal-Gamse, C.; Fu, H.; Smith, D. F.; Doms, R. W.; Geng, Y. *Glycobiology* **2010**, *20*, 280–286.
158. Morley, S. L.; Pollard, A. J. *Vaccine* **2001**, *20*, 666–687.
159. Astronomo, R. D.; Burton, D. R. *Nat. Rev. Drug Discovery* **2010**, *9*, 308–324.
160. Danishefsky, S. J.; Allen, J. R. *Angew. Chem., Int. Ed.* **2000**, *39*, 836–863.
161. Kudryashov, V.; Glunz, P. W.; Williams, L. J.; Hintermann, S.; Danishefsky, S. J.; Lloyd, K. O. *Proc. Natl. Acad. Sci. U.S.A.* **2001**, *98*, 3264–3269.
162. Gilewski, T.; Ragupathi, G.; Bhuta, S.; Williams, L. J.; Musselli, C.; Zhang, X. F.; Bencsath, K. P.; Panageas, K. S.; Chin, J.; Hudis, C. A.; Norton, L.; Houghton, A. N.; Livingston, P. O.; Danishefsky, S. J. *Proc. Natl. Acad. Sci. U.S.A.* **2001**, *98*, 3270–3275.
163. Ragupathi, G.; Cappello, S.; Yi, S. S.; Canter, D.; Spassova, M.; Bornmann, W. G.; Danishefsky, S. J.; Livingston, P. O. *Vaccine* **2002**, *20*, 1030–1038.

Downloaded by PENNSYLVANIA STATE UNIV on June 14, 2012 | http://pubs.acs.org
Publication Date (Web): June 12, 2012 | doi: 10.1021/bk-2012-1102.ch006

Downloaded by UNIV OF DELAWARE MORRIS LIB on June 13, 2012 | http://pubs.acs.org
Publication Date (Web): June 12, 2012 | doi: 10.1021/bk-2012-1102.ch007

Chapter 7

Toward a Carbohydrate-Based HIV-1 Vaccine

**Leopold Kong,[1,†] Jean-Philippe Julien,[1,†] Daniel Calarese,[1]
Christopher Scanlan,[2,5] Hing-Ken Lee,[3] Pauline Rudd,[5,‡]
Chi-Huey Wong,[3,4] Raymond A. Dwek,[5] Dennis R. Burton,[2]
and Ian A. Wilson[1,4,*]**

**[1]Department of Molecular Biology, [2]Department of Immunology,
[3]Department of Chemistry, The Scripps Research Institute,
10550 North Torrey Pines Road, La Jolla, CA 92037
[4]Skaggs Institute for Chemical Biology, The Scripps Research Institute,
10550 North Torrey Pines Road, La Jolla, CA, 92037
[5]The Glycobiology Institute, Department of Biochemistry, University of
Oxford, Oxford, United Kingdom
[*]wilson@scripps.edu
[†]Both authors contributed equally
[‡]Present address NIBRT Dublin Oxford Glycobiology Laboratory,
NIBRT - The National Institute for Bioprocessing Research & Training,
Fosters Avenue, Mount Merrion, Blackrock, Co. Dublin, Ireland**

Despite over almost three decades of active research since the discovery of HIV-1 as the infectious agent causing AIDS, an effective vaccine that protects against the virus has not been forthcoming. In this chapter, we begin with a discussion on barriers against eliciting a strong immune response against carbohydrates. We then describe novel technologies arising from the field of glycobiology that are helping researchers overcome them. With that background in place, we move into an introduction on the biochemical structure and biological role of the HIV-1 envelope glycoprotein gp160. We describe how the immune system recognizes it and develop an argument for the application of a carbohydrate vaccine. Analysis of the carbohydrates on gp160 follows leading to detailed descriptions of the high-resolution structures of glycan specific HIV-1 broadly neutralizing antibodies. How these structures inform a

new generation of carbohydrate-based HIV-1 vaccines are then discussed in detail.

Difficulty in Eliciting an Immune Response to Carbohydrates

While cellular immunity is highly correlated with viral control (*1*–*5*), an effective, prophylactic vaccine would need to induce a long-lasting and potent humoral immune response against a broad range of viral strains (*6*–*8*). Much of the research in HIV-1 immunogen design has focused on the protein portions of its envelope glycoprotein. However, with the recent discovery of many broadly neutralizing antibodies that recognize the glycan portions (*9*, *10*), substantial efforts are now being directed towards a carbohydrate vaccine.

Generally, carbohydrates elicit weak, short-term immune responses with little IgG class switching or establishment of B-cell memory [reviewed in (*11*, *12*)]. Several factors can be attributed to this limited response. There is generally *no CD4$^+$ T-cell help* for carbohydrates so B-cell activation would have to rely on the poorly understood CD4-independent mechanisms that only apply for certain types of antigens. The *low affinity* of protein-carbohydrate interactions places a physical constraint on the crucial step of B-cell activation. Furthermore, many carbohydrates on pathogens are similar to those on *self-proteins* (proteins from the host organism), preventing normal immune cells that have undergone clonal deletion to recognize them. Finally, a given glycoprotein may carry a wide *heterogeneity* of sugar types at a particular location, thus presenting multiple distinct isoforms of a potentially immunogenic surface that dilutes the immune response.

i. Lack of CD4 Help

The adaptive humoral immune response requires the activation of B-cells by relatively high affinity interactions between antigens and B-cell receptors (BCR) typically followed by activating signals from CD4$^+$ T-cells. However, CD4$^+$ T-cells only activate B-cells decorated with MHC class II molecules presenting, for the most part, peptide fragments from the antigen. Furthermore, these antigen-specific CD4$^+$ T-cells need to be primed first by professional antigen presenting cells such as dendritic cells and macrophages also with peptide bound MHC class II molecules. This requirement for “peptide” means carbohydrates by themselves would require alternate B-cell activation mechanisms. One such mechanism involves repetitive and densely arrayed carbohydrate antigens that are able to cluster B-cell receptors and generate a signal that activates the B-cell without T-cell help (*13*, *14*). However, not all carbohydrate antigens can be presented in this manner, and in the case of a licensed carbohydrate vaccine using the capsular polysaccharide of pneumococcal bacteria, it is only effective in healthy adults and not in children under 2 years of age or the elderly (*15*). Notable exceptions to carbohydrates not being presentable on MHC class II molecules are certain zwitterionic capsular polysaccharides that are able to be presented by these molecules (*16*).

Downloaded by UNIV OF DELAWARE MORRIS LIB on June 13, 2012 | http://pubs.acs.org
Publication Date (Web): June 12, 2012 | doi: 10.1021/bk-2012-1102.ch007

Downloaded by UNIV OF DELAWARE MORRIS LIB on June 13, 2012 | http://pubs.acs.org
Publication Date (Web): June 12, 2012 | doi: 10.1021/bk-2012-1102.ch007

ii. Low Affinity of Protein-Glycan Interactions

Protein-glycan interactions typically involve the same kinds of van der Waals and hydrophilic interactions found at protein-protein interfaces (*17*). However, while protein-protein interactions can achieve nanomolar affinities, especially in antibody-antigen association, protein-glycan interactions generally have much lower affinities (*18*). However, many glycan binding proteins such as naturally occurring lectins still achieve high apparent affinity through multivalency (*19–21*). For example, concanavilin A binds to individual high mannose glycans at ~ 600 nM, but can achieve 37.5 nM when the glycans are densely clustered (*18*).

A possible reason for this low affinity is the inherent flexibility of glycans. Even though there are energy minimal rotamers for certain torsion angles on the glycan, low energy configurations are wide ranging (*22*). Conformationally fixing a glycan would therefore incur a large entropy cost. Binding to an already idealized glycan conformation to minimize energy cost in addition to an extensive hydrogen bonding network at the interface may be an alternative to using avidity for a high affinity interaction.

However, since high affinity protein-glycan interactions are not commonly found in nature, it may be difficult to generate this type of response through vaccination. Such a physical constraint severely limits the ability of the B-cell receptors to respond to a glycan epitope and, hence, limits the evolution of soluble antibodies (IgG, IgA) that could potently neutralize a pathogen harboring glycans. Nevertheless, some Ig classes of antibodies have higher valencies; IgM can display up to ten combining sites, whereas IgG has only two.

The avidity derived from two combining sites (i.e. two Fab molecules, which are the antigen binding portions of an immunoglobulin) may approach the product of the individual binding constants of the Fabs. This potential bivalency can give an apparent affinity for a glycan ligand, comparable to that of a protein epitope (for example a 10^3 dissociation constant for each Fab could maximally give rise to a 10^6 Ka for the IgG directed against a polysaccharide epitope).

However, for optimal multivalent binding to occur, the epitope(s) must be orientated in such a way that allows simultaneous interaction of two or more Fabs with the antigen surface (*23*). Therefore, clustered glycans or repetitive polysaccharides are much more likely to elicit high affinity antibodies than dispersed, monovalent glycan epitopes.

iii. Similarity of Carbohydrates on Many Pathogens to Self-Antigens

Many pathogens cover their surface with glycans that resemble the structures present in the host. Some bacterial glycosyl transferases appear to have evolved, convergently, with their host, to produce glycans that mimic host carbohydrates. For example, the glycosyl transferases of some streptococcal pathogens appear to have evolved a convergent functionality with their host to produce glycosaminoglycans similar to that of the host (*24*).

Alternatively, most surface proteins from membrane viruses are glycosylated by the addition of 'self'-glycans to viral proteins by the host glycosylation apparatus itself. Many highly pathogenic viruses are heavily glycosylated, including Influenza (*25*), Ebola (*26–28*), HIV (*29–33*) and Hepatitis (*34*). The extent to which the self-glycan coating limits the humoral immune response is unknown, but the decoration of pathogen surfaces with self-glycans is a widespread phenotype, suggesting a functional role in immune evasion.

iv. Heterogeneity of Pathogen Glycosylation

Glycosylation exhibits multiple levels of heterogeneity. First, the N-linked glycosylation sequon (Asn-X-Thr/Ser) is not used at 100% frequency, and never when X is a Pro (*35*). When it is used, a pre-made $Man_9GlcNAc_2$ glycan is attached to the protein in the endoplasmic reticulum. However, once the glycoprotein is passed into the Golgi body, a host of enzymes process the glycans into different forms in an almost stochastic manner dependent on the accessibility of its glycans to the enzymes (*36–40*).

Therefore, the Asn residue, in the same protein, from the same cell line, can often be glycosylated by diverse carbohydrate moieties, yielding a second level of heterogeneity. In different cell lines, a different spectrum of glycoforms may arise. The distribution of glycoforms is determined by the distribution of available glycan processing enzymes, which is in turn mainly dependent on the cell type and its surrounding micro-environment. Therefore, the exact carbohydrate structures present on virus may depend on the tissue(s) infected, rather than being an inherent property of the pathogen, adding a third layer of heterogeneity. Such microheterogeneity may well dilute the immunogenicity of a particular epitope (*38*). Some exceptions are viruses that bud directly from the ER, such as Hepatitis C, which would contain mostly Man_9 glycans. Bacteria and fungi generally synthesize their own glycans, and are, therefore, less influenced by the host.

New Approaches to Old Challenges

Despite the natural difficulties in eliciting a robust immune response against glycans, carbohydrates are successfully being used as effective vaccines. For example, carbohydrate vaccines have been licensed for use against Haemophilus influenza, Neisseria meningitides, Salmonella typhi and Streptococcus pneumonia (*12*). In recent years, technological advances in glycobiology have greatly improved their effectiveness and expanded their application by directly circumventing many of the problems described in the previous section.

i. Overcoming the Lack of CD4 Help

A simple solution to lack of CD4+ T-Cell help is the conjugation of the carbohydrate antigen to a protein carrier. However, for a long time, the availability of pure, chemically activated antigen carbohydrates that can be used for conjugation were greatly limited due to the technical difficulties involved in

Downloaded by UNIV OF DELAWARE MORRIS LIB on June 13, 2012 | http://pubs.acs.org
Publication Date (Web): June 12, 2012 | doi: 10.1021/bk-2012-1102.ch007

purification and synthesis of the material. With the development of reactivity based one-pot synthesis, in which a glycan is made within a single container using a sequence of reactions, and solid support synthesis, a method that is similar to peptide synthesis involving protection/deprotection reactions to guide the addition of specific glycan moieties, gram quantities of various carbohydrate antigens can now be prepared with reasonable effort (*41*, *42*). The quality control of carbohydrate purity has also greatly improved with the newer mass spectrometry and glycan array technologies that are able to analyze with great sensitivity a large range of carbohydrate molecules even when attached to protein (*43–45*).

Using these methods, conjugated carbohydrates can now be prepared in high quality and quantities. Priming and boosting injections with this material greatly enhance the magnitude and persistence of the immune response (*46*). In cases where this may not be enough, highly immunogenic proteins such as cholera and tetanus toxoids can be used as carriers with strong adjuvant activity (*11*). Minimal CD4+ T-cell peptide can also be used along with TLR-stimulating haptens as a reductionist approach (*11*). This, along with optimizing the use of various adjuvants, has become a promising avenue towards overcoming the lack of CD4 help for most carbohydrate antigens.

Downloaded by UNIV OF DELAWARE MORRIS LIB on June 13, 2012 | http://pubs.acs.org
Publication Date (Web): June 12, 2012 | doi: 10.1021/bk-2012-1102.ch007

ii. Resolving Low Affinity of Protein-Glycan Interactions

In some cases, high affinity protein-glycan interactions may not be needed for the purpose of the vaccine, especially when the glycan antigen in question is highly clustered and arrayed on the target against which the vaccine was made. In those cases, the local concentration of the carbohydrate antigen may be so much higher than the antibody that the antibodies would be trapped in the bound form given a reasonable dissociation constant. However, when this is not the case, strategies are devised to achieve multivalency on the antibody so that the apparent affinity can be raised sufficiently. For those immunogens, the antigenic portions would need to be repetitively arrayed in dense clusters so as to enhance the chances of a B-cell receptor recognizing more than one carbohydrate at the same time. One advantage of this approach is that, in a dense cluster of carbohydrates, they scaffold each other to reduce the conformational flexibility that may be a cause for the low affinity glycan-carbohydrate interactions. Another advantage of this approach is that it could trigger CD4+ T-cell independent activation of B-cells, potentially boosting the immunogenicity on top of whatever CD4 help it acquires from various protein carriers.

It has been shown that the type and density of neighboring carbohydrates affects the affinity of carbohydrate antibodies (*47*). Thus, for these multivalent immunogens, it would be desirable to have different carbohydrates presented at the same time in specific ratios or arrayed in particular geometries to achieve the exact clustering that optimizes the immune response. With the use of structure-based design and chemistries that offer selective conjugation to different residues, optimizing the presentation of several carbohydrates on a single carrier can be achieved.

iii. Circumventing the Similarity of Carbohydrates on Pathogens to Self-Antigens

For many bacterial pathogens, the oligosaccharide units that form the basis for antibody recognition are distinct from self-carbohydrates. These differences can be attributed to the unique bacterial enzyme, which synthesize the capsular polysaccharides. Perhaps for this reason, the *N. meningitides* B strain has proved harder to combat because the structural linkage of polysialic acid is present in neuronal tissue (Table 1). The species and sub-type specificity of glycosylation is important. For example, immunity raised by C-type meningococcal vaccines is not generally reactive against the B-type polysaccharide antigen. Thus, differences in glycosylation allow self to be discriminated from non-self and, conversely, small differences in polysaccharide antigens, within a bacterial species, allow the persistence of vaccine-resistant sub-types. Fortunately, with the advent of greatly improved carbohydrate synthesis technologies, many of these issues can be overcome with the isolation of the particular sugars required for specific vaccinated responses.

Table 1. Carbohydrate epitope on various pathogens.

Pathogen	***Carbohydrate Epitope***	***Ref***
Neisseria meningitides A	(1-6)-N-acetyl-D-mannosamine-1-phosphate	(*50*)
Neisseria meningitides B	(2-8) polysialic acid[a]	(*51*)
Neisseria meningitides C	(2-9) polysialic acid	(*51*)
Haemophilus Influenzae B	polyribosyl ribitol-phosphate (PRP)	(*52*)
Staphylococcus aureus	Type 5: [-4-3-O-Ac-β-D-ManNac(1-4)-α-L-FucNAc-(1-3)-β-D-FucNAc-(1-)]n Type 8: [-3-4-O-Ac-β-D-ManNac(1-3)-α-L-FucNAc-(1-3)-β-D-FucNAc-(1-)]n	(*53*)
Salmonella typhi	[-4) 3-O-Ac-α-D-GalNAc-(1-]n	(*54*, *55*)
Streptococcus pneumonia	β-D-Glcp-(1-6)-[α-D-NeupNAc-(2-3)-β-D-Galp-(1-4)]-β-D-GlcpNAc-(1-3)-β-D-Galp-(1-4)	(*56*)

[a] also present in mammalian neuronal polysialic acid

Downloaded by UNIV OF DELAWARE MORRIS LIB on June 13, 2012 | http://pubs.acs.org
Publication Date (Web): June 12, 2012 | doi: 10.1021/bk-2012-1102.ch007

For viral pathogens that use host-processed glycans, this problem is much exacerbated. However, some pathogens, such as Epstein-Barr virus (*48*), Hepatitis C virus (*34*) and HIV (*49*), are decorated with unusually dense clusters of N-linked glycosylation that are generally not found in host glycoproteins. Details for exploiting this phenomenon are discussed in later sections.

iv. Outwitting the Heterogeneity of Pathogen Glycosylation

The potentially overwhelming diversity of glycosylation found on the exterior of eukaryotic glycoproteins may not be found within the capsid antigens of a single bacterium. Generally, a few repeating polysaccharide units can be isolated as a major neutralizing determinant on a bacterial surface (Table 1), as evidenced by their utility in vaccine design. Thus, glycan microheterogeneity probably does not significantly undermine the antibody response to bacterial antigens to the same extent as in eukaryotic glycosylation. However, this problem is real and significant for the animal viruses that hijack the eukaryotic protein expression machinery.

One approach towards a solution is achieving completely homogenous glycosylation on the immunogen. That way, at least, the immune response is not diluted by the glycan microheterogeneity. In this context, complete homogeneity would mean close to 100% usage of N-linked glycosylation sequons, as well as close to 100% equivalence of the glycoforms. This may be possible with the use of pure, synthetic glycans that are chemically activated for conjugation to protein (*57*). An alternative less laborious approach would be to use cocktails of glycosidase enzymes on the expression system in order to partially guide the enzymatic trimming of glycans (*58*). For example, the use of kifunensine at appropriate concentrations would yield proteins with mostly $Man_9GlcNAc_2$ glycans. Cell lines with various glycosidase mutations such as the GnTI- 293T cells that limit glycosylation to $Man_{5-9}GlcNAc_2$, can also be used for this purpose. However in these alternative methods, 100% sequon usage cannot be guaranteed.

HIV-1 Envelope Glycoprotein: Structure and Biology

The sole target of the humoral immune response on HIV-1 is the envelope glycoprotein gp160 because it is the only exposed viral protein on its membrane. An appreciation for the structure and biological role of gp160 would aid in understanding the antibody responses against it [reviewed in (*59*, *60*)]. HIV-1 gp160 is cleaved by cellular proteases into two proteins (gp41, which includes the transmembrane domain, and gp120, which is solely surface exposed) that remain non-covalently bound as a heterodimer. The final product on the viral surface is a homotrimeric complex made of gp41/gp120 heterodimers (Figure 1). While an atomic-resolution structure of gp160 trimer is not yet available, crystal structures of loop deleted gp120 core monomer, scaffolded gp120 loops and gp41 fragments in complex with various ligands have been solved over the years (*61–67*). Lower resolution cryo-electron microscopy (cryo-EM) reconstructions of the trimer are also available that can be used to fit higher resolution crystal structures to model envelope glycoprotein complex (*68*).

Downloaded by UNIV OF DELAWARE MORRIS LIB on June 13, 2012 | http://pubs.acs.org
Publication Date (Web): June 12, 2012 | doi: 10.1021/bk-2012-1102.ch007

Downloaded by UNIV OF DELAWARE MORRIS LIB on June 13, 2012 | http://pubs.acs.org
Publication Date (Web): June 12, 2012 | doi: 10.1021/bk-2012-1102.ch007

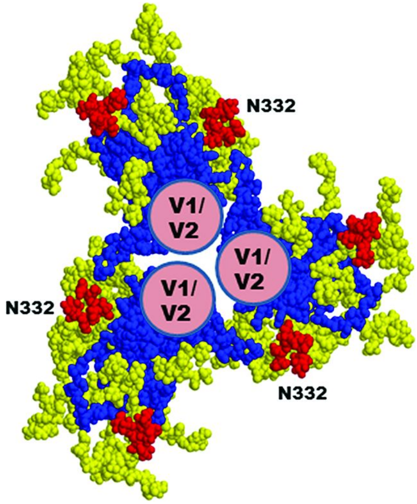

Figure 1. Proposed model for trimeric gp120, based on information in (69), with the protein core shown in blue and N-linked glycan chains in yellow. The glycans attached to Asn^{332} (labeled) and Asn^{392}, which form the primary attachment sites for 2G12, are indicated in red. This figure depicts a view of the trimeric gp120 as seen from the host cell membrane. The V1/V2 loops and attached carbohydrates are located at the apex of the trimer and are represented as spheres due to the current absence of structural information for this domain in the context of gp120. (see color insert)

Viral entry into cells begins when conserved regions of gp120 bind the CD4 receptor, inducing conformational changes that allow for the subsequent binding of a coreceptor (typically the CCR5 or CXCR4 membrane protein) of a host cell (such as CD4$^+$ T cells or macrophages). Once gp120 is bound, it is believed that more conformational changes take place that involve gp120 monomers being shed from the gp41 trimer in conjunction with the fusion peptides from the gp41 trimer inserting themselves into the lipid bilayer of the host cell. This is then followed by a “snapping shut” of the gp41 trimer into a compact six stranded coiled-coil complex that juxtaposes the host and viral membranes, allowing fusion to occur (Figure 2) [reviewed in (*59*)].

Antibody Responses against the Envelope Glycoprotein

When the first crystal structure of gp120 was solved, it was combined with extensive antibody epitope mapping experiments to produce a rough picture of the humoral immune response against the viral protein (*71*). From the data, it was convenient to divide the surface of core gp120 into three faces, each with different kinds of antibody responses against it: a region targeted predominantly by non-neutralizing antibodies (non-neutralizing face), a region targeted by antibodies that exhibit neutralizing activity (neutralizing face), and a region on which no antibodies seemed to bind (silent face).

Downloaded by UNIV OF DELAWARE MORRIS LIB on June 13, 2012 | http://pubs.acs.org
Publication Date (Web): June 12, 2012 | doi: 10.1021/bk-2012-1102.ch007

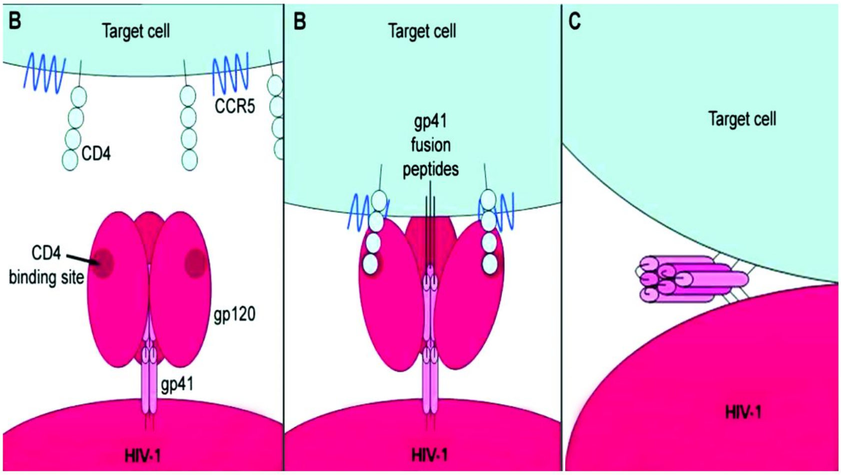

Figure 2. HIV-1 entry into the host cell. A) Components of HIV-1 entry into the host cell. On the surface of the virus is a homotrimeric pre-fusion complex made up of gp41/gp120 heterodimers. Gp120 has a recessed CD4 binding pocket (labeled). B) gp120 binds to CD4 and the CCR5 coreceptor, which signals gp41 to change conformation and insert its fusion peptides into the host cell. C) gp120 is subsequently shed from gp41, and gp41 undergoes a large conformational change causing it to snap shut into a six helix coiled-coil bundle. This activation of the spring-loaded mechanism brings the viral membrane and host cell membrane in close contact and allows the virus to fuse with the host cell. Figure adapted from (70). (see color insert)

The non-neutralizing face corresponds to what is called the inner domain of gp120, a portion of the protein that faces the center of the trimer. Therefore, antibodies against this region would not neutralize the virus because, within the trimer, it is occluded by neighboring subunits. Similarly, in the trimer complex, the gp41 protein is mainly sequestered by gp120 and only transiently exposed during the fusion process. This partial exposure of gp41 in the pre-fusogenic state (gp120 bound) results in low antigenicity, as it is sterically difficult for an antibody to bind gp41. This allows the important fusion machinery of gp41 to remain hidden until the moment of infection.

The neutralizing face of gp120 corresponds to the interface between inner and outer domains, but predominantly consists of outer domain surface. This surface is also where the receptor CD4 binds to and is a recessed region containing many conserved residues (*64*). Despite being somewhat hidden by the trimer, this surface is functionally constrained to being exposed and sequence conserved for binding its host receptor; it is, therefore, an ideal target for neutralizing antibody responses and vaccine design. Indeed, many CD4 binding site (CD4bs) broadly neutralizing monoclonal antibodies have been isolated and structurally characterized, with VRC01 being able to neutralize over 90% of known HIV-1 strains (*65*). A host of newly designed immunogens focusing on this neutralizing face may be successful in re-eliciting broadly neutralizing responses against the CD4bs by vaccination.

Proximal to the neutralizing face is a large surface of gp120 that is most exposed to the solvent, and perhaps, to antibody responses. However, at the time of the first epitope mapping onto the core structure, no antibodies were found to bind to this region and as such, it was labeled the "silent" face. Because this is also the portion of gp120 that is most heavily decorated with N-linked glycans, these carbohydrates were identified as the prime suspects for silencing the immune response. Despite this, broadly neutralizing antibody 2G12 that directly binds to a cluster of high mannose glycans on the silent face was isolated and structurally characterized (*72*). Much more recently, broadly neutralizing antibodies PG9 and PG16 (*10*), as well as a panel of broadly neutralizing antibodies (PGT 121-3, 125-8, 130-1, 135-7, 143-5) were isolated from several HIV-1 patients (*9*). These antibodies were all found to have a glycan-dependent epitope and, therefore, it appears that at least a portion of the silent face is targeted by a broad and potent activity from the immune response. Taking into account the structural characterization of antibody-glycan interactions, carbohydrate-containing immunogens, therefore, offer a promising approach towards re-eliciting such anti-HIV-1 immune responses by vaccination.

HIV Env Glycosylation

The unique features of the N-linked glycosylation on gp160 exacerbate some of the barriers against eliciting strong immune responses towards carbohydrates, but also offer special opportunities that may facilitate the development of a carbohydrate vaccine.

The most blatant feature is the high density of the sugar array or glycan shield surrounding the exposed envelope proteins gp120 and gp41. A remarkable interplay of selection pressures to optimize exposure of receptor binding sites on the one hand and to cover protein surfaces to evade antibody responses on the other hand results in the crowding of 15-32 glycosylation sites on the limited solvent-exposed protein surface of gp120 alone (*71*, *73*). This comprises close to half the molecular weight of gp120 and, when packed into a trimer, the glycans are so crowded that their enzymatic processing may be sterically inhibited (*31*, *32*, *74–76*). Indeed, recent studies investigating glycosylation on gp120 trimers show predominantly oligomannose forms (*77*). This implies that the level of glycan density at the center of the silence face in a monomer is achieved for every glycan on the trimer.

As expected from the discussion in the previous sections, there are advantages conferred from presenting an unusually dense cluster of high mannose glycans to the immune system. First, this is rare in host proteins, so this partially overcomes the possibility of self-tolerance. Second, because the glycosyltransferase enzymes process the glycans within the glycan shield with difficulty, the glycans appear somewhat homogenous in terms of glycoforms (*77*). Third, these glycans are so tightly packed that their conformation may be limited, increasing the chances for higher affinity interactions with protein by lowering the entropy cost of binding.

Downloaded by UNIV OF DELAWARE MORRIS LIB on June 13, 2012 | http://pubs.acs.org
Publication Date (Web): June 12, 2012 | doi: 10.1021/bk-2012-1102.ch007

However, despite these advantages, carbohydrate antibodies against gp120 glycans are not commonly elicited according to common antibody detection assays. One possible reason is that glycans on gp120 appear homogenous by themselves, but they are quite heterogeneous when compared to different mutational variants. This is difficult to appreciate because, overall, despite the high mutation rate of HIV-1, the locations of the N-linked glycosylation sites in gp120 are generally well conserved between different isolates and clades (*78*). However, no one site is found in all isolates and even the most conserved glycosylation motifs display significant heterogeneity. The dispensable nature of individual sites was highlighted by a study where each of the 24 N-linked sites of a gp120 were individually deleted (*79*). The resulting mutant viruses generally showed little or no decrease in activity, although they had varying effects on neutralization. Indeed, only if we compare gp120 from viruses at different time points of infection do we truly see effect of variation over time in the glycans. Studies show that differences in terms of antibody escape between early and later viruses are significantly affected by mutational changes at glycan sites (*73*, *80*). Unexpectedly, changes to some of these glycan sites are able to affect antibody binding in extremely distal regions, suggesting that small, local changes to the glycan shield can affect its global conformation.

Altogether, these observations suggest that the conformations that the glycans adopt on gp120 are influenced by each other because they are so tightly packed together. For carbohydrate vaccine design, this emphasizes the importance of glycan conformation in addition to chemical identity. The only way to account for these conformational constraints is through structural characterization of glycans on gp120, preferably in complex with broadly neutralizing glycan specific antibodies.

Downloaded by UNIV OF DELAWARE MORRIS LIB on June 13, 2012 | http://pubs.acs.org
Publication Date (Web): June 12, 2012 | doi: 10.1021/bk-2012-1102.ch007

Structural Basis of Antibody Recognition of gp120 Glycans

Two specific antibody binding regions have been determined on gp120 glycans. One is a cluster of oligomannose glycans on the outer domain of gp120 that is recognized by the neutralizing antibody 2G12, as well as by the newly discovered PGT121-123, PGT125-128, PGT130-131 and PGT135-137 antibodies. The second site of glycan recognition is located at the apex of the trimer, in the V1/V2 region of gp120. Broadly neutralizing antibodies PG9, PG16, PGT141-145 and CH01-CH04 have been implicated in the recognition of this site (*9*, *10*, *81*). The detailed interaction between antibodies and these two gp120 glycan sites are now discussed in detail.

2G12 neutralizes potently many HIV-1 isolates of clade B, but few HIV-1 isolates of clade C, for which the glycan arrangement varies significantly from that of clade B viruses. Investigation of the 2G12 epitope has illuminated surprising structural and immunological similarities between the outer domain of gp120 and the immunogenic carbohydrate surfaces of other pathogens (*45*, *51*, *52*). Mutagenesis studies on gp120 revealed that only substitutions that remove the N-linked glycosylation sites of gp120 had a significant effect on 2G12 affinity. Substitutions removing the sequences for some N-linked glycosylation sequons on the silent face of gp120 were sufficient to prevent 2G12 attachment. Comparison of mutagenesis data with 2G12 escape mutants and sequence alignments of sequences known to be bound by 2G12 identified a small cluster of gp120 glycans as the basis of the 2G12 epitope.

Treatment of gp120 with mannosidases (exoglycosidases, which remove terminal sugars from gp120) demonstrated that the removal of non-reducing Manα1-2Man sugars from gp120 was sufficient to abrogate 2G12 binding. Consistent with these data, the 2G12-gp120 interaction could be inhibited by D-mannose. Additionally, 2G12 binding to gp120 could be inhibited by Manα1-2Man, but not by Manα1-3, 4 or 6 di-mannose (*78*, *82*).

Further research has elucidated the specific interactions between 2G12 and its carbohydrate ligand. The crystal structures of the Fab fragments of 2G12 with $Man_9GlcNAc_2$ and with Manα1-2Man showed an extraordinary configuration where the variable heavy domains are domain-swapped between two Fabs (Figure 4) (*83*). Further biochemical and biophysical evidence (such as cryo-electron microscopy, analytical ultracentrifugation, gel filtration, and alanine mutagenesis) suggested that this domain-swapped dimer of Fabs is the natural, functional form of the 2G12 antibody. Interestingly, domain-swapping was found to be mediated by only a few mutations from a putative germline precursor, with V_H residues A14 and E75 being most critical, as well as I19 at the $V_H/V_{H'}$ interface and P113 in the elbow region (*84*). The consequence of this unusual configuration creates an entirely novel architecture for an IgG. As opposed to a classical Y- or T-shaped IgG, the 2G12 IgG would have to be linear in order to accommodate the domain swap of the variable heavy domains (Figure 3).

The crystal structures give us a detailed look at the molecular interactions between 2G12 and its carbohydrate ligands (Figure 4B-inset). The primary combining site is a pocket, which binds mainly to the Manα1-2Man at the tip of the D1 arm of a $Man_9GlcNAc_2$ moiety. Additional interactions are also found between 2G12 and the mannose 3 and 4 sugars of the $Man_9GlcNAc_2$, which explains why 2G12 has higher affinity for $Man_9GlcNAc_2$ than Manα1-2Man. These additional interactions also give 2G12 specificity for the Manα1-2Man of the D1 arm of a $Man_9GlcNAc_2$. In addition to the primary combining sites, a novel potential binding surface was created at the interface between the two variable heavy domains. At this interface, non-crystallographically unique $Man_9GlcNAc_2$ moieties can be found binding to 2G12 via their D2 arms (Figure 4B). These protein-carbohydrate interactions are not observed in a Manα1-2Man crystal structure and, therefore, may only represent a secondary low affinity binding site that has a different specificity than Manα1-2Man.

Recently, two new antibodies closely interacting with gp120 glycans were isolated from cell lines of HIV-1 infected individuals and their gp120 epitopes were structurally characterized. PGT128 is capable of potently neutralizing approximately 70% of circulating HIV-1 viruses by recognizing an epitope at the base of the gp120 V3 loop (*9*). On the other hand, via recognition of a gp120 epitope located on the V1/V2 loops of gp120, PG9 potently neutralizes approximately 75% of circulating HIV-1 isolates (*10*). As in the case of 2G12, glycosidase treatment of gp120 and/or treatment of viruses with glycosidase inhibitors resulted in the loss of PGT128 and PG9 binding and neutralization,

Downloaded by UNIV OF DELAWARE MORRIS LIB on June 13, 2012 | http://pubs.acs.org
Publication Date (Web): June 12, 2012 | doi: 10.1021/bk-2012-1102.ch007

therefore implicating the recognition of glycans in the interaction. However, whereas 2G12 only recognizes clustered α1-2 linked mannose termini on gp120, it was subsequently found that both PGT128 and PG9 evolved to recognize a part glycan/part protein epitope via interactions with moieties of the entire glycan length. This mode of interaction has been described as the penetration of the HIV-1 glycan shield to further access recessed protein epitopes (*61*, *67*).

Downloaded by UNIV OF DELAWARE MORRIS LIB on June 13, 2012 | http://pubs.acs.org
Publication Date (Web): June 12, 2012 | doi: 10.1021/bk-2012-1102.ch007

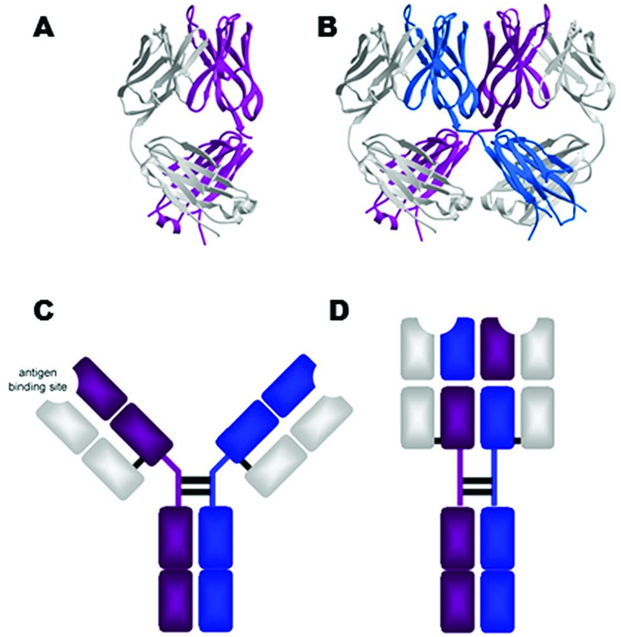

Figure 3. Comparison of a typical and domain-swapped antibody. A) Structure of a typical Fab molecule, with the heavy chain shown in purple and light chain in silver. B) Novel structure of the Fab 2G12 dimer, with variable heavy domains swapped between the two Fab molecules (83). The heavy chains of the two Fabs are shown in purple and blue, and the light chains are colored silver. C) The structure of a typical Y-shaped IgG1. D) Structure of 2G12 IgG1. The swapping of the variable heavy domains between the two Fab molecules causes the IgG to adopt a linear conformation. This unusual linear conformation of 2G12 IgG has been observed by cryo-electron microscopy (83, 85). Figures were generated using Molscript (86) and Raster3D (87). (see color insert)

Downloaded by UNIV OF DELAWARE MORRIS LIB on June 13, 2012 | http://pubs.acs.org
Publication Date (Web): June 12, 2012 | doi: 10.1021/bk-2012-1102.ch007

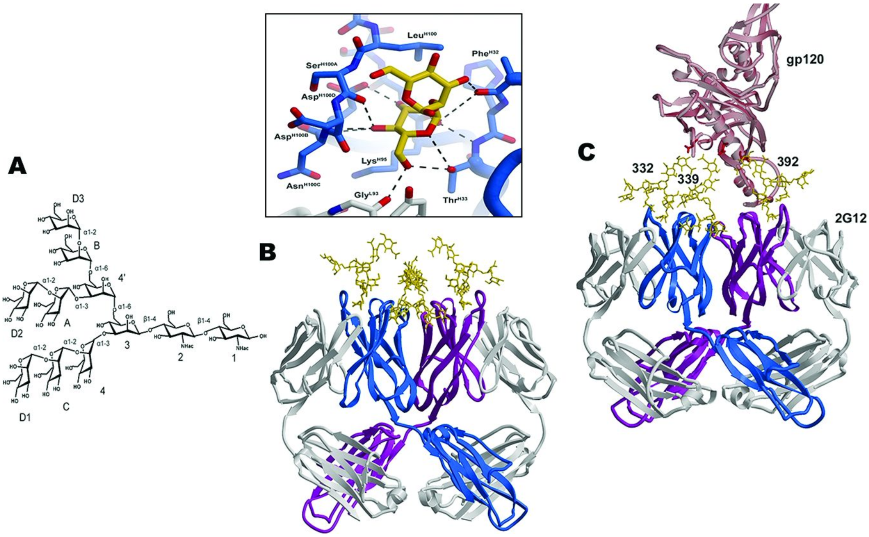

Figure 4. A) Structure of $Man_9GlcNAc_2$. This moiety contains three arms, D1, D2 and D3. B) Structure of Fab 2G12 with $Man_9GlcNAc_2$ (83). The carbohydrate is shown in a yellow stick model. A $Man_9GlcNAc_2$ moiety is bound in the primary combining sites of both Fabs. In addition, two non-crystallographically unique $Man_9GlcNAc_2$ moeities also bind at the interface between the variable heavy domains of the two Fabs. The inset details the interactions between the primary 2G12 antibody combining site and Manα1-2Man (83). The Fab heavy and light chains are shown in blue and silver, respectively. The Manα1-2Man is bound in a pocket made up of the L3, H1, H2, and H3 CDR loops of Fab 2G12. Potential hydrogen bonds between Fab 2G12 and Manα1-2Man are shown with dashed lines. C) Model of 2G12 glycan recognition of gp120 (83). The Fab 2G12 + $Man_9GlcNAc_2$ structure docks onto the previously determined structure for gp120 (63) (shown in red), almost perfectly spanning the N-linked glycosylation sites implicated as most critical for 2G12 binding. In this model, the $Man_9GlcNAc_2$ moieties in the primary combining sites are unchanged from the determined crystal structure, and the Man_9 moiety at the interface between the two Fabs has been slightly modified to show the potential for its origin to be Asn^{339}. This model shows that 2G12 has attained a high level of affinity and specificity to gp120 by adopting a conformation to recognize and bind the carbohydrate cluster. Figures were generated using Molscript (86) and Raster3D (87). (see color insert)

As revealed by structural studies, the PGT128 epitope consists of three components: 1) a Man$_{8/9}$ glycan at gp120 position Asn^{332}; 2) residues of a secondary glycan at gp120 position Asn^{301}; and 3) the backbone residues of the gp120 V3 C-terminus (*67*) (Figure 5). PGT128 buries 449 Å^2, 328 Å^2 and 305 Å^2 of surface area on these three regions, respectively. Thus, the PGT128 epitope is approximately 72% glycan and 28% protein. The relatively high affinity for the PGT128-glycan interaction with a Man$_{8/9}$ glycan at gp120 position Asn^{332} is explained by the formation of 16 hydrogen bonds, predominantly with the D1 and D3 arms mannoses. Most of the interactions between PGT128 and the two glycans are mediated by residues located in CDRs H1, H2, H3, L3 and FR3. A particularly interesting feature of PGT128 is a six-residue insertion in CDR H2 that allows the antibody to penetrate between the Asn^{301} and the Asn^{332} glycans. Furthermore, a crucial disulfide bond between PGT128 CDR H1 and CDR H2 creates a hydrophobic ridge where to support interactions with the two GlcNAc residues of the Asn^{301} glycan. Recognition by PGT128 of glycans at gp120 positions Asn^{301} and Asn^{332}, therefore, involves all of the glycan face, from the GlcNAc core all the way to the mannose tips.

Downloaded by UNIV OF DELAWARE MORRIS LIB on June 13, 2012 | http://pubs.acs.org
Publication Date (Web): June 12, 2012 | doi: 10.1021/bk-2012-1102.ch007

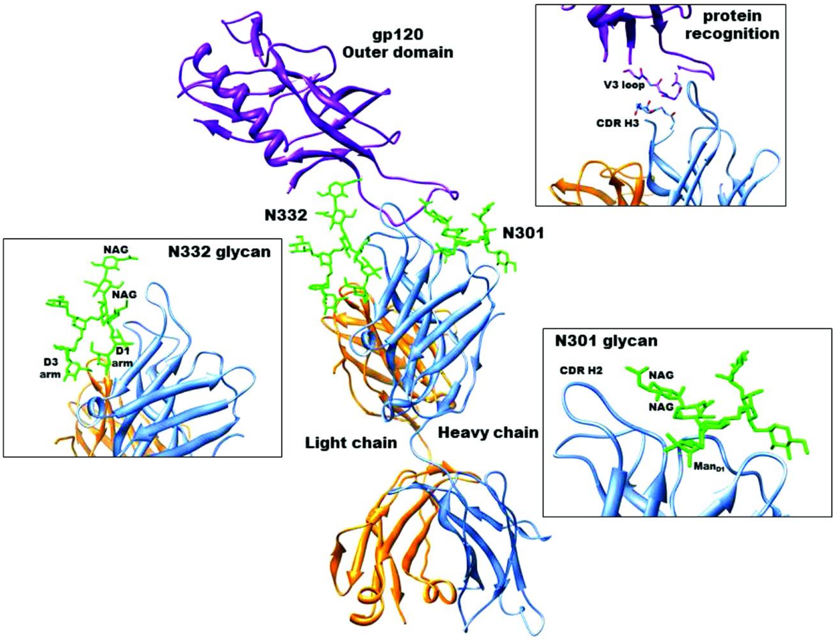

Figure 5. The recognition of gp120 by PGT128 consists of interactions with two glycans and the base of the V3 loop. The heavy chain and light chain of PGT128 are shown in blue and orange, respectively. The gp120 outer domain is rendered in purple, whereas the glycans being recognized are depicted as green sticks. Details of the three different interactions taking place are shown in the insets. PGT128 makes primary interactions with the glycan at position Asn^{332} via contacts with the GlcNAc moieties, as well as with mannose residues in the D1 and D3 arms. Secondary interactions take place with the glycan at position Asn^{301} and the residues of the V3 loop (shown in a backbone representation). Images were produced with the program Chimera (88) using PDB ID 3TYG (67). (see color insert)

Downloaded by UNIV OF DELAWARE MORRIS LIB on June 13, 2012 | http://pubs.acs.org
Publication Date (Web): June 12, 2012 | doi: 10.1021/bk-2012-1102.ch007

The gp120 epitope recognized by the PG9 antibody also consists of two glycans and a protein component (*61*). The main glycan engaged by PG9 is located at position N160 of the β-strand adjacent to the gp120 V1 loop (Figure 6). This glycan is of the $Man_5GlcNAc_2$ type and buries 489 Å^2 on PG9, which consists of 42% of the total PG9 epitope. There are 11 hydrogen bonds mediating the millimolar affinity interaction between PG9 and 5 saccharide moieties spanning from the core GlcNAc of $Man_5GlcNAc_2$ all the way to the two mannoses at the tip of the D2 and D3 arms. The secondary glycan recognized by PG9 is located at either position Asn^{156} or Asn^{173}, depending on the HIV-1 isolate recognized. It buries 337 Å^2 and 189 Å^2 of surface area on PG9, respectively. Finally, via its hammerhead CDR H3 motif, PG9 interacts closely with the C strand of gp120, which is adjacent to the V2 loop. The parallel β-strand stacking interaction accounts for approximately 31% of the total buried surface epitope. Interestingly, key electrostatic interactions take place between two sulfated tyrosine residues in the unusually long CDR H3 (28 amino acids) of PG9 and cationic residues in the gp120 V1/V2 domain. Structural studies of the PG9-gp120 interaction, therefore, indicate that this antibody mediates its broad neutralization via recognition of an epitope consisting of up to 69% glycan, as well as key backbone and electrostatic interactions taking place in a recessed epitope.

An interesting feature of the glycan recognition by the anti-HIV-1 broadly neutralizing antibodies 2G12, PGT128 and PG9 is their ability to be promiscuous in regards to which glycans they contact. Indeed, as seen in the 2G12 crystal structure, two non-crystallographically unique $Man_9GlcNAc_2$ moeities are found at the interface between the variable heavy domains of the two Fabs, which suggests different modes of glycan interaction at this position. For PGT128, it has been shown that although the gp120 glycan at position Asn^{332} is absolutely essential for recognition, the glycan at position Asn^{301} can potentially be replaced by that at position Asn^{295} (*67*). Similarly, as mentioned above, PG9 interacts primarily with the gp120 glycan at position Asn^{160}, but the secondary glycan binding site can be occupied by either glycan Asn^{156} or Asn^{173}, which are spatially located in almost identical positions when one of the two sites is not glycosylated. Promiscuity of glycan binding displayed by these antibodies is a feature that has most likely evolved to deal with the constantly evolving glycosylation profile on HIV-1 gp120.

The novel architecture of the 2G12 antibody is an unexpected immunological solution to the problem of specific binding to a carbohydrate cluster. The 2G12 antibody is able to bind with high affinity to gp120 because it binds divalently, with the geometrical spacing between the two primary combining sites (~35 Å) precisely aligned to the spacing of the carbohydrate ligands on gp120. In fact, docking of the 2G12+ $Man_9GlcNAc_2$ structure onto gp120 shows that the $Man_9GlcNAc_2$ moieties found in the primary combining sites perfectly span the previously implicated N-linked glycosylation sites (specifically Asn^{332} and Asn^{392}) on gp120 (Figure 4C). Most importantly, 2G12 shows that the immune system is capable of directing a high affinity antibody response specific against a self glycan that is arranged as a non-self cluster.

Downloaded by UNIV OF DELAWARE MORRIS LIB on June 13, 2012 | http://pubs.acs.org
Publication Date (Web): June 12, 2012 | doi: 10.1021/bk-2012-1102.ch007

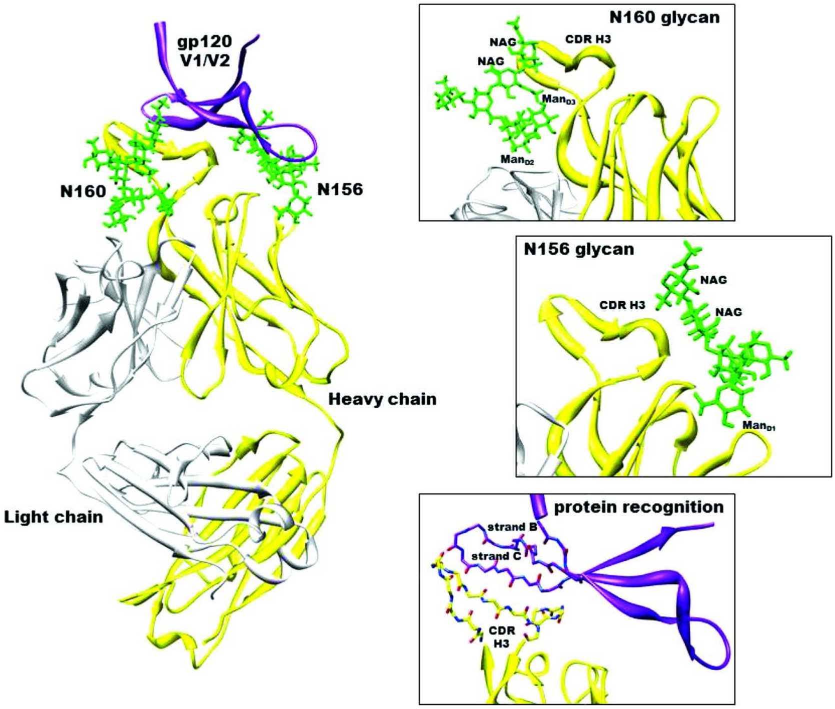

Figure 6. Antibody PG9 recognizes the gp120 V1/V2 region by interacting with two glycans and a strand. The PG9 heavy chain is colored in yellow whereas the PG9 light chain is rendered in gray. The gp120 V1/V2 protein domain and its glycans are colored in purple and green, respectively. The insets are close-up views of the antibody-glycan interactions taking place with moieties along the whole glycan face at positions Asn^{160} and Asn^{156}. The protein interaction is mediated by parallel β-strand stacking between the PG9 CDR H3 and the gp120 V1/V2 strand B (shown as a backbone representation), as well as by electrostatic interactions (not shown). Images were rendered with the program Chimera (88) using PDB ID 3U4E (61). (see color insert)

PGT128 and PG9 have also evolved exceptional novel features to provide an immunological solution for HIV-1 neutralization. To access a recessed protein epitope shielded by glycans on gp120, PGT128 and PG9 evolved a six-residue insertion in the CDR H2 and a 28-residue CDR H3, respectively. This protruding loop from the antibody paratope allows insertion through two glycans by making extensive interactions with moieties along the entire face of the glycans. It is interesting how the immune recognition of two glycans and a β-strand has emerged for two distinct locations on gp120: the base of the V3 loop on the gp120 outer domain and the gp120 V1/V2 loop at the trimer apex.

Downloaded by UNIV OF DELAWARE MORRIS LIB on June 13, 2012 | http://pubs.acs.org
Publication Date (Web): June 12, 2012 | doi: 10.1021/bk-2012-1102.ch007

Immunological Properties of the 2G12, PGT128 and PG9 Epitopes

The glycans on gp120 bound by broadly neutralizing antibodies are somewhat unusual and show some of the features that may overcome barriers to eliciting a robust immune response towards carbohydrates discussed in previous sections:

i) Some of the gp120 N-linked sites are fairly well conserved, explaining the ability of 2G12, PG128 and PG9 to recognize and neutralize a wide range HIV-1 isolates. For example, the two glycans at the center of the 2G12, PGT128 and PG9 epitopes, Asn^{160} and Asn^{332} are 93% and 73% conserved in circulating HIV-1 isolates, respectively. The close packing of these conserved sites limits the accessibility of the ER/Golgi enzymes to modify the basic oligomannose structure. Thus, multiple levels of glycan heterogeneity found at these sites on gp120 are significantly reduced.

ii) The dense clustering of oligomannoses is conceptually, if not chemically, similar to the repetitive glycans on many bacterial surfaces. This clustering is highly unusual and not previously observed in any mammalian (self) glycoproteins. Therefore, the recognition of this particular cluster of self glycans (which would individually normally be tolerated) by 2G12, PGT128 and PG9 can be explained by the close arrangement of the individual self glycans into a novel non-self cluster.

iii) The high avidity required for strong protein-carbohydrate interactions can be supported by the multivalent presentation on gp120. In addition, high affinity and specificity is achieved by adding a small protein component to the carbohydrate epitope in the case of PGT128 and PG9.

These features of gp120 glycosylation then open the door for design of carbohydrate-based HIV vaccines which utilize clustered carbohydrates as the immunogens to elicit 2G12, PGT128 and/or PG9-like antibody responses.

Glycan Immunogens

Since the discovery of the broadly neutralizing antibody 2G12 and the characterization of its gp120 carbohydrate epitope, a few laboratories have designed immunogens to present a self-glycan in a non-self cluster in attempts to re-elicit 2G12-like antibodies by vaccination. As the discovery of the PGT128 and PG9 carbohydrate/peptide epitopes is much more recent, immunogen design for these specific epitopes remains in infancy stages, but will surely see rapid development in the coming years.

Efforts in 2G12 immunogen design have mainly focused on presenting $Man_9GlcNAc_2$ (or a similar, cross-reactive carbohydrate) as a cluster in a geometry similar to that found on the gp120 envelope glycoprotein of HIV. One approach investigators have taken is to synthesize Man_9-containing glycopeptides (*89–92*). The creation of these glycopeptides provides a protein scaffold in which to display the carbohydrate as a multivalent array. The peptide portion can also provide classical CD4$^+$ T-cell help. However, in immunization assays in two different animal species, despite showing high levels of anti-carbohydrate antibodies, the recovered sera failed to recognize gp120 and neutralize HIV-1 (*91*).

Another group has used a reactivity-based one-pot synthesis approach to synthesize various Manα1-2Man containing oligomannoses (*82*). This approach provides non-self carbohydrates that are cross-reactive with Man$_9$GlcNAc$_2$. Two oligomannose candidates were discovered: a tetrasaccharide which mimics the D1 arm of Man$_9$GlcNAc$_2$ and a pentasaccharide which mimics the D2+D3 arms of Man$_9$GlcNAc$_2$. The D1 and D2+D3 arm oligomannoses are capable of inhibiting 2G12 binding to gp120 at levels nearly equivalent to that of Man$_9$. Also, from the surprising observation that 2G12 binds monosaccharide D-fructose with higher affinity than D-mannose, a designed set of nonself, synthetic monosaccharides were shown to be potent antigens and to have enhanced immunogenicity in vaccination studies (*93*). However, the recovered antibodies in this study failed to bind this glycan motif when present on gp120.

Several groups have created non-protein and whole protein scaffolds that present synthetic oligomannoses to further mimic the carbohydrate cluster epitope of gp120. Examples include 1) gold nanoparticles coated with self-assembled monolayers of synthetic oligomannosides (*94*); 2) neoglycoconjugates made of flexible polyamidoamine (PAMAM) displaying clustered HIV-1 related oligomannose carbohydrates (*95*); 3) self-assembly of oligosaccharides tagged with peptide nucleic acids (PNAs) onto DNA templates (*96*); 4) neoglycoconjugates displaying variable copy numbers of mannoses on bovine serum albumin (BSA) molecules by conjugation to Lys residues (*97*); 5) oligomannose dendrons, which display multivalent oligomannoses in high density (*98*); and 6) attachment of three Man$_9$GlcNAc$_2$ moieties on a maleimide cluster which is anchored to a cholic acid molecule (*82*) (Figure 7). In this last example, the final product is a molecule that displays three Man$_9$GlcNAc$_2$ moieties at a geometry similar to that of the N332, N339, and N392 carbohydrates of gp120. Indeed, this template-assembled Man9 cluster is capable of binding 2G12 46-fold better than a single Man$_9$GlcNAc$_2$ molecule. However, even when some of these multivalent carbohydrate scaffolds were covalently coupled to protein carriers and formulated with adjuvants, some generated oligomannose-specific IgG antibodies in immunization studies but none were able to significantly neutralize HIV-1 (e.g. (*95*)).

Finally, further encouraging immunogen design, studies revealed that a triple mutant *Saccharomyces cerevisiae* strain that expresses high-mannose glycoproteins could be used in vaccination studies to induce antibodies that bind to high-mannose glycans presented on the HIV envelope, but only when they are displayed on kifunensine-treated Env trimers (making most glycans Man$_9$GlcNAc$_2$), and not on native HIV-1 viruses (*100–103*). These antibodies could also potently and broadly neutralize viruses produced under kifunensine conditions, but not native HIV-1 viruses. In this case, most of the barriers against eliciting anti-carbohydrate responses were overcome. However, the exact conformational specificity required for gp120 binding was not accounted for with this rather bulk approach of introducing myriad different glycoproteins from the

Downloaded by UNIV OF DELAWARE MORRIS LIB on June 13, 2012 | http://pubs.acs.org
Publication Date (Web): June 12, 2012 | doi: 10.1021/bk-2012-1102.ch007

Downloaded by UNIV OF DELAWARE MORRIS LIB on June 13, 2012 | http://pubs.acs.org
Publication Date (Web): June 12, 2012 | doi: 10.1021/bk-2012-1102.ch007

yeast, highlighting the importance of fine structural determinants for engineering an appropriate immunogen.

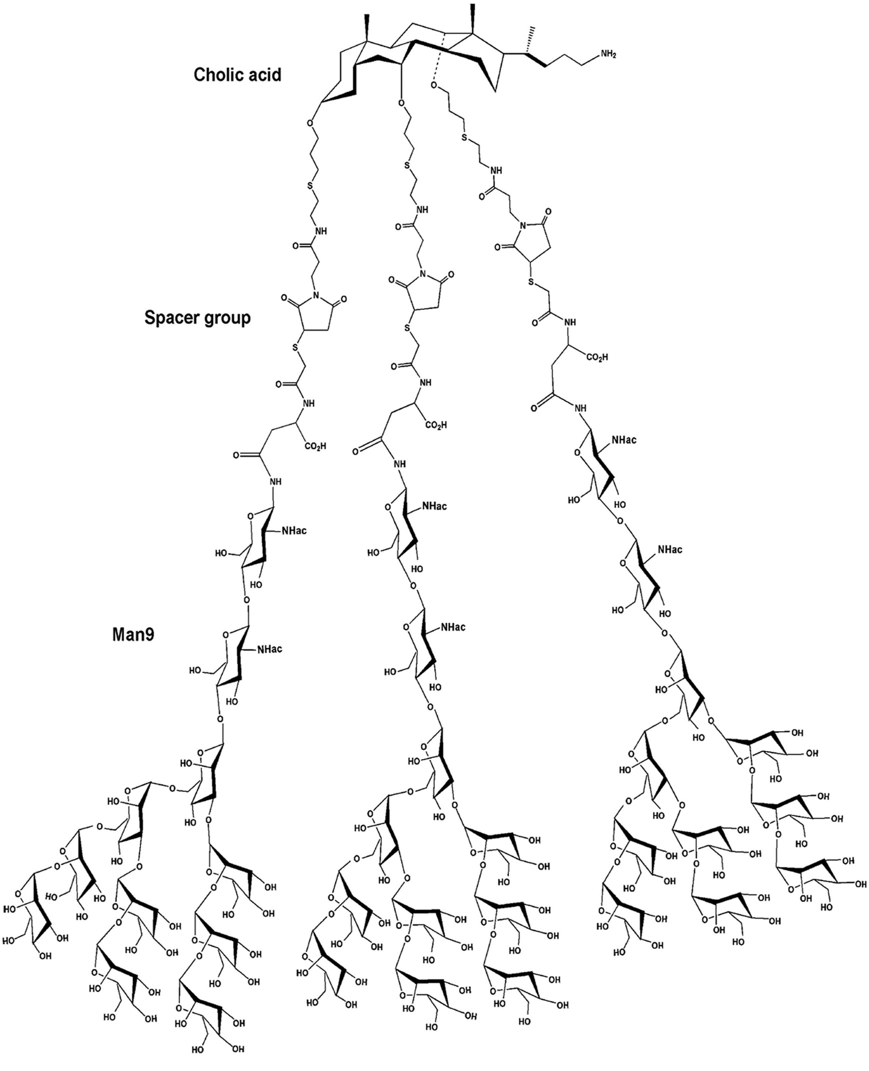

Figure 7. Structure of a designed oligomannose cluster (99). Three $Man_9GlcNAc_2$ *moieties were attached to a maleimide cluster. This cluster is attached via a spacer group onto a rigid template, cholic acid. The final product is a molecule that displays a* $Man_9GlcNAc_2$ *cluster resembling that on gp120.*

Clearly, despite creative research and significant advancement over the years, further investigations are still needed to improve the mimicry of the gp120 carbohydrate epitope for HIV-1 immunogen design. Crystal structures of PGT 128 and PG9 antibodies bound to glycans on the virus will certainly provide new approaches towards this enterprise.

Acknowledgments

Support is acknowledged from NIH GM46192 (IAW), AI33292 (DRB), the International AIDS Vaccine Initiative (IAVI), and a joint TSRI/Oxford University graduate program (CS). JPJ is the recipient of a Canadian Institutes of Health Research Fellowship. This is publication #16877-MB from The Scripps Research Institute.

References

1. Goulder, P. J.; Watkins, D. I. Impact of MHC class I diversity on immune control of immunodeficiency virus replication. *Nat. Rev. Immunol.* **2008**, *8*, 619–30.
2. Klein, M. R.; van Baalen, C. A.; Holwerda, A. M.; Kerkhof Garde, S. R.; Bende, R. J.; Keet, I. P.; Eeftinck-Schattenkerk, J. K.; Osterhaus, A. D.; Schuitemaker, H.; Miedema, F. Kinetics of Gag-specific cytotoxic T lymphocyte responses during the clinical course of HIV-1 infection: a longitudinal analysis of rapid progressors and long-term asymptomatics. *J. Exp. Med.* **1995**, *181*, 1365–72.
3. Harrer, T.; Harrer, E.; Kalams, S. A.; Elbeik, T.; Staprans, S. I.; Feinberg, M. B.; Cao, Y.; Ho, D. D.; Yilma, T.; Caliendo, A. M.; Johnson, R. P.; Buchbinder, S. P.; Walker, B. D. Strong cytotoxic T cell and weak neutralizing antibody responses in a subset of persons with stable nonprogressing HIV type 1 infection. *AIDS Res. Hum. Retroviruses* **1996**, *12*, 585–92.
4. Borrow, P.; Lewicki, H.; Hahn, B. H.; Shaw, G. M.; Oldstone, M. B. Virus-specific CD8+ cytotoxic T-lymphocyte activity associated with control of viremia in primary human immunodeficiency virus type 1 infection. *J. Virol.* **1994**, *68*, 6103–10.
5. Koup, R. A.; Safrit, J. T.; Cao, Y.; Andrews, C. A.; McLeod, G.; Borkowsky, W.; Farthing, C.; Ho, D. D. Temporal association of cellular immune responses with the initial control of viremia in primary human immunodeficiency virus type 1 syndrome. *J. Virol.* **1994**, *68*, 4650–5.
6. Mascola, J. R.; Lewis, M. G.; Stiegler, G.; Harris, D.; VanCott, T. C.; Hayes, D.; Louder, M. K.; Brown, C. R.; Sapan, C. V.; Frankel, S. S.; Lu, Y.; Robb, M. L.; Katinger, H.; Birx, D. L. Protection of Macaques against pathogenic simian/human immunodeficiency virus 89.6PD by passive transfer of neutralizing antibodies. *J. Virol.* **1999**, *73*, 4009–18.
7. Mascola, J. R.; Stiegler, G.; VanCott, T. C.; Katinger, H.; Carpenter, C. B.; Hanson, C. E.; Beary, H.; Hayes, D.; Frankel, S. S.; Birx, D. L.; Lewis, M. G.

Downloaded by UNIV OF DELAWARE MORRIS LIB on June 13, 2012 | http://pubs.acs.org
Publication Date (Web): June 12, 2012 | doi: 10.1021/bk-2012-1102.ch007

Protection of macaques against vaginal transmission of a pathogenic HIV-1/SIV chimeric virus by passive infusion of neutralizing antibodies. *Nat. Med.* **2000**, *6*, 207–10.

8. Baba, T. W.; Liska, V.; Hofmann-Lehmann, R.; Vlasak, J.; Xu, W.; Ayehunie, S.; Cavacini, L. A.; Posner, M. R.; Katinger, H.; Stiegler, G.; Bernacky, B. J.; Rizvi, T. A.; Schmidt, R.; Hill, L. R.; Keeling, M. E.; Lu, Y.; Wright, J. E.; Chou, T. C.; Ruprecht, R. M. Human neutralizing monoclonal antibodies of the IgG1 subtype protect against mucosal simian-human immunodeficiency virus infection. *Nat. Med.* **2000**, *6*, 200–6.
9. Walker, L. M.; Huber, M.; Doores, K. J.; Falkowska, E.; Pejchal, R.; Julien, J. P.; Wang, S. K.; Ramos, A.; Chan-Hui, P. Y.; Moyle, M.; Mitcham, J. L.; Hammond, P. W.; Olsen, O. A.; Phung, P.; Fling, S.; Wong, C. H.; Phogat, S.; Wrin, T.; Simek, M. D.; Koff, W. C.; Wilson, I. A.; Burton, D. R.; Poignard, P. Broad neutralization coverage of HIV by multiple highly potent antibodies. *Nature* **2011**, *477*, 466–70.
10. Walker, L. M.; Phogat, S. K.; Chan-Hui, P. Y.; Wagner, D.; Phung, P.; Goss, J. L.; Wrin, T.; Simek, M. D.; Fling, S.; Mitcham, J. L.; Lehrman, J. K.; Priddy, F. H.; Olsen, O. A.; Frey, S. M.; Hammond, P. W.; Miiro, G.; Serwanga, J.; Pozniak, A.; McPhee, D.; Manigart, O.; Mwananyanda, L.; Karita, E.; Inwoley, A.; Jaoko, W.; Dehovitz, J.; Bekker, L. G.; Pitisuttithum, P.; Paris, R.; Allen, S.; Kaminsky, S.; Zamb, T.; Moyle, M.; Koff, W. C.; Poignard, P.; Burton, D. R. Broad and Potent Neutralizing Antibodies from an African Donor Reveal a New HIV-1 Vaccine Target. *Science* **2009**.
11. Hecht, M. L.; Stallforth, P.; Silva, D. V.; Adibekian, A.; Seeberger, P. H. Recent advances in carbohydrate-based vaccines. *Curr. Opin. Chem. Biol.* **2009**, *13*, 354–9.
12. Astronomo, R. D.; Burton, D. R. Carbohydrate vaccines: developing sweet solutions to sticky situations? *Nat. Rev. Drug Discovery* **2010**, *9*, 308–24.
13. Mond, J. J.; Lees, A.; Snapper, C. M. T cell-independent antigens type 2. *Annu. Rev. Immunol.* **1995**, *13*, 655–692.
14. Snapper, C. M.; Mond, J. J. A model for induction of T cell-independent humoral immunity in response to polysaccharide antigens. *J. Immunol.* **1996**, *157*, 2229–2233.
15. Ada, G.; Isaacs, D. Carbohydrate-protein conjugate vaccines. *Clin. Microbiol. Infect.* **2003**, *9*, 79–85.
16. Kalka-Moll, W. M. Zwitterionic polysaccharides stimulate T cells by MHC class II-dependent interactions. *J. Immunol.* **2002**, *169*, 6149–6153.
17. Bundle, D. R.; Young, N. M. Carbohydrate-protein interactions in antibodies and lectins. *Curr. Opin. Struct. Biol.* **1992**, *2*, 666–673.
18. Liang, P. H.; Wang, S. K.; Wong, C. H. Quantitative analysis of carbohydrate-protein interactions using glycan microarrays: determination of surface and solution dissociation constants. *J. Am. Chem. Soc.* **2007**, *129*, 11177–84.
19. Dam, T. K.; Roy, R.; Das, S. K.; Oscarson, S.; Brewer, C. F. Binding of multivalent carbohydrates to concanavalin A and Dioclea grandiflora lectin. Thermodynamic analysis of the "multivalency effect". *J. Biol. Chem.* **2000**, *275*, 14223–30.

Downloaded by UNIV OF DELAWARE MORRIS LIB on June 13, 2012 | http://pubs.acs.org
Publication Date (Web): June 12, 2012 | doi: 10.1021/bk-2012-1102.ch007

Downloaded by UNIV OF DELAWARE MORRIS LIB on June 13, 2012 | http://pubs.acs.org
Publication Date (Web): June 12, 2012 | doi: 10.1021/bk-2012-1102.ch007

20. Dam, T. K.; Roy, R.; Page, D.; Brewer, C. F. Negative cooperativity associated with binding of multivalent carbohydrates to lectins. Thermodynamic analysis of the "multivalency effect". *Biochemistry (Mosc).* **2002**, *41*, 1351–8.
21. Monsigny, M.; Mayer, R.; Roche, A. C. Sugar-lectin interactions: sugar clusters, lectin multivalency and avidity. *Carbohydr. Lett.* **2000**, *4*, 35–52.
22. Carver, J. P. Oligosaccharides [mdash] How can flexible molecules act as signals. *Pure Appl. Chem.* **1993**, *65*, 763–770.
23. Mammen, M.; Choi, S. K.; Whitesides, G. M. Polyvalent interactions in biological systems: Implications for design and use of multivalent ligands and inhibitors. *Angew. Chem., Int. Ed.* **1998**, *37*, 2754.
24. DeAngelis, P. L. Evolution of glycosaminoglycans and their glycosyltransferases: Implications for the extracellular matrices of animals and the capsules of pathogenic bacteria. *Anat. Rec.* **2002**, *268*, 317–26.
25. Wilson, I. A.; Skehel, J. J.; Wiley, D. C. Structure of the haemagglutinin membrane glycoprotein of influenza virus at 3 A resolution. *Nature* **1981**, *289*, 366–73.
26. Feldmann, H.; Nichol, S. T.; Klenk, H. D.; Peters, C. J.; Sanchez, A. Characterization of filoviruses based on differences in structure and antigenicity of the virion glycoprotein. *Virology* **1994**, *199*, 469–73.
27. Jeffers, S. A.; Sanders, D. A.; Sanchez, A. Covalent modifications of the ebola virus glycoprotein. *J. Virol.* **2002**, *76*, 12463–72.
28. Lin, G.; Simmons, G.; Pohlmann, S.; Baribaud, F.; Ni, H.; Leslie, G. J.; Haggarty, B. S.; Bates, P.; Weissman, D.; Hoxie, J. A.; Doms, R. W. Differential N-linked glycosylation of human immunodeficiency virus and Ebola virus envelope glycoproteins modulates interactions with DC-SIGN and DC-SIGNR. *J. Virol.* **2003**, *77*, 1337–46.
29. Zhu, X.; Borchers, C.; Bienstock, R. J.; Tomer, K. B. Mass spectrometric characterization of the glycosylation pattern of HIV-gp120 expressed in CHO cells. *Biochemistry (Mosc).* **2000**, *39*, 11194–204.
30. Kuster, B.; Wheeler, S. F.; Hunter, A. P.; Dwek, R. A.; Harvey, D. J. Sequencing of N-linked oligosaccharides directly from protein gels: in-gel deglycosylation followed by matrix-assisted laser desorption/ionization mass spectrometry and normal-phase high-performance liquid chromatography. *Anal. Biochem.* **1997**, *250*, 82–101.
31. Mizuochi, T.; Spellman, M. W.; Larkin, M.; Solomon, J.; Basa, L. J.; Feizi, T. Carbohydrate structures of the human-immunodeficiency-virus (HIV) recombinant envelope glycoprotein gp120 produced in Chinese-hamster ovary cells. *Biochem. J.* **1988**, *254*, 599–603.
32. Mizuochi, T.; Spellman, M. W.; Larkin, M.; Solomon, J.; Basa, L. J.; Feizi, T. Structural characterization by chromatographic profiling of the oligosaccharides of human immunodeficiency virus (HIV) recombinant envelope glycoprotein gp120 produced in Chinese hamster ovary cells. *Biomed. Chromatogr.* **1988**, *2*, 260–70.
33. Feizi, T.; Larkin, M. AIDS and glycosylation. *Glycobiology* **1990**, *1*, 17–23.
34. Iacob, R. E.; Perdivara, I.; Przybylski, M.; Tomer, K. B. Mass spectrometric characterization of glycosylation of hepatitis C virus E2 envelope

Downloaded by UNIV OF DELAWARE MORRIS LIB on June 13, 2012 | http://pubs.acs.org
Publication Date (Web): June 12, 2012 | doi: 10.1021/bk-2012-1102.ch007

glycoprotein reveals extended microheterogeneity of N-glycans. *J. Am. Soc. Mass Spectrom.* **2008**, *19*, 428–44.

35. Kasturi, L.; Chen, H.; Shakin-Eshleman, S. H. Regulation of N-linked core glycosylation: use of a site-directed mutagenesis approach to identify Asn-Xaa-Ser/Thr sequons that are poor oligosaccharide acceptors. *Biochem. J.* **1997**, *323*, 415–9.
36. Hossler, P.; Mulukutla, B. C.; Hu, W. S. Systems analysis of N-glycan processing in mammalian cells. *PloS ONE* **2007**, *2*, e713.
37. Opdenakker, G.; Rudd, P. M.; Ponting, C. P.; Dwek, R. A. Concepts and principles of glycobiology. *FASEB J.* **1993**, *7*, 1330–7.
38. Rudd, P. M.; Dwek, R. A. Glycosylation: heterogeneity and the 3D structure of proteins. *Crit. Rev. Biochem. Mol. Biol.* **1997**, *32*, 1–100.
39. Van den Steen, P.; Rudd, P. M.; Dwek, R. A.; Opdenakker, G. Concepts and principles of O-linked glycosylation. *Crit. Rev. Biochem. Mol. Biol.* **1998**, *33*, 151–208.
40. Rudd, P. M.; Elliott, T.; Cresswell, P.; Wilson, I. A.; Dwek, R. A. Glycosylation and the immune system. *Science* **2001**, *291*, 2370–6.
41. Sears, P.; Wong, C. H. Toward automated synthesis of oligosaccharides and glycoproteins. *Science* **2001**, *291*, 2344–2350.
42. Seeberger, P. H. Automated oligosaccharide synthesis. *Chem. Soc. Rev.* **2008**, *37*, 19–28.
43. Adams, E. W.; Ratner, D. M.; Bokesch, H. R.; McMahon, J. B.; O'Keefe, B. R.; Seeberger, P. H. Oligosaccharide and glycoprotein microarrays as tools in HIV glycobiology; glycan-dependent gp120/protein interactions. *Chem. Biol.* **2004**, *11*, 875–81.
44. Blixt, O. Printed covalent glycan array for ligand profiling of diverse glycan binding proteins. *Glycobiology* **2004**, *14*, 1072–1072.
45. Raman, R.; Raguram, S.; Venkataraman, G.; Paulson, J. C.; Sasisekharan, R. Glycomics: an integrated systems approach to structure-function relationships of glycans. *Nat. Methods* **2005**, *2*, 817–824.
46. Avci, F. Y.; Li, X.; Tsuji, M.; Kasper, D. L. A mechanism for glycoconjugate vaccine activation of the adaptive immune system and its implications for vaccine design. *Nat. Med.* **2011**, *17*, 1602–9.
47. Liang, C. H.; Wang, S. K.; Lin, C. W.; Wang, C. C.; Wong, C. H.; Wu, C. Y. Effects of Neighboring Glycans on Antibody-Carbohydrate Interaction. *Angew. Chem., Int. Ed.* **2011**.
48. Szakonyi, G.; Klein, M. G.; Hannan, J. P.; Young, K. A.; Ma, R. Z.; Asokan, R.; Holers, V. M.; Chen, X. S. Structure of the Epstein-Barr virus major envelope glycoprotein. *Nat. Struct. Mol. Biol.* **2006**, *13*, 996–1001.
49. Mizuochi, T.; Matthews, T. J.; Kato, M.; Hamako, J.; Titani, K.; Solomon, J.; Feizi, T. Diversity of oligosaccharide structures on the envelope glycoprotein gp 120 of human immunodeficiency virus 1 from the lymphoblastoid cell line H9. Presence of complex-type oligosaccharides with bisecting N-acetylglucosamine residues. *J. Biol. Chem.* **1990**, *265*, 8519–24.
50. Liu, T. Y.; Gotschlich, E. C.; Jonssen, E. K.; Wysocki, J. R. Studies on the meningococcal polysaccharides. I. Composition and chemical properties of the group A polysaccharide. *J. Biol. Chem.* **1971**, *246*, 2849–58.

Downloaded by UNIV OF DELAWARE MORRIS LIB on June 13, 2012 | http://pubs.acs.org
Publication Date (Web): June 12, 2012 | doi: 10.1021/bk-2012-1102.ch007

51. Bhattacharjee, A. K.; Jennings, H. J.; Kenny, C. P.; Martin, A.; Smith, I. C. Structural determination of the sialic acid polysaccharide antigens of Neisseria meningitidis serogroups B and C with carbon 13 nuclear magnetic resonance. *J. Biol. Chem.* **1975**, *250*, 1926–32.
52. Nahm, M. H.; Kim, K. H.; Anderson, P.; Hetherington, S. V.; Park, M. K. Functional capacities of clonal antibodies to Haemophilus influenzae type b polysaccharide. *Infect. Immun.* **1995**, *63*, 2989–94.
53. Robbins, J. B.; Schneerson, R.; Horwith, G.; Naso, R.; Fattom, A. Staphylococcus aureus types 5 and 8 capsular polysaccharide-protein conjugate vaccines. *Am. Heart J.* **2004**, *147*, 593–8.
54. Szu, S. C.; Li, X. R.; Stone, A. L.; Robbins, J. B. Relation between structure and immunologic properties of the Vi capsular polysaccharide. *Infect. Immun.* **1991**, *59*, 4555–61.
55. Szu, S. C.; Stone, A. L.; Robbins, J. D.; Schneerson, R.; Robbins, J. B. Vi capsular polysaccharide-protein conjugates for prevention of typhoid fever. Preparation, characterization, and immunogenicity in laboratory animals. *J. Exp. Med.* **1987**, *166*, 1510–24.
56. Brisson, J. R.; Uhrinova, S.; Woods, R. J.; van der Zwan, M.; Jarrell, H. C.; Paoletti, L. C.; Kasper, D. L.; Jennings, H. J. NMR and molecular dynamics studies of the conformational epitope of the type III group B Streptococcus capsular polysaccharide and derivatives. *Biochemistry (Mosc).* **1997**, *36*, 3278–92.
57. van Kasteren, S. I.; Kramer, H. B.; Gamblin, D. P.; Davis, B. G. Site-selective glycosylation of proteins: creating synthetic glycoproteins. *Nat. Protoc.* **2007**, *2*, 3185–94.
58. Scanlan, C. N.; Ritchie, G. E.; Baruah, K.; Crispin, M.; Harvey, D. J.; Singer, B. B.; Lucka, L.; Wormald, M. R.; Wentworth, P., Jr.; Zitzmann, N.; Rudd, P. M.; Burton, D. R.; Dwek, R. A. Inhibition of mammalian glycan biosynthesis produces non-self antigens for a broadly neutralising, HIV-1 specific antibody. *J. Mol. Biol.* **2007**, *372*, 16–22.
59. Knipe, D. M.; Howley, P. M. *Fields Virology*; Lippincott Williams & Wilkins: Philadelphia, 2007.
60. Zwick, M. B.; Labrijn, A. F.; Wang, M.; Spenlehauer, C.; Saphire, E. O.; Binley, J. M.; Moore, J. P.; Stiegler, G.; Katinger, H.; Burton, D. R.; Parren, P. W. Broadly neutralizing antibodies targeted to the membrane-proximal external region of human immunodeficiency virus type 1 glycoprotein gp41. *J. Virol.* **2001**, *75*, 10892–905.
61. McLellan, J. S.; Pancera, M.; Carrico, C.; Gorman, J.; Julien, J. P.; Khayat, R.; Louder, R.; Pejchal, R.; Sastry, M.; Dai, K.; O'Dell, S.; Patel, N.; Shahzad-Ul-Hussan, S.; Yang, Y.; Zhang, B.; Zhou, T.; Zhu, J.; Boyington, J. C.; Chuang, G. Y.; Diwanji, D.; Georgiev, I.; Do Kwon, Y.; Lee, D.; Louder, M. K.; Moquin, S.; Schmidt, S. D.; Yang, Z. Y.; Bonsignori, M.; Crump, J. A.; Kapiga, S. H.; Sam, N. E.; Haynes, B. F.; Burton, D. R.; Koff, W. C.; Walker, L. M.; Phogat, S.; Wyatt, R.; Orwenyo, J.; Wang, L. X.; Arthos, J.; Bewley, C. A.; Mascola, J. R.; Nabel, G. J.; Schief, W. R.; Ward, A. B.; Wilson, I. A.; Kwong, P. D. Structure of HIV-1 gp120

Downloaded by UNIV OF DELAWARE MORRIS LIB on June 13, 2012 | http://pubs.acs.org
Publication Date (Web): June 12, 2012 | doi: 10.1021/bk-2012-1102.ch007

V1/V2 domain with broadly neutralizing antibody PG9. *Nature* **2011**, *480*, 336–343.

62. Huang, C. C.; Tang, M.; Zhang, M. Y.; Majeed, S.; Montabana, E.; Stanfield, R. L.; Dimitrov, D. S.; Korber, B.; Sodroski, J.; Wilson, I. A.; Wyatt, R.; Kwong, P. D. Structure of a V3-containing HIV-1 gp120 core. *Science* **2005**, *310*, 1025–8.
63. Kwong, P. D.; Wyatt, R.; Majeed, S.; Robinson, J.; Sweet, R. W.; Sodroski, J.; Hendrickson, W. A. Structures of HIV-1 gp120 envelope glycoproteins from laboratory-adapted and primary isolates. *Structure* **2000**, *8*, 1329–39.
64. Kwong, P. D.; Wyatt, R.; Robinson, J.; Sweet, R. W.; Sodroski, J.; Hendrickson, W. A. Structure of an HIV gp120 envelope glycoprotein in complex with the CD4 receptor and a neutralizing human antibody. *Nature* **1998**, *393*, 648–59.
65. Zhou, T.; Georgiev, I.; Wu, X.; Yang, Z. Y.; Dai, K.; Finzi, A.; Kwon, Y. D.; Scheid, J. F.; Shi, W.; Xu, L.; Yang, Y.; Zhu, J.; Nussenzweig, M. C.; Sodroski, J.; Shapiro, L.; Nabel, G. J.; Mascola, J. R.; Kwong, P. D. Structural basis for broad and potent neutralization of HIV-1 by antibody VRC01. *Science* **2010**, *329*, 811–7.
66. Zhou, T.; Xu, L.; Dey, B.; Hessell, A. J.; Van Ryk, D.; Xiang, S. H.; Yang, X.; Zhang, M. Y.; Zwick, M. B.; Arthos, J.; Burton, D. R.; Dimitrov, D. S.; Sodroski, J.; Wyatt, R.; Nabel, G. J.; Kwong, P. D. Structural definition of a conserved neutralization epitope on HIV-1 gp120. *Nature* **2007**, *445*, 732–7.
67. Pejchal, R.; Doores, K. J.; Walker, L. M.; Khayat, R.; Huang, P. S.; Wang, S. K.; Stanfield, R. L.; Julien, J. P.; Ramos, A.; Crispin, M.; Depetris, R.; Katpally, U.; Marozsan, A.; Cupo, A.; Maloveste, S.; Liu, Y.; McBride, R.; Ito, Y.; Sanders, R. W.; Ogohara, C.; Paulson, J. C.; Feizi, T.; Scanlan, C. N.; Wong, C. H.; Moore, J. P.; Olson, W. C.; Ward, A. B.; Poignard, P.; Schief, W. R.; Burton, D. R.; Wilson, I. A. A potent and broad neutralizing antibody recognizes and penetrates the HIV glycan shield. *Science* **2011**, *334*, 1097–103.
68. Liu, J.; Bartesaghi, A.; Borgnia, M. J.; Sapiro, G.; Subramaniam, S. Molecular architecture of native HIV-1 gp120 trimers. *Nature* **2008**, *455*, 109–13.
69. Kwong, P. D.; Wyatt, R.; Sattentau, Q. J.; Sodroski, J.; Hendrickson, W. A. Oligomeric modeling and electrostatic analysis of the gp120 envelope glycoprotein of human immunodeficiency virus. *J. Virol.* **2000**, *74*, 1961–72.
70. Montefiori, D.; Moore, J. P. HIV vaccines. Magic of the occult? *Science* **1999**, *283*, 336–7.
71. Wyatt, R.; Kwong, P. D.; Desjardins, E.; Sweet, R. W.; Robinson, J.; Hendrickson, W. A.; Sodroski, J. G. The antigenic structure of the HIV gp120 envelope glycoprotein. *Nature* **1998**, *393*, 705–11.
72. Sanders, R. W.; Venturi, M.; Schiffner, L.; Kalyanaraman, R.; Katinger, H.; Lloyd, K. O.; Kwong, P. D.; Moore, J. P. The mannose-dependent epitope for neutralizing antibody 2G12 on human immunodeficiency virus type 1 glycoprotein gp120. *J. Virol.* **2002**, *76*, 7293–305.
73. Wei, X.; Decker, J. M.; Wang, S.; Hui, H.; Kappes, J. C.; Wu, X.; Salazar-Gonzalez, J. F.; Salazar, M. G.; Kilby, J. M.; Saag, M. S.;

Downloaded by UNIV OF DELAWARE MORRIS LIB on June 13, 2012 | http://pubs.acs.org
Publication Date (Web): June 12, 2012 | doi: 10.1021/bk-2012-1102.ch007

Komarova, N. L.; Nowak, M. A.; Hahn, B. H.; Kwong, P. D.; Shaw, G. M. Antibody neutralization and escape by HIV-1. *Nature* **2003**, *422*, 307–12.

74. Allan, J. S.; Coligan, J. E.; Barin, F.; McLane, M. F.; Sodroski, J. G.; Rosen, C. A.; Haseltine, W. A.; Lee, T. H.; Essex, M. Major glycoprotein antigens that induce antibodies in AIDS patients are encoded by HTLV-III. *Science* **1985**, *228*, 1091–4.
75. Geyer, H.; Holschbach, C.; Hunsmann, G.; Schneider, J. Carbohydrates of human immunodeficiency virus. Structures of oligosaccharides linked to the envelope glycoprotein 120. *J. Biol. Chem.* **1988**, *263*, 11760–7.
76. Ratner, L.; Haseltine, W.; Patarca, R.; Livak, K. J.; Starcich, B.; Josephs, S. F.; Doran, E. R.; Rafalski, J. A.; Whitehorn, E. A.; Baumeister, K.; et al. Complete nucleotide sequence of the AIDS virus, HTLV-III. *Nature* **1985**, *313*, 277–84.
77. Doores, K. J.; Bonomelli, C.; Harvey, D. J.; Vasiljevic, S.; Dwek, R. A.; Burton, D. R.; Crispin, M.; Scanlan, C. N. Envelope glycans of immunodeficiency virions are almost entirely oligomannose antigens. *Proc. Natl. Acad. Sci. U.S.A.* **2010**, *107*, 13800–5.
78. Scanlan, C. N.; Pantophlet, R.; Wormald, M. R.; Ollmann Saphire, E.; Stanfield, R.; Wilson, I. A.; Katinger, H.; Dwek, R. A.; Rudd, P. M.; Burton, D. R. The broadly neutralizing anti-human immunodeficiency virus type 1 antibody 2G12 recognizes a cluster of alpha1-->2 mannose residues on the outer face of gp120. *J. Virol.* **2002**, *76*, 7306–21.
79. Ohgimoto, S.; Shioda, T.; Mori, K.; Nakayama, E. E.; Hu, H.; Nagai, Y. Location-specific, unequal contribution of the N glycans in simian immunodeficiency virus gp120 to viral infectivity and removal of multiple glycans without disturbing infectivity. *J. Virol.* **1998**, *72*, 8365–70.
80. Dacheux, L.; Moreau, A.; Ataman-Onal, Y.; Biron, F.; Verrier, B.; Barin, F. Evolutionary dynamics of the glycan shield of the human immunodeficiency virus envelope during natural infection and implications for exposure of the 2G12 epitope. *J. Virol.* **2004**, *78*, 12625–37.
81. Bonsignori, M.; Hwang, K. K.; Chen, X.; Tsao, C. Y.; Morris, L.; Gray, E.; Marshall, D. J.; Crump, J. A.; Kapiga, S. H.; Sam, N. E.; Sinangil, F.; Pancera, M.; Yongping, Y.; Zhang, B.; Zhu, J.; Kwong, P. D.; O'Dell, S.; Mascola, J. R.; Wu, L.; Nabel, G. J.; Phogat, S.; Seaman, M. S.; Whitesides, J. F.; Moody, M. A.; Kelsoe, G.; Yang, X.; Sodroski, J.; Shaw, G. M.; Montefiori, D. C.; Kepler, T. B.; Tomaras, G. D.; Alam, S. M.; Liao, H. X.; Haynes, B. F. Analysis of a clonal lineage of HIV-1 envelope V2/V3 conformational epitope-specific broadly neutralizing antibodies and their inferred unmutated common ancestors. *J. Virol.* **2011**, *85*, 9998–10009.
82. Lee, H. K.; Scanlan, C. N.; Huang, C. Y.; Chang, A. Y.; Calarese, D. A.; Dwek, R. A.; Rudd, P. M.; Burton, D. R.; Wilson, I. A.; Wong, C. H. Reactivity-based one-pot synthesis of oligomannoses: defining antigens recognized by 2G12, a broadly neutralizing anti-HIV-1 antibody. *Angew. Chem., Int. Ed.* **2004**, *43*, 1000–3.
83. Calarese, D. A.; Scanlan, C. N.; Zwick, M. B.; Deechongkit, S.; Mimura, Y.; Kunert, R.; Zhu, P.; Wormald, M. R.; Stanfield, R. L.; Roux, K. H.; Kelly, J. W.; Rudd, P. M.; Dwek, R. A.; Katinger, H.; Burton, D. R.; Wilson, I. A.

Downloaded by UNIV OF DELAWARE MORRIS LIB on June 13, 2012 | http://pubs.acs.org
Publication Date (Web): June 12, 2012 | doi: 10.1021/bk-2012-1102.ch007

Antibody domain exchange is an immunological solution to carbohydrate cluster recognition. *Science* **2003**, *300*, 2065–71.

84. Huber, M.; Le, K. M.; Doores, K. J.; Fulton, Z.; Stanfield, R. L.; Wilson, I. A.; Burton, D. R. Very few substitutions in a germ line antibody are required to initiate significant domain exchange. *J. Virol.* **2010**, *84*, 10700–7.
85. Schulke, N.; Vesanen, M. S.; Sanders, R. W.; Zhu, P.; Lu, M.; Anselma, D. J.; Villa, A. R.; Parren, P. W.; Binley, J. M.; Roux, K. H.; Maddon, P. J.; Moore, J. P.; Olson, W. C. Oligomeric and conformational properties of a proteolytically mature, disulfide-stabilized human immunodeficiency virus type 1 gp140 envelope glycoprotein. *J. Virol.* **2002**, *76*, 7760–76.
86. Kraulis, P. J. MOLSCRIPT: A Program to Produce Both Detailed and Schematic Plots of Protein Structures. *J. Appl. Crystallogr.* **1991**, *24*, 946–950.
87. Merritt, E. A. B. D. J. Raster3D Photorealistic Molecular Graphics'. *Methods Enzymol.* **1997**, *277*, 505–524.
88. Pettersen, E. F.; Goddard, T. D.; Huang, C. C.; Couch, G. S.; Greenblatt, D. M.; Meng, E. C.; Ferrin, T. E. UCSF Chimera--a visualization system for exploratory research and analysis. *J. Comput. Chem.* **2004**, *25*, 1605–12.
89. Mandal, M.; Dudkin, V. Y.; Geng, X.; Danishefsky, S. J. In pursuit of carbohydrate-based HIV vaccines, part 1: The total synthesis of hybrid-type gp120 fragments. *Angew. Chem., Int. Ed.* **2004**, *43*, 2557–61.
90. Geng, X.; Dudkin, V. Y.; Mandal, M.; Danishefsky, S. J. In pursuit of carbohydrate-based HIV vaccines, part 2: The total synthesis of high-mannose-type gp120 fragments--evaluation of strategies directed to maximal convergence. *Angew. Chem., Int. Ed.* **2004**, *43*, 2562–5.
91. Joyce, J. G.; Krauss, I. J.; Song, H. C.; Opalka, D. W.; Grimm, K. M.; Nahas, D. D.; Esser, M. T.; Hrin, R.; Feng, M.; Dudkin, V. Y.; Chastain, M.; Shiver, J. W.; Danishefsky, S. J. An oligosaccharide-based HIV-1 2G12 mimotope vaccine induces carbohydrate-specific antibodies that fail to neutralize HIV-1 virions. *Proc. Natl. Acad. Sci. U.S.A.* **2008**, *105*, 15684–9.
92. Wang, J.; Li, H.; Zou, G.; Wang, L. X. Novel template-assembled oligosaccharide clusters as epitope mimics for HIV-neutralizing antibody 2G12. Design, synthesis, and antibody binding study. *Org. Biomol. Chem.* **2007**, *5*, 1529–40.
93. Doores, K. J.; Fulton, Z.; Hong, V.; Patel, M. K.; Scanlan, C. N.; Wormald, M. R.; Finn, M. G.; Burton, D. R.; Wilson, I. A.; Davis, B. G. A nonself sugar mimic of the HIV glycan shield shows enhanced antigenicity. *Proc. Natl. Acad. Sci. U.S.A.* **2010**, *107*, 17107–12.
94. Marradi, M.; Di Gianvincenzo, P.; Enriquez-Navas, P. M.; Martinez-Avila, O. M.; Chiodo, F.; Yuste, E.; Angulo, J.; Penades, S. Gold nanoparticles coated with oligomannosides of HIV-1 glycoprotein gp120 mimic the carbohydrate epitope of antibody 2G12. *J. Mol. Biol.* **2011**, *410*, 798–810.
95. Kabanova, A.; Adamo, R.; Proietti, D.; Berti, F.; Tontini, M.; Rappuoli, R.; Costantino, P. Preparation, characterization and immunogenicity of HIV-1 related high-mannose oligosaccharides-CRM197 glycoconjugates. *Glycoconjugate J.* **2010**, *27*, 501–13.

96. Gorska, K.; Huang, K. T.; Chaloin, O.; Winssinger, N. DNA-templated homo- and heterodimerization of peptide nucleic acid encoded oligosaccharides that mimick the carbohydrate epitope of HIV. *Angew. Chem., Int. Ed.* **2009**, *48*, 7695–700.
97. Astronomo, R. D.; Lee, H. K.; Scanlan, C. N.; Pantophlet, R.; Huang, C. Y.; Wilson, I. A.; Blixt, O.; Dwek, R. A.; Wong, C. H.; Burton, D. R. A glycoconjugate antigen based on the recognition motif of a broadly neutralizing human immunodeficiency virus antibody, 2G12, is immunogenic but elicits antibodies unable to bind to the self glycans of gp120. *J. Virol.* **2008**, *82*, 6359–68.
98. Wang, S. K.; Liang, P. H.; Astronomo, R. D.; Hsu, T. L.; Hsieh, S. L.; Burton, D. R.; Wong, C. H. Targeting the carbohydrates on HIV-1: Interaction of oligomannose dendrons with human monoclonal antibody 2G12 and DC-SIGN. *Proc. Natl. Acad. Sci. U.S.A.* **2008**, *105*, 3690–5.
99. Li, H.; Wang, L. X. Design and synthesis of a template-assembled oligomannose cluster as an epitope mimic for human HIV-neutralizing antibody 2G12. *Org. Biomol. Chem.* **2004**, *2*, 483–8.
100. Agrawal-Gamse, C.; Luallen, R. J.; Liu, B.; Fu, H.; Lee, F. H.; Geng, Y.; Doms, R. W. Yeast-elicited cross-reactive antibodies to HIV Env glycans efficiently neutralize virions expressing exclusively high-mannose N-linked glycans. *J. Virol.* **2011**, *85*, 470–80.
101. Dunlop, D. C.; Bonomelli, C.; Mansab, F.; Vasiljevic, S.; Doores, K. J.; Wormald, M. R.; Palma, A. S.; Feizi, T.; Harvey, D. J.; Dwek, R. A.; Crispin, M.; Scanlan, C. N. Polysaccharide mimicry of the epitope of the broadly neutralizing anti-HIV antibody, 2G12, induces enhanced antibody responses to self oligomannose glycans. *Glycobiology* **2010**, *20*, 812–23.
102. Luallen, R. J.; Fu, H.; Agrawal-Gamse, C.; Mboudjeka, I.; Huang, W.; Lee, F. H.; Wang, L. X.; Doms, R. W.; Geng, Y. A yeast glycoprotein shows high-affinity binding to the broadly neutralizing human immunodeficiency virus antibody 2G12 and inhibits gp120 interactions with 2G12 and DC-SIGN. *J. Virol.* **2009**, *83*, 4861–70.
103. Luallen, R. J.; Lin, J.; Fu, H.; Cai, K. K.; Agrawal, C.; Mboudjeka, I.; Lee, F. H.; Montefiori, D.; Smith, D. F.; Doms, R. W.; Geng, Y. An engineered *Saccharomyces cerevisiae* strain binds the broadly neutralizing human immunodeficiency virus type 1 antibody 2G12 and elicits mannose-specific gp120-binding antibodies. *J. Virol.* **2008**, *82*, 6447–57.

Downloaded by UNIV OF DELAWARE MORRIS LIB on June 13, 2012 | http://pubs.acs.org
Publication Date (Web): June 12, 2012 | doi: 10.1021/bk-2012-1102.ch007

Downloaded by UNIV OF GUELPH LIBRARY on June 14, 2012 | http://pubs.acs.org
Publication Date (Web): June 12, 2012 | doi: 10.1021/bk-2012-1102.ch008

Chapter 8

Cationic Polysaccharides in the Treatment of Pathogenic *Candida* Infections

Avital Mazar Ben-Josef, David Platt, and Eliezer Zomer[*]

Pro-Pharmaceuticals, 7 Wells Avenue, Newton, MA 02459
[*]**zomer@galectintherapeutics.com**

A heat stable complex polysaccharide (molecular weight of 4300 Da) purified from the cell wall of the fungus *Mucor rouxii* (CPM) and a cationic polysaccharide from crab chitin (CPP) are potent antifungal agents both *in vitro* and *in vivo*. These compounds possess several highly desirable characteristics for the next generation of antifungal agents. First, being novel compounds, unrelated to the existing antifungal drugs, there is no cross resistance between the compounds and the currently used antifungal agents. Second is the importance of the rapidity of action, low MIC (Minimum Inhibitory Concentration) values and the lethal effect of these compounds against a wide spectrum of pathogenic yeasts. This will help reduce treatment duration and the development of untoward effects. Third, these compounds are heat and light-stable, making them promising to use for topical applications as was proven by the *in vivo* experiments with CPP. Fourth, being a large molecule with highly charged residues, these compounds are acting on external targets of the cell membrane. Thus, it is unlikely to develop resistance to CPM by the efflux mechanism that is a major cause of drug resistance in microorganisms including fungi.

Introduction

Commensally microorganisms considered to be the normal microflora of our body surfaces can become opportunistic pathogens responsible for severe and often fatal infections in humans (*1–3*). The expansion in numbers of fungal

In Glycobiology and Drug Design; Klyosov, A.;
ACS Symposium Series; American Chemical Society: Washington, DC, 2012.

Downloaded by UNIV OF GUELPH LIBRARY on June 14, 2012 | http://pubs.acs.org
Publication Date (Web): June 12, 2012 | doi: 10.1021/bk-2012-1102.ch008

infections is also due to an expanding population of immunocompromised patients from diseases like AIDS, or many therapeutics such as steroid and chemo therapies, and advances in organ transplantation that facilitate fungal invasion. The prevalence of hospital acquired infections has almost doubled in recent years and now accounts for 10-15%, of which nosocomial infections with pathogenic yeast are responsible for up to 70% of the cases (*4*).

The increased frequency, severity, and number of fungal species identified as pathogens have further created a critical need for new, safe, anti-fungal drugs. Today, the most commonly used drugs for systemic and local fungal infections are amphotericin B (AMB) and azole agents (*5*). AMB is still the drug of choice in many systemic mycoses due to its broad spectrum and fungicidal activity. However, AMB is nephro-toxic and is administered intravenously only (*6*). The triazoles, fluconazole and itraconazole, have a broad spectrum of activity, can be administered orally, and are considered less toxic than AMB. However, azoles are fungistatic, and drug resistance has become a significant problem (*7–12*).

The Compounds

Cationic Polysaccharide from *Mucor rouxii*

The polysaccharide purified from the cell wall of the fungus *Mucor rouxii* (CPM), is a heat stable complex carbohydrate with an estimated molecular weight of 4.3 Kd. The purified polysaccharide is composed of glucosamine residues with the majority connected through a 1,4 beta glucosidic bond (Scheme 1), and the minority has either a 3,4 or 4,6 glucosidic bond with about 5% *N*-acetylated residues.

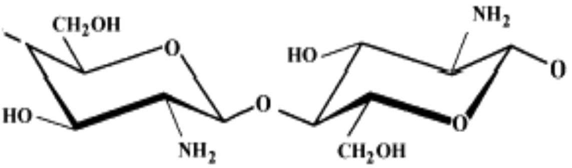

Scheme 1. Structural units of polyglucosamine consist mostly of D-glucosamine units connected in beta-1,4 bond configuration.

Cationic Polysaccharide From Crab Chitin

This polysaccharide is available commercially as deacetylated chitin (chitosan) with over 95% 2-amino-2-deoxy-D-glucopyranose. The polymer' monomeric units are bound through a 1,4 beta glycosidic bond (Scheme 2). A 1% solution of this polymer was prepared by dissolving it in mild hydrochloric acid at room temperature. This soluble preparation was combined with sodium pyrithionate (CPP) at acidic pH at 5 to 1 ratio (w/w) to study potential synergistic effect.

Downloaded by UNIV OF GUELPH LIBRARY on June 14, 2012 | http://pubs.acs.org
Publication Date (Web): June 12, 2012 | doi: 10.1021/bk-2012-1102.ch008

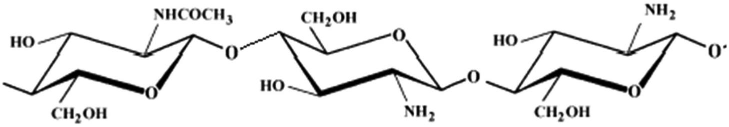

Scheme 2. Structural units of chitosan consist mostly of D-glucosamine units connected in beta 1-4 bond configuration with about 5% N acetyl-D-glucosamine.

In Vitro Activity

CPM was proven to possess a remarkable in vitro fungicidal activity against a wide spectrum of azole-resistant *Candida* with apparently no cross-resistance with any currently used antifungal agents (*13*). Its broad anti-*Candida* activity is well comparable to that of AMB; however, the fungicidal activity of CPM is faster than that of AMB. Use of CPM in concentrations of 8 and 16 times fold greater than the Minimum Inhibitory Concentration (MIC) (5 and 10 μg/ml), resulted in the killing of 99.6% and 99.9%, respectively, of *Candida albicans* within 15 minutes of exposure. Using AMB in similar concentrations resulted in 99.9% killing after 4 hours for *C. albicans and C. glabrata* (Fig. 1 & 2). CPM possess a very narrow therapeutic range (MIC = 0.078 – 0.321 μg/ml) in all 112 *Candida* species (Table 1) that were tested including Azole–resistant species (*13*).

Like CPM, CPP was evaluated for in-vitro anti-*Candida* activity and demonstrated superior *in vitro* fungicidal activity against a wide spectrum of pathogenic yeasts, including azole-resistant isolates. The MIC's of CPP for *C. albicans* were found to be similar or one dilution lower than that of CPM, with a MIC of 0.156-0.312 μg/ml.

Mode of Action

In recent years, the role of carbohydrates in biological interactions has been increasingly recognized (*14*). Carbohydrate-binding receptors, initiating diverse signal transduction pathways, have been described in hepatocytes (*15*), alveolar macrophages (*16*) and other systems (*17*). Many animal lectins contain carbohydrate-recognition domains (CRDs) (*18*), which specifically recognize a variety of sugars. The mannose-binding protein, for instance, is a serum lectin that binds to the surface of yeasts and bacteria and mediates an innate immune response (*15*, *19*). It recognizes and binds to mannose, N-acetyl-glucosamine and L-fucose with approximately equal affinities (*20*). This process is achieved, in part, by clustering of several CRDs, each with its own sugar binding site.

In the case of the macrophage mannose receptor, the full affinity for the yeast mannan can only be attained when five of the eight CRDs are present (*21*). Many of these lectins require calcium for binding activity (C-type lectins). At the binding site of these C-type lectins, specific oligosaccharide equatorial hydroxyl groups act as coordination ligands and bind to Ca^{2+}. An example of the latter would be the binding of the antifungal agents from the *pradimicins* family, that bind to the yeast cell wall through the mannopyranoside-binding site in the presence of Ca^{2+} (*22*). On the other hand, calcium and magnesium are also known to inhibit a number of aminoglycoside-membrane interactions including those with bacterial, plasma and subcellular membranes (*23*, *24*).

Table 1. In vitro susceptibilities of *C. albicans* and non-*albicans* Candida to Cationic Polysaccharide from *Mucor rouxii* (CPM).

Organisms	*Antifungal agent*	*MIC Range (μg/ml)*
C. albicans (29 tested)	CPM	0.156-0.312
C. parapsilosis (10)	CPM Fluconazole	0.078-0.312 0.16-20
C. glabrata (15)	CPM Ketoconazole Fluconazole	0.078-10.00 0.01-6.3 1.25-40
C. tropicalis (10)	CPM Fluconazole	0.039-0.312 0.63-80
C. lusitaniae (10)	CPM Fluconazole	0.156-0.312 0.31-20
C. krusie (12)	CPM Fluconazole	0.039-0.312 0.16-80
c. guillermondii (10)	CPM Fluconazole	0.078-0.312 5-10
C. kefyr (5)	CPM	0.156-0.312
C. stellatoidea (4)	CPM	0.312
C. rugosa (2)	CPM Fluconazole	0.312 5
C. lambica (1)	CPM Fluconazole	0.078 20
C. paratropicalis (1)	CPM	0.312
C. lipolitica (1)	CPM	0.312
Saccharomyces cerevisiae (2)	CPM	0.156

Downloaded by UNIV OF GUELPH LIBRARY on June 14, 2012 | http://pubs.acs.org
Publication Date (Web): June 12, 2012 | doi: 10.1021/bk-2012-1102.ch008

Downloaded by UNIV OF GUELPH LIBRARY on June 14, 2012 | http://pubs.acs.org
Publication Date (Web): June 12, 2012 | doi: 10.1021/bk-2012-1102.ch008

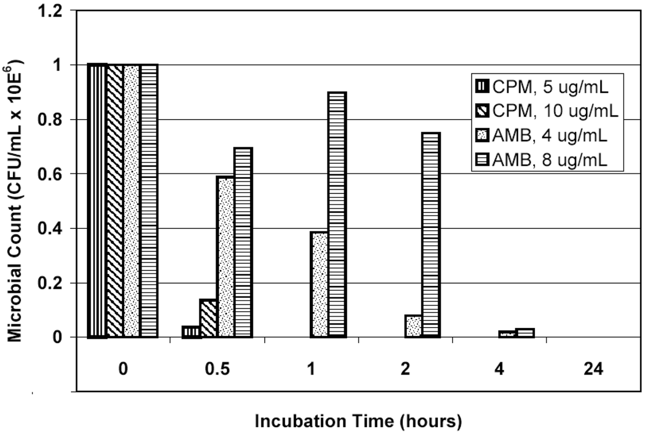

Figure 1. Comparison of fungicidal activity of cationic polysaccharide from Mucor rouxii (CPM) and Amphotericin b (AMB) – for C. albicans

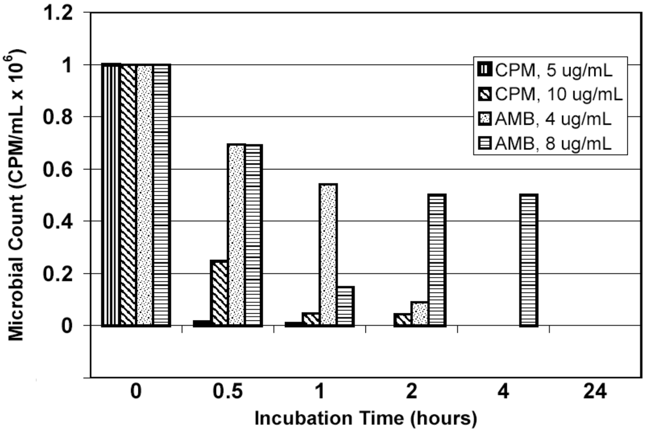

Figure 2. Comparison of fungicidal activity of cationic polysaccharide from Mucor rouxii (CPM) and amphotericin b (AMB) – for C. glabrata

Downloaded by UNIV OF GUELPH LIBRARY on June 14, 2012 | http://pubs.acs.org
Publication Date (Web): June 12, 2012 | doi: 10.1021/bk-2012-1102.ch008

The high-affinity sites for aminoglycoside-membrane interaction were identified as the acidic phospholipids of the membrane (*25*, *26*), and the binding is due to a charge interaction between those polycationic antibiotics and the anionic head of the acidic phospholipids. Divalent cations can interfere with these reactions.

Although the exact mechanism of action of CPM is not fully understood, it seems that a few steps are involved that affect critical functions within the yeast cell. These steps take place concurrently and rapidly.

The first step involves the aggregation of the yeast cells. The aggregate formation reaches a plateau within 60 minutes. This aggregation process can be inhibited with the addition of high concentration of calcium (1-5 g/L). The effect of calcium on CPM is a direct one. Calcium will bind directly to CPM and will inhibit its ability to bind to the yeast cell. However, the binding of calcium to CPM is loose enough and the calcium can be removed by dialysis.

Simultaneously, the second step involves the binding of CPM to the cell wall by means of carbohydrate-recognition domains. CPM is a relatively large size molecule. It is very unlikely that a compound of that size that also holds highly charged residues would be able to penetrate the yeast cell membrane and accumulate inside the cell. However, it may easily penetrate the relatively non-selective fungal cell wall and gain access to the cytoplasmic membrane. This binding of CPM to the cell wall is very tight (Fig. 3), as was shown by the lack of displacement of radioactive labeled CPM when washed with excess of unlabeled CPM (*27*).

The rapid irreversible action of the compound suggests the accessibility of a cellular target(s). The purified membrane fractions from *C. albicans* contain 10-12 membrane proteins. Binding studies reveal that radioactive CPM failed to bind to purified membrane fraction under denaturing conditions. Thus it is likely that the compound may be acting on a non-protein component(s) of the plasma membrane.

Further proof of this theory was demonstrated when *C. albicans* protoplasts were exposed to inhibitory concentrations of CPM. In the absence of CPM, *C. albicans* protoplasts were able to regenerate and produce colony forming units (CFUs). However, exposure of the proto-plasts to CPM in concentration of 10μg/ml resulted in 99% inhibition of the production of CFUs within 30minutes (Fig. 4). These results corresponded well with the percentage of killing observed when whole cells were exposed to CPM at the same concentration. Furthermore, when examining the physical appearance of the exposed protoplasts, complete lysis of the protoplasts was observed within 60 min of exposure, even in the presence of 1 M sorbitol (*28*).

Although it is not clear which component(s) of the plasma membrane interact with CPM, this indirect interaction affects the action of the proton translocating ATPase pump (H^+ -ATPase). The H^+ -ATPase of fungi is a plasma membrane located, ATP-driven proton pump belonging to the p-type ATPase superfamily. To date, 211 members (ranging from 646 to 1956 amino acids in size) of the P-type ATPase have been identified in a wide spectrum of organisms ranging from archeabacteria to man (*29*, *30*).

Downloaded by UNIV OF GUELPH LIBRARY on June 14, 2012 | http://pubs.acs.org
Publication Date (Web): June 12, 2012 | doi: 10.1021/bk-2012-1102.ch008

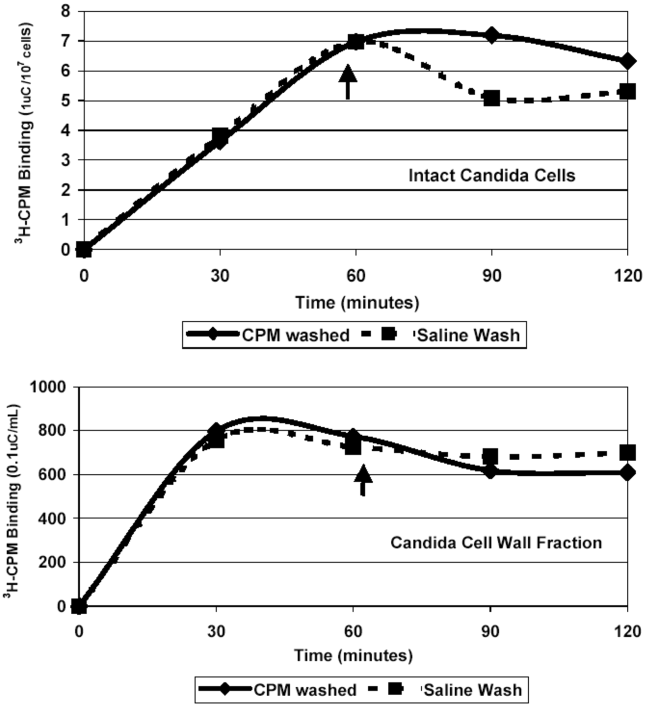

Figure 3. Effect of washing with unlabelled cationic polysaccharide from Mucor rouxii (CPM) on the uptake/binding of [^{3}H]cpm in intact cells (a) and in cell-wall fraction (b). The arrow indicates the time of addition of a 150-fold excess of unlabelled CPM. ♦ Washed with unlabelled CPM; ■ unwashed

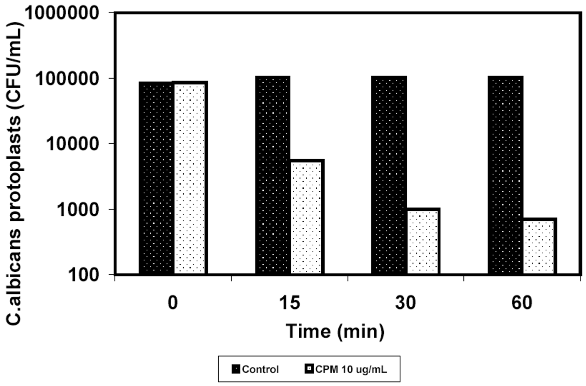

Figure 4. Effect of cationic polysaccharide from Mucor rouxii (CPM) on C. albicans protoplasts.

Downloaded by UNIV OF GUELPH LIBRARY on June 14, 2012 | http://pubs.acs.org
Publication Date (Web): June 12, 2012 | doi: 10.1021/bk-2012-1102.ch008

The charged substrates, the P-type ATPase translocate includes Na^+, K^+, Ca^+, Mg^{2+}, Cd^+, H^+ and phospholipids. Based on their substrate specificity, the ion translocating P-type ATPases are grouped into five (types I - V) families (30). The distinguishing feature of the P-type ATPases is the formation of a phosphorylated enzyme intermediate during the reaction cycle (hence they are called P-type). The phosphorylation of the enzyme invariably involves an aspartic acid residue of a highly conserved motif which consists of DKTGT (*29–31*).

The number of P-type ATPases present in an organism is highly variable, ranging from just a few (pathogenic bacteria), seven to nine (free living bacteria), as many as 16 in *Saccharomyces cerevisiae*, to more than 30 members in plants and animals. Studies with the *S. cerevisiae* H^+ -ATPase revealed that it is an integral protein of which greater than 80% is exposed to the cytoplasmic side of the cell, 15% is estimated to be associated with the lipid bilayer forming 10 membrane spanning helical regions while the remaining 5% of the protein is exposed to the extra cytoplasmic side of the cell (*32*).

The plasma membrane H^+ -ATPase plays an essential role in fungal cell physiology (*31*). This ion translocating enzyme is mainly responsible for maintaining the electrochemical proton gradient necessary for nutrient uptake and the regulation of the intracellular pH of fungal cells (*31*). Interference with its function will lead to cell death.

Glucose-induced acidification of the external medium by carbon-starved yeast cells is a convenient measure of H^+ -ATPase-mediated proton pumping. CPM was found to inhibit the acidification of external medium by *Candida* species in a concentration dependent manner (Fig. 5). It is important to note the inhibition of H^+ -ATPase function was achieved at the MIC concentrations of CPM. AMB, which is known to interact with the sterol component of the membrane, had no significant effect on H^+ -ATPase.

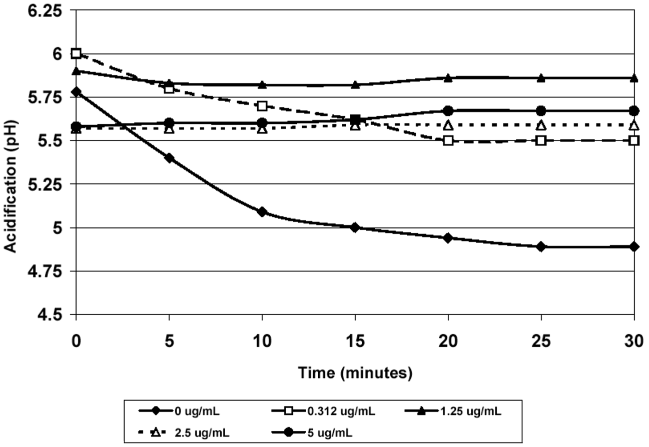

Figure 5. Effect of cationic polysaccharide from Mucor rouxii (CPM) on the proton pumping (as measured by the acidification of external medium) of C. albicans.

However, studies of purified fractions of *C. albicans* plasma membrane, which measured the enzymatic activity specifically, showed that the inhibition of the pump activity by CPM is an indirect one. The enzymatic activity was measured by the liberation of inorganic phosphate via the hydrolysis of ATP. The ATP hydrolysis was not inhibited by CPM (Fig. 6A) (*28*). On the other hand, 5 µg/ml of vanadate, a known inhibitor of H^+ -ATPase, almost completely inhibited the liberation of inorganic phosphate by ATP hydrolysis, suggesting an indirect effect of CPM on H^+ -ATPase (Fig 6B) (*28*).

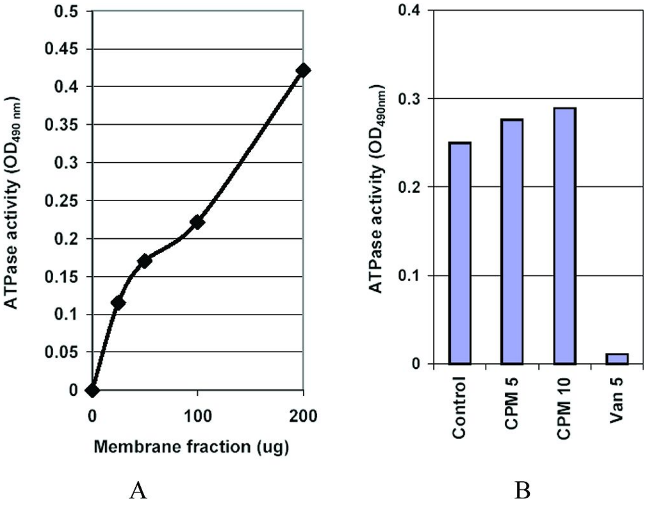

Figure 6. Effect of cationic polysaccharide from Mucor rouxii (CPM) on ATP hydrolysis by purified membrane fraction from C. albicans. (A) Relationship between the amount of membrane fraction and H^+-ATPase activity. (B) Effect of CPM and vanadate on ATP hydrolysis by purified fraction.

In Vivo Activity

The therapeutic effect of the combination of chitosan and pyrithione was tested on cutaneous candidiasis caused by *C.albicans* in guinea pigs.

A total of 175 female Duncan-Hartley guinea pigs were used to study the therapeutic efficacy of CPP. Among laboratory animals, guinea pigs were found to be very susceptible to cutaneous candidiasis. The therapeutic efficacy of CPP, as a 4% aqueous solution, was tested in treating cutaneous infection of *C. albicans*, and was compared to commercially available miconazole 2% (Table 2) (*33*). With short-duration therapy of 1 to 3 days, CPP 4% showed significantly better results than treatment with miconazole 2% (P = 0.0012 and 0.0071, on days 1 and 3 respectively). With long-duration therapy of 5 and 7 days, there were no significant differences between the two drugs.

Downloaded by UNIV OF GUELPH LIBRARY on June 14, 2012 | http://pubs.acs.org
Publication Date (Web): June 12, 2012 | doi: 10.1021/bk-2012-1102.ch008

Downloaded by UNIV OF GUELPH LIBRARY on June 14, 2012 | http://pubs.acs.org
Publication Date (Web): June 12, 2012 | doi: 10.1021/bk-2012-1102.ch008

Table 2. Therapeutic efficiency of topical treatment with sodium pyrithionate (CPP) compared with miconazole 2% in cutaneous candidiasis assessed by the number of culture-positive skin biopsies at completion of therapy.

Number of days treated	***1***	***3***	***5***	***7***
Negative control (not treated)	77/80	73/100	40/60	61/70
Negative control (treated with PBS)	20/20	20/20	20/20	ND
Positive control (miconazole 2%)	6/80[c]	5/90[b]	1/60	0/80[a]
CPP 0.125%	34/40[d]	0/40	ND	ND
CPP 0.25%	1/40	0/40	ND	ND
CPP 0.5%	5/40	0/40	1/40	3/40
CPP 1%	2/40	0/40	0/40	1/40
CPP 4%	0/130[c]	0/120[b]	0/100	0/80

[a] $P = 0.0145$. [b] $P = 0.0071$. [c] $P = 0.0012$. [d] $P = 0.0000$.

The efficacy of CPP was found to be concentration dependent, and application of CPP 0.125% for 1 day proved to be ineffective in clearing the infection. However, when the treatment period was extended to 3 days, even this low concentration of CPP cleared the infection in all tested animals (*33*).

Conclusion

Further studies of the mode of action of cationic polysaccharide from *Mucor rouxii* and the soluble chitosan and combination with pyrithione are essential for the development of this novel complex carbohydrate as an antifungal agent. This compound and its derivative possess several highly desirable characteristics for the next generation of antifungal agents. First, being novel compounds, unrelated to the existing antifungal drugs, there is no cross resistance between the compounds and the currently used antifungal agents. Second is the importance of the rapidity of action, low MIC values and the lethal effect of this compound against a wide spectrum of pathogenic yeasts. This will help reduce treatment duration and the development of untoward effects. Third, these compounds are heat and light-stable, making them ideal to use for topical applications as was proven by the in vivo experiments with CPP. Fourth, being a large molecule with highly charged residues, these compounds are acting on external targets of the cell membrane. Thus, it is unlikely to develop resistance to CPM by the efflux mechanism that is a major cause of drug resistance in microorganisms including fungi.

In summary, CPM and CPP are potent antifungal agents both in vitro and in vivo. These compounds hold great promise to become clinically useful.

Note

This chapter previously appeared in *Carbohydrate Drug Design* (ACS Symposium Series 932), edited by Klyosov et al. and published in 2006.

References

1. Bodey, G. P. The emergence of fungi as major hospital pathogens. *J. Hosp. Infect.* **1988**, *11*, 411–26.
2. Banerjee, S. N.; Enori, T. G.; Culver, D. H. Secular trends in noscomial primary bllodstream infections in the United States, 1980-1989. *Am. J. Med.* **1991**, *91* (Suppl. 3B), 86S–9S.
3. Edwards, J. R. Invasive Candida infections: evolution of a fungal pathogen. *New Engl. J. Med.* **1991**, *324*, 1060–2.
4. Bech-sague, C. M.; Jarvis, W. R. The national Nosocomial Infections Surveillance System. Secular trends in the epidemiology of mosocomial infections in the United States, 1890-1990. *J. Infect. Dis.* **1993**, *267*, 1247–51.
5. Polak, A.; Hartman, P. G. Antifungal chemotherapy are we winning? *Prog. Drug Res.* **1991**, *37*, 31–269.
6. Gallis, H. A.; Drew, H.; Pickard, W. W. Amphotericin B: 30 years of experience. *Rev. Infect. Dis.* **1990**, *12*, 308–329.
7. Baily, G. G.; Perry, F. M.; Denning, D. W.; Mandel, B. K. Fluconazole resistance candidosis in an HIV cohort. *AIDS* **1994**, *8*, 787–92.
8. Komshian, S. V.; Uwaydah, A.; Sobel, J. D.; Crane, L. R. Fungemia caused by Candida species and Torulopsis glabrata in hospitalized patients. Frequent charchcteristic, and evaluation of factors influencing outome. *Rev. Infect. Dis.* **1989**, *11*, 379–90.
9. Nobre, G.; Mences, E.; Charrua, M.; Cruz, O. Ketoconazole resistance in Torulopsis glabrata. *Mycopathologia* **1989**, *107*, 51–5.
10. Vazquez, J. A.; Lynch, M.; Sobel, J. D. In vitro activity of a new pneumocandin antifungal agent, L-733,560 against azole-susceptible and resistant Candida and Torulopsis species. *Antimicrob. Agents Chemother.* **1995**, *39*, 2689–91.
11. Warnock, D.; et al. Fluconazole resistance in Candida glabrata. *Lancet* **1988**, *I*, 1310.
12. Wingard, J. R.; et al. Increase in Candida krusi infection among patient with bone marrow transplantation and neutropenia treared prophylactically with fluconazole. *New Engl. J. Med.* **1991**, *18*, 1274–77.
13. Mazar Ben-Josef, A.; Manavnthu, E. K.; Platt, D.; Sobel, J. D. In vitro activity of CAN-296: a naturally occurring complex carbohydrate. *J. Antibiot.* **1997**, *50*, 71–7.
14. Drickamer, K.; Taylor, M. E. Biology of animal lectins. *Annu. Rev. Cell Biol.* **1993**, *9*, 237–64.
15. Morell, A. G.; et al. Physical and chemical studies on ceruloplasmin: V. metabolic studies on sialic acid-free ceruloplasmin in vivo. *J. Biol. Chem.* **1968**, *243*, 155–9.

Downloaded by UNIV OF GUELPH LIBRARY on June 14, 2012 | http://pubs.acs.org
Publication Date (Web): June 12, 2012 | doi: 10.1021/bk-2012-1102.ch008

16. Stahl, P.; et al. Receptor-mediated pinocytosis of mannose glyconjugates by macrophages: charhcterization and evidence for receptor recycling. *Cell* **1980**, *19*, 207–15.
17. Fischer, H. D.; Gonzales-Noriega, A.; Sly, W. S.; Morre, D. J. Phosphomannosyl-enzyme receptors in rat liver. Subcellular distribution and role in intracellular transport of lysosymal enzymes. *J. Biol. Chem.* **1980**, *255*, 9608–15.
18. Lee, Y. C. Biochemistry of carbohydrate-protein interaction. *FASEB J.* **1992**, *6*, 3193–200.
19. Drickamer, K. Ca++ - dependent sugar recognition by animal lectins. *Biochem. Soc. Trans.* **1996**, *24*, 146–50.
20. Lee, R. T.; et al. Ligand-binding characteristic of rat serum-type mannose-binding protein (MBP-A). Homology of binding site architecture with mammalian and chicken hepatic lectins. *J. Biol. Chem.* **1991**, *266*, 4810–15.
21. Drikamer, K. Recognition of complex carbohydrate by Ca^{2+} -dependent animal lectins. *Biochem. Soc. Trans.* **1993**, *21*, 456–9.
22. Sawada, Y.; et al. Calcium-dependent anticandidal action of pradimicin A. *J. Antibiot.* **1990**, *43*, 715–21.
23. Humes, H. D.; Sastrasinh, M.; Weinberg, J. M. Calcium is a competitive inhibitor of gentamicin-renal membranebinding interactions and dietary calcium supplementation protects against gentamicin nephrotoxicity. *J. Clin. Invest.* **1984**, *73*, 134–47.
24. Weinberg, J. M.; Humes, H. D. Mechanisms of Gentamicin-induced dysfunction of renal mitochondria. 1. Effects on mitochondrial respiration. *Arch. Biochem. Biophys.* **1980**, *205*, 222–31.
25. Sastrasinh, M.; Knauss, T. C.; Weinberg, J. M.; Humes, H. D. Identification of the aminoglycoside binding site in rat renal brush border membrane. *J. Pharmacol. Exp. Ther.* **1982**, *222*, 350–8.
26. Schacht, J. Isolation of an aminoglycoside receptor from guinea pig inner ear tissues and kidney. *Arch. Oto-Rhino-Laryngol.* **1979**, *224*, 129–34.
27. Mazar Ben-Josef, A.; Manavnthu, E. K.; Platt, D.; Sobel, J. D. Involvement of calcium inhibitable binding to the cell wall in the fungicidal activity of CPM. *J. Antimicrob. Chemother.* **1999**, *44*, 217–222.
28. Mazar Ben-Josef, A.; Manavnthu, E. K.; Platt, D.; Sobel, J. D. Proton translocating ATPase mediated fungicidal activity of a novel complex carbohydrate: CAN-296. *Int. J. Antimicrob. Agents* **2000**, *13*, 287–95.
29. Moller, J. V.; Juul, B.; Le Maire, M. Structural organization, ion transport, and energy transduction of P-type ATPase. *Biochem. Biophys. Acta* **1996**, *1286*, 1–51.
30. Axelsen, K. B.; Palmgren, M. G. Evolution of substrate specificities in the p-type ATPase superfamily. *J. Mol. Evol.* **1998**, *46*, 84–101.
31. Serrano, R. M. Structure and function of proton translocating ATPase in plasma membranes of plantes and fungi. *Biochem. Biophys. Acta.* **1988**, *947*, 1–28.

Downloaded by UNIV OF GUELPH LIBRARY on June 14, 2012 | http://pubs.acs.org
Publication Date (Web): June 12, 2012 | doi: 10.1021/bk-2012-1102.ch008

32. Perlin, D. S.; Harber, J. E. Genetic approaches to structure-function analysis in the yeast plasma membrane H^+ -ATPase. *Adv. Mol. Cell Biol.* **1998**, *23A*, 143–66.
33. Mazar Ben-Josef, A.; Cutright, J. L.; Manavnthu, E. K.; Sobel, J. D. CAN-296P is effective against cutaneous candidiasis in guinea pigs. *Int. J. Antimicrob. Agents* **2003**, *22*, 168–171.

Downloaded by UNIV OF GUELPH LIBRARY on June 14, 2012 | http://pubs.acs.org
Publication Date (Web): June 12, 2012 | doi: 10.1021/bk-2012-1102.ch008

Downloaded by UNIV OF GUELPH LIBRARY on June 13, 2012 | http://pubs.acs.org
Publication Date (Web): June 12, 2012 | doi: 10.1021/bk-2012-1102.ch009

Chapter 9

Synthetic Methods To Incorporate α-Linked 2-Amino-2-Deoxy-D-Glucopyranoside and 2-Amino-2-Deoxy-D-Galactopyranoside Residues into Glycoconjugate Structures

Robert J. Kerns* and Peng Wei

Division of Medicinal and Natural Products Chemistry, University of Iowa, Iowa City, Iowa 52242
***robert-kerns@uiowa.edu**

Numerous bioactive glycoconjugates contain D-glucosamine and D-galactosamine residues within their core structures. Diverse protecting group strategies for the 2-amino group of these sugars that impart neighboring group participation in the glycosylation process afford many strategies for the stereoselective synthesis of beta-linked (1,2-*trans*) glycosides. In contrast, stereoselective synthesis of alpha-linked (1,2-*cis*) glycosides of D-glucosamine and D-galactosamine has historically been more challenging because of a more limited repertoire of effective glycosylation methodologies, including a limited number of protecting group or latentiation strategies for the 2-amine group and poor consistency of stereocontrol and yield during glycosylation reactions. Synthetic methods to form alpha-linked glycosides of D-glucosamine and D-galactosamine are presented here, with a focus on the application and utility of both new methods and old strategies toward the synthesis of bioactive natural glycoconjugates and their analogs.

Overview of the 2-Amino-2-deoxy-D-hexopyranosides D-Glucosamine and D-Galactosamine

Numerous bioactive saccharides and glycoconjugates contain 2-amino-2-deoxy-D-hexopyranoside residues as an integral component of their molecular

In Glycobiology and Drug Design; Klyosov, A.;
ACS Symposium Series; American Chemical Society: Washington, DC, 2012.

structure (*1–3*). Many of these glycoconjugates contain the beta-linked isomer of the 2-amino-2-deoxy-D-hexopyranoside sugar residue. In particular, *O*-substituted derivatives of the 2-acetamido-2-deoxy-ß-D-glucopyranoside (*N*-acetyl-ß-D-glucosamine) and 2-acetamido-2-deoxy-ß-D-galactopyranoside (*N*-acetyl-ß-D-galactosamine) core residues are found as constituents in a diverse array of prokaryotic and eukaryotic glycoconjugate structures (Figure 1). In contrast to the diverse types of glycoconjugates that contain variably substituted beta-linked D-glucosamine and D-galactosamine residues, alpha-linked D-glucosamine and D-galactosamine residues are found in a more limited number of structural classes, or structural types, of bioactive glycoconjugates (Figure 1).

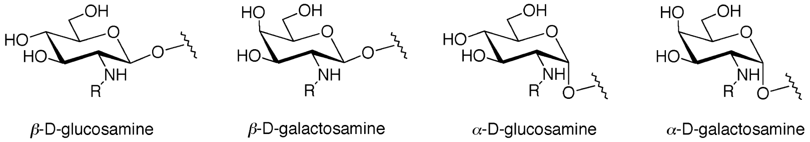

Figure 1. Structures of α- and β-glycosides of D-glucosamine and D-galactosamine. These 2-amino sugars are present in many bioactive natural products glycosidically linked to glycan or aglycone structures. The 2-amino groups are typically R = Ac, H, or SO_3^-, although other N-substituted derivatives are known. The 3, 4, and 6 hydroxyls can be substituted with saccharide residues or other functional groups such as OSO_3^-, NH_2, etc.

The more limited distribution in the number of unique structures containing alpha-linked D-glucosamine and D-galactosamine residues is offset, however, by the high level of molecular diversity found within many of the classes of bioactive structures containing these alpha-linked 2-amino sugars. For example, *N*-acetyl and *N*-sulfo substituted α-D-glucosamine residues are a core component of heparin and heparan sulfate, while *N*-acetyl-α-D-galactosamine is an important constituent of *O*-linked glycopeptide and glycoprotein structures. Within each of these types or classes of bioactive glycoconjugates, there are many structural variations through either the substituents on the 2-amino sugar or in the structure, sequence, substitution pattern, and/or linking position of additional sugar residues attached to the amino sugar. Thus, efficient and versatile methods to introduce variably substituted and differentially modified α-D-glucosamine and α-D-galactosamine residues into glycoconjugate structures are vital to the synthesis of many important bioactive glycoconjugates and their structural analogs.

Bioactive Glycoconjugates That Contain Alpha-Linked D-Glucosamine or Alpha-Linked D-Galactosamine Residues within Their Core Structure

Alpha-linked glycosides of D-glucosamine and D-galactosamine and their diversely substituted derivatives are important structural constituents in a significant number of bioactive natural products. Examples representative of

Downloaded by UNIV OF GUELPH LIBRARY on June 13, 2012 | http://pubs.acs.org
Publication Date (Web): June 12, 2012 | doi: 10.1021/bk-2012-1102.ch009

the different classes of bioactive glycoconjugates containing these alpha-linked 2-amino sugars are shown (Figure 2).

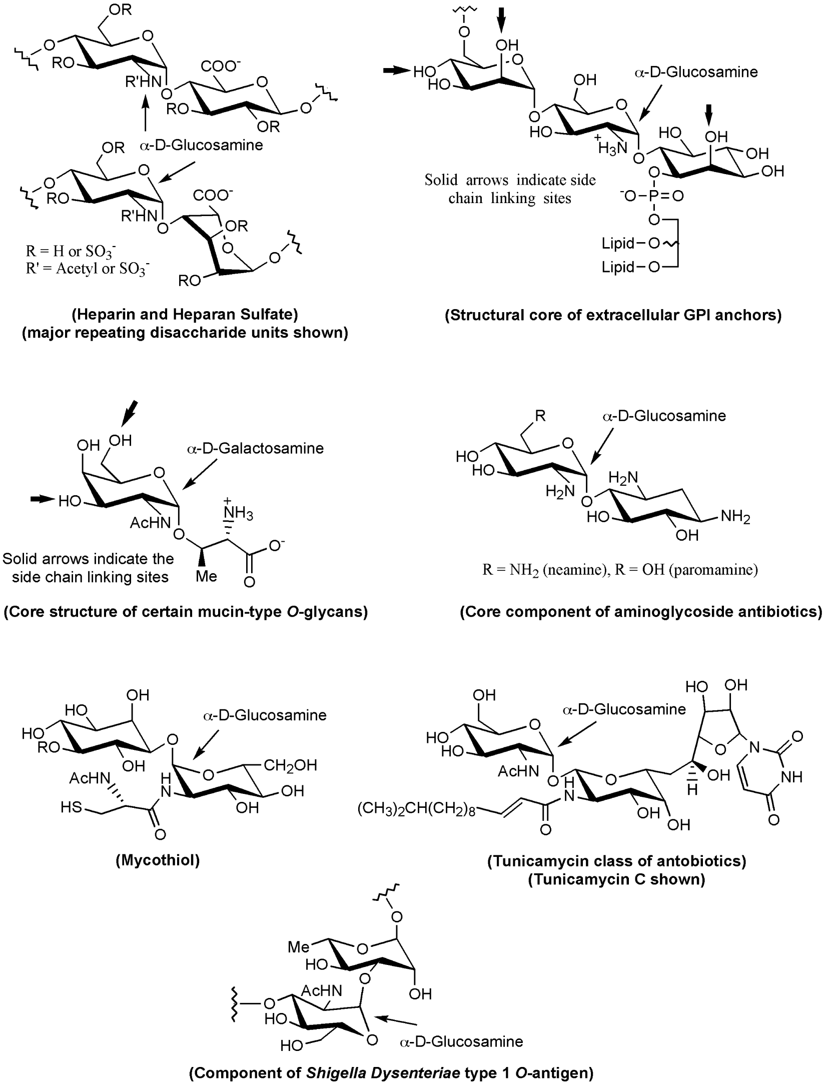
α-D-Glucosamine
COO⁻
OR
RO
R'HN
α-D-Glucosamine
α-D-Galactosamine
α-D-Glucosamine
α-D-Glucosamine
α-D-Glucosamine
α-D-Glucosamine
Lipid–O
Lipid–O
AcHN
HS
(CH3)2CH(CH2)8
Me

R = H or SO_3^-
R' = Acetyl or SO_3^-

(Heparin and Heparan Sulfate)
(major repeating disaccharide units shown)

Solid arrows indicate side chain linking sites

(Structural core of extracellular GPI anchors)

Solid arrows indicate the side chain linking sites

(Core structure of certain mucin-type *O*-glycans)

R = NH_2 (neamine), R = OH (paromamine)

(Core component of aminoglycoside antibiotics)

(Mycothiol)

(Tunicamycin class of antobiotics)
(Tunicamycin C shown)

(Component of *Shigella Dysenteriae* type 1 *O*-antigen)

Figure 2. Representative bioactive natural glycoconjugates that contain alpha-linked D-glucosamine or alpha-linked D-galactosamine residues as a core component of their structure.

Heparin and heparan sulfate are structurally similar members of the glycosaminoglycan class of acidic polysaccharides (*4*). Heparin is primarily found in the granules of mast cells and has been employed therapeutically for decades as an anticoagulant agent. Heparan sulfate is found on the surface of nearly all mammalian cell types where it plays a profound role in numerous

Downloaded by UNIV OF GUELPH LIBRARY on June 13, 2012 | http://pubs.acs.org
Publication Date (Web): June 12, 2012 | doi: 10.1021/bk-2012-1102.ch009

Downloaded by UNIV OF GUELPH LIBRARY on June 13, 2012 | http://pubs.acs.org
Publication Date (Web): June 12, 2012 | doi: 10.1021/bk-2012-1102.ch009

physiological processes (*4*). Natural heparin and heparan sulfate sequences as well as analogs and mimics of these structures have been the focus of many syntheses with the goal of developing therapeutic agents that selectively bind heparin/heparan-sulfate-binding proteins.

The tunicamycins (*5*) and aminoglycosides (*6*) are structural classes of natural antibiotics that are bacterial in origin (Figure 2). Certain aminoglycosides have found clinical utility. The continued development of efficient synthesis of these antibiotics and their analogs holds promise for the development of new antibiotics.

Mucin-type *O*-glycans are representative of a major class of *O*-linked glycopeptide/glycoprotein structures, where alpha-linked D-galactosamine affords a key linkage to serine or threonine amino acid residues (Figure 2) (*7*, *8*). Certain core structures of the mucin-type *O*-glycans also contain alpha-linked D-galactosamine residues attached to the 3-position or the 6-position of the amino acid-linked D-galactosamine residue. Efficient formation of these alpha-linked D-galactosamine conjugates has been extensively studied in efforts to synthesize and evaluate the biological function of numerous cell-surface glycopeptide structures and as vaccine candidates (*9*).

A wide variety of different oligosaccharide structures are found on the surface of bacteria in the form of capsular polysaccharides, lipooligosaccharides and lipopolysaccharides, of which the alpha-linked D-glucosamine containing *O*-antigen structure found on the surface of *Shigella dysenteriae* is shown (Figure 2) (*10*). Mycothiol is a low molecular weight thiol found intracellularly in most actinomycetes including mycobacteria, where it serves as an antioxidant by maintaining a reducing environment (Figure 2) (*11*). The biosynthesis and metabolism of mycothiol is a putative new target for antituberculosis drug development. The glycosylphosphatidylinositols (GPIs) are a diverse family of glycolipids expressed by eukaryotic cell types, where they serve to anchor extracellular protein and other glycoconjugate structures to the cell membrane (*12*). The core structure of a representative membrane protein GPIs anchor is shown (Figure 2).

General Considerations for Stereochemical Control in the Glycosidation of D-Glucosamine and D-Galactosamine Using Traditional Glycosyl Donor Approaches

Formation of the beta glycosidic linkage of various D-glucosamine and D-galactosamine glycosyl donors during the introduction of these residues into glycoconjugate structures typically relies on the use of protecting groups for the 2-amino group that afford neighboring group participation in the glycosylation reaction (Figure 3) (*13*). A C-2 participating group provides anchimeric assistance and thus stereochemical control to afford 1,2-trans glycoside products. Many amine protecting groups that participate in glycosylation of 2-amino-2-deoxy-D-hexopyranoside derivatives to afford the 1,2-trans product are known, which affords numerous orthogonal protection/deprotection strategies. An occasional exception to the above-described role of C-2 participating groups arises with select donor activation systems employed during glycosylation of

Downloaded by UNIV OF GUELPH LIBRARY on June 13, 2012 | http://pubs.acs.org
Publication Date (Web): June 12, 2012 | doi: 10.1021/bk-2012-1102.ch009

certain D-galactosamine derivatives. These derivatives have large or bulky protecting groups on the C-4 hydroxyl moiety that may impede formation of the beta glycoside by sterically hindering attack of the acceptor molecule from the same face of the amino sugar. In these unique cases the steric effect of the C-4 substituent appears to override the C-2 participating effect to afford high yields of the alpha-linked (1,2-*cis*) glycoside.

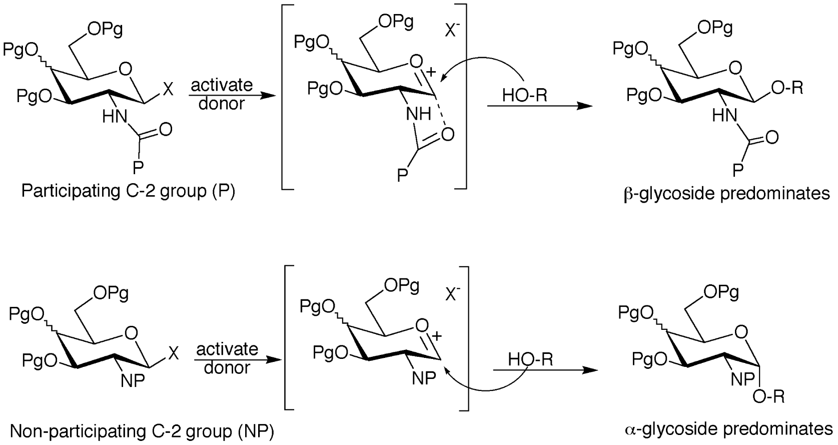

Figure 3. The effect of C-2 participating groups and non-participating groups typically observed in glycosidic bond forming reactions of D-glucosamine and D-galactosamine derivatives using traditional glycosyl donor activation strategies.

In contrast to the stereochemical control typically afforded by a neighboring group during the formation of 1,2-*trans* glycosides, introduction of D-glucosamine and D-galactosamine residues as their 1,2-cis (alpha-linked) glycosides into glycoconjugate structures using tradition glycosylation strategies cannot, in principal, possess a participating substituent at the C-2 position. Therefore, in order to preferentially obtain the 1,2-*cis* glycoside product an amine protecting group or a latent form of amine that will not participate in the glycosylation reaction is requisite at the C-2 position of the glycosyl donor (Figure 3). The fundamental principles of stereocontrol during the synthesis of 1,2-*cis* glycosides, with a focus on 2-*O*-sugars, have been recently reviewed (*14*).

Discussed throughout the various sections below are a number of putative non-participating C-2 groups that have been employed over the years with varied success in the synthesis of the alpha-linked (1,2-*cis*) glycosides of D-glucosamine and D-galactosamine. Furthermore, a variety of unique glycosyl donor strategies and novel glycoside bond forming methodologies that do not fit the tradition donor activation approaches shown in Figure 3 have also been developed and exploited toward the synthesis glycoconjugates containing α-D-glucosamine and/or α-D-galactosamine residues.

Downloaded by UNIV OF GUELPH LIBRARY on June 13, 2012 | http://pubs.acs.org
Publication Date (Web): June 12, 2012 | doi: 10.1021/bk-2012-1102.ch009

Overview of 2-Azido Sugars in the Synthesis of α-Linked Glycosides of D-Glucosamine and D-Galactosamine

The most common strategies employed over the years for incorporating α-D-glucosamine and α-D-galactosamine residues into glycoconjugate structures utilize an appropriate glycosyl donor or other functionalized saccharide having a protected or latent amine-precursor at the C-2 position, where formation of the glycosidic bond affords the desired alpha-linked glycoside. Subsequent chemical transformation of the C-2 substituent affords the desired 2-amino substituent. For roughly 30 years the azide group has served as a non-participating C-2 substituent and has provided the most versatile method in the synthesis of alpha-linked glycosides of D-glucosamine and D-galactosamine (Figure 3, NP = N_3). Indeed, appropriately substituted 2-azido sugars have been employed in at least one, and in many cases all reports describing total synthesis of individual glycoconjugates containing α-D-glucosamine or α-D-galactosamine residues (see Figures 2 and 4).

The chemical compatibility of a wide range of glycosyl donors and anomeric activation chemistries employed for glycosylation reactions using 2-azido-2-deoxy-D-hexopyranoside donors affords broad applicability of the 2-azido group. Furthermore, the azido group can be efficiently and selectively converted to amine using a variety of chemical methods, affording a range of orthogonal protecting group strategies with numerous other protecting groups employed in glycoconjugate synthesis.

While 2-azido derivatives of D-glucosamine and D-galactosamine glycosyl donors have served well for many years, synthesis of variably *O*-protected 2-azido glycosyl donors can be lengthy, and costly. Furthermore, careful control of solvent and temperature while comparing varied anomeric leaving groups will often yield a final synthesis of the alpha-linked conjugate with good to high stereoselectivity but rarely stereospecificity. Indeed, as shown in Figures 4-10, the 2-azido sugars are versatile and consistent in affording desired alpha-linked glycoside, but overall stereoselectivity and yield are often limited.

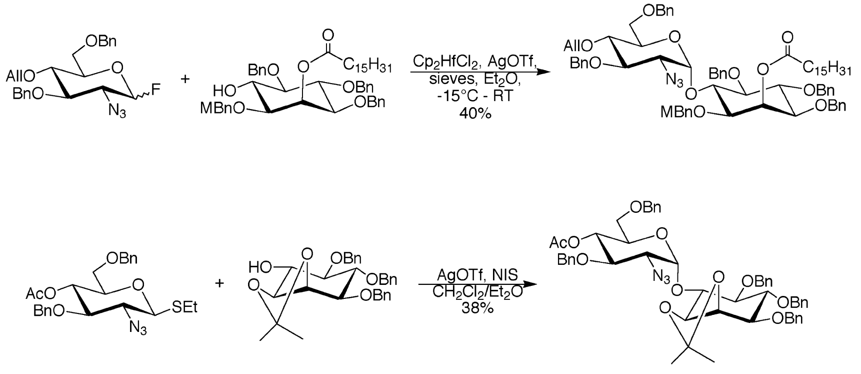

Figure 4. Glycosylation reactions published during 2002 that demonstrate the coupling of 2-azido-2-deoxy-D-glucopyranose donors to inositol structures toward the synthesis of GPI core structures (15, 16).

Downloaded by UNIV OF GUELPH LIBRARY on June 13, 2012 | http://pubs.acs.org
Publication Date (Web): June 12, 2012 | doi: 10.1021/bk-2012-1102.ch009

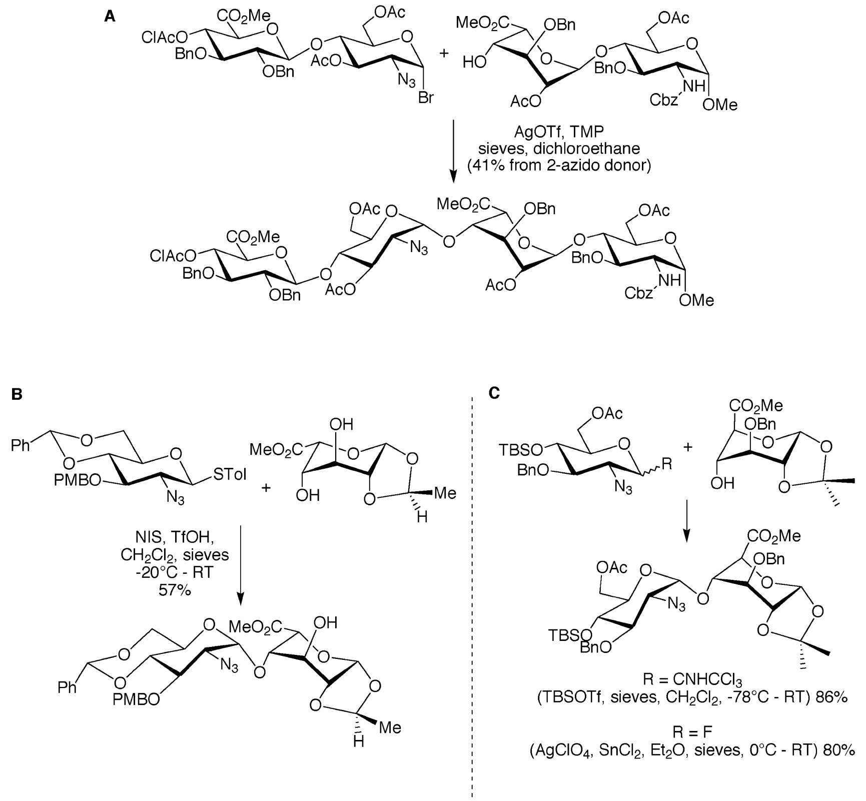
A
ClAcO
CO_2Me
BnO
OBn
OAc
AcO
N_3
Br
+
MeO_2C
OBn
HO
AcO
BnO
OAc
NH
Cbz
OMe
AgOTf, TMP
sieves, dichloroethane
(41% from 2-azido donor)
B
Ph
PMBO
N_3
STol
+
MeO_2C
OH
OH
Me
H
NIS, TfOH,
CH_2Cl_2, sieves
-20°C - RT
57%
C
TBSO
BnO
OAc
N_3
R
+
CO_2Me
OBn
OH
R = $CNHCCl_3$
(TBSOTf, sieves, CH_2Cl_2, -78°C - RT) 86%
R = F
($AgClO_4$, $SnCl_2$, Et_2O, sieves, 0°C - RT) 80%

Figure 5. Select examples showing the application of 2-azido-2-deoxy-D-glucopyranosyl donors toward the synthesis of heparin and heparan sulfate oligosaccharide sequences. Panel A) Original coupling methodology reported by Petitou et al toward the synthesis of the first synthetic heparin-based anticoagulant (Fondaparinux) to be approved for clinical use (17). Panel B) The regioselective and stereoselective glycosylation of a conformationally locked iduronic acid diol reported in 2004 (18). Panel C) Comparison of two anomeric activation strategies employed in the glycosylation of a conformationally locked glucuronic acid residue reported in 2002 (19).

Because of the wide application of 2-azido sugars in the synthesis of bioactive glycoconjugates containing alpha-linked D-glucosamine and D-galactosamine residues, these donors and various donor strategies have been covered in many glycosylation reviews. Outlined below in Figures 4-10 are representative examples showing application of the 2-azide substituted D-glucosamine and D-galactosamine glycosyl donors in the formation of alpha-linked glycosides in the synthesis of the bioactive glycoconjugates presented in Figure 2. Examples shown in Figures 4-10 were chosen from literally thousands of examples to display a sample of various anomeric groups and activation strategies employed with 2-azido sugars to form alpha-linked glycosides. These examples also exemplify the need for new synthetic methods that afford more consistent stereochemical control for the introduction of alpha-linked D-glucosamine and D-galactosamine into the structure of bioactive glycoconjugates and their analogs.

Downloaded by UNIV OF GUELPH LIBRARY on June 13, 2012 | http://pubs.acs.org
Publication Date (Web): June 12, 2012 | doi: 10.1021/bk-2012-1102.ch009

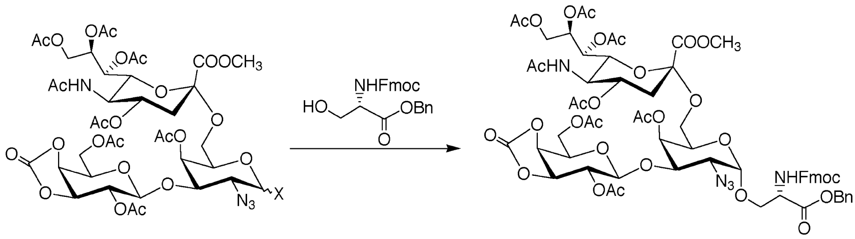

X = α-Br; activation = $AgClO_4$, CH_2Cl_2, RT; yield = 70% (2.6/1: α/β)
X = β-O(CNH)CCl_3; activation = BF_3OEt_2, THF, -30°C; yield = 65% (12/1: α/β)
X = 1/1-α/β -O(CNH)CCl_3; activation = BF_3OEt_2, THF, -30°C; yield = 66% (4/1: α/β)
X = 1/1-α/β -OP(OEt)$_2$; activation = BF_3OEt_2, THF, -30°C; yield = 30% (30/1: α/β)

Figure 6. Example from a 1997 report showing different donor strategies compared during the synthesis of a tumor-associated mucin motif (20). In this example a fully elaborated 2-azido-2-deoxy-D-galactose glycan was employed to form the alpha-linkage to serine. There are hundreds of reports for the coupling of variably protected monosaccharides of 2-azido-2-deoxy-D-glactopyranosyl donors to serine and/or threonine followed by subsequent elaboration of the glycan on the core glycopeptide structure.

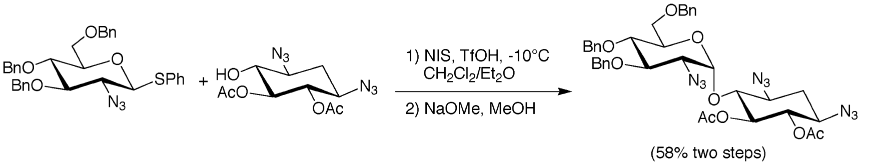

Figure 7. Glycosylation reaction reported in 1999 demonstrating the use of a non-participating 2-azide group in forming the alpha-linked glucosamine pseudodisaccharide core of aminoglycoside antibiotics, neamine (21)

Downloaded by UNIV OF GUELPH LIBRARY on June 13, 2012 | http://pubs.acs.org
Publication Date (Web): June 12, 2012 | doi: 10.1021/bk-2012-1102.ch009

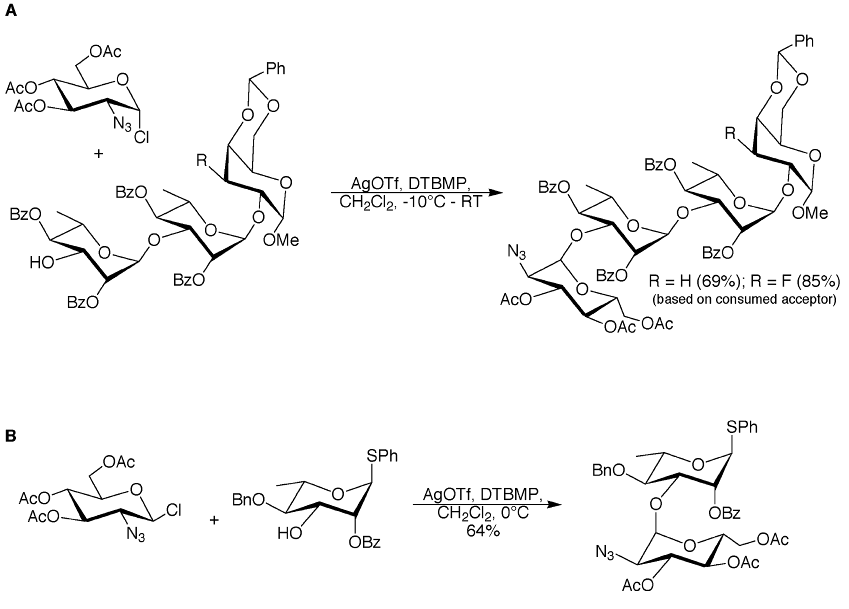
A
OAc
AcO
AcO
O
N3
Cl
+
Ph
O
O
R
BzO
BzO
O
O
HO
O
O
BzO
BzO
OMe
AgOTf, DTBMP,
CH2Cl2, -10°C - RT
R = H (69%); R = F (85%)
(based on consumed acceptor)
B
Cl
SPh
BnO
HO
OBz
AgOTf, DTBMP,
CH2Cl2, 0°C
64%
N3
OAc

Figure 8. Two coupling reactions reported in 1998 that utilize the non-participating 2-azide group to obtain the alpha-linkage of D-glucosamine in the synthesis of Shigella dysenteriae type 1 O-specific polysaccharide structures toward the potential development of vaccines against Shigella dysenteriae type 1. Panel A) Penultimate glycosidic coupling toward tetrasaccharide fragments, deoxygenated and fluorinated at a terminal galactose residue (22) Panel B) Initial coupling to afford a core disaccharide intermediate for further chain elongation (23).

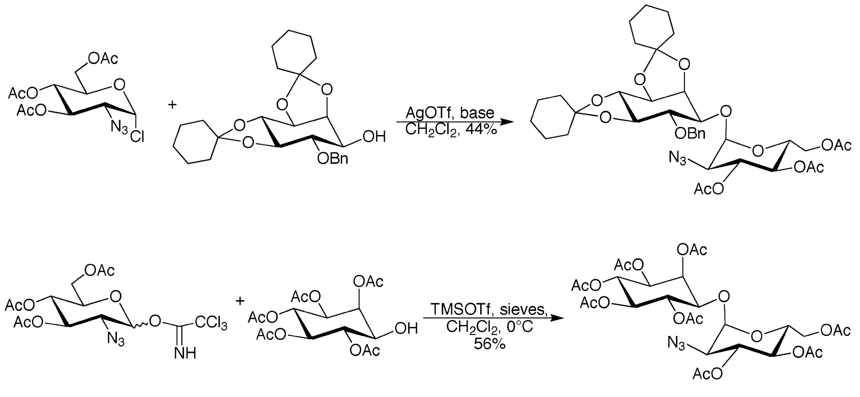
OAc
AcO
AcO
O
N3
Cl
+
O
O
OH
OBn
AgOTf, base
CH2Cl2, 44%
OBn
N3
AcO
OAc
O
CCl3
NH
OH
TMSOTf, sieves,
CH2Cl2, 0°C
56%

Figure 9. Synthesis of key intermediates in the synthesis of mycothiol employing 2-azido-2-deoxy-D-glucopyranosyl donors. Top) From a 2003 report describing the synthesis of structures used to evaluate the substrate specificity of AcGI deacetylase found in M. tuberculosis (24). Bottom) Key synthetic step in the first total synthesis of mycothiol and mycothiol disulfide reported in 2002 (25).

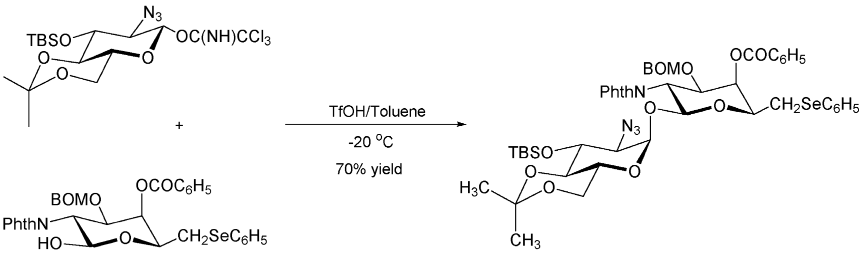

Figure 10. Example from a 1993 report showing synthesis of the 1,1-linked core disaccharide of tunicamycin employing a 2-azido donor to afford the alpha-linked D-glucosamine residue (26).

Downloaded by UNIV OF GUELPH LIBRARY on June 13, 2012 | http://pubs.acs.org
Publication Date (Web): June 12, 2012 | doi: 10.1021/bk-2012-1102.ch009

Why Are Old and New Alternatives to the 2-Azido Strategy for Forming Alpha-Linked Glycosides of D-Glucosamine and D-Galactosamine Important?

The use of 2-azido-2-deoxy glycosyl donors of D-glucose and D-galactose in the formation of 1,2-*cis* glycosides revolutionized the synthesis of glycoconjugates containing α-D-glucosamine and α-D-galactosamine residues. The versatility of the 2-azido group as a non-participating C-2 substituent has dramatically facilitated laboratory-scale synthesis of bioactive glycoconjugates and their analogs toward understanding biological function and exploring structure-activity-relationships. However, the cost, number of synthetic steps, and often low efficiency in preparing various 2-azido glycosyl donors is considered a major drawback to application of this methodology to the large scale synthesis of single target structures. In addition, while extremely versatile and reliable, alpha/beta ratios of the resulting glycosides generated using 2-azido glycosyl donors can range from exceptional to modest depending on the donor activation system and the acceptor alcohol. Because of these limitations, efforts continue toward the development of new methods for the efficient and stereoselective introduction of alpha-linked glycosides of D-glucosamine and D-galactosamine into glycoconjugate structures.

Over the past 40-plus years a fairly large number of methods have been intentionally developed or peripherally observed to afford alpha-linked glycosides of D-glucosamine and D-galactosamine, albeit often with mixed results from a versatility and consistency standpoint. As the pharmaceutical potential and therapeutic reality of synthetic glycoconjugates continues to grow, the cost and efficiency of synthesizing specific clinical candidates on large scale will necessitate evaluation of the most appropriate approach to prepare specific glycoconjugates on an industrial scale. Here, versatility of a method becomes secondary to cost and industrial scale efficiently in preparing the target structure. In this context, it is expected that old, new and even aberrant strategies that have been shown to afford alpha-linked glycosides of D-glucosamine and D-galactosamine derivatives may ultimately yield the most direct and cost effective syntheses of specific target structures.

In the sections below we discuss our work as well as the work of many other groups over many years that have yielded a somewhat under appreciated number and diverse strategies to introduce alpha-linked glycosides of D-glucosamine and D-galactosamine into glycoconjugate structures. It is possible that no current or future method will achieve the versatility of 2-azido sugars in the synthetic formation of alpha-linked glycosides of D-glucosamine and D-galactosamine derivatives. However, each of the unique methods presented below has its own advantages and disadvantages; and may ultimately afford the simplicity, cost effectiveness and chemical compatibility required for the large-scale synthesis of individual pharmaceutical glycoconjugates.

Downloaded by UNIV OF GUELPH LIBRARY on June 13, 2012 | http://pubs.acs.org
Publication Date (Web): June 12, 2012 | doi: 10.1021/bk-2012-1102.ch009

Alternatives to 2-Azido Sugars: Methods for Forming Alpha-Linked Glycosides of D-Glucosamine and D-Galactosamine and Application of These Methods in the Synthesis of Bioactive Glycoconjugates

Fused-Ring 2,3-Oxazolidinone Protection of Phenyl 2-Amino-2-deoxy-1-thio-glucopyrano-sides: A C-2 Non-Participating Group Strategy

In 2001 we reported the utility of ring-fused 2,3-oxazolidinone derivatives of phenyl 2-amino-2-deoxy-1-thio-glucopyranosides in the synthesis of alpha-linked glucosamine derivatives (Figure 11) (*27*). A notable feature of this class of alpha-selective D-glucosaminyl donors is a high yield and versatile synthesis; where the oxazolidinone group affords simultaneous protection of the 2-*N* and 3-*O* positions (Figure 11).

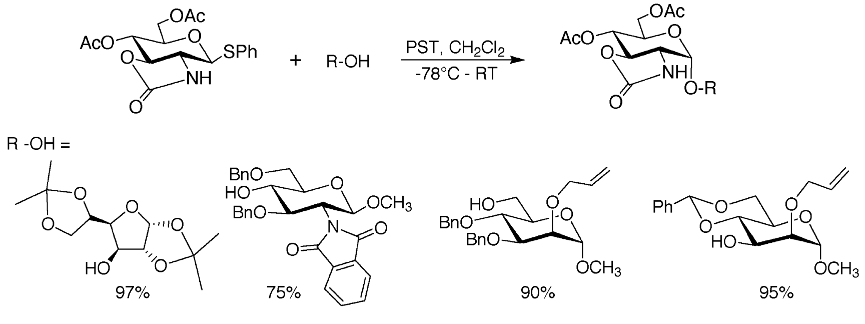

Figure 11. Ring-fused 2,3-oxazolidinone derivatives of phenyl 2-amino-2-deoxy-1-thio-glucopyranosides afford alpha-linked glycosides of D-glucosamine.

The ring-fused 2,3-oxazolidinones have also been shown to serve as versatile intermediates for more complex protecting group manipulations. Selective opening of the oxazolidinone ring with alcohols affords selective deprotection of the 3-hydroxyl group with concomitant protection of the 2-amine group as the carbamate, affording entry into thioglycoside donors bearing *N*-protection capable of neighboring group participation in the formation of beta-linked glycosides.

In addition, entry into the D-galactosamine series of thioglycoside donors from 2,3-oxazolidinone protected glucosamine derivatives is readily achieved through inversion of stereochemistry at the C-4 position (Figure 12) (*27*).

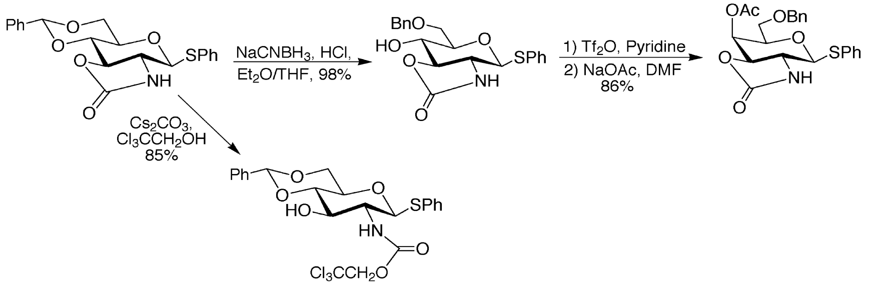
NaCNBH$_3$, HCl,
Et$_2$O/THF, 98%
1) Tf$_2$O, Pyridine
2) NaOAc, DMF
86%
Cs$_2$CO$_3$,
Cl$_3$CCH$_2$OH
85%
SPh
NH
BnO
HO
OAc
OBn
Ph
HN
Cl$_3$CCH$_2$O

Figure 12. Ring fused 2,3-oxazolidinone derivatives of D-glucosamine are readily converted into D-galactosamine derivatives and C-2-carbamate derivatives, the later of which are putative participating groups for the formation of beta-glycosides.

Glycosylation of a variety of sugar acceptors using a ring-fused 2,3-oxazolidinone protected thioglycoside donor of glucosamine upon activation with phenylsulfenyl triflate was shown to afford high yield, stereoselective, formation of the alpha-linked glycosides (Figure 11). This methodology has been applied to the formation of the repeating disaccharide unit of heparan sulfate and synthesis of alpha-linked serine and threonine derivatives (Figure 13) (*27*, *28*).

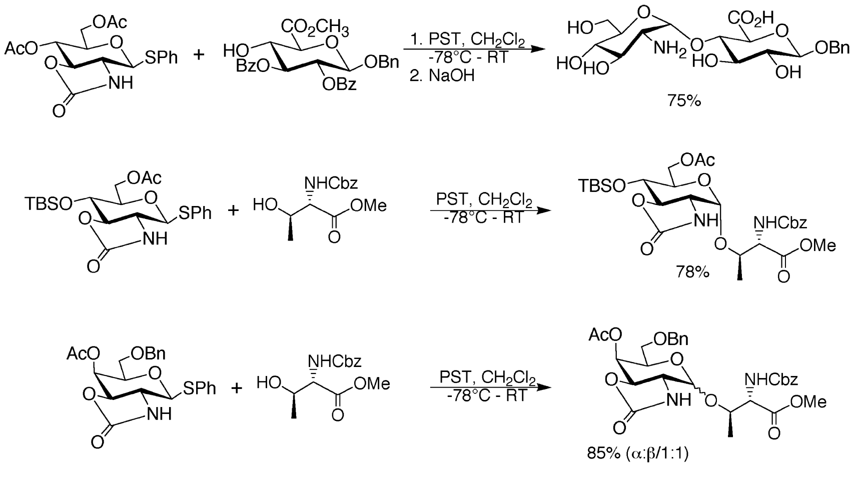
1. PST, CH$_2$Cl$_2$
-78°C - RT
2. NaOH
75%
CO$_2$CH$_3$
BzO
OBz
OBn
NH$_2$
CO$_2$H
OH
TBSO
NHCbz
OMe
PST, CH$_2$Cl$_2$
-78°C - RT
78%
85% (α:β/1:1)

Figure 13. Examples of the application of ring-fused 2,3-oxazolidinone protected thioglycoside donors in the synthesis of a heparan sulfate disaccharide and alpha-linked conjugates with amino acid residues.

Downloaded by UNIV OF GUELPH LIBRARY on June 13, 2012 | http://pubs.acs.org
Publication Date (Web): June 12, 2012 | doi: 10.1021/bk-2012-1102.ch009

The utility of a ring-fused 2,3-oxazolidinone protected phenyl 2-amino-2-deoxy-1-thio-glucopyranoside as glycosyl acceptor for a variety of glucuronic acid glycosyl donors in high yield has also been shown, demonstrating stability of the oxazolidinone protecting group to a number of different glycosyl donor activation methods (Figure 14).

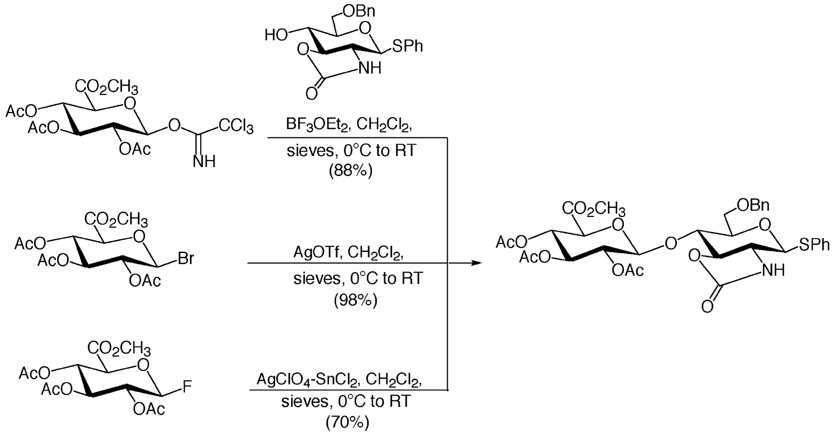

Figure 14. Chemical compatibility of ring-fused 2,3-oxazolidinone protection to a variety of glycosylation procedures.

Limitations of 2,3-oxazolidinone protected sugars in the synthesis of alpha-linked glycosides of D-glucosamine and D-galactosamine are evident. First, the 2,3-oxazolidinone protected thioglycoside donors are fairly low in reactivity, requiring phenylsulfenyl triflate activation, which is not a readily obtainable and employable reagent. Furthermore, deactivation of these donors through certain substituents at the 4 and 6 positions has been shown to render some donors virtually unreactive (*28*). To date the stereoselectivity of 2,3-oxazolidinone protected donors in the D-galactosamine series has been modest to poor. Finally, application of these donors to stepwise glycosylation methodologies as required for oligosaccharide synthesis may be complicated by varied levels of *N*-glycosylation of the oxazolidinone ring (*28*). Continued efforts to overcome these limitations are now focused on evaluating the effect of *N*-substituted 2,3-oxazolidone protection on the stereoselective formation of glycosides.

Downloaded by UNIV OF GUELPH LIBRARY on June 13, 2012 | http://pubs.acs.org
Publication Date (Web): June 12, 2012 | doi: 10.1021/bk-2012-1102.ch009

Downloaded by UNIV OF GUELPH LIBRARY on June 13, 2012 | http://pubs.acs.org
Publication Date (Web): June 12, 2012 | doi: 10.1021/bk-2012-1102.ch009

Nitro-D-galactal Based Strategies for the Synthesis of Glycoconjugates Containing Alpha-Linked 2-Amino-2-deoxy-D-galactopyranosides

Building on early work by Lemieux and others in the field of glycal and galactal chemistry, Schmidt and coworkers have recently expanded chemical methodology for the Michael-type addition of hydroxy nucleophiles to 2-nitro-D-galactal derivatives to afford alpha-linked *O*-glycosides of D-galactosamine (*29*–*33*). Fully *O*-benzyl protected 2-nitro-D-galactal has been reported to afford excellent yields of alpha-linked galactosides upon treatment of monosaccharides, serine, or threonine derivatives with strong base (Figure 15) (*30*, *31*, *33*). Subsequent reduction of the nitro group followed by acetylation of the resulting amine affords efficient formation of the alpha-linked 2-acetamido-2-deoxy-D-galactopyranosides in high overall yields.

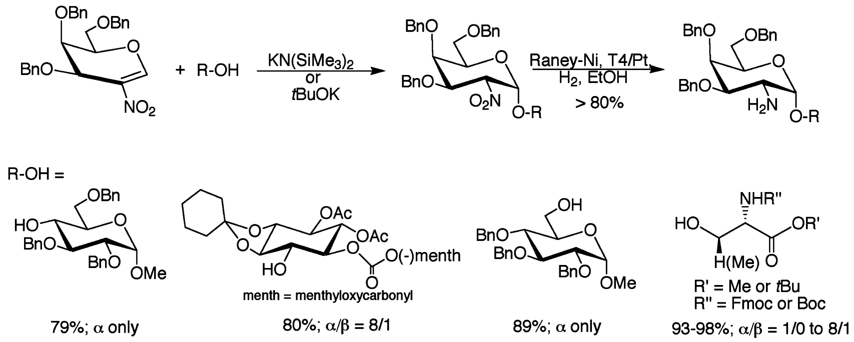
OBn
OBn
O
BnO
NO2
+ R-OH
KN(SiMe3)2
or
tBuOK
BnO
OBn
O
BnO
O2N
O-R
Raney-Ni, T4/Pt,
H2, EtOH
> 80%
BnO
OBn
O
BnO
H2N
O-R
R-OH =
OBn
HO
O
BnO
BnO
OMe
79%; α only
OAc
O
OAc
O
O
HO
O(-)menth
O
menth = menthyloxycarbonyl
80%; α/β = 8/1
OH
BnO
O
BnO
BnO
OMe
89%; α only
NHR"
HO
OR'
H(Me) O
R' = Me or tBu
R" = Fmoc or Boc
93-98%; α/β = 1/0 to 8/1

Figure 15. Michael-type addition of alcohols to 2-nitro-D-galactal derivatives followed by reduction of the nitro group affords alpha-linked glycosides of D-galactosamine derivatives.

The 2-nitro-D-galactal methodology has been elaborated using a C-6 *O*-differentiated 2-nitro-D-galactal intermediate to form an alpha-linked 2-acetamido-2-deoxy-D-galactopyranosyl linked threonine conjugate in the synthesis of a sialylated mucin-type *O*-glycan as shown (Figure 16) (*32*, *33*). Based on these early, albeit limited reports, this methodology is anticipated to be a highly useful addition to the synthetic arsenal for synthesizing bioactive glycoconjugates containing the alpha-linked galactosamine residues. Efficient formation of the requisite nitro galactals and the strong base employed to form the glycosidic bond will present potential limitations of this methodology in certain glycoconjugate systems.

Downloaded by UNIV OF GUELPH LIBRARY on June 13, 2012 | http://pubs.acs.org
Publication Date (Web): June 12, 2012 | doi: 10.1021/bk-2012-1102.ch009

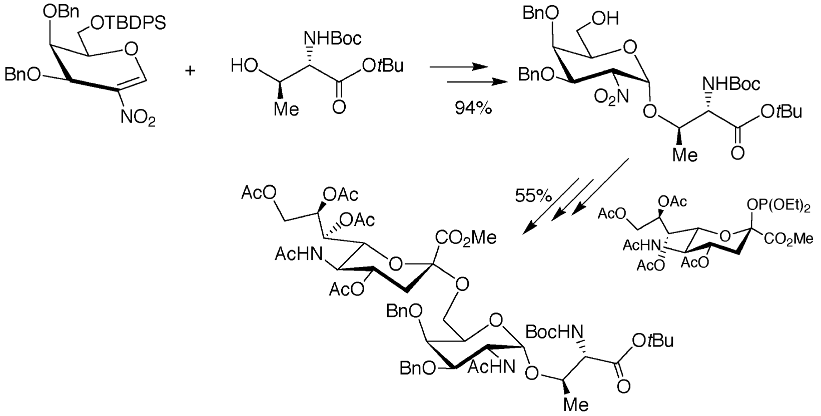
OBn
OTBDPS
O
BnO
NO2
+
NHBoc
HO
OtBu
Me
O
94%
BnO
OH
O
BnO
O2N
O
NHBoc
OtBu
Me
O
55%
AcO
OAc
OAc
OP(OEt)2
O
CO2Me
AcHN
AcO
AcO
OAc
OAc
CO2Me
AcHN
O
AcO
O
BnO
O
BocHN
OtBu
BnO
AcHN
O
O
Me

Figure 16. Application of the 2-nitro-D-galactal methodology in the synthesis of a sialylated mucin-type O-glycan (32, 33).

The 2,4-Dintrophenyl Moiety as a Putative Non-Participating Group for the 2-Amino Group in D-Glucosamine and D-Galactosamine Glycosyl Donors

The 2,4-dinitrophenyl group was investigated over 40 years ago as a non-participating protecting group for the 2-amine functionality in formation of alpha-linked (1,2-*cis*) glycosides of D-glucosamine (Figure 17) (*34*). Application of 2-(2,4-dinitrophenyl amino donors in the synthesis of alpha-linked disaccharides of 2-amino-2-deoxy-D-glucopyranoside has afforded mixed results, where stereocontrol is highly dependent on the activation system employed to activate glycosyl halide donor (*13*).

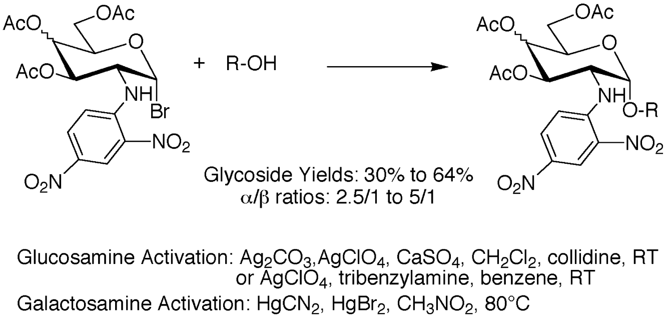
AcO
OAc
O
AcO
NH
Br
NO2
O2N
+ R-OH
AcO
OAc
O
AcO
NH
O-R
NO2
O2N

Glycoside Yields: 30% to 64%
α/β ratios: 2.5/1 to 5/1

Glucosamine Activation: Ag_2CO_3,$AgClO_4$, $CaSO_4$, CH_2Cl_2, collidine, RT
or $AgClO_4$, tribenzylamine, benzene, RT
Galactosamine Activation: $HgCN_2$, $HgBr_2$, CH_3NO_2, 80°C

Figure 17. Overview of 2-(2,4-dinitrophenyl)amino protected D-glucosamine and D-galactosamine derivatives as potential alpha-selective glycosyl donors.

Syntheses employing 2,4-dinitrophenyl protection of the 2-amino group in D-glucosamine and D-galactosamine donor residues have been reported for a number of bioactive natural product structures including trehalosamine analogs (*35*), aminoglycosides (*36*), glycosylated amino acids (*37*), and glycosylated inositols (*38*, *39*). The coupling reactions employed in these syntheses are exemplified by those shown (Figure 18). Future applications of this approach to the synthesis of alpha-linked glycosides are likely to be limited because relatively low yields and modest enantioselectivity are observed compared to other methods.

Downloaded by UNIV OF GUELPH LIBRARY on June 13, 2012 | http://pubs.acs.org
Publication Date (Web): June 12, 2012 | doi: 10.1021/bk-2012-1102.ch009

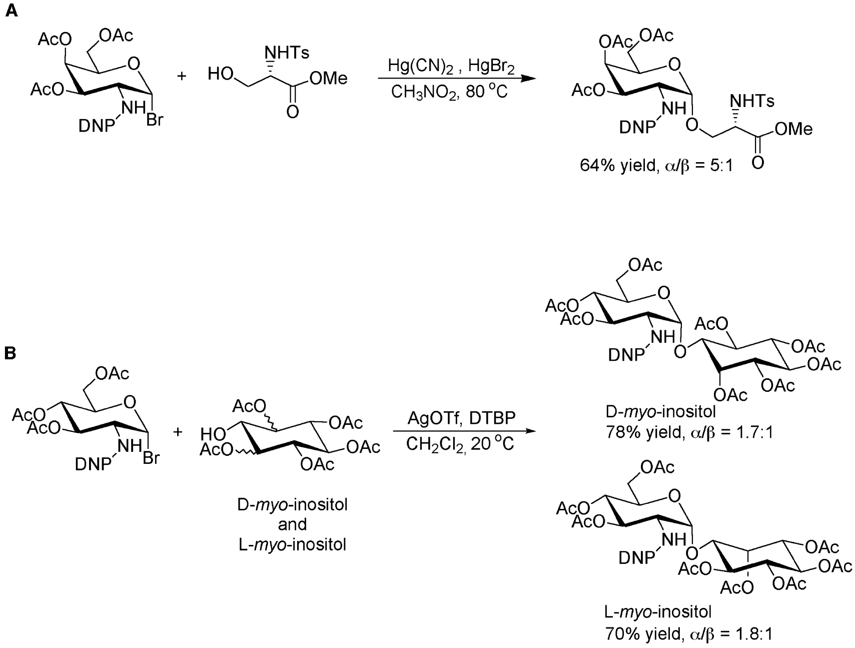
A
AcO
OAc
O
AcO
NH
DNP
Br
+
NHTs
HO
OMe
O
Hg(CN)2 , HgBr2
CH3NO2, 80 °C
OAc
OAc
O
AcO
NH
DNP
O
NHTs
OMe
O
64% yield, α/β = 5:1
B
OAc
AcO
AcO
O
NH
DNP
Br
+
AcO
HO
AcO
OAc
OAc
OAc
D-*myo*-inositol
and
L-*myo*-inositol
AgOTf, DTBP
CH2Cl2, 20 °C
OAc
AcO
AcO
O
NH
DNP
O
AcO
OAc
OAc
OAc
OAc
D-*myo*-inositol
78% yield, α/β = 1.7:1
OAc
AcO
AcO
O
NH
DNP
O
AcO
OAc
OAc
AcO
OAc
L-*myo*-inositol
70% yield, α/β = 1.8:1

Figure 18. Select coupling reactions employing 2-(2,4-dinitrophenyl)amino glycosyl donors investigated toward the synthesis of natural bioactive glycoconjugates. Panel A) Formation of the α-O-glycopeptide linkage with a serine residue employing DNP protected 2-amino-2-deoxy-D-galactopyranosyl bromide donor (37). Panel B) Application of DNP protected donors reported in 2002 for studies toward the synthesis of mycothiol derivatives (38).

Downloaded by UNIV OF GUELPH LIBRARY on June 13, 2012 | http://pubs.acs.org
Publication Date (Web): June 12, 2012 | doi: 10.1021/bk-2012-1102.ch009

Methoxybenzylidene (Arylimino) Protection for the 2-Amino Group of D-Glucosamine Donors as a Putative Non-Participating Moiety

Protection of the 2-amine group of 2-amino sugar donors through formation of arylimino moieties was initially employed under the premise that the arylimine group represented a potential non-participating group for the formation of 1,2-*cis* glycosides. Early application of this strategy toward the early synthesis of bioactive natural products such as aminoglycosides (*40–42*), heparin (*43*), and teichoic acid degradation products (*44*) employed *O*-protected 2-(4-methoxybenzylideneamino) glycosyl bromides as donor residues (Figure 19). Importantly, the stereochemical outcome of these glycosylations using the 2-(4-methoxybenzylideneamino) protected donors appears to be strongly dependent on the system employed in donor activation, with mercury(II)cyanide affording modest yields of the desired alpha-linked glycoconjugates (*13*).

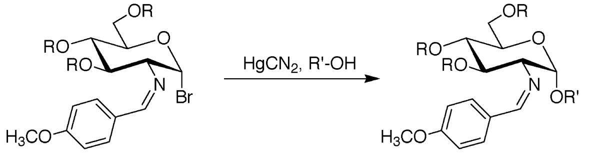

Figure 19. Arylimino protection of the 2-amine group as a putative non-participating C-2 moiety for the synthesis of alpha-linked 2-amino sugars.

Further evaluation of this methodology in the 1990s during application of this coupling strategy toward synthesis of heparin-like oligosaccharides revealed a possible alternative pathway for formation of the alpha-linked glycosides as a result of mercuric cyanide activation, indicating the 2-imino group does display neighboring group participation during glycosylation reactions (*45*).

In 1989 the stereoselective glycosidation of a 2-(4-methoxybenzylideneamino) protected pentenyl glycoside was reported using a series of monosaccharide acceptors (Figure 20, Panel A) (*46*). Here, alpha-linked disaccharides were obtained in good yields (60-64%) with the exception of a 4-hydroxy-galactose derivative that afforded 68% yield of 1:1 α/β mixture. Subsequently, a 4,6-benzylidene protected pentenyl glycoside bearing a C-2 4-methoxybenzylideneamino group was employed in the synthesis of an alpha-linked 2-amino-2-deoxy-D-glucosylinositol intermediate, which was employed in synthesis of the pentasaccharide core of the protein membrane anchor found in *Trypanosoma brucei* (Figure 20 Panel B) (*47*).

Downloaded by UNIV OF GUELPH LIBRARY on June 13, 2012 | http://pubs.acs.org
Publication Date (Web): June 12, 2012 | doi: 10.1021/bk-2012-1102.ch009

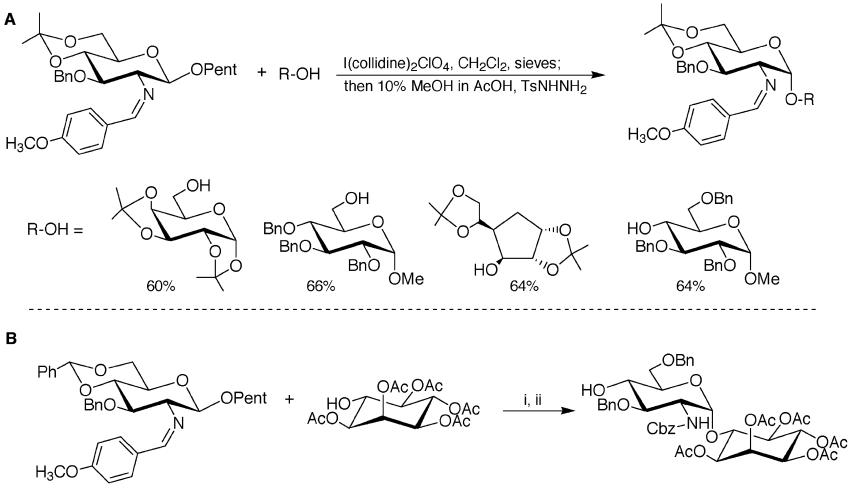

(i) I(collidine)$_2$ClO$_4$, CH$_2$Cl$_2$, sieves; then 10% MeOH in AcOH, TsNHNH$_2$; then Et$_3$N, Cbz-Cl; 65%
(ii) NaBH$_3$(CN), THF-Et$_2$O, HCl, sieves; 75%

Figure 20. Application of 1-O-pentenyl glycosyl donors bearing a C-2 arylimino moiety as a latent amine group. (Panel A) Application to the synthesis of alpha-linked disaccharides (46). (Panel B) Application to the synthesis of a α-D-glucosaminyl-inositol intermediate that was further elaborated to prepare the pentasaccharide core of a GPI anchor of Trypanosoma brucei (47).

C-2-Oximino Protection as a Putative Non-Participating Moiety for the 2-Amino Group of D-Glucosamine and D-Galactosamine Glycosyl Donors

The utility of glycal-derived oximino derivatives of hexopyranosides in preparing glycosides of 2-amino-2-deoxy-D-hexopyranosides was first introduced in the 1960s (*48*). Formation of a nitroso dimer by addition of nitrosyl chloride to glycal followed by condensation with monosaccharides as well as simple alcohols selectively afforded good yields of alpha-linked 2-oximino glycosides (Figure 21). Reduction of the resulting oximino functionality ultimate determines stereochemistry of the C-2-amine group. Utility of this methodology in the synthesis of 1,2-cis and 1,2-trans glycosides has been reviewed (*13*). This methodology was employed in early syntheses of aminoglycoside antibiotics (*49–52*) and proposed antigenic teichoic acid structures of *Staphylococcus aureus* (*53*). Alpha-linked glycosides were typically obtained in 30% to 50% yields during these syntheses.

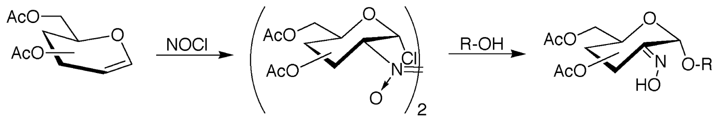

Figure 21. Early methodology employing glycal-derived 2-oximino dimers for the formation of alpha-linked glycosides of 2-amino sugars.

Downloaded by UNIV OF GUELPH LIBRARY on June 13, 2012 | http://pubs.acs.org
Publication Date (Web): June 12, 2012 | doi: 10.1021/bk-2012-1102.ch009

A variation of this method has also been employed, where a C-2 oximino ester is prepared as a putative non-participating C-2 protecting group for traditional promoter-mediated glycosidation of a glycosyl donor. For example, in 1985 Lichtenthaler *et al* reported the coupling of an oximino ester containing disaccharide donor with a monosaccharide acceptor to afford the alpha-linked trisaccharide product in 77% yield (Figure 22, panel A) (*54*). In 1997 Karpiesiuk and Banaszek employed a 2-oximino derivatized glucosyl bromide toward synthesis of the 1,1-linked disaccharide component in tunicamycin antibiotics (Figure 22, Panel B) (*55*, *56*). It must be noted that alpha selectivity in this coupling strategy is sensitive to the donor activation system (activating agent and solvent). Beta-glycosides of the 2-oximino sugars often prevailed until optimal conditions were found to form the alpha-linked glycoside (*54–56*), and could even be optimized to preferentially afford high yields of beta glycosides (*57*).

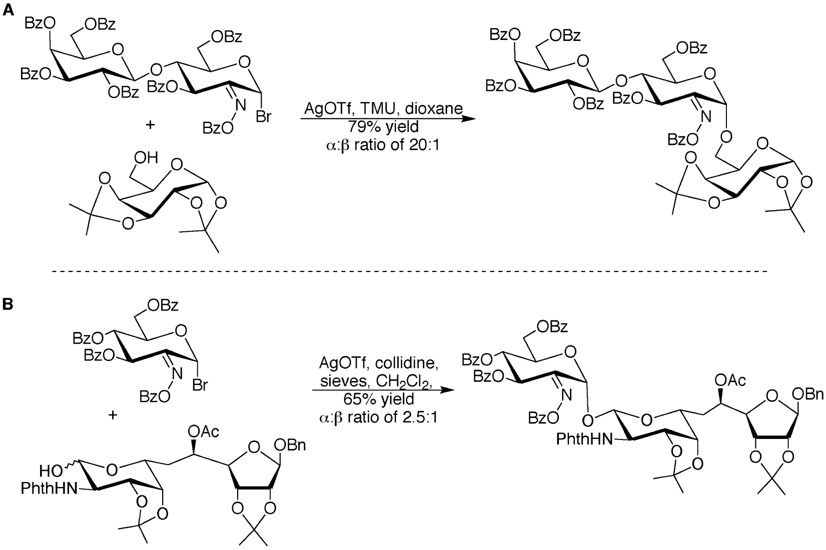

Figure 22. Application of glycosyl donors bearing a 2-oximino ester group in the synthesis of a trisaccharide (panel A), and synthesis of the 1,1-disaccharide of tunicamycin (Panel B).

N-Acetyl 1-Diazirine Glycosyl Donors

Vasella and coworkers have reported the formation of alpha-linked glycosides of *N*-acetyl-D-glucosamine and *N*-acetyl-D-allosamine *via* photolysis of C-1-diazirine derivatives of 2-acetamido-2-deoxy-D-glucopyranose and 2-acetamido-2-deoxy-D-allopyranose (Figure 23) (*58*, *59*). This glycosidation strategy is based on photolytic or thermolytic generation of glycosylidene carbenes in the presence of alcohol to afford the *O*-linked glycoside. Employing simple alcohols of different Pka at varied concentrations and temperatures of photolysis provided fair to excellent yields of the alpha-linked

2-acetamido products (*59*). The only alpha-linked disaccharide of a 2-acetamido-2-deoxy-D-hexopyranoside derivative prepared using this method employed 1,2:5,6-di-*O*-isopropylidene-α-D-glucofuranose as the acceptor alcohol, affording a modest 30% yield of the alpha-linked product and significant recovery of the unreacted glucofuranose (*59*). This method does not require the use of a chemical promoter and accommodates use of the *N*-acetylated monosaccharide aziridine, which eliminates the need to modify the 2-amino group after glycoside bond formation to obtain the 1,2-cis glycosides of *N*-acetyl products. However, modest yields appear to be a limiting factor. In addition, synthesis of the diazirine sugars is a non-trivial multi-step process that requires preparation of appropriate hydroxyl-protected ring-opened oximes in order to obtain the requisite glyconohydroximo-lactone intermediates.

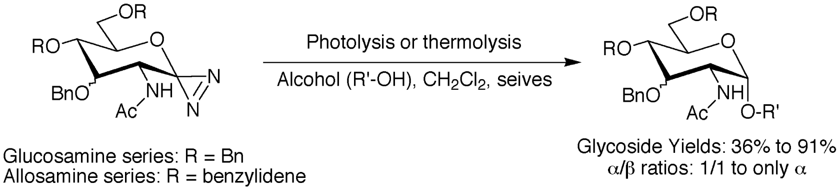
RO
OR
O
BnO
NH
Ac
N
N
Photolysis or thermolysis
Alcohol (R'-OH), CH2Cl2, seives
RO
OR
O
BnO
NH
Ac
O-R'
Glucosamine series: R = Bn
Allosamine series: R = benzylidene
Glycoside Yields: 36% to 91%
α/β ratios: 1/1 to only α

Figure 23. Pictorial representation of Vasella's methodology to utilize glycosylidene carbene-based glycosyl donors in the synthesis of glycosides of N-acetylated D-glucosamine.

Downloaded by UNIV OF GUELPH LIBRARY on June 13, 2012 | http://pubs.acs.org
Publication Date (Web): June 12, 2012 | doi: 10.1021/bk-2012-1102.ch009

Formation of Alpha-Linked Glycosides from D-Glucosamine and D-Galactosamine Glycosyl Donors Bearing C-2 *N*-Alkoxycarbonyl Moieties That Traditionally Afford Beta-Linked Glycosides

Glycosylation reactions using 2-amino-2-deoxy-D-glucopyranosyl and D-galactopyranosyl donors bearing *N*-alkoxycarbonyl (carbamate) protection of the 2-amine group typically afford beta-linked (1,2-*trans*) glycosides, owing to participation of the alkoxycarbonyl group during the glycosylation reaction. However, alpha-selective glycosylation has been reported for certain 2-alkoxycarbonyl protected glycosyl donors under specific conditions. For example in 1990 Higashi *et al* reported good yields and excellent stereoselectivity in obtaining alpha glycosides upon activating an *N*-Troc protected 2-amino-2-deoxy-α-D-glucopyranosyl bromide with zinc halides or silver perchlorate (Figure 24) (*60*). As would be anticipated, good yields and excellent stereoselectivity in forming the beta-linked (1,2-*trans*) glycosides of 2-*N*-Troc substituted glycosyl donors is achieved under alternative activation conditions (*60*, *61*). Based on this report it is somewhat surprising that activation of *N*-Troc protected 2-amino-2-deoxy-α-D-glucopyranosyl bromides with zinc halides has not been employed in more syntheses of alpha-linked 2-amino-2-deoxy-α-D-glycopyranosides. Although versatility of the 2-azido methodologies and extensive use of 2-*N*-alkoxycarbonyl protection of 2-amino-D-glucopyranosides and 2-amino-D-galactopyranosides to afford the 1,2-*trans* (beta) glycosidic linkage likely overshadow this potentially useful unique system.

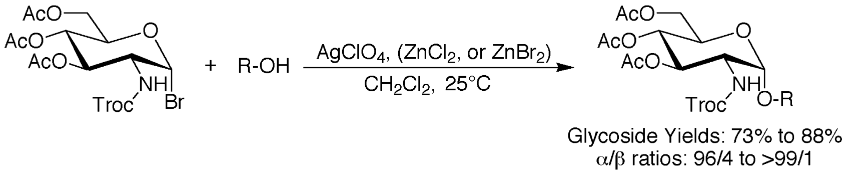
AcO
AcO
AcO
O
NH
Troc
Br
+
R-OH
AgClO4, (ZnCl2, or ZnBr2)
CH2Cl2, 25°C
AcO
AcO
AcO
O
NH
Troc
O-R
Glycoside Yields: 73% to 88%
α/β ratios: 96/4 to >99/1

Figure 24. Activation of N-Troc protected 2-amino-2-deoxy-D-glucopyranosyl bromides under specific conditions has been shown to afford unexpectedly high stereoselectivity and yields of the alpha-linked glycoside products (60).

A 1990 report by Kolar *et al* also showed good yields and stereoselectivity in formation of non-natural etoposide derivatives, where activation of 2-*N*-benzyloxycarbonyl 1-α-lactols with boron trifluoride etherate in dichloromethane afforded the alpha-linked glycosides (Figure 25) (*62*). The corresponding beta glycosides were preferentially formed when ethyl acetate or ethyl acetate-dichloromethane were employed as reaction solvent. Mutarotation studies demonstrated the stereoselectivity observed in this coupling reaction was controlled by solvent-dependent α/β equilibrium of the 2-*N*-Cbz protected lactol under glycosylation conditions.

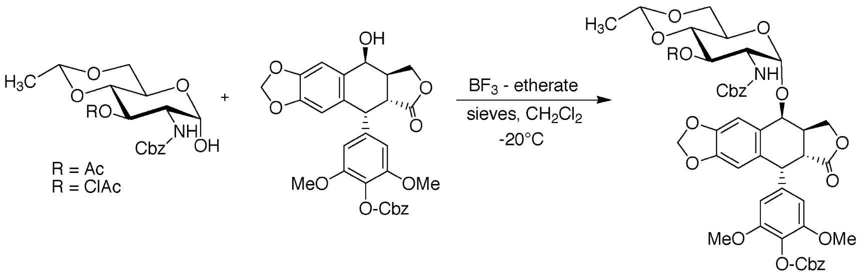

Figure 25. Reported alpha-selective glycosylation where the C-2 amine substituent bears a benzyloxycarbonyl protecting group (62).

In 2003 Imamura *et.al* reported a potentially more general approach to achieving stereoselective formation of 2-amino-2-deoxy-α-D-galactopyranosides using D-galactosamine donors possessing 2-*N*-alkoxycarbonyl and other 2-*N*-acyl protecting groups (*63*). In this approach a 4,6-*O*-di-*tert*-butylsilylene protected thiophenyl glycoside bearing *N*-Troc protection of the C-2 amine group was shown to yield alpha-selective glycosylation of a trisaccharide, two monosaccharides, and two serine derivatives (Figure 26) (*63*). Alpha-selective glycosylation of alcohols in modest to high yields was also imparted by the 4,6-*O*-di-*tert*-butylsilylene protecting group for derivatives having *N*-Phthaloyl and *N*-Acetyl protection of the 2-amino group. It is notable that the corresponding 4,6-*O*-benzylidene derivatives did not show similar alpha-directing properties.

Downloaded by UNIV OF GUELPH LIBRARY on June 13, 2012 | http://pubs.acs.org
Publication Date (Web): June 12, 2012 | doi: 10.1021/bk-2012-1102.ch009

Downloaded by UNIV OF GUELPH LIBRARY on June 13, 2012 | http://pubs.acs.org
Publication Date (Web): June 12, 2012 | doi: 10.1021/bk-2012-1102.ch009

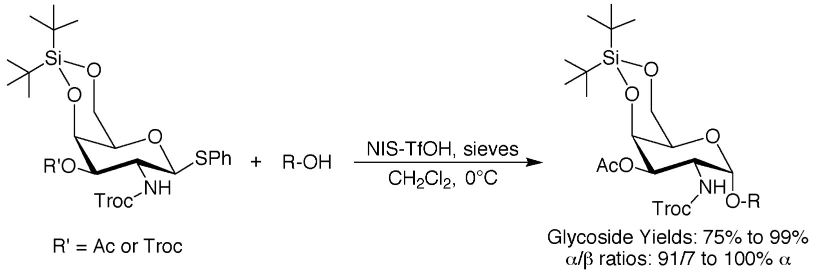
R'O
SPh
Troc
NH
Si
O
+ R-OH
NIS-TfOH, sieves
CH2Cl2, 0°C
AcO
NH
Troc
O-R
R' = Ac or Troc
Glycoside Yields: 75% to 99%
α/β ratios: 91/7 to 100% α

Figure 26. The 4,6-O-di-tert-butylsilylene protecting group has been shown to direct alpha-selective glycosylation of 1-thio galactosaminyl donors even in the presence of participating groups on the C-2 Nitrogen (63).

Certain 2-acetamido-2-deoxy-D-glucopyranosyl donors have been shown to afford alpha-linked glycosides under thermal glycosylation conditions (*64*, *65*). Thermal glycosylation of alcohols employing 2-acetamido-2-deoxy-3,4,6-tri-*O*-acetyl-α-D-glucopyranosyl chloride at high temperatures (160°C-180°C) in the presence of acid scavengers including α-methylstyrene or N,N,N′,N′-tetramethylurea preferentially afforded alpha-linked products in modest yield (Figure 27, Panel A) (*64*). A complication with this reaction system is acylation of the acceptor alcohol, which presumably forms as a result of intermolecular acetate transfer at high temperatures. At lower temperatures beta-linked products predominate and loss of acceptor to acetylation is minimized.

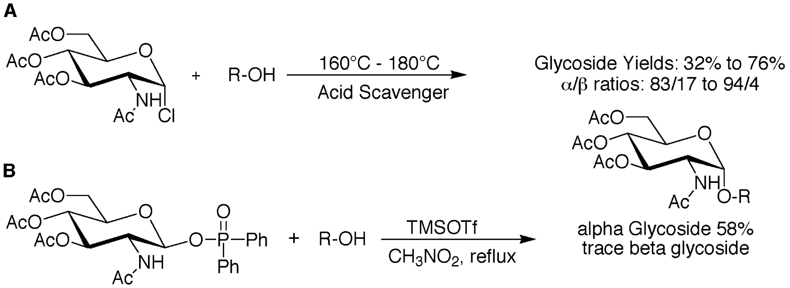
A
AcO
AcO
AcO
O
NH
Ac
Cl
+ R-OH
160°C - 180°C
Acid Scavenger
Glycoside Yields: 32% to 76%
α/β ratios: 83/17 to 94/4
O-R
B
O-P-Ph
Ph
+ R-OH
TMSOTf
CH3NO2, reflux
alpha Glycoside 58%
trace beta glycoside

Figure 27. Thermal glycosylation strategies that have been shown to afford alpha-linked glycosides of N-acetyl-D-glucosamine derivatives.

In 2000 an alpha-selective thermal glycosylation was reported using acetyl-protected 2-acetamido-2-deoxy-ß-D-glucopyranosyl diphenylphosphinate donor activated with TMSOTf in refluxing nitromethane (Figure 27, Panel B) (*65*). Although stereoselectivity for the alpha-linked product appears high, only modest overall yield of the glycoside is obtained. In theory, an advantage of the thermal glycosylation using 2-acetamido glycosyl donors is the glycosylation product contains the intact *N*-acetyl substituent at the C-2 position, thus avoiding manipulation of a latent C-2 amine substituent after glycoside bond formation to obtain *N*-acetyl derivatized alpha-linked products. In practice, it is anticipated that the high temperatures, modest yields, and sometimes modest stereoselectivity of these current thermal glycosylation strategies, when compared to the alternative glycosylation strategies, will limit application of these methods to the synthesis of more complex bioactive glycoconjugates containing alpha-linked 2-acetamido-2-deoxy-α-D-glycopyranoside residues.

Utility of Miscellaneous 1-OH Glycosyl Donors

Glycosylation by way of direct activation of 1-OH sugar derivatives is of interest because such approaches eliminate the need to prepare reactive glycosyl donors. One example of this strategy was discussed above (Figure 25). Koto *et al* reported the synthesis of α-linked glycosides of 2-azido-3,4,6-tri-*O*-benzyl-2-deoxy-D-glucose and using 2-azido-3,4,6-tri-*O*-benzyl-2-deoxy-D-galactose through *in situ* activation of the lactol employing *p*-nitrobenzenesulfonyl chloride (NsCl)-silver triflate-triethylamine as the activation system (Figure 28) (*66*). Modest yields and stereoselectivity were achieved.

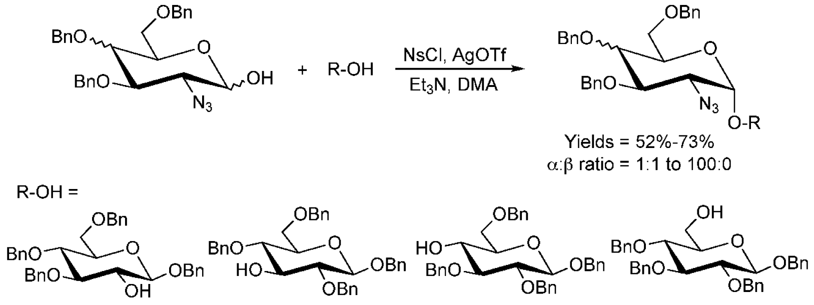

Figure 28. Synthesis of alpha-linked disaccharides employing the free lactol of 2-azido-2-deoxy-D-glucopyranose and 2-azido-2-deoxy-D-galactopyranose reported in 1999 (66).

In general, the existence of an *N*-acetyl group at the C-2 position of hexopyranosyl glycosyl donors preferentially affords β-glycosides upon glycosylation due to anchimeric participation of the *N*-acetyl group. However, Fisher-type glycosidation of *N*-acetyl-D-glucosamine (Figure 29) using *n*-octanol or allyl alcohol with boron trifluoride etherate activation and acetonitrile as solvent has been shown to afford the corresponding α-glycosides with modest yields and good stereoselectivity (*67*, *68*).

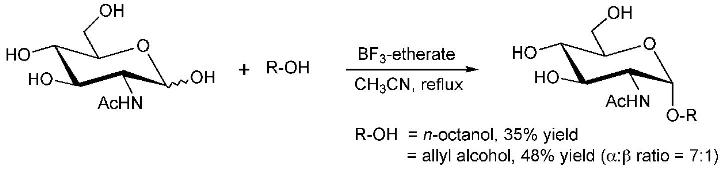
OH
HO
O
HO
OH
AcHN
+ R-OH
BF3-etherate
CH3CN, reflux
O-R
R-OH = n-octanol, 35% yield
= allyl alcohol, 48% yield (α:β ratio = 7:1)

Figure 29. Examples of Fisher-type glycosidation of N-acetyl-D-glucosamine using simple alcohols.

Downloaded by UNIV OF GUELPH LIBRARY on June 13, 2012 | http://pubs.acs.org
Publication Date (Web): June 12, 2012 | doi: 10.1021/bk-2012-1102.ch009

A suitable α-linked spacer at the reducing end of D-galactosamine derivatives has been employed for conjugation of this saccharide residue to macromolecular carriers. For example, the introduction of a α-linked spacer into *N*-acetyl-D-galactosamine has been achieved using Fisher glycosidation as shown (Figure 30). Here, heating *N*-acetyl-D-galactosamine in 2-bromoethanol or 3-bromo-1-propanol at 60-70°C in the presence of catalytic hydrogen chloride afforded the alpha glycosides in good yield and stereoselectivity (*69*, *70*).

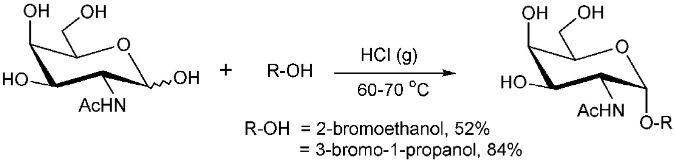

Figure 30. Formation of simple alpha-linked glycoside of N-acetyl-D-galactosamine using Fisher glycosidation.

The later two methods described above are applicable to the formation of glycosides using simple alcohols during the early steps of a synthesis. These methods are typically used to cap the anomeric position rendering a stable glycoside or to introduce a stable glycosidic moiety bearing requisite functional groups for additional, non-glycosidic, conjugation chemistry.

Methods To Obtain Alpha-Linked Aryl *O*-Glycosides of D-Glucosamine and D-Galactosamine

The occurrence of aryl *O*-glycosides in nature and the biological activities of these glycoconjugates makes them attractive targets in synthetic organic chemistry. However, due to reduced nucleophilicity of a phenolic hydroxyl group compared to other alcohols, formation of aryl *O*-glycosides typically requires modification of traditional glycosylation strategies. The synthesis of aryl-*O* 2-amino-2-deoxy-β-D-glycosides have been extensively reported, with the corresponding α-glycosides generally presented as side products obtained during these syntheses. However, aryl-*O* glycosides of 2-amino-2-deoxy-α-D-glucopyranose and 2-amino-2-deoxy-α-D-galactopyranose have been synthesized in excellent yields under specific conditions. For example, in 2004 Nishiyama *et al* reported good yields and stereoselectivity in formation of phenyl 2-amino-2-deoxy-α-D-glucopyranoside, the core structure of glycocinnasperimicin D (*71*). Glycosidation of peracetylated D-glucosamine with phenol using catalytic tin (IV) chloride in CH_2Cl_2 (Figure 31) proceeded smoothly to afford a 4:1 (α:β) anomeric mixture of phenyl glycosides in 87% yield. The stereoselectivity in this glycosylation is reversed using TMSOTf in ether, affording a 1:9 (α:β) anomeric mixture of phenyl glycoside in 50% yield.

Downloaded by UNIV OF GUELPH LIBRARY on June 13, 2012 | http://pubs.acs.org
Publication Date (Web): June 12, 2012 | doi: 10.1021/bk-2012-1102.ch009

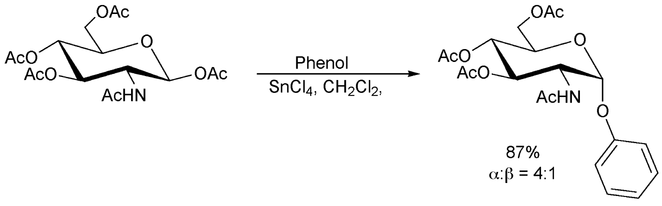

Figure 31. Direct conversion of peracetylated D-glucosamine to alpha-linked aryl-O-glycosides reported in 2004 (71).

In 2003 Schmidt and co-workers reported good yields and excellent stereoselectivity in obtaining aryl-*O* glycosides of 2-acetamido-2-deoxy-α-D-galactopyranosides employing the Michael-type addition of phenols to nitro-D-galactal (*29*). Here, *O*-benzyl protected 2-nitro-D-galactal was treated with commercially available *N*-Boc protected tyrosine methyl ester in toluene in the presence of a catalytic amount of potassium *tert*-butoxide, affording stereoselective formation of the α-anomer (α/β = 40/1) in 82% yield (Figure 32). No racemization of the tyrosine moiety was observed under the reaction conditions. Selective reduction of the nitro group with platinised Raney nickel followed by acetylation provided the final 2-acetamido-2-deoxy-α-D-galactopyranoside product (*29*).

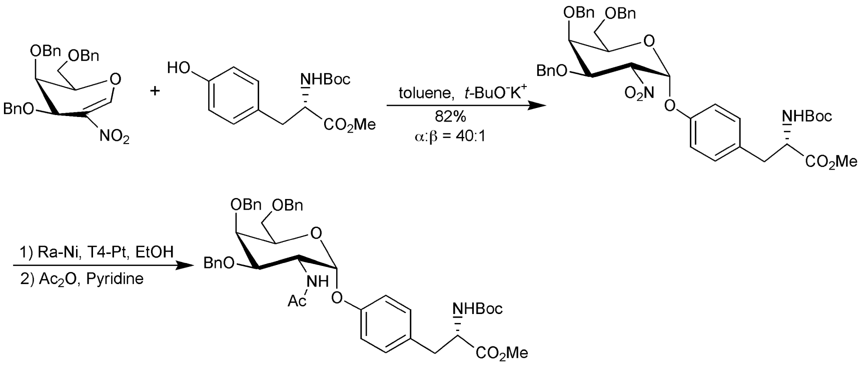

Figure 32. Example of the Michael-type addition of phenols to 2-nitro-D-galactal derivatives reported in 2003 as a method to obtain alpha-linked aryl-O-glycosides of D-galactosamine derivatives (29).

Araki and coworkers reported a straightforward approach to obtaining aryl *O*-glycosides of D-glucosamine and D-galactosamine *via* use of the non-participating C-2 azide group (Figure 33) (*72*). The 1-*O*-acetyl and 1-chloro glycosyl donors were coupled with ethyl *p*-hydroxycinnamate using a number of different activation strategies. Modest yields were obtained while preferentially affording the α-glycosides.

Downloaded by UNIV OF GUELPH LIBRARY on June 13, 2012 | http://pubs.acs.org
Publication Date (Web): June 12, 2012 | doi: 10.1021/bk-2012-1102.ch009

Downloaded by UNIV OF GUELPH LIBRARY on June 13, 2012 | http://pubs.acs.org
Publication Date (Web): June 12, 2012 | doi: 10.1021/bk-2012-1102.ch009

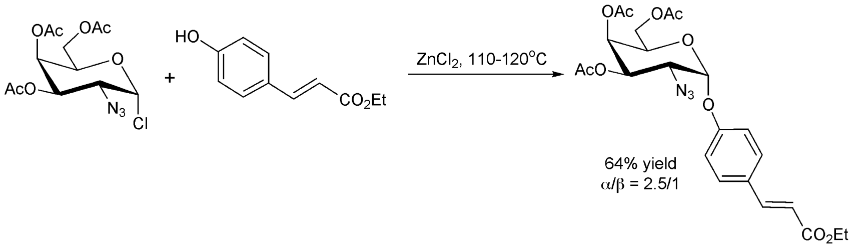

Figure 33. One example of conditions reported for aryl O-glycoside synthesis employing the non-participating 2-azide moiety (72).

An Alternative Route for the Stereoselective Introduction of Alpha-Linked 2-Amino-2-deoxy-D-hexopyranosides into Glycoconjugate Structures

The use of fully *O*-protected D-glucosyl and D-galactosyl donors in alpha-selective glycoside bond formation followed by the introduction of an amine or amine precursor has also found utility in glycoconjugate synthesis. Introduction of the amine group or latent amine group is typically achieved through nucleophilic displacement of a C-2 leaving group such as triflate. One example of this indirect strategy for obtaining alpha-linked glycosides of D-glucosamine or D-galactosamine employed by Fraser-Reid in the synthesis of a prototype GPI of *P. falciparum* is shown (Figure 34) (*73*, *74*).

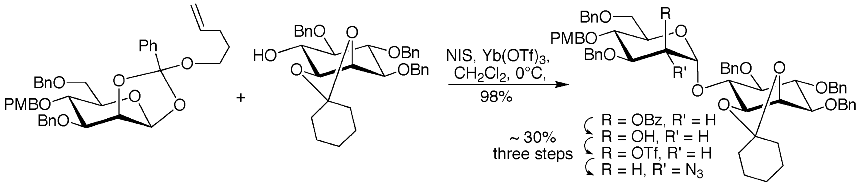

Figure 34. Incorporation of a 2-azido-2-deoxy-α-D-glucopyranoside residue into a GPI precursor structure where the 2-azide group (latent amine group) is introduced after formation of the requisite alpha glycosidic linkage.

Note

This chapter previously appeared in *Carbohydrate Drug Design* (ACS Symposium Series 932), edited by Klyosov et al. and published in 2006.

References

1. Dwek, R. A. *Chem. Rev.* **1996**, *96*, 683–720.
2. Casu, B.; Lindahl, U. *Adv. Carbohydr. Chem. Biochem.* **2001**, *57*, 159–206.
3. Davis, B. G. *Chem. Rev.* **2002**, *102*, 579–601.
4. Rabenstein, D. L. *Nat. Prod. Rep.* **2002**, *19*, 312–331.
5. *Tunicamycin*; Tamura, G., Ed.; Scientific Press: Tokyo, Japan, 1982.

6. *Aminoglycoside Antibiotics*; Umezawa, H., Hooper, I. R., Eds.; Springer-Verlag: New York, Heidelberg, 1982.
7. Hart, G. W.; Haltiwanger, R. S.; Holt, G. D.; Kelly, W. G. *Annu. Rev. Biochem.* **1989**, *58*, 841–874.
8. Montreuil, J. *Adv. Carbohydr. Chem. Biochem.* **1980**, *37*, 157–223.
9. Taylor, C. M. *Tetrahedron* **1998**, *54*, 11317–11362.
10. Sturm, S.; Jann, B.; Fortnagel, P.; Timmis, K. N. *Microbial Pathogenesis* **1986**, *1*, 307–324.
11. Newton, G. L.; Arnold, K.; Price, M. S.; Sherrill, C.; Delcardayre, S. B.; Aharonowitz, Y.; Cohen, G.; Davies, J.; Fahey, R. C.; Davis, C. *J. Bacteriol.* **1996**, 1990.
12. Ferguson, M. A. J.; Williams, A. F. *Annu. Rev. Biochem.* **1988**, *57*, 285–320.
13. Banoub, J.; Boullanger, P.; Lafont, D. *Chem. Rev.* **1992**, *92*, 1167–1195.
14. Demchenko, A. V. *Curr. Org. Chem.* **2003**, *7*, 35–79.
15. Schofield, L.; Hewitt, M. C.; Evans, C.; Siomas, M.-A.; Seeberger, P. H. *Nature* **2002**, *418*, 785–789.
16. Xue, J.; Guo, Z. *Bioorg. Med. Chem. Lett.* **2002**, *12*, 2015–2018.
17. Petitou, M.; Duchaussoy, P.; Lederman, I.; Choay, J.; Jacquinet, J.-C.; Sinay, P.; Torri, G. *Carbohydr. Res.* **1987**, *167*, 67–75.
18. Yu, H. N.; Furukawa, J.-I.; Ikeda, T.; Wong, C. H. *Org. Lett.* **2004**, *6*, 723–726.
19. Orgueira, H. A.; Bartolozzi, A.; Schell, P.; Seeberger, P. H. *Angew. Chem., Int. Ed.* **2002**, *41*, 2129–2131.
20. Sames, D.; Chen, X.-T.; Danishefsky, S. J. *Nature* **1997**, *389*, 587–591.
21. Greenberg, W. A.; Priestley, E. S.; Sears, P. S.; Alper, P. B.; Rosenbohm, C.; Hendrix, M.; Hung, S.-C.; Wong, C.-H. *J. Am. Chem. Soc.* **1999**, *121*, 6527–6541.
22. Mulard, L. A.; Glaudemans, C. P. J. *Carbohydr. Res.* **1998**, *311*, 121–133.
23. Pozsgay, V. *J. Org. Chem.* **1998**, *63*, 5983–5999.
24. Nicholas, G. M.; Eckman, L. L.; Kovac, P.; Otero-Quintero, S.; Bewley, C. A. *Bioorg. Med. Chem.* **2003**, *11*, 2641–2647.
25. Lee, S.; Rosazza, J. P. N. *Org. Lett.* **2004**, *6*, 365–368.
26. Myers, A. G.; Gin, D. Y.; Rogers, D. H. *J. Am. Chem. Soc.* **1993**, *115*, 2036–2038.
27. Benakli, K.; Zha, C.; Kerns, R. J. *J. Am. Chem. Soc.* **2001**, *123*, 9461–9462.
28. Kerns, R. J.; Zha, C.; Benakli, K.; Liang, Y.-Z. *Tetrahedron Lett.* **2003**, *44*, 8069–8072.
29. Khodair, A. I.; Winterfeld, G. A.; Schmidt, R. R. *Eur. J. Org. Chem.* **2003**, 1847–1852.
30. Das, J.; Schmidt, R. R. *Eur. J. Org. Chem.* **1998**, 1609–1613.
31. Winterfeld, G. A.; Ito, Y.; Ogawa, T.; Schmidt, R. R. *Eur. J. Org. Chem.* **1999**, 1167–1171.
32. Winterfeld, G. A.; Schmidt, R. R. *Angew. Chem., Int. Ed.* **2001**, *40*, 2654–2657.
33. Winterfeld, G. A.; Khodair, A. I.; Schmidt, R. R. *Eur. J. Org. Chem.* **2003**, 1009–1021.
34. Lloyd, P. F.; Stacey, M. *Tetrahedron* **1960**, *9*, 116–124.

Downloaded by UNIV OF GUELPH LIBRARY on June 13, 2012 | http://pubs.acs.org
Publication Date (Web): June 12, 2012 | doi: 10.1021/bk-2012-1102.ch009

Downloaded by UNIV OF GUELPH LIBRARY on June 13, 2012 | http://pubs.acs.org
Publication Date (Web): June 12, 2012 | doi: 10.1021/bk-2012-1102.ch009

35. Ogawa, S.; Shibata, Y. *Carbohydr. Res.* **1988**, *176*, 309–315.
36. Umezawa, S.; Koto, S. *Bull. Chem. Soc. Jpn.* **1966**, *39*, 2014–2017.
37. Kaifu, R.; Osawa, T. *Carbohydr. Res.* **1977**, *58*, 235–239.
38. Jardine, M. A.; Spies, H. S. C.; Nkambule, C. M.; Gammon, D. W.; Steenkamp, D. J. *Bioorg. Med. Chem.* **2002**, *10*, 875–881.
39. Plourde, R.; d'Alarcao, M. *Tetrahedron Lett.* **1990**, *31*, 2693–2696.
40. Umezawa, S.; Sana, H.; Tsuchiya, T. *Bull. Chem. Soc. Jpn.* **1975**, *48*, 556–559.
41. Watanabe, I.; Tsuchiya, T.; Takase, T.; Umezawa, S.; Umezawa, H. *Bull. Chem. Soc. Jpn.* **1977**, *50*, 2369–2374.
42. Harayama, A.; Tsuchiya, T.; Umezawa, S. *Bull. Chem. Soc. Jpn.* **1979**, *52*, 3626–3628.
43. Wolfrom, M. L.; Tomomatsu, H.; Szarek, W. A. *J. Org. Chem.* **1966**, *31*, 1173–1178.
44. Hardy, F. E.; Buchanan, J. G.; Baddiley, J. *J. Chem. Soc.* **1963**, 3360–3366.
45. Marra, A.; Sinay, P. *Carbohydr. Res.* **1990**, *200*, 319–337.
46. Mootoo, D. R.; Fraser-Reid, B. *Tetrahedron Lett.* **1989**, *30*, 2363–2366.
47. Mootoo, D. R.; Konradsson, P.; Fraser-Reid, B. *J. Am. Chem. Soc.* **1989**, *111*, 8540–8542.
48. Lemieux, R. U.; Nagabhushan, T. L.; O'Neill, I. K. *Tetrahedron Lett.* **1964**, *29*, 1909–1916.
49. Paulsen, H.; Stadler, P.; Todter, F. *Chem. Ber.* **1977**, *110*, 1925–1930.
50. Kugelman, M.; Mallams, A. K.; Vernay, H. F.; Crowe, D. F.; Detre, G.; Tanabe, M.; Yasuda, D. M. *J. Chem. Soc., Perkin Trans. I* **1976**, 1097–1113.
51. Kugelman, M.; Mallams, A. K.; Vernay, H. F. *J. Chem. Soc., Perkin Trans. I* **1976**, 1113–1126.
52. Kugelman, M.; Mallams, A. K.; Vernay, H. F. *J. Chem. Soc., Perkin Trans. I* **1976**, 1126–1134.
53. Loureau, J.-M.; Boullanger, P.; Descotes, G. *Eur. J. Med. Chem.* **1985**, *20*, 455–458.
54. Lichtenthaler, F. W.; Kaji, E. *Liebigs Ann. Chem.* **1985**, 1659–1668.
55. Karpiesiuk, W.; Banaszek, A. *Carbohydr. Res.* **1994**, *261*, 243–253.
56. Karpiesiuk, W.; Banaszek, A. *Carbohydr. Res.* **1997**, *299*, 245–252.
57. Kaji, E.; Lichtenthaler, F. W.; Nishino, T.; Yamane, A.; Zen, S. *Bull. Chem. Soc. Jpn.* **1988**, *61*, 1291–1297.
58. Vasella, A. *Pure Appl. Chem.* **1993**, *65*, 731–752.
59. Vasella, A.; Witzig, C. *Helv. Chim. Acta* **1995**, *78*, 1971–1982.
60. Higashi, K.; Nakayama, K.; Soga, T.; Shioya, E.; Uoto, K.; Kusama, T. *Chem. Pharm. Bull.* **1990**, *38*, 3280–3282.
61. Ellervik, U.; Magnusson, G. *Carbohydr. Res.* **1996**, *280*, 251–260.
62. Kolar, C.; Dehmel, K.; Wolf, H. *Carbohydr. Res.* **1990**, *206*, 219–231.
63. Imamura, A.; Ando, H.; Korogi, S.; Tanabe, G.; Muraoka, O.; Ishida, H.; Kiso, M. *Tetrahedron Lett.* **2003**, *44*, 6725–6728.
64. Nishizawa, M.; Shimomoto, W.; Momil, F.; Yamada, H. *Tetrahedron Lett.* **1992**, *33*, 1907–1908.
65. Kadokawa, J.-I.; Nagaoka, T.; Ebana, J.; Tagaya, H.; Chiba, K. *Carbohydr. Res.* **2000**, *327*, 341–344.

66. Koto, S.; Asami, K.; Hirooka, M.; Nagura, K.; Takiazawa, M.; Yamamoto, S.; Okamoto, N.; Sato, M.; Tajima, H.; Yoshida, T.; Nonaka, N.; Sato, T.; Zen, S.; Yago, K.; Tomonaga, F. *Bull. Chem. Soc. Jpn.* **1999**, *72*, 765–777.
67. Wong, C.-H.; Hendrix, M.; Manning, D. D.; Rosenbohm, C.; Greenberg, W. A. *J. Am. Chem. Soc.* **1998**, *120*, 8319–8327.
68. Aguilera, B.; Romero-Ramirez, L.; Abad-Rodriguez, J.; Corrales, G.; Nieto-Sampedro, M.; Fernandez-Mayoralas, A. *J. Med. Chem.* **1998**, *41*, 4599–4606.
69. George, S. K.; Holm, B.; Reis, C. A.; Schwientek, T.; Clausen, H.; Kihlberg, J. *J. Chem. Soc., Perkin Trans. I* **2001**, 880–885.
70. Spijker, N. M.; Keuning, C. A.; Hooglugt, M.; Veeneman, G. H.; van Boeckel, C. A. A. *Tetrahedron* **1996**, *52*, 5945–5960.
71. Nishiyama, T.; Ichikawa, Y.; Isobe, M. *Synlett* **2004**, 89–92.
72. Araki, K.; Hashimoto, H.; Yoshimura, J. *Carbohydr. Res.* **1982**, *109*, 143–160.
73. Lu, J.; Jayaprakash, K. N.; Fraser-Reid, B. *Tetrahedron Lett.* **2004**, *45*, 879–882.
74. Lu, J.; Jayaprakash, K. N.; Schlueter, U.; Fraser-Reid, B. *J. Am. Chem. Soc.* **2004**, *126*, 7540–7547.

Downloaded by UNIV OF GUELPH LIBRARY on June 13, 2012 | http://pubs.acs.org
Publication Date (Web): June 12, 2012 | doi: 10.1021/bk-2012-1102.ch009

Downloaded by OHIO STATE UNIV LIBRARIES on June 14, 2012 | http://pubs.acs.org
Publication Date (Web): June 12, 2012 | doi: 10.1021/bk-2012-1102.ch010

Chapter 10

Systematic Synthesis of Aminosugars and Their Stereoselective Glycosylation

Jinhua Wang and Cheng-Wei Tom Chang*

**Department of Chemistry and Biochemistry, Utah State University,
0300 Old Main Hill, Logan, Utah 84322-0300**
***tom.chang@usu.edu**

Carbohydrate synthesis is one of the most formidable tasks in organic synthesis. The synthesis of aminosugar libraries for practical applications represents an even greater challenge. Nevertheless, through the use of standardized protocols and a divergent synthetic approach, systematic procedures have been developed. The advantage of employing two separate aminosugar libraries for stereoselective glycosylation has also been demonstrated in the library construction of pyranmycin and kanamycin B analogues. However, there are several aspects that still require applicable solutions. There is no convenient synthesis of 2-aminopyranose that will favor the stereospecific formation of α-glycosidic bond. The deoxygenation method that is compatible with the presence of an azido group, stereospecific glycosylation for the formation of α-glycosidic bond, and a convenient protocol for the stereoselective glycosylation of 2-deoxyglycopyranoses are several such examples that still need further perfection. This overview considers systematic synthesis of aminosugars, including general synthetic protocols and divergent synthesis of both glycosyl trichloroacetimidate library and phenylthioglucopyranoside library, stereoselective glycosylation, including formation of β-glycosidic and α-glycosidic bonds, exemplified with preparation of Pyranmycin and Kanamycin libraries.

In Glycobiology and Drug Design; Klyosov, A.;
ACS Symposium Series; American Chemical Society: Washington, DC, 2012.

Downloaded by OHIO STATE UNIV LIBRARIES on June 14, 2012 | http://pubs.acs.org
Publication Date (Web): June 12, 2012 | doi: 10.1021/bk-2012-1102.ch010

Introduction

Synthesis of oligosaccharides and glycoconjugates has become increasingly important for the elucidation of their biological functions. Aminosugar, as one of the main components of these diverse glycoconjugates, has attracted burgeoning interest (*1–8*). Aminosugars are a group of structurally diverse unusual sugars bearing amino substitution on a normal sugar scaffold. Aminosugars can be found in bacteria, plant, and some mammalian cells, exerting unique but essential biological functions (*2–8*). Therefore, if there is a library of aminosugars available, a modular approach can be readily employed to construct a library of novel aminosugar-containing glycoconjugates for exploring important activities of interest in areas like biology, chemistry, and medicine. This strategy is termed glycodiversification or glycorandomization, a concept with fruitful applications (Figure 1).

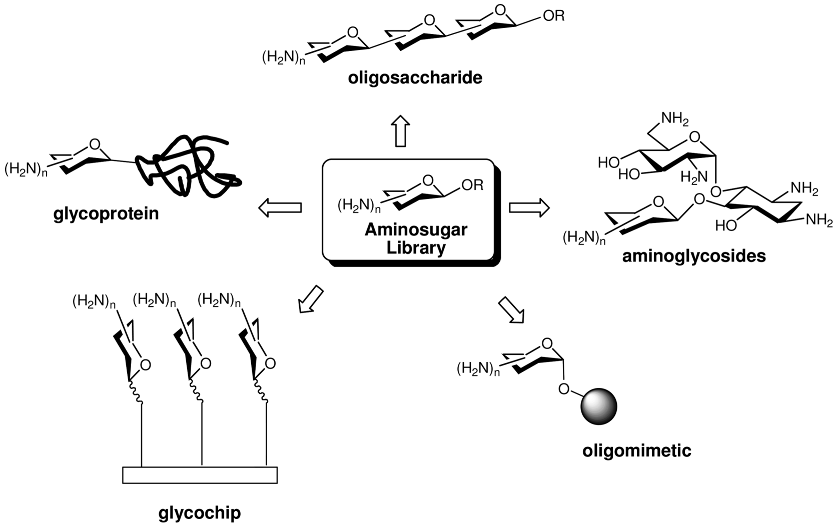

Figure 1. Prospective Glycoconjugates from Glycodiversification

In order to materialize the applications of aminosugar-containing glycoconjugates, numerous efforts have been devoted to the synthesis of aminosugars (*9–11*). Normal sugars, such as glucose, galactose, and mannose, are commonly used as the starting material for the chemical synthesis of aminosugars due to their intrinsic chirality, availability in large quantity, and lower cost. For the synthesis and application of aminosugars, two major issues are typically needed to be resolved properly: protective group manipulation including both hydroxyl and amino groups, and the stereoselective glycosylation.

Protective group manipulations are necessary to achieve regiospecific reactions for the aminosugar synthesis. For example, the hydroxyl groups which are not involved in the glycosylation must be masked. Protective groups, especially at the C-2 position, will affect not only the reactivity of the glycosyl

Downloaded by OHIO STATE UNIV LIBRARIES on June 14, 2012 | http://pubs.acs.org
Publication Date (Web): June 12, 2012 | doi: 10.1021/bk-2012-1102.ch010

donor during glycosylation, but also the stereoselectivity. Amino groups often require different reagents for protection and deprotection as compared to hydroxyl groups, creating more synthetic complications. Meanwhile, the protection of the anomeric position must be treated separately from the protection at other positions since it has to be stable enough to endure the reagents and conditions needed for the incorporation of amino groups. Nevertheless, the anomeric group is preferred to be labile so it can be activated at mild conditions for glycosylation. These two requirements regarding the anomeric groups work against each other (Figure 2). All these subtle demands make the preparation and utilization of aminosugars an extremely challenging and time-consuming task.

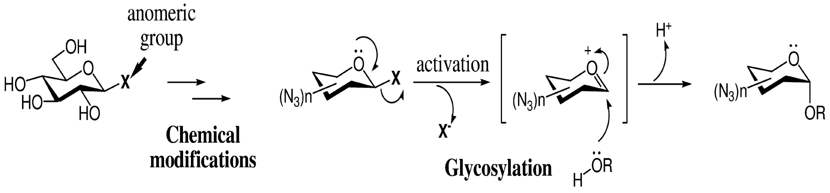

x group needs to be **stable** enough to endure the conditions for chemical modifications while being **labile** enough to be activated for glycosylation.

Figure 2. Challenges in Making the Aminosugar Donors

In addition, there are many reported methods for the preparation of specific aminosugars (*9–11*). However, the general protocols or methods that will allow the synthesis of other aminosugars for different applications are not available. As a result, when initiating a synthesis for a desired aminosugar, one may still need to contribute a significant amount of effort in searching and optimizing the best approach among the vast number of documented prior reports. There may not be an ideal answer for this issue. Nevertheless, we wish to provide some solution to alleviate the synthetic burden through our efforts in this area. In this article, we will focus on the identification of general protocols that can be used for the systematic construction of two libraries of aminopyranoses, and provide a brief coverage of their use in the preparation of novel aminoglycosides, pyranmycins and kanamycin analogues.

1. Synthesis of Aminosugars

1.1. Choice of Starting Sugars

Based on a survey of current reviews, glycosyl donors can be generally classified into thirteen types based on the anomeric functional groups and their activating methods (Table 1) (*12–16*). The predominantly used methods among them include glycosyl halide [e.g., (*17*, *18*)], thioglycoside [e.g., (*19–24*)], trichloroimidate (*15*, *25*, *26*), and 1-*O*-acyl sugar [e.g., (*27*, *28*)].

Downloaded by OHIO STATE UNIV LIBRARIES on June 14, 2012 | http://pubs.acs.org
Publication Date (Web): June 12, 2012 | doi: 10.1021/bk-2012-1102.ch010

Table 1. Commonly Used Anomeric Functional Groups Employed in Glycosyl Donors

Name	Structures	Stability in epimerization conditions	Stability in hydride or radical-mediated deoxygenation	Stability in azido group substitution
Glycosyl Halide	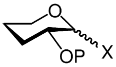 X = F, Cl or Br	Not stable	Not stable	Not stable
Thioglycoside	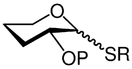	Stable	Not stable in radical-mediated deoxygenation	Stable
1-*O*-Acyl Sugar	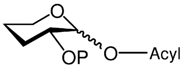	Could be stable	Not stable in hydride-mediated deoxygenation	Could be stable
Ortho Ester	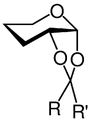	Stable	Stable	Stable
1-*O*- and *S*-Carbonate	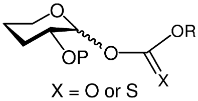 X = O or S	Not stable	Not stable	Not stable
Trichloroacetimidate	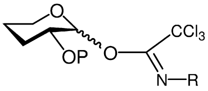	Not stable	Not stable	Not stable
4-Pentenyl Glycoside	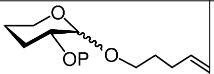	Stable	Not stable in radical-mediated deoxygenation	Stable
Phosphate Derivatives	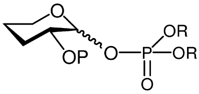	Not stable	Not stable	Not stable
Sulfoxide	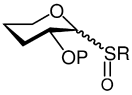	Not stable in the presence of Tf_2O	Not Stable	Could be stable
1-*O*-Silylated Glycoside	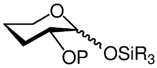	Could be stable	Could be stable	Could be stable
1,2-Anhydro Sugar	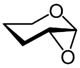	Not stable	Not stable	Not stable
1-Hydroxyl Sugar	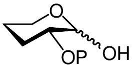	Not stable	Not stable	Not stable
Glycal	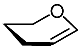	Stable	Not stable	Stable

Downloaded by OHIO STATE UNIV LIBRARIES on June 14, 2012 | http://pubs.acs.org
Publication Date (Web): June 12, 2012 | doi: 10.1021/bk-2012-1102.ch010

However, when considering the systematic synthesis of aminosugars, and their glycosylation, not all these donors are suitable. As shown in Table 1, most of the commonly employed glycosyl donors, such as glycosyl halides, glycosyl acetates, and glycosyl trichloroacetamidates, are not stable enough for the procedures of aminosugar synthesis, especially the incorporation of amino group and deoxygenation. 4-Pentenyl glycoside and glycal could be ideal options. Nevertheless, it is not very cost effective to use these molecules for the preparation of corresponding materials in large quantity.

In addition, the "armed" and "disarmed" effects of protecting groups and azido groups on the reactivity of pyranose further limit the options for suitable donors (*29*, *30*). The reactivity of glycosyl donors can be enhanced with an electron-donating protecting group, such as Bn, leading to the term: armed glycosyl donor. On the other hand, having an electron-withdrawing protecting group, such as Ac, Bz, or azido group, will decrease the reactivity of the glycosyl donor, which is termed as a disarmed donor.

One solution toward this problem is to have a rigid anomeric group that will enable the incorporation of an amino group and other modifications. After which, the anomeric group can be transformed into those functional groups that can serve as glycosyl donors. Following this strategy, methyl glucopyranosides that have a relatively stable anomeric methoxy group, and are available at lower cost, are commonly employed for synthesis of aminosugars. Combining with the concept of divergent synthesis, our group has examined a panel of reagents and completed the synthesis of 4- and/or 6-aminopyranoses. A general protocol with modest to excellent yields for converting diverse modified methyl glycosides into acetyl glycosides was also developed. Acetyl glycopyranosides can be transformed into two different glycosyl donors, glycosyl trichloroacetimidate and phenylthioglycosides, for "disarmed" and "armed" pyranoses following the reported procedures (Scheme 1) (*31*).

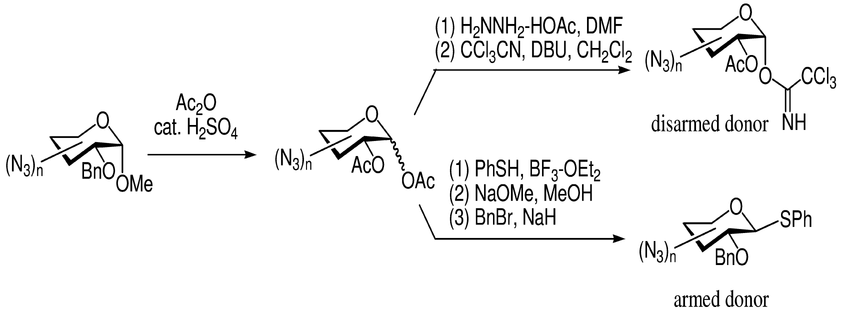

Scheme 1. General Procedure for the Synthesis of Glycosyl Donors

1,2:5,6-di-*O*-isopropylidine-D-glucofuranose is another important starting material since it gives immediate access to the modifications at the 3-OH group. Also, because it can be selectively hydrolyzed to 1,2-*O*-isopropylidine derivatives, further manipulation leading to the synthesis of 3,6-diaminopyranose can be readily achieved (Scheme 2) (*32*). Glucosamine is commonly used for the synthesis of 2-aminopyranoses since it has an amino group at the C-2 position and is of lower cost than galactosamine [e.g., (*33*)].

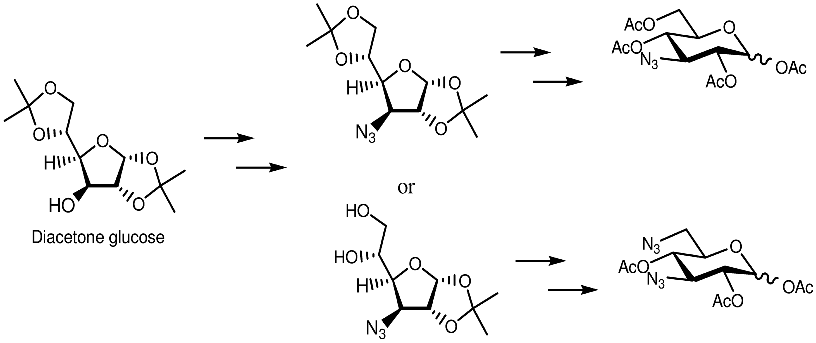

Scheme 2. Examples of Modification of 1,2:5,6-Di-O-isopropylidine-D-glucofuranose

Arylthio or alkylthio groups are resistant toward many organic operations used in aminosugar synthesis, and can be activated for glycosylation directly. Therefore, arylthio or alkylthio-glycosides are often used for the synthesis of aminosugars and corresponding derivatives (*24*). Although ethylthioglycopyranoside, tolylthioglycopyranoside or phenylthioglycopyranoside are expensive to purchase, these compounds can be prepared in large quantities from treating glycose pentaacetate with the corresponding ethanethiol, thiophenol, or *p*-thiocresol under the catalysis of Lewis acids [e.g., (*34*, *35*)]. Our group favors the use of phenylthioglycopyranoside for two reasons. First, unlike ethylthioglycopyranoside, phenylthioglycopyranoside is easy to crystallize and thereby avoids the formidable task of column chromatography. Second, to ensure the completed conversion of glycosyl acetate to the corresponding thioglycoside, excess thiol is often required (*36*) (Note: this recent publication has used 60 mol% MeSSMe for the synthesis of methylthioglycoside. However, the maximum scale for the reported synthesis is 20g. In order to facilitate the library construction of phenylthioglycosides, it is preferable to start from 100 – 200g scale). The excess thiophenol can be readily removed by co-evaporating with other organic solvents, and subsequently bleached for proper disposal. (Note: we have developed method for large-scale synthesis of phenylthioglycosides (100 – 200 g scale), and the product can be purified via recrystallization). However, *p*-thiocresol is a solid at room temperature, making its removal more challenging.

The overall strategy of constructing aminosugar libraries is summarized in Scheme 3. We prefer the use of disarmed trichloroacetimidate glycosyl donor for the formation of the β-glycosidic bond, and armed phenylthio glycosyl donor for the formation of the α-glycosidic bond. In general, trichloroacetimidate donors are more reactive than phenylthio glycosyl donors. Thus, the electron-withdrawing effect in the disarmed donors can be better countered by the higher reactivity of trichloroacetimidate glycosyl donor, while the electron-donating effect in the phenylthio glycosyl donors is advantageous for the less reactive disarmed donors.

Downloaded by OHIO STATE UNIV LIBRARIES on June 14, 2012 | http://pubs.acs.org
Publication Date (Web): June 12, 2012 | doi: 10.1021/bk-2012-1102.ch010

Downloaded by OHIO STATE UNIV LIBRARIES on June 14, 2012 | http://pubs.acs.org
Publication Date (Web): June 12, 2012 | doi: 10.1021/bk-2012-1102.ch010

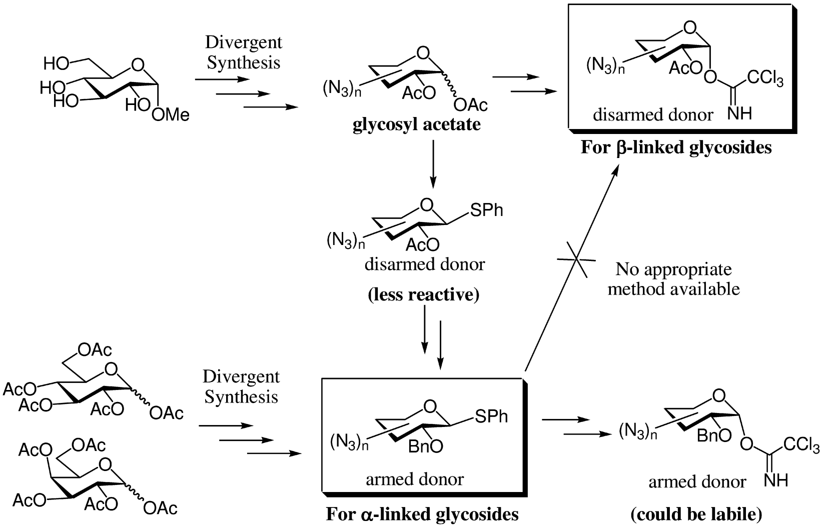

Scheme 3. Overall Concept of Aminosugar Construction

Azido group incorporated glycosyl acetates that can be derived from methyl glucoside are better for the synthesis of disarmed donors bearing an acetyl protecting group at C-2 position, which is designed for the formation of β-linked glycosides. If necessary, these glycosyl acetates can also be converted into phenylthioglycosides. Although the disarmed donors like phenylthioglycosides can be less reactive and give rise to unsatisfactory yield in glycosylation, they can be converted to more reactive armed donors with Bn protecting groups favoring the formation of α-linked glycosides.

Based on our experience, however, it would be more convenient and cost effective to synthesize azido groups incorporated phenylthioglycosides from glucose pentaacetate or galacto pentaacetate. The disadvantage is that these glycosides can only lead to the synthesis of armed donors. To our knowledge and through our unsuccessful attempts, there is no simple method to convert armed donors into disarmed donors once the Bn groups have been incorporated. Incorporation of Bn groups prior to azido group incorporation is, however, necessary since acetyl groups are not stable enough under the chemical conditions employed. The reactivity of armed phenylthio glycosyl donors can be further enhanced by converting the phenylthio group into a trichloroacetimidate group. Nevertheless, such highly reactive armed donors could be too reactive to be properly purified in some of the aminosugar constructs.

1.2. General Synthetic Protocols

To achieve divergent synthesis of aminosugar, four synthetic transformations for the development of general protocols should be considered in advance: regioselective protection and deprotection of hydroxyl groups (for example: cleavage of *O*-benzylidine acetale), epimerization of hydroxyl group, azido (amino) group incorporation, and regioselective deoxygenation. As long as the general protocols for the above-mentioned reactions can be established, a systematic approach for the synthesis designed aminosugars can be envisioned.

1.2.1. Synthesis and Regioselective Cleavage of O-Benzylidine Acetales

There are many protecting groups for pyranoses reported in the literature (*37*, *38*). We are especially interested in the benzylidene-type of protecting group because the 4,6-benzylidene pyranoses can lead to several regioselectively deprotected pyranoses, which is valuable in our divergent synthetic approach (Scheme 4). For example, by using appropriate solvent and reducing agent, the 4,6-benzylidene-protected pyranose can lead to the synthesis of derivatives with either 4-OH or 6-OH (*39*). Alternatively, hydrolysis of benzylidene results in the expose of 4,6-dihydroxyl groups (*40*). In our opinion, the selective protection methods have been well developed for many pyranoses, such as glucose, galactose, and mannose, and hence will not be discussed in detail in this article.

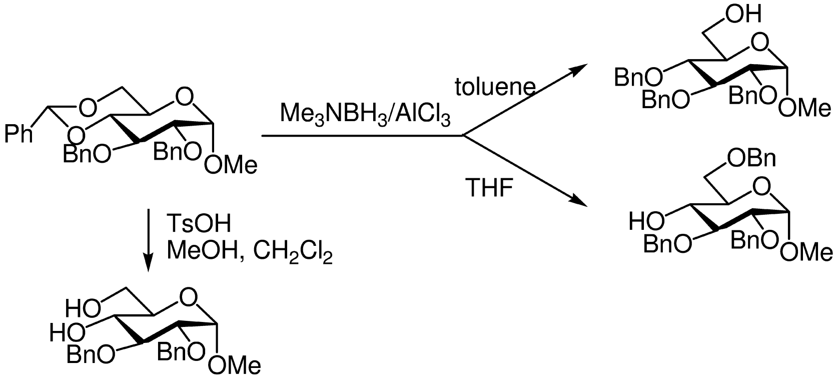

Scheme 4. Sample of Regioselective Opening of 4,6-O-Benzelidene Acetals

1.2.2. Epimerization of Hydroxyl Group

Since the substitution of a hydroxyl group with a nucleophile is often carried out via S_N2 substitution, it is often necessary to stereoselectively epimerize a hydroxyl group on a pyranose scaffold that will allow the installation of the nucleophile with the desired stereochemistry. Four out of five hydroxyl groups in hexopyranose are chiral, therefore stereoselectively epimerizing a hydroxyl group on the glucopyranose and galactopyranose scaffold is essential to expand the possibilities for more sugar manipulation.

There are many well-established methods in the literature, which can be grouped into two types including oxidation-reduction and nucleophilic substitution processes. The former involves an oxidation of a hydroxyl group to

Downloaded by OHIO STATE UNIV LIBRARIES on June 14, 2012 | http://pubs.acs.org
Publication Date (Web): June 12, 2012 | doi: 10.1021/bk-2012-1102.ch010

a keto group followed by stereoselective hydride reduction. In this method, the vicinal protecting groups may influence the stereoselectivity (*41*).

It is also worthy to point out that oxidation of a hydroxyl group using Swern oxidation and reduction of ketone using $NaBH_4$ are compatible to the presence of phenylthiol and azido groups, respectively.

The second method involves converting the secondary hydroxyl group into a leaving group using Tf_2O followed by S_N2 substitution using, for example, OAc^- or NO_2^-, as the nucleophiles. While Tf_2O may activate glycosyl sulfoxide, it is compatible to the presence of phenylthio group. Thus, both oxidation-reduction and nucleophilic substitution reactions can be applied in the synthesis of a glycosyl trichloroacetimidate library and phenyl thioglucopyranoside library. Three commonly used protocols in our laboratory are summarized in Table 2.

Downloaded by OHIO STATE UNIV LIBRARIES on June 14, 2012 | http://pubs.acs.org
Publication Date (Web): June 12, 2012 | doi: 10.1021/bk-2012-1102.ch010

Table 2. Common Protocols for Epimerization of Hydroxyl Group

Types of Transformations	*Examples of Reagents*	*Comments*	*Refs*
Oxidation/reduction (Swern oxidation)	(1) $(COCl)_2$, DMSO DIPEA (2) $NaBH_4$	Vicinal protecting groups (*i.e.* Bn) are essential for the selectivity. However, the selectivity may vary among different sugars. Others (*i.e.* Bz) may offer lower or no selectivity toward epimerization.	(*41*)
S_N2 substitution	(1) Tf_2O (2) $(n\text{-Bu})_4N^+NO_2^-$	$(n\text{-Bu})_4N^+NO_2^-$ can be soluble in CH_2Cl_2, providing better results than reagents like $NaNO_2$. In general, this method offers stereospecific epimerization.	e.g., (*42*, *43*)
S_N2 substitution	(1) Tf_2O (2) $(n\text{-Bu})_4N^+OAc^-$ (3) hydrolysis of OAc	$(n\text{-Bu})_4N^+OAc^-$ can be soluble in CH_2Cl_2, providing better result than reagent like KOAc or CsOAc. In general, this method offers stereospecific epimerization.	e.g., (*44*)

1.2.3. Azido Group Incorporation

The amino group needs to be protected in order to make the synthesis of the glycosyl donor and glycosylation feasible. We favor use of the azido group as an amino group surrogate for the synthesis of aminosugars (or azidosugars). There are several advantages that make the azido group a popular choice. First, the azido group is relatively stable to many reductive and oxidative conditions. Second, unlike the carbamate type protecting group for amines, azido compounds have good solubility in organic media, allowing an expedient chromatographic purification. Third, azido groups can be converted into amino groups conveniently by hydrogenation or the Staudinger reaction. More importantly, an azido group can be easily installed from an activated hydroxyl group via S_N2 substitution and, unlike amino group, no sequential protection is needed. Substitution of a hydroxyl group using the amino or carbamate-protected amino groups as the nucleophiles can be relatively difficult since the protected amino group is not a good nucleophile, while a free amino group can act as a base and cause undesired elimination. Finally, the azido group can be applied to the "click" chemistry creating more diversification opportunities [e.g., (*45–49*)].

Despite the advantage of easy manipulation, one-pot method for the incorporation of azido group is not recommended since it often generates a mixture that complicates the purification of the desired product. In the two-step method, selective tosylation of a primary hydroxyl group in the presence of secondary hydroxyl groups is one of the advantages of employing TsCl. The commonly used protocols are summarized in Table 3.

Table 3. Common Protocols for Azide Substitution

Types of Transformations	*Reagents*	*Typical Conditions*	*Types of Hydroxyl Groups*	*Notes*	*Refs*
One-pot	DPPA (or HN_3), PPh_3 and DEAD	-40° to 0°C, overnight	1° and 2°	Complex mixture may be obtained, difficult to purify	e.g., (*50*)
Two-step	(1) TsCl (2) NaN_3	(1) 0°C to R.T., overnight (2) 80°C, overnight	1° (2° tosylate is difficult to be replaced with N_3^-)	Can be used for selective azide substitution	(*51*)
Two-step	(1) MsCl (2) NaN_3	(1) 0°C to R.T., couple hours (2) 120°C, overnight	1° and 2°	MsCl is cheaper than Tf_2O	e.g., (*52*)
Two-step	(1) Tf_2O (2) NaN_3	(1) 0°C, 0.5 hour (2) R.T., overnight	1° and 2°	Most expedient	(*51*)

Downloaded by OHIO STATE UNIV LIBRARIES on June 14, 2012 | http://pubs.acs.org
Publication Date (Web): June 12, 2012 | doi: 10.1021/bk-2012-1102.ch010

Downloaded by OHIO STATE UNIV LIBRARIES on June 14, 2012 | http://pubs.acs.org
Publication Date (Web): June 12, 2012 | doi: 10.1021/bk-2012-1102.ch010

1.2.4. Regioselective Deoxygenation

Many aminosugars contain the features of deoxygenation. Table 4 summarizes the common protocols for regioselective deoxygenation in the literature. Since azido groups can be reduced under conditions of hydride reduction (e.g. $LiAlH_4$) or radical-initiated deoxygenation (e.g. Barton reduction or dehalogenation) ((*53*, *54*) and references cited therein), deoxygenation generally proceeds before the introduction of the azido group.

Table 4. Common Protocols for Regioselective Deoxygenation

Types of Transformations	Reactions	References
6-deoxy	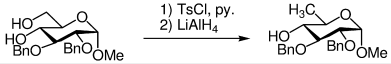	51
4-deoxy	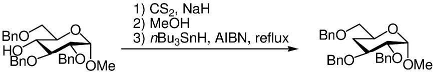	53 and cited therein
3-deoxy	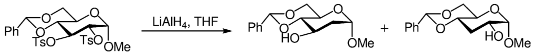	55
3-deoxy	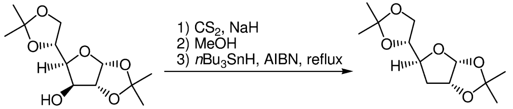	53 and cited therein
2-deoxy	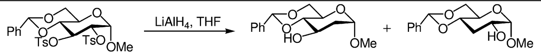	55
2-deoxy	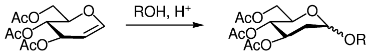	56
4,6-dideoxy	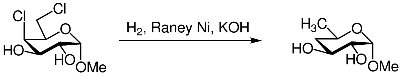	54

1.3. Divergent Synthesis of Glycosyl Trichloroacetimidate Library

The synthesis of our glycosyl trichloroacetimidate aminosugar library began with the commercially available methyl glucopyranoside (Scheme 5). Benzylidine protection, followed by benzylation of C-2 and C-3 hydroxyl groups (*39*, *40*), yielded compound **1**. Compound **1** was treated with $NaBH_3CN/HCl$ in THF to selectively deprotect the C-4 hydroxyl group providing compound **2** (*39*, *40*). Triflation followed by azide substitution of compound **2** generated azidosugar **3** in the *galacto*-configuration. Epimerization of the 4-OH of **2** was achieved with Swern oxidation and $NaBH_4$ reduction offering compound **4**, which allowed a S_N2 azide substitution that furnished azidosugar, **5** in the desired *gluco*-configuration.

Downloaded by OHIO STATE UNIV LIBRARIES on June 14, 2012 | http://pubs.acs.org
Publication Date (Web): June 12, 2012 | doi: 10.1021/bk-2012-1102.ch010

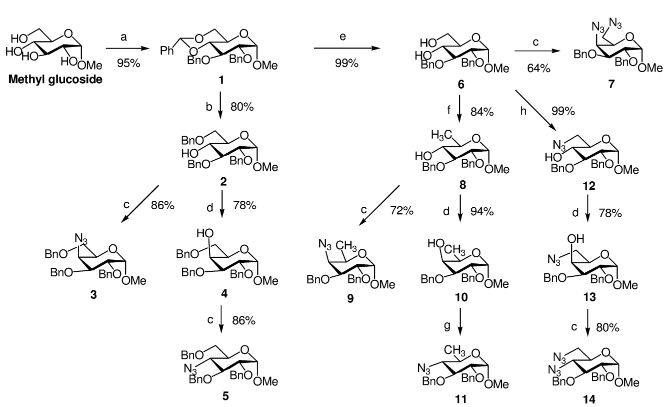

Conditions: (a) (1) $PhCH(OMe)_2$, $TsOH\text{-}H_2O$, DMF, (2) BnBr, NaH, TBAI, THF; (b) $BH_3\text{-}Me_3N$, $AlCl_3$, THF; (c) (1) Tf_2O, py., CH_2Cl_2, (2) NaN_3, DMF; (d) $(COCl)_2$, DMSO, DIPEA, (2) $NaBH_4$, MeOH; (e) $TsOH\text{-}H_2O$, MeOH; (f) (1) TsCl, py, (2) $LiAlH_4$, THF; (g) (1) MsCl, Et_3N, CH_2Cl_2, (2) NaN_3, DMF; (h) (1) TsCl, py, (2) NaN_3, DMF.

Scheme 5. Divergent Synthesis of Glycosyl Trichloroacetimidate Library

In another route, compound **1** was treated with TsOH to give compound **6** with free hydroxyl groups at the C-4 and C-6 positions, which branched into three distinct routes. In the first route, triflation followed by azide substitution of compound **6** provided azidosugar **7** with C-4 and C-6 diazido substituted. In the second route, compound **6** was selectively deoxygenated at the C-6 position by sequential tosylation and $LiAlH_4$ reduction. Compound **8** was subjected to azide substitution generating azidosugar, **9** with C-6 deoxygenation in the *galacto*-configuration. Alternatively, compound **8** underwent the Swern oxidation/$NaBH_4$ reduction protocol to invert the C-4 hydroxyl group that allowed the synthesis of azidosugar, **11** with C-6 deoxygenation in the *gluco*-configuration. In the last path, compound **6** was treated with TsCl, followed by azide substitution to selectively place an azido group on the C-6 position. The free C-4 hydroxyl group in the equatorial position of compound **12** was converted to the axial position yielding compound **13**, which enabled the synthesis of azidosugar **14** with C-4 and C-6 diazido in the *gluco*-configuration.

As described in the previous section, the anomeric methoxy group and all the benzyl groups of these azidosugars can be converted into acetyl groups using Ac_2O with a catalytic amount of H_2SO_4 (Scheme 1). The resulting acetyl glycosides can then be transformed into the glycosyl trichloroacetimidate as the glycosyl donor (*31*), which could then be coupled to the acceptor of choice.

1.4. Divergent Synthesis of Phenylthioglucopyranoside Library

By employing the philosophy of divergent synthesis, and phenylthioglucopyranoside as the starting material, the other library, thioglycopyranoside-based aminosugar library can be constructed in a similar fashion (Scheme 6). We modify the literature procedure, which allows the purification of phenylthioglucopyranoside via recrystallization, and hence

Downloaded by OHIO STATE UNIV LIBRARIES on June 14, 2012 | http://pubs.acs.org
Publication Date (Web): June 12, 2012 | doi: 10.1021/bk-2012-1102.ch010

enables its large scale synthesis (*34–36*) [Note: we have developed method for large-scale synthesis of phenylthioglycosides (100 – 200 g scale), and the product can be purified via recrystallization].

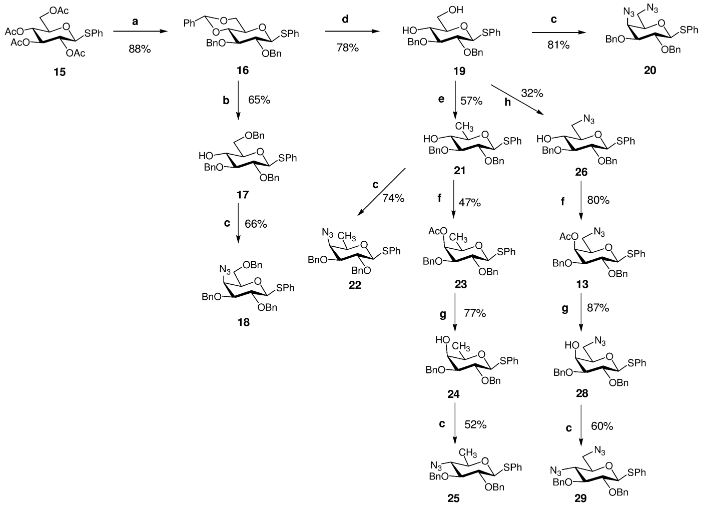

Conditions: (a) (1) NaOMe, MeOH, (2) PhCH(OMe)$_2$, TsOH-H$_2$O, DMF, (3) BnBr, NaH, TBAI, THF; (b) BH$_3$-Me$_3$N, AlCl$_3$, THF; (c) (1) MsCl, Et$_3$N, DMAP, CH$_2$Cl$_2$, (2) NaN$_3$, DMF; (d) TsOH-H$_2$O, MeOH/CH$_2$Cl$_2$; (e) (1) TsCl, py, (2) LiAlH$_4$, THF; (f) (1) Tf$_2$O, py, CH$_2$Cl$_2$, (2) *n*-Bu$_4$NOAc, CH$_2$Cl$_2$; (g) K$_2$CO$_3$, MeOH; (h) (1) TsCl, py, (2) NaN$_3$, DMF.

Scheme 6. Divergent Synthesis of Phenylthioglucopyranoside Library

To avoid the cumbersome epimerization of C-4 free hydroxyl, an alternative route is to use the 2,3-di-*O*-benzyl-4,6-*O*-benzylidene-1-phenylthio-β-D-galactopyranoside instead of glucopyrano-side as starting material (Scheme 7).

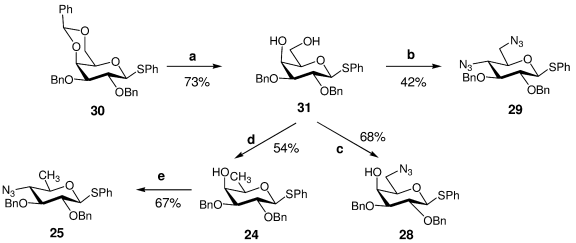

Conditions: (a) TsOH-H$_2$O, MeOH/CH$_2$Cl$_2$; (b) (1) Tf$_2$O, py, CH$_2$Cl$_2$, (2) NaN$_3$, DMF; (c) (1) TsCl, py, (2) NaN$_3$, DMF; (d) (1) TsCl, py, (2) LiAlH$_4$, THF; (e) (1) MsCl, Et$_3$N, DMAP, CH$_2$Cl$_2$, (2) NaN$_3$, DMF.

Scheme 7. Alternative Synthesis Route

As mentioned previously, the C-3 azido group-incorporated sugars can be synthesized from 1,2:5,6-di-*O*-isopropylidine-D-glucofuranose. Further manipulations can be used to synthesize 3,6- or 3,4-diazidopyranoses (Scheme 8).

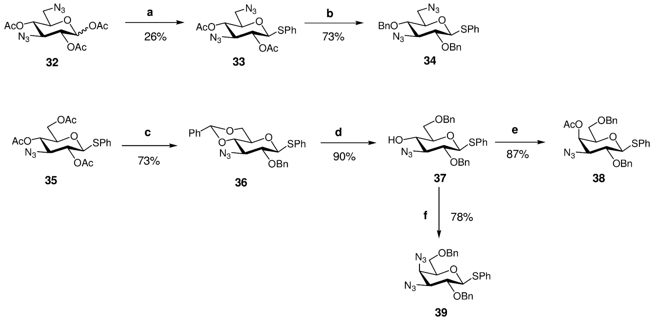

Conditions: (a) PhSH, BF_3-OEt_2, CH_2Cl_2; (b) (1) NaOMe, MeOH, (2) BnBr, NaH, TBAI, THF; (c) (1) NaOMe, MeOH, (2) $PhCH(OMe)_2$, TsOH-H_2O, DMF, (3) BnBr, NaH, TBAI, THF; (d) BH_3-Me_3N, $AlCl_3$, THF; (e) (1) Tf_2O, py, CH_2Cl_2, (2) n-Bu_4NOAc, CH_2Cl_2; (f) (1) Tf_2O, py, CH_2Cl_2, (2) NaN_3, DMF.

Scheme 8. Synthesis of C3-azido Phenylthioglucopyranoside Compounds

2. Stereoselective Glycosylation

2.1. Background in Glycosylation

The development of methodologies for efficient glycosylation reaction, especially *O*-glycosylation reaction, has been a major issue for practical synthesis of oligosaccharides and glycoconjugates. As a result, intense research activities have been devoted to the study of stereoselective glycosylation. However, stereochemical problems in glycosidic bond formation have not been solved completely (*12*, *14*, *57–59*).

Based on the general structure of pyranoses and the chirality of the anomeric center, four possible products can be formed (Figure 3) ((*60*) and references cited therein). The glycosylation, which involves α and β *manno*-type pyranose has been studied extensively by Crich [e.g., (*61–65*)]. Therefore, we will only discuss the α- and β- linkage of *gluco*-type.

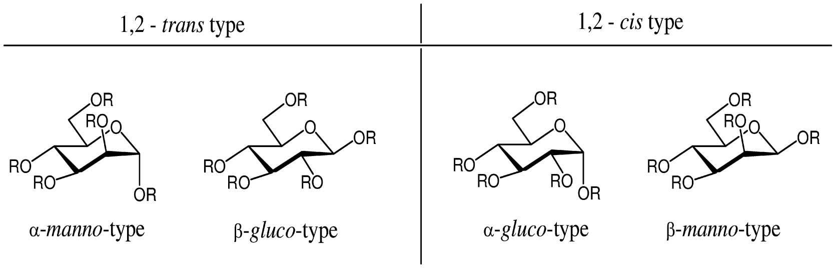

Figure 3. Four Possible Products of Glycosidation

Downloaded by OHIO STATE UNIV LIBRARIES on June 14, 2012 | http://pubs.acs.org
Publication Date (Web): June 12, 2012 | doi: 10.1021/bk-2012-1102.ch010

Downloaded by OHIO STATE UNIV LIBRARIES on June 14, 2012 | http://pubs.acs.org
Publication Date (Web): June 12, 2012 | doi: 10.1021/bk-2012-1102.ch010

2.1.1. Anomeric Effect

In substituted cyclohexanes, the substituents usually prefer the equatorial position due to the steric effects (Figure 4). In rings containing oxygen atoms and with adjacent electronegative substituents there is a preference for this substituent to be *axial*. This is referred as the anomeric effect (*66*). The anomeric effect favors the formation of kinetic product, the α-anomer, for most glycosides.

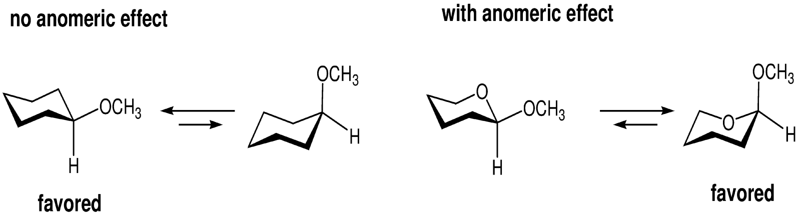
no anomeric effect
with anomeric effect
OCH3
H
O
favored
favored

Figure 4. Anomeric Effect

2.1.2. Protecting Group on O-2 of the Glycosyl Donor

The stereospecific formation of a β-glycosidic bond can be achieved by the presence of an acyl protecting group at the *O*-2 position via neighboring group participation (Figure 5). The formation of an α-glycosidic bond is, however, more challenging, despite great advances. The stereocontrolled synthesis of α-glycosides can be affected by factors such as electronic effects, steric hindrance, solvent, and conformation. To our knowledge, there is no satisfactory general protocol for stereospecific glycosylation for formation of an α-glycosidic bond despite numerous efforts.

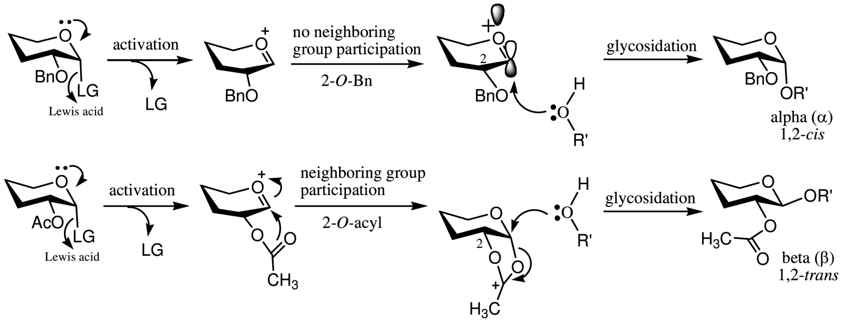
BnO
LG
Lewis acid
activation
LG
no neighboring group participation
2-O-Bn
glycosidation
H
R'
OR'
alpha (α) 1,2-cis
AcO
neighboring group participation
2-O-acyl
CH3
H3C
beta (β) 1,2-trans

Figure 5. Common Mechanism for Glycosidation and the Associated Selectivity

Downloaded by OHIO STATE UNIV LIBRARIES on June 14, 2012 | http://pubs.acs.org
Publication Date (Web): June 12, 2012 | doi: 10.1021/bk-2012-1102.ch010

2.2. Formation of β-Glycosidic Bond: Preparation of Pyranmycin Library

As mentioned previously, our group favors the use of glycosyl trichloroacetimidate library as the glycosyl donor for the formation of β-glycosidic bond leading to the development of the pyranmycin library, a library of neomycin B analogues (Figure 6).

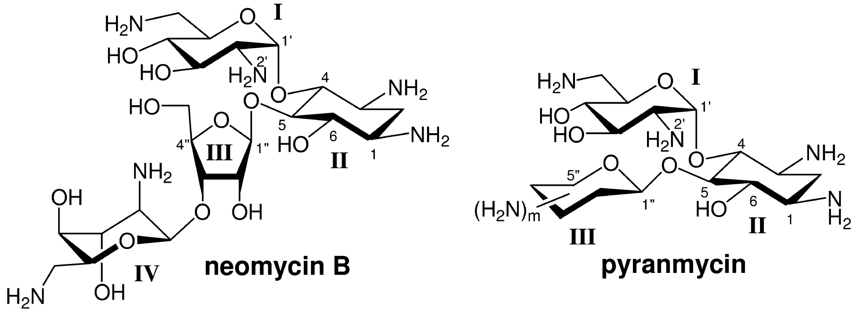

Figure 6. Structures of Neomycin B and Pyranmycin

Neomycin belongs to a group of aminoglycoside antibiotics containing a 4,5-disubstituted 2-deoxystreptamine core (ring II) and has been used against both gram-positive and gram-negative bacteria for more than fifty yearsbv (*5*, *67–69*). The neomycin exerts its antibacterial activity by binding selectively to the A-site decoding region of the 16S ribosomal RNA of bacteria, and thereby disrupts the protein synthesis of these microorganisms.

The design of pyranmycin contains a ring III pyranose that is linked to the *O*-5 of neamine (rings I and II) via a β-glycosidic bond. It is known that neomycin is labile under acidic conditions due to the presence of a glycosidic bond from the ring III furanose. As a result, neomycin degrades readily into less active neamine (rings I and II) and inactive neobiosamine (rings III and IV). Since the corresponding glycosidic bond of pyranmycin is made from a pyranose, this gives pyranmycin better stability to acidic conditions (*70*). Therefore, replacement of neobiosamine with a pyranose will yield a novel aminoglycoside with improved stability in acidic media.

Reported study has also showed that an intramolecular hydrogen bonding between the 2′-amino group of ring I and the *O*-4″ atom of ring III helps to orient ring I for specific binding toward RNA (*71*). Thus, the attachment of ring III via a β-glycosidic bond is crucial in offering the intramolecular hydrogen bonding similar to that in the neomycin. Therefore, our glycosyl trichloroacetimidate library is ideal for incorporation of the desired β-linked pyranoses. With the appropriate neamine aglycon, we have prepared a library of pyranmycin that show comparable activity against *Escherichia coli* (ATCC 25922) and *Staphylococcus aureus* (ATCC 25923) (Scheme 9) (*31*, *51*, *72–74*).

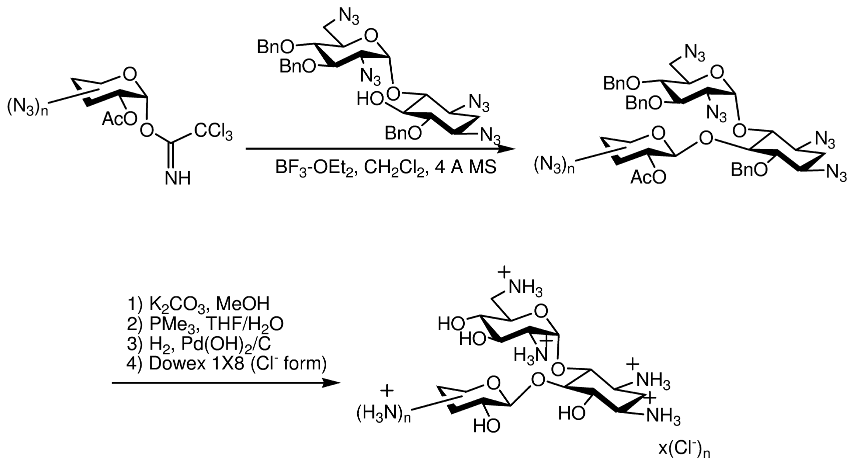

Scheme 9. Synthesis of Pyranmycin Library

2.3. Formation of α-Glycosidic Bond: Preparation of Kanamycin Library

Kanamycin belongs to a group of aminoglycoside antibiotics with 4,6-disubstituted 2-deoxystreptamine (Figure 7) (*5*, *67–69*). Like neomycin, kanamycin also exerts prominent antibacterial activity against both gram positive and gram negative susceptible strains of bacteria. Nevertheless, kanamycin has become clinically obsolete due to the emergence of aminoglycoside resistant bacteria [e.g., (*75–78*). In order to revive the activity of kanamycin against drug resistant bacteria, numerous attempts have been devoted to the chemical modification of kanamycin (*67–69*, *79–81*). Except for a few publications (*82*, *83*), most works use various carbamates as protecting groups for kanamycin resulting in the production of kanamycin with polycarbamate groups. Two drawbacks were often encountered: the poor solubility of polycarbamates, which produce great difficulties in purification and characterization of these compounds, and the limited options for structural modifications imposed by the kanamycin scaffold.

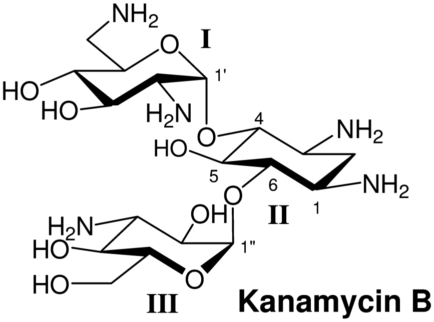

Figure 7. Structures of Kanamycin B

Downloaded by OHIO STATE UNIV LIBRARIES on June 14, 2012 | http://pubs.acs.org
Publication Date (Web): June 12, 2012 | doi: 10.1021/bk-2012-1102.ch010

The α-glycosidic bond between rings II and III is important as the kanamycin analogous with a β-glycosidic bond manifests much weaker antibacterial activity (*84*). Having a 2-*O*-Bn group, our phenylthioglycoside library is preferable for the formation of the needed α-glycosidic bond due to the anomeric effect. The neamine acceptor underwent regiospecific glycosylation at the *O*-6 position resulting in the desired 4,6-disubstituted 2-deoxystreptamine motif. The optimal stereo-selectivity for the formation of the α-glycosidic bond can be accomplished by carrying out the reaction in a solution of Et_2O and CH_2Cl_2 in a 3 : 1 ratio (similar solvent effect in the selectivity of glycosylation can be found in (*85*)). The desired α-glycosylated compounds were often mixed with their inseparable β-epimer. After hydrolysis of the acetyl groups, the triols can be obtained in good purity and improved α/β ratio. The final products (in pure α form or α/β from 10/1 to 7/1) were synthesized as chloride salts using the Staudinger reaction followed by hydrogenation and ion-exchange (Scheme 10) (*86*, *87*). A library of kanamycin B has been prepared via the concept of glycodiversification. These compounds also show comparable activity against *Escherichia coli* (ATCC 25922) and *Staphylococcus aureus* (ATCC 25923).

Downloaded by OHIO STATE UNIV LIBRARIES on June 14, 2012 | http://pubs.acs.org
Publication Date (Web): June 12, 2012 | doi: 10.1021/bk-2012-1102.ch010

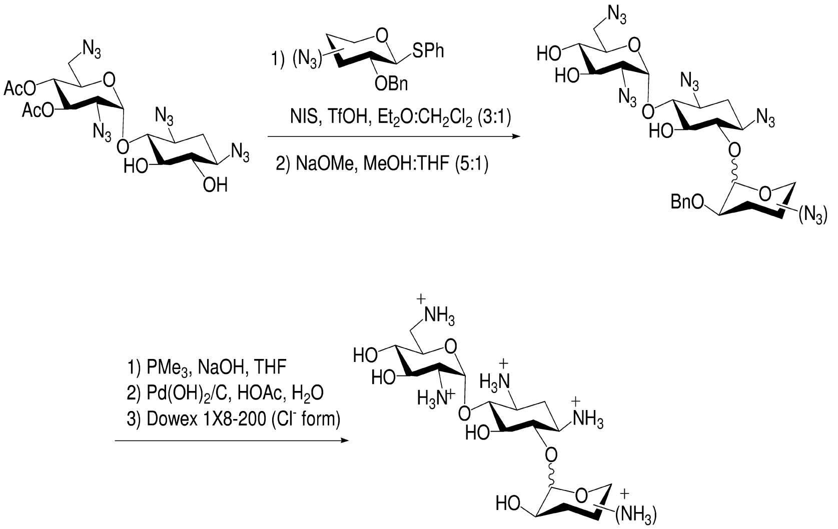

Scheme 10. Synthesis of Kanamycin Analogue Library

3. Conclusion

Carbohydrate synthesis is one of the most formidable tasks in organic synthesis. The synthesis of aminosugar libraries for practical applications represents an even greater challenge. Nevertheless, through the use of standardized protocols and a divergent synthetic approach, systematic procedures have been developed. The advantage of employing two separate aminosugar libraries for stereoselective glycosylation has also been demonstrated in the library construction of pyranmycin and kanamycin B analogues. It is our hope that part of the problem associated with the synthesis and application of aminosugars can be resolved. However, there are several aspects that still require applicable solutions. For example, there is no convenient synthesis of 2-aminopyranose that will favor the stereospecific formation of α-glycosidic bond. The deoxygenation method that is compatible with the presence of an azido group, stereospecific glycosylation for the formation of α-glycosidic bond, and a convenient protocol for the stereoselective glycosylation of 2-deoxyglycopyranoses are several such examples that still need further perfection.

Downloaded by OHIO STATE UNIV LIBRARIES on June 14, 2012 | http://pubs.acs.org
Publication Date (Web): June 12, 2012 | doi: 10.1021/bk-2012-1102.ch010

Note

This is an updated version of a chapter that previously appeared in *Carbohydrate Drug Design* (ACS Symposium Series 932), edited by Klyosov et al. and published in 2006.

References

1. Dwek, R. A. *Chem. Rev.* **1996**, *96*, 683–720.
2. Kirschning, A.; Bechthold, A. F.-W.; Rohr, J. *Top. Curr. Chem.* **1997**, *188*, 1–84.
3. Johnson, D. A.; Liu, H.-W. *Curr. Opin. Chem. Biol.* **1998**, *2*, 642–649.
4. Weymouth-Wilson, A. C. *Nat. Prod. Rep.* **1997**, 99–110.
5. Hooper, I. R. *Aminoglycoside Antibiotics*; Springer-Verlag: New York, 1982.
6. Priebe, W.; Van, N. T.; Burke, T. G.; Perez-Soler, R. *Anticancer Drugs* **1993**, *4*, 37–48.
7. Lothstein, L.; Sweatman, T, W.; Priebe, W. *Bioorg. Med. Chem. Lett.* **1995**, *5*, 1807–1812.
8. Kren, V.; Martinkova, L. *Curr. Med. Chem.* **2001**, *8*, 1313–1338.
9. Brimacombe, J. S. *Angew. Chem., Int. Ed.* **1971**, *10*, 236–248.
10. Umezawa, S.; Tsuchiya, T. In *Aminoglycoside Antibiotics*; Springer-Verlag: New York, 1982; pp 37−110.
11. Jurczak, J. In *Preparative Carbohydrate Chemistry*; Hanessian, S., Ed.; Marcel Dekker, Inc.: NewYork, 1997; pp 595−614.
12. Toshima, K.; Tatsuta, K. *Chem. Rev.* **1993**, *93*, 1503–1531.
13. Nicolaou, K. C.; Mitchell, H. J. *Angew. Chem., Int. Ed.* **2001**, *40*, 1576–1624.
14. Paulsen, H. *Angew. Chem., Int. Ed.* **1982**, *21*, 155–173.
15. Schmidt, R. R. *Angew. Chem., Int. Ed.* **1986**, *25*, 212–235.
16. Demchenko, A. V. *Synlett* **2003**, *9*, 1225–1240.
17. Lemieux, R. U.; Hendriks, K. S.; Stick, R. V.; James, K. *J. Am. Chem. Soc.* **1975**, *97*, 4056–4062.
18. Paulsen, H. *Angew. Chem., Int. Ed.* **1982**, *21*, 184–201.
19. Nicolaou, K. C.; Seitz, S. P.; Papahatjis, D. P. *J. Am. Chem. Soc.* **1983**, *105*, 2430–2434.

20. Konradsaon, P.; Udodong, U. E.; Fraeer-Reid, B. *Tetrahedron Lett.* **1990**, *31*, 4313–4316.
21. Vwneman, G. H.; van Leeuwen, S. H.; van Boom, J. H. *Tetrahedron Lett.* **1990**, *31*, 1331–1334.
22. Dasgupta, F.; Garegg, P. J. *Carbohydr. Res.* **1988**, *177*, c13–c17.
23. Fugedi, P.; Garegg, P. J. *Carbohydr. Res.* **1986**, *149*, c9–c12.
24. Garegg, P. J. *Adv. Carbohydr. Chem. Biochem.* **1997**, *52*, 179–205.
25. Halcomb, R. L.; Boyer, S. H.; Danishefeky, S. J. *Angew. Chem., Int. Ed.* **1992**, *31*, 338–340.
26. Nicolaou, K. C.; Schreiner, E. P.; Iwabuchi, Y.; Suzuki, T. *Angew. Chem., Int. Ed.* **1992**, *31*, 340–342.
27. Jutten, P.; Scharf, H. D.; Raabe, G. *J. Org. Chem.* **1991**, *56*, 7144–7149.
28. Gurjar, M. K.; Viswanadham, G. *Tetrahedron Lett.* **1991**, *32*, 6191–6194.
29. Zhang, Z.; Ollmann, I. R.; Ye, X.-S.; Wischnat, R.; Baasov, T.; Wong, C.-H. *J. Am. Chem. Soc.* **1999**, *121*, 734–753.
30. Ye, X.-S.; Wong, C.-H. *J. Org. Chem.* **2000**, *65*, 2410–2431.
31. Chang, C.-W. T.; Hui, Y.; Elchert, B.; Wang, J.; Li, J.; Rai, R. *Org. Lett.* **2002**, *4*, 4603–4606.
32. Schmidt, O. T. *Methods Carbohydr. Chem.* **1963**, *2*, 318.
33. Alper, P. B.; Hung, S.-C.; Wong, C.-H. *Tetrahedron Lett.* **1996**, *37*, 6029–6032.
34. Tai, C.-A.; Kulkarni, S. S.; Hung, S.-C. *J. Org. Chem.* **2003**, *68*, 8719–8722.
35. Benakli, K.; Zha, C.; Kerns, R. J. *J. Am. Chem. Soc.* **2001**, *123*, 9461–9462.
36. Mukhopadhyay, B.; Kartha, K. P. R.; Russell, D. A.; Field, R. A. *J. Org. Chem.* **2004**, *69*, 7758–7760.
37. Greene, T. W.; Wuts, P. G. M. *Protective groups in Organic Synthesis*, 3rd ed.; John Wiley & Sons: New York, 1998.
38. Kocienski, P. J. *Protective groups*; Georg Thieme Verlag: Stuttgart, New York, 1994.
39. Garegg, P. J. In *Preparative Carbohydrate Chemistry*; Hanessian, S., Ed.; Marcel Dekker, Inc.: New York, 1997; pp 53−67.
40. Garegg, P. J. *Pure Appl. Chem.* **1984**, *56*, 845–858.
41. Chang, C.-W. T.; Hui, Y.; Elchert, Y. *Tetrahedron Lett.* **2001**, *42*, 7019–7023.
42. Poirot, E.; Chang, A. H. C.; Horton, D.; Kovac, P. *Carbohydr. Res.* **2001**, *334*, 195–205.
43. Marcaurelle, L. A.; Bertozzi, C. R. *J. Am. Chem. Soc.* **2001**, *123*, 1587–1595.
44. Dohi, H.; Nishida, Y.; Furuta, Y.; Uzawa, H.; Yokoyama, S.-I.; Ito, S.; Mori, H.; Kobayashi, K. *Org. Lett.* **2002**, *4*, 355–357.
45. Tornoe, C. W.; Christensen, C.; Meldal, M. *J. Org. Chem.* **2002**, *67*, 3057–3064.
46. Kuijpers, B. H. M.; Groothuys, S.; Keereweer, A. R.; Quaedflieg, P. J. L. M.; Blaauw, R. H.; Delft, F. L.; Rutjes, F. P. J. T. *Org. Lett.* **2004**, *6*, 3123–3126.
47. Yang, J.; Hoffmeister, D.; Liu, L.; Fu, X.; Thorson, J. S. *Bioorg. Med. Chem.* **2004**, *12*, 1577–1584.
48. Lin, H.; Walsh, C. T. *J. Am. Chem. Soc.* **2004**, *126*, 13998–14003.

Downloaded by OHIO STATE UNIV LIBRARIES on June 14, 2012 | http://pubs.acs.org
Publication Date (Web): June 12, 2012 | doi: 10.1021/bk-2012-1102.ch010

49. Mocharla, V. P.; Colasson, C.; Lee, L. V.; Röper, S.; Sharpless, K. B.; Wong, C.-H.; Kolb, H. C. *Angew. Chem., Int. Ed.* **2005**, *44*, 116–120.
50. Tanaka, K. S. E.; Winters, G. C.; Batchelor, R. J.; Einstein, F. W. B.; Bennet, A. J. *J. Am. Chem. Soc.* **2001**, *123*, 998–999.
51. Elchert, B.; Li, J.; Wang, J.; Hui, Y.; Rai, R.; Ptak, R.; Ward, P.; Takemoto, J. Y.; Bensaci, M.; Chang, C.-W. T. *J. Org. Chem.* **2004**, *69*, 1513–1523.
52. Takayanagi, M.; Flessner, T.; Wong, C.-H. *J. Org. Chem.* **2000**, *65*, 3811–3815.
53. Barton, D. H. R.; Ferreira, J. A.; Jaszberenyi, J. C. In *Preparative Carbohydrate Chemistry*; Hanessian, S., Ed.; Marcel Dekker, Inc.: New York, 1997; pp 151−172.
54. Szarek, W. A.; Kong, X. In *Preparative Carbohydrate Chemistry*; Hanessian, S., Ed.; Marcel Dekker, Inc.: New York, 1997; pp 105−125.
55. Chang, C.-W. T.; Clark, T.; Ngaara, M. *Tetrahedron Lett.* **2001**, *42*, 6797–6801.
56. Sabesan, S.; Neira, S. *J. Org. Chem.* **1991**, *56*, 5468–5472.
57. Boons, G. J. *Tetrahedron* **1996**, *52*, 1095–1121.
58. Jung, K.-H.; Muller, M.; Schmidt, R. R. *Chem. Rev.* **2000**, *100*, 4423–4442.
59. Hanessian, S.; Lou, B. *Chem. Rev.* **2000**, *100*, 4443–4463.
60. Schmidt, R. R. Jung, K.-H. In *Preparative Carbohydrate Chemistry*; Hanessian, S., Ed.; Marcel Dekker, Inc.: New York, 1997; pp 283−313.
61. Crich, D.; Sun, S. *J. Am. Chem. Soc.* **1998**, *120*, 435–436.
62. Crich, D.; Sun, S. *J. Org. Chem.* **1997**, *62*, 1198–1199.
63. Crich, D.; Smith, M. *Org. Lett.* **2000**, *2*, 4067–4069.
64. Crich, D.; Smith, M. *J. Am. Chem. Soc.* **2001**, *123*, 9015–9020.
65. Crich, D. In *Glycochemistry Principles, Synthesis, and Applications*; Wang, P. G., Bertozzi, C. R., Eds.; Marcel Dekker, Inc.: 2001; pp 53−75.
66. Lemieux, R. U. *Pure Appl. Chem.* **1971**, *25*, 527–548.
67. Haddad, J; Kotra, L. P.; Mobashery, S. In *Glycochemistry Principles, Synthesis, and Applications*; Wang, P. G., Bertozzi, C. R., Eds.; Marcel Dekker, Inc.: 2001; pp 307−351.
68. Wang, J.; Chang, C.-W. T. Design, Chemical Synthesis, and Antibacterial Activity of Kanamycin and Neomycin Class Aminoglycoside Antibiotics. In *Aminoglycoside Antibiotics*; Arya, D. P., Ed.; John Wiley & Sons, Inc.: 2007; pp 141−180.
69. Li, J.; Chang, C.-W. T. *Anti-Infect. Agents Med. Chem.* **2006**, *5*, 255–271.
70. Bochkov, A. F.; Zaikov, G. E. *Chemistry of the O-Glycosidic Bond: Formation and Cleavage*; Pergamon Press: Elmsford, New York, 1979.
71. Fourmy, D.; Recht, M. I.; Blanchard, S. C.; Puglisi, J. D. *Science* **1996**, *274*, 1367–1371.
72. Wang, J.; Li, J.; Tuttle, D.; Takemoto, J.; Chang, C.-W. T. *Org. Lett.* **2002**, *4*, 3997–4000.
73. Li, J.; Wang, J.; Hui, Y.; Chang, C.-W. T. *Org. Lett.* **2003**, *5*, 431–434.
74. Wang, J.; Li, J.; Czyryca, P. G.; Chang, H.; Kao, J.; Chang, C.-W. T. *Bioorg. Med. Chem. Lett.* **2004**, *4*, 4389–4393.
75. Mingeot-Leclercq, M.-P.; Glupczynski, Y.; Tulkens, P. M. *Antimicrob. Agents Chemother.* **1997**, *43*, 727–737.

Downloaded by OHIO STATE UNIV LIBRARIES on June 14, 2012 | http://pubs.acs.org
Publication Date (Web): June 12, 2012 | doi: 10.1021/bk-2012-1102.ch010

76. Kotra, L. P.; Haddad, J.; Mobashery, S. *Antimicrob. Agents Chemother.* **2000**, *44*, 3249–3256.
77. Cohen, M. L. *Science* **2002**, *257*, 1050–1055.
78. Neu, H. C. *Science* **2002**, *257*, 1064–1072.
79. Tanaka, H.; Nishida, Y.; Furuta, Y.; Kobayashi, K. *Bioorg. Med. Chem. Lett.* **2002**, *12*, 1723–1726.
80. Hanessian, S.; Tremblay, M.; Swayze, E. E. *Tetrahedron* **2003**, *59*, 983–993.
81. Hanessian, S.; Kornienko, A.; Swayze, E. E. *Tetrahedron* **2003**, *59*, 995–1007.
82. Seeberger, P. H.; Baumann, M.; Zhang, G.; Kanemitsu, T.; Swayze, E. E.; Hofstadler, S. A.; Griffey, R. H. *Synlett* **2003**, 1323–1326.
83. Chou, C.-H.; Wu, C.-S.; Chen, C.-H.; Lu, L.-D.; Kulkarni, S. S.; Wong, C.-H.; Hung, S.-C. *Org. Lett.* **2004**, *6*, 585–588.
84. Suami, T.; Nashiyama, S.; Ishikawa, Y.; Katsura, S. *Carbohydr. Res.* **1976**, *52*, 187–196.
85. Greenberg, W. A; Priestley, E. S.; Sears, P. S.; Alper, P. B.; Rosenbohm, C.; Hendrix, M.; Hung, S.-C.; Wong, C.-H. *J. Am. Chem. Soc.* **1999**, *121*, 6527–6541.
86. Li, J.; Wang, J.; Czyryca, P. G.; Chang, H.; Orsak, T. W.; Evanson, R.; Chang, C.-W. T. *Org. Lett.* **2004**, *6*, 1381–1384.
87. Wang, J.; Li, J.; Chen, H.-N.; Chang, H.; Tanifum, C. T.; Liu, H.-H.; Czyryca, P. G.; Chang, C.-W. T. *J. Med. Chem.* **2005**, *48*, 6271–6285.

Downloaded by OHIO STATE UNIV LIBRARIES on June 14, 2012 | http://pubs.acs.org
Publication Date (Web): June 12, 2012 | doi: 10.1021/bk-2012-1102.ch010

Downloaded by OHIO STATE UNIV LIBRARIES on June 13, 2012 | http://pubs.acs.org
Publication Date (Web): June 12, 2012 | doi: 10.1021/bk-2012-1102.ch011

Chapter 11

Practical Applications of Computational Studies of the Glycosylation Reaction

Dennis M. Whitfield[1,*] and Tomoo Nukada[2]

[1]Institute for Biological Sciences, National Research Council Canada,
100 Sussex Dr., Ottawa, Ontario, Canada K1A 0R6
[2]The Institute for Physical and Chemical Research (RIKEN), Wako-shi,
351-01 Saitama, Japan
[*]Dennis.Whitfield@nrc-cnrc.gc.ca

A qualitative summary of our canonical vector representation of the conformations of six membered rings and its quantitative application to sugar pyranose rings is presented first. This representation is illustrated for the results of Density Functional Theory (DFT) optimized structures of per *O*-methylated D-*lyxo*, D-*manno* and D-*gluco*-configured oxacarbenium ions where two conformers are consistently found. Nucleophilic attack modelled with methanol is found to lead to intramolecular hydrogen bonding from the hydroxylic proton to electronegative oxygens of the oxacarbenium ion. As well, the ring conformation is found to change with the C-5-O-5--C-1-C-2 torsion angle moving from nearly planar in the isolated cations to more negative values in the case of α-approach and to more positive values for β-attack. This can be favorable or unfavorable depending on the protecting groups present with for example 4,6-benzylidene protection favoring β-attack with D-*manno*-configured ions whereas for D-*gluco*-configured ions α-approach is favorable. Extending the DFT studies to 2-*O*-acetyl analogues finds similar pairs of cations and raises the important issue of the order of ring inversion or O-2 bond rotation during the formation of ring inverted dioxolenium ions which in some cases are calculated to be very stable. Finally, an example using complex constraints is described which led to the design and development of 2,6-dimethylbenzoyl and

In Glycobiology and Drug Design; Klyosov, A.;
ACS Symposium Series; American Chemical Society: Washington, DC, 2012.

2,6-dimethoxybenzoyl as *O*-2 protecting groups which greatly minimize the acyl transfer side reaction.

Introduction

Organic chemistry has a long established principle that by understanding the mechanism of a reaction it should be possible to optimize that reaction. What we wish to present in this chapter is a synopsis of our attempts to understand the mechanism of glycosylation reactions with the goal of optimizing this important reaction. Our technique is the use of modern computational methods, see experimental. Since it is not possible to investigate all aspects of the glycosylation reaction we have focussed on the role of ring conformations. It is hoped that our results will assist experimentalists like us and our collaborators to develop better glycosylation technologies.

This chapter is divided into four sections. The first outlines the new algebra that we have developed to describe the conformations of 6-membered rings that dominate the chemistry of carbohydrates (*1*). The second section shows our current understanding of the conformations of pyranose sugars with all ether protecting groups. The third section considers the implications of section 2 when C-2 is substituted with an acyl group capable of neighboring group participation. The fourth section considers a side reaction, namely acyl transfer to the acceptor alcohol, that is a problematic side reaction associated with neighboring group participation. This is not the chronological order in which these studies were made. It is, however, a more logical choice and should provide the reader with a logical progression of our ideas.

Quantitative Description of Pyranose Ring Conformation Following the IUPAC Nomenclature

In this communication we characterize each pyranose conformer which is derived from the output of a density functional theory (DFT) calculation by a system that uses the familiar IUPAC nomenclature. This definition is not deduced from a 3-dimensional view of a graphical representation of a molecule. In practice the differentiation of a skew conformer from a boat conformer is difficult by visual examination of graphical models. Instead, our definition is based on a numerical basis. We first introduce the concepts of our new definition method. A detailed description is given in (*1*), here we attempt to give a sufficiently simple explanation that all chemists can use.

Why do we need a new definition? The reason follows from the ambiguities of visual examination which partly results from the fact that traditional pyranose ring conformation characterizations are qualitative (*2*). These traditional methods describe visual conformational changes based on symmetry elements, which are intuitively easy to understand, but it is not easy to describe conformational interconversions qualitatively with these methods.

On the other hand, quantitative characterizations have been also developed (e.g., (*3*, *4*)). These quantitative methods are mathematically precise and afford

Downloaded by OHIO STATE UNIV LIBRARIES on June 13, 2012 | http://pubs.acs.org
Publication Date (Web): June 12, 2012 | doi: 10.1021/bk-2012-1102.ch011

a set of numbers which is unique to one pyranose conformation. The basic idea of all of these methods is a projection of pyranose endocyclic torsion angles onto a trigonometric orthonormal system. Such projections use a kind of Fourier transformation and this mathematical rigor insures their preciseness. These mathematical methods are advantageous for a quantitative recognition. However, they lack the visual significances that qualitative methods have. Our new definition aims to have both the visual significance familiar to an organic chemists and the quantitative preciseness for computational purposes.

In particular we aim to elucidate the mechanisms of both enzymatic and experimental glycosylations with computational chemistry. These processes involve conformational changes. of pyranose rings and so we need a robust method to calculate these changes. We also should provide conformational figures which researchers in many fields can easily understand. Therefore, we come to need a new definition having advantages both of qualitative and quantitative methods.

Downloaded by OHIO STATE UNIV LIBRARIES on June 13, 2012 | http://pubs.acs.org
Publication Date (Web): June 12, 2012 | doi: 10.1021/bk-2012-1102.ch011

Quantitative Description of Pyranose Ring Conformation Following the IUPAC Conformational Nomenclature

Since internal ring dihedral angles give the best descriptions of ring distortions, we choose to use the set of six endocyclic dihedral angles as a geometrical parameter. We use the following definitions τ_1(C-1C-2--C-3C-4), τ_2(C-2C-3--C-4C-5), τ_3(C-3C-4--C-5O-5), τ_4(C-4C-5--O-5C-1), τ_5(C-5O-5--C-1C-2) and τ_6(O-5C-1--C-2C-3). A six dimensional space containing only these sets is a closed vector space which includes torsion angle sets of all typical conformations, namely, chairs, boats, skew-boats, half-chairs, and envelopes.

A basic concept of Fourier transformation is a projection of XYZ-Cartesian coordinates onto another orthonormal system. We reasoned that we could use a direct projection of any set onto the vector space defined by sets of typical conformer's torsion angles. As a first step, we should make this vector space defined by typical conformers conforming to the IUPAC conformational nomenclature. This procedure amounts to making quantitative representations of visual conformational changes which chemists can intuitively understand.

Canonical Vector Space and Redundancy Vector Space

We define the canonical vector space (a vector space defined by typical conformers) on the basis of a 3-dimensional sphere as qualitatively analyzed by Hendrickson (*5*). The interrelation diagram among typical conformers can be described as in Figure 1. The two chair conformers occupy the poles and the pseudo-rotation plane consisting of the skew and boat conformers is situated at the mid-point between the two chairs. Any axis connected to the two chairs is orthogonal to the pseudo-rotation plane in this spherical representation. It is therefore easily realized that this canonical vector space could be represented with three basic canonical vectors.

Downloaded by OHIO STATE UNIV LIBRARIES on June 13, 2012 | http://pubs.acs.org
Publication Date (Web): June 12, 2012 | doi: 10.1021/bk-2012-1102.ch011

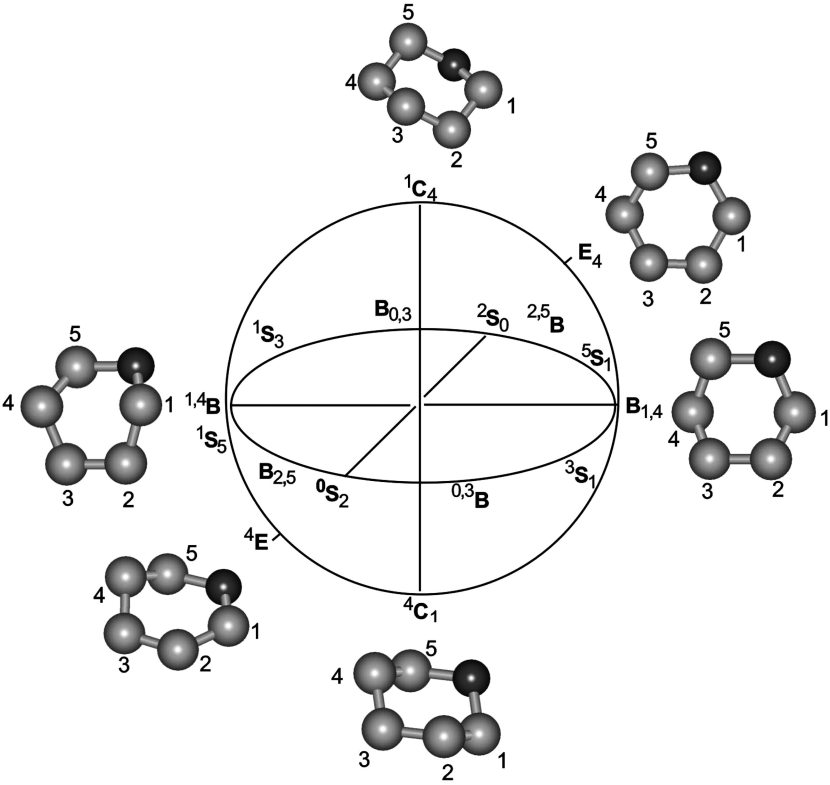

Figure 1. Spherical representation of pyranose conformations. The equatorial circle corresponds to pseudo-rotation.

By contrast, the number of components in the set are the six dihedral angles. Note that older qualitative characterizations use two molecular symmetry elements (σ-plane or C_2-axis). Such qualitative figures give us several hints for making appropriate canonical vectors. That is, each conformer's canonical vector should maintain an adequate symmetry. The presence of symmetry elements means that the sum of components in a canonical vector should be equal to 0. Based on these concepts, we define basic canonical vectors shown in Table 1. In order to precisely conform to the IUPAC convention we adopt 60° as a maximum torsion angle value according to Prelog and Cano (*6*, *7*).

For fitting to chemist's intuition, we define a transition conformer, a half-chair, that is situated at a middle point between chair and skewboat. In a similar manner, the envelope conformers are situated at a middle point between chair and boat, see E_4 and ^4E in Figure 1. By definition the canonical vector space presented by these vectors is isomorphic to 3 dimensional space. This means any point of canonical vector space can be represented adequately by three fundamental vectors. We can handle canonical vectors with the methods of three dimensional Euclidean space vectors. Any point in this space can be described as in equation 1.

Downloaded by OHIO STATE UNIV LIBRARIES on June 13, 2012 | http://pubs.acs.org
Publication Date (Web): June 12, 2012 | doi: 10.1021/bk-2012-1102.ch011

Table 1. Endocyclic torsion angles of 38 basic canonical conformations.

Conformer	τ_1	τ_2	τ_3	τ_4	τ_5	τ_6
$^{1}C_{4}$	60.0	-60.0	60.0	-60.0	60.0	-60.0
$^{4}C_{1}$	-60.0	60.0	-60.0	60.0	-60.0	60.0
$^{1,4}B$	0.0	60.0	-60.0	0.0	60.0	-60.0
$B_{2,5}$	60.0	0.0	-60.0	60.0	0.0	-60.0
$^{O,3}B$	60.0	-60.0	0.0	60.0	-60.0	0.0
$B_{1,4}$	0.0	-60.0	60.0	0.0	-60.0	60.0
$^{2,5}B$	-60.0	0.0	60.0	-60.0	0.0	60.0
$B_{O,3}$	-60.0	60.0	0.0	-60.0	60.0	0.0
$^{1}S_{5}$	30.0	30.0	-60.0	30.0	30.0	-60.0
$^{O}S_{2}$	60.0	-30.0	-30.0	60.0	-30.0	-30.0
$^{3}S_{1}$	30.0	-60.0	30.0	30.0	-60.0	30.0
$^{5}S_{1}$	-30.0	-30.0	60.0	-30.0	-30.0	60.0
$^{2}S_{O}$	-60.0	30.0	30.0	-60.0	30.0	30.0
$^{1}S_{3}$	-30.0	60.0	-30.0	-30.0	60.0	-30.0
$^{1}H_{2}$	45.0	-15.0	0.0	-15.0	45.0	-60.0
$^{3}H_{2}$	60.0	-45.0	15.0	0.0	15.0	-45.0
$^{3}H_{4}$	45.0	-60.0	45.0	-15.0	0.0	-15.0
$^{5}H_{4}$	15.0	-45.0	60.0	-45.0	15.0	0.0
$^{5}H_{O}$	0.0	-15.0	45.0	-60.0	45.0	-15.0
$^{1}H_{O}$	15.0	0.0	15.0	-45.0	60.0	-45.0
$^{4}H_{5}$	-15.0	45.0	-60.0	45.0	-15.0	0.0
$^{O}H_{5}$	0.0	15.0	-45.0	60.0	-45.0	15.0
$^{O}H_{1}$	-15.0	0.0	-15.0	45.0	-60.0	45.0
$^{2}H_{1}$	-45.0	15.0	0.0	15.0	-45.0	60.0
$^{2}H_{3}$	-60.0	45.0	-15.0	0.0	-15.0	45.0
$^{4}H_{3}$	-45.0	60.0	-45.0	15.0	0.0	15.0
^{1}E	30.0	0.0	0.0	-30.0	60.0	-60.0
E_{2}	60.0	-30.0	0.0	0.0	30.0	-60.0
^{3}E	60.0	-60.0	30.0	0.0	0.0	-30.0
E_{4}	30.0	-60.0	60.0	-30.0	0.0	0.0
^{5}E	0.0	-30.0	60.0	-60.0	30.0	0.0
E_{O}	0.0	0.0	30.0	-60.0	60.0	-30.0

Continued on next page.

Downloaded by OHIO STATE UNIV LIBRARIES on June 13, 2012 | http://pubs.acs.org
Publication Date (Web): June 12, 2012 | doi: 10.1021/bk-2012-1102.ch011

Table 1. (Continued). Endocyclic torsion angles of 38 basic canonical conformations.

Conformer	τ_1	τ_2	τ_3	τ_4	τ_5	τ_6
^4E	-30.0	60.0	-60.0	30.0	0.0	0.0
E_5	0.0	30.0	-60.0	60.0	-30.0	0.0
^OE	0.0	0.0	-30.0	60.0	-60.0	30.0
E_1	-30.0	0.0	0.0	30.0	-60.0	60.0
^2E	-60.0	30.0	0.0	0.0	-30.0	60.0
E_3	-60.0	60.0	-30.0	0.0	0.0	30.0

P is a point in the canonical space. **Ec** is a vector among chair, envelope, or half-chair basic canonical vectors.

Ea, **Eb**, (**Ea** ≠ **Eb**, **Ec** ≠ **Eb**, **Ec** ≠ **Ea**) are two arbitrary orthogonal basic canonical vectors.

fa, fb and fc are scalar coefficients.

$$\mathbf{P} = \mathrm{fa}\cdot\mathbf{Ea} + \mathrm{fb}\cdot\mathbf{Eb} + \mathrm{fc}\cdot\mathbf{Ec} \qquad (\mathbf{1})$$

Since any vector in this canonical space can be presented by a linear combination of three basic canonical vectors this canonical space is a vector space. Therefore, we can define metric characters, inner product and absolute value in the same manner as those of a vector space.

$|\mathbf{E}|^2 = (\mathbf{E}, \mathbf{E})$, $|\mathbf{E}|>0$, an absolute value of vector **E**, (**E**,**E**) inner product.

We also use another metric character corresponding to an angle between two vectors of Euclidean space.

$$F = (\mathbf{E},\mathbf{P})/|\mathbf{E}|\cdot|\mathbf{P}|, \quad 0 \leq F \leq 1 \qquad (\mathbf{2})$$

The scalar, F, in equation (2) is an indicator of closeness between two vectors. When we want to assign a conformation of a vector in a simple way, it is straightforward to calculate F between the vector and each basic canonical vector shown in Table 1. A basic canonical vector giving maximum F is closest to the target vector. When F is equal to 0, the two vectors are orthogonal to each other. For example, a chair vector is orthogonal to any vector, skew or boat, in the pseudo-rotational plane.

For quantitative definition of this canonical space, we defined three basic canonical vectors, namely, $\mathbf{^1C_4}$, $\mathbf{^0S_2}$, and $\mathbf{^{1,4}B}$ vectors as basis sets. These vectors are orthogonal to each other and can be used as reference ideal conformers in chemist's discussions. This basis set selection, one chair, one skewboat and one boat, from the pseudo-rotation plane is in line with the qualitative figure of Hendrickson. Of course, 11 other combinations are available for this purpose.

The three orthogonal basis sets confirm a straightforward recognition because of being isomorphic to three dimensional Euclidean space.

We have discussed that for example an idealized pyranose conformation corresponding exactly to one of the IUPAC standard conformations should have a symmetry element. However, real molecules we encounter are distorted from such exact symmetric conformations. We define redundancy vectors, which are residual vectors out of a projection with the canonical vectors (three basis sets, chair, skew-boat, and boat). This redundancy is not significant in carbohydrate pyranose rings. It is, however, not negligible for some six-membered rings involving transition metals where bond lengths and bond angles are far from equal or tetrahedral respectively.

We have not precisely analyzed the details of these redundancy vectors. From our basic ideas about canonical vector space, we predict that during motions of pyranose rings, these molecules produce the redundancy in cases of symmetrical motions being energetically disfavored. This redundancy appears to originate from breaking the structural symmetry of the molecule. Most carbohydrate pyranose molecules are only slightly asymmetric and therefore they only produce small amounts of redundancy. We define 3 redundancy basis set vectors as in Table 2.

Downloaded by OHIO STATE UNIV LIBRARIES on June 13, 2012 | http://pubs.acs.org
Publication Date (Web): June 12, 2012 | doi: 10.1021/bk-2012-1102.ch011

Table 2. Redundancy vectors.

Vector	τ_1	τ_2	τ_3	τ_4	τ_5	τ_6
Red1	60	60	60	60	60	60
Red2	0	60	60	0	60	60
Red3	60	30	-30	-60	-30	30

Each redundancy vector is orthogonal to any of the canonical vectors and is orthogonal to the other two redundancy vectors. With redundancy basis set vectors, six-membered rings could not be built. We consequently present a conformer with using a set of endocyclic torsion angles.

P a vector of endocyclic torsion angles on an arbitrary conformation.

$^{1}\boldsymbol{C_4}$ the canonical vector of conformation $^{1}C_4$ in Table 1.

$^{0}\boldsymbol{S_2}$ the canonical vector of conformation $^{O}S_2$ in Table 1.

$^{1,4}\boldsymbol{B}$ the canonical vector of conformation $^{1,4}B$ in Table 1.

Red1, **Red2**, **Red3**, the redundancy vectors in Table 2.

f1, f2, f3, f4, f5, f6 scalar coefficients.

$$\mathbf{P} = \mathrm{f1}\cdot{}^{1}\boldsymbol{C_4} + \mathrm{f2}\cdot{}^{0}\boldsymbol{S_2} + \mathrm{f3}\cdot{}^{1,4}\boldsymbol{B} + \mathrm{f4}\cdot\mathbf{Red1} + \mathrm{f5}\cdot\mathbf{Red2} + \mathrm{f6}\cdot\mathbf{Red3} \qquad (\mathbf{3})$$

With equation (3), one conformer is mapped uniquely to the vector space which is built by three canonical basis set vectors and three redundancy basis set vectors. A convenient method of conformational characterization is to use only the first three terms, three canonical basis set vectors in the equation (3).

Downloaded by OHIO STATE UNIV LIBRARIES on June 13, 2012 | http://pubs.acs.org
Publication Date (Web): June 12, 2012 | doi: 10.1021/bk-2012-1102.ch011

So, a pyranose conformation and a conformational change can be represented with XYZ-coordinates or polar coordinates. As mentioned above, we make a new definition method which has advantages both of quantitative and qualitative methods.

Quantitative methods have advantages for illustrating pyranose conformational changes. Our new method inherits this strong point. Distortions from initial conformers can be visually and quantitatively understood with our method from the magnitude and type of distortion. For example we have used this canonical vector space for a constraint in molecular dynamic simulations of pyranose conformation change. Since we are interested in glycosylation reactions we need also to consider bond breaking and bond forming therefore with this quantitative formulation we can use such constraints in quantum molecular dynamics (*8*).

Permethylated Glycopyranosyl Oxacarbenium Ions - The Two Conformer Hypothesis

We confine our discussion in Sections two to four, to glycosylation reactions between pyranose sugars in which one sugar acts as an electrophilic donor reacting with a nucleophilic alcohol. This encompasses most, but not all experimental methods for glycosylation.

Early kinetic studies showed that, except for reactions of very strong nucleophiles where true S_N2 kinetics could be observed, most glycosylation reactions have considerable S_N1 character (*9*). This strongly implies that glycopyranosyl oxacarbenium ions are likely formed as intermediates or transitions states (TS). In all such cases the anomeric carbon must obtain appreciable sp^2 character. In most donors before activation the anomeric carbon is sp^3 hybridized and in the product glycosides it is also sp^3 hybridized. Therefore as a glycosylation reaction proceeds the anomeric carbon proceeds from sp^3 to sp^2 and back to sp^3. These changes have pronounced consequences for the conformation of the 6-membered pyranose ring.

It should be noted that the classical 5-coordinate *anti* S_N2 TS also requires the anomeric carbon to obtain a transient planar conformation. Although the details are clearly different, the concepts are similar. To describe these ring conformational changes we use the formalism developed in Section 1.

In a real glycosylation reaction the donor must be activated by a promoter or catalyst in a solvent. The reaction must also be kept free of adventitious water and any other nucleophiles that could compete with the alcoholic acceptor. As well, the proton of the acceptor must be transferred and some base must ultimately take up these protons. These realities make the reaction much more complicated than our models. However, it is our goal to assess the importance of the pyranose ring conformation especially in the intermediates and TS of the reaction.

The progress of glycosylation reactions is difficult to follow experimentally and usually the most one can measure is the disappearance of starting material and the appearance of products as a function of time. Importantly, it is difficult to detect transient intermediates if they are formed. In fact, in most cases all the data that is reported is the overall yield and the α:β ratio of the products. Typically, predominant or exclusive formation of one isomer is attributed to S_N2 attack on a reactive intermediate and approximately 50:50 α:β mixtures attributed to non-specific attack on a free oxacarbenium ion i.e. S_N1. Thus, it was a great surprise to us to discover that calculated intermediates between glycopyranosyl oxacarbenium ions and the achiral nucleophile methanol exhibited marked stereoselectivity.

Furthermore, in all cases studied to date the calculated intermediate with the lowest energy corresponds to the generally preferred anomer of the product. This unanticipated result led us to completely revise our thinking about the origin of the stereochemistry of glycosylation reactions.

How do we calculate these intermediates? First for these examples, we choose *O*-methyl substituted glycopyranosyl oxacarbenium ions[i] by suitable *in silico* modifications to optimized chair conformations of the parent per *O*-methyl glycopyranose. With these species there are no hydroxyls and hence no intramolecular hydrogen bonding. Conformations with intramolecular hydrogen bonding are found as the lowest energy ones by gas phase calculations of neutral monosaccharides and this factor may obscure other factors influencing reactivity (*10–14*).

Methyl is also the smallest possible protecting group and begins to address the important issue of the effect of protecting groups on reactivity. In agreement with other calculations of permethylated sugars and experimental studies with model compounds, the preferred conformation of secondary *O*-methyl substituents is to have the methyl carbon *syn* to the sugar methane (*15*). These species with these *O*-methyl conformations are then subjected to minimization using Density Functional Theory (DFT) calculations. Visual analysis of graphical images of this first optimized structure is then performed to check for side chain orientations.

All appropriate side chain conformations are altered until a good structure is found which is then checked to be a minima by frequency calculations. These calculations include a continuum solvent (parameterized to CH_2Cl_2) correction and energies are corrected for Zero Point Energy (ZPE). Alternatively, different conformations may be generated by *in silico* modifications of one of the 38 standard IUPAC conformations of tetrahydropyran followed by the DFT optimization with side chain optimization process described above. These 38 conformations are shown in Table 1.

The DFT calculations were carried out with the Amsterdam Density Functional (ADF) program system, ADF2000 (*16–20*). The atomic orbitals were described as an uncontracted double-ζ Slater function basis set with a single-ζ polarization function on all atoms which were taken from the ADF library. The 1s electrons on carbon and oxygen were assigned to the core and treated by the frozen core approximation. A set of s, p, d, f, and g Slater functions centered on all nuclei were used to fit the electron density, and to evaluate the Coulomb and exchange potentials accurately in each SCF cycle.

The local part of the V_{xc} potential (LDA) was described using the VWN parameterization (*21*), in combination with the gradient corrected (CGA) Becke's functional (*22*) for the exchange and Perdew's function for correlation (BP86) (*23*). The CGA approach was applied self-consistently in geometry optimizations. Second derivatives were evaluated numerically by a two point formula. The

Downloaded by OHIO STATE UNIV LIBRARIES on June 13, 2012 | http://pubs.acs.org
Publication Date (Web): June 12, 2012 | doi: 10.1021/bk-2012-1102.ch011

solvation parameters were dielectric constant ε =9.03, ball radius =2.4 angstroms, with atomic radii of C=1.7, O=1.4 and H=1.2 angstroms.

As a first example consider 2,3,4-tri-*O*-methyl-D-lyxopyranosyl cation, **1**. Two conformers were found that differ by ring inversion, see Figure 2. One conformer, **B0**, is the $^4H_3$ conformation, long considered a probable conformation for such glycopyranosyl oxacarbenium ions. In terms of the C, B and S terms (Section 1) it is $^4C_1$ 0.573, $B_{2,5}$ 0.059 and $^1S_3$ 0.389 i.e. approximately half a chair and half a twist boat therefore a half chair; $^4H_3$ 0.778. The second conformer, **B1**, has the $^3H_4$ conformation which is $^1C_4$ 0.580, $B_{2,5}$ 0.100 and $^3S_1$ 0.486 and therefore $^3H_4$ 0.972. In this conformation the substituents at O-3 and O-4 are pseudo-axial whereas the substituent at O-2 is pseudo-equatorial. The terms with small coefficients show not only how the dominant conformation is distorted but precisely measure the degree of distortion.

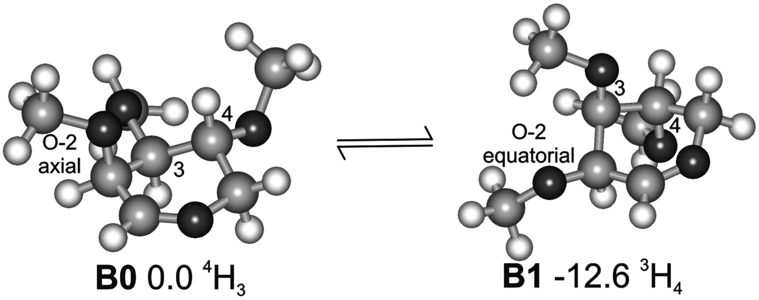

*Figure 2. Ball and Stick Representations of 2,3,4-tri-O-methyl-D-lyxopyranosyl cation, **1**, in its **B0** and **B1** Conformations, showing relative energies in kJ mol^{-1}*

Considering that axial substituents are normally considered to be destabilizing it is surprisingly that this **B1** conformer is calculated to be 12.6 kJ mol^{-1} more stable than **B0**. This energy difference is sufficiently high that, if the barrier separating these conformers is low enough, and the lifetime of these ions is long enough, than **B1** should be the dominant species present. Specific solvation, ion-pairing, nucleophile preassociation and the effects of different protecting groups are all expected to modify this intrinsic selectivity. Note, for most synthetic purposes even if all ether protecting groups are used the stereoelectronic effects of protecting groups are expected to have an effect. This result, i.e. two conformers, does give the experimentalist a place to start their analysis from, which is our present goal.

Consideration of α or β-nucleophilic attack on **B0** and **B1** of **1** leads to four cases to consider. Using methanol as model nucleophile in order to avoid most issues of the stereoelectronic effects of protecting groups of the acceptor on stereoselectivity DFT calculations of the four possible cases were made (*24–26*). Values are: **1**(**B0**)+αMeOH -19.3 kJ mol^{-1}, **1**(**B0**)+βMeOH -48.9 (-20.9) kJ mol^{-1}, **1**(**B1**)+αMeOH -35.6 (-17.6) kJ mol^{-1}, **1**(**B1**)+βMeOH -64.6 (-36.6) kJ mol^{-1} (in brackets corrected for H-bonding, see below).

The results are best viewed by looking at the spherical representation of the conformations of 6-membered rings, see Figure 3. This shows the changes in conformation from the isolated cation to the ion:dipole complexes. Examination

Downloaded by OHIO STATE UNIV LIBRARIES on June 13, 2012 | http://pubs.acs.org
Publication Date (Web): June 12, 2012 | doi: 10.1021/bk-2012-1102.ch011

Downloaded by OHIO STATE UNIV LIBRARIES on June 13, 2012 | http://pubs.acs.org
Publication Date (Web): June 12, 2012 | doi: 10.1021/bk-2012-1102.ch011

of a number of such complexes has led to the recognition of two important variables (*27*). One factor is intramolecular hydrogen bonding between the nucleophilic hydroxyl proton and the electronegative atoms of the oxacarbenium ions especially in cases where the species have appreciable hydronium ion character. The relative energetics of this effect are over estimated because intermolecular hydrogen bonding is not considered but it still is considered to be an important factor.

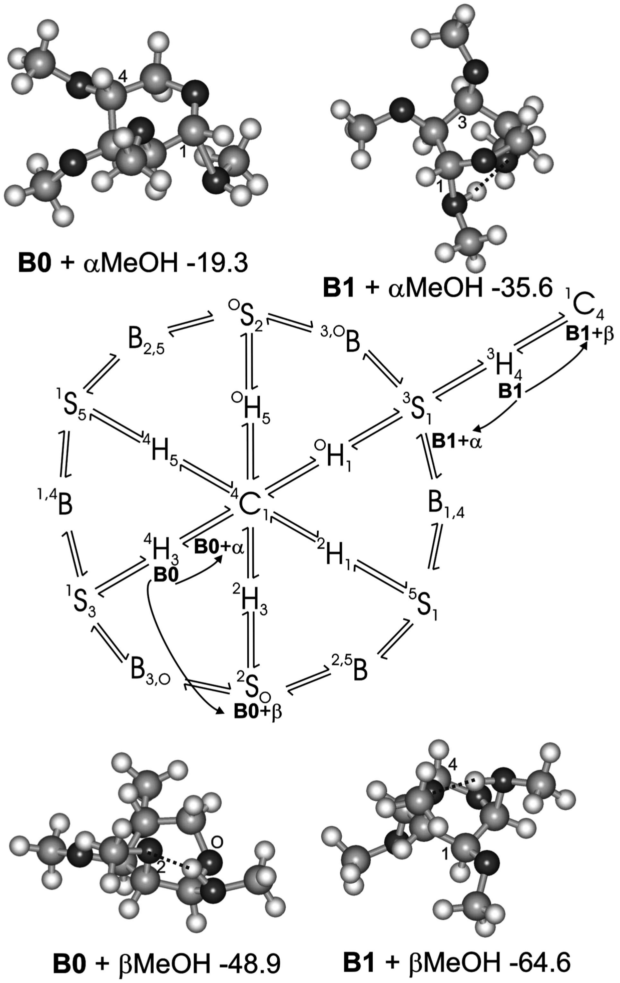
4
1
B0 + αMeOH -19.3
3
1
B1 + αMeOH -35.6
$^{1}C_{4}$
B1+β
$^{O}S_{2}$
$B_{2,5}$
$^{3,O}B$
$^{3}H_{4}$
B1
$^{1}S_{5}$
$^{O}H_{5}$
$^{3}S_{1}$
B1+α
$^{4}H_{5}$
$^{O}H_{1}$
$^{1,4}B$
$^{4}C_{1}$
$B_{1,4}$
$^{4}H_{3}$
B0+α
B0
$^{2}H_{1}$
$^{1}S_{3}$
$^{2}H_{3}$
$^{5}S_{1}$
$B_{3,O}$
$^{2,5}B$
$^{2}S_{O}$
B0+β
4
O
2
1
B0 + βMeOH -48.9
B1 + βMeOH -64.6

*Figure 3. Planar Representation of the Spherical Representation of Pyranose Ring Conformations Showing the Positions of the Parent **B0** and **B1** Conformers of **1** and the results of α- or β-Attack. Ball and Stick Representations of the Resulting Ion:Dipole Complexes of **1** and Methanol, showing relative energies in kJ mol^{-1}.*

Downloaded by OHIO STATE UNIV LIBRARIES on June 13, 2012 | http://pubs.acs.org
Publication Date (Web): June 12, 2012 | doi: 10.1021/bk-2012-1102.ch011

Secondly, the change in pyranosyl ring conformation from the isolated cation to the ion:dipole complex can be favorable or unfavorable. In all the isolated cations the C-5-O-5--C-1-C-2 (τ_5) torsion angle is nearly planar, for **1** **B0** it is -10.6° and for **1** **B1** it is 5.2°. For the D-sugars considered so far, this torsion angle increases for β-attack and decreases for α-attack.

For **1** α-attack ion:dipole complexes shift the pyranosyl ring conformation by lowering the C-5-O-5--C-1-C-2 torsion angle by 9° and 44.9° for **B0** and **B1** respectively. Whereas β-attack raises it by 31.7° and 45.2° for **B0** and **B1**. Both β-complexes allow for hydrogen bonding with the **B0** conformer exhibiting an acutely angled H-bond to the pseudo-axial O-2 and for the **B1** conformer a nearly linear H-bond to the pseudo-axial O-3 was found.

For α-attack on **B1** a H-bond to pseudo-axial O-4 was found, whereas for α-attack on **B0** no hydrogen bonds were found. Ball and stick representations of these structures are shown in Figure 3. The result of these effects is to put the **B0** + αMeOH in a $^4C_1$ conformer which is close to the starting $^4H_3$ whereas **B0** + βMeOH shifts to the less favourable ^2S_O conformer. This **B0** + αMeOH conformation is favourable for α-attack but the absence of hydrogen bonding probably underestimates the stability of this complex.

On the other hand the **B1** + αMeOH is in the unfavourable $^3S_1$ conformation whereas the **B1** + βMeOH is in the favourable $^1C_4$ chair as well as having a strong intramolecular hydrogen bond. Therefore it is not surprising that this is predicted to be the most stable complex and hence β-glycosides are predicted to be the preferred products. Indeed our experimental results with a 2,3,4-tri-*O*-benzyl-D-lyxopyranosyl donor predominantly give β-glycosides.

D-lyxopyranose has the same configurations at C-2, C-3 and C-4 as D-mannopyranose and from the results with **1** could be expected to preferentially yield β-glycosides in glycosilation reactions. Since even ether protected D-mannopyranosyl donors usually give predominantly α-glycosides this suggests an important stereodirecting role for the substituent at C-5 in hexopyranoses. DFT calculations on 2,3,4,6-tetra-*O*-methyl- mannopyranosyl cation **2** provide some support for this hypothesis (*28*).

Again two conformers that differ by ring inversion were found for the *manno* cation. With **B0** characterized as $^4C_1$ 0.566, $B_{2,5}$ 0.043 and $^1S_3$ 0.397 therefore $^4H_3$ 0.793 and the inverted **B1** conformations characterized as $^1C_4$ 0.522, $^{O,3}B$ 0.432 and $^5S_1$ 0.048 therefore ^3E 0.864 (ΔE 1.9 kJ mol^{-1}). The ^3E conformation is near in configurational space to $^3H_4$ as visualized on the planar representation of the spherical representation, Figure 4a. The calculated C-5--C-6 torsion angle defined as ω_H (H-5C-5--C-6O-6) was found to be -178.7° (gg) for **B0** and -50.8° (gt) for **B1**. This shift for **B1** perhaps reflects the pseudo-axial orientation of O4.

Downloaded by OHIO STATE UNIV LIBRARIES on June 13, 2012 | http://pubs.acs.org
Publication Date (Web): June 12, 2012 | doi: 10.1021/bk-2012-1102.ch011

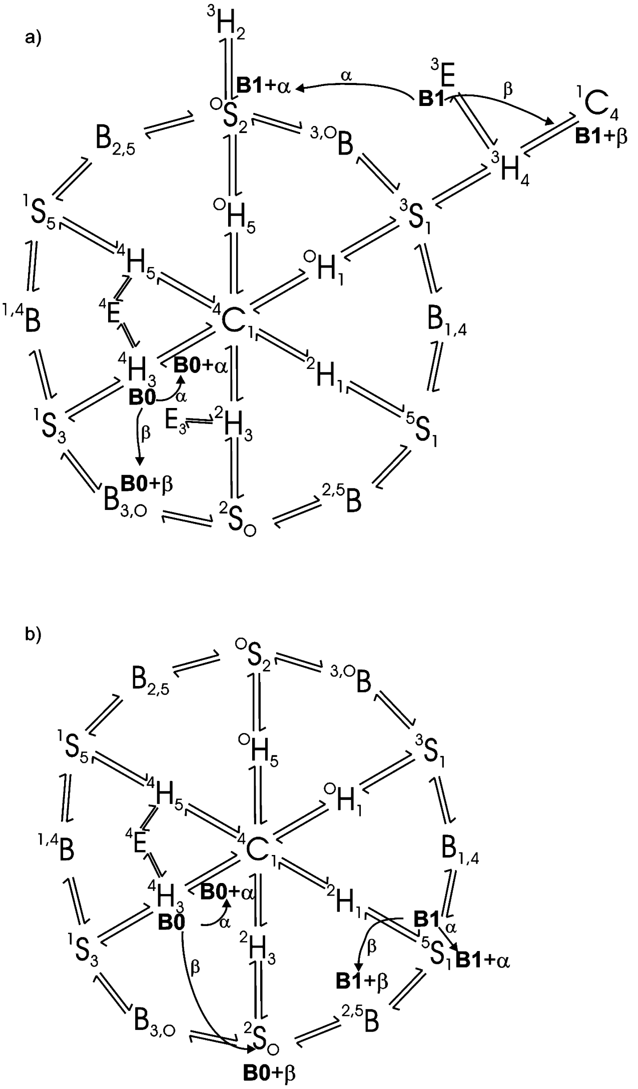
a)
$^{3}H_{2}$
B1+α
α
^{3}E
B1
β
$^{1}C_{4}$
B1+β
$^{O}S_{2}$
$B_{2,5}$
$^{3,O}B$
$^{3}H_{4}$
$^{1}S_{5}$
$^{O}H_{5}$
$^{3}S_{1}$
$^{4}H_{5}$
$^{O}H_{1}$
$^{1,4}B$
^{4}E
$^{4}C_{1}$
$B_{1,4}$
$^{4}H_{3}$
B0+α
$^{2}H_{1}$
B0
α
β
E_{3}
$^{2}H_{3}$
$^{1}S_{3}$
$^{5}S_{1}$
B0+β
$B_{3,O}$
$^{2}S_{O}$
$^{2,5}B$
b)
$^{O}S_{2}$
$B_{2,5}$
$^{3,O}B$
$^{1}S_{5}$
$^{O}H_{5}$
$^{3}S_{1}$
$^{4}H_{5}$
$^{O}H_{1}$
$^{1,4}B$
^{4}E
$^{4}C_{1}$
$B_{1,4}$
$^{4}H_{3}$
B0+α
$^{2}H_{1}$
B0
α
B1
α
β
$^{2}H_{3}$
$^{1}S_{3}$
$^{5}S_{1}$
B1+α
B1+β
$B_{3,O}$
$^{2}S_{O}$
$^{2,5}B$
B0+β

Figure 4. Planar Representation of the Spherical Representation of Pyranose Ring Conformations Showing the Positions of the Parent ***B0*** *and* ***B1*** *Conformers of* ***2*** *and* ***3*** *plus the Consequences of α- or β-Attack on Each. Top (a) Man* ***2*** *and Bottom (b)* ***3****.*

For **2** the β-face complexes are calculated to be more stable than those for α-face complexes. Values are: **2**(**B0**)+αMeOH -21.3 kJ mol^{-1}, **2**(**B0**)+βMeOH -51.3 (-23.3) kJ mol^{-1}, **2**(**B1**)+αMeOH -30.9 kJ mol^{-1}, **2**(**B1**)+βMeOH -49.5 (-21.5) kJ mol^{-1} (in brackets corrected for H-bonding). Most of this extra stabilization comes from hydrogen bonding to O-6 even though this forces the ring into a $B_{O,3}$ (**B0**) or an inverted $^{1}C_{4}$ (**B1**) conformations, respectively. The second consequence of hydrogen bonding is a shorter O_m--C-1 bond length. Values are: **2**(**B0**)+αMeOH 1.860 Å, **2**(**B0**)+βMeOH 1.498 Å, **2**(**B1**)+αMeOH 1.672 Å, **2**(**B1**)+βMeOH 1.510 Å.

Previously, we had estimated the energetic contribution of hydrogen bonding to be 28 kJ mol^{-1} by calculating for a deoxy analogue in the same conformation as the parent oxygen containing hydrogen bond accepting compound (*27*). These "corrected" values show the expected trend of α more favorable than β for mannopyranosyl donors.

Similar DFT calculations with 2,3,4,6-tetra-*O*-methyl-glucopyranosyl cation **3** test the effect of the configuration at C-2. Again two conformers were found with **3**(**B0**) characterized as $^{4}C_{1}$ 0.507, $B_{2,5}$ 0.015 and $^{1}S_{3}$ 0.509 therefore $^{4}H_{3}$ 1.013 and **3**(**B1**) characterized as $^{1}C_{4}$ 0.188, $B_{O,3}$ 0.117 and $^{5}S_{1}$ 0.779 (ΔE 4.8 kJ mol^{-1}). In this case $^{5}S_{1}$ is relatively far, see Figure 4b, from $^{3}H_{4}$. Examination of Figure 5h shows that this conformation allows O-2 to be pseudo-equatorial while O-3, O-4 and C-6 are pseudo-axial. This limited selection of results suggests that having O-2 in a pseudo-equatorial conformation stabilizes the oxacarbenium ion. This unanticipated result is a direction for future investigations.

Hydrogen bonding is found for **3**(**B0**)+βMeOH and **3**(**B1**)+βMeOH to O-6 and for **3**(**B1**)+αMeOH to O-4. The corresponding energies are: **3**(**B0**)+αMeOH -43.4 kJ mol^{-1}, **3**(**B0**)+βMeOH -56.2 (-28.2) kJ mol^{-1}, **3**(**B1**)+αMeOH -55.3 (-27.3) kJ mol^{-1} and **3**(**B1**)+βMeOH -43.0 (-15.0) kJ mol^{-1}. Thus, including H-bonding shows a preference for β-glycosides whereas without it a preference for α-glycosides. The torsion angle τ_5 is 0.3° for **B0** changing to -39.5° and 35.3° for α- and β-attack respectively whereas for **B1** τ_5 changes from -4.6° to -38.1° and 23.3° for α- and β-attack respectively.

For **1** to **3** and for several other sugars (unpublished and below) this trend of finding two conformers for the glycopyranosyl oxacarbenium ions which differ by ring inversion appears to be general. We have named this the Two Conformer Hypothesis. This hypothesis leads to four cases to consider when examining the α:β selectivity.

The resulting ion:dipole complexes with the model nucleophile methanol have as distinguishing characteristics intramolecular hydrogen bonding and ring conformational changes characterized by a decrease in C-5-O-5--C-1-C-2 (τ_5) for α-attack and an increase for β-attack on D-sugars from nearly planar configurations in the isolated cations. These conformational changes may be favorable or unfavorable depending on the conformations involved. These changes depend on the configuration of the sugar and the protecting groups.

Downloaded by OHIO STATE UNIV LIBRARIES on June 13, 2012 | http://pubs.acs.org
Publication Date (Web): June 12, 2012 | doi: 10.1021/bk-2012-1102.ch011

Downloaded by OHIO STATE UNIV LIBRARIES on June 13, 2012 | http://pubs.acs.org
Publication Date (Web): June 12, 2012 | doi: 10.1021/bk-2012-1102.ch011

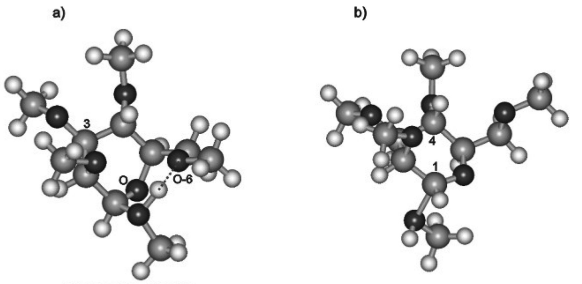

2 B0 β-MeOH $B_{3,O}$ **2** B0 α-MeOH $^4C_1$

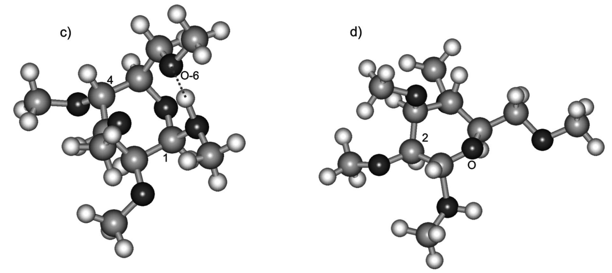

2 B1 β-MeOH $^1C_4$ **2** B1 α-MeOH $^OS_2$

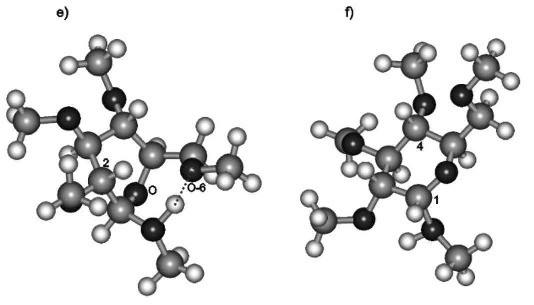

3 B0 β-MeOH ^2S_O **3** B0 α-MeOH $^4C_1$

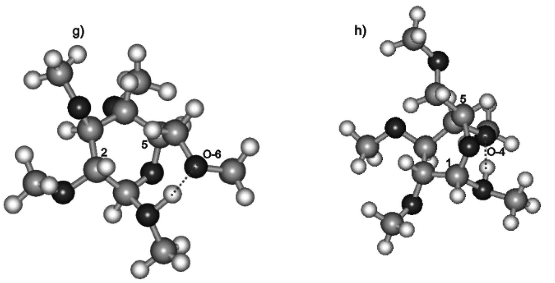

3 B1 β-MeOH $^{2,5}B$ **3** B1 α-MeOH $^5S_1$

*Figure 5. Ball and Stick Representations of the Ion:Dipole Complexes of **2** (a-d) and **3** (e-h) plus Methanol.*

Downloaded by OHIO STATE UNIV LIBRARIES on June 13, 2012 | http://pubs.acs.org
Publication Date (Web): June 12, 2012 | doi: 10.1021/bk-2012-1102.ch011

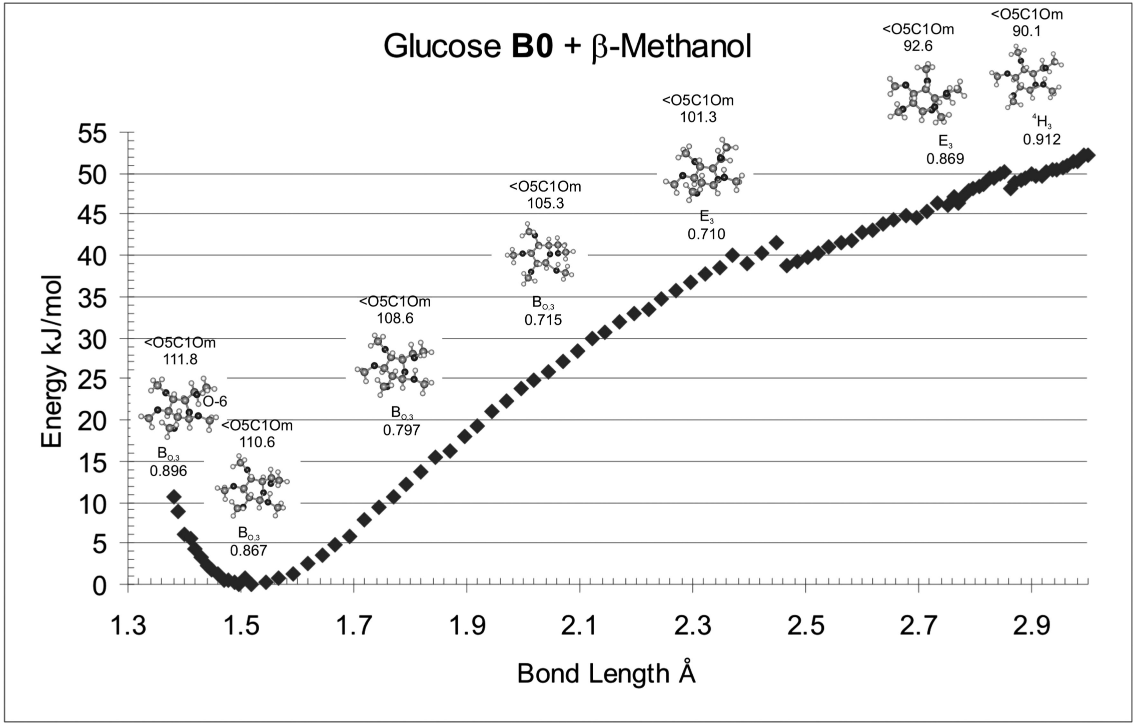

*Figure 6. Variation of the Energy as a Function of the C-1--O_m Bond length for Glc **3** Plus β-Methanol. The minimum is set to 0.0 kJ mol^{-1}. Optimizations include a continuum dielectric correction parameterized to CH_2Cl_2.*

Among other factors that could be studied, one variable that could be expected to be important is the variation of overall energy with the distance between the nucleophilic oxygen and the anomeric carbon, O_m--C-1. We have investigated this degree of freedom by systematically varying this "bond length" while allowing all other degrees of freedom to optimize by starting at the minima found in Figure 5 and varying this distance either forward or backward between 1.38 and 3.0 Å in small increments. Figure 6 shows one such study for the case of **3** plus βMeOH where each data point is a full constrained DFT optimization. We identified several technical problems with this study such as the discontinuities at long C-1--O_m bond lengths associated with changes in the ring conformation. However, in this case the complex does dissociate to the expected $^4H_3$ conformation at long C-1--O_m bond lengths. Several conclusions can be made from these studies.

In all cases including the one in Figure 6 the minima are shallow as in this case the region from about 1.42-1.68 Å is within 5 kJ mol^{-1} of the minimum. As mentioned above, this complex shows considerable hydronium ion character. Indeed at short separations the hydrogen bonded hydroxyl proton transfers to its oxygen acceptor, in this case O-6. Since many glycosylation reactions are done in the absence of bases this type of intramolecular proton transfer is highly plausible in real reactions.

Ultimately such species would transfer to the molecular sieves or other weakly basic components in the reaction mixtures. A third trend is apparent in all cases and is related to the O_m-C-1-O-5 bond angle. At large separations this angle is near 90° whereas at shorter separations it approaches the tetrahedral angle. We attribute this to a change from a π-complex to a σ-complex reflecting the hybridization changes at C-1 from sp^2 to sp^3.

The two factors, namely intramolecular hydrogen bonding and pyranose ring conformational changes, each suggest strategies for optimizing the stereoselectivity of glycosylation reactions. The possibility of hydrogen bonding could be stabilized or destabilized by the general principle of small electron donating (type 1) protecting groups favoring such interactions and large electron withdrawing (type 2) protecting groups disfavoring such interactions.

For *lyxo*-configured pyranoses β-glycosylation should be favoured by type 1 protecting groups at O-3 and perhaps O-2. Similarly for both **2** and **3**, type 1 groups should be at O-6 to favor β-glycosylation. Changing to type 2 groups should have the opposite effects. There is some experimental evidence for *gluco* configured donors that these observations are valid (*29–31*). Clearly more detailed studies are necessary. The possibility of fixing the ring conformation by for example fusing an additional ring to it could then lead to the stabilization of one of the two families of conformers.

Downloaded by OHIO STATE UNIV LIBRARIES on June 13, 2012 | http://pubs.acs.org
Publication Date (Web): June 12, 2012 | doi: 10.1021/bk-2012-1102.ch011

Downloaded by OHIO STATE UNIV LIBRARIES on June 13, 2012 | http://pubs.acs.org
Publication Date (Web): June 12, 2012 | doi: 10.1021/bk-2012-1102.ch011

Table 3. Conformational Descriptions, Selected Geometric Parameters and relative energies of Cations 4 and 5 and their methanol adducts (α and β).

Species	*Chair*	*Boat*	*Skew-Boat*	*Half-Chair Envelope*	*C-1--O_m Å*	*<O-5C-1O_m°*	*<C-5O-5--C-1C-2°*	*E kJ mol^{-1}*
Man								
4(B)	$^4C_1$ 0.052	**$B_{2,5}$ 0.834**	$^1S_3$ 0.090	-	-	-	2.2	0.0[a]
4 - β	$^1C_4$ 0.024	$^{O,3}B$ 0.251	**$^1S_5$ 0.970**	-	1.632	107.4	15.4	-51.5
4 - α	$^4C_1$ 0.111	**$B_{2,5}$ 0.825**	$^3S_1$ 0.018	-	2.298	96.3	-7.7	-13.5
Glc								
5(B)	$^4C_1$ 0.483	$^{1,4}B$ 0.495	$^OS_2$ 0.046	**^4E 0.967**	-	-	-0.4	0.0[a]
5 - β	$^4C_1$ 0.344	$^{1,4}B$ 0.629	$^OS_2$ 0.046	**^4E 0.688**	2.222	97.9	16	-18.9
5 - α	**$^4C_1$ 0.780**	$^{O,3}B$ 0.018	$^1S_5$ 0.266	-	1.645	108.1	-39.8	-67.2

[a] The energy of solvated methanol is added to that of solvated **B** and then set to 0.0 kJ mol^{-1}.

Further the fused ring could lead to preferential glycosylation of one face over the other. Experimentally the 4,6-benzylidene derivatives of mannose and glucose are known under particular experimental conditions to give predominantly β- or α-glycosides respectively (*32–38*). To study this we have done DFT optimizations on 4,6-*O*-benzylidene-2,3-di-*O*-methyl-D-mannopyranosyl (**4**) and 4,6-*O*-benzylidene-2,3-di-*O*-methyl-D-glucopyranosyl (**5**) cations (*27*). The data presented in Table 3 show that these experimental observations are consistent with the ring conformational changes associated with changes in τ_5. A pictorial representation is shown in Figure 7. There are some related systems where similar control may be operative (*39–41*). The use of fused rings or other mechanisms to stabilize one oxacarbenium ion ring conformation appears to be an experimental strategy that could be further exploited.

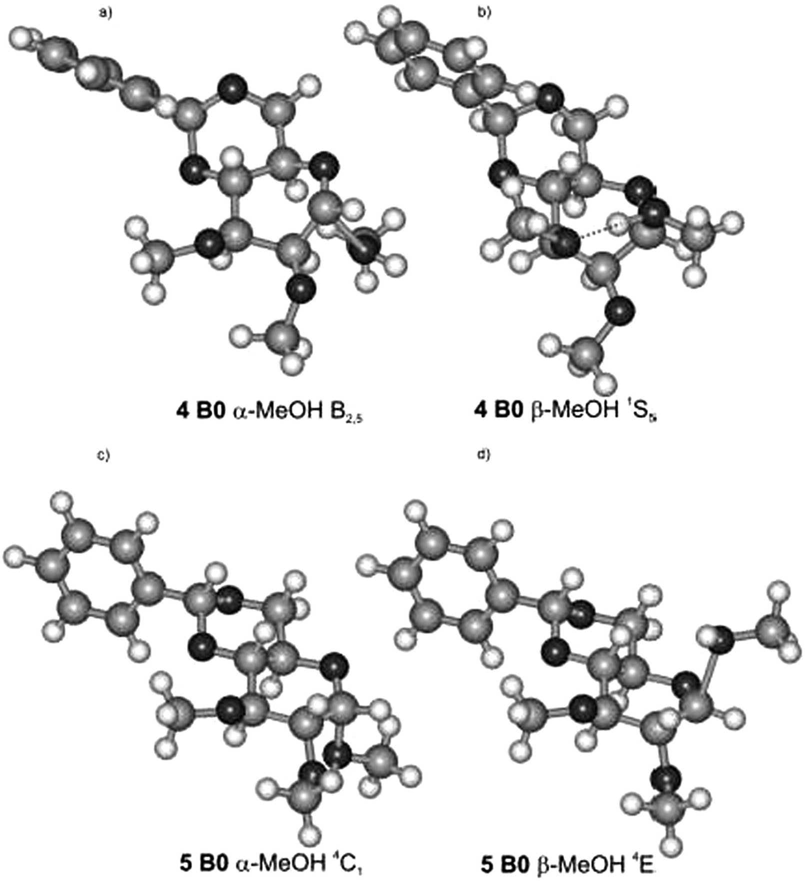

4 B0 α-MeOH $B_{2,5}$ **4 B0** β-MeOH $^{1}S_{5}$

5 B0 α-MeOH $^{4}C_{1}$ **5 B0** β-MeOH ^{4}E

*Figure 7. Ball and Stick Representation of Calculated Cations of 4,6-Benzylidene Protected Man **4** and Glc **5** Showing the Favorable (β for **4** and α for **5**) and Unfavorable (α for **4** and β for **5**) Ring Changes Resulting from α- or β-attack of Methanol.*

Downloaded by OHIO STATE UNIV LIBRARIES on June 13, 2012 | http://pubs.acs.org
Publication Date (Web): June 12, 2012 | doi: 10.1021/bk-2012-1102.ch011

Neighboring Group Participation from O-2

It has long been recognized that putting an acyl group adjacent to the anomeric carbon, in our examples on O-2, has a pronounced affect on reactions at the anomeric carbon. Lemieux showed that by successively substituting chlorine on the methyl carbon of a 2-*O*-acetyl substituted hexopyranosyl donor that the reactivity markedly decreased (*42*). Thus, the kinetic barrier to forming oxacarbenium ions is increased by the electron withdrawing groups.

The second major effect is that the carbonyl oxygen, O-7, can directly interact with C-1 to form a dioxolenium ion species (*43*, *44*). Such ions have been prepared and detected in solution and the solid state (*45–47*). One such 5-membered ring was found to be almost exactly planar in the solid state (*48*). Our DFT calculations of this species also found a planar geometry (*49*). In fact in all the cases we have calculated so far such rings are nearly planar. Accommodating this planarity has consequences for the fused pyranose ring.

When we started our studies of these neighboring groups systems we expected to be able to find a 5-coordinate *anti* S_N2 TS. Such TS are the conventional explanation for the 1,2-*trans* stereochemistry often but not always observed with O-2 acyl protecting groups (*50–56*). Our aim was to study the effect of various protecting groups on this TS such as studying different acyl groups in order to optimize the experimental choices. Unfortunately, in spite of numerous attempts we have never found this TS. It may be that our models are too simple and that inclusion of specific solvation and/or counterions may be necessary to stabilize this type of TS. However, our studies of these dioxolenium ions has led to some interesting observations that may be of interest.

One such observation is illustrated by the data in Table 4 where the results for DFT calculations on 2-*O*-acetyl-3,4,6-tri-*O*-methyl-D-glucopyranosyl **6**, mannopyranosyl **7** and galactopyranosyl **8** oxacarbenium ions are given. Species **6** and **7** are the 2-*O*-acetyl-analogues of **2** and **3**. As can be readily observed their respective **B0** and **B1** ring conformations ($^4H_3$ and $^5S_1$ for **6** and $^4H_3$ and ^3E for **7**) are very similar to those for **2** and **3**. For **6** **B0** is more stable as for **3** but for **7** **B1** is calculated to be more stable in contrast to **2**.

Note that these **B0** and **B1** ring conformations have the O-2 acetyl group in its favoured conformation which is with the carbonyl oxygen syn to the methine at C-2, see Figure 8 (*57*). In all calculated pyranose structures with secondary esters this is found to be the minimum energy conformation. In either of these conformations if the ester rotates than the ring can close to form the dioxolenium ion. For *gluco* configured **6** this leads to two species **C0** and **C1** with conformations characterized as $^4H_5$ 0.813 and $^3S_1$ 0.654 respectively i.e. two conformers that differ by ring inversion.

Similarly for *manno* configured **7** two species characterized as $^4C_1$ 0.792 and $^1C_4$ 0.678, see Figure 9, and for *galacto* configured **8** two species characterized as $^4H_5$ 0.737 and $^1C_4$ 0.836 were found, see Figure 10. Intriguingly for **6** **C0** is energetically favored by about 10 kJ mol^{-1} and for **8** **C0** is still energetically favored but by about 40 kJ mol^{-1} whereas for **7** **C0** and **C1** are nearly isoenergetic (< 1 kJ mol^{-1}) i.e. all three configurational isomers are different.

Downloaded by OHIO STATE UNIV LIBRARIES on June 13, 2012 | http://pubs.acs.org
Publication Date (Web): June 12, 2012 | doi: 10.1021/bk-2012-1102.ch011

Downloaded by OHIO STATE UNIV LIBRARIES on June 13, 2012 | http://pubs.acs.org
Publication Date (Web): June 12, 2012 | doi: 10.1021/bk-2012-1102.ch011

Table 4. Ring Conformations of 2-*O*-Acetyl-3,4,6-tri-*O*-methyl-D-Glucopyranosyl 6, Mannopyranosyl 7 and Galactopyranosyl 8 and 9 Oxacarbenium Ions.

Species	τ_1 °	τ_2 °	τ_3 °	τ_4 °	τ_5 °	τ_6 °	*Chair*	*Boat*	*Skew-Boat*	*Half-Chair Envelope*	*Energy kJ mol^{-1}*
6B0	-42.9	61.0	-50.2	21.3	-3.9	15.6	$^{4}C_{1}$ 0.541	$B_{2,5}$ 0.055	$^{1}S_{3}$ 0.473	**$^{4}H_{3}$ 0.946**	0.0[a]
6B1	-9.5	-34.3	59.5	-40.0	-4.6	31.8	$^{1}C_{4}$ 0.244	$B_{O,3}$ 0.044	**$^{5}S_{1}$ 0.752**	-	7.2
6C0	-26.9	51.3	-65.3	56.2	-31.6	16.7	$^{4}C_{1}$ 0.689	$^{O,3}B$ 0.040	$^{1}S_{5}$ 0.406	**$^{4}H_{5}$ 0.813**	-32.5
6C1	24.5	-52.1	43.0	-3.0	-26.3	14.2	$^{1}C_{4}$ 0.228	$^{2,5}B$ 0.149	**$^{3}S_{1}$ 0.654**	^{5}E 0.298	-23.2
7B0	-43.6	60.1	-46.7	17.0	-0.7	14.7	$^{4}C_{1}$ 0.508	$B_{2,5}$ 0.023	$^{1}S_{3}$ 0.493	**$^{4}H_{3}$ 0.986**	0.0[a]
7B1	54.9	-60.6	37.9	-7.6	3.2	-28.7	$^{1}C_{4}$ 0.536	$^{O,3}B$ 0.436	$^{5}S_{1}$ 0.079	**^{3}E 0.873**	-12.5
7C0	-26.3	37.6	-57.3	70.0	-58.0	35.8	$^{4}C_{1}$ 0.792	$^{1,4}B$ 0.004	$^{O}S_{2}$ 0.359	-	-30.0
7C1	46.4	-57.6	50.7	-33.0	24.4	-32.0	$^{1}C_{4}$ 0.678	$^{2,5}B$ 0.022	$^{3}S_{1}$ 0.273	-	-29.1
8B0	-52.3	65.2	-45.9	12.9	-0.8	22.1	$^{4}C_{1}$ 0.553	$^{2,5}B$ 0.065	$^{1}S_{3}$ 0.533	**$^{4}H_{3}$ 1.067**	0.0[a]
8B1	35.9	-47.6	66.8	-69.8	61.9	-46.9	$^{1}C_{4}$ 0.913	$B_{1,4}$ 0.023	$^{2}S_{O}$ 0.284	-	5.5
8C0	-37.1	59.6	-65.7	48.9	-27.0	21.6	$^{4}C_{1}$ 0.722	$B_{O,3}$ 0.087	$^{1}S_{5}$ 0.369	**$^{4}H_{5}$ 0.737**	-38.8
8C1	31.8	-43.4	59.2	-67.3	56.9	-38.2	**$^{1}C_{4}$ 0.824**	$B_{1,4}$ 0.031	$^{2}S_{O}$ 0.293	-	0.3
9B0	-59.6	35.4	7.6	-33.4	7.7	40.7	$^{4}C_{1}$ 0.242	$B_{1,4}$ 0.022	**$^{2}S_{O}$ 0.771**	-	0.0[a]
9C0	-51.6	33.1	17.5	-58.3	40.9	15.7	$^{1}C_{4}$ 0.045	$^{1,4}B$ 0.170	**$^{2}S_{O}$ 0.908**	-	-20.1
9C1	22.1	17.6	-58.3	62.4	-21.4	-22.3	$^{4}C_{1}$ 0.320	**$B_{2,5}$ 0.688**	$^{3}S_{1}$ 0.032	-	-55.2

[a] Energy of this species set to 0.0 kJ mol^{-1}. Total energies **6B0** 18 442.1, **7B0** 18 425.9 and **8B0** 18430.3.

Downloaded by OHIO STATE UNIV LIBRARIES on June 13, 2012 | http://pubs.acs.org
Publication Date (Web): June 12, 2012 | doi: 10.1021/bk-2012-1102.ch011

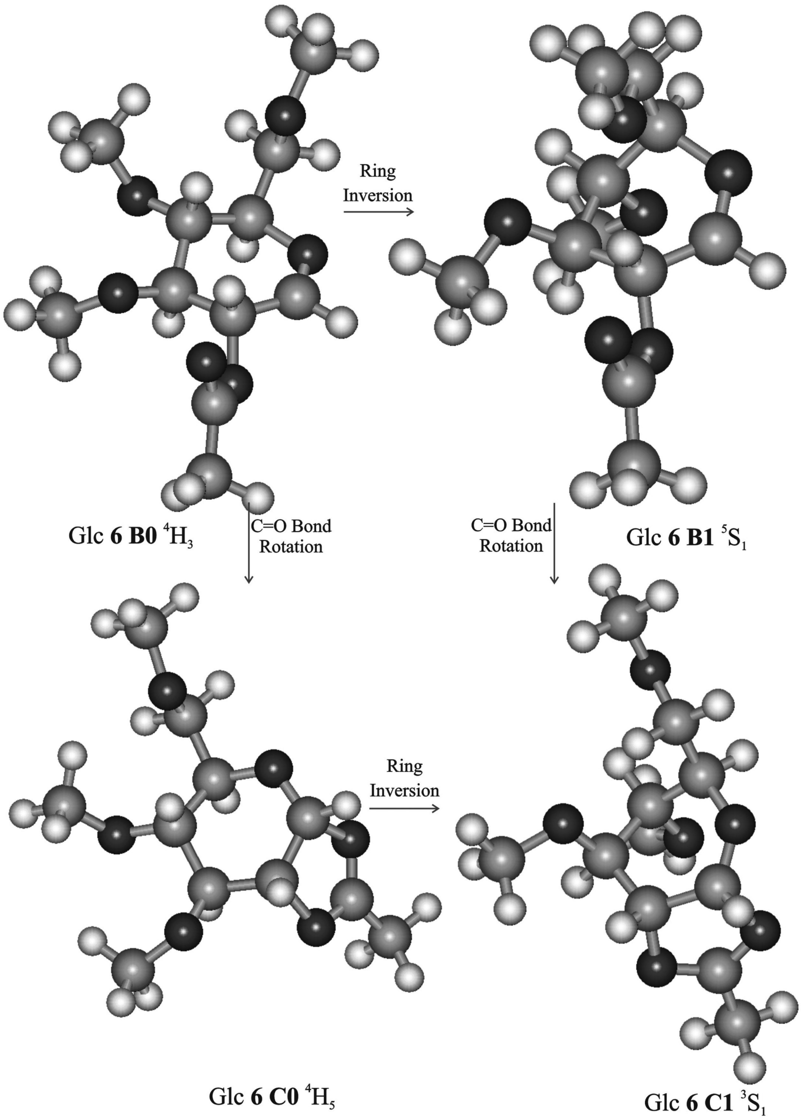
Ring Inversion
Glc 6 B0 $^4H_3$
C=O Bond Rotation
C=O Bond Rotation
Glc 6 B1 $^5S_1$
Ring Inversion
Glc 6 C0 $^4H_5$
Glc 6 C1 $^3S_1$

*Figure 8. Ball and Stick Representations of the **B0**, **B1**, **C0** and **C1** Species of Glc **6**.*

Downloaded by OHIO STATE UNIV LIBRARIES on June 13, 2012 | http://pubs.acs.org
Publication Date (Web): June 12, 2012 | doi: 10.1021/bk-2012-1102.ch011

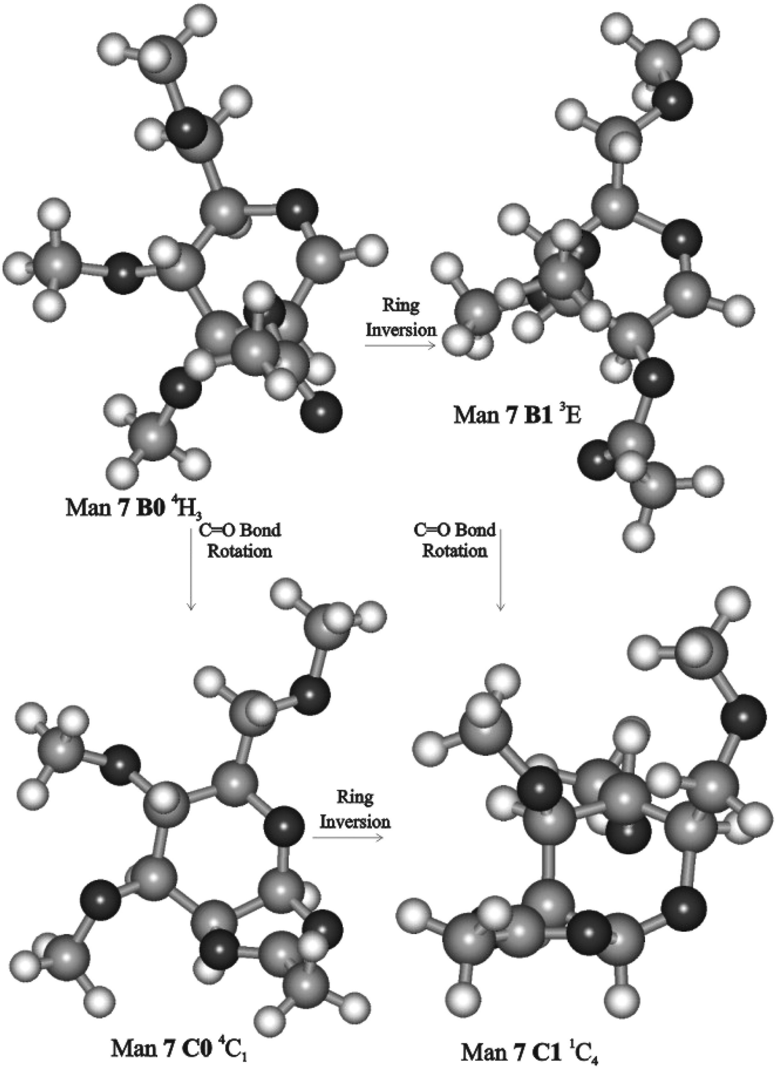
Ring Inversion
Man 7 **B1** ^{3}E
Man 7 **B0** $^{4}H_{3}$
C=O Bond Rotation
C=O Bond Rotation
Ring Inversion
Man 7 **C0** $^{4}C_{1}$
Man 7 **C1** $^{1}C_{4}$

*Figure 9. Ball and Stick Representations of the **B0**, **B1**, **C0** and **C1** Species of Man 7.*

Downloaded by OHIO STATE UNIV LIBRARIES on June 13, 2012 | http://pubs.acs.org
Publication Date (Web): June 12, 2012 | doi: 10.1021/bk-2012-1102.ch011

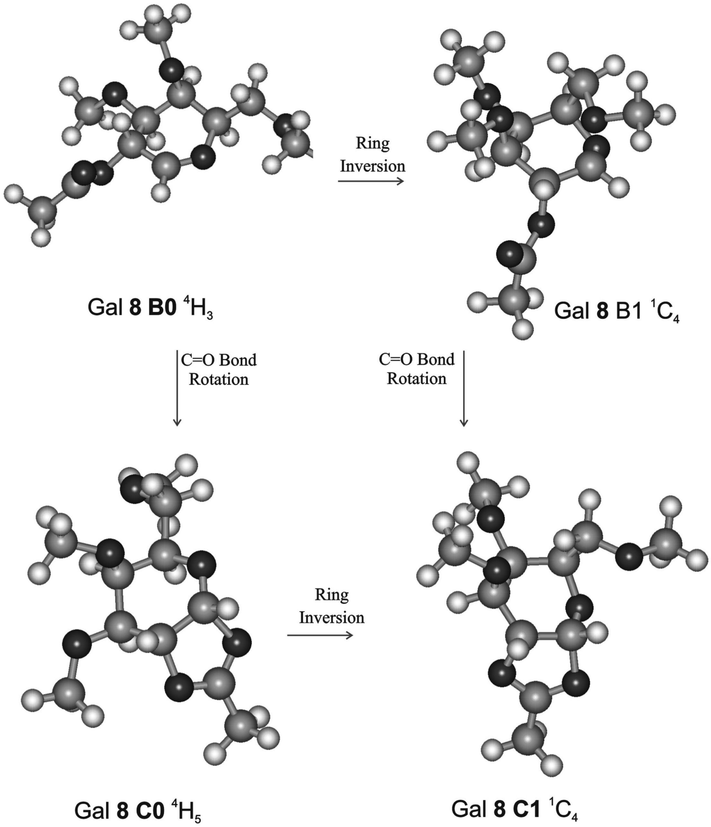

*Figure 10. Ball and Stick Representations of the **B0**, **B1**, **C0** and **C1** Species of Gal **8**.*

We have previously studied both experimentally (*58*) and computationally 2-*O*-acyl-derivatives of galactopyranose. In particular we have made extensive DFT studies of 2,6-di-*O*-acetyl-3,4-isopropylidene-D-galactopyranosyl cation **9**. In these cases the same trends as for **8** were found but **C0** and **C1** have different conformations. Furthermore, the conversion of **B**'s to **C**'s for **9** was studied computationally using the formulations developed in Section 1 to enable DFT dynamic calculations. These results strongly supported a model where ring inversion preceded carbonyl ring closure and where the barrier to ring inversion is the main kinetic barrier (estimated barrier height 34 kJ mol^{-1}) (*8*).

We have also studied the **C1** to **C0** interconversion to assess if this would shed some light on finding the *anti* S_N2 TS. In all conformers of the pyranose ring the C-1--O-7 did not appreciably lengthen. Therefore, from these studies we tentatively conclude that C-1--O-7 bond disassociation precedes ring inversion for the glycosylation process. In the extreme case this would be the same as

Downloaded by OHIO STATE UNIV LIBRARIES on June 13, 2012 | http://pubs.acs.org
Publication Date (Web): June 12, 2012 | doi: 10.1021/bk-2012-1102.ch011

nucleophilic attack on the isolated **B1**, not **B0** (for **9**). Since some degree of nucleophilic preassociation is probable and since this can only occur on the expected *trans* face this can partly explain the observed stereoselectivity. The cases where some cis (occasionally predominant) glycosylation occurs could be the result of attack on **B1**.

In reactions with very strong nucleophiles or cases where excess (e.g. solvolysis conditions) nucleophile is used attack on the first formed **B0** may out compete ring inversion and ring closure to **C** and therefore lead to anomeric mixtures. The order of reaction via **B** or **C** (i.e. ring inversion before or after carbonyl rotation) for derivatives other than *galacto* configured **9** is not known and is an active area of research for us (see Fig. 11).

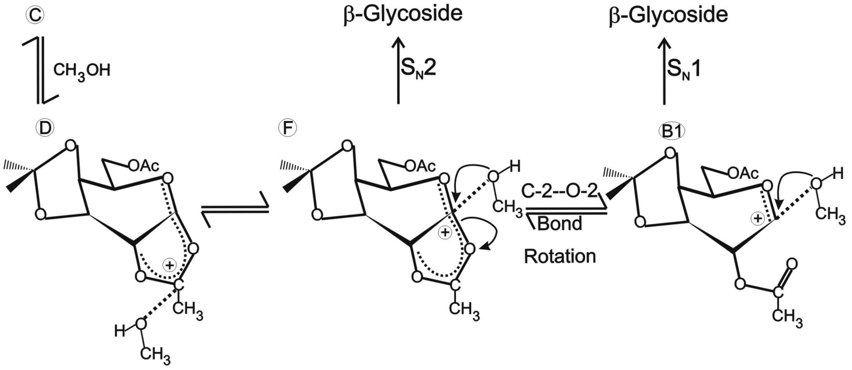

*Figure 11. Schematic Representation of Possible Intermediates in Neighboring Group Glycosylation Reactions of **9**.*

Although entirely speculative at this point this observation of two conformers for dioxolenium ions and the possibility that at least in some cases ring inversion precedes 5-membered ring closure may assist in the comprehension of some cases in the literature. For example, it has been shown that n-pentenyl orthoesters can give rise to different glycosylation products than those derived from otherwise identically protected n-pentenyl glycoside donors (*59–61*). An interpretation following from our data would be that the dioxolenium ion formed by each process have different conformations and hence different reactivity.

Similar explanations may apply to cases where oligosaccharide donors with 2-acyl groups show different stereoselectivities depending on the anomericity of the sugar linkage attached to the reducing end sugar (*62*, *63*).

Downloaded by OHIO STATE UNIV LIBRARIES on June 13, 2012 | http://pubs.acs.org
Publication Date (Web): June 12, 2012 | doi: 10.1021/bk-2012-1102.ch011

Again, it would seem possible that different conformations of the reducing end sugar could be formed after activation that have different reactivities. A detailed study of these possibilities appears warranted.

Acyl Transfer as a Side Reaction to Neighboring Group Participation

Our study of **9** was prompted by a glycosylation of the polymer linker combination, monomethyl ether of polyethylene glycol-dioxyxylene (MPEGDOXOH), with the donor ethyl 2,6-di-*O*-benzoyl-3,4-isopropylidene-1-thio-β-D-galactopyranoside, **10**. This glycosylation under a large variety of conditions led to a complex mixture of products. For example, under conventional NIS/triflic acid conditions the desired polymer bound glycoside **11** was obtained in <40 % yield. The remaining products can be attributed to the side reaction know as acyl transfer. These include: the benzoylated acceptor MPEGDOXOBz, the 2-OH glycoside analogue of **11** namely **12** and β1,2-linked oligomers, **13**, of the donor, see Figure 12. This side reaction is long known but little recognized. It is obvious that for successful polymer-supported synthesis where high yields and high purity are mandatory this side reaction is very unproductive. Since polymer-supported oligosaccharide synthesis is a major endeavour in our research groups (*64*, *65*) we devoted considerable effort to discovering the mechanism of this reaction.

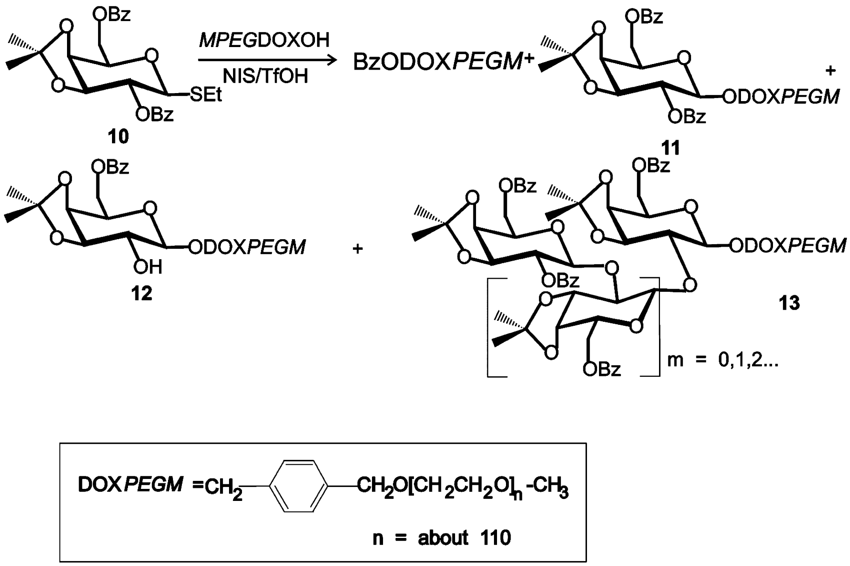

*Figure 12. Schematic Representation Showing Polymer-supported Glycosylation Reaction with Donor **10** Resulting in >60% Benzoyl Transfer Related Products.*

Downloaded by OHIO STATE UNIV LIBRARIES on June 13, 2012 | http://pubs.acs.org
Publication Date (Web): June 12, 2012 | doi: 10.1021/bk-2012-1102.ch011

After considering a large number of possibilities including most of the suggested mechanisms in the literature we found a mechanism that starts from ion:dipole complex **D** and is triggered by proton transfer to O-2 followed by several bond breaking and bond forming reactions, see Figure 13.

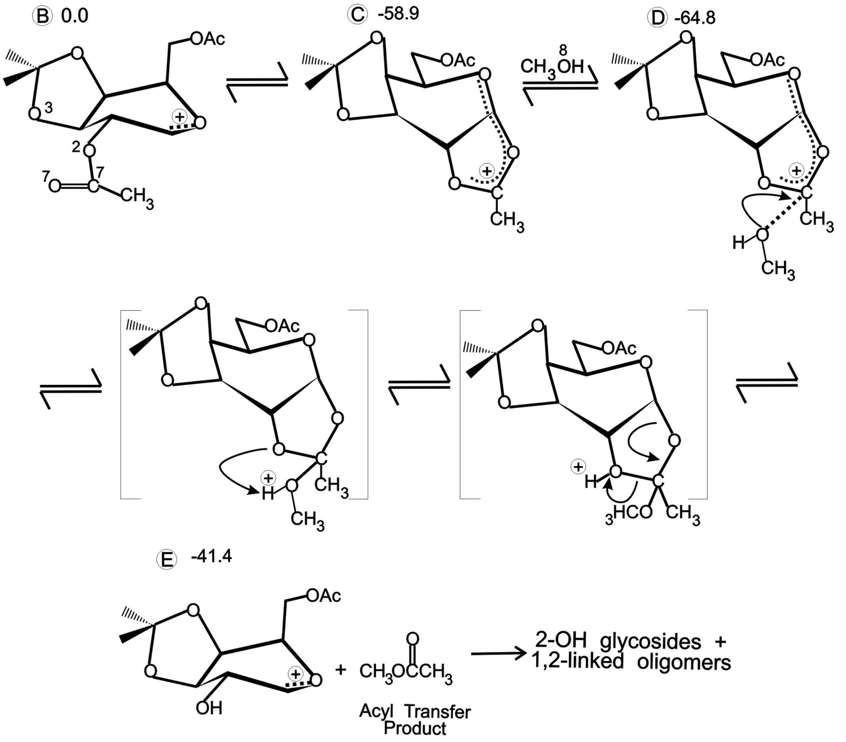

Figure 13. Schematic Representation of Mechanism for Acyl Transfer Triggered by Proton

Consideration of the LUMO's of **B**'s and **C**'s suggests that for **B**'s nucleophilic attack should occur at C-1 where as for **C**'s it should occur at C-7, the former carbonyl carbon of the dioxolenium ion. Ion:dipole complexes **D** have long bonds to this carbon from the nucleophilic oxygen, O-8. In order to model this reaction we developed a procedure that uses complex constraints. This complex constraint is a linear combination of the bond lengths that are formed or broken during the reaction, see equation 4:

$$Q = r_1 - r_2 + r_3 - r_4 + r_5 - r_6 \qquad \textbf{(4)}$$

where, r_1 through r_6 are defined in Figure 14.

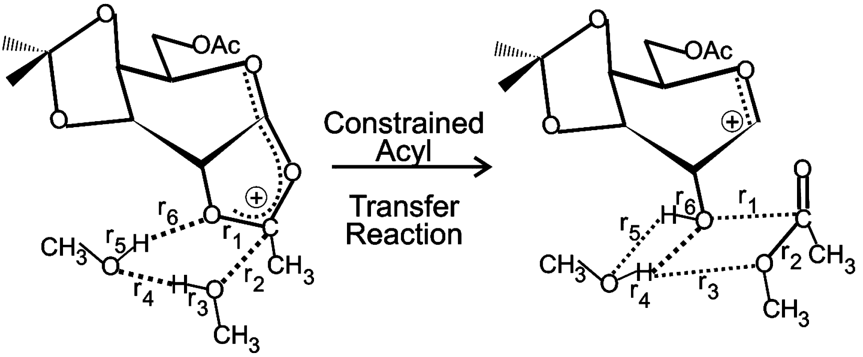

Figure 14. Bond Lengths (r_1 to r_6) used for the Constrained Acyl Transfer Reaction

The mechanism that results starts by having the O-8--C-7 bond length shorten. This shortening has the result that the complex develops appreciable hydronium ion character and hence most of the positive charge moves to the nucleophilic hydroxyl. In the presence of base this species could undergo proton transfer to form a stable orthoester. In the absence of added base this proton can transfer to another oxygen. In order to find a low enough barrier to proton transfer we had to introduce a relay molecule which in our case is another methanol but in the real reaction could be any species with an exchangeable hydrogen.

The second step in our mechanism is the transfer of the hydroxylic proton to the relay molecule followed by transfer to O-2. The 1st proton transfer is concurrent with O-8--C-7 covalent bond formation. The first TS is associated with the 2nd proton transfer. Once transferred the O-2--C-7 bond breaks with the positive charge now mostly on C-7. This process is associated with a second TS. Finally the O-7--C-1 breaks to lead to an ion:dipole complex of the newly formed ester and a 2-OH analogue of **B** i.e. **E**. The 2-OH glycosides and β1,2-linked oligomers are assumed to arise from **E** but this has not been studied in detail.

We studied this mechanism using the same constrained methodology with four different acyl groups namely formyl, acetyl, benzoyl and pivaloyl. These were chosen since experimental evidence from our collaborators has shown that acyl transfer decreases in the order formyl > acetyl > benzoyl > pivaloyl (*66*). Our studies found exactly the same mechanism for all 4 analogues including the location of the two TS's and the order of bond forming and bond breaking. This was highly surprising considering that the constraint in no way influenced this outcome and therefore we regard these results as quite convincing.

Detailed examination of the various steps and intermediates led to two interesting observations. The first is shown in Figure 16 that shows a portion of the calculated structures of ion dipole complexes **D**. In these structures one can see that the O-7--C-1 bond length correlates with the ease of acyl transfer. The O-7--C-1 is longest for formyl and shortest for benzoyl and pivaloyl. This is not an intuitive result and demonstrates the power of calculations to find novel correlations. Correlations only suggest causation and do not prove it. We come back to this correlation after examining the second point.

Downloaded by OHIO STATE UNIV LIBRARIES on June 13, 2012 | http://pubs.acs.org
Publication Date (Web): June 12, 2012 | doi: 10.1021/bk-2012-1102.ch011

Graphical examination of the second TS for the benzoyl case, see Figure 15e, suggested to us that 2,6-substitution of the benzoyl ring might further restrict rotation about the C-7--C (substituent bond C_{ipso} for benzoyl). This idea prompted us to first calculate and then prepare 2,6-disubstituted analogues **14** and **15** of benzoate **10**. In their calculated **D** structures the O-7-- C-1 is even shorter than for unsubstituted benzoyl suggesting an electronic component to this effect, see Figures 16e and f. More importantly under the same reaction conditions that resulted in >60% benzoyl transfer the 2,6-dimethylbenzoyl donor **14** exhibited no detectable transfer to give glycoside **16** in nearly quantitative yield and the 2,6-dimethoxybenzoyl donor **15** exhibited 8% transfer and >90% glycoside **17**.

Downloaded by OHIO STATE UNIV LIBRARIES on June 13, 2012 | http://pubs.acs.org
Publication Date (Web): June 12, 2012 | doi: 10.1021/bk-2012-1102.ch011

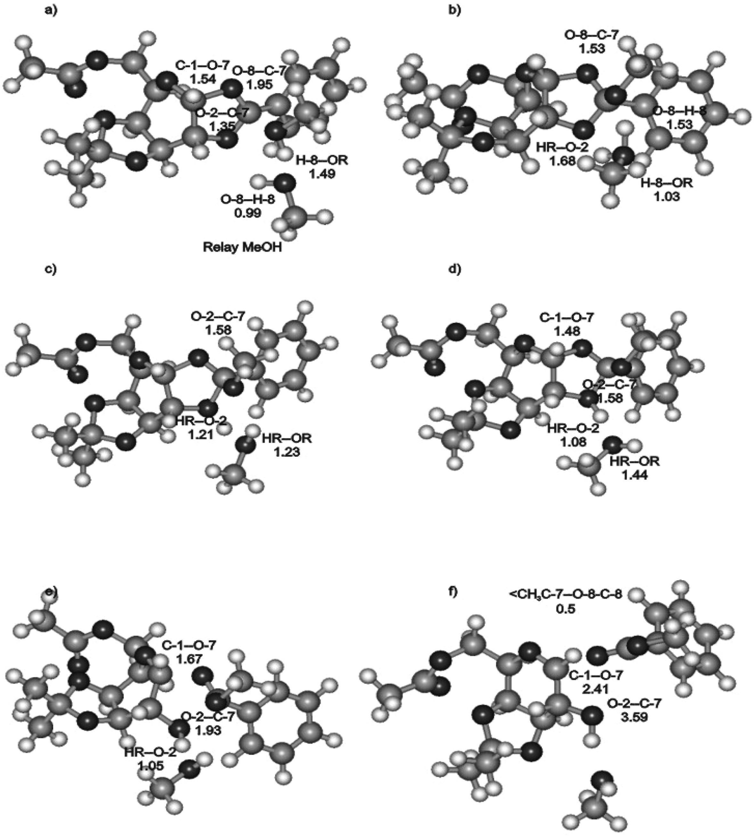
a)
C-1–O-7
1.54
O-8–C-7
1.95
O-2–C-7
1.35
H-8–OR
1.49
O-8–H-8
0.99
Relay MeOH
b)
O-8–C-7
1.53
O-8–H-8
1.53
HR–O-2
1.68
H-8–OR
1.03
c)
O-2–C-7
1.58
HR–O-2
1.21
HR–OR
1.23
d)
C-1–O-7
1.48
O-2–C-7
1.58
HR–O-2
1.08
HR–OR
1.44
e)
C-1–O-7
1.67
O-2–C-7
1.93
HR–O-2
1.05
f)
<CH₃C-7–O-8-C-8
0.5
C-1–O-7
2.41
O-2–C-7
3.59

Figure 15. Ball and Stick Representations of Snapshots of the Calculated Mechanism of Acyl Transfer. The Acyl Group is Benzoyl. Starting Structure Showing Relay MeOH (a) Proton Transfer to Relay O and Formation of O-7--C-7 bond (b) 1st TS with Proton being Transferred to O-2 (c) Proton Transferred to O-2 (d) 2nd TS and breaking of O-2--C-7 bond (e) Final structure with bond C-1--O7 broken too, note cis conformation of ester (f).

Downloaded by OHIO STATE UNIV LIBRARIES on June 13, 2012 | http://pubs.acs.org
Publication Date (Web): June 12, 2012 | doi: 10.1021/bk-2012-1102.ch011

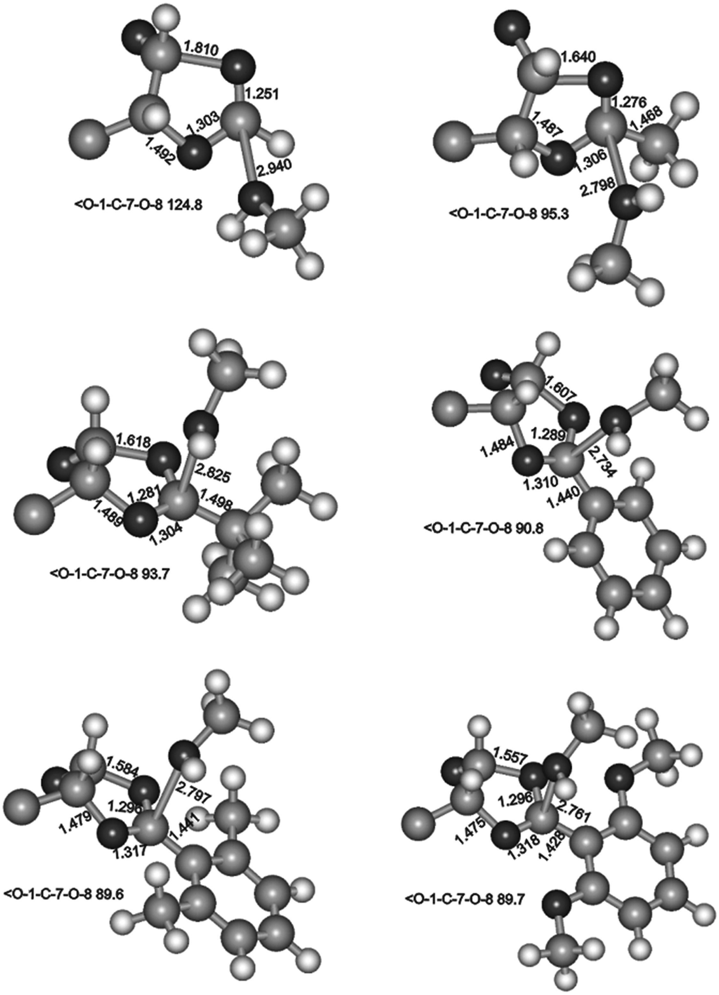
1.810
1.251
1.303
1.492
2.940
<O-1-C-7-O-8 124.8
1.640
1.276
1.468
1.487
1.306
2.798
<O-1-C-7-O-8 95.3
1.618
2.825
1.281
1.498
1.489
1.304
<O-1-C-7-O-8 93.7
1.607
1.289
1.484
2.734
1.310
1.440
<O-1-C-7-O-8 90.8
1.584
2.797
1.296
1.479
1.441
1.317
<O-1-C-7-O-8 89.6
1.557
1.296
2.761
1.475
1.318
1.428
<O-1-C-7-O-8 89.7

Figure 16. Portions of the Calculated Structures for Intermediates ***D****: Formyl (a) Acetyl (b) Benzoyl (c) Pivaloyl (d) 2,6-dimethylbenzoyl (e) and 2,6-dimethoxybenzoyl (f).*

The 2,6-dimethoxybenzoates are easier to remove than 2,6-dimethylbenzoate to yield the diol **18** and so are the protecting group of choice, see Figure 17. Further improvements can likely be made by adding an electron withdrawing group in the 4-position. Thus we have gone from a calculated TS to a modified protecting group that eliminates this side reaction having first done the calculations before the experiment.

Downloaded by OHIO STATE UNIV LIBRARIES on June 13, 2012 | http://pubs.acs.org
Publication Date (Web): June 12, 2012 | doi: 10.1021/bk-2012-1102.ch011

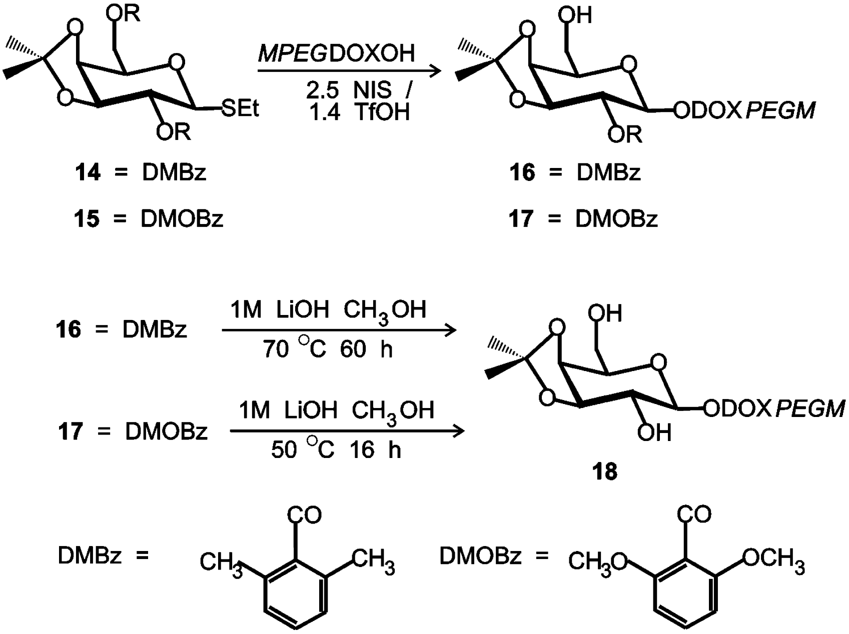
OR
SEt
OR
*MPEG*DOXOH
2.5 NIS /
1.4 TfOH
OH
ODOX*PEGM*
OR
14 = DMBz
15 = DMOBz
16 = DMBz
17 = DMOBz
16 = DMBz
1M LiOH CH3OH
70 °C 60 h
17 = DMOBz
1M LiOH CH3OH
50 °C 16 h
OH
ODOX*PEGM*
OH
18
DMBz =
CO
CH3
CH3
DMOBz =
CO
CH3O
OCH3

Figure 17. Structures and Reactions of Protecting Groups that Minimize Acyl Transfer Developed from a Calculated TS.

Conclusion

It is our hope that organic chemists will use our quantitative method of describing pyranose ring conformations. The examples shown here show how this aids in defining the probable conformations of the common glycopyranosyl oxacarbenium ions. Our calculations support a model where such ions are found in at least two different conformations that depend on the protecting groups and the configuration. This ability to exist in two different conformations is a probable explanation for some of the experimental observations on glycosylation reactions. Furthermore, it is anticipated that experimentalists should be able to take advantage of this idea to design stereoselective glycosylation reactions.

Note

This chapter previously appeared in *Carbohydrate Drug Design* (ACS Symposium Series 932), edited by Klyosov et al. and published in 2006.

Acknowledgments

The authors gratefully acknowledge the use of the VPP770 Fujitsu parallel computer situated in the RIKEN Computer Center. This work was partly supported by the iHPC multiscale modeling initiative of the NRC.

References

1. Bérces, A.; Whitfield, D. M.; Nukada, T. *Tetrahedron* **2001**, *57*, 477.
2. Stoddart, J. F. *Stereochemistry of Carbohydrates*; Wily-Interscience: New York, 1971.
3. Cremer, D.; Pople, J. A. *J. Am. Chem. Soc.* **1975**, *97*, 1354.
4. Haasnot, C. G. A. *J. Am. Chem. Soc.* **1992**, *114*, 882.
5. Hendrickson, J. B. *J. Am. Chem. Soc.* **1967**, *89*, 7047.
6. Klyne, W.; Prelog, V. *Experimentia* **1960**, *16*, 521.
7. Cano, F. H.; Foces-Foces, C.; Garcia-Binoco, S. *Tetrahedron* **1977**, *35*, 797.
8. Bérces, A.; Nukada, T.; Whitfield, D. M. *J. Am. Chem. Soc.* **2001**, *123*, 5460.
9. Rhind-Tutt, A. J.; Vernon, C. A. *J. Chem. Soc., Part 2* **1960**, 4637.
10. Bennet, A. J. *J. Chem. Soc., Perkin Trans 2* **2002**, 1207.
11. Barrows, S. E.; Dulles, F. J.; Cramer, C. J.; French, A. D.; Truhlar, D. G. *Carbohydr. Res.* **1995**, *276*, 219.
12. Whitfield, D. M. *J. Mol. Struct.(Theochem)* **1997**, *395*, 53.
13. Polavarapu, P. L.; Ewig, C. S. *J. Comput. Chem.* **1992**, *13*, 1255.
14. Jeffrey, G. A. *J. Mol. Struct.* **1990**, *237*, 75.
15. Mendonca, A.; Johnson, G. P; French, A. D.; Laine, R. A. *J. Phys. Chem. A* **2002**, *106*, 4115.
16. Baerends, E. J.; Ellis, D. E.; Ros, P. *Chem. Phys.* **1973**, *2*, 41.
17. te Velde, G.; Baerends, E. J. *J. Comput. Phys.* **1992**, *99*, 84.
18. Fonseca Guerra, C.; Snijders, J. G.; te Velde, G.; Baerends, E. J. *Theor. Chim. Acta* **1998**, *99*, 391.
19. Versiuis, L.; Ziegler, T. *J. Chem. Phys.* **1988**, *88*, 322.
20. Fan, L.; Ziegler, T. *J. Chem. Phys.* **1992**, *96*, 9005.
21. Vosko, S. H.; Wilk, L.; Nusair, M. *Can. J. Phys.* **1980**, *58*, 1200.
22. Becke, A. D. *Phys. Rev. A* **1988**, *38*, 3098.
23. Perdew, J. P. *Phys. Rev. B* **1986**, *34*, 7506.
24. Spijker, N. M.; Basten, J. E. M.; van Boeckel, C. A. A. *Recl. Trav. Chim. Pays-Bas* **1993**, *112*, 611.
25. Spijker, N. M.; van Boeckel, C. A. A. *Angew. Chem., Int. Ed. Engl.* **1991**, *30*, 180.
26. Green, L. G.; Ley, S. V. In *Carbohydrates in Chemistry and Biology*; Ernst, B., Hart, G. W., Sinaÿ, P., Eds.; Wiley-VCH Weinheim: 2000; Vol. 1, p 427.
27. Nukada, T.; Bérces, A.; Whitfield, D. M. *Carbohydr. Res.* **2002**, *337*, 765.
28. Nukada, T.; Bérces, A.; Wang, L.; Zgierski, M. Z.; Whitfield, D. M. *Carbohydr. Res.* **2005**, *340*, 841.
29. Maroušek, V.; Lucas, T. J.; Wheat, P. E.; Schuerch, C. *Carbohydr. Res.* **1978**, *60*, 85.
30. Houdier, S.; Vottero, P. J. A. *Carbohydr. Res.* **1992**, *232*, 349.
31. Fréchet, J. M.; Schuerch, C. *J. Am. Chem. Soc.* **1972**, *94*, 604.
32. Abdel-Rahman, A. A.-H.; Jonke, S.; El Ashry, E. S. H.; Schmidt, R. R. *Angew. Chem., Int. Ed.* **2002**, *41*, 2972.
33. Crich, D.; Cai, W. *J. Org. Chem.* **1999**, *64*, 4926.
34. Crich, D.; Li, H. *J. Org. Chem.* **2000**, *65*, 801.

Downloaded by OHIO STATE UNIV LIBRARIES on June 13, 2012 | http://pubs.acs.org
Publication Date (Web): June 12, 2012 | doi: 10.1021/bk-2012-1102.ch011

Downloaded by OHIO STATE UNIV LIBRARIES on June 13, 2012 | http://pubs.acs.org
Publication Date (Web): June 12, 2012 | doi: 10.1021/bk-2012-1102.ch011

35. Weingart, R.; Schmidt, R. R. *Tetrahedron Lett.* **2000**, *41*, 8753.
36. Yun, M.; Shin, Y.; Chun, K. H.; Nam Shin, J. E. *Bull. Korean Chem. Soc.* **2000**, *21*, 562.
37. Crich, D.; Dudkin, V. *Org. Lett.* **2000**, *2*, 3941.
38. Ito, Y.; Ohnishi, Y.; Ogawa, T.; Nakahara, Y. *Synlett* **1998**, 1102.
39. Tamura, S.; Abe, H.; Matsuda, A.; Shuto, S. *Angew. Chem., Int. Ed.* **2003**, *42*, 1021.
40. Yule, J. E.; Wong, T. C.; Gandhi, S. S.; Qiu, D.; Riopel, M. A; Koganty, R. R. *Tetrahedron Lett.* **1995**, *36*, 6839.
41. Toshima, K.; Nozaki, Y.; Tatsuta, K. *Tetrahedron Lett.* **1991**, *32*, 6887.
42. Lemieux, R. U. *Adv. Carbohydr. Chem.* **1954**, *9*, 1.
43. Lemieux, R. U. *Chem. Can.* **1964**, *16*, 14.
44. Wulff, G.; Röhle, G. *Angew. Chem., Int. Ed. Engl.* **1974**, *13*, 157.
45. Wallace, J. E.; Schroeder, L. R. *J. Chem. Soc., Perkin Trans 2* **1977**, 795.
46. Paulsen, H.; Herold, C. P. *Chem. Ber.* **1970**, *103*, 2450.
47. Crich, D.; Dai, Z.; Gastaldo, S. *J. Org. Chem.* **1999**, *64*, 5224.
48. Paulsen, H.; Dammeyer, R. *Chem. Ber.* **1973**, *106*, 2324.
49. Nukada, T.; Bérces, A.; Zgierski, M. Z.; Whitfield, D. M. *J. Am. Chem. Soc.* **1998**, *120*, 13291.
50. Toshima, K.; Tatsuta, K. *Chem. Rev.* **1993**, *93*, 1503.
51. Sinaÿ, P. *Pure Appl. Chem.* **1991**, *63*, 519.
52. Schmidt, R. R. *Pure Appl. Chem.* **1989**, *61*, 1257.
53. Paulsen, H. *Chem. Soc. Rev.* **1984**, *13*, 15.
54. Ogawa, T. *Chem. Soc. Rev.* **1994**, *23*, 397.
55. Kochetkov, N. E. *Stud. Nat. Prod. Chem.* **1994**, *14*, 201.
56. Demchenko, A. V. *Curr. Org. Chem.* **2003**, *7*, 35.
57. Schweizer, W. B.; Dunitz, J. D. *Helv. Chim. Acta* **1982**, *65*, 1547.
58. Nukada, T.; Bérces, A.; Whitfield, D. M. *J. Org. Chem.* **1999**, *64*, 9030.
59. Fraser-Reid, B.; Grimme, S.; Piacenza, M.; Mach, M; Schlueter, U. *Chem. Eur. J.* **2003**, *9*, 4687.
60. Fraser-Reid, B.; López, J. L.; Radhakrishnan, K. V.; Nandakumar, M. V.; Gómez, A. M.; Uriel, C. *J. Chem. Soc., Chem. Commun.* **2002**, 2104.
61. Mach, M.; Schlueter, U.; Mathew, F.; Fraser-Reid, B.; Hazen, K. C. *Tetrahedron* **2002**, *58*, 7345.
62. Zeng, Y.; Ning, J.; Kong, F. *Tetrahedron Lett.* **2002**, *43*, 3729.
63. Zeng, Y.; Ning, J.; Kong, F. *Carbohydr. Res.* **2003**, *338*, 307.
64. Hanashima, S.; Manabe, S.; Ito, Y. *Synlett* **2003**, 979.
65. Yan, F.; Gilbert, M.; Wakarchuk, W. W.; Brisson, J. R.; Whitfield, D. M. *Org. Lett.* **2001**, *3*, 3265.
66. Bérces, A.; Whitfield, D. M.; Nukada, T.; do Santos, Z. I.; Obuchowska, A.; Krepinsky, J. J. *Can. J. Chem.* **2004**, *82*, 1157.

Subject Index

A

- Acadesine, 8
- Acarbose, 14
- Acyl transfer, glycosylation reaction, 312, 312*f*, 313*f*, 314*f*, 315*f*, 317*f*
- Alpha-linked aryl O-glycosides, 258
- Alpha-linked D-galactosamine, 236, 237*f*, 249*f*
- Alpha-linked D-glucosamine, 236, 237*f*, 249*f*
- Alpha-linked glycosides, 245, 245*f*, 248*f*, 258*f*
  - formation, 254
- 2-Amino-2-deoxy-D-galactopyranoside, 235, 236*f*
  - glycosidation, 238
- 2-Amino-2-deoxy-D-glucopyranoside, 235, 236*f*
  - 2-azido sugars, 240
  - glycosidation, 238
- 2-Amino-2-deoxy-D-hexopyranosides, 235, 260, 260*f*
- Aminosugars, 21
  - anomeric effect, 279, 279*f*
  - anomeric functional groups, 268*t*
  - azide substitution, 274*t*
  - construction, 271*s*
  - 1,2:5,6-di-O-isopropylidine-D-glucofuranose modification, 270*s*
  - donors, 267*f*
  - glycoconjugates, 266*f*
  - glycosyl donors, 269*s*
  - glycosyl trichloroacetimidate library, 276*s*
  - hydroxyl group epimerization, 272, 273*t*
  - O-benzelidene acetals, 272*s*
  - overview, 265
  - phenylthioglucopyranoside library, 277*s*
  - regioselective deoxygenation, 275*t*
  - stereoselective glycosylation, 278
    - α-glycosidic bond formation, 281
    - β-glycosidic bond formation, 280
    - kanamycin library preparation, 281
    - pyranmycin library preparation, 280
  - synthesis, 267
    - glycosyl trichloroacetimidate library, 275
    - phenylthioglucopyranoside library, 276
    - starting sugar choice, 267
    - synthetic protocols, 271
- Amphotericin B, 8
- Anomeric effect, aminosugars, 279, 279*f*
- Anomeric functional groups, aminosugars, 268*t*
- Anthracyclines
  - antitumor activity, 144
    - multiple injection regimen, 145
    - single injection regimen, 145
  - cytotoxicity, 150
  - DoxoDavanat, 146
    - synthesis, 148*s*, 150*s*
  - Galactomycin, 140
    - antitumor activity, 146*t*
  - overview, 131
  - structure, 134*f*, 136*f*
- Arthritis, galectin therapy, 49
- Arylimino protection, bioactive glycoconjugates, 251*f*
- Aryl O-glycoside synthesis, 260*f*
- Asthma, galectin therapy, 47
- Azide substitution, aminosugars, 274*t*
- 2-Azido-2-deoxy-D-galactopyranose, 257*f*
- 2-Azido-2-deoxy-D-glucopyranose, 257*f*
- 2-Azido sugars, 240
  - alternatives, 245
- Azithromycin, 15

B

- β-Galactosidase daunorubicin prodrug activation, 139*f*
- β-Glucuronide daunorubicin prodrug activation, 138*f*
- Bioactive glycoconjugates
  - alpha-linked aryl O-glycosides, 258
  - alpha-linked D-galactosamine, 236, 237*f*, 249*f*
  - alpha-linked D-glucosamine, 236, 237*f*, 249*f*
  - alpha-linked glycosides, 245, 245*f*, 248*f*, 258*f*
    - formation, 254
  - aryl O-glycoside synthesis, 260*f*
  - arylimino protection, 251*f*
  - 2-azido sugars, 240
    - alternatives, 245
  - 2-azido-2-deoxy-D-galactopyranose, 257*f*
  - 2-azido-2-deoxy-D-glucopyranose, 257*f*
  - coupling reactions, 243*f*

Downloaded by 89.163.35.42 on June 13, 2012 | http://pubs.acs.org
Publication Date (Web): June 12, 2012 | doi: 10.1021/bk-2012-1102.ix002

Downloaded by 89.163.35.42 on June 13, 2012 | http://pubs.acs.org
Publication Date (Web): June 12, 2012 | doi: 10.1021/bk-2012-1102.ix002

  C-2-oximino protection, 252
  2,4-dintrophenyl moiety, 249
  fused-ring 2,3-oxazolidinone, 245, 246*f*, 247*f*
  glycosidation, 238
  glycosylation reactions, 240*f*, 242*f*
  methoxybenzylidene protection, 251
  N-acetyl 1-diazirine glycosyl donors, 253
  N-acetyl-D-glucosamine, 257*f*
  nitro-D-galactal based strategies, 248
  1-OH glycosyl donors, 257
  overview, 235
  select coupling reactions, 250*f*
  thermal glycosylation strategies, 256*f*

C

Cancer
  carbohydrate-assisted chemotherapy, 16
  colon cancer, 99
  galectins-based diagnostics, 33
Carbohydrate antigens, 162
  2G12, 162, 165, 168
  PG9, 163
  PG16, 163
  PGT series monoclonal antibodies, 163
Carbohydrate-assisted chemotherapy, 16
Carbohydrate-based HIV vaccines, 3
  carbohydrate antigens, 162, 165
    2G12, 162, 168
    PG9, 163
    PG16, 163
    PGT series monoclonal antibodies, 163
  HIV-1 glycopeptides, 173, 174*f*, 175*f*, 176*f*
  HIV-1 Gp120 glycosylation, 159
  HIV-1 N-glycosylation, 161
    ligands, 161
  oligomannose synthesis, 168, 169*f*, 170*f*, 171*f*, 172*f*
  oligosaccharide binding, 165, 166*f*, 167*f*
  overview, 157
  synthetic glycoconjugate immunogens, 175
Carbohydrate-based HIV-1 vaccines, 18
  CD4$^+$ T-cells, 188, 190
  2G12, 199*f*, 200*f*, 204
  glycan immunogens, 204
  gp120 glycans antibody recognition, 194*f*, 195*f*, 197, 201*f*
  HIV Env glycosylation, 196
  HIV-1 envelope glycoprotein, 193
    antibody responses, 194
  immune response eliciting, 188
  overview, 187
  pathogen glycosylation heterogeneity, 190, 193
  pathogen similarity, 189, 192, 192*t*
  PG9, 203*f*, 204
  PGT128, 204
  protein-glycan interactions, 189, 191
Carbohydrates
  aminosugars, 21
  carbohydrate-assisted chemotherapy, 16
  computational studies, 22
  drugs, 4
    disaccharides, 10
    macrolides, 15
    monosaccharide conjugates, 4
    oligosaccharides, 12
    polysaccharides, 12
    trisaccharides, 11
  galectins, 17
  HIV-1 vaccines, 18
  infections, 20
  overview, 3
  polysaccharides, 20
Cardiovascular diseases, galectin therapy, 47
Carminomycin conjugates synthesis, 142*s*
Cationic polysaccharides
  crab chitin, 220
  D-glucosamine, 221*s*
  Mucor rouxii, 220, 222*t*, 223*f*, 225*f*, 226*f*, 227*f*
  overview, 219
  polyglucosamine, 220*s*
  sodium pyrithionate, 228*t*
  in vitro activity, 221
  in vivo activity, 227
CD4$^+$ T-cells, 188, 190
Clarithromycin, 15
Clindamycin, 9
COLO 205, 100*t*, 101*t*, 102*t*, 104*t*
Colon cancer, 99
C-2-oximino protection, 252
Crab chitin, 220

D

Dalteparin, 13
Danaparoid, 13
Daunorubicin, 5
DAVANAT, 44*f*, 69
  anti-cancer efficacy enhancement, 98
  binding, 111, 113*f*, 114*f*

Downloaded by 89.163.35.42 on June 13, 2012 | http://pubs.acs.org
Publication Date (Web): June 12, 2012 | doi: 10.1021/bk-2012-1102.ix002

- chemistry, 91
- COLO 205, 100*t*, 101*t*, 102*t*, 104*t*
- drug administration, 109
- drug formulation, 109
- effect, 99, 101*f*, 102, 103*f*, 105*f*
- 5-Fluorouracil, 93, 98
  - efficacy, 99, 101*f*, 102, 104, 108*f*
- HT-29, 105*t*, 106*t*
- identification, 92
- isolation, 92
- mucositis, 127
- mutagenicity, 93
- overview, 89
- patients tolerance, 124*t*
- phase I clinical studies, 120
- phase II clinical studies, 125
- pre-clinical efficacy, 98
- pre-clinical in vivo toxicity, 96
  - non-clinical safety studies, 96
- purification, 92
- radiolabel studies, 115
  - tissue distribution, 115, 117*t*
- statistical methods, 110
- tumor volumes, 100*t*, 101*t*
- *See also* Galactomannan polysaccharide (GM-CT-01)

D-Glucosamine, 221*s*
Digoxin, 11
2,4-Dintrophenyl moiety, 249
1,2:5,6-Di-O-isopropylidine-D-glucofuranose modification, 270*s*
Dirithromycin, 15
DoxoDavanat, 146
- synthesis, 148*s*, 150*s*

Doxorubicin, 5, 144*f*
- ED_{50}, 150*t*

Doxorubicin conjugates synthesis, 142*s*, 143*s*

E

ED_{50}, 150*t*
Enoxaparin, 13
Epirubicin, 5
Erythromycin, 15
Etoposide, 9

F

Fludarabine phosphate, 6
5-Fluorouracil, 93, 98
- efficacy, 99, 101*f*, 102, 104, 108*f*

Fused-ring 2,3-oxazolidinone, 245, 246*f*, 247*f*

G

2G12, 199*f*, 200*f*, 204
Galactomannan polysaccharide (GM-CT-01)
- accelerated thermal stability, 80*t*
- analytical identification, 74
- building blocks, 73*f*
- clinical studies, 84
- ^{13}C-NMR spectrum, 75*f*, 77*t*
- compatibility, 82
- final formulation composition, 73
- ^{1}H NMR spectra, 74*f*, 76*f*
- HPLC, 79*f*
- manufacturing, 73
- molecular weight determination, 77
- overview, 69
- physical description, 72
- pre-clinical data, 84
- quantitation, 77
- stability, 80
- stereochemical configuration, 73*f*
- ZIMM plot, 78*f*
- *See also* DAVANAT

Galactomannans, activation, 147*s*
Galactomycin, 140
- antitumor activity, 146*t*

Galectin blockers, galectin therapy, 40
Galectin ligands molecules, 40
Galectins, 17
- academic publications, 27*f*
- clinical manifestations
  - immune response, 32
  - inflammation, 30
  - tumor angiogenesis, 28
- diagnostics
  - cancer, 33
  - heart failure, 36
  - liver diseases, 38
- ligand specificity, 111
- targeted drug design
  - overview, 25
  - therapeutics, 33
- therapy
  - arthritis, 49
  - asthma, 47
  - cardiovascular diseases, 47
  - galactomannans, 43
  - galectin blockers, 40
  - malignant gliomas, 52
  - pathology indicators, 52

Downloaded by 89.163.35.42 on June 13, 2012 | http://pubs.acs.org
Publication Date (Web): June 12, 2012 | doi: 10.1021/bk-2012-1102.ix002

potentiality, 53
Gemcitabine, 6
Glycan immunogens, 204
Glycosylation reaction
  acyl transfer, 312, 312*f*, 313*f*, 314*f*, 315*f*, 317*f*
  O-2, 306, 307*t*, 308*f*, 309*f*, 310*f*
  overview, 287
  permethylated glycopyranosyl oxacarbenium ions, 294, 296*f*, 301*f*, 304*t*, 305*f*
  pyranose ring conformation, 288, 290*f*, 297*f*, 299*f*
    canonical vector space, 289, 291*t*
    redundancy vector space, 289, 293*t*
Glycosyl donors, aminosugars, 269*s*
Glycosyl trichloroacetimidate library, aminosugars, 276*s*
Glycosylation reactions, bioactive glycoconjugates, 240*f*, 242*f*
GM-CT-01. *See* Galactomannan polysaccharide (GM-CT-01)
Gp120 glycans antibody recognition, 194*f*, 195*f*, 197, 201*f*

H

Heart failure, galectins-based diagnostics, 36
Heparin, 13
HIV Env glycosylation, 196
HIV-1 envelope glycoprotein, 193
  antibody responses, 194
HIV-1 glycopeptides, 173, 174*f*, 175*f*, 176*f*
HIV-1 Gp120 glycosylation, 159
HIV-1 N-glycosylation, 161
  effects, 161
  ligands, 161
HT-29, 105*t*, 106*t*
Hydroxyl group epimerization, aminosugars, 272, 273*t*

I

Idarubicin, 5
Immune response, galectins, 32
Infections, polysaccharides, 20
Inflammation, galectins, 30

L

Lactulose, 10
Lincomycin, 9
Liver diseases, galectins-based diagnostics, 38

M

Malignant gliomas, galectin therapy, 52
MCP. *See* Modified citrus pectin (MCP)
Methoxybenzylidene protection, 251
Modified citrus pectin (MCP), 41
Monosaccharide conjugates
  anthracycline antibiotics, 5
  nucleosides, 5
  nucleotides, 5
  polyenes, 8
Mucor rouxii, 220, 222*t*, 223*f*, 225*f*, 226*f*, 227*f*
Mucositis, 127

N

N-acetyl 1-diazirine glycosyl donors, 253
N-acetyl-D-glucosamine, 257*f*
Neomycin, 13
Nitro-D-galactal based strategies, 248
3′N-L-lysyl-doxorubicin synthesis, 149*s*

O

O-2, glycosylation reaction, 306, 307*t*, 308*f*, 309*f*, 310*f*
O-benzelidene acetals, aminosugars, 272*s*
1-OH glycosyl donors, 257
Oligomannose synthesis, 168, 169*f*, 170*f*, 171*f*, 172*f*, 206*f*
Oligosaccharide binding, 165, 166*f*, 167*f*
Oligosaccharides
  complex oligosaccharides, 13
  heparin, 12

P

Pathogen glycosylation heterogeneity, 190, 193
Pathology indicators, galectin therapy, 52
Pentosan polysulfate, 13

Pentostatin, 10
Permethylated glycopyranosyl oxacarbenium ions, glycosylation reaction, 294, 296*f*, 301*f*, 304*t*, 305*f*
PG9, 203*f*, 204
PGT128, 204
Phenylthioglucopyranoside library, aminosugars, 277*s*
Polyglucosamine, 220*s*
Polysaccharides, infections, 20
Protein-glycan interactions, 189, 191
Pyranose ring conformation, glycosylation reaction, 288, 290*f*, 297*f*, 299*f*
  canonical vector space, 289, 291*t*
  redundancy vector space, 289, 293*t*

R

Regioselective deoxygenation, aminosugars, 275*t*
Ribavirin, 7
13-(R,S)-Dihydrodaunorubicin, monosaccharide conjugates synthesis, 141*s*

S

Sodium pyrithionate, 228*t*
Stavudine, 6
Stereoselective glycosylation, aminosugars, 278
  α-glycosidic bond formation, 281
  β-glycosidic bond formation, 280
  kanamycin library preparation, 281
  pyranmycin library preparation, 280
Streptomycin, 13
Sucralfate, 10
Synthetic glycoconjugate immunogens, 175

T

Thermal glycosylation strategies, bioactive glycoconjugates, 256*f*
Tinzaparin, 13
Tobramycin, 11
Tumor angiogenesis, galectins, 28

V

Vancomycin, 10

Downloaded by 89.163.35.42 on June 13, 2012 | http://pubs.acs.org
Publication Date (Web): June 12, 2012 | doi: 10.1021/bk-2012-1102.ix002